ISSN: 2150-4091 (Print), 2150-4105 (Online) Volume 2, Number 4, April 2010

Scientific Research

Natural Science

ISSN: 2150-4091

Editor-in-Chief
Kuo-Chen Chou

www.scirp.org/journal/ns/

Journal Editorial Board

ISSN: 2150-4091 (Print) ISSN: 2150-4105 (Online)

http://www.scirp.org/journal/ns/

Vol.2, No.4, 247-417 (2010) Natural Science

TABLE OF CONTENTS

Volume 2, Number 4, April 2010

Natural Science

Journal Information

SUBSCRIPTIONS

The *Natural Science* (Online at Scientific Research Publishing, www.SciRP.org) is published monthly by Scientific Research Publishing, Inc., USA.

Subscription rates:

Print: $50 per copy.
To subscribe, please contact Journals Subscriptions Department, E-mail: sub@scirp.org

SERVICES

Advertisements
Advertisement Sales Department, E-mail: service@scirp.org

Reprints (minimum quantity 100 copies)
Reprints Co-ordinator, Scientific Research Publishing, Inc., USA.
E-mail: sub@scirp.org

COPYRIGHT

PRODUCTION INFORMATION

For manuscripts that have been accepted for publication, please contact:
E-mail: ns@scirp.org

Vol.2, No.4, 247-291 (2010)
doi:10.4236/ns.2010.24036

Natural Science

Genetic structure associated with diversity and geographic distribution in the USDA rice world collection

Hesham A. Agrama[1], WenGui Yan[2]*, Melissa Jia[2], Robert Fjellstrom[2], Anna M. McClung[2]

[1]University of Arkansas, Rice Research and Extension Center, Stuttgart, USA
[2]USDA-ARS, Dale Bumpers National Rice Research Center, Stuttgart, USA; Wengui.Yan@ars.usda.gov

Received 14 December 2009; revised 13 January 2010; accepted 26 January 2010.

ABSTRACT

Cultivated rice (*Oryza sativa* L.) is structured into five genetic groups, *indica, aus, tropical japonica*, *temperate japonica* and *aromatic*. Genetic characterization of rice germplasm collections will enhance their utilization by the global research community for improvement of rice. The USDA world collection of rice germplasm that was initiated in 1904 has resulted in over 18,000 accessions from 116 countries, but their ancestry information is not available. A core subset, including 1,763 accessions representing the collection, was genotyped using 72 genome-wide SSR markers, and analyzed for genetic structure, genetic relationship, global distribution and genetic diversity. Ancestry analysis proportioned this collection to 35% *indica*, 27% *temperate japonica*, 24% *tropical japonica*, 10% *aus* and 4% *aromatic*. Graphing model-based ancestry coefficients demonstrated that *tropical japonica* showed up mainly in the American continents and part of the South Pacific and Oceania, and *temperate japonica* in Europe and the North Pacific far from the equator, which matched the responses to temperature. *Indica* is adapted to the warm areas of Southern Asia, South China, Southeast Asia, South Pacific and Central Africa and around the equator while *aus* and *aromatic* are special types of rice that concentrates in Bangladesh and India. *Indica* and *aus* were highly diversified while *temperate* and *tropical japonicas* had low diversity, indicated by average alleles and private alleles per locus. *Aromatic* has the most polymorphic information content. *Indica* and *aromatic* were genetically closer to *tropical japonica* than *temperate japonica*. This study of global rice has found significant population stratification generally corresponding to major geographic regions of the world.

Keywords: Genetic Structure; Rice Ancestry; Germplasm Collection; Molecular Diversity; Global Distribution

1. INTRODUCTION

Rice (*Oryza sativa* L) is one of the earliest domesticated crop species and has become the one of the world's most widely grown crops. Rice consumption constitutes about 20% of the world's caloric intake, and in Asian countries, where over half of the world's population lives, rice represents over 50% of the calories consumed [1]. Because of its small genome size, rice became the first crop species to have its genome completely sequenced [2,3] and thus has become a model system for other grass species.

Oryza rufipogon, a member of more than 20 wild species in the genus *Oryza* [4,5], is commonly regarded as the wild progenitor of cultivated rice, *O. sativa*, which is divided into two sub-species: *indica* and *japonica*. *Indica* is the predominant subspecies representing about 80% of the world rice crop, and the remaining 20% is *japonica* [6]. The two sub-species differ distinctly in morphological and genetic characteristics [7] and their hybrids are highly sterile [8]. As a result, a wide compatibility gene is necessary to utilize hybrid vigor between the two sub-species [9], which is greater than the vigor within either sub-species alone. This classification confirms the empirical distinction between them, which the Chinese recognized in literature as early as 100 AD [10] and called 'Hsian' for *indica* and 'Jing or Geng' for *japonica* [11]. The domestication from *O. rufipogon* to two sub-species of *O. sativa* is believed to have occurred several times [12], but more recent studies indicate a single domestication [13].

Molecular markers and more recently, high throughput genome sequence efforts, have dramatically increased the capability to characterize genetic diversity and population structure in plant germplasm pools [14]. Early studies divided the cultivated rice into six groups: *indica, japonica, aus, aromatic, rayada* and *ashima* [11]. *Rayada* and *ashima* are floating types of rice limited in special areas of Bangladesh and India. The former is responsive to photo-period, but the latter is not. *Aus*, drought-tolerant rice cultivars grown in Bangladesh and West Bengal, is further differentiated from *indica*. *Japonica* has been divided into three groups: *tropical japonica* or *javanica*, *temperate japonica* and *aromatic* [12, 15-17]. Because *Rayada* and *ashima* are minor and limited, research efforts have concentrated on five subgroups: *indica, aus, tropical japonica, temperate japonica*, and *aromatic* [12,15,17].

Genetic incompatibility between *indica* and *japonica* results in hybrid sterility [8,9,18,19]. Thus, hybrid rice which exhibits a yield advantage of 15 to 20 percent over the best traditional cultivars [20,21] has been limited to parents within each sub-species [22]. However, because heterosis between the two sub- species, as observed in vegetative growth, panicle size and spikelets per panicle, is so pronounced, scientists consistently make an effort to overcome the sexual barrier [8,9, 18,19]. Analyses of genetic structure and relationships based on genetic differentiation in rice help design breeding strategies and overcome the sexual barrier for utilizing inter-subspecies heterosis. This subject has attracted numerous studies on five- model structure in rice genetics [11,12,15-17,23-26]. However, these studies were based on an evaluation of limited set of diverse materials ranging from 72 [16] to 330 accessions [24] instead of a complete worldwide collection. The only study on a complete rice collection was done by Zhang *et al*. [27], where ecotypes in both *indica* and *japonica* of the China national collection were analyzed.

Genetic structure is usually inferred using the model-based clustering algorithms implemented in STRUCTURE [28-30] and TESS [31]. Admixture coefficients of population as the outputs of STRUCTURE or TESS analyses could be integrated in other programs to demonstrate geographical structure of populations [32]. These computer programs have been widely used for analysis of genetic structure in rice [17,23,24].

The rice world collection in the USDA National Plant Germplasm System (NPGS) started in 1904 [33] and contains over 18,000 accessions from 116 countries representing 12 *Oryza* species with 99% originating from *O. sativa* [34]. However, ancestry information is not available for these accessions. A core subset including 10% of the collection has proven to well represent the whole collection [35], so is a good subset for genetic assessment of the collection.

Using genotypic information of the core subset generated by 72 genome-wide SSR markers, the objectives of this study were to 1) characterize genetic structure of ancestry population, 2) analyze geographic distribution of each population in rice growing areas of the world, and 3) describe genetic diversity and specialty in each of the populations, including average alleles distinct and private to a population in the USDA rice world collection. The resulting information could help design genetic strategies for gene transfer among genetic populations and utilization of hybrid vigor between genetic populations.

2. MATERIALS AND METHODS

2.1. Materials and Genotyping

Advantages for using core subset strategy in germplasm characterization and management of a large collection have been well documented [35,36]. A core collection of 1,794 accessions was developed using a stratified random sampling method [37]. Evaluation of the core collection has been applied to 14 characteristics with agronomic and quality importance [35], and resistance to biotic and abiotic stresses including straighthead disorder [38]. Genetic information resulted from this study combining with phenotypic evaluations would help understand this collection. This core collection genotyped by 72 single sequence repeat (SSR) markers was studied for our objectives. Purification of each core accession was conducted using single plant selection to remove 'heterogeneity' for genotyping purpose [39]. The SSR markers were distributed over the entire rice genome about every 30 cM in genetic distance [39]. Total genomic DNA was extracted using a rapid alkali extraction procedure [40] from a bulk of five plants representing each accession. PCR amplifications of the markers followed the protocol described by Agrama *et al.* [39]. DNA samples were separated on an ABI Prism 3730 DNA analyzer according to the manufacturer's instructions (Applied Biosystems, Foster City, CA, USA). Fragments were sized and binned into alleles using GeneMapper v. 3.7 software.

Nine accessions were excluded from analysis because of their unknown (four accessions) and uncertain (two) originations and failure during processing (three) as well as 22 other species. The remaining 1,763 accessions of *Oryza sativa* were analyzed using the following methods. Structural ancestry of each accession was inferred by 40 reference cultivars that have known structural information, which are marked in the **Supplementary Table**. There were 17 core accessions, 19 cultivars commercialized in the U.S. and four in China, respectively. Two of the core accessions originated in the U.S. as well. Forty reference cultivars had five *aromatic*, three *aus*, eight *indica*, four *temperate japonica* and 20 *tropical japonica* types described by Garris *et al*. [17], Agrama and Eizenga [23], Agrama and Yan [41], Mackill [6] and McNally *et al*. [42]. Twenty-one U.S. reference cultivars included one *indica* (Jasmine 85), two *temperate japonicas* grown in California (M201 and M202), and 18 *tropical japonicas* commercialized in the southern states.

Each country from which germplasm originated was grouped in the geographic region according to the United Nations Statistics Division (http://unstats.un.org/unsd/methods/m49/m49regin.htm). Latitude and longitude of each accession were downloaded from the USDA Germplasm Resources Information Network (GRIN, www.ars-grin.gov) when available. They were inferred using coordinate location of the state or province where it was collected if the location is marked in the GRIN. Otherwise, the location was inferred using the location of its capital city for the accession to be collected.

2.2. Statistical Analysis

Genotypic data of 72 SSR markers for 1,763 core accessions plus additional 23 reference cultivars were used to decide putative number of structures at first. Genetic structure was inferred using the admixture analysis model-based clustering algorithms implemented in TESS v. 2.1 [31]. TESS implements a Bayesian clustering algorithm for spatial population genetics. Multi-locus genotypes were analyzed with TESS using the Markov Chain Monte Carlo (MCMC) method, with the F-model and a ψ value of 0.6 which assumes 0.0 as non-informative spatial prior. To estimate the K number of ancestral-genetic populations and the ancestry membership proportions of each individual in the cluster analysis, the algorithm was run 50 times, each run with a total of 70.000 sweeps and 50.000 burn-in sweeps for each K value from 2 to 9. For each run we computed the Deviance Information Criterion (DIC), the log-likelihood value [43] and rate of change in the log-likelihood value (ΔK) [44], which are the model-complexity penalized measures to show how well the model fits the data. The putative number of populations was obtained when the DIC and ΔK values were the smallest and estimates of data likelihood were the highest in 10% of the runs. Similarity coefficients between runs and the average matrix of ancestry membership were calculated using CLUMPP v. 1.1 [45].

Each accession in the core collection was grouped to a specific cluster or population by its K value resulted from cluster analysis using TESS. The sub- species ancestry of each K was inferred by the reference cultivars for *indica*, *aus*, *aromatic*, *temperate japonica*, and *tropical japonica* rice. Analysis of molecular variance (AMOVA) [46] was used to calculate variance components within and among the populations obtained from TESS in the collection. Estimation of variance components was performed using the software ARLEQUIN 3.0 [47]. The AMOVA-derived Φ_{ST} [48] is analogous to Wright's F statistics differing only in their assumption of heterozygosity [49]. Φ_{ST} provides an effective estimate of the amount of genetic divergence or structuring among populations [46]. Significance of variance components was tested using a non-parametric procedure based on 1,000 random permutations of individuals. The computer package ARLEQUIN was used to estimate pair-wise F_{ST} [50] for the five populations obtained from TESS.

Multivariate analysis such as principle coordinates analysis (PCA) provides techniques for classifying the inter-relationship of measured variables among populations. Multivariate geo-statistical methods combine the advantages of geo-statistical techniques and multivariate analysis while incorporating spatial or temporal correlations and multivariate relationships to detect and map different sources of spatial variation on different scales [51,52]. Geographical spatial interpolation of principal coordinates of latitude and longitude and admixture ancestry matrix coefficients (Ks) calculated in TESS for each accession were represented by kriging method [32] as implemented in the R statistical packages 'spatial', 'maps' and 'fields' [53,54] for visualizing distribution in the world map.

Principal coordinates analysis (PCA) was conducted using GenAlex 6.2 [55] software to structure the core collection genotyped by 72 SSR markers, and generate the PCA. Geo-statistical and geographic analysis was based on CNT coordinates of latitude and longitude where a core accession originated using the R statistical packages. Polymorphism information content (PIC) and number of alleles per locus in each sub-species population were estimated using PowerMarker software [56]. Number of distinct alleles in each population and number of alleles private to each population that is not found in other populations, were calculated using ADZE program (Allelic Diversity AnalyZEr) [57]. ADZE uses the rarefaction method to trim unequal accessions to the same standardized sample size, a number equal to the smallest accessions across the populations.

3. RESULTS

3.1. Number of Populations and Their Ancestries

Structural analysis for 1,763 accessions in the USDA rice core collection plus 23 reference cultivars genotyped with 72 molecular markers using TESS program [31] resulted in the most sharp variation of both the log-likelihood value Deviance Information Criterion (DIC) and its change rate (ΔK) till the putative number (K) of populations reached five, indicating the most likelihood structure of the collection (**Figure 1**). The inferred ancestry estimate of each accession in each K is presented in the **Supplementary Table** (**Sup Table**). Similarly, principle coordinates (PC) analysis of Nei's genetic

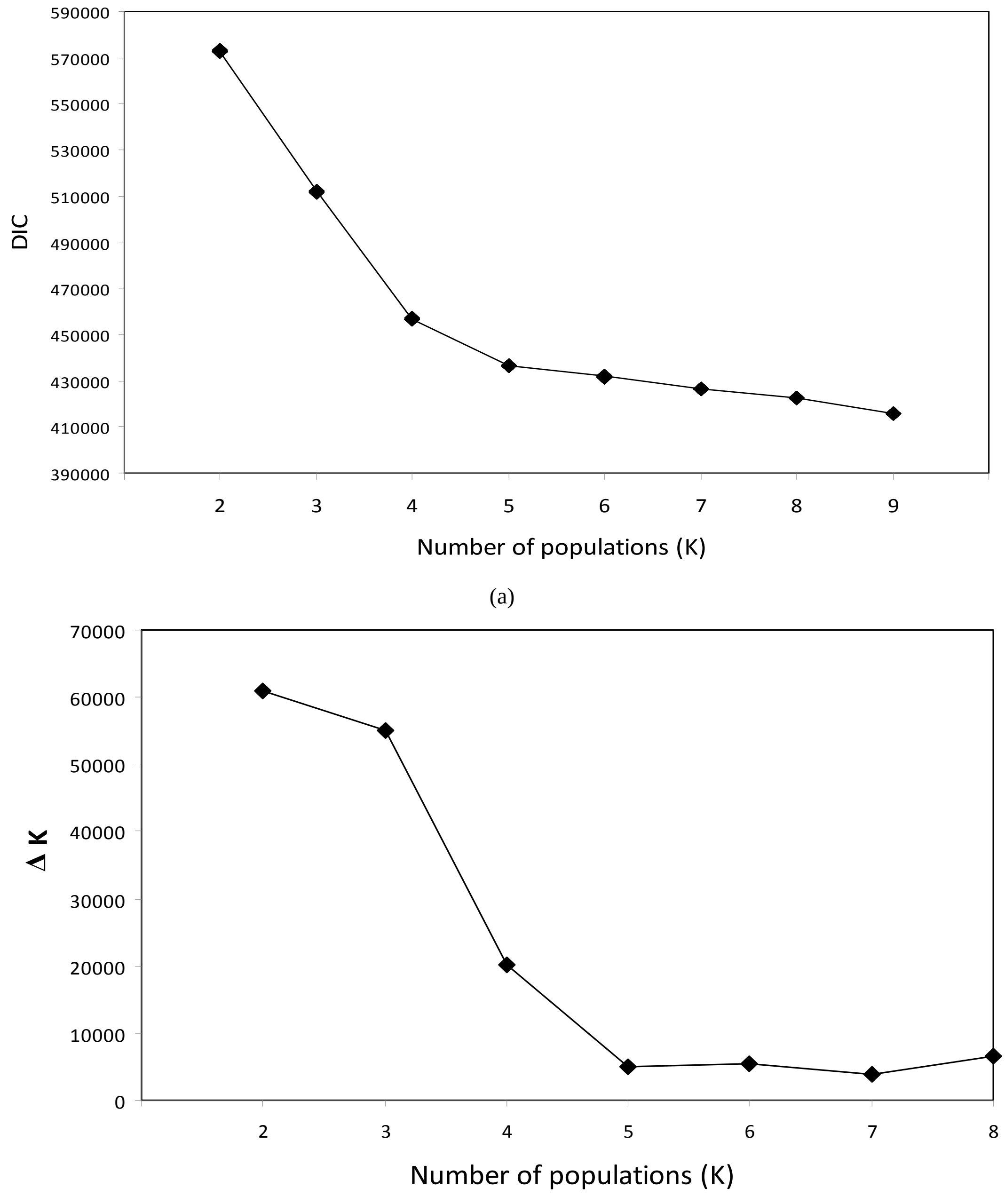

Figure 1. Five populations should be structured based on (a) the log-likelihood values (Deviance Information Criterion, DIC) and (b) the change rate of log-likelihood values (ΔK) for estimated number of populations over 50 structure replicated runs using TESS program. A plateau of DIC and maximum ΔK indicate the most likely number of populations.

distance [58,59] classified the core accessions into five clusters by PC1 and PC2 including 71% of total variances (**Figure 2**). Both structure and PC analyses indicated that five populations sufficiently explained the genetic relationship in the core collection. Analysis of molecular variance (AMOVA) showed that 38% of the variance was due to genetic differentiation among the populations (**Table 1**). The remaining 62% of the variance was due to the differences within the populations. The variances among and within the populations were highly significant ($P < 0.001$).

Among 40 reference cultivars, 20 that are known *tropical japonica* (TRJ) were classified in K1, four known *temperate japonica* (TEJ) in K2, eight known

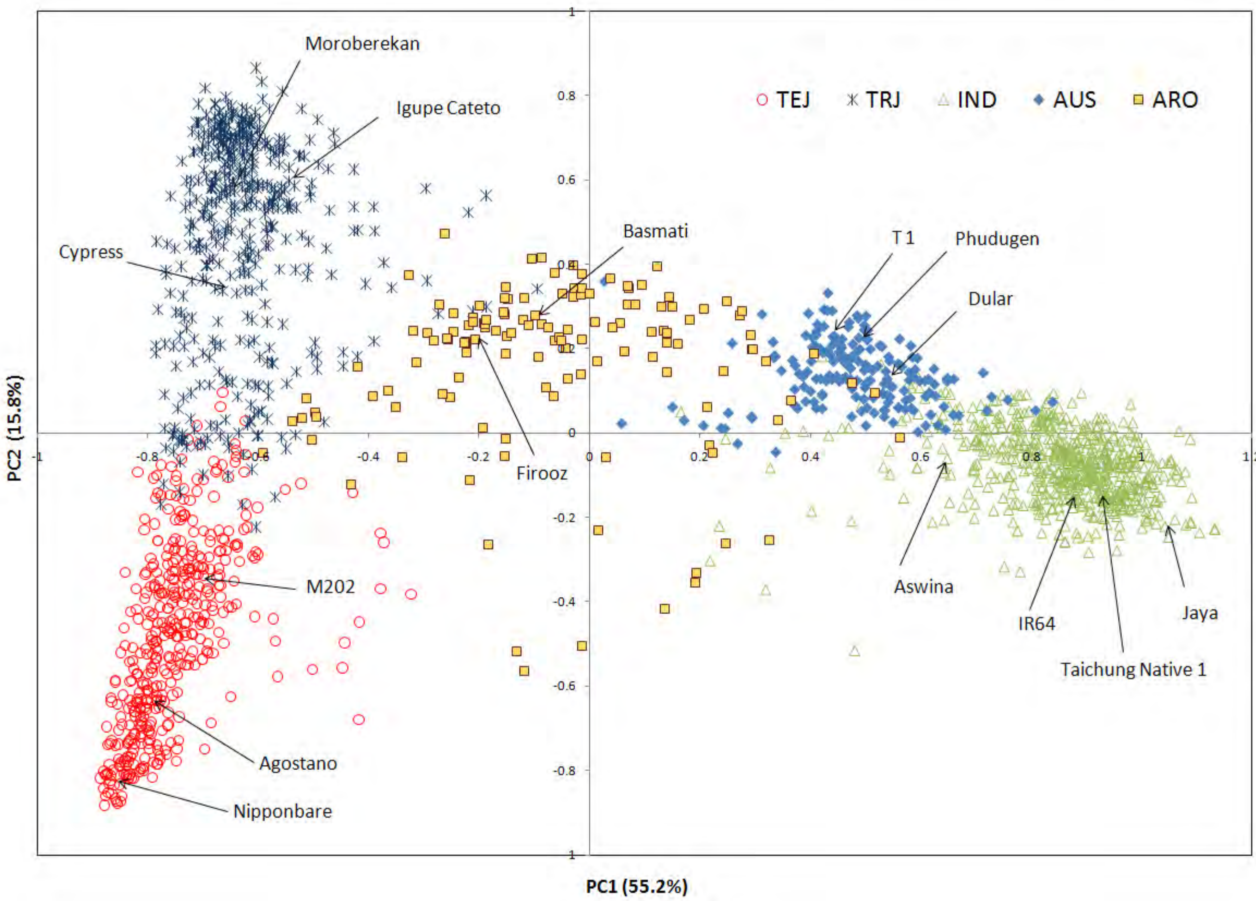

Figure 2. Principle coodinates analysis of five populations inferred by highlighted reference cultivars (*temperate japonica* – TEJ, *tropical japonica* – TRJ, *indica* - IND, *aus* - *AUS and aromatic* - ARO) for 1,763 core accessions genotyped with 72 SSR markers (Data presented in **Supplementary Table**).

indica (IND) in K3, three known *aus* (AUS) in K4 and five known *aromatic* (ARO) in K5 (**Sup Table**), indicating the correspondent ancestry of each population. Based on the references, each accession was clearly assigned to a single population when its inferred ancestry estimate was 0.6 or larger, the cutoff criterion used by Garris *et al*. [17] (**Supplementary Table**), and admixture between populations when its estimate was less than 0.6 (**Sup Table**). Admixture was based on proportion of the estimate, i.e. GSOR 310002 was assigned TEJ-TRJ because of its estimate 0.5227 in K2 and 0.4770 in K1.

K1 or *tropical japonica* population included 351 (19.9%) absolute accessions, 40 (2.3%) admixtures with K2 or *temperate japonica* population, 26 (1.5%) admixtures with K3 or *indica* and one admixture with K4 or *aus*. In K2, 419 (23.8%) accessions had absolute ancestry, 52 (2.9%) admixed with K1 and eight admixed with other populations. K3 or *indica* population had 620 (35.1%) accessions among which 590 were clearly assigned, twelve admixed with K4, eight admixed with each of K1 and K2 and two with K5. One hundred sixty-one (9.1%) accessions were clearly grouped in K4, 13 were admixed with K3 and one admixed with K5 or *aromatic* population. Sixty-three (4.0%) accessions were clearly structured in K5, five were admixed with K2 and three admixed with other populations.

3.2. Genetic Relationship and Global Distribution of Ancestry Populations

All pair-wise estimates of F_{ST} using AMOVA for the populations were highly significant ranging from 0.240 between *tropical japonica* and *aromatic* to 0.517 between *temperate japonica* and *aus* (**Table 2**). *Indica* was about equally distant from *aromatic* and *aus*, but more distant from *temperate japonica* and *tropical japonica*. *Aus* and *indica* were mostly differentiated from *temperate japonica*. However, *temperate japonica*, *tropical japonica* and *aromatic* were close to each other in comparison with others. These relationships were consistent with structure analysis revealed by the PCA (**Figure 2**).

Table 1. Analysis of molecular variance (AMOVA) for the 1,763 core accessions and 23 reference cultivars for five populations (*aromatic*, *aus*, *indica*, *temperate japonica* and *tropical japonica*) based on 72 SSR markers.

Source	df	SS	MS	Est.Var.	%	Φ_{ST}	P-value[a]
Among Pops	4	57383	14346	43	38	0.38	<0.001
Within Pops	1781	124086	70	70	62	0.62	<0.001
Total	1785	181470		112	100		

[a]Probability of obtaining a more extreme random value computed from non-parametric procedures (1,000 permutations).

Table 2. Pairwise estimates of F_{ST} (lower diagonal) and their corresponding probability values (upper diagonal) for five rice populations, K5 - *aromatic* (ARO), K4 - *aus* (AUS), K3 - *indica* (IND), K2 - *temperate japonica* (TEJ) and K1 - *tropical japonica* (TRJ) for 1,763 core accessions genotyped with 72 SSR markers based on 999 permutations.

	ARO	AUS	IND	TEJ	TRJ
ARO		0.001	0.001	0.001	0.001
AUS	0.253		0.001	0.001	0.001
IND	0.284	0.308		0.001	0.001
TEJ	0.317	0.517	0.500		0.001
TRJ	0.240	0.475	0.462	0.273	

Among 418 accessions of *tropical japonica* rice in the collection, the majority is collected from Africa (100 or 24%) and South America (88 or 21%), followed by Central America (15%), North America (13%), South Pacific (6%), Southeast Asia and Oceania (5% each) (**Figure 3(a)**, **Sup Table**). The remaining accessions scattered in other regions. North America had 70 accessions in total and 55 were grouped in *tropical japonica*, which was the highest percentage (79%) among 14 regions, followed by Central America (56%), Africa (49%) and South America (41%). Among 112 countries, the U.S. in North America had the highest percentage (92%) of accessions, followed by Cote d'lvoire and Zaire (91%) in Africa and Puerto Rico (72%) in Central America.

Most *temperate japonica* rice is collected from Western and Eastern Europe (20% each), followed by North Pacific (14%), South America (10%), Central Asia (7%) and North China (7%) (**Figure 3(b)**, **Sup Table**). Similarly, Western and Eastern Europe had the highest percentage (85% each) of *temperate japonica*, followed by North Pacific (55%) and South America (20%). Hungary accessions had the highest percentage (97%), followed by Italy (89%), Russian Federation and Portugal (83% each).

Based on United Nations' classification, region China includes Mongolia, Hong Kong, Taiwan and China itself. Most *indica* rice (25%) is collected from region China, followed by the Southern Asia (14%), South America (13%), Southeast Asia and Africa (10% each) (**Figure 3(c)**, **Sup Table**). Region China had the highest percentage (72%) of *indica*, followed by South Pacific (57%), Southeast Asia (53%), Southern Asia (38%) and Africa (29%). Also, country China had the highest percentage (84%) of *indica*, followed by Columbia (81%), Sri Lanka (80%) and Philippines (68%).

About half of the *aus* rice in the collection was sampled from the Southern Asia (48%), followed by Africa (16%), Middle East (11%), South America and Southeast Asia (7% each) (**Figure 3(d)**, **Sup Table**). Southern Asia had the highest percentage (40%) of *aus*, followed by Middle East (21%), Africa (14%) and Southeast Asia (10%). Bangladesh had the highest percentage (63%) of *AUS*, followed by Iraq (64%), Pakistan (49%) and India (40%).

Aromatic rice in the collection originated mainly from Pakistan (20%) and Afghanistan (13%) in the Southern Asia and Azerbaijan (15%) in Central Asia, representing 37%, 44% and 57% of total core accessions from these countries, respectively (**Figure 3(e)**, **Sup Table**).

3.3. Genetic Diversity of Ancestry Populations

Average alleles per locus were the highest in *indica*, followed by *aus*, *aromatica*, *tropical japonica* and *temperate japonica* (**Figure 4**). *Indica* had 45% more alleles per locus than *temperate japonica*. *Aromatic* had the highest polymorphic information content (PIC), followed by *aus*, *indica*, *tropical japonica* and *temperate japonica*. The PIC value of *temperate japonica* was 72% less than that of *aromatic*. Similarly after standardizing sample size for five populations, *indica* had the most alleles per locus (7.95), which was close to *aus* (7.76) and *aromatic* (7.44) (**Figure 5(a)**). *Tropical* (6.53) and *temperate japonica* (5.66) had much less alleles per locus than those three populations. Private alleles per locus in a population are unique to others. *Aus* (1.01) had the most private alleles, which was similar to indica (0.93) and much more than *tropical japonica* (0.50), *temperate japonica* (0.34) and *aromatic* (0.20) (**Figure 5(b)**).

4. DISCUSSIONS

Rice grown in the west belt of the U.S. belongs to *temperate japonica* and in the south belt to *tropical japonica* [6,17]. However, a consistent effort has been applied to

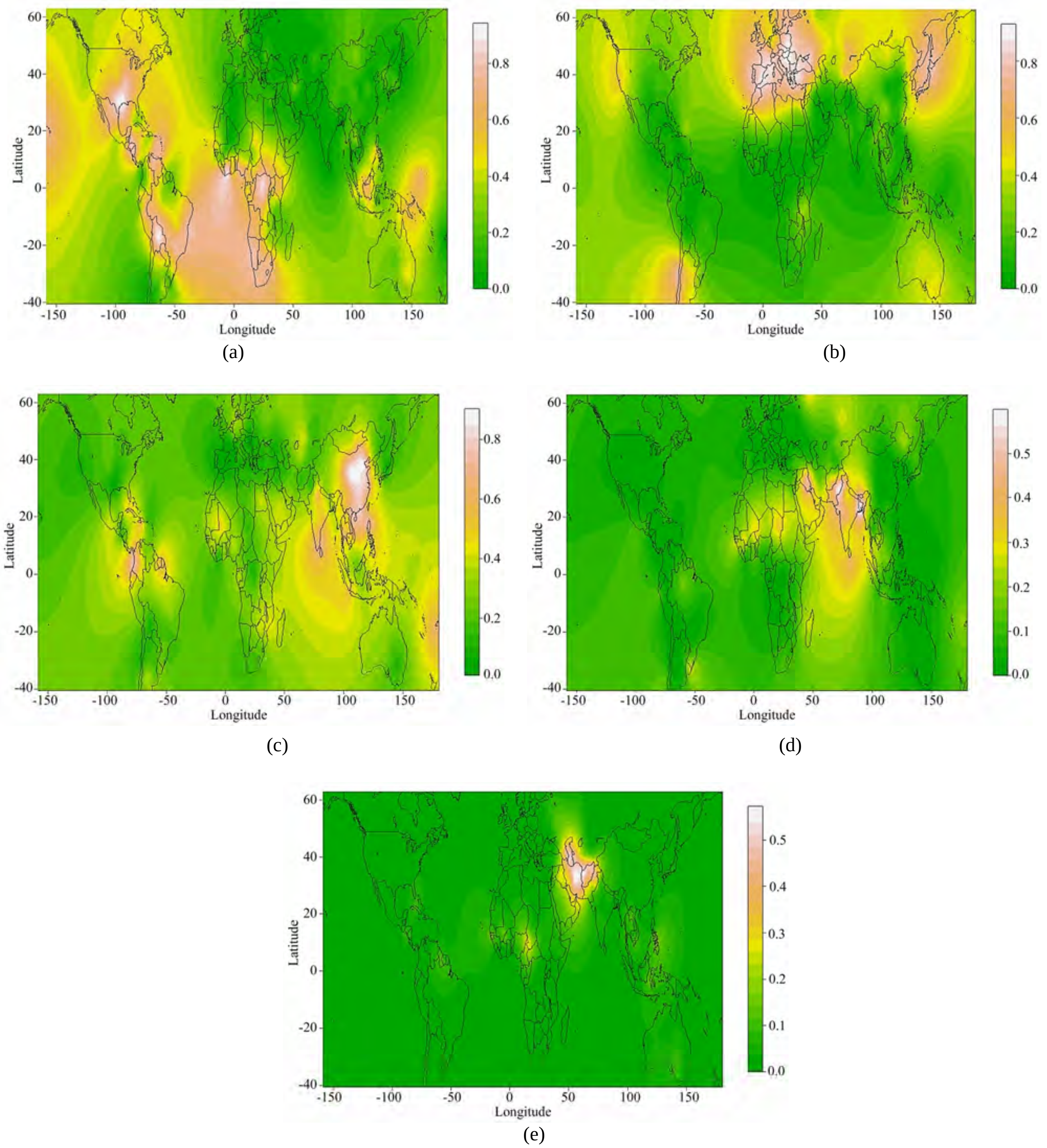

Figure 3. Global distribution of core accessions in each population resulted from cluster analysis and inferred by reference cultivars based on geographical coordinates of latitude and longitude in (a) K1 (*tropical japonica* – TRJ); (b) K2 (*temperate japonica* – TEJ); (c) K3 (*indica* – IND); (d) K4 (*aus* – AUS); and (e) K5 (*aromatic* – ARO) (Data presented in **Supplementary Table**).

collect rice germplasm in a global scope for maximizing genetic diversity in the USDA rice germplasm collection. As a result, this collection holds over 18,000 accessions introduced from 116 countries at present. This study demonstrated that the collection contains 35% *indica*, 27% *temperate japonica*, 24% *tropical japonica*, 10% *aus* and 4% *aromatic*. This was the first time to completely structure a worldwide collection using molecular

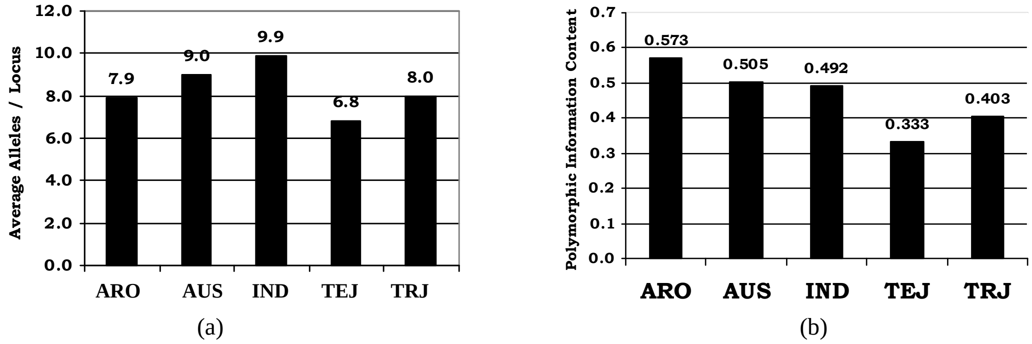

Figure 4. Genetic diversity analysis for five populations resulted from cluster analysis and inferred by reference cultivars K1 (*tropical japonica* – TRJ), K2 (*temperate japonica* – TEJ), K3 (*indica* – IND), K4 (*aus* – AUS) and K5 (*aromatic* – ARO).

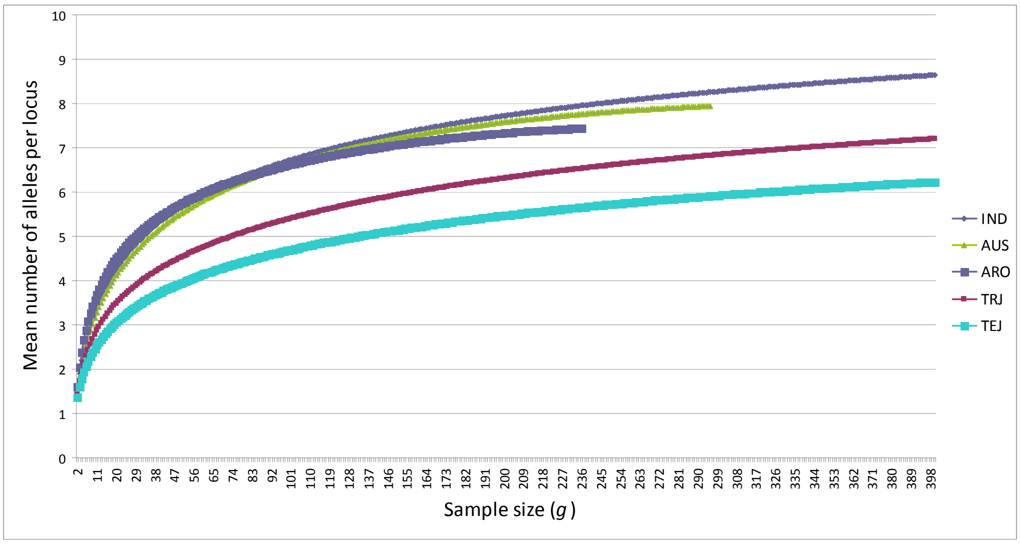

(a)

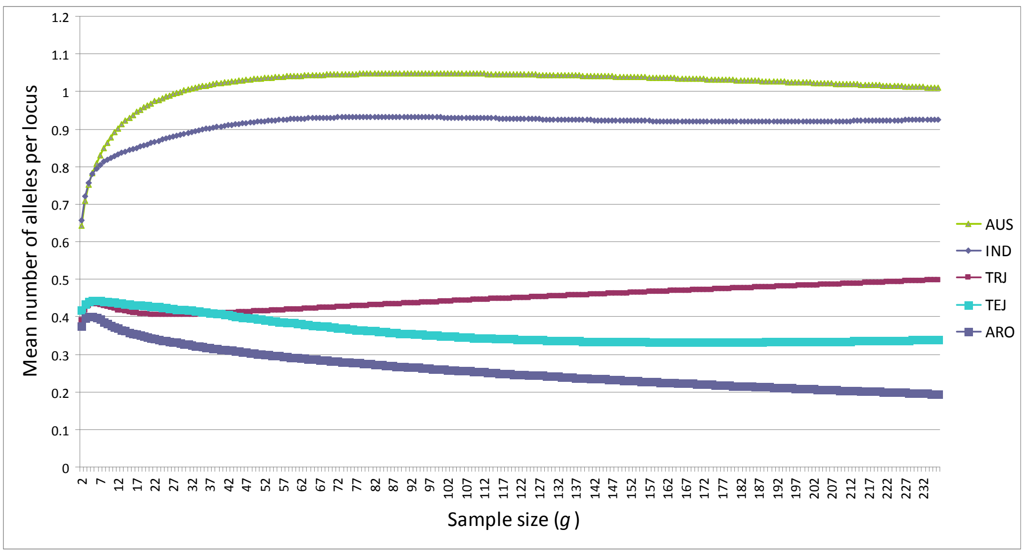

(b)

Figure 5. The mean number of (a) distinct alleles per locus and (b) private alleles per locus to each of five populations, K1 (tropical japonica – TRJ), K2 (temperate japonica – TEJ), K3 (indica – IND), K4 (aus – AUS) and K5 (aromatic – ARO), as functions of standardized sample size g.

tools. The information generated in this study could help design genetic strategies for gene transfer, evidenced by a similar study in maize (*Zea mays* L.) [60].

In general, *indica* is grown in tropical and subtropical regions of low latitude and low altitude with warmer climate conditions, while *japonica* in high altitudes or temperate regions of high latitudes with cooler climate conditions. As indicated by the name, *tropical japonica* is more tolerant to warm climate conditions than *temperate japonica*. *Temperate japonica* is predominantly grown across Northeast Asia, Europe, Western U.S. and Australia, while *tropical japonica* is most common in Southeast Asia, Southern China, Southern U.S., and the uplands of Latin America and Africa [22]. *Aromatic* is special fragrant rice such as 'Basmati' type of cultivars grown in the Himalayan region including Pakistan, Nepal and India. Both *aus* and *aromatic* are small groups and concentrated in Bangladesh and India. *Indica* is grown on about 80% of the world's total rice area with the remaining 20% *japonica* [6]. In fact, *indica* and *japonica* cultivars can be found sympatric in many areas. In mountainous regions of Bhutan, Nepal and Yunnan Province of China, *indica* is grown at lower elevations and *japonica* at higher elevations. Occasionally, *indica* and *japonica* cultivars can be found in the same village or same field [61].

Occurrence or distribution of *indica* and *japonica* cultivars is largely affected by human activity. During the Indonesian expansion to Madagascar, many *tropical japonica* cultivars grown locally and *indica* cultivars from South Asia were introduced [62]. A consequence of these waves of introduction of rice is inter-subspecific (*indica*/*japonica*) hybridization, resulting in a variety group specific to Madagascar. The aforementioned distribution of rice groups has completely depended on germplasm survey and exploration. Through the USDA rice world collection we are able to visualize the global distribution of each group of accessions and their genetic differences, using structural analysis of molecular markers with geographical regions. This visualization highly matches with the survey reported previously [12,15-17,62]. This matching is evident that molecular information can be utilized for geographic study which is usually done by investigation or survey that is more costly in time and money than the lab work for molecular data. This study of global rice has found significant stratification generally corresponding to major geographic regions of the world. Stratification in plant diversity panels and breeding populations appears to resemble the level found in many studies. For example, sixteen of 21 studied populations were differentiated into three or more subgroups using STRUCTURE [63]. To provide an additional, and rather different, type of algorithm against which to compare our structure, we also analyzed the data using principal coordinates analysis (PCA). It has been shown [64] that the resolution of PCA methods and STRUCTURE are quite similar in many cases.

Genetic differentiation between *indica* and *japonica* is ancient, resulting in a sterility barrier associated with the hybrids between these two subspecies except when wide compatibility genes are present [8,9,22]. The barrier limits commercial hybrid rice within each subspecies. However, development of *indica*/*japonica* hybrids has showed immense yield potential compared with intra-subspecies hybrids due to genome diversity. Hybrid vigor or heterosis is expressed as a function of additive, dominant and epistatic gene effects which is positively associated with gene diversity [65]. The more genetically distant the parents are, the stronger heterosis should be expected. As a result, genetic diversity and relationship among these types of rice will help design breeding strategies for overcoming sexual barrier and optimizing heterosis on characteristics with agronomic importance.

Indica is about equally and genetically distant to *aus* and *aromatic*, but far away from *temperate japonica* and *tropical japonica*. *Indica* is highly diversified, as indicated by the most alleles per locus and the second most private alleles per locus and the third most polymorphic information content (PIC) among the five groups. *Tropical japonica* is close to *aromatic* and *temperate japonica*, but far from *aus* and *indica*. *Tropical japonica* has the second lowest alleles per locus and PIC. *Temperate japonica* is genetically farther from *indica* than *tropical japonica* and has the lowest PIC and average alleles and private alleles per locus among the five groups. *Aus* is mostly distant from *temperate japonica* and then from *tropical japonica, indica and aromatic*, and has the most private alleles per locus and the second most average alleles per locus and PIC. *Aromatic* has the closest genetic relationship to *tropical japonica*, which is similar to *aus* and *indica*, and then to *temperate japonica*. In terms of genetic diversity, *aromatic* has the most PIC.

We confirmed that *japonica* is genetically less diversified than *indica* and its diversity is even smaller in *temperate japonica* than in *tropical japonica*. However, our results could not completely agree with the division of *aromatic* from *japonica*, concluded previously because F_{ST} of *aromatic* with *temperate japonica* (0.317) is larger than that with *indica* (0.284). Hybrid sterility between *indica* and *japonica* occurs because of their genetic distance. Therefore, a wide-compatibility gene has to be adapted for good seed set. *Indica* is closer to *tropical japonica* than *temperate japonica*. The genetic relationship makes sense, because almost all the cultivars bred in the Southern U.S., which belongs to *tropical japonica* [6], are widely compatible for the inter-subspecies crosses [66]. In other words, the wide-compatibility genes popularly exist in *tropical japonica* rice. Similarly, *aromatic* is widely compatible for the inter-subspecies crosses, demonstrated by successfully bred aromatic hybrid rice, Chuanxiang [67]. Furthermore, genetic diversity in *japonica* can be enriched along with improvement of fragrance using wide compatibility because *aromatic* was more diversified than *japonica*, especially *temperate japonica*.

In conclusion, characterization of the USDA rice world collection for genetic structure will better serve the global rice community for cultivar improvements in rice, especially hybrid rice because this collection is internationally available, free of charge and restrictions for research purposes. Seed may be requested via www.ars-grin.gov for the whole collection, and http://www.ars.usda.gov/Main/docs.htm?docid=8318 for the core collection.

5. ACKNOWLEDGEMENTS

The authors thank Kenneth Olsen, Karen Moldenhauer, Farman Jodari and Ellen McWhirter for critical review, and Tiffany Sookaserm, Tony Beaty, Aaron Jackson, Yao Zhou, BiaoLin Hu, XiaoBai Li and LiMeng Jia for technical assistance.

REFERENCES

[1] FAO (2005) FAOSTAT data. http://faostat.fao.org/site/346/DesktopDefault.aspx?PageID=346.

[2] Yu, J., Hu, S.N., Wang, J., Wong, G.K., Li, S.G., *et al*. (2002) A draft sequence of the rice genome (*Oryza sativa* L. ssp *Indica*). *Science*, **296(5565)**, 79-92.

[3] Goff, S.A., Ricke, D., Lan, T.H., Presting, G. and Wang, R.L. (2002) A draft sequence of the rice genome (*Oryza sativa* L. ssp *Japonica*). *Science*, **296(5565)**, 92-100.

[4] Khush, G.S. (1997) Origin, dispersal, cultivation and variation of rice. *Plant Molecular Biology*, **35(1-2)**, 25-34.

[5] Vaughan, D.A. (1989) The genus *Oryza* L: Current status of taxonomy. *IRRI Research Paper Series*, **138**, 1-21.

[6] Mackill, D.J. (1995) Classifying japonica rice cultivars with RAPD markers. *Crop Science*, **35(3)**, 889-894.

[7] Zhang, Q.F., Maroof, M.A.S., Lu, T.Y. and Shen, B.Z. (1992) Genetic diversity and differentiation of *Indica* and *Japonica* rice detected by RFLP analysis. *Theoretical and Applied Genetics*, **83(4),** 495-499.

[8] Zhang, Q.F., Liu, K.D., Yang, G.P., Maroof, M.A.S., Xu, C.G. and Zhou, Z.Q. (1997) Molecular marker diversity and hybrid sterility in Indica-Japonica rice crosses. *Theoretical and Applied Genetics*, **95(1-2),** 112-118.

[9] Williams, C.E., Yanagihara, S., McCouch, S.R., Mackill, D.J. and Ronald, P.C. (1997) Predicting success of Indica/Japonica crosses in rice, based on a PCR marker for the S-5^n allele at a hybrid-sterility locus. *Crop Science*, **37(6)**, 1910-1912.

[10] Matsuo, T., Futsuhara, Y., Kikuchi, F. and Yamaguchi, H. (1997) Science of the rice plant. Food and Agriculture Policy Research Center, Tokyo.

[11] Glaszmann, J.C. (1987) Isozymes and classification of Asian rice varieties. *Theoretical and Applied Genetics*, **74(1)**, 21-30.

[12] Izawa, T. (2008) The process of rice domestication: A new model based on recent data. *Rice*, **1(2)**, 127-134.

[13] Vaughan, D.A., Lu, B.R. and Tomooka, N. (2008) Was Asian rice (*Oryza sativa*) domesticated more than once? *Rice*, **1(1)**, 16-24.

[14] Joshi, S.P., Gupta, V.S., Aaggarwal, R.K., Ranjekar, P.K. and Brar, D.S. (2000) Genetic diversity and phylogenetic relationship as revealed by inter simple sequence repeat (ISSR) polymorphism in the genus *Oryza*. *Theoretical and Applied Genetics*, **100(8)**, 1311-1320.

[15] Kovach, M.J., Sweeney, M.T. and McCouch, S.R. (2007) New insights into the history of rice domestication. *Trends in Genetics*, **23(11)**, 578-587.

[16] Caicedo, A.L., Williamson, S.H., Hernandez, R.D. and Boyko, A. (2007) Genome-wide patterns of nucleotide polymorphism in domecticated rice. *PloS Genetics*, **3(9)**, 1745-1756.

[17] Garris, A.J., Tai, T.H., Coburn, J., Kresovich, S. and McCouch, S. (2005) Genetic structure and diversity in Oryza sativa L. *Genetics*, **169(3)**, 1631-1638.

[18] Li, H.B., Zhang, Q., Liu, A.M., Zou, J.S. and Chen, Z.M. (1996) A genetic analysis of low-temperature-sensitive sterility in Indica-Japonica rice hybrids. *Plant Breeding*, **115(5)**, 305-309.

[19] Xiao, J., Li, J., Yuan, L. and McCouch, S.R. (1996) Genetic diversity and its relationship to hybrid performance and heterosis in rice as revealed by PCR-based markers. *Theoretical and Applied Genetics*, **92(6)**, 637-643.

[20] Xu, Y.B. (2003) Developing marker-assisted selection strategies for breeding hybrid rice. In: Janick, J., Ed., *Plant Breeding Reviews*, John Wiley & Sons, Inc., Hoboken, **23**, 73-174.

[21] FAO (Food and Agriculture Organization of the United Nations) (2004) Rice is life. *International Year of Rice* '04, Rome, 22-27 November 2004.

[22] Negrao, S., Oliveira, M.M., Jena, K.K. and Mackill, D. (2008) Integration of genomic tools to assist breeding in the *japonica* subspecies of rice. *Molecular Breeding*, **22(2)**, 159-168.

[23] Agrama, H.A. and Eizenga, G.C. (2008) Molecular diversity and genome-wide linkage disequilibrium patterns in a worldwide collection of *Oryza sativa* and its wild relatives. *Euphytica*, **160(3)**, 339-355.

[24] Thomson, M.J., Septiningsin, E.M., Suwardjo, F., Santoso, T.J., Silitonga, T.S. and McCouch, S.R. (2007) Genetic diversity analysis of traditional and improved Indonesian rice (*Oryza sativa* L.) germplasm using microsatellite markers. *Theoretical and Applied Genetics*, **114(3)**, 559-568.

[25] Jayamani, P., Negrao, S., Martins, M., Macas, B. and Oliveira, M.M. (2007) Genetic relatedness of Portuguese rice accessions from diverse origins as assessed by microsatellite markers. *Crop Science*, **47(2)**, 879-886.

[26] Xu, Y.B., Beachell, H. and McCouch, S.R. (2004) A marker-based approach to broading the genetic base of rice in the USA. *Crop Science*, **44(6)**, 1947-1959.

[27] Zhang, D., Zhang, H., Wang, M., Sun, J., Qi, Y., Wang, F., Wei, X., Han, L., Wang, X. and Li, Z. (2009) Genetic structure and differentiation of *Oryza sativa* L. in China revealed by microsatellites. *Theoretical and Applied Ge-*

netics, **119(6)**, 1105-1117.

[28] Pritchard, J.K., Stephens, M. and Donnelly, P. (2000) Inference of population structure using multilocus genotype data. *Genetics*, **155(2)**, 945-959.

[29] Falush, D., Stephens, M. and Pritchard, J.K. (2003) Inference of population structure using multilocus genotype data: Linked loci and correlated allele frequencies. *Genetics*, **164(4)**, 1567-1587.

[30] Falush, D., Stephens, M. and Pritchard, J.K. (2007) Inference of population structure using multilocus genotype data: Dominant markers and null alleles. *Molecular Ecology Notes*, **7(4)**, 574-578.

[31] Chen, C., Durand, E., Forbes, F. and François, O. (2007) Bayesian clustering algorithms ascertaining spatial population structure: A new computer program and a comparison study. *Molecular Ecology Notes*, **7(5)**, 747-756.

[32] François, O., Blum, M.G.B., Jakobsson, M. and Rosenberg, N.A. (2008) Demographic history of European populations of Arabidopsis thaliana. *PLoS Genetics*, **4(5)**, 75.

[33] Bockelman, H.E., Dilday, R.H., Yan, W.G. and Wesenberg, D.M. (2003) Germplasm collection, preservation and utilization. In: Smith, C.W. and Dilday, R.H., Ed., *Rice Origin, History, Technology and Production*, John Wiley & Sons, Inc., Hoboken, 597-625.

[34] NPGS (2009) Summary statistics of holdings for *Oryza*. http://www.ars-grin.gov/cgi-bin/npgs/html/stats/genussite.pl?Oryza

[35] Yan, W.G., Rutger, J.N., Bryant, R.J., Bockelman, H.E., Fjellstrom, R.G., Chen, M.H., Tai, T.H. and McClung, A.M. (2007) Development and evaluation of a core subset of the USDA rice (*Oryza sativa* L.) germplasm collection. *Crop Science*, **47(2)**, 869-878.

[36] Grenier, C., Hamon, P. and Bramel-Cox, P.J. (2001) Core collection of sorghum: II. Comparison of three random sampling strategies. *Crop Science*, **41(1)**, 241-246.

[37] Yan, W.G., Rutger, J.N., Bockelman, H.E. and Tai, T.H. (2004a) Development of a core collection from the USDA rice germplasm collection. In: Norman, R.J., Meullenet, J.F. and Moldenhauer, K.A.K., Ed., *Rice Research Studies* 2003, University Arkansas, Agricultural Experiment Station, Research Series, **517**, 88-96.

[38] Yan, W.G., Rutger, J.N., Bockelman, H.E. and Tai, T.H. (2004b) Germplasm accessions resistant to straighthead in the USDA rice core collection. In Norman, R.J., Meullenet, J.F. and Moldenhauer, K.A.K. (eds.) *Rice Research Studies* 2003, University Arkansas, Agricultural Experiment Station Research Series, **517**, 97-102.

[39] Agrama, H.A., Yan, W.G., Lee, F.N., Fjellstrom, R., Chen, M., Jia, M. and McClung, A. (2009) Genetic assessment of a mini-core developed from the USDA rice genebank. *Crop Science*, **49,** 1336-1346.

[40] Xin, Z., Velten, J.P., Oliver, M.J. and Burke, J.J. (2003) High-throughput DNA extraction method suitable for PCR. *BioTechniques*, **34(4)**, 820-826.

[41] Agrama, H.A. and Yan, W.G. (2009) Genetic diversity and relatedness of rice cultivars resistant to straighthead disorder. *Plant Breeding*, **128(4)**.

[42] McNally, K.L., Bruskiewich, R., Mackill, D., Buell, C.R., Leach, J.E. and Leung, H. (2006) Sequencing multiple and diverse rice varieties: Connecting whole-genome variation with phenotypes. *Plant Physiology*, **141(1)**, 26-31.

[43] Spiegelhalter, D.J., Best, N.G., Carlin, B.P. and van Der, L.A. (2002) Bayesian measures of model complexity and fit (with discussion). *Journal of the Royal Statistical Society B*, **64**, 583-639.

[44] Evanno, G., Regnaut, S. and Goudet, J. (2005) Detecting the number of clusters of individuals using the software structure: a simulation. *Molecular Ecology*, **14(8)**, 2611-2620.

[45] Jakobsson, M. and Rosenberg, N.A. (2007) CLUMPP: A cluster matching and permutation program for dealing with label switching and multimodality in analysis of population structure. *Bioinformatics*, **23(14)**, 1801-1806.

[46] Excoffier, L., Smouse, P.E. and Quattro, J.M. (1992) Analysis of molecular variance inferred from metric distances among DNA haplotypes: Application to human mitochondrial DNA restriction sites. *Genetics*, **131(2)**, 479-491.

[47] Schneider, S., Roessli, D. and Excoffier, L. (2000) Arlequin: A software for population genetic data. Genetics and Biometry Laboratory, University of Geneva, Switzerland.

[48] Weir, B. and Cockerham, C.C. (1984) Estimating *F* statistics for the analysis of population structure. *Evolution*, **38(6)**, 1358-1370.

[49] Paun, O., Greilhuber, J., Temsch, E.M. and Hörandl, E. (2006) Patterns, sources and ecological implications of clonal diversity in apomictic Ranunculus carpaticola (Ranunculus auricomus complex, Ranunculaceae). *Molecular Ecology*, **15(4)**, 897-910.

[50] Goudet, J. (1995) FSTAT (version 1.2): A computer program to calculate F statistics. *Journal of Heredity*, **86(6)**, 485-486.

[51] Goovaerts, P. (1992) Factorial kriging analysis: A useful tool for exploring the structure of multivariate spatial soil information. *Journal of Soil Science*, **43,** 597-619.

[52] Wackernagel, H. (1994) Cokriging versus kriging in regionalized multivariate data analysis. *Geoderma*, **62(1)**, 83-92.

[53] Venables, W.N. and Ripley, B.D. (1998) Modern applied statistics with S+. 2nd Edition, Springer, New York.

[54] Venables, W.N., Smith, D.M. and R Development Core Team (2008) Notes on R: A programming environment for data analysis and graphics version 2.8.1. R Foundation for Statistical Computing, Vienna.

[55] Peakall, R. and Smouse, P.E. (2006) GenAlEx 6: Genetic analysis in Excel. Population genetic software for teaching and research. *Molecular Ecology Notes*, **6(1)**, 288-295.

[56] Liu, K. and Muse, S. (2005) PowerMarker: An integrated analysis environment for genetic marker analysis. *Bioinformatics*, **21(9)**, 2128-2129.

[57] Szpiech, Z.A., Jacksson, M. and Rosenbreg, N.A. (2008) ADZE: A rarefaction approach for counting alleles private to combinations of populations. *Bioinformatics*, **24(21)**, 2498-2504.

[58] Nei, M. (1973) The theory and estimation of genetic distance. In: Morton, N.E., Ed., *Genetic Structure of Populations*. University Press of Hawaii, Honolulu, 45-54.

[59] Nei, M. (1978) Estimation of average heterozygosity and genetic distance from a small number of individuals. *Genetics*, **89(3)**, 583-590.

[60] Vigouroux, Y., Glaubitz, J.C., Matsuoka, Y., Goodman, M.M., Sanchez, J. and Doebley, J. (2008) Population

structure and genetic diversity of new world maize races assessed by DNA microsatellites. *American Journal of Botany*, **95**, 1240-1253.

[61] Morishima, H. (1989) Intra-population genetic diversity in landrace of rice. *Proceedings of the* 6*th International Congress of SABRAO*, Tsukuba, 25 August 1989.

[62] Vaughan, D.A., Miyazaki, S. and Miyashita, K. (2004) The rice genepool and human migrations. In: Werner, D., Ed., *Biological Resources and Migration*, Springer, Berlin, 1-11.

[63] Sneller, C.H., Mather, D.E. and Crepieux, S. (2009) Analytical approaches and population types for finding and utilizing QTL in complex plant populations. *Crop Science*, **49(5)**, 363-390.

[64] Patterson, N., Price, A.L. and Reich, D. (2006) Population structure and eigenanalysis. *PLoS Genetics*, **2(12)**.

[65] Melchinger, A.E., Utz, H.F., Piepho, H.P., Zeng, Z.B. and Schon, C.C. (2007) The role of epistasis in the manifestation of heterosis: A systems-oriented approach. *Genetics*, **177**, 1815-1825.

[66] Luo, L., Yin, C., Mei, H. and Wu, Y. (1996) Wide compatibility and agronomic performance of southern US rice cultivars in China. *Proceedings of* 26*th Rice Technical Working Group*, San Antonio, 25-28 February 1996, 80-81.

[67] Sun, S.X., Gao, F.Y., Lu, X.J., Wu, X.J., Wang, X.D., Ren, G.J. and Luo, H. (2008) Genetic analysis and gene fine mapping of aroma in rice (*Oryza sative* L. Cyperales, Poaceae). *Genetics and Molecular Biology*, **31(2)**, 532-538.

SUPPLEMENTARY TABLE

Ancestry coefficients (K value) for each accession in the USDA rice core collection with genetic stock number (GSOR NO), accession number (ACNO)

GSOR NO	ACP	ACNO	Cultivar name	Country	Region	Received	Ancestry	K1-TRJ	K2-TEJ	K3-IND	K4-AUS	K5-ARO
310001	CIor	8	Ostiglia	Italy	Western_Europe	1904-3-1	IND	0.0024	0.0022	0.9946	0.0006	0.0001
310002	CIor	1160	GPNO 967	Guatemala	Central_America	1904-12-1	TEJ-TRJ	0.4770	0.5227	0.0002	0.0001	0.0001
310003	CIor	1664	WC 3398	Mexico	North_America	1909-7-1	TRJ	0.9989	0.0006	0.0003	0.0000	0.0001
310004	CIor	2168	WC 3420	Guatemala	Central_America	1915-12-1	TRJ	0.9992	0.0005	0.0001	0.0001	0. 0001
310005	CIor	2174	WC 3423	Guatemala	Central_America	1915-12-1	TRJ	0.9991	0.0008	0.0001	0.0000	0.0001
310006	CIor	2181	Nacaome	Honduras	Central_America	1915-12-1	TRJ	0.9959	0.0032	0.0002	0.0002	0.0004
310007	CIor	2490	Karang Serang	Indonesia	South_Pacific	1914-12-1	TRJ	0.7466	0.1808	0.0627	0.0006	0.0093
310008	CIor	4191	Quinanda Pollopot	Philippines	South_Pacific	1916-12-1	TRJ	0.9986	0.0010	0.0001	0.0001	0.0002
310009	CIor	4616	GPNO 1645	Philippines	South_Pacific	1916-12-1	IND	0.0140	0.0080	0.9778	0.0001	0.0001
310010	CIor	5249	Coray 4	Honduras	Central_America	1916-12-1	TRJ	0.9949	0.0039	0.0005	0.0003	0.0005
310011	CIor	5256	Arroz en Granza	Guatemala	Central_America	1916-12-1	IND	0.0013	0.0006	0.9627	0.0062	0.0292
310012	CIor	5390	Jimoca	Peru	South_America	1920-12-1	TRJ	0.8011	0.1986	0.0001	0.0001	0.0001
310013	CIor	5798	WC 4431	Panama	Central_America	1925-12-1	TRJ	0.9986	0.0010	0.0002	0.0000	0.0002
310014	CIor	6332	GPNO 2016	Japan	North_Pacific	1928-12-1	AUS	0.0001	0.0002	0.0006	0.9990	0.0001
310015	CIor	7155	Mayang Khang	Indonesia	South_Pacific	1928-12-1	IND	0.0005	0.0003	0.9988	0.0003	0.0001
310016	CIor	7203	Indonesia Seln	Indonesia	South_Pacific	1928-12-1	TRJ	0.6117	0.2818	0.0956	0.0005	0.0104
310017	CIor	7352	Shinshu	Japan	North_Pacific	1928-12-1	IND	0.0004	0.0005	0.9984	0.0006	0.0001
310018	CIor	8320	DELREX	United States	North_America	1943-7-17	TRJ	0.9793	0.0012	0.0002	0.0001	0.0191
310019	CIor	8635	Romay	Peru	South_America	1946-7-20	TRJ-TEJ	0.5460	0.4535	0.0002	0.0001	0.0001
310020	CIor	9032	E B Gopher	United States	North_America	1954-3-10	TRJ	0.9990	0.0007	0.0001	0.0001	0.0001
310021	CIor	9043	PR 325	Puerto Rico	Central_America	1954-3-10	TRJ	0.9993	0.0004	0.0002	0.0000	0.0001
310022	CIor	9044	PR 358	Puerto Rico	Central_America	1954-3-10	TRJ	0.9986	0.0010	0.0002	0.0000	0.0001
310023	CIor	9049	RD 218	Dominican Republic	Central_America	1954-3-10	TRJ-TEJ	0.5221	0.4776	0.0001	0.0000	0.0001
310024	CIor	9100	B53R3540	Thailand	Southeast_Asia	1954-3-1	ARO	0.0002	0.0001	0.0004	0.0003	0.9990
310025	CIor	9113	B4564A2-11-4-3	United States	North_America	1954-3-1	TRJ	0.9956	0.0040	0.0002	0.0000	0.0002
310026	CIor	9132	B459A3-13-1-2-2	United States	North_America	1954-3-1	TRJ	0.9994	0.0004	0.0001	0.0001	0.0001
310027	CIor	9182	S4517A3-49B-123-4	United States	North_America	1954-3-1	TRJ	0.9993	0.0005	0.0001	0.0000	0.0001
310028	CIor	9219	SD 120	Puerto Rico	Central_America	1954-12-1	TEJ	0.0004	0.9995	0.0001	0.0000	0.0000
310029	CIor	9220	RD 208	Puerto Rico	Central_America	1954-12-1	TRJ	0.9993	0.0005	0.0001	0.0000	0.0001
310030	CIor	9222	PR 378	Puerto Rico	Central_America	1954-12-1	TRJ	0.9969	0.0029	0.0001	0.0000	0.0001
310031	CIor	9323	BC V-2-14	United States	North_America	1954-3-1	TEJ	0.1003	0.8992	0.0004	0.0001	0.0001
310032	CIor	9352	WC 1018	Panama	Central_America	1954-3-1	TRJ	0.9987	0.0010	0.0001	0.0001	0.0002
310033	CIor	9391	49C965	United States	North_America	1957-12-1	TRJ	0.9780	0.0217	0.0002	0.0001	0.0001
310034	CIor	9484	Stg 56655-28	United States	North_America	1961-1-1	TRJ	0.9432	0.0007	0.0536	0.0019	0.0006
310035	CIor	9509	Stg 58-2158	United States	North_America	1961-1-1	TRJ	0.9949	0.0047	0.0003	0.0000	0.0001
310036	CIor	9544	BLUEBELLE	United States	North_America	1962-1-1	TRJ	0.9992	0.0006	0.0001	0.0000	0.0001
310037	CIor	9636	Stg 625377	United States	North_America	1966-12-1	TRJ	0.8797	0.1199	0.0003	0.0000	0.0001
310038	CIor	9644	Stg 9544-32	United States	North_America	1966-12-1	TRJ	0.9990	0.0008	0.0001	0.0000	0.0001
310039	CIor	9723	C 5560	Thailand	Southeast_Asia	1969-12-1	TRJ-TEJ-ARO	0.4661	0.3323	0.0081	0.0006	0.1928
310040	CIor	9733	FORTUNA	Puerto Rico	Central_America	1969-12-1	TRJ	0.9989	0.0009	0.0001	0.0000	0.0001
310041	CIor	9778	1-14-1-3-2	Australia	Oceania	1969-12-1	TEJ-TRJ	0.4807	0.5190	0.0001	0.0000	0.0001
310042	CIor	9824	B6334A2-1-2	United States	North_America	1970-12-1	TRJ	0.6655	0.3342	0.0001	0.0001	0.0001
310043	CIor	9838	Stg 687914	United States	North_America	1971-12-1	TRJ	0.9990	0.0008	0.0001	0.0000	0.0001
310044	CIor	9838	71Cr-5247	United States	North_America	1972-12-1	TRJ	0.7176	0.2822	0.0001	0.0000	0.0001
310045	CIor	9979	LEAH	United States	North_America	1981-10-30	TRJ	0.8053	0.0010	0.0015	0.1565	0.0357
310046	CIor	11009	GPNO 254	United States	North_America	1977-12-1	TRJ-TEJ	0.5895	0.4097	0.0002	0.0002	0.0005
310047	CIor	12010	Catibos	Philippines	South_Pacific	1904-12-1	TRJ	0.9276	0.0705	0.0009	0.0002	0.0008
310048	CIor	12017	CI 1160-1	Guatemala	Central_America	1904-12-1	TEJ	0.0004	0.9994	0.0001	0.0000	0.0000
310049	CIor	12018	CI 1168-2	Guatemala	Central_America	1904-12-1	TRJ	0.9598	0.0399	0.0001	0.0001	0.0001
310050	CIor	12020	Vintula	Guyana	South_America	1904-12-1	TRJ	0.9981	0.0010	0.0005	0.0001	0.0003

310051	CIor	12053	15	Iran	Mideast	1914-12-1	TRJ	0.9806	0.0004	0.0179	0.0002	0.0009
310052	CIor	12153	Quinimpol	Philippines	South_Pacific	1916-12-1	TRJ	0.8467	0.1528	0.0002	0.0001	0.0002
310053	CIor	12180	M'Bale Selection	Kenya	Africa	1920-12-1	TRJ	0.9865	0.0130	0.0001	0.0001	0.0003
310054	CIor	12285	Santaro Selection	Japan	North_Pacific	1947-3-1	TEJ	0.3242	0.6668	0.0074	0.0005	0.0012
310055	CIor	12321	RD 209	Puerto Rico	Central_America	1954-12-1	TRJ	0.9992	0.0005	0.0002	0.0000	0.0000
310056	CIor	12325	PR 398	Puerto Rico	Central_America	1954-12-1	TRJ-TEJ	0.5784	0.4211	0.0003	0.0001	0.0001
310057	PI	2E+05	WC 3395	Jamaica	Central_America	1954-8-18	TRJ	0.9856	0.0139	0.0001	0.0002	0.0001
310058	CIor	12425	Sadri Type	Iraq	Mideast	1949-12-1	ARO	0.0003	0.0005	0.0001	0.0002	0.9989
310059	CIor	12454	CHIKANARI 2	Japan	North_Pacific	1955-6-1	TEJ	0.0006	0.9993	0.0001	0.0000	0.0000
310060	CIor	12466	Criollo Selection	Mexico	North_America	1955-12-1	TRJ	0.9972	0.0024	0.0002	0.0001	0.0001
310061	CIor	12469	Mojito	Bolivia	South_America	1957-12-1	TRJ	0.9991	0.0006	0.0001	0.0001	0.0001
310062	CIor	12496	PI 298965-2	Australia	Oceania	1964-12-1	TRJ-TEJ	0.5216	0.4781	0.0002	0.0001	0.0001
310063	CIor	12498	PI 298967-1	Australia	Oceania	1964-12-1	TEJ-TRJ	0.4768	0.5229	0.0001	0.0001	0.0001
310064	CIor	12505	PR 433	Puerto Rico	Central_America	1954-12-1	TRJ	0.9992	0.0005	0.0002	0.0000	0.0001
310065	CIor	12510	Puang Nigern	Thailand	Southeast_Asia	1947-12-1	TRJ	0.9991	0.0007	0.0002	0.0000	0.0001
310066	CIor	12526	Chong Kuc Tae Pyang	Korea_ South	North_Pacific	1947-3-1	TEJ-TRJ	0.4544	0.5351	0.0026	0.0017	0.0062
310067	PI	15547	WC 2634	Tanzania	Africa	1905-3-21	TEJ	0.2295	0.7702	0.0001	0.0001	0.0001
310068	PI	45598	WC 747	St. Lucia	Central_America	1917-10-15	TRJ	0.9991	0.0003	0.0002	0.0003	0.0000
310069	PI	49880	502	Zaire	Africa	1920-4-1	TRJ	0.9878	0.0118	0.0001	0.0001	0.0002
310070	PI	61718	Shala	Turkistan	Central_Asia	1924-9-1	IND	0.0002	0.0002	0.9993	0.0001	0.0001
310071	PI	67155	Safed	India	Southern_Asia	1926-5-1	AUS	0.0001	0.0001	0.0003	0.9995	0.0001
310072	PI	136125	Pata de Gallinazo	Ecuador	South_America	1940-3-25	TRJ	0.9960	0.0037	0.0003	0.0000	0.0000
310073	PI	141750	Fortuna Negro	Peru	South_America	1941-5-9	TRJ	0.7861	0.2081	0.0038	0.0016	0.0004
310074	PI	141755	Mejicano	Peru	South_America	1941-5-9	TRJ	0.9992	0.0006	0.0001	0.0000	0.0001
310075	PI	141757	Tambo	Peru	South_America	1941-5-9	IND	0.0004	0.0009	0.9973	0.0005	0.0009
310076	PI	153454	WC 4203	Russian Federation	Eastern_Europe	1946-2-5	TEJ	0.0008	0.9990	0.0001	0.0001	0.0000
310077	PI	154449	Daido	Mongolia	China	1946-5-10	TEJ	0.3422	0.6556	0.0009	0.0004	0.0009
310078	PI	154452	Saku	Mongolia	China	1946-5-10	TRJ	0.6238	0.3760	0.0001	0.0000	0.0001
310079	PI	154453	Kon Suito	Mongolia	China	1946-5-10	TEJ	0.0028	0.9086	0.0001	0.0019	0.0866
310080	PI	154464	TAICHU MOCHI 59	Taiwan	China	1946-5-10	TRJ	0.7859	0.0052	0.0066	0.0113	0.1910
310081	PI	154478	Natapasume	Taiwan	China	1946-5-10	IND	0.0045	0.0158	0.9761	0.0004	0.0033
310082	PI	154563	TAINO 33	Taiwan	China	1946-5-10	TEJ	0.0003	0.9996	0.0001	0.0000	0.0000
310083	PI	154680	KANAN NO. 3	Taiwan	China	1946-5-10	TEJ	0.0004	0.9993	0.0001	0.0000	0.0001
310084	PI	155222	Rz No. 111	Zaire	Africa	1946-7-19	IND	0.0011	0.0022	0.9963	0.0002	0.0002
310085	PI	155419	Apure	Venezuela	South_America	1946-7-29	TRJ	0.9953	0.0030	0.0013	0.0002	0.0002
310086	PI	155989	WC 2810	Micronesia	Oceania	1946-9-1	TRJ	0.9983	0.0012	0.0004	0.0001	0.0001
310087	PI	155990	WC 2811	Micronesia	Oceania	1946-9-1	TRJ	0.9992	0.0005	0.0002	0.0001	0.0001
310088	PI	157294	Kama Okoshi	Japan	North_Pacific	1947-2-18	TEJ-TRJ	0.4577	0.5340	0.0019	0.0021	0.0042
310089	PI	157296	Ka Oe Chal	Korea_ South	North_Pacific	1947-2-18	TEJ-TRJ	0.4550	0.5334	0.0026	0.0023	0.0068
310090	PI	157317	Miyanishiki	Japan	North_Pacific	1947-2-18	TEJ-TRJ	0.4336	0.5659	0.0002	0.0002	0.0001
310091	PI	157326	Owari Mochi	Japan	North_Pacific	1947-2-18	TEJ-TRJ	0.3916	0.5234	0.0012	0.0006	0.0832
310092	PI	157326	Ryuc-u 13	Japan	North_Pacific	1947-2-18	TRJ-TEJ	0.5227	0.4689	0.0081	0.0002	0.0001
310093	PI	157372	Tokyo Shino Mochi	Japan	North_Pacific	1947-2-18	TEJ-TRJ	0.4820	0.5089	0.0018	0.0022	0.0052
310094	PI	157386	Yung Chong Omochi	Korea_ South	North_Pacific	1947-2-18	TEJ	0.3407	0.6588	0.0002	0.0002	0.0002
310095	PI	157894	BALILLA	Italy	Western_Europe	1947-3-1	TEJ	0.0003	0.9996	0.0001	0.0000	0.0001
310096	PI	160403	Choh Chang 303 Hao	China	China	1947-11-25	IND	0.0002	0.0012	0.9980	0.0002	0.0004
310097	PI	160448	Leng Shwei Ku Choh	China	China	1947-11-25	IND	0.0008	0.0008	0.9957	0.0020	0.0006
310098	PI	160590	Yang Ku Tsi	China	China	1947-11-25	IND	0.0014	0.0017	0.9963	0.0003	0.0003
310099	PI	160688	Leng Kwang	China	China	1947-11-25	IND	0.0046	0.0005	0.9947	0.0001	0.0001
310100	PI	160700	Ao Chiu 2 Hao	China	China	1947-11-25	IND	0.0009	0.0002	0.9987	0.0001	0.0001
310101	PI	161564	Criollo Apure	Venezuela	South_America	1947-12-26	TRJ	0.7477	0.0007	0.0006	0.0005	0.2505
310102	PI	161567	Criollo Chivacoa 2	Venezuela	South_America	1947-12-26	TRJ	0.9965	0.0030	0.0003	0.0002	0.0001
310103	PI	161571	Precoz de Machiques	Venezuela	South_America	1947-12-26	TRJ	0.9986	0.0010	0.0003	0.0000	0.0001
310104	PI	162115	NORIN 8	Japan	North_Pacific	1948-2-1	TEJ	0.0004	0.9995	0.0001	0.0000	0.0000
310105	PI	162131	SUITO NORIN 3	Japan	North_Pacific	1948-2-1	TEJ	0.0003	0.9995	0.0001	0.0000	0.0000
310106	PI	163336	Bergreis	Austria	Western_Europe	1948-4-21	TEJ	0.0010	0.9987	0.0001	0.0001	0.0002

310107	PI	163575	1021	Guatemala	Central_America	1948-4-1	TRJ	0.9992	0.0004	0.0002	0.0001	0.0002
310108	PI	165610	WC 3777	Honduras	Central_America	1948-6-1	TRJ	0.9988	0.0009	0.0001	0.0001	0.0001
310109	PI	167928	RINALDO BERSANI	Italy	Western_Europe	1948-9-1	TEJ	0.0158	0.9839	0.0001	0.0000	0.0001
310110	PI	168945	Bomba	Spain	Western_Europe	1948-11-1	TEJ-TRJ	0.4944	0.5049	0.0004	0.0002	0.0001
310111	PI	168946	Bombilla	Spain	Western_Europe	1948-11-1	TEJ	0.1930	0.8062	0.0006	0.0001	0.0001
310112	PI	170885	Tehran	Iran	Mideast	1948-11-1	ARO	0.1199	0.0003	0.0004	0.0025	0.8769
310113	PI	175015	EAN 3	Portugal	Western_Europe	1949-2-1	TEJ	0.0007	0.9991	0.0001	0.0001	0.0001
310114	PI	175018	Muga	Portugal	Western_Europe	1949-2-1	TEJ	0.0007	0.9991	0.0000	0.0000	0.0001
310115	PI	177221	6257	Turkey	Mideast	1949-3-1	TEJ	0.3031	0.6965	0.0001	0.0001	0.0002
310116	PI	180175	Early 1600	Peru	South_America	1949-4-1	TEJ	0.0066	0.7746	0.2184	0.0003	0.0002
310117	PI	180178	LAMBAYEQUE NO. 2	Peru	South_America	1949-4-1	IND	0.0003	0.0004	0.8658	0.1300	0.0034
310118	PI	223894	Berenj	Afghanistan	Southern_Asia	1955-2-24	ARO	0.0014	0.0061	0.0002	0.0003	0.9920
310119	PI	185800	BG 79	Guyana	South_America	1950-1-3	ARO	0.0003	0.0004	0.0002	0.0001	0.9990
310120	PI	185811	*T 1	Guyana	South_America	1950-1-3	AUS	0.0002	0.0001	0.0003	0.9992	0.0002
310121	PI	187077	ALLORIO	Italy	Western_Europe	1950-2-28	TEJ	0.0003	0.9996	0.0000	0.0000	0.0000
310122	PI	187078	Chines	Portugal	Western_Europe	1950-2-28	TEJ	0.0011	0.9986	0.0001	0.0001	0.0000
310123	PI	189452	D. Sancho	Portugal	Western_Europe	1950-5-1	TEJ	0.2847	0.7150	0.0001	0.0001	0.0001
310124	PI	189466	Barbado	Portugal	Western_Europe	1950-5-1	TEJ	0.0055	0.9944	0.0001	0.0000	0.0001
310125	PI	190192	WC 3531	Ecuador	South_America	1950-7-1	TRJ	0.9968	0.0029	0.0003	0.0000	0.0000
310126	PI	198624	Catetao Dourado	Peru	South_America	1951-10-1	TRJ	0.9991	0.0007	0.0001	0.0000	0.0001
310127	PI	198625	Secano Brazil	Peru	South_America	1951-10-1	TRJ	0.9993	0.0005	0.0001	0.0000	0.0001
310128	PI	199539	Agulha Branco Medio	El Salvador	Central_America	1952-3-6	TRJ	0.9992	0.0006	0.0001	0.0001	0.0001
310129	PI	199540	Agulha Branco	El Salvador	Central_America	1952-3-6	TRJ	0.9993	0.0004	0.0002	0.0000	0.0001
310130	PI	199551	Matao Lizo	El Salvador	Central_America	1952-3-6	TRJ	0.9993	0.0004	0.0001	0.0001	0.0001
310131	PI	199553	Secano do Brazil	El Salvador	Central_America	1952-3-6	TRJ	0.9988	0.0006	0.0002	0.0001	0.0003
310132	PI	201175	Blue Nile	South Africa	Africa	1952-5-1	TRJ	0.9945	0.0050	0.0002	0.0000	0.0002
310133	PI	201902	NP 125	India	Southern_Asia	1952-6-1	AUS	0.0010	0.0002	0.0005	0.9981	0.0003
310134	PI	202864	BERLIN	Costa Rica	Central_America	1952-9-1	IND	0.0554	0.0011	0.9428	0.0005	0.0002
310135	PI	214076	Buffalo	Jamaica	Central_America	1954-2-11	TEJ-TRJ	0.4489	0.5508	0.0001	0.0000	0.0001
310136	PI	215409	Sanakevelle	Liberia	Africa	1954-4-9	TRJ	0.9982	0.0016	0.0001	0.0000	0.0001
310137	PI	215482	RAZZA 77	Italy	Western_Europe	1954-4-13	TEJ	0.1601	0.8396	0.0002	0.0001	0.0001
310138	PI	215485	Vialone	Italy	Western_Europe	1954-4-13	TEJ	0.0041	0.9956	0.0001	0.0000	0.0001
310139	PI	215520	MARATELLI	Italy	Western_Europe	1954-4-19	TEJ	0.0004	0.9995	0.0001	0.0000	0.0001
310140	PI	215880	TAICHU 153	Taiwan	China	1954-4-28	IND	0.0001	0.0001	0.9997	0.0001	0.0000
310141	PI	215917	TAINAN 5	Taiwan	China	1954-4-28	TEJ	0.0003	0.9995	0.0001	0.0000	0.0000
310142	PI	215952	TAINAN IKU 510	Taiwan	China	1954-4-28	TEJ	0.0004	0.9994	0.0001	0.0001	0.0001
310143	PI	215983	TAKAO 26	Taiwan	China	1954-4-28	TEJ	0.0003	0.9995	0.0002	0.0000	0.0000
310144	PI	220214	British Honduras Creole	Belize	Central_America	1954-7-30	TRJ	0.9988	0.0006	0.0004	0.0001	0.0001
310145	PI	220268	SERENDAH KUNING	Malaysia	South_Pacific	1954-8-6	TRJ	0.9995	0.0003	0.0001	0.0000	0.0001
310146	PI	220485	WC 3396	Jamaica	Central_America	1954-8-18	TRJ	0.9991	0.0006	0.0001	0.0001	0.0001
310147	PI	220486	WC 3397	Jamaica	Central_America	1954-8-18	TRJ	0.9991	0.0005	0.0002	0.0001	0.0001
310148	PI	220872	Criollo de Chirgua 3	Venezuela	South_America	1954-9-15	TRJ	0.9993	0.0004	0.0002	0.0000	0.0001
310149	PI	220873	Criollo de la Fia	Venezuela	South_America	1954-9-15	TRJ	0.9995	0.0003	0.0001	0.0000	0.0001
310150	PI	220874	Criollo de la Victoria	Venezuela	South_America	1954-9-15	TRJ	0.9994	0.0004	0.0001	0.0000	0.0001
310151	PI	222453	Yodanya	Myanmar	Southeast_Asia	1954-12-2	IND	0.0008	0.0005	0.9980	0.0006	0.0001
310152	PI	223484	JAPONESITO DE TRES MESES SEL. F.A.	Argentina	South_America	1955-1-24	TEJ	0.1956	0.8041	0.0002	0.0001	0.0001
310153	PI	223484	VICTORIA TARDIO F.A.	Argentina	South_America	1955-1-24	TEJ	0.2533	0.7463	0.0002	0.0001	0.0001
310154	PI	223497	1201	Afghanistan	Southern_Asia	1955-1-24	IND	0.0003	0.0002	0.9992	0.0002	0.0001
310155	PI	223512	Shali-i-Mahin	Afghanistan	Southern_Asia	1955-1-24	ARO	0.0004	0.0005	0.0004	0.3865	0.6123
310156	PI	223612	Sel. No. 388	Uruguay	South_America	1955-2-8	TEJ-TRJ	0.4532	0.5465	0.0001	0.0001	0.0001
310157	PI	224903	SHIMOTSUKI	Japan	North_Pacific	1955-4-20	TEJ	0.0010	0.9987	0.0001	0.0000	0.0001
310158	PI	224906	SHIN 7	Japan	North_Pacific	1955-4-20	TEJ	0.0002	0.9996	0.0000	0.0000	0.0000
310159	PI	224943	Eiko	France	Western_Europe	1955-4-19	TEJ	0.0009	0.9989	0.0000	0.0001	0.0001
310160	PI	226183	RIKUTO NORIN 11	Japan	North_Pacific	1955-6-6	TEJ	0.3941	0.6029	0.0020	0.0003	0.0006

310161	PI	226204	SHIMIZU MOCHI	Japan	North_Pacific	1955-6-6	TEJ	0.0222	0.9731	0.0010	0.0003	0.0034
310162	PI	226305	GIZA 14	Egypt	Mideast	1955-6-8	AUS	0.0020	0.0002	0.0003	0.9967	0.0007
310163	PI	226308	YABANI MON-TAKHAB 7	Egypt	Mideast	1955-6-8	TEJ	0.0006	0.9991	0.0001	0.0001	0.0001
310164	PI	226329	C1-6-5-3	Mexico	North_America	1955-6-10	TEJ	0.0076	0.7290	0.2632	0.0001	0.0001
310165	PI	226424	C6-116-5-3	Mexico	North_America	1955-6-10	TRJ-TEJ	0.5678	0.4319	0.0002	0.0000	0.0001
310166	PI	226427	C6-146-4-1	Mexico	North_America	1955-6-10	TRJ	0.6343	0.3651	0.0004	0.0001	0.0001
310167	PI	226435	C6-221-4-4	Mexico	North_America	1955-6-10	AUS	0.0004	0.0002	0.0005	0.9988	0.0001
310168	PI	231633	Murasaki Daikoku	Japan	North_Pacific	1956-3-13	TEJ	0.0010	0.9988	0.0001	0.0001	0.0001
310169	PI	231643	Desvauxii	Former Soviet Union	Eastern_Europe	1956-3-13	TEJ	0.0007	0.9990	0.0001	0.0001	0.0001
310170	PI	231645	Dunganica	Former Soviet Union	Eastern_Europe	1956-3-13	TEJ	0.0002	0.9996	0.0001	0.0000	0.0000
310171	PI	231648	Italica Alef	Former Soviet Union	Eastern_Europe	1956-3-13	TEJ	0.0004	0.9985	0.0003	0.0006	0.0002
310172	PI	233083	NABATAT ASMAR	Egypt	Mideast	1956-5-1	TRJ	0.6572	0.3424	0.0002	0.0001	0.0001
310173	PI	233663	LOMELLO	Italy	Western_Europe	1956-6-5	TEJ	0.1373	0.8625	0.0001	0.0000	0.0001
310174	PI	233880	GIZA 35	Egypt	Mideast	1956-7-6	TEJ-TRJ	0.4817	0.5083	0.0087	0.0007	0.0006
310175	PI	238497	YAMANI SEL M.A.	Argentina	South_America	1957-3-27	TEJ	0.0005	0.9994	0.0000	0.0000	0.0000
310176	PI	303681	I KUNG PAO 5-3-4	Taiwan	China	1964-12-22	IND	0.0005	0.0011	0.9979	0.0003	0.0001
310177	PI	240651	AP 439	Venezuela	South_America	1957-6-10	TRJ	0.9965	0.0032	0.0001	0.0000	0.0001
310178	PI	241372	583	Ecuador	South_America	1957-7-17	TRJ	0.9979	0.0014	0.0005	0.0001	0.0001
310179	PI	242801	Aguja	Bolivia	South_America	1957-10-10	TRJ	0.9994	0.0003	0.0001	0.0000	0.0000
310180	PI	242802	Cola de Burro	Bolivia	South_America	1957-10-10	TRJ	0.9991	0.0005	0.0001	0.0000	0.0002
310181	PI	242804	Mojito Colorado	Bolivia	South_America	1957-10-10	TRJ	0.9995	0.0003	0.0001	0.0000	0.0000
310182	PI	242805	Noventa Dias Blanco	Bolivia	South_America	1957-10-10	TRJ	0.9994	0.0004	0.0001	0.0000	0.0000
310183	PI	242806	Noventa Dias Colo-rado	Bolivia	South_America	1957-10-10	TRJ	0.9988	0.0005	0.0006	0.0001	0.0001
310184	PI	242807	Palo Morado	Bolivia	South_America	1957-10-10	TRJ	0.9969	0.0013	0.0010	0.0005	0.0003
310185	PI	242809	Pico de Pato	Bolivia	South_America	1957-10-10	TRJ	0.9983	0.0014	0.0001	0.0001	0.0001
310186	PI	244684	Dima	Cuba	Central_America	1957-12-20	IND	0.0094	0.0003	0.9800	0.0026	0.0077
310187	PI	245354	48	Cuba	Central_America	1958-1-31	TRJ-IND-ARO	0.5018	0.0345	0.2590	0.0262	0.1786
310188	PI	247946	Catibao Dourado	Costa Rica	Central_America	1958-5-15	TRJ	0.9994	0.0004	0.0001	0.0000	0.0001
310189	PI	247948	Dourado Aguilia	Costa Rica	Central_America	1958-5-15	TRJ	0.9992	0.0003	0.0003	0.0001	0.0001
310190	PI	247949	WC 3513	Costa Rica	Central_America	1958-5-15	TRJ	0.9990	0.0005	0.0004	0.0001	0.0001
310191	PI	247956	Cuba 65	Cuba	Central_America	1958-5-15	TRJ	0.9988	0.0009	0.0001	0.0000	0.0002
310192	PI	248522	R 82	Italy	Western_Europe	1958-6-6	TEJ	0.0071	0.9925	0.0001	0.0001	0.0003
310193	PI	260661	Milketan 20	Philippines	South_Pacific	1959-9-23	TRJ-IND-TEJ	0.4476	0.1891	0.3353	0.0040	0.0239
310194	PI	263751	WC 4430	Costa Rica	Central_America	1960-3-2	TRJ-IND	0.5909	0.0056	0.3685	0.0320	0.0030
310195	PI	263808	Nickerie 19	Suriname	South_America	1960-3-7	IND-TRJ-AUS	0.3151	0.0033	0.5146	0.1666	0.0004
310196	PI	263813	81B/25	Suriname	South_America	1960-3-7	IND	0.0881	0.0136	0.7553	0.1419	0.0011
310197	PI	263816	140-4-1-2-5	Suriname	South_America	1960-3-7	TRJ-IND-AUS	0.4484	0.0007	0.3473	0.2021	0.0016
310198	PI	263832	K12 C/48	Suriname	South_America	1960-3-7	IND-ARO-TRJ	0.1319	0.0006	0.5916	0.0011	0.2747
310199	PI	263833	K12 C/53	Suriname	South_America	1960-3-7	IND	0.0005	0.0012	0.9981	0.0002	0.0001
310200	PI	264242	Chin Chin	Panama	Central_America	1960-3-18	IND	0.0003	0.0009	0.9985	0.0001	0.0001
310201	PI	264243	WC 1909	Japan	North_Pacific	1960-3-18	TRJ	0.9264	0.0712	0.0016	0.0000	0.0007
310202	PI	264750	Campesino	Venezuela	South_America	1960-3-13	TRJ	0.9989	0.0007	0.0002	0.0000	0.0001
310203	PI	265108	Italica Agostano	Poland	Eastern_Europe	1960-4-27	TEJ	0.0039	0.9956	0.0001	0.0001	0.0003
310204	PI	265110	Italica Carolina	Poland	Eastern_Europe	1960-4-27	TEJ	0.0005	0.9990	0.0001	0.0001	0.0002
310205	PI	265111	Italica M1	Poland	Eastern_Europe	1960-4-27	TEJ	0.0005	0.9992	0.0001	0.0001	0.0001
310206	PI	265113	Italica Oobie	Poland	Eastern_Europe	1960-4-27	IND	0.0004	0.0006	0.9988	0.0001	0.0001
310207	PI	265114	Erythroceros Hok-kaido	Poland	Eastern_Europe	1960-4-27	TEJ	0.0044	0.9953	0.0001	0.0001	0.0002
310208	PI	265116	Zerawchanica Karatalski	Poland	Eastern_Europe	1960-4-27	TEJ	0.0007	0.9990	0.0001	0.0001	0.0001
310209	PI	266121	KUBANSKIJ 140	Russian Federation	Eastern_Europe	1960-6-8	TEJ	0.0052	0.8765	0.0004	0.0003	0.1176
310210	PI	266122	KRASNODARSKIJ 424	Russian Federation	Eastern_Europe	1960-6-8	TEJ	0.0019	0.9978	0.0002	0.0000	0.0001
310211	PI	267996	Pergonil 15	Portugal	Western_Europe	1960-9-7	TEJ	0.0030	0.9964	0.0003	0.0002	0.0001

310212	PI	269938	Girba Jowal	Pakistan	Southern_Asia	1960-11-29	TEJ-ARO-TRJ	0.1644	0.4589	0.0721	0.0426	0.2620
310213	PI	274574	Alvario	Portugal	Western_Europe	1961-5-12	TEJ	0.3257	0.6308	0.0045	0.0379	0.0012
310214	PI	274577	Campino	Portugal	Western_Europe	1961-5-12	TRJ	0.9991	0.0006	0.0001	0.0000	0.0001
310215	PI	275452	44	Guyana	South_America	1961-6-20	TEJ	0.0006	0.9993	0.0001	0.0000	0.0001
310216	PI	276154	SML 242	Suriname	South_America	1961-8-3	IND	0.0022	0.0011	0.9949	0.0015	0.0003
310217	PI	276860	Laat	Suriname	South_America	1961-9-29	IND	0.0015	0.0004	0.7615	0.2360	0.0006
310218	PI	277262	SC 70	Tanzania	Africa	1961-11-8	TRJ	0.9990	0.0007	0.0002	0.0000	0.0001
310219	PI	277414	Red Khosha Cerma	Afghanistan	Southern_Asia	1961-11-20	ARO	0.0003	0.0006	0.0004	0.0012	0.9976
310220	PI	277415	Safut Khosha	Afghanistan	Southern_Asia	1961-11-20	AUS	0.0001	0.0002	0.0003	0.9992	0.0002
310221	PI	279375	Carola	France	Western_Europe	1962-2-19	TEJ	0.1538	0.8452	0.0004	0.0004	0.0002
310222	PI	279971	BARAGGIA	Italy	Western_Europe	1962-3-28	TEJ	0.0086	0.9911	0.0001	0.0001	0.0002
310223	PI	279983	MONTICELLI	Italy	Western_Europe	1962-3-28	TEJ	0.0014	0.9984	0.0001	0.0000	0.0001
310224	PI	279991	WC 2493	Italy	Western_Europe	1962-3-28	TEJ	0.0038	0.9959	0.0001	0.0001	0.0001
310225	PI	280001	STIRPE 82 CHIAP-PELLI	Italy	Western_Europe	1962-3-28	TEJ	0.0118	0.9879	0.0001	0.0001	0.0001
310226	PI	281630	NORIN 11	Japan	North_Pacific	1962-6-12	TEJ	0.0005	0.9993	0.0001	0.0001	0.0001
310227	PI	281760	Fanny	France	Western_Europe	1962-7-5	TEJ	0.0348	0.9649	0.0001	0.0000	0.0002
310228	PI	281789	2	Chile	South_America	1962-7-6	TEJ	0.0004	0.9993	0.0001	0.0001	0.0001
310229	PI	281791	4	Chile	South_America	1962-7-6	TEJ	0.0005	0.9993	0.0001	0.0001	0.0001
310230	PI	281844	Kam Bau Ngan	Hong Kong	China	1962-7-10	IND	0.0093	0.0038	0.9840	0.0026	0.0003
310231	PI	281845	Lo Shu Ngar	Hong Kong	China	1962-7-10	IND	0.0303	0.0030	0.9660	0.0005	0.0003
310232	PI	282171	ARPA SHALI	Uzbekistan	Central_Asia	1962-7-23	TEJ	0.0015	0.9979	0.0001	0.0004	0.0002
310233	PI	282172	BULGAR TAJFA-JTA	Bulgaria	Eastern_Europe	1962-7-23	TEJ	0.0002	0.9996	0.0001	0.0000	0.0001
310234	PI	282196	PRECOCE ALLO-RIO	Hungary	Eastern_Europe	1962-7-23	TEJ	0.0152	0.9836	0.0001	0.0008	0.0002
310235	PI	282207	UZ ROSZ 5	Uzbekistan	Central_Asia	1962-7-23	TEJ	0.0242	0.9479	0.0004	0.0069	0.0206
310236	PI	282210	UZ ROSZ 269	Uzbekistan	Central_Asia	1962-7-23	TEJ	0.0004	0.9994	0.0001	0.0000	0.0001
310237	PI	282767	Jappein Tunkungo	Senegal	Africa	1962-8-28	IND	0.0012	0.0009	0.9755	0.0220	0.0005
310238	PI	282769	R 75	Senegal	Africa	1962-8-28	TRJ	0.9572	0.0010	0.0406	0.0007	0.0006
310239	PI	282771	*Iguape Cateto	Senegal	Africa	1962-8-28	TRJ	0.9311	0.0004	0.0677	0.0008	0.0001
310240	PI	282947	TAICHUNG 33	Taiwan	China	1962-9-11	TRJ-TEJ	0.5168	0.4724	0.0105	0.0001	0.0003
310241	PI	291430	UZ ROSZ M38	Uzbekistan	Central_Asia	1963-6-6	TEJ	0.1578	0.8413	0.0001	0.0000	0.0007
310242	PI	291438	Kirman	Hungary	Eastern_Europe	1963-6-6	TEJ	0.0452	0.8022	0.0001	0.0003	0.1521
310243	PI	291478	Italica Livorno	Hungary	Eastern_Europe	1963-6-6	TEJ	0.0006	0.9990	0.0001	0.0002	0.0001
310244	PI	291481	Cin Szen No. 5	Hungary	Eastern_Europe	1963-6-6	TEJ	0.0010	0.9987	0.0001	0.0001	0.0001
310245	PI	291484	Tscchan Tzun Uman	Hungary	Eastern_Europe	1963-6-6	TEJ	0.2792	0.7201	0.0001	0.0002	0.0005
310246	PI	291491	Gun Lu	Hungary	Eastern_Europe	1963-6-6	TEJ	0.0613	0.9384	0.0001	0.0001	0.0001
310247	PI	291526	Romanica	Hungary	Eastern_Europe	1963-6-6	TEJ	0.0390	0.9591	0.0005	0.0003	0.0011
310248	PI	291535	Pembe 62	Hungary	Eastern_Europe	1963-6-6	TEJ	0.0006	0.9991	0.0001	0.0001	0.0001
310249	PI	291542	P 6 Africana	Hungary	Eastern_Europe	1963-6-6	TEJ	0.0010	0.9988	0.0001	0.0000	0.0001
310250	PI	291636	MUTSU HIKARI	Japan	North_Pacific	1963-6-13	TEJ	0.0004	0.9993	0.0001	0.0001	0.0001
310251	PI	291640	FUKU SUKE	Japan	North_Pacific	1963-6-13	TEJ	0.0004	0.9980	0.0004	0.0004	0.0007
310252	PI	294370	PANBIRA	Bangladesh	Southern_Asia	1963-12-9	AUS	0.0002	0.0001	0.0017	0.9980	0.0000
310253	PI	294397	TAIPEI WOO CO	Taiwan	China	1963-12-9	IND	0.0005	0.0001	0.9992	0.0001	0.0001
310254	PI	294421	Ambar	Iraq	Mideast	1963-12-13	ARO	0.0008	0.0006	0.0002	0.0010	0.9974
310255	PI	294423	GHRAIBA	Iraq	Mideast	1963-12-13	AUS	0.0006	0.0006	0.0007	0.9979	0.0001
310256	PI	297556	Rexora	Mozambique	Africa	1964-5-8	IND	0.0015	0.0029	0.9949	0.0006	0.0001
310257	PI	297557	Til	Mozambique	Africa	1964-5-8	TRJ	0.9956	0.0038	0.0003	0.0000	0.0003
310258	PI	298958	XB-6	Australia	Oceania	1964-7-7	TRJ-TEJ	0.5036	0.4961	0.0002	0.0001	0.0001
310259	PI	303646	WC 4419	Honduras	Central_America	1965-1-11	TRJ	0.9989	0.0007	0.0002	0.0000	0.0002
310260	PI	304221	2-1-2-3-1	Australia	Oceania	1965-2-19	TEJ-TRJ	0.4211	0.5786	0.0002	0.0001	0.0001
310261	PI	304222	1-7-1-1-3	Australia	Oceania	1965-2-19	TRJ-TEJ	0.5342	0.4653	0.0002	0.0001	0.0001
310262	PI	312645	I Geo Tze	Taiwan	China	1966-3-22	IND	0.0002	0.0003	0.9992	0.0002	0.0001
310263	PI	313075	138-1-1	Chile	South_America	1966-4-7	TEJ	0.0881	0.8634	0.0412	0.0056	0.0016
310264	PI	315640	Nilo 47	El Salvador	Central_America	1966-6-29	TRJ	0.8154	0.1843	0.0002	0.0000	0.0001
310265	PI	315644	Nilo 48A	El Salvador	Central_America	1966-6-29	TRJ	0.7878	0.2119	0.0002	0.0000	0.0001
310266	PI	315649	45-5-6	El Salvador	Central_America	1966-6-29	TRJ-IND	0.4821	0.0099	0.3949	0.1128	0.0004

310267	PI	315651	45-5-17	El Salvador	Central_America	1966-6-29	TRJ-IND	0.4637	0.0076	0.4079	0.1203	0.0005
310268	PI	315652	45-5-18	El Salvador	Central_America	1966-6-29	TRJ-IND	0.4981	0.0041	0.3997	0.0976	0.0005
310269	PI	317316	JUMA 1	Dominican Republic	Central_America	1966-11-8	TEJ-TRJ	0.4682	0.5306	0.0008	0.0001	0.0002
310270	PI	317525	1300	Madagascar	Africa	1966-11-18	TEJ	0.0005	0.9994	0.0001	0.0000	0.0000
310271	PI	318642	CHUGOKU 31	Japan	North_Pacific	1967-2-14	TEJ	0.0009	0.9569	0.0001	0.0408	0.0013
310272	PI	319515	Mo. V65-S93	Mexico	North_America	1967-4-10	TRJ	0.9992	0.0005	0.0002	0.0001	0.0000
310273	PI	319699	Hassawi	Saudi Arabia	Mideast	1967-4-27	IND	0.0002	0.0006	0.9986	0.0006	0.0000
310274	PI	321142	IR 334-17-1-3-1	Philippines	South_Pacific	1967-7-12	IND	0.1760	0.0011	0.8177	0.0003	0.0049
310275	PI	321331	IR 154-123-1-1-1	Philippines	South_Pacific	1967-7-12	IND	0.1849	0.0010	0.8135	0.0004	0.0002
310276	PI	325821	Khao Khao	Thailand	Southeast_Asia	1968-2-23	IND	0.0009	0.0013	0.9973	0.0002	0.0002
310277	PI	326028	Yongkwang	Korea_ South	North_Pacific	1968-3-4	TEJ	0.0003	0.9995	0.0001	0.0000	0.0001
310278	PI	326029	AMBER 33	Iraq	Mideast	1968-3-5	ARO	0.0004	0.0007	0.0002	0.0011	0.9976
310279	PI	326033	NAYIMA 45	Iraq	Mideast	1968-3-5	AUS	0.0002	0.0007	0.0005	0.9982	0.0004
310280	PI	330479	SUWON 82	Korea_ South	North_Pacific	1968-5-15	TEJ	0.0005	0.9993	0.0001	0.0001	0.0001
310281	PI	330625	Triomphe du Maroc	Morocco	Mideast	1968-5-20	TEJ	0.0003	0.9995	0.0001	0.0001	0.0001
310282	PI	330641	68-2	France	Western_Europe	1968-5-24	TEJ	0.0124	0.9873	0.0000	0.0000	0.0002
310283	PI	331519	IR 151-P136-2-3	Philippines	South_Pacific	1968-7-12	IND	0.3041	0.0059	0.6897	0.0001	0.0003
310284	PI	331548	IR 293-6-2-1	Philippines	South_Pacific	1968-7-12	IND	0.1506	0.0069	0.8079	0.0338	0.0007
310285	PI	338107	IR 532-1-47	Philippines	South_Pacific	1968-11-6	IND	0.0003	0.0002	0.9988	0.0006	0.0001
310286	PI	339730	KULU	Australia	Oceania	1969-2-4	TRJ-TEJ	0.5324	0.4673	0.0001	0.0001	0.0001
310287	PI	340884	392-12-8-4	Spain	Western_Europe	1969-2-18	TEJ	0.0004	0.9995	0.0000	0.0000	0.0000
310288	PI	340888	Dosel	Spain	Western_Europe	1969-2-18	TEJ	0.0340	0.9645	0.0014	0.0001	0.0001
310289	PI	340889	DH-1	Spain	Western_Europe	1969-2-18	TEJ	0.0004	0.9994	0.0001	0.0000	0.0001
310290	PI	340894	22-5-12-11	Spain	Western_Europe	1969-2-18	TEJ	0.0005	0.9992	0.0001	0.0002	0.0001
310291	PI	340896	Peladilla	Spain	Western_Europe	1969-2-18	TEJ	0.0011	0.9987	0.0001	0.0000	0.0001
310292	PI	343835	SHUHO	Japan	North_Pacific	1969-7-16	TEJ	0.0003	0.9996	0.0000	0.0000	0.0000
310293	PI	343840	WOMBAT	Australia	Oceania	1969-7-16	TEJ	0.0943	0.9051	0.0004	0.0001	0.0001
310294	PI	345805	IR 583-14-3-3-1	Philippines	South_Pacific	1969-8-13	IND	0.0003	0.3228	0.6767	0.0002	0.0001
310295	PI	346409	ALLORIO LAMBDA	France	Western_Europe	1969-11-6	TEJ	0.1195	0.8802	0.0001	0.0000	0.0001
310296	PI	346442	50770	Guyana	South_America	1969-11-25	IND	0.0002	0.0002	0.9991	0.0005	0.0001
310297	PI	346446	50778	Guyana	South_America	1969-11-25	TRJ	0.8427	0.0005	0.1504	0.0039	0.0026
310298	PI	346448	51779	Guyana	South_America	1969-11-25	IND	0.0037	0.0003	0.9909	0.0013	0.0039
310299	PI	346818	ALDEBARAN AG 1	Argentina	South_America	1969-12-10	TEJ-TRJ	0.4590	0.5406	0.0002	0.0000	0.0001
310300	PI	346819	BLUE ROSE SEL M.A.	Argentina	South_America	1969-12-10	IND	0.2667	0.1277	0.6054	0.0002	0.0000
310301	PI	346827	H57-3-1	Argentina	South_America	1969-12-10	TEJ	0.3945	0.6048	0.0006	0.0001	0.0001
310302	PI	346831	H62-3-1	Argentina	South_America	1969-12-10	TRJ-IND-TEJ	0.3942	0.2814	0.3242	0.0001	0.0002
310303	PI	346845	H71-11-1	Argentina	South_America	1969-12-10	TEJ	0.3885	0.6111	0.0002	0.0001	0.0001
310304	PI	346847	H73-8-1	Argentina	South_America	1969-12-10	TRJ	0.6706	0.3291	0.0002	0.0001	0.0001
310305	PI	346849	H74-2-1	Argentina	South_America	1969-12-10	TEJ	0.0351	0.9648	0.0001	0.0000	0.0001
310306	PI	346927	VILKID ZIRE	Azerbaijan	Central_Asia	1969-12-24	TEJ	0.0004	0.9994	0.0001	0.0000	0.0001
310307	PI	348779	IR 510-15-1-1-2-1	Philippines	South_Pacific	1970-3-6	IND-TRJ-TEJ	0.3180	0.2987	0.3830	0.0002	0.0001
310308	PI	348905	UZ ROS 269	Uzbekistan	Central_Asia	1918-3-5	TEJ	0.0006	0.9992	0.0001	0.0000	0.0001
310309	PI	348908	AZ ROS 637	Azerbaijan	Central_Asia	1918-3-5	TEJ	0.0006	0.9087	0.0022	0.0464	0.0420
310310	PI	348909	SADRI MA-SALINSKIJ	Azerbaijan	Central_Asia	1918-3-5	ARO	0.0009	0.2740	0.0003	0.0002	0.7246
310311	PI	350295	Biser 1	Bulgaria	Eastern_Europe	1970-5-28	TEJ	0.0004	0.9994	0.0001	0.0001	0.0001
310312	PI	350296	Carina	Bulgaria	Eastern_Europe	1970-5-28	TEJ	0.0005	0.9993	0.0001	0.0001	0.0001
310313	PI	350297	Iskra	Bulgaria	Eastern_Europe	1970-5-28	TEJ	0.0003	0.9995	0.0001	0.0000	0.0001
310314	PI	350300	Plovdiv	Bulgaria	Eastern_Europe	1970-5-28	TEJ	0.0007	0.9991	0.0001	0.0000	0.0001
310315	PI	350301	Slava	Bulgaria	Eastern_Europe	1970-5-28	TEJ	0.0415	0.9583	0.0001	0.0000	0.0001
310316	PI	373450	ARC 10299	India	Southern_Asia	1972-3-27	AUS	0.0004	0.0002	0.1122	0.8872	0.0001
310317	PI	353723	IARI 6626	India	Southern_Asia	1970-5-4	AUS	0.0003	0.0002	0.1497	0.8434	0.0064
310318	PI	353746	IARI 7449	India	Southern_Asia	1970-5-4	AUS	0.0003	0.0002	0.0813	0.9179	0.0003
310319	PI	357051	BC5-55	India	Southern_Asia	1971-1-12	IND	0.0002	0.0002	0.6719	0.0111	0.3167
310320	PI	366134	CENTURY PATNA 231	United States	North_America	1971-8-30	TRJ	0.9968	0.0029	0.0001	0.0000	0.0002

310322	PI	369811	Pinde Gogo Wierie	Suriname	South_America	1972-2-1	TRJ	0.9907	0.0012	0.0053	0.0018	0.0011
310323	PI	372046	P881-12-4-B	Colombia	South_America	1972-4-11	IND	0.0071	0.0259	0.9655	0.0011	0.0004
310324	PI	372054	P855-B-3-B	Colombia	South_America	1972-4-11	IND	0.1404	0.0008	0.8581	0.0001	0.0006
310325	PI	372921	2-43-3	Iran	Mideast	1972-5-21	ARO	0.0004	0.0022	0.0002	0.0002	0.9971
310326	PI	373102	IR 1103-15-8-5-3-3-3	Philippines	South_Pacific	1972-3-27	IND	0.0101	0.0895	0.9002	0.0002	0.0001
310327	PI	373136	52/16-0-2	Papua New Guinea	Oceania	1972-3-27	TRJ	0.9791	0.0028	0.0026	0.0151	0.0003
310328	PI	373139	E-425	Senegal	Africa	1972-3-27	TRJ	0.9920	0.0008	0.0006	0.0022	0.0044
310329	PI	373141	GPNO 15007	Senegal	Africa	1972-3-27	TRJ	0.6583	0.3413	0.0001	0.0001	0.0001
310330	PI	373166	Qiparat	Philippines	South_Pacific	1972-3-27	TRJ	0.9550	0.0173	0.0005	0.0146	0.0126
310331	PI	373194	Agbede	Nigeria	Africa	1972-3-27	TRJ	0.9950	0.0045	0.0003	0.0001	0.0002
310332	PI	373203	Tchibanga	Gabon	Africa	1972-3-27	IND	0.0002	0.0001	0.9996	0.0001	0.0000
310333	PI	373204	Bungara	Rwanda	Africa	1972-3-27	TRJ	0.9972	0.0024	0.0002	0.0000	0.0002
310334	PI	373205	TONO BREA ENANO 5	Dominican Republic	Central_America	1972-3-27	IND	0.0362	0.0008	0.9616	0.0007	0.0008
310335	PI	373206	Sika	Cameroon	Africa	1972-3-27	TRJ	0.9923	0.0003	0.0053	0.0018	0.0003
310336	PI	373222	Chao Puak Deng	Laos	Southeast_Asia	1972-3-27	IND	0.0003	0.0004	0.9989	0.0003	0.0002
310337	PI	373232	Khao Phoi	Laos	Southeast_Asia	1972-3-27	TRJ-TEJ-ARO	0.4374	0.3301	0.0066	0.0008	0.2251
310338	PI	373249	Khao Luang	Laos	Southeast_Asia	1972-3-27	TRJ-TEJ-ARO	0.4451	0.2902	0.0593	0.0005	0.2048
310339	PI	373282	Kh. Mack Ko	Laos	Southeast_Asia	1972-3-27	TRJ-TEJ-ARO	0.4725	0.2986	0.0205	0.0006	0.2077
310340	PI	373289	Chao Hay b	Laos	Southeast_Asia	1972-3-27	IND	0.0001	0.0001	0.9997	0.0001	0.0000
310341	PI	373313	Khao Hao	Laos	Southeast_Asia	1972-3-27	IND	0.0010	0.0014	0.8388	0.1586	0.0002
310342	PI	439117	NIQUEN	Chile	South_America	1980-1-1	TEJ	0.0355	0.9639	0.0005	0.0001	0.0000
310343	PI	373703	Deng Mak Tek	Laos	Southeast_Asia	1972-3-27	IND-TRJ	0.4380	0.0547	0.5015	0.0035	0.0023
310344	PI	373746	Chao Khao	Laos	Southeast_Asia	1972-3-27	AUS	0.0005	0.0002	0.0745	0.9245	0.0003
310345	PI	373761	J.P. 5	Australia	Oceania	1972-3-27	TEJ	0.0005	0.9993	0.0001	0.0000	0.0001
310346	PI	373764	Bakukut	Malaysia	South_Pacific	1972-3-27	TRJ	0.9906	0.0085	0.0003	0.0003	0.0003
310347	PI	373768	Kandioya	Malaysia	South_Pacific	1972-3-27	TRJ	0.9961	0.0036	0.0001	0.0001	0.0002
310348	PI	373771	C 8429	Papua New Guinea	Oceania	1972-3-27	TRJ	0.9121	0.0868	0.0003	0.0003	0.0004
310349	PI	373772	C 8432	Papua New Guinea	Oceania	1972-3-27	TRJ	0.9925	0.0064	0.0007	0.0003	0.0002
310350	PI	373774	C 8435	Papua New Guinea	Oceania	1972-3-27	IND	0.0000	0.0000	0.9998	0.0001	0.0000
310351	PI	373795	Warrangal Culture 1252	India	Southern_Asia	1972-3-27	IND	0.0002	0.0005	0.9463	0.0528	0.0002
310352	PI	373799	Padi Bangka	Malaysia	South_Pacific	1972-3-27	TRJ	0.9900	0.0089	0.0003	0.0003	0.0004
310353	PI	373801	Goh Chi Sai	Malaysia	South_Pacific	1972-3-27	AUS	0.0044	0.0043	0.3616	0.6294	0.0002
310354	PI	373816	Padi Pohon Batu	Malaysia	South_Pacific	1972-3-27	TRJ	0.8855	0.1123	0.0004	0.0010	0.0008
310355	PI	373819	Padi Thinop	Malaysia	South_Pacific	1972-3-27	TRJ	0.8248	0.0841	0.0010	0.0022	0.0879
310356	PI	373832	Padi Amur	Malaysia	South_Pacific	1972-3-27	TRJ	0.7424	0.2495	0.0010	0.0003	0.0069
310357	PI	373900	Besudi Long-Grain	Afghanistan	Southern_Asia	1972-3-27	ARO	0.0003	0.0002	0.0002	0.0005	0.9987
310358	PI	373940	Lawangeen	Afghanistan	Southern_Asia	1972-7-3	ARO	0.0005	0.0010	0.0003	0.0003	0.9980
310359	PI	373941	Maien Garm	Afghanistan	Southern_Asia	1972-7-3	ARO	0.0006	0.0825	0.0002	0.0003	0.9164
310360	PI	374810	KAKAI 203	Hungary	Eastern_Europe	1972-8-16	IND-TEJ	0.0019	0.4532	0.5440	0.0007	0.0002
310361	PI	374813	SDS-7	Hungary	Eastern_Europe	1972-8-16	TEJ	0.0173	0.9821	0.0001	0.0001	0.0003
310362	PI	376527	IR 1614-168-2-2	Philippines	South_Pacific	1972-7-13	IND	0.0004	0.0005	0.9988	0.0002	0.0001
310363	PI	377570	P773-44-3-1	Colombia	South_America	1972-12-11	IND	0.0002	0.0002	0.9994	0.0001	0.0001
310364	PI	377620	Purple Puttu	India	Southern_Asia	1972-12-12	AUS	0.0002	0.0006	0.0020	0.9969	0.0002
310365	PI	377750	Nauta	Peru	South_America	1973-1-18	TRJ	0.9990	0.0006	0.0003	0.0000	0.0000
310366	PI	378096	P726-287-2-1	Colombia	South_America	1973-2-22	IND	0.0004	0.0003	0.9991	0.0001	0.0001
310367	PI	378102	P 738-97-3-1	Colombia	South_America	1973-2-22	IND	0.0002	0.0004	0.9990	0.0003	0.0001
310368	PI	378108	P 761-40-2-1	Colombia	South_America	1973-2-22	IND	0.0004	0.0004	0.9991	0.0001	0.0000
310369	PI	385322	Usen	Kenya	Africa	1974-2-5	IND	0.0006	0.0001	0.9992	0.0001	0.0001
310370	PI	439626	Sundensis	Kazakhstan	Central_Asia	1980-2-1	IND	0.0092	0.0090	0.9815	0.0003	0.0001
310371	PI	385326	*JAYA	India	Southern_Asia	1974-2-5	IND	0.0000	0.0000	0.9998	0.0001	0.0000
310372	PI	385345	RD-1	Thailand	Southeast_Asia	1974-2-5	IND	0.0002	0.0002	0.9994	0.0001	0.0001
310373	PI	385417	*Basmati Sufaid	Pakistan	Southern_Asia	1974-2-20	ARO	0.0003	0.0004	0.0008	0.0107	0.9878
310374	PI	385447	Chak 48	Pakistan	Southern_Asia	1974-2-20	ARO	0.0003	0.0003	0.0001	0.0002	0.9991

310375	PI	385489	B35	Pakistan	Southern_Asia	1974-2-20	AUS	0.0001	0.0002	0.0005	0.9990	0.0002
310376	PI	385537	Dhan Sufaid	Pakistan	Southern_Asia	1974-2-20	AUS	0.0004	0.0002	0.0009	0.9981	0.0005
310377	PI	385588	Jhona	Pakistan	Southern_Asia	1974-2-20	AUS	0.0002	0.0002	0.0015	0.9980	0.0002
310378	PI	385609	P 293	Pakistan	Southern_Asia	1974-2-20	AUS	0.0002	0.0001	0.0003	0.9993	0.0002
310379	PI	385643	Dhan Baggi	Pakistan	Southern_Asia	1974-2-20	AUS	0.0002	0.0002	0.0003	0.9991	0.0002
310380	PI	385722	P 79	India	Southern_Asia	1974-2-20	AUS	0.0002	0.0002	0.0003	0.9993	0.0001
310381	PI	385826	NC 1/536	Pakistan	Southern_Asia	1974-2-20	AUS	0.0001	0.0001	0.0002	0.9995	0.0001
310382	PI	385830	Ratua Red Nehri	Pakistan	Southern_Asia	1974-2-20	AUS	0.0002	0.0001	0.0002	0.9993	0.0001
310383	PI	385837	Ratua	Pakistan	Southern_Asia	1974-2-20	AUS	0.0001	0.0002	0.0013	0.9982	0.0001
310384	PI	385881	Saunfi Sarian	Pakistan	Southern_Asia	1974-2-20	AUS	0.0001	0.0002	0.0002	0.9993	0.0002
310385	PI	388243	Ponta Rubra	Portugal	Western_Europe	1974-3-5	TEJ	0.0009	0.9989	0.0001	0.0001	0.0001
310386	PI	388257	Chagas 4	Brazil	South_America	1974-3-5	TEJ	0.2289	0.7707	0.0002	0.0001	0.0001
310387	PI	388279	Ban To	Japan	North_Pacific	1974-3-5	TEJ	0.0023	0.9975	0.0001	0.0000	0.0001
310388	PI	388298	Polman	India	Southern_Asia	1974-3-5	AUS	0.0001	0.0001	0.0003	0.9994	0.0001
310389	PI	388304	Won Son Zo No. 11	Korea	North_Pacific	1974-3-5	IND	0.0002	0.0003	0.9994	0.0001	0.0000
310390	PI	388346	GPNO 19314	Brazil	South_America	1974-3-5	AUS	0.0003	0.0001	0.0002	0.9992	0.0002
310391	PI	388355	Assaw	China	China	1974-3-5	TEJ	0.3353	0.6642	0.0004	0.0001	0.0001
310392	PI	388389	Choeii-ine	Japan	North_Pacific	1974-3-5	TEJ	0.3525	0.6375	0.0009	0.0053	0.0038
310393	PI	388391	Chokei Wase	Japan	North_Pacific	1974-3-5	TEJ-TRJ	0.4390	0.5558	0.0022	0.0013	0.0018
310394	PI	388392	Chu Cheng	Korea	North_Pacific	1974-3-5	IND	0.0003	0.0001	0.9995	0.0001	0.0001
310395	PI	388423	GPNO 16379	Micronesia	Oceania	1974-3-5	IND	0.0002	0.0001	0.9996	0.0001	0.0001
310396	PI	388426	Chacareiro	Argentina	South_America	1974-3-5	IND	0.0348	0.2047	0.7600	0.0004	0.0001
310397	PI	388427	Chacareiro Uruguay	Uruguay	South_America	1974-3-5	TEJ	0.0032	0.9954	0.0004	0.0002	0.0007
310398	PI	388433	Du Zung Zione No. 119	Korea	North_Pacific	1974-3-5	TEJ	0.0022	0.9971	0.0002	0.0001	0.0004
310399	PI	388436	Doble Carolina	Uruguay	South_America	1974-3-5	AUS	0.0002	0.0002	0.0003	0.9991	0.0002
310400	PI	388458	Gun Do No. 82	Korea_ South	North_Pacific	1974-3-5	TEJ-TRJ	0.4798	0.5112	0.0025	0.0020	0.0045
310401	PI	388466	HIRAYAMA	Japan	North_Pacific	1974-3-5	TEJ	0.0151	0.9683	0.0001	0.0001	0.0164
310402	PI	388467	Huk Pi	Korea	North_Pacific	1974-3-5	TEJ-TRJ	0.3726	0.5544	0.0689	0.0009	0.0032
310403	PI	388489	Kanou	Brazil	South_America	1974-3-5	IND	0.0008	0.0003	0.9984	0.0003	0.0002
310404	PI	388492	Ken Yen	China	China	1974-3-5	IND	0.0003	0.0004	0.9990	0.0001	0.0001
310405	PI	388507	Miga	Brazil	South_America	1974-3-5	TRJ	0.8186	0.1812	0.0001	0.0000	0.0001
310406	PI	388528	No Iku No. 1774	Taiwan	China	1974-3-5	TEJ	0.0151	0.9841	0.0004	0.0004	0.0001
310407	PI	388540	No. Ordem Lista 81	Brazil	South_America	1974-3-5	TRJ	0.6591	0.3406	0.0001	0.0001	0.0001
310408	PI	388542	No. Ordem Lista 85	Brazil	South_America	1974-3-5	TEJ-TRJ	0.4606	0.5388	0.0004	0.0001	0.0001
310409	PI	388550	Oh Bada No. 133	Brazil	South_America	1974-3-5	TRJ	0.8467	0.1117	0.0370	0.0043	0.0003
310410	PI	388593	UZ ROSZ 2831	Uzbekistan	Central_Asia	1974-3-5	TEJ-TRJ	0.4289	0.5709	0.0001	0.0000	0.0001
310411	PI	388606	IGUAPE AGULHA	Brazil	South_America	1974-3-5	TRJ	0.9966	0.0029	0.0002	0.0002	0.0002
310412	PI	389010	Kung Shun	Taiwan	China	1974-9-1	TRJ	0.9984	0.0010	0.0002	0.0001	0.0003
310413	PI	389019	CHIANUNG 242	Taiwan	China	1974-9-1	IND	0.0005	0.0002	0.9992	0.0001	0.0001
310414	PI	389036	Ai Chueh Li	Taiwan	China	1974-9-1	IND	0.0074	0.0122	0.9790	0.0008	0.0005
310415	PI	389037	Ai Chueh Ta Pai Ku	Taiwan	China	1974-9-1	IND	0.0101	0.0004	0.9889	0.0002	0.0004
310416	PI	389164	CHIEM CHANH	Vietnam	Southeast_Asia	1974-9-1	IND	0.0773	0.0079	0.8681	0.0011	0.0456
310417	PI	389165	BAU 157	Vietnam	Southeast_Asia	1974-9-1	IND	0.0355	0.0008	0.9619	0.0005	0.0013
310418	PI	389177	Nep Vai	Vietnam	Southeast_Asia	1974-9-1	IND	0.0126	0.0003	0.9849	0.0005	0.0016
310419	PI	389200	CAU PHU XUYEN 264	Vietnam	Southeast_Asia	1974-9-1	IND	0.0075	0.0003	0.9496	0.0183	0.0242
310420	PI	389234	Thang 10	Vietnam	Southeast_Asia	1974-9-1	IND	0.0189	0.0007	0.9251	0.0102	0.0451
310421	PI	389266	Giau Dumont	Vietnam	Southeast_Asia	1974-9-1	IND	0.0067	0.0006	0.9214	0.0127	0.0586
310422	PI	389336	Ukoku	China	China	1974-9-1	IND	0.0020	0.0032	0.9926	0.0007	0.0015
310423	PI	389467	Hung Fan Goo	China	China	1974-9-1	IND	0.0002	0.0001	0.9994	0.0001	0.0001
310424	PI	389548	833-5691-11	China	China	1974-9-1	IND	0.0005	0.0007	0.9982	0.0004	0.0002
310425	PI	389637	Bir Co Tsan	China	China	1974-9-1	IND	0.0002	0.0005	0.9989	0.0003	0.0001
310426	PI	389707	Hung Co Man	China	China	1974-9-1	IND	0.0002	0.0006	0.9988	0.0003	0.0001
310427	PI	389812	Fa Yu Tao	China	China	1974-9-1	IND	0.0003	0.0005	0.9990	0.0001	0.0001
310428	PI	389876	Sipirasikkam	Indonesia	South_Pacific	1974-9-1	TRJ	0.9525	0.0360	0.0007	0.0073	0.0035
310429	PI	389921	Choku Chai	Hong Kong	China	1974-9-1	IND	0.0523	0.0003	0.9462	0.0010	0.0003
310430	PI	389925	Chun Chu Cho	Hong Kong	China	1974-9-1	IND	0.0005	0.0008	0.9965	0.0017	0.0006

310431	PI	389926	Glutinous	Hong Kong	China	1974-9-1	TRJ	0.9485	0.0509	0.0002	0.0001	0.0003
310432	PI	389931	Phnat Tuk	Cambodia	Southeast_Asia	1974-9-1	TEJ	0.0023	0.9974	0.0001	0.0001	0.0001
310433	PI	389932	Rit Ankrong	Cambodia	Southeast_Asia	1974-9-1	IND	0.0044	0.0007	0.9213	0.0005	0.0730
310434	PI	389935	Chantas Phlouk B. Phlg	Cambodia	Southeast_Asia	1974-9-1	IND-TEJ	0.0010	0.3093	0.5093	0.1791	0.0013
310435	PI	389945	Angkrang	Cambodia	Southeast_Asia	1974-9-1	IND-TEJ	0.0022	0.3908	0.4952	0.1114	0.0004
310436	PI	389989	Zayas Bazan	Cuba	Central_America	1974-9-1	IND	0.0003	0.0004	0.9989	0.0004	0.0000
310437	PI	391181	Che Shau Nan Bir	China	China	1974-11-20	TRJ	0.9993	0.0004	0.0001	0.0000	0.0001
310438	PI	391199	3287	Taiwan	China	1974-11-20	IND	0.0005	0.0003	0.9990	0.0001	0.0001
310439	PI	391216	3997	Haiti	Central_America	1974-11-20	TRJ-IND-AUS	0.3983	0.0006	0.3600	0.2409	0.0002
310440	PI	391218	TJ	Guyana	South_America	1974-11-20	IND	0.0018	0.0010	0.9964	0.0007	0.0001
310441	PI	391260	Ambalalava 1283	Madagascar	Africa	1974-11-20	IND	0.0008	0.0006	0.9982	0.0003	0.0001
310442	PI	391264	PD 46	Sri Lanka	Southern_Asia	1974-11-20	IND	0.0013	0.0002	0.9981	0.0003	0.0001
310443	PI	391272	OKSHITMAYIN	Myanmar	Southeast_Asia	1974-11-20	TRJ-TEJ	0.5025	0.3721	0.0345	0.0902	0.0007
310444	PI	391326	Chibica	Mozambique	Africa	1974-11-20	TEJ	0.1418	0.8579	0.0001	0.0000	0.0002
310445	PI	391375	59	Philippines	South_Pacific	1974-11-20	TRJ-TEJ	0.5477	0.4519	0.0002	0.0000	0.0001
310446	PI	391691	Acheh	Malaysia	South_Pacific	1974-11-27	IND	0.0014	0.0032	0.9948	0.0004	0.0001
310447	PI	391756	Sukananadi B	Indonesia	Oceania	1974-11-27	TEJ	0.0003	0.9995	0.0001	0.0000	0.0000
310448	PI	391827	Lantjang	Indonesia	Oceania	1974-11-27	IND	0.0003	0.0002	0.9992	0.0003	0.0000
310449	PI	391859	Gambiaka Sebela	Mali	Africa	1974-11-27	TEJ	0.0003	0.9996	0.0001	0.0000	0.0000
310450	PI	391861	Kihogo	Tanzania	Africa	1974-11-27	TEJ	0.0003	0.9996	0.0001	0.0000	0.0000
310451	PI	391891	Tjina	Indonesia	Oceania	1974-11-27	IND	0.0001	0.0003	0.9994	0.0001	0.0001
310452	PI	391943	Sabharaj	Bangladesh	Southern_Asia	1974-11-27	IND	0.0018	0.0214	0.9761	0.0006	0.0002
310453	PI	392085	CHONTALPA 16	Mexico	North_America	1974-12-31	TRJ-IND	0.5148	0.0682	0.4148	0.0022	0.0001
310454	PI	392089	JUMA 18	Dominican Republic	Central_America	1974-12-31	IND	0.0003	0.0006	0.9987	0.0001	0.0003
310455	PI	392247	Bahia	Spain	Western_Europe	1974-12-24	TEJ	0.0003	0.9996	0.0001	0.0000	0.0000
310456	PI	392534	GPNO 27792	Peru	South_America	1975-2-3	TEJ-TRJ	0.4831	0.5054	0.0104	0.0007	0.0004
310457	PI	392540	Unhlatuzi Valley Sugar	South Africa	Africa	1975-2-3	TRJ	0.6885	0.0449	0.0011	0.2586	0.0069
310458	PI	392543	Nang Mon	Thailand	Southeast_Asia	1975-2-3	TEJ	0.0017	0.9979	0.0003	0.0000	0.0001
310459	PI	392559	TONG SANGKER	Cambodia	Southeast_Asia	1975-2-3	TRJ	0.9990	0.0007	0.0001	0.0001	0.0001
310460	PI	392565	NEW GUINEA	Fiji	Oceania	1975-2-3	TEJ	0.0003	0.9996	0.0001	0.0000	0.0000
310461	PI	392576	NGAKYAUK	Myanmar	Southeast_Asia	1975-2-3	TEJ	0.0004	0.9994	0.0001	0.0000	0.0001
310462	PI	392579	NEANG MEAS	Cambodia	Southeast_Asia	1975-2-3	ARO	0.0006	0.0008	0.0002	0.0009	0.9975
310463	PI	392582	BAWKU WHITE	Ghana	Africa	1975-2-3	AUS	0.0004	0.0002	0.0003	0.9990	0.0002
310464	PI	392597	DISSI N 14	Mali	Africa	1975-2-3	AUS-IND	0.0010	0.0006	0.4084	0.5897	0.0003
310465	PI	392626	FA YIU TSAI	Hong Kong	China	1975-2-3	AUS	0.0001	0.0001	0.0006	0.9991	0.0001
310466	PI	392647	G Bonota	Liberia	Africa	1975-2-3	AUS	0.0002	0.0002	0.0003	0.9992	0.0001
310467	PI	392656	Kahago ex Mwaba-gale 1/146	Tanzania	Africa	1975-2-3	TEJ	0.0007	0.9991	0.0001	0.0000	0.0001
310468	PI	392688	Jambaram Vermelho	Guinea-Bissau	Africa	1975-2-3	AUS	0.0003	0.0001	0.0003	0.9991	0.0001
310469	PI	392690	Iaca	Guinea-Bissau	Africa	1975-2-3	AUS	0.0003	0.0002	0.0007	0.9986	0.0002
310470	PI	392691	Iaca Escuro	Guinea	Africa	1975-2-3	AUS	0.0004	0.0002	0.0006	0.9985	0.0003
310471	PI	392694	PATNAI 6	Myanmar	Southeast_Asia	1975-2-3	AUS	0.0005	0.0002	0.0008	0.9983	0.0002
310472	PI	392702	Gazi	Fiji	Oceania	1975-2-3	IND	0.0004	0.0002	0.7255	0.2736	0.0003
310473	PI	392757	Nang Rum Trang	Vietnam	Southeast_Asia	1975-2-3	TEJ	0.0004	0.9994	0.0001	0.0000	0.0001
310474	PI	392773	Lua Trang	Vietnam	Southeast_Asia	1975-2-3	TEJ	0.0009	0.9988	0.0001	0.0000	0.0001
310475	PI	392813	K8C-263-3	Suriname	South_America	1975-2-3	IND	0.0658	0.0005	0.9134	0.0185	0.0018
310476	PI	392880	TAITUNG 328	Taiwan	China	1975-2-3	TEJ-TRJ	0.4301	0.5634	0.0014	0.0007	0.0045
310477	PI	392914	BIRIBRA	Ghana	Africa	1975-2-3	IND	0.0004	0.0011	0.8555	0.1426	0.0004
310478	PI	393036	EMATA A 16-34	Myanmar	Southeast_Asia	1975-2-3	IND	0.0003	0.0002	0.9970	0.0020	0.0005
310479	PI	281788	1	Chile	South_America	1962-7-6	TEJ	0.0003	0.9993	0.0001	0.0001	0.0001
310480	PI	393180	Djimoron	Guinea	Africa	1975-2-3	IND	0.0006	0.0006	0.8223	0.1747	0.0018
310481	PI	393292	Anandi	India	Southern_Asia	1975-2-3	IND	0.0003	0.0009	0.9985	0.0002	0.0001
310482	PI	400081	Elliott	Liberia	Africa	1975-5-7	TRJ	0.9987	0.0010	0.0002	0.0001	0.0001
310483	PI	400090	OS 4	Nigeria	Africa	1975-5-7	ARO-TRJ	0.3984	0.0005	0.0005	0.0007	0.5999
310484	PI	400095	RT 1095-S26	Senegal	Africa	1975-5-7	TRJ	0.9987	0.0011	0.0001	0.0001	0.0000
310485	PI	400116	Perum Karuppan	Sri Lanka	Southern_Asia	1975-5-7	IND	0.0046	0.0075	0.9869	0.0009	0.0001

310486	PI	400157	PULUT NANGKA 016	Indonesia	South_Pacific	1975-4-23	IND	0.0007	0.0005	0.9983	0.0004	0.0001
310487	PI	400322	SIGADIS	Indonesia	South_Pacific	1975-6-3	IND	0.0004	0.0006	0.9984	0.0004	0.0002
310488	PI	400345	U.V.S. Unblatuzi	South Africa	Africa	1975-6-3	IND	0.0003	0.0008	0.9985	0.0004	0.0001
310489	PI	400398	Chun 118-33	China	China	1975-6-3	IND	0.0002	0.0001	0.9995	0.0001	0.0001
310490	PI	400424	Si Jih Goo	China	China	1975-6-3	IND	0.0002	0.0001	0.9994	0.0003	0.0000
310491	PI	400575	Mendi	Ghana	Africa	1975-6-3	IND	0.0012	0.0004	0.9980	0.0004	0.0001
310492	PI	400662	Janeri	Nepal	Southern_Asia	1975-6-3	IND	0.0046	0.0015	0.9929	0.0008	0.0002
310493	PI	400670	WW 3/200	Netherlands	Western_Europe	1975-6-3	IND-TRJ	0.3673	0.0235	0.5800	0.0287	0.0004
310494	PI	400672	WW 8/2290	Netherlands	Western_Europe	1975-6-3	TRJ-IND-AUS	0.4892	0.0035	0.3463	0.1574	0.0036
310495	PI	400714	Subdesvauxii Vase	Portugal	Western_Europe	1975-6-3	TEJ	0.2644	0.7352	0.0003	0.0001	0.0001
310496	PI	400718	Kathmandu Valley No. 1 Selection	Nepal	Southern_Asia	1975-6-3	IND	0.0007	0.0007	0.9981	0.0003	0.0001
310497	PI	400725	Dourado	El Salvador	Central_America	1975-6-3	TRJ	0.9987	0.0010	0.0002	0.0000	0.0001
310498	PI	400728	H 17 Tardio	Argentina	South_America	1975-6-3	TEJ	0.1419	0.8579	0.0001	0.0000	0.0001
310499	PI	400732	H-29-31	Argentina	South_America	1975-6-3	IND	0.0011	0.0005	0.9982	0.0001	0.0001
310500	PI	400772	VARY LAVA 9	Madagascar	Africa	1975-6-3	TRJ	0.7697	0.0011	0.0839	0.1452	0.0001
310501	PI	400778	Precoz Verde 1061	Madagascar	Africa	1975-6-3	IND-TEJ	0.0004	0.4846	0.5135	0.0012	0.0003
310502	PI	400779	Pirititovo 1417	Madagascar	Africa	1975-6-3	TRJ-IND	0.5494	0.0013	0.3661	0.0828	0.0004
310503	PI	400780	Manga Kely 694	Madagascar	Africa	1975-6-3	IND-AUS	0.0340	0.0121	0.5990	0.3548	0.0002
310504	PI	400782	Bengaly Morino 120	Madagascar	Africa	1975-6-3	IND	0.0071	0.0008	0.6054	0.3865	0.0002
310505	PI	401431	CHING YUEH 1	China	China	1975-6-10	TEJ	0.0007	0.9989	0.0002	0.0000	0.0001
310506	PI	402519	ARLESIENNE	France	Western_Europe	1975-6-19	TEJ	0.2091	0.7902	0.0004	0.0000	0.0002
310507	PI	402636	LEUANG HAWN	Thailand	Southeast_Asia	1975-8-4	TEJ	0.0005	0.9992	0.0001	0.0001	0.0001
310508	PI	402638	923	Madagascar	Africa	1975-8-4	TRJ-IND-AUS	0.4921	0.0012	0.3851	0.1213	0.0003
310509	PI	402758	Bantia	Liberia	Africa	1975-8-4	TRJ	0.9987	0.0009	0.0002	0.0001	0.0001
310510	PI	402789	BLUE STICK	Fiji	Oceania	1975-8-4	TEJ	0.0104	0.9875	0.0019	0.0001	0.0001
310511	PI	402795	BOM DIA	Guinea-Bissau	Africa	1975-8-4	AUS	0.0003	0.0002	0.0012	0.9982	0.0001
310512	PI	402858	CA 497/V/7	Chad	Africa	1975-8-4	TRJ	0.9966	0.0032	0.0001	0.0001	0.0001
310513	PI	403091	DJ 53	Bangladesh	Southern_Asia	1975-8-4	AUS	0.0001	0.0002	0.0004	0.9992	0.0001
310514	PI	403161	DM 56	Bangladesh	Southern_Asia	1975-8-4	AUS	0.0001	0.0001	0.0003	0.9993	0.0001
310515	PI	403289	Nam Dawk Mai	Thailand	Southeast_Asia	1975-8-4	IND	0.0015	0.0007	0.9964	0.0006	0.0008
310516	PI	403375	EKARIN YAHINE	Myanmar	Southeast_Asia	1975-8-4	TEJ	0.0003	0.9995	0.0001	0.0000	0.0000
310517	PI	403383	FA LOH PAK	Hong Kong	China	1975-8-4	IND	0.0002	0.0001	0.9995	0.0001	0.0000
310518	PI	403401	Gaza	Mozambique	Africa	1975-8-4	IND	0.0010	0.0006	0.7097	0.2882	0.0005
310519	PI	403422	GUYANE 1	Chad	Africa	1975-8-4	IND	0.0003	0.0816	0.7512	0.1667	0.0002
310520	PI	403427	Gonabaru	Nigeria	Africa	1975-8-4	IND	0.0318	0.0020	0.9110	0.0033	0.0520
310521	PI	403471	HON CHIM	Hong Kong	China	1975-8-4	IND	0.0049	0.0007	0.8722	0.0047	0.1175
310522	PI	403483	Risotto	Hungary	Eastern_Europe	1975-8-4	TEJ	0.0169	0.9828	0.0001	0.0000	0.0002
310523	PI	403499	Hokjo 97	Korea_ South	North_Pacific	1975-8-4	TEJ	0.0143	0.9744	0.0001	0.0001	0.0111
310524	PI	403534	Zaneli	Nepal	Southern_Asia	1975-8-4	TRJ-TEJ	0.5181	0.4759	0.0049	0.0006	0.0005
310525	PI	403565	India Pa Lil 92	Sierra Leone	Africa	1975-8-4	IND	0.0013	0.0007	0.6781	0.3197	0.0003
310526	PI	403597	Jhona 5716	Pakistan	Southern_Asia	1975-8-4	IND	0.1518	0.0025	0.8448	0.0003	0.0006
310527	PI	403615	JST 58	Morocco	Mideast	1975-8-4	TEJ-AUS-IND	0.0899	0.4086	0.1917	0.3094	0.0004
310528	PI	403621	J 312	United States	North_America	1975-8-4	IND	0.0002	0.0003	0.9994	0.0001	0.0000
310529	PI	403635	Kan Tien Ju	China	China	1975-8-4	IND	0.0007	0.0008	0.9981	0.0003	0.0001
310530	PI	403641	KARATOLSZKIJ	Kazakhstan	Central_Asia	1975-8-4	AUS	0.0001	0.0002	0.0002	0.9994	0.0002
310531	PI	403644	Kaukau	Mali	Africa	1975-8-4	IND-AUS	0.0010	0.0021	0.5744	0.4223	0.0002
310532	PI	403675	Lang Shwei Keng	China	China	1975-8-4	IND	0.0002	0.0002	0.9993	0.0002	0.0001
310533	PI	403703	MAKALIOKA 752	Madagascar	Africa	1975-8-4	IND	0.0168	0.0322	0.6868	0.2641	0.0002
310534	PI	405078	HSIEN CHU 56	Taiwan	China	1975-10-27	TEJ	0.0005	0.9994	0.0001	0.0000	0.0000
310535	PI	406033	CA 435/B/5/1	Chad	Africa	1975-11-13	TRJ	0.9966	0.0031	0.0001	0.0001	0.0001
310536	PI	406034	CA 902/B/2/1	Chad	Africa	1975-11-13	AUS	0.0007	0.0004	0.0016	0.9970	0.0003
310537	PI	406061	Donduni Kunluz	Afghanistan	Southern_Asia	1975-11-13	ARO	0.0006	0.0003	0.0025	0.0007	0.9958
310538	PI	406079	PI 184675-4	Iran	Mideast	1975-11-13	ARO	0.0004	0.0006	0.0002	0.0002	0.9987
310539	PI	406575	Segadis	Mali	Africa	1976-1-6	IND	0.0003	0.0006	0.9983	0.0006	0.0001
310540	PI	406577	T442-57	Thailand	Southeast_Asia	1976-1-6	IND	0.0004	0.0003	0.9992	0.0001	0.0000

310541	PI	408369	BR51-243-1	Bangladesh	Southern_Asia	1975-12-1	IND	0.0008	0.0002	0.9973	0.0016	0.0001
310542	PI	408371	BR51-319-9	Bangladesh	Southern_Asia	1975-12-1	IND	0.0008	0.0003	0.9984	0.0004	0.0001
310543	PI	408378	CR 1113	Costa Rica	Central_America	1975-12-1	IND	0.0005	0.0006	0.9975	0.0004	0.0010
310544	PI	408385	B441B-24-4-5-1	Indonesia	South_Pacific	1975-12-1	IND	0.0076	0.0009	0.9842	0.0073	0.0000
310545	PI	408401	B462B-PN-31-2	Indonesia	South_Pacific	1975-12-1	IND	0.1100	0.0005	0.8890	0.0004	0.0001
310546	PI	408406	MAHSURI	Malaysia	South_Pacific	1975-3-1	IND	0.0014	0.0014	0.9967	0.0003	0.0002
310547	PI	408410	HUALLAGA	Peru	South_America	1975-12-1	IND	0.0004	0.0001	0.9992	0.0002	0.0000
310548	PI	408567	BKN 6820-6-3-2	Thailand	Southeast_Asia	1975-12-1	IND	0.1068	0.0005	0.8920	0.0006	0.0001
310549	PI	408608	BG 90-2	Sri Lanka	Southern_Asia	1975-12-1	IND	0.0001	0.0001	0.9996	0.0002	0.0000
310550	PI	412785	Daudzai	Pakistan	Southern_Asia	1976-6-30	ARO	0.0004	0.0002	0.0017	0.0635	0.9343
310551	PI	412913	Mit Da Rae	Korea_ South	North_Pacific	1976-7-20	IND	0.0137	0.0006	0.9839	0.0004	0.0015
310552	PI	413737	YR 73	Australia	Oceania	1976-7-19	TRJ	0.6518	0.3151	0.0271	0.0051	0.0009
310553	PI	414002	205	Iran	Mideast	1976-12-1	ARO	0.0005	0.0011	0.0002	0.0002	0.9980
310554	PI	414007	223	Iran	Mideast	1976-12-1	ARO	0.0005	0.0009	0.0001	0.0001	0.9982
310555	PI	414238	COLOMBIA 1	Colombia	South_America	1976-12-13	TRJ-IND-TEJ	0.5632	0.1931	0.2145	0.0002	0.0290
310556	PI	414545	Emanaye Carambak	Senegal	Africa	1975-10-17	TRJ	0.9983	0.0012	0.0003	0.0001	0.0001
310557	PI	414712	H 5	Sri Lanka	Southern_Asia	1977-2-15	IND	0.0003	0.0005	0.8706	0.1284	0.0002
310558	PI	415667	Amposta	Puerto Rico	Central_America	1977-4-21	TEJ	0.0007	0.9990	0.0003	0.0001	0.0000
310559	PI	418224	SUNBONNET	Swaziland	Africa	1977-6-20	TRJ	0.9973	0.0023	0.0001	0.0000	0.0002
310560	PI	419448	Thangone	Laos	Southeast_Asia	1977-8-7	IND	0.2542	0.0035	0.7264	0.0006	0.0154
310561	PI	420140	Azaurel	Venezuela	South_America	1977-10-18	IND	0.0003	0.0002	0.9992	0.0003	0.0001
310562	PI	420194	Higueyano	Dominican Republic	Central_America	1977-9-12	TRJ	0.9948	0.0046	0.0002	0.0003	0.0002
310563	PI	420241	JUMA 58	Dominican Republic	Central_America	1977-9-29	IND	0.0001	0.0002	0.9997	0.0001	0.0000
310564	PI	420800	KAOHSIUNG-SHEN 12	Taiwan	China	1977-12-30	IND	0.0007	0.0020	0.9942	0.0027	0.0003
310565	PI	420936	Sequial	Spain	Western_Europe	1977-12-1	TEJ	0.0544	0.9454	0.0001	0.0000	0.0001
310566	PI	420960	INIAP 7	Ecuador	South_America	1977-12-14	IND	0.0002	0.0001	0.9996	0.0001	0.0000
310567	PI	420965	TIKAL 2	Guatemala	Central_America	1977-12-14	IND	0.0002	0.0001	0.9996	0.0001	0.0000
310568	PI	422204	GPNO 26345	Morocco	Mideast	1977-11-21	TEJ	0.0013	0.9974	0.0007	0.0005	0.0001
310569	PI	422208	Patna	Morocco	Mideast	1977-11-21	TEJ	0.0973	0.9024	0.0001	0.0000	0.0001
310570	PI	422209	RAZZA 82	Italy	Western_Europe	1977-11-21	TEJ	0.0018	0.9980	0.0001	0.0001	0.0001
310571	PI	422211	Sesia	Portugal	Western_Europe	1977-11-21	TRJ-TEJ	0.4708	0.4210	0.1079	0.0002	0.0001
310572	PI	422213	Triomphe	Morocco	Mideast	1977-11-21	TEJ	0.0005	0.9993	0.0001	0.0001	0.0001
310573	PI	422214	Varyla	Madagascar	Africa	1977-11-21	TRJ	0.6615	0.3381	0.0002	0.0001	0.0001
310574	PI	422244	SM II	Malaysia	South_Pacific	1978-9-5	IND	0.0003	0.0004	0.9992	0.0001	0.0001
310575	PI	422518	Gros Riz	Haiti	Central_America	1978-9-5	IND	0.0048	0.0004	0.9904	0.0039	0.0004
310576	PI	429749	PUSA 33	India	Southern_Asia	1978-9-25	IND	0.0004	0.0013	0.9978	0.0002	0.0003
310577	PI	429862	GPNO 22232	Germany	Western_Europe	1978-9-28	IND	0.0001	0.0002	0.9996	0.0001	0.0000
310578	PI	430134	IRAT 10	Cote D'Ivoire	Africa	1978-10-10	TRJ	0.6307	0.3678	0.0002	0.0009	0.0004
310579	PI	430253	TONO BREA 408	Dominican Republic	Central_America	1978-11-15	IND	0.0001	0.0002	0.9995	0.0001	0.0001
310580	PI	430312	Pratao Precoce	Brazil	South_America	1978-11-30	TRJ	0.9991	0.0006	0.0001	0.0000	0.0001
310581	PI	430315	Precocinho	Brazil	South_America	1978-11-30	TRJ	0.9993	0.0006	0.0001	0.0000	0.0001
310582	PI	430330	Batatais	Brazil	South_America	1978-11-30	TRJ	0.9992	0.0007	0.0001	0.0000	0.0000
310583	PI	430331	17465-4	Fiji	Oceania	1978-11-30	IND	0.0002	0.0002	0.9992	0.0002	0.0001
310584	PI	430333	17752	Fiji	Oceania	1978-11-30	IND	0.0009	0.0010	0.9978	0.0002	0.0001
310585	PI	430340	Sautu	Fiji	Oceania	1978-11-30	IND	0.1048	0.0004	0.8926	0.0021	0.0002
310586	PI	430382	Baluola II	Zaire	Africa	1978-12-4	TRJ	0.9985	0.0009	0.0003	0.0001	0.0001
310587	PI	430390	Imbolo II	Zaire	Africa	1978-12-4	TRJ	0.9961	0.0014	0.0015	0.0005	0.0004
310588	PI	430397	Onu B	Zaire	Africa	1978-12-4	TRJ	0.9910	0.0049	0.0014	0.0003	0.0024
310589	PI	430400	OS 6/M	Zaire	Africa	1978-12-4	TRJ	0.6858	0.0007	0.1078	0.2056	0.0002
310590	PI	430404	R 29/1	Zaire	Africa	1978-12-4	TRJ	0.9979	0.0005	0.0005	0.0009	0.0002
310591	PI	430420	R 89	Zaire	Africa	1978-12-4	TRJ	0.9985	0.0011	0.0002	0.0001	0.0001
310592	PI	430424	R 92/1	Zaire	Africa	1978-12-4	IND	0.0001	0.0001	0.9996	0.0001	0.0000
310593	PI	430430	R 98	Zaire	Africa	1978-12-4	TRJ	0.9245	0.0740	0.0011	0.0002	0.0002
310594	PI	430431	R 98/1	Zaire	Africa	1978-12-4	TRJ	0.9758	0.0239	0.0002	0.0000	0.0001
310595	PI	430436	R 99/3	Zaire	Africa	1978-12-4	TRJ	0.9107	0.0886	0.0005	0.0001	0.0001

310596	PI	430439	R 100/2	Zaire	Africa	1978-12-4	TRJ	0.9989	0.0005	0.0004	0.0000	0.0001
310597	PI	430689	KAR 2	Korea_ South	North_Pacific	1978-12-28	TEJ	0.0008	0.9990	0.0000	0.0001	0.0000
310598	PI	430936	Red	Pakistan	Southern_Asia	1978-12-29	AUS-IND-TEJ	0.0007	0.1476	0.2928	0.4970	0.0618
310599	PI	430981	Nema	Iraq	Mideast	1978-12-29	ARO	0.0009	0.0012	0.0044	0.0005	0.9930
310600	PI	430982	Shima	Iraq	Mideast	1978-12-29	AUS	0.0005	0.0003	0.3752	0.6227	0.0013
310601	PI	431024	Cat 1747	Russian Federation	Eastern_Europe	1978-12-29	IND	0.0007	0.0004	0.9988	0.0001	0.0001
310602	PI	431031	P 817	Russian Federation	Eastern_Europe	1978-12-29	IND	0.0003	0.0030	0.8401	0.1565	0.0001
310603	PI	431034	P 820	Russian Federation	Eastern_Europe	1978-12-29	AUS	0.0003	0.0003	0.0002	0.9990	0.0001
310604	PI	431045	Mahiwan Karsh Mir	Pakistan	Southern_Asia	1978-12-29	AUS	0.0001	0.0001	0.0007	0.9990	0.0001
310605	PI	431084	Dsi Sel Dangar Shah	Myanmar	Southeast_Asia	1978-12-29	IND	0.0004	0.0018	0.8594	0.1383	0.0001
310606	PI	431085	UVS Sel Medgoscer	Switzerland	Western_Europe	1978-12-29	TRJ-IND	0.5502	0.0009	0.4485	0.0001	0.0003
310607	PI	431093	Yabani Pearl	Egypt	Mideast	1978-12-29	AUS-IND	0.0012	0.0006	0.3981	0.5986	0.0015
310608	PI	431107	VARY LAVA 16	Madagascar	Africa	1978-12-29	AUS	0.0008	0.0007	0.0010	0.9972	0.0004
310609	PI	431161	Egypt 4	Egypt	Mideast	1978-12-29	IND	0.0199	0.0012	0.9706	0.0009	0.0074
310610	PI	431162	Egypt 5	Egypt	Mideast	1978-12-29	IND	0.0195	0.0011	0.9666	0.0010	0.0118
310611	PI	431176	Dee Geo Gen	Taiwan	China	1978-12-29	AUS-IND	0.0025	0.0036	0.4738	0.5194	0.0007
310612	PI	431202	Uz Begohef 2	Uzbekistan	Central_Asia	1978-12-29	IND	0.0006	0.0015	0.9975	0.0004	0.0001
310613	PI	431203	Subdi Chroa Kora Muazah Tolinsty	Kazakhstan	Central_Asia	1978-12-29	TRJ	0.7043	0.2954	0.0001	0.0001	0.0001
310614	PI	431208	Ae Kylick	Azerbaijan	Central_Asia	1978-12-29	IND	0.0002	0.0005	0.9988	0.0002	0.0003
310615	PI	431210	Dichroa Alef Uslkij	Kazakhstan	Central_Asia	1978-12-29	IND	0.0002	0.0003	0.9984	0.0003	0.0008
310616	PI	431212	Zeraschcivica Sroches Krothearny Snij	Former Soviet Union	Eastern_Europe	1978-12-29	IND	0.0002	0.0001	0.9996	0.0001	0.0000
310617	PI	431213	Krosheaynit Zeravse Kamica Primen Skit 6	Russian Federation	Eastern_Europe	1978-12-29	AUS-IND-TRJ	0.1538	0.0036	0.3793	0.4609	0.0025
310618	PI	431218	Known Kros 358	Kazakhstan	Central_Asia	1978-12-29	IND	0.0027	0.0009	0.9962	0.0001	0.0001
310619	PI	431235	P 1041	Former Soviet Union	Eastern_Europe	1978-12-29	IND	0.0004	0.0008	0.9986	0.0002	0.0001
310620	PI	431242	P 1048	Former Soviet Union	Eastern_Europe	1978-12-29	ARO	0.0008	0.2428	0.0002	0.0001	0.7561
310621	PI	431243	P 1049	Former Soviet Union	Eastern_Europe	1978-12-29	ARO	0.0008	0.0005	0.1744	0.0006	0.8238
310622	PI	431287	Doom Zero	Iran	Mideast	1978-12-29	TEJ-IND	0.0254	0.5634	0.4109	0.0002	0.0001
310623	PI	431288	Muse Tu Rum	Iran	Mideast	1978-12-29	ARO	0.0003	0.0003	0.0001	0.0001	0.9991
310624	PI	431339	P 1289	Turkey	Mideast	1978-12-29	TEJ	0.0006	0.9991	0.0002	0.0001	0.0001
310625	PI	403224	DNJ 140	Bangladesh	Southern_Asia	1975-8-4	AUS	0.0002	0.0006	0.0004	0.9987	0.0001
310626	PI	431352	P 1302	Turkey	Mideast	1978-12-29	TEJ	0.0049	0.9948	0.0002	0.0001	0.0001
310627	PI	431362	P 1312	Turkey	Mideast	1978-12-29	TEJ	0.0191	0.9805	0.0002	0.0001	0.0001
310628	PI	431371	P 1321	Turkey	Mideast	1978-12-29	IND	0.0002	0.0001	0.9995	0.0002	0.0000
310629	PI	431410	P 1360	Turkey	Mideast	1978-12-29	TEJ	0.0052	0.9946	0.0001	0.0000	0.0000
310630	PI	431499	BKN 6987-68-14	Thailand	Southeast_Asia	1979-2-1	IND	0.0003	0.0010	0.9985	0.0001	0.0001
310632	PI	432578	IR 4482-5-3-9-5	Philippines	South_Pacific	1979-3-1	IND	0.0736	0.0019	0.8242	0.1001	0.0002
310633	PI	433493	ARGO 9	Italy	Western_Europe	1979-5-1	TEJ	0.2044	0.7953	0.0001	0.0000	0.0001
310634	PI	433508	RADON 2	Italy	Western_Europe	1979-5-1	TEJ	0.0614	0.9378	0.0002	0.0001	0.0005
310635	PI	433850	IM 16	Nigeria	Africa	1979-6-1	TRJ	0.9992	0.0004	0.0002	0.0001	0.0001
310636	PI	433852	IRAT 8	Cote D'Ivoire	Africa	1979-6-1	IND	0.0001	0.0001	0.9997	0.0001	0.0000
310637	PI	433855	M 4	Nigeria	Africa	1979-6-1	TRJ	0.9990	0.0007	0.0002	0.0000	0.0001
310638	PI	433900	IRAT 104	Cote D'Ivoire	Africa	1979-7-1	TRJ	0.9986	0.0010	0.0002	0.0001	0.0001
310639	PI	433901	IRAT 105	Cote D'Ivoire	Africa	1979-7-1	TEJ	0.3569	0.6403	0.0006	0.0005	0.0018
310640	PI	433907	IRAT 112	Cote D'Ivoire	Africa	1979-7-1	TRJ	0.9994	0.0004	0.0002	0.0001	0.0001
310641	PI	433908	IRAT 113	Cote D'Ivoire	Africa	1979-7-1	TRJ	0.9986	0.0012	0.0001	0.0001	0.0000
310642	PI	433913	IRAT 132	Cote D'Ivoire	Africa	1979-7-1	TRJ	0.9992	0.0005	0.0002	0.0000	0.0001
310643	PI	433915	IRAT 134	Cote D'Ivoire	Africa	1979-7-1	TRJ	0.8462	0.1531	0.0004	0.0001	0.0001
310644	PI	433919	IRAT 139	Cote D'Ivoire	Africa	1979-7-1	TRJ	0.9990	0.0007	0.0001	0.0000	0.0001
310645	PI	434632	*MOROBEREKAN	Guinea	Africa	1979-7-1	TRJ	0.9970	0.0006	0.0022	0.0001	0.0001
310646	PI	435977	Nucleoryza	Austria	Western_Europe	1979-7-1	TEJ	0.0005	0.9993	0.0001	0.0000	0.0000
310647	PI	436587	Yu Hua Tsan	China	China	1979-7-1	IND	0.0003	0.0001	0.9993	0.0003	0.0001
310648	PI	439026	IR 400	Zimbabwe	Africa	1979-10-1	IND	0.0003	0.0008	0.9985	0.0004	0.0001

310649	PI	439046	BALA	India	Southern_Asia	1980-1-1	IND	0.0010	0.0007	0.9017	0.0964	0.0002
310650	PI	439085	PR 106	India	Southern_Asia	1980-1-1	IND	0.0641	0.0013	0.9343	0.0001	0.0002
310651	PI	439106	CH 126-129	Chile	South_America	1980-1-1	TEJ	0.0005	0.9993	0.0001	0.0000	0.0001
310652	PI	439107	CH 153-138	Chile	South_America	1980-1-1	TEJ	0.0166	0.9832	0.0001	0.0000	0.0000
310653	PI	439109	CH 242-32	Chile	South_America	1980-1-1	IND	0.0002	0.0002	0.9989	0.0005	0.0002
310654	PI	439110	CH 271-131	Chile	South_America	1980-1-1	TEJ	0.0658	0.9340	0.0000	0.0000	0.0000
310655	PI	439111	CH 272-132	Chile	South_America	1980-1-1	IND	0.0040	0.0035	0.9901	0.0004	0.0020
310656	PI	439123	CR 373-2-1-1	Egypt	Mideast	1979-8-1	TEJ	0.0003	0.9995	0.0001	0.0000	0.0001
310657	PI	439125	CR 418-3-12	Egypt	Mideast	1979-8-1	IND	0.1357	0.0041	0.8595	0.0001	0.0006
310658	PI	439127	CR 561-4-2-1	Egypt	Mideast	1979-8-1	IND	0.0015	0.0249	0.9723	0.0010	0.0002
310659	PI	439146	YNA 223	Egypt	Mideast	1979-8-1	TEJ	0.0003	0.9910	0.0071	0.0015	0.0001
310660	PI	439616	Nigro Apiculata	Sweden	Western_Europe	1980-2-1	TEJ	0.0046	0.9936	0.0002	0.0001	0.0015
310661	PI	439621	Azerbaidjanica	Azerbaijan	Central_Asia	1980-2-1	TEJ	0.0016	0.9972	0.0001	0.0001	0.0010
310662	PI	439623	Affinis	Kazakhstan	Central_Asia	1980-2-1	TEJ	0.2957	0.7035	0.0003	0.0003	0.0003
310663	PI	439624	Kasakstanica	Kazakhstan	Central_Asia	1980-2-1	IND	0.0036	0.0076	0.9880	0.0006	0.0001
310664	PI	439628	Parnelli	Korea_ North	North_Pacific	1980-2-1	TEJ	0.3383	0.6596	0.0008	0.0005	0.0008
310665	PI	439630	Melanotrix	Tajikistan	Central_Asia	1980-2-1	TEJ	0.0640	0.6672	0.0002	0.0003	0.2684
310666	PI	439635	Astarinica	Azerbaijan	Central_Asia	1980-2-1	ARO	0.0028	0.0202	0.0947	0.0019	0.8804
310667	PI	439646	Arpa Shaly Mestnyj	Uzbekistan	Central_Asia	1980-2-1	TEJ	0.0011	0.9981	0.0001	0.0004	0.0003
310668	PI	439650	Bak Saly Mestnyj	Azerbaijan	Central_Asia	1980-2-1	ARO-TEJ	0.0013	0.4541	0.0001	0.0002	0.5443
310669	PI	439662	DUBOVSKIJ 129	Russian Federation	Eastern_Europe	1980-2-1	TEJ	0.1602	0.6908	0.0001	0.0003	0.1486
310670	PI	439683	KUBANETS 508	Russian Federation	Eastern_Europe	1980-2-1	TEJ	0.0121	0.8788	0.0002	0.0005	0.1085
310671	PI	439687	Linia 84 Icar	Romania	Eastern_Europe	1980-2-1	TEJ	0.0020	0.9975	0.0001	0.0001	0.0004
310672	PI	439708	Naruha	Japan	North_Pacific	1980-2-1	AUS	0.0002	0.0002	0.0005	0.9989	0.0002
310673	PI	439711	Pirinae 69	Former Yugoslavia	Eastern_Europe	1980-2-1	IND-TEJ	0.0021	0.4385	0.5589	0.0004	0.0001
310674	PI	439725	Slavianskij	Bulgaria	Eastern_Europe	1980-2-1	TEJ	0.1344	0.8653	0.0003	0.0000	0.0000
310675	PI	442135	GIZA 172	Egypt	Mideast	1980-4-1	TEJ	0.0003	0.9996	0.0000	0.0000	0.0001
310676	PI	442970	IR 34	Philippines	South_Pacific	1980-5-1	IND	0.0003	0.0005	0.9985	0.0004	0.0003
310677	PI	446914	STEGARU 65	Romania	Eastern_Europe	1980-8-1	TEJ	0.0009	0.9985	0.0001	0.0001	0.0003
310680	PI	430977	Halwa Gose Red	Iraq	Mideast	1978-12-29	AUS	0.0014	0.0013	0.0030	0.9938	0.0004
310681	PI	389101	Shuan Leu Shan Goo	Taiwan	China	1974-9-1	ARO-TEJ	0.0750	0.3521	0.0055	0.0027	0.5646
310682	PI	458435	Bersani	Turkey	Mideast	1981-3-1	TEJ	0.0073	0.9924	0.0002	0.0001	0.0001
310683	PI	458468	IITA 130	Nigeria	Africa	1981-3-1	TRJ	0.9986	0.0009	0.0003	0.0001	0.0001
310684	PI	458472	IITA 164	Nigeria	Africa	1981-3-1	TRJ	0.8035	0.0016	0.0010	0.0904	0.1035
310685	PI	458823	BR-IRGA-410	Brazil	South_America	1981-4-1	IND	0.0045	0.0054	0.9895	0.0002	0.0004
310686	PI	460635	Pratao	Brazil	South_America	1981-6-1	TRJ	0.9980	0.0015	0.0003	0.0000	0.0001
310687	PI	464597	IR 9660-48-1-1-2	Philippines	South_Pacific	1981-11-1	IND	0.0000	0.0001	0.9998	0.0001	0.0000
310688	PI	464616	MILYANG 56	Korea_ South	North_Pacific	1981-11-1	IND	0.0025	0.0672	0.9296	0.0003	0.0004
310689	PI	464621	RAEGYEONG	Korea_ South	North_Pacific	1981-11-1	IND	0.0003	0.1169	0.8826	0.0001	0.0001
310690	PI	464636	PI464636	Korea_ South	North_Pacific	1981-11-1	IND	0.0074	0.0167	0.9749	0.0003	0.0006
310691	PI	490789	UA 1038	Nigeria	Africa	1984-8-1	TRJ	0.9986	0.0010	0.0002	0.0001	0.0001
310692	PI	490792	Tox 177-1-2-B	Nigeria	Africa	1984-8-1	TRJ	0.9555	0.0006	0.0435	0.0003	0.0001
310693	PI	493131	Bakiella 1	Sri Lanka	Southern_Asia	1984-12-1	IND	0.0005	0.0006	0.9959	0.0028	0.0002
310694	PI	493132	Balislus	Senegal	Africa	1984-12-1	IND	0.0008	0.0006	0.9984	0.0001	0.0001
310695	PI	503060	15906	Colombia	South_America	1986-2-1	IND	0.0326	0.0872	0.8795	0.0003	0.0004
310696	PI	503073	16776	Colombia	South_America	1986-2-1	IND	0.0395	0.1128	0.8464	0.0007	0.0006
310697	PI	503090	17335	Colombia	South_America	1986-2-1	IND	0.0369	0.0030	0.9599	0.0002	0.0001
310698	PI	503133	19954	Colombia	South_America	1986-2-1	IND	0.0003	0.0032	0.9960	0.0003	0.0002
310699	PI	504478	TATSUMIMOCHI	Japan	North_Pacific	1986-8-1	TEJ	0.0012	0.9898	0.0076	0.0012	0.0001
310700	PI	505386	IR 31779-112-1-2-2-3	Philippines	South_Pacific	1986-11-18	IND	0.0042	0.0012	0.9932	0.0013	0.0001
310701	PI	505387	IR 31802-48-2-2	Philippines	South_Pacific	1986-11-18	IND	0.0001	0.0001	0.9992	0.0003	0.0002
310702	PI	549224	Jumli dhan	Nepal	Southern_Asia	1984-12-13	TEJ-TRJ-ARO	0.3166	0.4287	0.0154	0.0532	0.1861
310703	PI	549253	N-2703	Nepal	Southern_Asia	1984-12-13	AUS	0.0013	0.0415	0.1413	0.8148	0.0011
310704	PI	560273	CT7378-2-1-3-1-4-M	Colombia	South_America	1990-1-24	TRJ	0.8938	0.0237	0.0823	0.0001	0.0001
310705	PI	564577	Zira	Kenya	Africa	1992-12-17	TRJ	0.9978	0.0012	0.0004	0.0005	0.0001

310706	PI	564581	Pulut Manjetti	Indonesia	Oceania	1992-12-17	TRJ	0.9989	0.0006	0.0002	0.0002	0.0001
310707	PI	574428	MEDUSA	Italy	Western_Europe	1992-7-29	TEJ	0.1471	0.8527	0.0001	0.0000	0.0001
310708	PI	574441	SILLA	Italy	Western_Europe	1992-7-29	TEJ	0.1839	0.8158	0.0001	0.0000	0.0001
310709	PI	574675	BR19	Bangladesh	Southern_Asia	1993-7-28	IND	0.0001	0.0001	0.9990	0.0009	0.0000
310710	PI	583842	OSOGOVKA	Macedonia	Eastern_Europe	1991-10-31	TEJ	0.0107	0.9890	0.0001	0.0000	0.0001
310711	PI	583845	MAKEDONIJA	Macedonia	Eastern_Europe	1993-11-3	TEJ	0.0454	0.9531	0.0013	0.0002	0.0001
310712	PI	584559	IRAT 13	Cote D'Ivoire	Africa	1991-7-5	TRJ	0.9992	0.0004	0.0002	0.0000	0.0001
310713	PI	584562	GHARIB	Iran	Mideast	1991-7-5	ARO-TEJ	0.0356	0.3990	0.0004	0.0003	0.5646
310714	PI	584564	TCHAMPA	Iran	Mideast	1991-7-5	AUS	0.0002	0.0053	0.0026	0.9916	0.0002
310715	PI	584566	PHUDUGEY	Bhutan	Southern_Asia	1991-7-5	AUS	0.0006	0.0001	0.0004	0.9988	0.0001
310716	PI	584583	GHATI KAMMA NANGARHAR	Afghanistan	Southern_Asia	1991-7-5	AUS	0.0001	0.0004	0.0006	0.9987	0.0002
310717	PI	584584	LUK TAKHAR	Afghanistan	Southern_Asia	1991-7-5	TEJ	0.0003	0.9704	0.0243	0.0045	0.0005
310718	PI	584588	M. BLATEC	Macedonia	Eastern_Europe	1991-10-31	TEJ	0.0090	0.9907	0.0001	0.0000	0.0002
310719	PI	584610	Fossa Av	Burkina Faso	Africa	1991-7-5	TRJ	0.9969	0.0027	0.0002	0.0001	0.0001
310720	PI	584612	PATE BLANC MN 1	Cote D'Ivoire	Africa	1991-7-5	TRJ	0.9988	0.0009	0.0002	0.0001	0.0001
310721	PI	584615	WIR 623	Uzbekistan	Central_Asia	1992-6-2	TEJ	0.0236	0.8598	0.0001	0.0001	0.1164
310722	PI	584619	WIR 1889	Kazakhstan	Central_Asia	1992-6-2	TEJ	0.0119	0.9293	0.0051	0.0450	0.0087
310723	PI	584624	WIR 3039	Tajikistan	Central_Asia	1992-6-2	TEJ	0.0031	0.7632	0.0001	0.0001	0.2336
310724	PI	584625	Ak Tokhum	Azerbaijan	Central_Asia	1992-6-2	ARO	0.0029	0.2764	0.0004	0.0005	0.7198
310725	PI	584626	Shato Lua	Azerbaijan	Central_Asia	1992-6-2	ARO	0.0011	0.1026	0.0002	0.0001	0.8959
310726	PI	584633	UZ ROS 2759	Uzbekistan	Central_Asia	1992-6-2	TEJ	0.0012	0.9986	0.0001	0.0000	0.0001
310727	PI	584634	WIR 3764	Uzbekistan	Central_Asia	1992-6-2	TEJ	0.0033	0.9961	0.0001	0.0002	0.0002
310728	PI	584639	Sirkat	Afghanistan	Southern_Asia	1992-6-2	AUS-ARO	0.0012	0.0004	0.0005	0.5753	0.4227
310729	PI	584652	ZEMCYZNYJ	Russian Federation	Eastern_Europe	1992-6-2	TEJ	0.0006	0.9993	0.0001	0.0000	0.0001
310730	PI	584667	JUMA 61	Dominican Republic	Central_America	1993-3-23	IND	0.0001	0.0002	0.9996	0.0001	0.0000
310731	PI	584668	ORYZICA LLANOS 5	Colombia	South_America	1993-3-23	IND	0.0057	0.0723	0.9215	0.0001	0.0004
310732	PI	584683	C 3CU77-1CU-2CU-2C U-2CU-SMCU2	Colombia	South_America	1993-3-23	IND	0.0024	0.0007	0.9958	0.0003	0.0008
310733	PI	584722	CT10323-21-6-M	Colombia	South_America	1993-3-23	IND	0.1008	0.1095	0.7885	0.0005	0.0007
310734	PI	584731	CNAX 5072-2-1-2B	Colombia	South_America	1993-3-23	IND	0.0814	0.0667	0.8514	0.0003	0.0002
310735	PI	584740	ANAYANSI	Panama	Central_America	1991-4-23	IND	0.0001	0.0001	0.9996	0.0001	0.0000
310736	PI	584741	ARAURE 1	Venezuela	South_America	1991-4-23	IND	0.0003	0.0002	0.9993	0.0002	0.0000
310737	PI	584744	CEA 2	Paraguay	South_America	1991-4-23	IND	0.0005	0.0601	0.9392	0.0001	0.0000
310738	PI	584746	CEA 3	Paraguay	South_America	1991-4-23	IND	0.0005	0.0005	0.9989	0.0001	0.0000
310739	PI	584750	EMPASC 103	Brazil	South_America	1991-4-23	IND	0.0003	0.0001	0.9995	0.0001	0.0000
310740	PI	584753	ORYZICA LLANOS 4	Colombia	South_America	1991-4-23	IND	0.1374	0.1234	0.7377	0.0003	0.0012
310741	PI	584755	PERLA	Cuba	Central_America	1991-4-23	IND	0.0008	0.0007	0.9983	0.0001	0.0001
310743	PI	596806	DIAMANTE	Chile	South_America	1990-1-24	TRJ-TEJ	0.5563	0.3662	0.0002	0.0769	0.0005
310744	PI	596808	Tropical Rice	Ecuador	South_America	1991-5-8	TEJ	0.0010	0.9984	0.0002	0.0003	0.0001
310745	PI	596813	WIR 3419	Azerbaijan	Central_Asia	1992-6-2	ARO	0.0011	0.0081	0.0002	0.0017	0.9890
310746	PI	596815	376	Cambodia	Southeast_Asia	1992-6-5	IND	0.0001	0.0002	0.9948	0.0049	0.0001
310747	PI	596818	BHIM DHAN	Nepal	Southern_Asia	1992-7-20	TEJ-TRJ-ARO	0.3775	0.4679	0.0325	0.0144	0.1078
310748	PI	596827	IR-44595	Nepal	Southern_Asia	1992-7-20	IND	0.0005	0.0002	0.9992	0.0001	0.0000
310749	PI	596846	IDIAP-863	Panama	Central_America	1993-4-14	IND	0.0038	0.0725	0.9235	0.0002	0.0001
310750	PI	596873	FARO 37	Nigeria	Africa	1993-8-23	IND	0.0002	0.0003	0.9993	0.0002	0.0001
310751	PI	596885	RP1821-5-17-2	India	Southern_Asia	1993-8-23	IND	0.0005	0.0001	0.9989	0.0001	0.0003
310752	PI	596908	ECIA 128	Cuba	Central_America	1993-8-23	IND	0.0015	0.0002	0.9978	0.0003	0.0003
310753	PI	596909	GZ1368-5-4	Egypt	Mideast	1993-8-23	IND	0.0005	0.0006	0.9988	0.0001	0.0001
310754	PI	596911	H232-44-1-1	Argentina	South_America	1993-8-23	TRJ	0.7860	0.0921	0.1216	0.0001	0.0002
310755	PI	596924	IR 53901-64-3-2-1	Philippines	South_Pacific	1993-8-23	IND	0.0001	0.0001	0.9997	0.0001	0.0000
310756	PI	596935	J355-6-2-1-1	Dominican Republic	Central_America	1993-8-23	IND	0.0014	0.0009	0.9947	0.0024	0.0006
310757	PI	596941	RP2151-173-1-8	India	Southern_Asia	1993-8-23	IND	0.0001	0.0001	0.9501	0.0492	0.0004
310758	PI	596946	TOPLOEA 58/76	Romania	Eastern_Europe	1993-8-23	TEJ	0.0010	0.9987	0.0001	0.0002	0.0001
310759	PI	596947	TOPLOEA 70/76	Romania	Eastern_Europe	1993-8-23	TEJ	0.0009	0.9989	0.0001	0.0001	0.0001

310760	PI	596977	CT6744-2-11-1-M-M	Chile	South_America	1993-8-23	TEJ	0.0325	0.8973	0.0697	0.0003	0.0002
310761	PI	597003	H239-103-1	Argentina	South_America	1993-8-23	TRJ	0.7633	0.1310	0.1048	0.0002	0.0007
310762	PI	597004	IRAT 44	Burkina Faso	Africa	1993-8-23	TRJ	0.9122	0.0796	0.0041	0.0029	0.0013
310763	PI	597024	79004-TR4-4-2-1-1	Turkey	Mideast	1993-8-23	TEJ	0.0125	0.9873	0.0001	0.0000	0.0001
310764	PI	597027	7913-TR34-1-1	Turkey	Mideast	1993-8-23	TEJ	0.0954	0.9042	0.0002	0.0001	0.0001
310765	PI	597029	80110-TR4-1-1	Turkey	Mideast	1993-8-23	TEJ	0.0958	0.9039	0.0001	0.0000	0.0001
310766	PI	597045	HD14	Australia	Oceania	1994-6-29	IND	0.0790	0.0009	0.9195	0.0005	0.0001
310767	PI	602606	HB-6-2	Hungary	Eastern_Europe	1994-8-7	TEJ	0.0009	0.9979	0.0001	0.0009	0.0002
310768	PI	602612	RINGOLA	Hungary	Eastern_Europe	1994-8-7	TEJ	0.0007	0.9991	0.0001	0.0001	0.0000
310769	PI	602622	SZ-958	Hungary	Eastern_Europe	1994-8-7	TEJ	0.0024	0.9971	0.0002	0.0002	0.0002
310770	PI	602625	MIYANG	China	China	1994-8-7	IND	0.0042	0.0071	0.9881	0.0005	0.0001
310771	PI	602635	WAB56-104	Cote D'Ivoire	Africa	1996-5-14	TRJ	0.9967	0.0015	0.0014	0.0002	0.0001
310772	PI	602651	CL SELECCION 56	Brazil	South_America	1996-5-14	IND	0.0046	0.0028	0.9916	0.0005	0.0005
310773	PI	602654	ECIA76-S89-1	Cuba	Central_America	1996-5-14	IND	0.0009	0.0002	0.9973	0.0011	0.0005
310774	PI	602661	WAB 502-13-4-1	Cote D'Ivoire	Africa	1996-5-14	TRJ	0.9599	0.0063	0.0041	0.0276	0.0021
310775	PI	602662	WAB 501-11-5-1	Cote D'Ivoire	Africa	1996-5-14	TRJ	0.9881	0.0068	0.0010	0.0031	0.0010
310776	PI	18920	Sultani	Egypt	Mideast	1906-7-5	TRJ	0.8507	0.1490	0.0002	0.0001	0.0001
310777	PI	37215	WC 3532	Peru	South_America	1914-2-17	TRJ	0.9994	0.0003	0.0002	0.0000	0.0001
310778	PI	37859	114b	Brazil	South_America	1914-4-13	TRJ	0.9992	0.0003	0.0003	0.0001	0.0001
310779	CIor	2169	GPNO 1106	Guatemala	Central_America	1915-6-1	TRJ	0.9994	0.0003	0.0002	0.0000	0.0001
310780	PI	596836	DARIJ 8	Russian Federation	Eastern_Europe	1992-9-25	TEJ	0.0009	0.9973	0.0001	0.0005	0.0012
310781	PI	51520	M'Bale	Kenya	Africa	1920-10-1	TRJ	0.9863	0.0132	0.0001	0.0001	0.0002
310782	CIor	5451	LADY WRIGHT	United States	North_America	1922-6-1	TRJ	0.7764	0.2234	0.0001	0.0000	0.0001
310783	CIor	5793	BLUE ROSE SU-PREME	United States	North_America	1925-6-1	TRJ-TEJ	0.5187	0.4811	0.0001	0.0001	0.0001
310784	PI	65884	Styk	Azerbaijan	Central_Asia	1926-1-1	ARO	0.0007	0.0041	0.0001	0.0001	0.9949
310785	PI	65894	Gidej	Azerbaijan	Central_Asia	1926-1-1	ARO	0.0050	0.0131	0.0396	0.0002	0.9421
310786	CIor	5883	EARLY PROLIFIC	United States	North_America	1926-6-1	TEJ-TRJ	0.4763	0.5234	0.0001	0.0000	0.0001
310787	PI	67148	Ziri	India	Southern_Asia	1926-5-1	AUS	0.0014	0.0009	0.0006	0.9970	0.0001
310788	PI	67153	Toga	India	Southern_Asia	1926-5-1	IND	0.0094	0.0004	0.9840	0.0042	0.0021
310789	CIor	7337	Pulutan	Philippines	South_Pacific	1928-6-1	TRJ	0.9157	0.0155	0.0022	0.0020	0.0646
310790	CIor	7375	Sze Guen Zim	China	China	1928-6-1	IND	0.0007	0.0009	0.9980	0.0003	0.0001
310791	CIor	7404	Kin Shan Zim	China	China	1928-6-1	IND	0.0023	0.0009	0.9958	0.0001	0.0009
310792	PI	100924	2476	China	China	1932-8-1	TEJ-TRJ	0.4090	0.5906	0.0002	0.0000	0.0001
310793	PI	130650	Amber	Australia	Oceania	1938-10-12	ARO	0.0011	0.0054	0.0002	0.0004	0.9928
310794	PI	130960	Benllok	Peru	South_America	1938-11-1	TEJ	0.0003	0.9996	0.0000	0.0000	0.0000
310795	PI	130961	EAS 3	Peru	South_America	1938-11-1	TRJ	0.9403	0.0593	0.0002	0.0001	0.0001
310796	PI	134053	Hiderisirazu	Japan	North_Pacific	1939-9-18	TEJ	0.2790	0.7181	0.0010	0.0005	0.0015
310797	PI	141754	Java Barba Azul	Peru	South_America	1941-5-9	TRJ	0.6393	0.2254	0.1127	0.0041	0.0185
310798	PI	154434	Mairaromu	Taiwan	China	1946-5-10	TEJ-TRJ	0.4147	0.5783	0.0014	0.0002	0.0054
310799	PI	154435	Ragasu	Taiwan	China	1946-5-10	TRJ-TEJ	0.5379	0.4009	0.0600	0.0003	0.0009
310800	PI	154441	Natara	Taiwan	China	1946-5-10	TEJ	0.0233	0.9071	0.0685	0.0003	0.0008
310801	PI	154481	Tobura	Taiwan	China	1946-5-10	TEJ-TRJ	0.4419	0.5552	0.0010	0.0004	0.0015
310802	PI	154531	Tamanishiki	Japan	North_Pacific	1946-5-10	TEJ	0.0006	0.9983	0.0001	0.0006	0.0004
310803	PI	154707	TAKAO 11	Taiwan	China	1946-5-10	IND	0.0313	0.0002	0.9682	0.0002	0.0001
310804	PI	155420	Chirgua 1	Venezuela	South_America	1946-7-29	TRJ	0.9983	0.0012	0.0003	0.0000	0.0001
310805	PI	155421	Chivacia 1	Venezuela	South_America	1946-7-29	TRJ	0.9991	0.0005	0.0001	0.0000	0.0002
310806	PI	155422	Delta Amacuro	Venezuela	South_America	1946-7-29	TRJ	0.9981	0.0003	0.0015	0.0001	0.0001
310807	PI	157292	Kokuta	Korea_ South	North_Pacific	1947-2-18	TEJ	0.3984	0.6011	0.0003	0.0001	0.0002
310808	PI	157380	Wase Shinshu	Japan	North_Pacific	1947-2-18	TRJ-TEJ	0.5811	0.4129	0.0022	0.0017	0.0021
310809	PI	157385	Yong Chal Byo	Korea_ South	North_Pacific	1947-2-18	TEJ	0.3293	0.6600	0.0084	0.0006	0.0018
310810	PI	157388	Ike Zawa	Korea_ South	North_Pacific	1947-2-18	TEJ-TRJ	0.4543	0.5337	0.0109	0.0005	0.0007
310811	PI	157390	Zui Ho	Japan	North_Pacific	1947-2-18	IND	0.0017	0.0011	0.9970	0.0002	0.0001
310812	CIor	2962	GPNO 1257	Philippines	South_Pacific	1916-6-1	TRJ	0.9988	0.0005	0.0003	0.0000	0.0004
310813	PI	157528	Pico Negro	El Salvador	Central_America	1947-2-24	TRJ	0.9980	0.0015	0.0002	0.0000	0.0002
310814	CIor	8913	Grassy	Haiti	Central_America	1947-6-1	TRJ	0.9988	0.0008	0.0002	0.0000	0.0001
310815	CIor	9041	PR 147	Puerto Rico	Central_America	1954-3-10	TRJ	0.9986	0.0006	0.0003	0.0001	0.0004

310816	CIor	9046	PR 403	Puerto Rico	Central_America	1954-3-10	TRJ	0.9983	0.0009	0.0003	0.0001	0.0004
310817	CIor	9107	S4511A2-49B-4-1	United States	North_America	1954-3-1	TRJ	0.9987	0.0008	0.0001	0.0001	0.0002
310818	CIor	9166	REXORO ROGUE	United States	North_America	1954-3-1	TRJ	0.9584	0.0413	0.0001	0.0000	0.0002
310819	CIor	9198	ARKROSE SELEC-TION	United States	North_America	1954-3-1	TRJ-TEJ	0.5469	0.4529	0.0001	0.0000	0.0001
310820	CIor	9226	B459A1-49-1-2-1	United States	North_America	1955-3-1	TRJ	0.9991	0.0007	0.0001	0.0000	0.0001
310821	CIor	9275	B4524A1-13	United States	North_America	1955-3-1	TRJ	0.9991	0.0005	0.0002	0.0001	0.0001
310822	CIor	9280	Short Century	United States	North_America	1955-3-1	TRJ	0.9504	0.0492	0.0001	0.0000	0.0003
310823	CIor	9287	WC 1006	Iraq	Mideast	1950-6-1	AUS	0.0002	0.0006	0.0005	0.9986	0.0003
310824	CIor	9402	B502A2-113-B3	United States	North_America	1957-6-1	TRJ	0.9991	0.0006	0.0001	0.0000	0.0002
310825	CIor	9425	C57-5043	United States	North_America	1958-6-1	TRJ	0.8581	0.1417	0.0001	0.0001	0.0001
310826	CIor	9436	Stg 563808	United States	North_America	1959-6-1	TRJ	0.9923	0.0074	0.0002	0.0000	0.0001
310827	CIor	9438	58C5091	United States	North_America	1959-6-1	TRJ	0.9904	0.0093	0.0002	0.0000	0.0001
310828	CIor	9538	B574A1-1-4	United States	North_America	1962-1-1	TRJ	0.9993	0.0005	0.0001	0.0000	0.0001
310829	CIor	9646	Stg 64M3390	United States	North_America	1967-6-1	TRJ	0.9690	0.0308	0.0001	0.0000	0.0002
310830	CIor	9650	Stg 63D1636	United States	North_America	1967-1-1	TRJ	0.9833	0.0165	0.0001	0.0000	0.0001
310831	CIor	9736	Zenith	Puerto Rico	Central_America	1969-6-1	TRJ	0.8195	0.1803	0.0001	0.0001	0.0000
310832	CIor	9812	Stg 664652	United States	North_America	1970-6-1	TRJ	0.9846	0.0135	0.0014	0.0002	0.0003
310833	CIor	9896	71Cr-308	United States	North_America	1972-6-1	TRJ	0.7580	0.2417	0.0002	0.0000	0.0001
310834	CIor	9949	Stg 70M6961	United States	North_America	1973-3-9	TRJ	0.7236	0.2761	0.0001	0.0001	0.0001
310835	CIor	9953	Stg 704905	United States	North_America	1973-3-9	TRJ	0.9980	0.0017	0.0001	0.0001	0.0002
310836	CIor	11030	GPNO 5055	United States	North_America	1977-6-1	TRJ	0.6461	0.1930	0.1608	0.0001	0.0001
310837	CIor	12030	Honduras	Honduras	Central_America	1908-6-1	TRJ	0.9994	0.0004	0.0001	0.0000	0.0001
310838	CIor	12052	Molok	Indonesia	South_Pacific	1914-6-1	TRJ-TEJ	0.5938	0.3466	0.0583	0.0004	0.0008
310839	CIor	12211	Arroz Creollo	Mexico	North_America	1926-6-1	TRJ	0.7575	0.0003	0.0002	0.2418	0.0002
310840	CIor	12234	Long Gnar Jim	United States	Oceania	1928-6-1	TRJ	0.9475	0.0517	0.0002	0.0001	0.0005
310841	CIor	12248	Byakkoku	Australia	Oceania	1938-6-1	IND	0.0005	0.0003	0.9987	0.0004	0.0001
310842	CIor	12250	Tile	Australia	Oceania	1938-6-1	TRJ	0.9311	0.0683	0.0002	0.0001	0.0003
310843	CIor	12277	Kerang Serang	Indonesia	South_Pacific	1946-6-1	TRJ	0.9288	0.0010	0.0698	0.0003	0.0001
310844	PI	157527	Criollo	El Salvador	Central_America	1947-2-24	TRJ	0.9905	0.0019	0.0019	0.0003	0.0054
310845	CIor	12342	CI 9489-3	United States	North_America	1961-12-1	TRJ	0.7456	0.2539	0.0003	0.0000	0.0002
310846	CIor	12492	Kao Chio Lin Chou	Taiwan	China	1962-6-1	IND	0.0024	0.0007	0.9943	0.0005	0.0021
310847	CIor	12532	PR 428	Puerto Rico	Central_America	1954-12-1	TEJ-IND-TRJ	0.1994	0.5697	0.2306	0.0002	0.0001
310848	PI	160410	Ho Yi Tiao	China	China	1947-11-25	IND	0.0030	0.0012	0.9954	0.0002	0.0001
310849	PI	160530	Pan Ju	China	China	1947-11-25	IND	0.0002	0.0001	0.9994	0.0002	0.0001
310850	PI	160650	Chiu Tien	China	China	1947-11-25	TEJ	0.0010	0.9987	0.0002	0.0000	0.0001
310851	PI	160737	Ai Chih Hsu	China	China	1947-11-25	TEJ	0.0009	0.9990	0.0001	0.0000	0.0000
310852	PI	160792	Hsin Shan Tien Swei 1 Hao	China	China	1947-11-25	TEJ	0.0003	0.9996	0.0001	0.0000	0.0001
310853	PI	160821	Ming Cheng 164	China	China	1947-11-25	TEJ	0.0007	0.8729	0.1261	0.0002	0.0001
310854	PI	160832	Chung Hsuan	China	China	1947-11-25	TRJ	0.8891	0.1105	0.0003	0.0000	0.0001
310855	PI	389922	See Mew	Hong Kong	China	1974-9-1	IND	0.0124	0.0025	0.9841	0.0003	0.0007
310856	PI	160871	WC 521	China	China	1947-11-25	TRJ	0.6653	0.2816	0.0524	0.0004	0.0004
310857	PI	160962	Ai Yeh Lu	China	China	1947-11-25	IND-TEJ-TRJ	0.2490	0.3272	0.4227	0.0001	0.0009
310858	PI	161566	Criollo Chirgua 3	Venezuela	South_America	1947-12-26	TRJ	0.9987	0.0003	0.0009	0.0000	0.0001
310859	PI	161568	Criollo La Fria	Venezuela	South_America	1947-12-26	IND	0.0005	0.0007	0.9980	0.0002	0.0006
310860	PI	161570	Morotuto	Venezuela	South_America	1947-12-26	TRJ	0.9995	0.0003	0.0001	0.0000	0.0001
310861	PI	162113	Niwahutaw Mochi	Japan	North_Pacific	1948-2-1	TEJ	0.0007	0.9992	0.0001	0.0000	0.0001
310862	PI	162144	SUITO NORIN 20	Japan	North_Pacific	1948-2-1	TEJ	0.0009	0.9988	0.0002	0.0000	0.0000
310863	PI	162177	Bul Zo	Korea_ South	North_Pacific	1948-2-1	TEJ	0.0017	0.9981	0.0002	0.0000	0.0000
310864	PI	162196	Du Jung Zyong	Korea_ South	North_Pacific	1948-2-1	IND	0.0003	0.0003	0.9992	0.0001	0.0001
310865	PI	162261	Mu Zo	Korea_ South	North_Pacific	1948-2-1	TEJ	0.0036	0.9962	0.0001	0.0001	0.0001
310866	PI	162311	Su Won 55	Korea_ South	North_Pacific	1948-2-1	TEJ	0.0061	0.9934	0.0002	0.0001	0.0002
310867	PI	162317	Su Won 72	Korea_ South	North_Pacific	1948-2-1	TRJ-TEJ	0.4998	0.4992	0.0002	0.0006	0.0002
310868	PI	162387	Zyouk Sin Ryouk	Korea_ South	North_Pacific	1948-2-1	TEJ	0.0005	0.9993	0.0001	0.0000	0.0001
310869	PI	164910	CUME MAN F.A.	Argentina	South_America	1948-6-6	TEJ-TRJ	0.4054	0.5942	0.0002	0.0002	0.0001
310870	PI	167930	Penbe	Turkey	Mideast	1948-9-1	TEJ	0.2085	0.7913	0.0001	0.0000	0.0001

310871	PI	168934	PI168934	Spain	Western_Europe	1948-10-18	TRJ	0.9991	0.0007	0.0001	0.0000	0.0001
310872	PI	168947	WC 2564	Spain	Western_Europe	1948-11-1	TEJ	0.0003	0.9996	0.0000	0.0000	0.0000
310873	PI	168948	Precoz Verde	Spain	Western_Europe	1948-11-1	TEJ-TRJ	0.4354	0.5643	0.0002	0.0001	0.0001
310874	PI	168949	Sellent	Spain	Western_Europe	1948-11-1	TEJ	0.0003	0.9996	0.0000	0.0000	0.0000
310875	PI	171971	27	Dominican Republic	Central_America	1948-12-1	TRJ	0.9993	0.0004	0.0001	0.0000	0.0001
310876	CIor	12312	REXARK ROGUE	United States	North_America	1954-6-1	TRJ	0.9988	0.0009	0.0002	0.0001	0.0001
310877	PI	175019	VIALONE NERO	Italy	Western_Europe	1949-2-1	TEJ	0.0034	0.9963	0.0001	0.0001	0.0001
310878	PI	176370	5490	Turkey	Mideast	1949-3-1	TEJ	0.0024	0.9974	0.0001	0.0000	0.0001
310879	PI	177224	6360	Turkey	Mideast	1949-3-1	TEJ	0.1408	0.8140	0.0001	0.0002	0.0449
310880	PI	177233	10340	Turkey	Mideast	1949-3-1	TEJ	0.0007	0.9990	0.0001	0.0001	0.0001
310881	PI	183700	10697	Turkey	Mideast	1949-7-27	TEJ	0.3504	0.6494	0.0001	0.0000	0.0000
310882	PI	184496	FUJISAKA 2	Japan	North_Pacific	1949-9-23	TEJ	0.0034	0.9963	0.0001	0.0001	0.0001
310883	PI	184506	Somewake	Japan	North_Pacific	1949-9-23	TEJ	0.0086	0.9904	0.0001	0.0001	0.0008
310884	PI	189451	Gilanica	Portugal	Western_Europe	1950-5-1	TEJ	0.3040	0.6957	0.0001	0.0000	0.0001
310885	PI	189458	Batatka	Portugal	Western_Europe	1950-5-1	TEJ-TRJ	0.4311	0.5681	0.0003	0.0001	0.0004
310886	PI	190617	WC 2656	Zaire	Africa	1950-9-1	TRJ	0.9776	0.0216	0.0006	0.0001	0.0002
310887	PI	198134	Buphopa	Myanmar	Southeast_Asia	1951-9-1	ARO-TEJ-TRJ	0.3052	0.3180	0.0041	0.0027	0.3701
310888	PI	199542	Boa Vista	El Salvador	Central_America	1952-3-6	TRJ	0.9639	0.0006	0.0350	0.0002	0.0004
310889	PI	199543	Brazilero Perla	El Salvador	Central_America	1952-3-6	TRJ	0.6595	0.3401	0.0001	0.0001	0.0001
310890	PI	199552	Peraiba	El Salvador	Central_America	1952-3-6	TRJ	0.9994	0.0004	0.0001	0.0000	0.0001
310891	PI	199554	Shapajillan	El Salvador	Central_America	1952-3-6	TRJ	0.9972	0.0025	0.0001	0.0001	0.0001
310892	PI	201838	Mamoriaka	Madagascar	Africa	1952-6-1	IND-AUS	0.0053	0.0014	0.5168	0.4760	0.0006
310893	PI	201839	SIKASSO B	Mali	Africa	1952-6-1	IND-AUS	0.0003	0.0085	0.5873	0.4025	0.0012
310894	PI	202968	Kinai No. 37	Japan	North_Pacific	1952-9-15	TEJ	0.0002	0.9997	0.0000	0.0000	0.0000
310895	PI	202992	NORIN 26	Japan	North_Pacific	1952-9-15	TEJ	0.0003	0.9967	0.0017	0.0007	0.0006
310896	PI	202994	NORIN 31	Japan	North_Pacific	1952-9-15	TEJ	0.0004	0.9995	0.0001	0.0000	0.0000
310897	PI	203095	RIKUTO TOUKAI MOCHI 27	Japan	North_Pacific	1952-9-29	TEJ-TRJ	0.4748	0.5172	0.0021	0.0013	0.0046
310898	PI	203282	Sacol 2	Chile	South_America	1952-10-27	TRJ-TEJ	0.5160	0.4836	0.0002	0.0001	0.0001
310899	PI	207010	LAMBAYEQUE 1	Peru	South_America	1953-4-8	AUS	0.0002	0.0001	0.0007	0.9989	0.0001
310900	PI	208450	Hasa	Nepal	Southern_Asia	1953-5-12	ARO-TEJ-TRJ	0.1315	0.3738	0.0016	0.0790	0.4141
310901	PI	208452	Juppa	Nepal	Southern_Asia	1953-5-12	IND	0.0006	0.0004	0.6534	0.3454	0.0002
310902	PI	209934	2	Taiwan	China	1953-8-13	TEJ	0.0004	0.9995	0.0001	0.0000	0.0000
310903	PI	209938	6	Taiwan	China	1953-8-13	TEJ	0.0004	0.9994	0.0001	0.0001	0.0000
310904	PI	214075	Palmira 8	Costa Rica	Central_America	1954-2-11	TRJ	0.9994	0.0003	0.0001	0.0000	0.0001
310905	PI	215477	Americano 1600	Italy	Western_Europe	1954-4-13	TEJ	0.0003	0.9995	0.0001	0.0000	0.0000
310906	PI	215478	Ardito	Italy	Western_Europe	1954-4-13	TEJ	0.1783	0.8214	0.0001	0.0000	0.0001
310907	PI	215517	Allorio 11	France	Western_Europe	1954-4-19	TEJ	0.0004	0.9995	0.0001	0.0000	0.0000
310908	PI	175013	ARDIZZONE	Italy	Western_Europe	1949-2-1	TEJ	0.0015	0.9976	0.0005	0.0004	0.0001
310909	PI	215937	TAINAN IKU 488	Taiwan	China	1954-4-28	IND	0.0002	0.0001	0.9994	0.0002	0.0001
310910	PI	215970	TAINO 38	Taiwan	China	1954-4-28	AUS-IND-TEJ-TRJ	0.1164	0.2561	0.3080	0.3193	0.0002
310911	PI	216011	TAKAO IKU 46	Taiwan	China	1954-4-28	TEJ	0.0002	0.9894	0.0089	0.0014	0.0000
310912	PI	216016	TAKAO IKU 51	Taiwan	China	1954-4-28	IND	0.0010	0.2832	0.7154	0.0002	0.0001
310913	PI	218238	WC 2702	Afghanistan	Southern_Asia	1954-6-14	IND-TEJ-ARO	0.0070	0.2262	0.5689	0.0005	0.1974
310914	PI	220706	WC 2685	Iran	Mideast	1954-8-31	ARO	0.0003	0.0005	0.0001	0.0001	0.9990
310915	PI	222454	ZALE	Myanmar	Southeast_Asia	1954-12-2	IND	0.0003	0.0001	0.9992	0.0003	0.0000
310916	PI	223456	Berenj-i-Mahin	Afghanistan	Southern_Asia	1955-2-4	ARO	0.0016	0.0006	0.0006	0.0006	0.9967
310917	PI	223457	Berenj-i-Luk	Afghanistan	Southern_Asia	1955-2-4	ARO	0.0012	0.0004	0.0003	0.0004	0.9976
310918	PI	223482	CHACARERO F.A.	Argentina	South_America	1955-1-24	TEJ	0.1813	0.8184	0.0001	0.0001	0.0001
310919	PI	223487	VICTORIA F.A.	Argentina	South_America	1955-1-24	TEJ	0.2962	0.7035	0.0001	0.0001	0.0001
310920	PI	223489	Yamani	Argentina	South_America	1955-1-24	TEJ	0.2192	0.7789	0.0016	0.0003	0.0001
310921	PI	224655	TOMINISHIKI	Japan	North_Pacific	1955-4-8	TEJ	0.0006	0.9991	0.0001	0.0001	0.0001
310922	PI	224813	HATSUNISHIKI	Japan	North_Pacific	1955-4-20	TEJ	0.0005	0.9992	0.0001	0.0001	0.0001
310923	PI	224834	KINUGASAWASE 121	Japan	North_Pacific	1955-4-20	TEJ	0.0005	0.9992	0.0001	0.0000	0.0001
310924	PI	224888	RIKUTO NORIN 4	Japan	North_Pacific	1955-4-20	TEJ-TRJ	0.3953	0.5988	0.0021	0.0016	0.0022

310925	PI	224899	SEKIYAMA	Japan	North_Pacific	1955-4-20	TEJ	0.0025	0.9967	0.0003	0.0002	0.0002
310926	PI	225744	Arroz Portugues	Portugal	Western_Europe	1955-5-11	TEJ	0.1374	0.8622	0.0001	0.0001	0.0002
310927	PI	226155	AKATSUKI MOCHI	Japan	North_Pacific	1955-6-6	TEJ	0.0009	0.9989	0.0001	0.0000	0.0001
310928	PI	226210	Teruju	Japan	North_Pacific	1955-6-6	TEJ	0.0050	0.9945	0.0001	0.0001	0.0002
310929	PI	226216	ZENNOO	Japan	North_Pacific	1955-6-6	TEJ	0.0007	0.9991	0.0001	0.0001	0.0001
310930	PI	226217	Mubo Aikoku	Japan	North_Pacific	1955-6-6	TEJ	0.0004	0.9994	0.0001	0.0001	0.0001
310931	PI	226307	Sab Ini	Egypt	Mideast	1955-6-8	TEJ	0.0060	0.9934	0.0001	0.0002	0.0003
310932	PI	226313	17-9-4	Mexico	North_America	1955-6-10	IND	0.0321	0.0587	0.9087	0.0002	0.0003
310933	PI	226317	C1-5-5-1	Mexico	North_America	1955-6-10	IND	0.0011	0.0005	0.7034	0.2943	0.0007
310934	PI	231176	Bulgare	France	Western_Europe	1956-1-30	TEJ	0.0061	0.9935	0.0001	0.0001	0.0003
310935	PI	231641	Amaura Alef	Former Soviet Union	Eastern_Europe	1956-3-13	TEJ	0.0022	0.9949	0.0001	0.0009	0.0019
310936	PI	231642	Caucasica	Former Soviet Union	Eastern_Europe	1956-3-13	TEJ	0.0009	0.9988	0.0001	0.0000	0.0001
310937	PI	231644	Dichroa	Former Soviet Union	Eastern_Europe	1956-3-13	TEJ	0.0020	0.9972	0.0003	0.0001	0.0005
310938	PI	231647	Ianthoceros	Former Soviet Union	Eastern_Europe	1956-3-13	TEJ	0.0003	0.9986	0.0004	0.0005	0.0002
310939	PI	231651	Rubra	Former Soviet Union	Eastern_Europe	1956-3-13	TEJ	0.0008	0.9986	0.0001	0.0001	0.0005
310940	PI	215840	SHINCHIKU NO. 124	Taiwan	China	1954-4-28	TEJ	0.0005	0.9993	0.0001	0.0000	0.0001
310941	PI	233289	Peta	Indonesia	South_Pacific	1956-5-10	IND	0.0001	0.0001	0.9994	0.0001	0.0002
310942	PI	236422	LATE CALORO	Australia	Oceania	1957-1-9	TEJ	0.0005	0.9993	0.0001	0.0000	0.0001
310943	PI	238119	COLUSA 180	Australia	Oceania	1957-3-21	TEJ	0.1591	0.8407	0.0001	0.0000	0.0001
310944	PI	238492	JAPONES GIGANTE SEL M.A.	Argentina	South_America	1957-3-27	TEJ	0.0586	0.9401	0.0011	0.0001	0.0001
310945	PI	240638	*Dular	India	Southern_Asia	1957-6-10	AUS	0.0004	0.0004	0.0025	0.9964	0.0002
310946	PI	240649	AP 423	Venezuela	South_America	1957-6-10	TRJ	0.9993	0.0005	0.0001	0.0000	0.0001
310947	PI	242808	Petacon	Bolivia	South_America	1957-10-10	TRJ	0.9990	0.0004	0.0004	0.0001	0.0001
310948	PI	242810	Sin Cuero	Bolivia	South_America	1957-10-10	TRJ	0.9953	0.0036	0.0007	0.0003	0.0001
310949	PI	244727	Esperanza	Cuba	Central_America	1957-12-30	IND	0.0044	0.0004	0.7386	0.2558	0.0008
310950	PI	245071	NANTON NO. 131	Taiwan	China	1958-1-16	TRJ-TEJ-ARO	0.5715	0.2173	0.0199	0.0045	0.1868
310951	PI	245352	45B	Cuba	Central_America	1958-1-31	ARO	0.0010	0.0029	0.0035	0.0010	0.9916
310952	PI	245353	47	Cuba	Central_America	1958-1-31	TRJ	0.6778	0.0034	0.1619	0.1566	0.0003
310953	PI	247885	Palman 246	Pakistan	Southern_Asia	1958-5-9	AUS	0.0002	0.0001	0.0002	0.9992	0.0002
310954	PI	247944	Canairo	Costa Rica	Central_America	1958-5-15	TEJ	0.1725	0.8270	0.0002	0.0001	0.0002
310955	PI	247945	Cateto Branco	Costa Rica	Central_America	1958-5-15	TRJ	0.9994	0.0002	0.0002	0.0001	0.0001
310956	PI	247954	Secano	Costa Rica	Central_America	1958-5-15	TRJ	0.9993	0.0004	0.0001	0.0001	0.0001
310957	PI	248516	*AGOSTANO	Italy	Western_Europe	1958-6-6	TEJ	0.0011	0.9986	0.0001	0.0001	0.0001
310958	PI	256340	2	Afghanistan	Southern_Asia	1959-3-31	ARO	0.0016	0.0019	0.0002	0.0002	0.9960
310959	PI	256989	HR 109	India	Southern_Asia	1959-4-21	TRJ-TEJ-IND	0.3636	0.2953	0.2616	0.0781	0.0015
310960	PI	263815	100-1-1-11	Suriname	South_America	1960-3-7	TRJ-IND-AUS	0.4935	0.0007	0.3116	0.1914	0.0028
310961	PI	265107	M 2	Poland	Eastern_Europe	1960-4-27	TEJ	0.0009	0.9810	0.0056	0.0093	0.0031
310962	PI	265109	Italica Banloc	Poland	Eastern_Europe	1960-4-27	TEJ	0.0010	0.9981	0.0001	0.0002	0.0006
310963	PI	266123	Sadri Belyi	Azerbaijan	Central_Asia	1960-6-8	ARO	0.0008	0.2262	0.0001	0.0002	0.7727
310964	PI	267993	Africano	Portugal	Western_Europe	1960-9-7	TEJ	0.0011	0.9987	0.0001	0.0000	0.0001
310965	PI	268003	Vary Tarva Osla	Portugal	Western_Europe	1960-9-7	TEJ	0.2134	0.7863	0.0001	0.0001	0.0001
310966	PI	271287	Perlita Jalapa	Guatemala	Central_America	1961-1-24	TRJ	0.9986	0.0010	0.0002	0.0000	0.0002
310967	PI	271672	*TAICHUNG NA-TIVE 1	Taiwan	China	1961-2-10	IND	0.0001	0.0001	0.9997	0.0001	0.0000
310968	PI	271888	Kakai Korai	Hungary	Eastern_Europe	1961-2-28	TEJ	0.0040	0.9947	0.0004	0.0002	0.0007
310969	PI	274494	143-24	Korea_ South	North_Pacific	1961-5-8	TEJ	0.0008	0.9990	0.0001	0.0000	0.0000
310970	PI	275429	TAICHUNG 176	Taiwan	China	1961-6-20	TEJ	0.0003	0.9993	0.0003	0.0000	0.0000
310971	PI	275442	Trionfo Fassone	Italy	Western_Europe	1961-6-20	TEJ	0.3013	0.6984	0.0002	0.0000	0.0001
310972	PI	233085	Yabani Montakhab 57	India	Southern_Asia	1956-5-1	TEJ	0.0003	0.9995	0.0001	0.0000	0.0000
310973	PI	275542	VARY LAVA 1302	Madagascar	Africa	1961-6-27	TEJ	0.3041	0.6954	0.0003	0.0001	0.0000
310974	PI	277235	TAICHUNG 122	Taiwan	China	1961-11-8	TEJ	0.0003	0.9996	0.0001	0.0000	0.0000
310975	PI	279120	Bir-Co	Taiwan	China	1962-2-5	IND	0.0081	0.0013	0.9897	0.0003	0.0007
310976	PI	279167	TAITUNG WOO TSAN	Taiwan	China	1962-2-5	IND	0.0002	0.0001	0.9995	0.0001	0.0000

310977	PI	279994	RIZZOTTO	Italy	Western_Europe	1962-3-28	TEJ	0.2364	0.7628	0.0006	0.0001	0.0001
310978	PI	280003	WC 4197	Italy	Western_Europe	1962-3-28	TEJ	0.0990	0.9008	0.0001	0.0000	0.0001
310979	PI	280674	Chokoto	Japan	North_Pacific	1962-5-3	IND	0.0002	0.0002	0.9993	0.0002	0.0001
310980	PI	281758	Cesariot	France	Western_Europe	1962-7-5	TEJ	0.0033	0.9965	0.0001	0.0000	0.0001
310981	PI	281759	CIGALON	France	Western_Europe	1962-7-5	TEJ	0.0003	0.9995	0.0001	0.0000	0.0000
310982	PI	281790	3	Chile	South_America	1962-7-6	TEJ	0.0004	0.9993	0.0001	0.0001	0.0001
310983	PI	281792	5	Chile	South_America	1962-7-6	TEJ	0.0005	0.9992	0.0001	0.0001	0.0001
310984	PI	282173	CSORNUJ	Hungary	Eastern_Europe	1962-7-23	TEJ	0.0785	0.9193	0.0015	0.0006	0.0001
310985	PI	282188	L.K.V.R.	Hungary	Eastern_Europe	1962-7-23	TEJ	0.0015	0.9981	0.0001	0.0002	0.0001
310986	PI	282191	OMIRT 168	Hungary	Eastern_Europe	1962-7-23	TEJ	0.0006	0.9990	0.0001	0.0002	0.0001
310987	PI	282200	SZANISZLO 2	Hungary	Eastern_Europe	1962-7-23	TEJ	0.0404	0.9593	0.0001	0.0000	0.0002
310988	PI	282203	SZEGEDI SZA-KALLAS 28	Uzbekistan	Central_Asia	1962-7-23	TEJ	0.0013	0.9981	0.0001	0.0002	0.0002
310989	PI	282217	Zolotje Vszhodu	Hungary	Eastern_Europe	1962-7-23	TEJ	0.3767	0.6141	0.0052	0.0013	0.0027
310990	PI	282768	R 67	Senegal	Africa	1962-8-28	TRJ	0.9991	0.0004	0.0002	0.0002	0.0001
310991	PI	283687	PATNAI 23	Myanmar	Southeast_Asia	1962-10-5	IND-TRJ	0.4859	0.0012	0.5123	0.0005	0.0001
310992	PI	286178	PG 503	El Salvador	Central_America	1963-1-28	TRJ	0.9994	0.0004	0.0001	0.0000	0.0000
310993	PI	291426	UZ ROSZ M8	Uzbekistan	Central_Asia	1963-6-6	TEJ	0.1149	0.8845	0.0002	0.0002	0.0001
310994	PI	291442	DUNGHAN SHALI	Uzbekistan	Central_Asia	1963-6-6	TEJ	0.0012	0.9979	0.0001	0.0006	0.0002
310995	PI	291489	Cs He Jao No. 1	Hungary	Eastern_Europe	1963-6-6	TEJ	0.0830	0.9064	0.0011	0.0033	0.0062
310996	PI	291529	BELLARDONE	Hungary	Eastern_Europe	1963-6-6	TEJ	0.0004	0.9995	0.0000	0.0000	0.0000
310997	PI	291539	LUSITANO	Portugal	Western_Europe	1963-6-6	TEJ	0.0022	0.9973	0.0001	0.0001	0.0002
310998	PI	291608	WC 4443	Bolivia	South_America	1963-6-13	TRJ	0.9995	0.0002	0.0001	0.0000	0.0001
310999	PI	291658	MI MASARI	Japan	North_Pacific	1963-6-13	TEJ	0.0011	0.9986	0.0001	0.0001	0.0001
311000	PI	298955	XB-2	Australia	Oceania	1964-7-7	TEJ-TRJ	0.4066	0.5930	0.0002	0.0001	0.0001
311001	PI	298959	XB-7	Australia	Oceania	1964-7-7	TEJ-TRJ	0.4958	0.5038	0.0002	0.0001	0.0001
311002	PI	298966	1-7-24-1-2	Australia	Oceania	1964-7-7	TEJ-TRJ	0.4850	0.5147	0.0002	0.0001	0.0001
311003	PI	307579	1-4-1-2-2-4	Australia	Oceania	1965-9-2	TRJ-TEJ	0.5570	0.4427	0.0001	0.0001	0.0001
311004	PI	275449	Precosur	Argentina	South_America	1961-6-20	TEJ	0.1966	0.8031	0.0001	0.0001	0.0001
311005	PI	312631	IR 8-296-2-1	Philippines	South_Pacific	1966-3-22	IND	0.0001	0.0002	0.9996	0.0001	0.0000
311006	PI	312644	T(N) Yu 7	Taiwan	China	1966-3-22	IND	0.0034	0.0438	0.9527	0.0001	0.0001
311007	PI	312760	RPP 31-3	Philippines	South_Pacific	1966-3-22	IND	0.0070	0.0011	0.9909	0.0004	0.0006
311008	PI	312776	WC 4643	Philippines	South_Pacific	1966-3-22	IND	0.0007	0.0001	0.9990	0.0001	0.0000
311009	PI	315646	Palo Gordo A	El Salvador	Central_America	1966-6-29	TRJ	0.7969	0.2028	0.0002	0.0000	0.0001
311010	PI	315647	43-5-10	El Salvador	Central_America	1966-6-29	TRJ-IND	0.5495	0.0023	0.3923	0.0550	0.0009
311011	PI	317514	342	Madagascar	Africa	1966-11-18	TRJ	0.9989	0.0005	0.0004	0.0002	0.0001
311012	PI	319494	WC 5015	Mexico	North_America	1967-4-10	TRJ	0.9967	0.0030	0.0002	0.0001	0.0001
311013	PI	319502	COTAXTLA A66	Mexico	North_America	1967-4-10	TRJ	0.9917	0.0077	0.0004	0.0001	0.0002
311014	PI	319504	WC 5023	Mexico	North_America	1967-4-10	TRJ-IND	0.5983	0.0033	0.3971	0.0003	0.0010
311015	PI	319521	C86-13-16-Cu2-Cu1-FV1-FV5	Mexico	North_America	1967-4-10	TRJ	0.7453	0.0249	0.2295	0.0001	0.0002
311016	PI	321183	IR 238	Philippines	South_Pacific	1967-7-12	IND	0.2048	0.0046	0.7471	0.0419	0.0016
311017	PI	321336	IR 126-6-3-1	Philippines	South_Pacific	1967-7-12	TRJ	0.9244	0.0005	0.0745	0.0005	0.0001
311018	PI	325909	IR 237-20-1	Philippines	South_Pacific	1968-2-29	IND	0.3961	0.0020	0.6010	0.0007	0.0002
311019	PI	326031	Choul	Iraq	Mideast	1968-3-5	AUS	0.0014	0.0014	0.0004	0.9960	0.0009
311020	PI	326143	K1790	Afghanistan	Southern_Asia	1968-3-8	TEJ	0.0020	0.9691	0.0005	0.0004	0.0280
311021	PI	330469	RAFFAELLO	Italy	Western_Europe	1968-5-15	TEJ	0.1594	0.8402	0.0001	0.0001	0.0002
311022	PI	331504	IR 547-54-1-2	Philippines	South_Pacific	1968-7-12	IND	0.2524	0.0011	0.7416	0.0034	0.0014
311023	PI	338033	IR 497-81-3-3-2	Philippines	South_Pacific	1968-11-6	TRJ	0.8012	0.0080	0.1906	0.0002	0.0001
311024	PI	338707	RP1 332	India	Southern_Asia	1969-1-9	IND	0.0001	0.0001	0.9998	0.0001	0.0000
311025	PI	338956	IR 647-PD1-C1	Philippines	South_Pacific	1969-1-15	IND	0.3496	0.0206	0.6292	0.0003	0.0003
311026	PI	340887	Colina	Spain	Western_Europe	1969-2-18	TEJ	0.0003	0.9996	0.0001	0.0000	0.0001
311027	PI	340890	Frances	Spain	Western_Europe	1969-2-18	TEJ	0.0004	0.9982	0.0012	0.0001	0.0001
311028	PI	340891	LISO	Spain	Western_Europe	1969-2-18	TEJ	0.0004	0.9993	0.0001	0.0001	0.0001
311029	PI	340893	Matususka	Spain	Western_Europe	1969-2-18	TEJ	0.0005	0.9994	0.0001	0.0001	0.0000
311030	PI	341933	Johiku No. 314	Japan	North_Pacific	1969-4-9	TEJ	0.0004	0.9994	0.0001	0.0000	0.0000
311031	PI	342650	Flown	Dominican Republic	Central_America	1969-4-30	TRJ	0.9990	0.0008	0.0001	0.0001	0.0001

311032	PI	346441	50638	Guyana	South_America	1969-11-25	IND	0.0001	0.0002	0.9993	0.0003	0.0001
311033	PI	346821	FORTUNA CORRI-ENTES SEL INTA	Argentina	South_America	1969-12-10	IND	0.0446	0.0014	0.9536	0.0001	0.0002
311034	PI	346823	LA PLATA GUALEYAN F.A.	Argentina	South_America	1969-12-10	TRJ-TEJ	0.5342	0.4655	0.0002	0.0001	0.0001
311035	PI	346830	H61-10-1	Argentina	South_America	1969-12-10	TEJ-TRJ	0.4361	0.5635	0.0002	0.0001	0.0001
311036	PI	312605	IR 3-122-1-1	Philippines	South_Pacific	1966-3-22	IND	0.0383	0.0004	0.9608	0.0004	0.0000
311037	PI	346859	H75-23-1	Argentina	South_America	1969-12-10	TRJ-TEJ	0.5981	0.4016	0.0001	0.0001	0.0001
311038	PI	346932	KUBAN 3	Russian Federation	Eastern_Europe	1969-12-24	TEJ	0.0008	0.9988	0.0001	0.0001	0.0002
311039	PI	348844	IR 1321-19	Philippines	South_Pacific	1970-3-6	TEJ	0.0008	0.7433	0.2557	0.0001	0.0001
311040	PI	348910	Ambarby White	Azerbaijan	Central_Asia	1918-3-5	ARO	0.0030	0.2621	0.0002	0.0003	0.7344
311041	PI	348912	ALAKULIAN	Kazakhstan	Central_Asia	1918-3-5	TEJ	0.0008	0.9988	0.0001	0.0002	0.0001
311042	PI	350338	IR 1314-28-1-2	Philippines	South_Pacific	1970-5-12	TEJ-IND	0.0004	0.5978	0.4017	0.0001	0.0001
311043	PI	350621	KC 16-2-5	Philippines	South_Pacific	1970-5-12	TEJ	0.1252	0.8710	0.0036	0.0001	0.0001
311044	PI	350664	IR 773A1-36-2-1-3	Philippines	South_Pacific	1970-5-12	IND	0.0178	0.0011	0.9726	0.0033	0.0052
311045	PI	353636	IARI 5753B	India	Southern_Asia	1970-5-4	IND-AUS	0.0001	0.0001	0.5115	0.4880	0.0002
311046	PI	353722	IARI 6621	India	Southern_Asia	1970-5-4	AUS	0.0012	0.0186	0.0823	0.8978	0.0001
311047	PI	353771	IARI 10376	India	Southern_Asia	1970-5-4	IND	0.0002	0.0003	0.9971	0.0023	0.0001
311048	PI	366346	IR 1561-106-5	Philippines	South_Pacific	1971-6-1	IND	0.0002	0.0004	0.9985	0.0008	0.0001
311049	PI	369804	Blakka Tere Thelma	Suriname	South_America	1972-2-1	TRJ	0.9948	0.0037	0.0004	0.0001	0.0011
311050	PI	369808	Guatakka	Suriname	South_America	1972-2-1	IND	0.3448	0.0360	0.6185	0.0004	0.0003
311051	PI	369809	Jinge Jinge zwp	Suriname	South_America	1972-2-1	IND	0.0002	0.0002	0.9994	0.0001	0.0000
311052	PI	369813	Samanis	Suriname	South_America	1972-2-1	ARO-IND	0.0011	0.0004	0.4607	0.0006	0.5372
311053	PI	369815	Wittie Sakka	Suriname	South_America	1972-2-1	IND	0.1319	0.1962	0.6713	0.0003	0.0002
311054	PI	370748	Naylamp	Peru	South_America	1972-3-7	IND	0.0002	0.0001	0.9996	0.0001	0.0000
311055	PI	371600	KAKAI 162	Hungary	Eastern_Europe	1972-3-14	TEJ	0.0031	0.9966	0.0001	0.0001	0.0001
311056	PI	372041	P859-17-14-B	Colombia	South_America	1972-4-11	IND	0.0590	0.0511	0.8892	0.0005	0.0002
311057	PI	372765	Murni	Malaysia	South_Pacific	1972-5-30	TRJ	0.9985	0.0004	0.0005	0.0005	0.0001
311058	PI	373014	1-39-3-1-3	Iran	Mideast	1972-3-27	TRJ	0.9992	0.0004	0.0002	0.0001	0.0001
311059	PI	373097	IR 1103-49-4-1-3-3-2	Philippines	South_Pacific	1972-3-27	TRJ	0.9979	0.0015	0.0003	0.0001	0.0002
311060	PI	373121	Hal Suduwi	Sri Lanka	Southern_Asia	1972-3-27	IND	0.0003	0.0016	0.7190	0.2790	0.0001
311061	PI	373160	Siryan	Philippines	South_Pacific	1972-3-27	IND	0.0001	0.0001	0.9932	0.0064	0.0003
311062	PI	373237	Khao Meuay	Laos	Southeast_Asia	1972-3-27	AUS	0.0002	0.0001	0.0025	0.9969	0.0002
311063	PI	373238	Mack Khoune	Laos	Southeast_Asia	1972-3-27	TRJ-TEJ-ARO	0.4056	0.3410	0.0142	0.0011	0.2380
311064	PI	373241	Khao Pick	Laos	Southeast_Asia	1972-3-27	IND	0.0002	0.0005	0.8508	0.1480	0.0004
311065	PI	373263	A6-10-37	Sri Lanka	Southern_Asia	1972-3-27	IND	0.0667	0.0011	0.9286	0.0009	0.0026
311066	PI	373283	Kh. Mack Fay	Laos	Southeast_Asia	1972-3-27	IND	0.0001	0.0001	0.9996	0.0001	0.0001
311067	PI	373295	Kh. Samdeuane	Laos	Southeast_Asia	1972-3-27	TRJ-TEJ	0.4936	0.3646	0.0129	0.0008	0.1281
311068	PI	346838	H64-9-1	Argentina	South_America	1969-12-10	TRJ	0.6677	0.3319	0.0002	0.0001	0.0001
311069	PI	373701	Lay Sort	Laos	Southeast_Asia	1972-3-27	TRJ	0.9945	0.0051	0.0002	0.0001	0.0002
311070	PI	373716	Med Noi	Laos	Southeast_Asia	1972-3-27	ARO	0.0017	0.0003	0.0006	0.0009	0.9965
311071	PI	373742	Y Kome	Laos	Southeast_Asia	1972-3-27	IND	0.0002	0.0004	0.9988	0.0005	0.0001
311072	PI	373763	FATEHPUR 4	Pakistan	Southern_Asia	1972-3-27	ARO	0.0013	0.0003	0.0005	0.0045	0.9934
311073	PI	373784	Tukan Tuna	Indonesia	Oceania	1972-3-27	IND	0.0001	0.0001	0.9998	0.0000	0.0000
311074	PI	373786	Mitak	Indonesia	Oceania	1972-3-27	TRJ	0.8148	0.0997	0.0063	0.0002	0.0790
311075	PI	373803	Padi Gabukon	Malaysia	South_Pacific	1972-3-27	IND	0.3114	0.0148	0.6735	0.0002	0.0001
311076	PI	373896	Sesilla	Bulgaria	Eastern_Europe	1972-3-27	IND	0.0002	0.0009	0.9983	0.0006	0.0001
311077	PI	373898	Uspeh	Bulgaria	Eastern_Europe	1972-3-27	TEJ	0.0004	0.9995	0.0001	0.0000	0.0000
311078	PI	373939	Gazan	Afghanistan	Southern_Asia	1972-7-3	TEJ	0.0020	0.6419	0.0002	0.0003	0.3556
311079	PI	373942	Qumanani	Afghanistan	Southern_Asia	1972-7-3	ARO	0.0006	0.0012	0.0002	0.0001	0.9979
311080	PI	376718	YRL-1	Australia	Oceania	1972-7-13	TEJ-TRJ	0.4356	0.5191	0.0425	0.0024	0.0003
311081	PI	376734	IR 1670-85-3-B	Philippines	South_Pacific	1972-7-13	IND	0.0004	0.3426	0.6563	0.0001	0.0005
311082	PI	385462	Hansraj	Pakistan	Southern_Asia	1974-2-20	ARO	0.0022	0.0006	0.0008	0.0717	0.9247
311083	PI	385571	Begum	Pakistan	Southern_Asia	1974-2-20	AUS	0.0003	0.0001	0.0002	0.9993	0.0001
311084	PI	385620	Mabla	Pakistan	Southern_Asia	1974-2-20	AUS	0.0002	0.0002	0.0006	0.9989	0.0002
311085	PI	385693	P 32	India	Southern_Asia	1974-2-20	AUS	0.0214	0.0015	0.0015	0.9350	0.0406
311086	PI	385772	Ratura Mushkan	Pakistan	Southern_Asia	1974-2-20	ARO	0.0013	0.0036	0.0002	0.0010	0.9938

311087	PI	385821	Ziri Palman	Pakistan	Southern_Asia	1974-2-20	AUS	0.0002	0.0002	0.0002	0.9993	0.0001
311088	PI	385844	Sathra 4	Pakistan	Southern_Asia	1974-2-20	AUS	0.0002	0.0001	0.0002	0.9994	0.0001
311089	PI	388274	ARBORIO	Italy	Western_Europe	1974-3-5	TEJ	0.0174	0.9824	0.0001	0.0000	0.0001
311090	PI	388282	Cheng Kin Sen Ko	China	China	1974-3-5	IND	0.0010	0.0013	0.9964	0.0010	0.0002
311091	PI	388297	2868	Brazil	South_America	1974-3-5	AUS	0.0013	0.0002	0.0003	0.9981	0.0002
311092	PI	388307	BC 1-1-1	United States	North_America	1974-3-5	TEJ-TRJ	0.4592	0.5405	0.0001	0.0000	0.0001
311093	PI	388400	GPNO 29157	China	China	1974-3-5	IND	0.0060	0.0047	0.9886	0.0002	0.0005
311094	PI	388435	Dae Ku	Korea	North_Pacific	1974-3-5	TEJ-TRJ	0.4598	0.5312	0.0024	0.0018	0.0047
311095	PI	388439	Ean No. 4	Portugal	Western_Europe	1974-3-5	TEJ	0.0004	0.9994	0.0001	0.0001	0.0001
311096	PI	388471	Hae Zo	Korea	North_Pacific	1974-3-5	IND	0.0002	0.0001	0.9995	0.0002	0.0001
311097	PI	388484	Indo Yiaia Lonica	Portugal	Western_Europe	1974-3-5	IND	0.0001	0.0001	0.9998	0.0001	0.0000
311098	PI	388490	Kwan Tone Zo Saeng No. 20	Korea	North_Pacific	1974-3-5	IND	0.0006	0.0007	0.9980	0.0003	0.0004
311099	PI	388495	Ku Mun Do No. 84	Korea	North_Pacific	1974-3-5	TRJ	0.9960	0.0038	0.0001	0.0000	0.0001
311100	PI	373403	ARC 6578	India	Southern_Asia	1972-3-27	AUS	0.0030	0.0039	0.0166	0.9759	0.0007
311101	PI	388554	Paraiba Chines Nova	Brazil	South_America	1974-3-5	IND	0.0002	0.0002	0.9989	0.0007	0.0001
311102	PI	388561	Roque HP	Brazil	South_America	1974-3-5	TEJ-TRJ	0.4498	0.5497	0.0002	0.0001	0.0002
311103	PI	388563	Sezia Uruguai	Uruguay	South_America	1974-3-5	TRJ	0.7305	0.2692	0.0002	0.0000	0.0001
311104	PI	388612	EEA 406	Brazil	South_America	1974-3-5	TRJ	0.8002	0.1990	0.0006	0.0002	0.0001
311105	PI	389069	Hsin Hsing Pai Ku	Taiwan	China	1974-9-1	IND	0.0005	0.0004	0.9974	0.0016	0.0002
311106	PI	389141	O Tre	Vietnam	Southeast_Asia	1974-9-1	IND	0.0004	0.0001	0.9926	0.0061	0.0007
311107	PI	389227	Giau Nghe 558	Vietnam	Southeast_Asia	1974-9-1	IND	0.0005	0.0003	0.9980	0.0008	0.0005
311108	PI	389251	Gie No. 1	Vietnam	Southeast_Asia	1974-9-1	IND	0.0607	0.0076	0.9192	0.0053	0.0073
311109	PI	389380	Shoa Ga Dau	China	China	1974-9-1	IND	0.0009	0.0002	0.9958	0.0030	0.0002
311110	PI	389774	Hunan Yochow Zone	China	China	1974-9-1	IND	0.0006	0.0004	0.9982	0.0008	0.0001
311111	PI	389863	99216	India	Southern_Asia	1974-9-1	AUS	0.0003	0.0002	0.0011	0.9983	0.0001
311112	PI	389920	Far Yu Jien	Hong Kong	China	1974-9-1	IND	0.0001	0.0002	0.9983	0.0013	0.0001
311113	PI	389923	Shui Ya Jien	Hong Kong	China	1974-9-1	IND	0.0002	0.0011	0.9964	0.0014	0.0009
311114	PI	389924	CHAI MEI	Hong Kong	China	1974-9-1	IND	0.0073	0.0016	0.9901	0.0004	0.0005
311115	PI	389927	Pai Hok Glutinous	Hong Kong	China	1974-9-1	IND	0.0007	0.0371	0.9618	0.0002	0.0001
311116	PI	389930	Lek Slek	Cambodia	Southeast_Asia	1974-9-1	IND	0.0020	0.0007	0.9971	0.0001	0.0001
311117	PI	389933	Tranoeup Beykher	Cambodia	Southeast_Asia	1974-9-1	IND	0.0004	0.0003	0.9951	0.0041	0.0002
311118	PI	390165	CADUNG KET	Vietnam	Southeast_Asia	1974-9-1	IND	0.0020	0.0015	0.8611	0.1338	0.0016
311119	PI	390176	Ba Tuc	Vietnam	Southeast_Asia	1974-9-1	TEJ	0.0004	0.9994	0.0001	0.0000	0.0000
311120	PI	390179	Cuc Cao Trang	Vietnam	Southeast_Asia	1974-9-1	IND	0.0001	0.0001	0.9996	0.0002	0.0001
311121	PI	390981	SRI MALAYSIA DUA	Malaysia	South_Pacific	1974-8-25	TEJ	0.0004	0.9994	0.0001	0.0001	0.0000
311122	PI	391209	Zwang Zo 46	Taiwan	China	1974-11-20	TRJ	0.9522	0.0473	0.0003	0.0001	0.0001
311123	PI	391214	10340	Italy	Western_Europe	1974-11-20	IND	0.0004	0.0003	0.9990	0.0002	0.0001
311124	PI	391215	3557	Puerto Rico	Central_America	1974-11-20	IND	0.0021	0.0008	0.9963	0.0007	0.0001
311125	PI	391217	4105	Iran	Mideast	1974-11-20	ARO	0.0005	0.0005	0.0001	0.0001	0.9988
311126	PI	391224	Yin Chan	Taiwan	China	1974-11-20	IND	0.0004	0.0009	0.9983	0.0003	0.0001
311127	PI	391230	Espinho 15	Brazil	South_America	1974-11-20	TRJ	0.9987	0.0006	0.0002	0.0000	0.0004
311128	PI	391234	AGULHA AMA-RELO	Brazil	South_America	1974-11-20	TRJ	0.9994	0.0004	0.0001	0.0001	0.0000
311129	PI	391254	H 25-36	Argentina	South_America	1974-11-20	IND	0.0019	0.0008	0.9971	0.0001	0.0002
311130	PI	391364	JIRASAR 280	India	Southern_Asia	1974-11-20	TEJ	0.0006	0.9988	0.0001	0.0003	0.0002
311131	PI	388520	Nao Traduzido No. 5	Brazil	South_America	1974-3-5	TEJ	0.2983	0.7014	0.0001	0.0001	0.0001
311132	PI	392086	CHONTALPA 437	Mexico	North_America	1974-12-31	IND	0.0051	0.0006	0.9940	0.0003	0.0000
311133	PI	392093	SINAOLOA A68-19C	Mexico	North_America	1974-12-31	IND	0.0003	0.0006	0.9989	0.0001	0.0002
311134	PI	392121	Sathi Basmati	Pakistan	Southern_Asia	1974-12-15	ARO	0.0011	0.0002	0.0011	0.0028	0.9948
311135	PI	392195	Kangni Type	Pakistan	Southern_Asia	1974-12-15	AUS	0.0002	0.0001	0.0003	0.9993	0.0001
311136	PI	392211	Coarse	Pakistan	Southern_Asia	1974-12-15	IND	0.0013	0.0015	0.6825	0.3145	0.0003
311137	PI	392225	Sugdasi Gharho	Pakistan	Southern_Asia	1974-12-15	ARO	0.0031	0.0007	0.0014	0.2160	0.7788
311138	PI	392545	Tono 112	Sierra Leone	Africa	1975-2-3	TEJ	0.0019	0.9978	0.0002	0.0001	0.0000
311139	PI	392563	PHCAR TIEN	Cambodia	Southeast_Asia	1975-2-3	TEJ	0.0003	0.9996	0.0000	0.0000	0.0000
311140	PI	392605	AKP 4	India	Southern_Asia	1975-2-3	IND	0.0082	0.0051	0.9782	0.0068	0.0017
311141	PI	392637	SORNAVARI	Mali	Africa	1975-2-3	AUS	0.0006	0.0002	0.0004	0.9987	0.0001

311142	PI	392649	PEROLA	Brazil	South_America	1975-2-3	TEJ	0.0025	0.9972	0.0003	0.0000	0.0000
311143	PI	392658	Bhadoia 684	Bangladesh	Southern_Asia	1975-2-3	TEJ	0.0044	0.9782	0.0001	0.0036	0.0137
311144	PI	392705	RADIN EBOS 33	Malaysia	South_Pacific	1975-2-3	IND	0.0005	0.0003	0.9986	0.0004	0.0002
311145	PI	392715	EMATA PIN-DOGALE	Myanmar	Southeast_Asia	1975-2-3	TRJ-IND-TEJ	0.5520	0.2073	0.2103	0.0004	0.0301
311146	PI	392718	SITPWA	Myanmar	Southeast_Asia	1975-2-3	TEJ	0.0002	0.9996	0.0001	0.0000	0.0000
311147	PI	392725	221/BC IV/1/178/3	Indonesia	Oceania	1975-2-3	TEJ	0.0004	0.9995	0.0001	0.0000	0.0000
311148	PI	392804	56-122-23	Thailand	Southeast_Asia	1975-2-3	TEJ	0.0005	0.9993	0.0001	0.0000	0.0001
311149	PI	392862	Bir 37 Thou Dau	China	China	1975-2-3	IND	0.0037	0.0818	0.9120	0.0008	0.0018
311150	PI	392883	Five Months	Guyana	South_America	1975-2-3	TRJ	0.9993	0.0005	0.0001	0.0000	0.0000
311151	PI	393070	TD 70	Thailand	Southeast_Asia	1975-2-3	IND	0.0034	0.0004	0.9945	0.0015	0.0003
311152	PI	393181	Rani	Fiji	Oceania	1975-2-3	IND	0.0003	0.0011	0.9984	0.0001	0.0001
311153	PI	399748	IR 2061-214-2-3	Philippines	South_Pacific	1975-5-7	IND	0.0003	0.0003	0.9985	0.0002	0.0008
311154	PI	399768	IR 2151-598-3-5	Philippines	South_Pacific	1975-5-7	IND	0.0014	0.0015	0.9968	0.0002	0.0001
311155	PI	400021	Jumula 2	Nepal	Southern_Asia	1975-5-7	IND	0.0001	0.0002	0.9994	0.0002	0.0001
311156	PI	400063	KRASNODAR 424	Russian Federation	Eastern_Europe	1975-5-7	TEJ	0.0011	0.9983	0.0001	0.0003	0.0002
311157	PI	400064	L-2270	Romania	Eastern_Europe	1975-5-7	TEJ	0.0007	0.9989	0.0002	0.0001	0.0002
311158	PI	400068	L-III-122	Romania	Eastern_Europe	1975-5-7	TEJ	0.0641	0.9350	0.0001	0.0002	0.0006
311159	PI	400072	L-IV-34	Romania	Eastern_Europe	1975-5-7	TEJ	0.0008	0.9988	0.0001	0.0001	0.0001
311160	PI	400096	SML KAPURI	Suriname	South_America	1975-5-7	TEJ	0.1606	0.8389	0.0001	0.0001	0.0003
311161	PI	391847	BRITISH GUIANA 79	Guyana	South_America	1974-11-27	IND	0.0030	0.0025	0.7691	0.2250	0.0004
311162	PI	400127	60-283	Guyana	South_America	1975-5-7	IND	0.0004	0.0003	0.9992	0.0001	0.0001
311163	PI	400473	Chuan Chu Tan Dau Bir	China	China	1975-6-3	IND	0.0003	0.0008	0.9982	0.0002	0.0004
311164	PI	400492	Chin Chin Goo	China	China	1975-6-3	IND	0.0004	0.0003	0.9989	0.0004	0.0001
311165	PI	400581	Man Taro Mai	Japan	North_Pacific	1975-6-3	TEJ	0.0023	0.7904	0.2069	0.0003	0.0001
311166	PI	400589	Bulu Pote	Indonesia	Oceania	1975-6-3	TEJ	0.0004	0.9995	0.0001	0.0000	0.0001
311167	PI	400607	TAINUNG 45	Taiwan	China	1975-6-3	IND	0.0107	0.0081	0.9801	0.0003	0.0007
311168	PI	400675	IR 9-60	Philippines	South_Pacific	1975-6-3	IND	0.0001	0.0001	0.9996	0.0001	0.0000
311169	PI	400678	Nilo 2	Suriname	South_America	1975-6-3	TRJ-IND	0.4956	0.0018	0.4993	0.0022	0.0012
311170	PI	400708	GPNO 23386	Taiwan	China	1975-6-3	TEJ	0.0004	0.7583	0.2411	0.0001	0.0001
311171	PI	400720	Ranga Khavli	Indonesia	Oceania	1975-6-3	ARO	0.0006	0.0006	0.0007	0.0036	0.9943
311172	PI	400738	SML APURA	Suriname	South_America	1975-6-3	IND	0.2271	0.0068	0.7538	0.0116	0.0008
311173	PI	400771	Manga 629	Madagascar	Africa	1975-6-3	IND-AUS	0.0085	0.0016	0.5916	0.3982	0.0001
311174	PI	400773	Vary Vato 275	Madagascar	Africa	1975-6-3	AUS	0.0001	0.0001	0.0006	0.9991	0.0001
311175	PI	400776	Tsilaitranakoho 706	Madagascar	Africa	1975-6-3	TRJ-AUS-IND	0.3654	0.0009	0.3109	0.3226	0.0003
311176	PI	400784	Pai K'o Hua Lon Toucheng	Taiwan	China	1975-6-3	IND	0.0001	0.0001	0.9997	0.0001	0.0000
311177	PI	401452	SUNG LIAO 2	China	China	1975-6-10	TEJ	0.0004	0.9993	0.0001	0.0001	0.0001
311178	PI	401458	29 LU 1	China	China	1975-6-10	IND	0.0002	0.0001	0.9996	0.0001	0.0000
311179	PI	402527	ACORNI	Suriname	South_America	1975-6-19	IND	0.2767	0.0057	0.6423	0.0650	0.0103
311180	PI	402673	Sapundali Local	India	Southern_Asia	1975-8-4	IND-AUS	0.0008	0.0022	0.5719	0.4189	0.0062
311181	PI	402689	Tauli	Nepal	Southern_Asia	1975-8-4	AUS	0.0002	0.0001	0.0005	0.9991	0.0001
311182	PI	402702	560A	Mali	Africa	1975-8-4	IND	0.0003	0.0005	0.9983	0.0007	0.0002
311183	PI	402705	WC 5730	Thailand	Southeast_Asia	1975-8-4	TRJ	0.9994	0.0004	0.0001	0.0000	0.0001
311184	PI	402752	Bang Tuey	Thailand	Southeast_Asia	1975-8-4	IND	0.0002	0.0003	0.9987	0.0006	0.0002
311185	PI	402794	Bombon	Spain	Western_Europe	1975-8-4	TEJ	0.2877	0.7101	0.0008	0.0001	0.0013
311186	PI	402860	CA 902/8/2/2	Chad	Africa	1975-8-4	TRJ	0.9987	0.0009	0.0002	0.0001	0.0001
311187	PI	402914	Cristal de Angola	Brazil	South_America	1975-8-4	IND	0.0014	0.0003	0.9980	0.0003	0.0001
311188	PI	402983	Dara	Indonesia	South_Pacific	1975-8-4	AUS	0.0008	0.0007	0.0006	0.9978	0.0001
311189	PI	403011	DD 62	Bangladesh	Southern_Asia	1975-8-4	AUS	0.0033	0.0005	0.3320	0.6639	0.0003
311190	PI	403241	Doble Carolina Rinaldo Barsani	Uruguay	South_America	1975-8-4	TEJ	0.0179	0.9818	0.0001	0.0001	0.0001
311191	PI	403306	DV 123	Bangladesh	Southern_Asia	1975-8-4	AUS	0.0001	0.0002	0.0003	0.9993	0.0001
311192	PI	403369	D 6-2-2	India	Southern_Asia	1975-8-4	IND	0.0028	0.0007	0.7496	0.2467	0.0002
311193	PI	403391	Java Long Grain	Indonesia	South_Pacific	1975-8-4	AUS	0.0002	0.0002	0.0007	0.9989	0.0001
311194	PI	403418	GIONG CHIEM 351	Vietnam	Southeast_Asia	1975-8-4	IND	0.0164	0.0005	0.9801	0.0006	0.0023
311195	PI	403425	GOIANA 465	Brazil	South_America	1975-8-4	TRJ	0.9983	0.0014	0.0001	0.0000	0.0001

311196	PI	403466	SHINRIKI 11	Japan	North_Pacific	1975-8-4	TEJ	0.0007	0.9941	0.0051	0.0000	0.0001
311197	PI	403521	IAC 9	Brazil	South_America	1975-8-4	TRJ	0.9993	0.0003	0.0001	0.0001	0.0002
311198	PI	403546	WC 6570	Spain	Western_Europe	1975-8-4	TEJ	0.3024	0.6974	0.0001	0.0001	0.0001
311199	PI	403596	Jhona 5715	Pakistan	Southern_Asia	1975-8-4	AUS	0.0002	0.0002	0.0002	0.9992	0.0001
311200	PI	403627	KALILA 50	Madagascar	Africa	1975-8-4	TRJ	0.9982	0.0014	0.0003	0.0001	0.0001
311201	PI	403640	KARATALSKIJ 86	Kazakhstan	Central_Asia	1975-8-4	TEJ	0.0012	0.9984	0.0001	0.0000	0.0002
311202	PI	403943	REIHO	Japan	North_Pacific	1975-9-5	IND	0.1190	0.0009	0.8787	0.0011	0.0004
311203	PI	404086	02.00.14	Japan	North_Pacific	1975-9-10	IND	0.0002	0.0001	0.9995	0.0001	0.0000
311204	PI	406035	CA 902/b/2/2	Chad	Africa	1975-11-13	TRJ	0.9959	0.0007	0.0020	0.0004	0.0010
311205	PI	406041	CTG 1516	Bangladesh	Southern_Asia	1975-11-13	AUS	0.0001	0.0001	0.0005	0.9993	0.0001
311206	PI	406073	79	Guyana	South_America	1975-11-13	ARO	0.0003	0.0003	0.0001	0.0002	0.9990
311207	PI	406074	NP 97	India	Southern_Asia	1975-11-13	AUS	0.0001	0.0001	0.0004	0.9993	0.0001
311208	PI	408365	BR51-114-2	Bangladesh	Southern_Asia	1975-12-1	IND	0.0010	0.0003	0.9937	0.0048	0.0001
311209	PI	408375	X69-56-12-19-6-3	Myanmar	Southeast_Asia	1975-12-1	IND	0.0024	0.0009	0.9961	0.0004	0.0002
311210	PI	408473	IR 2151-745-3-1	Philippines	South_Pacific	1975-6-1	IND	0.0388	0.0095	0.9509	0.0006	0.0002
311211	PI	408559	BW 191	Sri Lanka	Southern_Asia	1975-5-1	IND	0.0130	0.0007	0.9737	0.0115	0.0011
311212	PI	408563	BKN 6323-17	Thailand	Southeast_Asia	1975-12-1	IND	0.0000	0.0001	0.9995	0.0003	0.0000
311213	PI	408591	BIPLAB	Bangladesh	Southern_Asia	1975-6-1	IND	0.0001	0.0003	0.9993	0.0003	0.0000
311214	PI	408642	IR 1514A-E597	Philippines	South_Pacific	1975-12-1	IND	0.0016	0.0014	0.9966	0.0004	0.0000
311215	PI	408673	KLG 6986-161-7	Thailand	Southeast_Asia	1975-12-1	IND	0.0012	0.0010	0.9972	0.0005	0.0001
311216	PI	412772	*BASMATI 802	Pakistan	Southern_Asia	1976-6-30	ARO	0.0005	0.0004	0.0009	0.3270	0.6712
311217	PI	412800	Sella Manzkhora	Pakistan	Southern_Asia	1976-6-30	IND	0.0588	0.0186	0.9173	0.0004	0.0048
311218	PI	412902	Mushkan	Pakistan	Southern_Asia	1976-6-30	ARO	0.0006	0.0005	0.0005	0.0020	0.9964
311219	PI	412914	SUWEON 258	Korea_ South	North_Pacific	1976-7-20	IND	0.0006	0.1113	0.8879	0.0001	0.0001
311220	PI	413734	YR 44	Australia	Oceania	1976-7-19	TRJ	0.9895	0.0056	0.0002	0.0001	0.0046
311221	PI	413818	CHINA 1039-3 DWARF MUTANT	Philippines	South_Pacific	1976-11-10	IND	0.0005	0.0005	0.9988	0.0002	0.0001
311222	PI	413890	AGAMI MONT 1	Egypt	Mideast	1976-11-10	TEJ	0.1950	0.8047	0.0001	0.0001	0.0001
311223	PI	413929	KN-1 B-361-BLK-2	Indonesia	South_Pacific	1976-11-10	IND	0.0002	0.0002	0.9995	0.0001	0.0000
311224	PI	414239	Colombia 2	Colombia	South_America	1976-12-13	TRJ-IND-TEJ	0.5823	0.1938	0.2007	0.0003	0.0229
311225	PI	414682	SLO 17	India	Southern_Asia	1977-2-2	IND	0.0002	0.0005	0.9918	0.0073	0.0001
311226	PI	415656	BALDO	Italy	Western_Europe	1977-4-25	TEJ	0.1082	0.8915	0.0001	0.0001	0.0001
311227	PI	415664	Sari Celtik	Turkey	Mideast	1977-4-25	TEJ	0.0060	0.9937	0.0001	0.0000	0.0001
311228	PI	415673	Galaxia	Puerto Rico	Central_America	1977-4-21	TRJ	0.9993	0.0004	0.0001	0.0000	0.0001
311229	PI	415674	Gema	Puerto Rico	Central_America	1977-4-21	TEJ-TRJ	0.4502	0.5351	0.0141	0.0005	0.0002
311230	PI	415675	Girona	Puerto Rico	Central_America	1977-4-21	TEJ	0.0054	0.9945	0.0001	0.0000	0.0000
311231	PI	415723	KAOHSIUNG 136	Taiwan	China	1977-4-15	TEJ	0.0005	0.9993	0.0001	0.0000	0.0001
311232	PI	415761	TAITUNG YU 303	Taiwan	China	1977-4-15	TEJ	0.0011	0.9649	0.0337	0.0002	0.0001
311233	PI	415773	TUNGLU YU 286	Taiwan	China	1977-4-15	TEJ	0.3586	0.6405	0.0004	0.0001	0.0004
311234	PI	415775	Wan Li Hsien	Taiwan	China	1977-4-15	IND	0.0002	0.0001	0.9986	0.0009	0.0002
311235	PI	415784	LAC 23	Liberia	Africa	1977-5-23	TRJ	0.9986	0.0011	0.0002	0.0001	0.0001
311236	PI	417820	B805D-MR-16-8-3	Indonesia	South_Pacific	1977-6-7	IND	0.0004	0.0003	0.9107	0.0010	0.0876
311237	PI	417833	BW248-1	Sri Lanka	Southern_Asia	1977-6-7	IND	0.0003	0.0116	0.9872	0.0005	0.0003
311238	PI	418205	Chen Chu Ai	Sierra Leone	Africa	1977-7-15	IND	0.0001	0.0002	0.9995	0.0001	0.0000
311239	PI	419447	Pratao Tipo Guedes	Brazil	South_America	1977-8-7	TRJ	0.9991	0.0007	0.0001	0.0000	0.0001
311240	PI	420143	Llanero 501	Venezuela	South_America	1977-10-18	TRJ	0.8615	0.0005	0.0001	0.0001	0.1378
311241	PI	420193	Cabrerita	Dominican Republic	Central_America	1977-9-12	IND	0.0004	0.0002	0.9992	0.0001	0.0001
311242	PI	420195	Marole	Dominican Republic	Central_America	1977-9-12	IND	0.0003	0.0002	0.9993	0.0003	0.0000
311243	PI	420954	Camponi SML	Suriname	South_America	1977-12-14	IND	0.1815	0.0015	0.8143	0.0017	0.0010
311244	PI	420961	INTI	Peru	South_America	1977-12-14	IND	0.0043	0.0073	0.9712	0.0015	0.0157
311245	PI	420968	Col. 10694	Turkey	Mideast	1977-11-30	TEJ	0.0207	0.8401	0.0001	0.0002	0.1388
311246	PI	420983	Thapachini	Nepal	Southern_Asia	1977-11-30	TEJ-TRJ	0.4823	0.5173	0.0001	0.0001	0.0002
311247	PI	429770	STIRPE	Brazil	South_America	1978-9-25	TEJ	0.1176	0.8822	0.0001	0.0000	0.0001
311248	PI	430251	Mingolo	Dominican Republic	Central_America	1978-11-15	IND	0.0002	0.0003	0.9916	0.0076	0.0003
311249	PI	430254	TONO BREA 439	Dominican Republic	Central_America	1978-11-15	IND	0.0001	0.0002	0.9995	0.0001	0.0001

311250	PI	430321	Priano Guaira	Brazil	South_America	1978-11-30	TRJ	0.9990	0.0007	0.0002	0.0000	0.0001
311251	PI	430323	CICA 4	Colombia	South_America	1978-11-30	IND	0.0001	0.0001	0.9998	0.0001	0.0000
311252	PI	430334	AJRAL	Fiji	Oceania	1978-11-30	IND	0.0004	0.0005	0.9988	0.0002	0.0001
311253	PI	430336	BILO	Fiji	Oceania	1978-11-30	IND	0.0002	0.0002	0.9994	0.0002	0.0000
311254	PI	430337	Boldgrain	Fiji	Oceania	1978-11-30	IND	0.0007	0.0003	0.9981	0.0008	0.0001
311255	PI	430339	Saraya	Fiji	Oceania	1978-11-30	AUS	0.0001	0.0011	0.0002	0.9986	0.0000
311256	PI	430384	BAMANGBA II	Zaire	Africa	1978-12-4	TRJ	0.9504	0.0482	0.0002	0.0004	0.0007
311257	PI	430385	Basala Baatka S-R	Zaire	Africa	1978-12-4	TRJ	0.9990	0.0006	0.0002	0.0001	0.0001
311258	PI	430387	Botika S/R	Zaire	Africa	1978-12-4	TRJ	0.9981	0.0013	0.0002	0.0001	0.0002
311259	PI	430388	Goli	Zaire	Africa	1978-12-4	TRJ	0.9988	0.0006	0.0003	0.0001	0.0001
311260	PI	430395	Mbiyo	Zaire	Africa	1978-12-4	TRJ	0.6825	0.2443	0.0560	0.0035	0.0137
311261	PI	430401	OS 16	Zaire	Africa	1978-12-4	TRJ	0.9991	0.0006	0.0001	0.0001	0.0001
311262	PI	430409	R 46/3	Zaire	Africa	1978-12-4	TRJ	0.9413	0.0583	0.0003	0.0001	0.0001
311263	PI	430441	R 101	Zaire	Africa	1978-12-4	TRJ	0.9917	0.0079	0.0002	0.0001	0.0001
311264	PI	430443	Sechele	Zaire	Africa	1978-12-4	TRJ	0.9912	0.0084	0.0001	0.0001	0.0002
311265	PI	430447	Zumbulu	Zaire	Africa	1978-12-4	TRJ	0.7484	0.1827	0.0685	0.0003	0.0002
311266	PI	430740	CO 13	India	Southern_Asia	1978-12-29	IND	0.0006	0.0005	0.7872	0.2116	0.0002
311267	PI	430915	Jan-38	Pakistan	Southern_Asia	1978-12-29	AUS	0.0001	0.0002	0.0004	0.9989	0.0004
311268	PI	430976	Shim Balte	Iraq	Mideast	1978-12-29	AUS	0.0001	0.0003	0.0003	0.9990	0.0002
311269	PI	430979	Shimla Early	Iraq	Mideast	1978-12-29	IND-AUS	0.0022	0.0324	0.5955	0.3698	0.0001
311270	PI	430991	Bara Peshanari	Pakistan	Southern_Asia	1978-12-29	ARO	0.0004	0.0006	0.0004	0.0007	0.9979
311271	PI	431009	Pachodi 460	India	Southern_Asia	1978-12-29	IND	0.0008	0.0005	0.9423	0.0561	0.0003
311272	PI	431061	Sadri Dum Sufaid	Iran	Mideast	1978-12-29	IND	0.0003	0.0045	0.9944	0.0004	0.0003
311273	PI	431062	Champa Zoodrus	Iran	Mideast	1978-12-29	AUS	0.0430	0.0005	0.0006	0.7653	0.1906
311274	PI	431065	Qari Bak	Iran	Mideast	1978-12-29	IND	0.0002	0.0004	0.9986	0.0007	0.0001
311275	PI	431082	Sia Bud Via	Thailand	Southeast_Asia	1978-12-29	IND-AUS	0.0026	0.0107	0.5926	0.3937	0.0005
311276	PI	431083	A 31 12 Late	Myanmar	Southeast_Asia	1978-12-29	IND-AUS	0.0026	0.0084	0.5944	0.3943	0.0003
311277	PI	431087	Ghoal Champa	Iran	Mideast	1978-12-29	IND	0.0002	0.0014	0.8625	0.1358	0.0001
311278	PI	431092	Montakcl	Egypt	Mideast	1978-12-29	AUS	0.0004	0.0002	0.0048	0.9944	0.0002
311279	PI	431111	WB 103	Pakistan	Southern_Asia	1978-12-29	AUS	0.0004	0.0003	0.3886	0.6096	0.0012
311280	PI	431125	NORIN 18	Japan	North_Pacific	1978-12-29	IND	0.0001	0.0001	0.9997	0.0001	0.0000
311281	PI	431128	A 152	Bangladesh	Southern_Asia	1978-12-29	IND-TRJ	0.3838	0.0357	0.5372	0.0202	0.0231
311282	PI	431158	Egypt 1	Egypt	Mideast	1978-12-29	IND	0.0155	0.0012	0.9706	0.0008	0.0119
311283	PI	431165	Palwan	Philippines	South_Pacific	1978-12-29	ARO	0.0005	0.0003	0.0003	0.0003	0.9985
311284	PI	431172	LA PLATA GENA F.A.	Argentina	South_America	1978-12-29	AUS	0.0002	0.0002	0.0004	0.9991	0.0001
311285	PI	431195	Vulgaris Ko Ch Azpasaly	Uzbekistan	Central_Asia	1978-12-29	IND	0.0006	0.0003	0.9989	0.0002	0.0001
311286	PI	431201	UZ ROS 59	Uzbekistan	Central_Asia	1978-12-29	IND	0.0006	0.0006	0.9984	0.0002	0.0001
311287	PI	431207	Guanicagust Soclri Masayensnif	Azerbaijan	Central_Asia	1978-12-29	IND	0.0020	0.0009	0.9969	0.0001	0.0001
311288	PI	431209	Italica Sojuzryi 244	Former Soviet Union	Eastern_Europe	1978-12-29	IND	0.0001	0.0001	0.9997	0.0001	0.0000
311289	PI	431227	Peroz	Iran	Mideast	1978-12-29	AUS	0.0002	0.0002	0.3158	0.6835	0.0002
311290	PI	431251	*Basmati	Pakistan	Southern_Asia	1978-12-29	ARO	0.0004	0.0003	0.0003	0.0005	0.9986
311291	PI	431267	HZ ROS 637	Uzbekistan	Central_Asia	1978-12-29	IND	0.0001	0.0001	0.9996	0.0001	0.0000
311292	PI	431293	Yukare	Japan	North_Pacific	1978-12-29	ARO	0.0004	0.0025	0.0001	0.0001	0.9969
311293	PI	431324	Tetep	Vietnam	Southeast_Asia	1978-12-29	ARO	0.0010	0.0006	0.1687	0.0014	0.8283
311294	PI	431328	CAS 209	Senegal	Africa	1978-12-29	IND	0.0002	0.0004	0.9992	0.0001	0.0000
311295	PI	431369	P 1319	Turkey	Mideast	1978-12-29	TEJ	0.0016	0.6372	0.1982	0.1627	0.0004
311296	PI	431420	C4-63	Philippines	South_Pacific	1978-12-29	IND	0.0001	0.0003	0.9993	0.0003	0.0000
311297	PI	431439	KT 29	Nepal	Southern_Asia	1978-12-29	AUS	0.0002	0.0002	0.0003	0.9992	0.0002
311298	PI	431482	Jek Chuey 159	Thailand	Southeast_Asia	1979-2-1	IND	0.0002	0.0008	0.9987	0.0003	0.0001
311299	PI	432553	Tsao A 057	China	China	1979-3-1	TEJ	0.0006	0.8322	0.1669	0.0001	0.0002
311300	PI	433509	RINGO	Italy	Western_Europe	1979-5-1	TEJ	0.0014	0.9983	0.0001	0.0000	0.0001
311301	PI	433512	ROMEO	Italy	Western_Europe	1979-5-1	TEJ	0.2352	0.7644	0.0002	0.0001	0.0002
311302	PI	433797	SL 22-613	Sierra Leone	Africa	1979-6-1	IND	0.3089	0.0005	0.6543	0.0303	0.0060
311303	PI	433808	SL 22-642	Sierra Leone	Africa	1979-6-1	IND	0.0011	0.0002	0.9983	0.0003	0.0001
311304	PI	433832	ADNY 11	Nigeria	Africa	1979-6-1	IND	0.0001	0.0001	0.9996	0.0001	0.0000

311305	PI	433843	IB 94	Nigeria	Africa	1979-6-1	TRJ	0.9991	0.0005	0.0003	0.0000	0.0001
311306	PI	433857	Mange 2	Nigeria	Africa	1979-6-1	IND	0.0001	0.0001	0.9996	0.0001	0.0001
311307	PI	433905	IRAT 110	Cote D'Ivoire	Africa	1979-7-1	TRJ	0.9618	0.0370	0.0004	0.0007	0.0001
311308	PI	433911	IRAT 116	Cote D'Ivoire	Africa	1979-7-1	TRJ	0.9987	0.0011	0.0001	0.0001	0.0001
311309	PI	433922	IRAT 142	Cote D'Ivoire	Africa	1979-7-1	TRJ	0.9185	0.0809	0.0003	0.0002	0.0001
311310	PI	439043	Archana	India	Southern_Asia	1980-1-1	IND	0.0002	0.0002	0.9941	0.0054	0.0000
311311	PI	439090	RATNAGIRI 68-1-1	India	Southern_Asia	1980-1-1	IND	0.0003	0.0003	0.9992	0.0002	0.0001
311312	PI	439113	CH 434-94	Chile	South_America	1980-1-1	AUS	0.0002	0.0001	0.0004	0.9993	0.0001
311313	PI	439118	Oro	Chile	South_America	1980-1-1	TEJ	0.0003	0.9995	0.0001	0.0000	0.0001
311314	PI	439119	Quella	Chile	South_America	1980-1-1	TEJ	0.0935	0.9063	0.0001	0.0000	0.0001
311315	PI	439121	ARABI	Egypt	Mideast	1979-8-1	TEJ-TRJ	0.4437	0.5172	0.0300	0.0088	0.0003
311316	PI	439131	GIZA 159	Egypt	Mideast	1979-8-1	TEJ	0.0092	0.9905	0.0001	0.0000	0.0002
311317	PI	439137	IR 1615-246	Philippines	South_Pacific	1979-8-1	IND	0.0006	0.0007	0.9986	0.0001	0.0001
311318	PI	439140	Nahda	Egypt	Mideast	1979-8-1	TEJ	0.0003	0.9996	0.0001	0.0000	0.0000
311319	PI	439144	YABANI LULU	Egypt	Mideast	1979-8-1	TEJ	0.0002	0.9997	0.0001	0.0000	0.0000
311320	PI	439617	Amaura	Russian Federation	Eastern_Europe	1980-2-1	TEJ	0.0021	0.9949	0.0003	0.0001	0.0026
311321	PI	439625	Vavilovi	Kazakhstan	Central_Asia	1980-2-1	TEJ	0.0013	0.9875	0.0011	0.0018	0.0084
311322	PI	439639	Chaltyk Champa	Iran	Mideast	1980-2-1	AUS	0.0001	0.0001	0.0004	0.9993	0.0002
311323	PI	439641	Ak Kylcik Mestnyj	Azerbaijan	Central_Asia	1980-2-1	TEJ	0.0009	0.9966	0.0008	0.0013	0.0004
311324	PI	439647	Astrahanskij Skoros-pelyi	Russian Federation	Eastern_Europe	1980-2-1	TEJ	0.0065	0.9928	0.0001	0.0002	0.0004
311325	PI	439649	Bajang Allorio	Italy	Western_Europe	1980-2-1	IND	0.0004	0.0004	0.9990	0.0002	0.0001
311326	PI	439661	DONSKOJ 2	Russian Federation	Eastern_Europe	1980-2-1	TEJ	0.0020	0.9972	0.0002	0.0001	0.0006
311327	PI	439669	Gasym Hany	Azerbaijan	Central_Asia	1980-2-1	ARO	0.0010	0.0050	0.0001	0.0002	0.9936
311328	PI	439670	Hodza Ahmat	Uzbekistan	Central_Asia	1980-2-1	TEJ	0.0052	0.7783	0.0001	0.0003	0.2161
311329	PI	439671	Hokkajdo	Russian Federation	Eastern_Europe	1980-2-1	TEJ	0.0018	0.9904	0.0002	0.0055	0.0021
311330	PI	439679	Kesa	Azerbaijan	Central_Asia	1980-2-1	ARO	0.0028	0.1079	0.1479	0.0007	0.7408
311331	PI	439730	UZBEKSKIJ 2	Uzbekistan	Central_Asia	1980-2-1	TEJ	0.0005	0.9993	0.0001	0.0001	0.0001
311332	PI	442136	YR 71003-9	Australia	Oceania	1980-4-1	TEJ	0.0826	0.8712	0.0458	0.0002	0.0002
311333	PI	442140	NAVILE	Italy	Western_Europe	1980-4-1	TEJ	0.0216	0.9781	0.0001	0.0000	0.0001
311334	PI	442953	E 425	Senegal	Africa	1980-5-1	TRJ	0.9993	0.0004	0.0001	0.0000	0.0001
311335	PI	442978	IR 1746-194-1-1-1	Philippines	South_Pacific	1980-5-1	AUS	0.0002	0.0001	0.0009	0.9988	0.0001
311336	PI	443001	DM 59	Bangladesh	Southern_Asia	1980-5-1	AUS	0.0001	0.0001	0.0005	0.9992	0.0001
311337	PI	445964	KAIRYOSHINKO	Japan	North_Pacific	1980-6-1	IND	0.0003	0.0002	0.9984	0.0010	0.0002
311338	PI	452428	MR 1	Malaysia	South_Pacific	1980-12-1	IND	0.0001	0.0001	0.9995	0.0002	0.0001
311339	PI	458462	Zoria	Turkey	Mideast	1981-3-1	TEJ	0.0004	0.9994	0.0001	0.0000	0.0001
311340	PI	458470	IITA 135	Nigeria	Africa	1981-3-1	TRJ	0.8781	0.0011	0.1206	0.0002	0.0001
311341	PI	458475	63-83	Cote D'Ivoire	Africa	1981-3-1	TRJ	0.9990	0.0006	0.0002	0.0001	0.0001
311342	PI	458478	RD 7	Thailand	Southeast_Asia	1981-4-1	IND	0.1253	0.0008	0.8728	0.0008	0.0002
311343	PI	458483	IET 6187	India	Southern_Asia	1981-4-1	IND	0.0004	0.0003	0.9243	0.0750	0.0001
311344	PI	458488	IR 9209-26-2	Philippines	South_Pacific	1981-4-1	IND	0.0002	0.0001	0.9996	0.0001	0.0000
311345	PI	458755	CRISTAL	France	Western_Europe	1981-4-1	TEJ	0.0231	0.9767	0.0001	0.0001	0.0001
311346	PI	459028	B 541B-PN-58-5-3-1	Indonesia	South_Pacific	1981-6-1	IND	0.0002	0.0001	0.9986	0.0010	0.0001
311347	PI	464599	IR 19759-21-3-3-2	Philippines	South_Pacific	1981-11-1	IND	0.0001	0.0001	0.9993	0.0004	0.0001
311348	PI	464623	SEOGWANGBYEO	Korea_ South	North_Pacific	1981-11-1	IND	0.0045	0.0261	0.9685	0.0003	0.0006
311349	PI	490796	Tox 782-20-1	Nigeria	Africa	1984-8-1	TRJ	0.9980	0.0012	0.0002	0.0004	0.0002
311350	PI	490805	Tox 1417-17-SB	Nigeria	Africa	1984-8-1	TRJ	0.9335	0.0049	0.0585	0.0029	0.0002
311351	PI	493134	Bungan B	Malaysia	South_Pacific	1984-12-1	TRJ	0.8392	0.1572	0.0010	0.0004	0.0023
311352	PI	493138	IR 10176-24-6-2	Philippines	South_Pacific	1984-12-1	IND	0.0002	0.0001	0.9983	0.0014	0.0000
311353	PI	494757	HUNAN EARLY DWARF NO. 3	China	China	1985-2-1	IND	0.0002	0.0001	0.9996	0.0001	0.0000
311354	PI	502690	Arroz en Granza 106 Selection	Guatemala	Central_America	1920-5-1	TRJ	0.7267	0.0026	0.2642	0.0050	0.0015
311355	PI	502967	GULFMONT	United States	North_America	1986-3-1	TRJ	0.9986	0.0004	0.0009	0.0001	0.0001
311356	PI	503036	CHAO LANG 1 HAO	China	China	1986-2-1	IND	0.0002	0.0002	0.9995	0.0001	0.0000
311357	PI	503051	14757	Colombia	South_America	1986-2-1	IND	0.0023	0.0850	0.9122	0.0003	0.0001
311358	PI	503068	16438	Colombia	South_America	1986-2-1	IND	0.0153	0.0687	0.9157	0.0001	0.0002

311359	PI	503119	17632	Colombia	South_America	1986-2-1	IND	0.0003	0.0004	0.9498	0.0489	0.0006
311360	PI	503137	19965	Colombia	South_America	1986-2-1	IND	0.0004	0.0025	0.9963	0.0006	0.0003
311361	PI	503157	G-158	Hungary	Eastern_Europe	1986-2-1	TEJ	0.0013	0.9984	0.0001	0.0001	0.0001
311362	PI	503169	UPL RI-5	Philippines	South_Pacific	1986-2-1	IND	0.0014	0.0253	0.9657	0.0065	0.0011
311363	PI	506225	78Y81	United States	North_America	1986-12-1	TRJ	0.6872	0.3126	0.0001	0.0000	0.0001
311364	PI	514666	SACHIMINORI	Japan	North_Pacific	1987-12-18	TEJ	0.0010	0.9988	0.0001	0.0000	0.0001
311365	PI	514668	TODOROKIWASE	Japan	North_Pacific	1987-12-18	TEJ	0.0006	0.9993	0.0001	0.0000	0.0000
311366	PI	536047	Te Qing	China	China	1989-4-10	IND	0.0005	0.0005	0.9986	0.0001	0.0002
311367	PI	543874	SLG 12	Japan	North_Pacific	1989-5-16	TEJ	0.0600	0.8018	0.0020	0.0014	0.1348
311368	PI	560216	FANNY DWARF	France	Western_Europe	1990-1-16	TEJ	0.0302	0.9694	0.0001	0.0000	0.0002
311369	PI	560217	TAINAN 5-72-536	Taiwan	China	1990-1-16	TEJ	0.0003	0.9995	0.0001	0.0000	0.0000
311370	PI	560268	CT6515-18-1-3-1-4	Colombia	South_America	1990-1-24	TRJ	0.7463	0.0805	0.1635	0.0079	0.0018
311371	PI	560276	ESTRELA	Colombia	South_America	1990-1-24	TRJ-TEJ	0.4987	0.4181	0.0813	0.0017	0.0002
311372	PI	560285	P 3084F4-56-2-2	Colombia	South_America	1990-1-24	IND	0.0007	0.0017	0.9970	0.0004	0.0002
311373	PI	560297	Santa Julia	Colombia	South_America	1990-12-12	IND	0.0004	0.0025	0.9553	0.0413	0.0006
311374	PI	564573	Podiratawee	Sri Lanka	Southern_Asia	1992-12-17	IND	0.0004	0.0006	0.9130	0.0856	0.0004
311375	PI	564578	N 11061-71	El Salvador	Central_America	1992-12-17	TRJ	0.7699	0.0005	0.2289	0.0006	0.0001
311376	PI	574421	EUROSE	Italy	Western_Europe	1992-7-29	TEJ	0.2160	0.7838	0.0001	0.0000	0.0001
311377	PI	574444	SORRISO	Italy	Western_Europe	1992-7-29	TEJ	0.3051	0.6946	0.0001	0.0001	0.0001
311378	PI	574445	STAR	Italy	Western_Europe	1992-7-29	TRJ	0.9893	0.0104	0.0001	0.0001	0.0001
311379	PI	574658	BR1	Bangladesh	Southern_Asia	1993-7-28	IND	0.0026	0.1774	0.8111	0.0086	0.0003
311380	PI	574680	BR24	Bangladesh	Southern_Asia	1993-7-28	IND	0.0714	0.0005	0.9256	0.0016	0.0010
311381	PI	575182	Jamir	Bangladesh	Southern_Asia	1993-7-28	AUS	0.0005	0.0119	0.0036	0.9834	0.0005
311382	PI	575212	Ghorbhai	Bangladesh	Southern_Asia	1993-7-28	AUS	0.0011	0.0011	0.0292	0.9678	0.0008
311383	PI	584555	DARMALI	Nepal	Southern_Asia	1991-7-5	TEJ-ARO-TRJ	0.1292	0.4689	0.0008	0.1083	0.2928
311384	PI	584557	CHAHORA 144	Pakistan	Southern_Asia	1991-7-5	IND-ARO	0.0007	0.0004	0.5800	0.0052	0.4137
311385	PI	584567	KAUKKYI ANI	Myanmar	Southeast_Asia	1991-7-5	TRJ	0.6494	0.3200	0.0256	0.0013	0.0038
311386	PI	584569	*FIROOZ	Iran	Mideast	1991-7-5	ARO	0.0005	0.0007	0.0011	0.0004	0.9973
311387	PI	584570	ARIAS	Indonesia	South_Pacific	1991-7-5	TRJ	0.8871	0.0787	0.0002	0.0020	0.0320
311388	PI	584572	GOTAK GATIK	Indonesia	South_Pacific	1991-7-5	TRJ	0.8334	0.0011	0.0192	0.0070	0.1393
311389	PI	584608	Dom Zard	Iran	Mideast	1991-7-5	ARO	0.0005	0.0007	0.0002	0.0002	0.9984
311390	PI	584611	Yancaousa	Cote D'Ivoire	Africa	1991-7-5	TRJ	0.9987	0.0010	0.0002	0.0001	0.0001
311391	PI	584613	Tres Meses	Brazil	South_America	1991-7-5	TRJ	0.9568	0.0009	0.0421	0.0002	0.0001
311392	PI	584618	WIR 1528	Azerbaijan	Central_Asia	1992-6-2	TEJ	0.0019	0.9972	0.0002	0.0001	0.0007
311393	PI	584629	Celiaj	Azerbaijan	Central_Asia	1992-6-2	TEJ	0.0137	0.9858	0.0001	0.0002	0.0003
311394	PI	584637	KROS 358	Kazakhstan	Central_Asia	1992-6-2	TEJ	0.0024	0.9972	0.0001	0.0001	0.0002
311395	PI	584644	SPALCIK	Russian Federation	Eastern_Europe	1992-6-2	TEJ	0.0004	0.9993	0.0002	0.0001	0.0000
311396	PI	584649	INTENSIVNYJ	Uzbekistan	Central_Asia	1992-6-2	TEJ	0.0005	0.9991	0.0002	0.0000	0.0001
311397	PI	584650	AVANGARD	Uzbekistan	Central_Asia	1992-6-2	TEJ	0.0018	0.9981	0.0001	0.0000	0.0001
311398	PI	584651	GORIZONT	Russian Federation	Eastern_Europe	1992-6-2	TEJ	0.0004	0.9991	0.0002	0.0001	0.0002
311399	PI	584660	AMISTAD 82	Colombia	South_America	1993-3-23	IND	0.0007	0.0008	0.9984	0.0001	0.0001
311400	PI	584661	CR1821	Costa Rica	Central_America	1993-3-23	IND	0.0020	0.0019	0.9766	0.0004	0.0191
311401	PI	584663	EL PASO L-144	Uruguay	South_America	1993-3-23	IND	0.0003	0.0003	0.9993	0.0001	0.0000
311402	PI	584666	INIAP 11	Ecuador	South_America	1993-3-23	IND	0.0001	0.0001	0.9996	0.0002	0.0000
311403	PI	584669	PANAMA 1048	Colombia	South_America	1993-3-23	IND	0.0005	0.0003	0.9987	0.0002	0.0003
311404	PI	584671	X-10	El Salvador	Central_America	1993-3-23	IND	0.0792	0.0027	0.9176	0.0003	0.0001
311405	PI	584678	HURI 282	Colombia	South_America	1993-3-23	IND	0.0005	0.0004	0.9989	0.0001	0.0001
311406	PI	584680	TAICHUNG SEN YU 10	Taiwan	China	1993-3-23	TEJ	0.0007	0.9989	0.0002	0.0001	0.0001
311407	PI	584688	CT9901-1-7-M	Colombia	South_America	1993-3-23	TRJ	0.8814	0.0136	0.1047	0.0002	0.0001
311408	PI	584742	ARAURE 4	Venezuela	South_America	1991-4-23	IND	0.0018	0.0655	0.9316	0.0002	0.0010
311409	PI	584743	CAMPECHE A 80	Mexico	North_America	1991-4-23	IND	0.0157	0.0015	0.9825	0.0001	0.0001
311410	PI	584751	ICTA VIRGINIA	Guatemala	Central_America	1991-4-23	IND	0.0005	0.0003	0.9991	0.0001	0.0000
311411	PI	584756	SAN MARTIN 86	Peru	South_America	1991-4-23	IND	0.0003	0.0016	0.9038	0.0002	0.0941
311412	PI	584757	SAN PEDRO	Bolivia	South_America	1991-4-23	IND	0.0002	0.0001	0.9995	0.0001	0.0000
311413	PI	596811	ROJOFOTSY 738	Madagascar	Africa	1991-7-5	IND	0.0024	0.0024	0.6012	0.3938	0.0002

311414	PI	596835	DAL'RIS 13	Russian Federation	Eastern_Europe	1992-9-25	TEJ	0.0004	0.9994	0.0001	0.0000	0.0001
311415	PI	596872	BR827-35-2-1	Bangladesh	Southern_Asia	1993-8-23	IND	0.0001	0.0002	0.9991	0.0005	0.0000
311416	PI	596893	VILLAGUAY P.A.	Argentina	South_America	1993-8-23	TRJ	0.6801	0.2514	0.0680	0.0003	0.0002
311417	PI	596902	CNTLR80076-44-1-1-1	Thailand	Southeast_Asia	1993-8-23	IND	0.0002	0.0002	0.9957	0.0035	0.0005
311418	PI	596906	CU8068	Cuba	Central_America	1993-8-23	IND	0.0006	0.0004	0.9989	0.0001	0.0001
311419	PI	596914	H256-76-1-1-1	Argentina	South_America	1993-8-23	TRJ	0.8207	0.1393	0.0361	0.0002	0.0036
311420	PI	596936	PNA1005-F4-88-1	Peru	South_America	1993-8-23	IND	0.0055	0.0073	0.9772	0.0042	0.0059
311421	PI	596960	C2764-10-2	Philippines	South_Pacific	1993-8-23	IND	0.0045	0.0001	0.9950	0.0004	0.0001
311422	PI	596975	CT6741-CA-14	Chile	South_America	1993-8-23	TEJ	0.2075	0.7921	0.0002	0.0001	0.0002
311423	PI	596990	IR 58614-B-B-8-2	Philippines	South_Pacific	1993-8-23	IND	0.0010	0.0004	0.9968	0.0011	0.0006
311424	PI	597058	BL 1	Japan	North_Pacific	1994-6-29	TEJ	0.0005	0.9406	0.0588	0.0000	0.0001
311425	PI	597078	B 4142	Philippines	South_Pacific	1994-6-29	TEJ-TRJ-IND	0.2529	0.5447	0.1722	0.0004	0.0299
311426	PI	602605	AGUSITA	Hungary	Eastern_Europe	1994-8-7	TEJ	0.0014	0.9980	0.0004	0.0001	0.0002
311427	PI	602608	HC-7-2	Hungary	Eastern_Europe	1994-8-7	TEJ	0.0014	0.9981	0.0003	0.0001	0.0001
311428	PI	602610	KARMINA	Hungary	Eastern_Europe	1994-8-7	TEJ	0.0010	0.8437	0.1550	0.0002	0.0001
311429	PI	602636	WAB56-57	Cote D'Ivoire	Africa	1996-5-14	TRJ	0.9034	0.0411	0.0549	0.0003	0.0003
311430	PI	602652	ECIA 66	Cuba	Central_America	1996-5-14	IND	0.0035	0.0012	0.9950	0.0002	0.0001
311431	PI	602666	PALLAGI 67	Hungary	Eastern_Europe	1995-11-1	TEJ	0.0025	0.9970	0.0001	0.0001	0.0004
311432	PI	608405	WU FENG LENG SHUI ZHAN	China	China	1995-7-6	IND	0.0033	0.0009	0.9955	0.0002	0.0001
311433	PI	608418	IR 54055-142-2-1-2-3	Philippines	South_Pacific	1996-5-14	IND	0.0001	0.0002	0.9991	0.0005	0.0001
311434	PI	608430	LINE III_ HANOI	Vietnam	Southeast_Asia	1997-9-10	TEJ	0.0444	0.8570	0.0003	0.0003	0.0980
311435	PI	608431	CM1_ HAIPONG	Vietnam	Southeast_Asia	1997-9-10	IND	0.0018	0.0004	0.9950	0.0012	0.0016
311436	PI	614980	ZHONGYU NO. 1	China	China	1996-9-5	IND	0.0013	0.0077	0.9908	0.0001	0.0001
311437	PI	615011	Guineandao	Guinea	Africa	1996-9-5	TRJ	0.7906	0.2088	0.0002	0.0003	0.0002
311438	PI	615012	2071-621-2	Liberia	Africa	1996-9-5	IND	0.0296	0.0009	0.9692	0.0001	0.0002
311439	PI	615028	4582	China	China	1996-9-5	IND	0.0015	0.0005	0.9978	0.0001	0.0002
311440	PI	615048	4641-2	China	China	1996-9-5	IND	0.0007	0.0002	0.9989	0.0001	0.0001
311441	PI	614956	GP-2	China	China	1996-9-5	IND	0.0003	0.0002	0.9994	0.0001	0.0001
311442	PI	614957	IR58025 B	Philippines	South_Pacific	1996-9-5	IND	0.0253	0.0098	0.9356	0.0243	0.0049
311443	PI	614958	GUI 99	China	China	1996-9-5	IND	0.0005	0.0135	0.9858	0.0001	0.0001
311444	PI	614959	R 312	China	China	1996-9-5	IND	0.0016	0.0004	0.9977	0.0002	0.0002
311445	PI	614960	Z 535	China	China	1996-9-5	IND	0.0151	0.0251	0.9595	0.0002	0.0001
311446	PI	614961	R 147	China	China	1996-9-5	IND	0.0010	0.0004	0.9949	0.0007	0.0030
311447	PI	614962	XIANGZHAOXIAN NO. 15	China	China	1996-9-5	IND	0.0906	0.0137	0.8934	0.0018	0.0005
311448	PI	614963	HUNANRUANMI	China	China	1996-9-5	IND	0.0089	0.0031	0.9797	0.0079	0.0004
311449	PI	614965	ZHONGYU NO. 6	China	China	1996-9-5	IND	0.0013	0.0009	0.9976	0.0001	0.0001
311450	PI	614966	ZHENSHAN 97	China	China	1996-9-5	IND	0.0001	0.0010	0.9987	0.0001	0.0000
311451	PI	614968	ZHONGYOUZAO NO. 3	China	China	1996-9-5	IND	0.0050	0.0754	0.9189	0.0002	0.0005
311452	PI	614969	CHAO 25	China	China	1996-9-5	IND	0.0002	0.0001	0.9995	0.0002	0.0000
311453	PI	614970	XIANGHU NO. 2	China	China	1996-9-5	TEJ-TRJ-IND	0.3081	0.4750	0.2139	0.0004	0.0027
311454	PI	614971	NINGHUI 18	China	China	1996-9-5	TEJ	0.0004	0.6047	0.3947	0.0001	0.0001
311455	PI	614972	QINGLIN NO. 9	China	China	1996-9-5	IND	0.0015	0.3592	0.6391	0.0001	0.0000
311456	PI	614973	ERXI NO. 149	China	China	1996-9-5	IND	0.0004	0.1171	0.8823	0.0001	0.0001
311457	PI	614974	TAIZHOU 1950	China	China	1996-9-5	TRJ-TEJ	0.5632	0.4361	0.0004	0.0000	0.0002
311458	PI	614975	TAIZHONGXIAN 255	China	China	1996-9-5	IND	0.0040	0.0042	0.9830	0.0075	0.0012
311459	PI	614978	71198	China	China	1996-9-5	IND	0.0004	0.0004	0.9989	0.0001	0.0001
311460	PI	614979	WUNONG NO. 2	China	China	1996-9-5	IND	0.0012	0.0016	0.9969	0.0002	0.0001
311461	PI	614982	MINGHUI 63	China	China	1996-9-5	IND	0.0012	0.0010	0.9975	0.0001	0.0002
311462	PI	614983	DALIDAO	China	China	1996-9-5	IND	0.0039	0.0549	0.9376	0.0005	0.0031
311463	PI	614984	ZHANG 32	China	China	1996-9-5	IND	0.0002	0.0003	0.9994	0.0001	0.0000
311464	PI	614987	TIEJING NO. 4	China	China	1996-9-5	IND	0.0065	0.0003	0.9924	0.0002	0.0006
311465	PI	614988	ZANUO NO. 1	China	China	1996-9-5	IND	0.0009	0.0013	0.9897	0.0044	0.0038
311466	PI	614989	KECHENGNUO NO. 4	China	China	1996-9-5	IND	0.0003	0.0006	0.9979	0.0002	0.0010

311467	PI	614990	JINNUO NO. 6	China	China	1996-9-5	IND	0.0003	0.0003	0.9993	0.0001	0.0001
311468	PI	614991	DIAN NO. 01	China	China	1996-9-5	IND	0.0134	0.0004	0.9852	0.0004	0.0006
311469	PI	614993	89-5	China	China	1996-9-5	TRJ	0.9967	0.0005	0.0023	0.0002	0.0002
311470	PI	614994	AIJIAONANTE	China	China	1996-9-5	IND	0.0004	0.0003	0.9991	0.0001	0.0001
311471	PI	614995	YOU NO. 51	China	China	1996-9-5	IND	0.0173	0.0132	0.9682	0.0004	0.0009
311472	PI	614996	FU NO. 83	China	China	1996-9-5	IND	0.0004	0.0001	0.9992	0.0002	0.0002
311473	PI	614997	DIANDUN 501	China	China	1996-9-5	IND	0.0030	0.0063	0.9898	0.0003	0.0006
311474	PI	614998	CHUNZHI NO. 11	China	China	1996-9-5	IND	0.0232	0.0005	0.9754	0.0004	0.0006
311475	PI	614999	TIE 90-1	China	China	1996-9-5	IND	0.0001	0.0006	0.9992	0.0001	0.0001
311476	PI	615003	SHENG 12	China	China	1996-9-5	IND	0.0005	0.0003	0.9990	0.0001	0.0001
311477	PI	615004	H 323	China	China	1996-9-5	IND	0.0098	0.0114	0.9786	0.0002	0.0000
311478	PI	615008	CDR 22	China	China	1996-9-5	IND	0.0029	0.0025	0.9943	0.0001	0.0002
311479	PI	615010	CDR 210	China	China	1996-9-5	IND	0.0035	0.0055	0.9903	0.0001	0.0006
311480	PI	615013	GUICHAO NO. 2	China	China	1996-9-5	IND	0.0002	0.0001	0.9995	0.0001	0.0001
311481	PI	615015	SHUFENG 121	China	China	1996-9-5	IND	0.0008	0.0006	0.9983	0.0001	0.0001
311482	PI	615021	4429-2	China	China	1996-9-5	IND	0.0002	0.0002	0.9991	0.0003	0.0001
311483	PI	615022	4484	China	China	1996-9-5	IND	0.0008	0.0002	0.9988	0.0001	0.0000
311484	PI	615033	4595	China	China	1996-9-5	IND	0.0002	0.0001	0.9996	0.0001	0.0000
311485	PI	615035	4597	China	China	1996-9-5	IND	0.0007	0.0003	0.9988	0.0001	0.0001
311486	PI	615036	4607	China	China	1996-9-5	IND	0.0006	0.0003	0.9991	0.0001	0.0001
311487	PI	615039	4612	China	China	1996-9-5	IND	0.0005	0.0003	0.9991	0.0000	0.0001
311488	PI	615041	4633	China	China	1996-9-5	IND	0.0007	0.0003	0.9989	0.0001	0.0001
311489	PI	615047	4641-1	China	China	1996-9-5	IND	0.0006	0.0002	0.9990	0.0001	0.0001
311490	PI	615049	4642	China	China	1996-9-5	IND	0.0007	0.0003	0.9988	0.0001	0.0001
311491	PI	615192	YOU-I B	China	China	1996-9-5	IND	0.0002	0.0016	0.9981	0.0001	0.0000
311492	PI	615193	JIN-23 B	China	China	1996-9-5	IND	0.0001	0.0001	0.9996	0.0001	0.0000
311493	PI	615194	BO B	China	China	1996-9-5	IND	0.0014	0.0005	0.9979	0.0001	0.0002
311494	PI	615195	R 647	China	China	1996-9-5	IND	0.0008	0.0005	0.9984	0.0002	0.0001
311495	PI	615196	CE 64	China	China	1996-9-5	IND	0.0005	0.0004	0.9986	0.0003	0.0001
311496	PI	615197	NANJING 11	China	China	1996-9-5	IND	0.0003	0.0002	0.9994	0.0001	0.0000
311497	PI	615198	CHUNJIANGZAO NO. 1	China	China	1996-9-5	TEJ	0.0008	0.9302	0.0684	0.0005	0.0001
311498	PI	615199	LUHONGZAO	China	China	1996-9-5	IND	0.0002	0.0078	0.9919	0.0002	0.0000
311499	PI	615200	ZHONG 156	China	China	1996-9-5	IND	0.0003	0.0029	0.9965	0.0002	0.0001
311500	PI	615201	ZHONGYOUWAN NO. 1	China	China	1996-9-5	IND	0.0123	0.0136	0.9736	0.0003	0.0003
311501	PI	615202	ZHONG 86-44	China	China	1996-9-5	IND	0.0034	0.0203	0.9762	0.0001	0.0001
311502	PI	615203	ZHONGYOUZAO NO. 5	China	China	1996-9-5	IND	0.0137	0.0180	0.9679	0.0001	0.0003
311503	PI	615204	ZHONG 413	China	China	1996-9-5	IND	0.0002	0.0002	0.9994	0.0001	0.0001
311504	PI	615206	MINKEZAO NO. 22	China	China	1996-9-5	IND	0.0002	0.0003	0.9991	0.0002	0.0002
311505	PI	615207	LONGQING NO. 3	China	China	1996-9-5	TRJ-TEJ	0.5983	0.3591	0.0346	0.0002	0.0078
311506	PI	615208	LUDAO	China	China	1996-9-5	IND	0.0002	0.0004	0.9992	0.0001	0.0000
311507	PI	615210	SHANGYU 394	China	China	1996-9-5	TEJ	0.0005	0.9994	0.0001	0.0001	0.0000
311508	PI	615211	W48-3	China	China	1996-9-5	IND	0.0194	0.0848	0.8948	0.0008	0.0002
311509	PI	615213	XIANDAN	China	China	1996-9-5	IND	0.0144	0.0014	0.9659	0.0124	0.0059
311510	PI	615214	DANWANBAO 24	China	China	1996-9-5	IND	0.0005	0.0004	0.9979	0.0011	0.0001
311511	PI	615215	MPH 501	China	China	1996-9-5	IND	0.0149	0.0012	0.9412	0.0028	0.0399
311512	PI	615217	II-32B	China	China	1996-9-5	IND	0.0002	0.0014	0.9982	0.0001	0.0000
311513	PI	615218	ZAO 402	China	China	1996-9-5	IND	0.0003	0.0007	0.9984	0.0004	0.0002
311514	PI	615219	CHAOYANG NO. 1	China	China	1996-9-5	IND	0.0001	0.0001	0.9996	0.0001	0.0000
311515	PI	615222	ZHONGBAI NO. 4	China	China	1996-9-5	IND	0.0003	0.0007	0.9975	0.0003	0.0012
311516	PI	615223	DUOYINGLIN-SHUIDAO	China	China	1996-9-5	IND	0.0003	0.0005	0.9990	0.0002	0.0001
311517	PI	404094	92.09.31	Japan	North_Pacific	1975-9-10	IND	0.0002	0.0001	0.9995	0.0001	0.0000
311518	PI	575114	Bhujon Kolpo	Bangladesh	Southern_Asia	1993-7-28	IND	0.0001	0.0004	0.9991	0.0004	0.0001
311519	PI	575186	Khoia	Bangladesh	Southern_Asia	1993-7-28	IND	0.0006	0.0006	0.9985	0.0001	0.0002
311520	PI	575209	Bogra	Bangladesh	Southern_Asia	1993-7-28	IND	0.0004	0.0003	0.9978	0.0013	0.0002
311521	PI	596931	IR 56450-28-2-2	Philippines	South_Pacific	1993-8-23	IND	0.0003	0.0003	0.9992	0.0001	0.0001

311522	PI	634219	IR59624-34-2-2	Philippines	South_Pacific	1996-5-14	TRJ	0.9977	0.0016	0.0006	0.0001	0.0001
311523	PI	634220	NJ70507	China	China	1996-5-14	IND	0.0002	0.0002	0.9995	0.0001	0.0000
311524	PI	634221	RP2199-16-2-2-1	India	Southern_Asia	1996-5-14	IND	0.0001	0.0001	0.9995	0.0002	0.0000
311525	PI	634222	S972B-22-1-3-1-1	Indonesia	South_Pacific	1996-5-14	IND	0.0002	0.0001	0.9995	0.0001	0.0000
311526	CIor	8915	Timonchette 3	Haiti	Central_America	1947-12-1	IND	0.0004	0.0025	0.6630	0.3339	0.0001
311527	CIor	12300	Bulk	Haiti	Central_America	1947-12-1	TRJ	0.9991	0.0005	0.0002	0.0001	0.0001
311528	PI	160639	WC 316	China	China	1947-11-25	IND	0.0006	0.0003	0.9810	0.0173	0.0008
311529	PI	162283	Sal B 10	Korea_ South	North_Pacific	1948-2-1	TEJ	0.0054	0.6485	0.3388	0.0065	0.0007
311530	PI	162284	Sal Bio 10	Korea_ South	North_Pacific	1948-2-1	TEJ	0.0014	0.9648	0.0319	0.0005	0.0013
311531	PI	167923	2046	Turkey	Mideast	1948-9-1	TEJ	0.0153	0.9782	0.0061	0.0002	0.0002
311532	PI	182254	Egyptian Wild Type	Turkey	Mideast	1949-6-1	TEJ	0.0003	0.9993	0.0001	0.0001	0.0002
311533	PI	189457	Rajado de Ponta Escura	Portugal	Western_Europe	1950-5-1	TEJ	0.0249	0.9518	0.0151	0.0078	0.0004
311534	PI	208449	Early No. 3	Nepal	Southern_Asia	1953-5-12	AUS	0.0005	0.0003	0.2165	0.7822	0.0005
311535	PI	223518	Shali-i-Luk	Afghanistan	Southern_Asia	1955-1-24	IND	0.0002	0.0001	0.9989	0.0006	0.0001
311536	PI	240640	THUYAMALLI	India	Southern_Asia	1957-6-10	IND	0.0001	0.0021	0.8458	0.1519	0.0001
311537	PI	245694	A 5	Japan	North_Pacific	1958-2-6	TEJ	0.0358	0.9626	0.0007	0.0007	0.0002
311538	PI	282390	PADANG TRENG-GANU 22	Malaysia	South_Pacific	1962-7-26	AUS	0.0007	0.0004	0.0009	0.9978	0.0001
311539	PI	352687	C.B. II	Japan	North_Pacific	1970-7-29	AUS	0.0002	0.0003	0.0030	0.9963	0.0002
311540	PI	353702	IARI 6196	India	Southern_Asia	1970-5-4	TEJ-ARO-TRJ	0.2460	0.4982	0.0004	0.0016	0.2538
311541	PI	353797	IARI 10840	India	Southern_Asia	1970-5-4	IND	0.0011	0.0007	0.8699	0.1281	0.0001
311542	PI	373040	MI-273M	Sri Lanka	Southern_Asia	1972-3-27	IND	0.0001	0.0042	0.7976	0.1979	0.0002
311543	PI	373116	LD 24	Sri Lanka	Southern_Asia	1972-3-27	IND	0.0002	0.0042	0.7986	0.1968	0.0002
311544	PI	373340	Gallawa	Sri Lanka	Southern_Asia	1972-3-27	AUS	0.0926	0.0005	0.0048	0.8957	0.0064
311545	PI	373341	Ittikulama	Sri Lanka	Southern_Asia	1972-3-27	AUS	0.0010	0.0118	0.0009	0.9844	0.0020
311546	PI	373346	Kaluwee	Sri Lanka	Southern_Asia	1972-3-27	AUS	0.0009	0.0080	0.0008	0.9888	0.0016
311547	PI	373347	Karayal	Sri Lanka	Southern_Asia	1972-3-27	AUS	0.0013	0.0018	0.0005	0.9881	0.0083
311548	PI	373551	ARC 10693	India	Southern_Asia	1972-3-27	AUS	0.0004	0.0009	0.0012	0.9974	0.0001
311549	PI	373800	DAWEBYAN	Myanmar	Southeast_Asia	1972-3-27	IND	0.0160	0.0024	0.8498	0.1314	0.0004
311550	PI	373813	Padi Pagalong	Malaysia	South_Pacific	1972-3-27	TRJ	0.8136	0.1791	0.0005	0.0025	0.0043
311551	PI	385323	Mad/S	Rwanda	Africa	1974-2-5	IND	0.0267	0.0032	0.6844	0.2854	0.0003
311552	PI	389845	Lun An Shun Geen Bir	China	China	1974-9-1	IND	0.0014	0.0014	0.9244	0.0605	0.0122
311553	PI	389879	Sigoendaba	Indonesia	South_Pacific	1974-9-1	IND	0.0170	0.0019	0.8395	0.1413	0.0003
311554	PI	389960	Srav Prapay	Cambodia	Southeast_Asia	1974-9-1	IND	0.0023	0.0031	0.9476	0.0029	0.0441
311555	PI	392531	Jaguary Zongo	El Salvador	Central_America	1975-2-3	IND	0.0006	0.0010	0.6615	0.3369	0.0001
311556	PI	392581	PHCAR SLA	Cambodia	Southeast_Asia	1975-2-3	AUS	0.0004	0.0002	0.0010	0.9983	0.0001
311557	PI	392603	CHETUA	Fiji	Oceania	1975-2-3	AUS	0.0002	0.0002	0.0005	0.9991	0.0001
311558	PI	392606	Gambiaka Kokoum	Burkina Faso	Africa	1975-2-3	AUS	0.0004	0.0005	0.0038	0.9952	0.0001
311559	PI	392612	PAUNG MALAUNG	Myanmar	Southeast_Asia	1975-2-3	AUS	0.0003	0.0002	0.0018	0.9976	0.0001
311560	PI	392633	CRISTAL 161	Chad	Africa	1975-2-3	AUS	0.0001	0.0001	0.0301	0.9696	0.0002
311561	PI	392768	Nang Bang Bentre	Vietnam	Southeast_Asia	1975-2-3	AUS	0.0002	0.0001	0.0042	0.9955	0.0001
311562	PI	392794	Khao Tot Long 227	Thailand	Southeast_Asia	1975-2-3	AUS	0.0001	0.0001	0.0003	0.9995	0.0001
311563	PI	393112	DNJ 179	Bangladesh	Southern_Asia	1975-2-3	AUS	0.0002	0.0004	0.0005	0.9987	0.0002
311564	PI	393440	Chien Hoa Khe	Vietnam	Southeast_Asia	1975-2-3	IND	0.0007	0.0008	0.9819	0.0162	0.0004
311565	PI	400274	517	Uruguay	South_America	1975-3-24	IND	0.0008	0.0013	0.9872	0.0056	0.0051
311566	PI	400275	518	Uruguay	South_America	1975-3-24	AUS-IND	0.0066	0.0032	0.4237	0.5653	0.0012
311567	PI	400276	519	Uruguay	South_America	1975-3-24	AUS-IND	0.0036	0.0016	0.3992	0.5944	0.0012
311568	PI	400277	520	Uruguay	South_America	1975-3-24	IND	0.0040	0.0007	0.9923	0.0018	0.0012
311569	PI	400411	Thou 20-72	China	China	1975-6-3	IND	0.0003	0.0006	0.9982	0.0007	0.0001
311570	PI	402631	Kalo Parame	Nepal	Southern_Asia	1975-8-4	AUS	0.0020	0.0008	0.0309	0.9655	0.0007
311571	PI	402691	Trandeup Kandir	Cambodia	Southeast_Asia	1975-8-4	AUS	0.0002	0.0002	0.0004	0.9991	0.0001
311572	PI	403082	DJ 24	Bangladesh	Southern_Asia	1975-8-4	AUS	0.0001	0.0001	0.0004	0.9993	0.0001
311573	PI	403114	DJ 102	Bangladesh	Southern_Asia	1975-8-4	AUS	0.0001	0.0002	0.0004	0.9993	0.0001
311574	PI	403121	DJ 123	Bangladesh	Southern_Asia	1975-8-4	AUS	0.0001	0.0000	0.0003	0.9995	0.0001
311575	PI	403151	DM 43	Bangladesh	Southern_Asia	1975-8-4	AUS	0.0001	0.0001	0.0088	0.9909	0.0001
311576	PI	403214	DNJ 121	Bangladesh	Southern_Asia	1975-8-4	AUS	0.0002	0.0002	0.0015	0.9979	0.0003

311577	PI	403235	DNJ 169	Bangladesh	Southern_Asia	1975-8-4	AUS	0.0001	0.0003	0.0183	0.9812	0.0001
311578	PI	403240	Doble Carolina Cesia	Uruguay	South_America	1975-8-4	AUS	0.0003	0.0001	0.0006	0.9989	0.0001
311579	PI	403304	DV 118	Bangladesh	Southern_Asia	1975-8-4	AUS	0.0001	0.0001	0.0003	0.9994	0.0001
311580	PI	403516	Iaca Claro	Guinea-Bissau	Africa	1975-8-4	TEJ-TRJ	0.4634	0.5355	0.0002	0.0004	0.0004
311581	PI	413900	S.R.	Sri Lanka	Southern_Asia	1976-11-10	IND	0.0003	0.0008	0.8490	0.1498	0.0001
311582	PI	414546	Banjul	Gambia	Africa	1976-10-17	IND	0.0950	0.0042	0.8781	0.0172	0.0055
311583	PI	418206	Bakula	Sierra Leone	Africa	1977-7-15	TRJ	0.9920	0.0030	0.0004	0.0013	0.0033
311584	PI	418208	Pa Fiele	Sierra Leone	Africa	1977-7-15	TRJ	0.9980	0.0016	0.0002	0.0001	0.0001
311585	PI	418210	Pa Kebile	Sierra Leone	Africa	1977-7-15	TRJ	0.9978	0.0014	0.0001	0.0002	0.0004
311586	PI	430909	Santhi 990	Pakistan	Southern_Asia	1978-12-29	ARO-IND-AUS	0.0014	0.0367	0.3358	0.2126	0.4134
311587	PI	430956	P 737	Pakistan	Southern_Asia	1978-12-29	IND	0.0004	0.0001	0.9979	0.0014	0.0001
311588	PI	430978	Amber Coarse	Iraq	Mideast	1978-12-29	AUS	0.0028	0.0014	0.0028	0.9928	0.0003
311589	PI	431005	Pachodi 427	India	Southern_Asia	1978-12-29	AUS	0.0004	0.0003	0.0033	0.9955	0.0005
311590	PI	431060	Sadri Siah Dum	Iran	Mideast	1978-12-29	AUS-IND	0.0077	0.0032	0.4766	0.5109	0.0016
311591	PI	431078	Heenat 13224	Sri Lanka	Southern_Asia	1978-12-29	AUS	0.0079	0.2917	0.0006	0.6687	0.0310
311592	PI	431204	UZ ROS 7-13	Uzbekistan	Central_Asia	1978-12-29	AUS	0.0002	0.0002	0.0025	0.9968	0.0003
311593	PI	431205	Italica Alef Ambeste Royj	Azerbaijan	Central_Asia	1978-12-29	AUS	0.0002	0.0002	0.0026	0.9965	0.0005
311594	PI	431206	Celhoea Kben Kyemy Zymestny	Uzbekistan	Central_Asia	1978-12-29	AUS	0.0002	0.0002	0.0030	0.9960	0.0006
311595	PI	431343	P 1293	Turkey	Mideast	1978-12-29	AUS	0.0041	0.0042	0.0026	0.9868	0.0022
311596	PI	433799	SL 22-620	Sierra Leone	Africa	1979-6-1	AUS	0.0006	0.0059	0.0072	0.9854	0.0009
311597	PI	433803	SL 22-632	Sierra Leone	Africa	1979-6-1	TRJ	0.9980	0.0012	0.0002	0.0003	0.0002
311598	PI	433818	SL 31-693	Sierra Leone	Africa	1979-6-1	TRJ	0.9958	0.0034	0.0002	0.0005	0.0001
311599	PI	433823	SL 31-709	Sierra Leone	Africa	1979-6-1	TRJ	0.9973	0.0010	0.0002	0.0007	0.0008
311600	PI	434614	Jyanak	Bhutan	Southern_Asia	1979-7-1	TEJ-ARO-TRJ	0.2398	0.4319	0.0021	0.0010	0.3252
311601	PI	439654	Bluebonnet 50-Calrose	Australia	Oceania	1980-2-1	IND	0.0033	0.0036	0.9884	0.0031	0.0015
311602	PI	449351	Riz Local	Burkina Faso	Africa	1980-6-1	AUS	0.0037	0.0017	0.3533	0.6402	0.0011
311605	PI	490783	UA 1012	Niger	Africa	1984-8-1	AUS	0.0012	0.0005	0.0015	0.9964	0.0005
311606	PI	549215	Dhan	Nepal	Southern_Asia	1984-12-13	IND	0.0004	0.0004	0.7301	0.2684	0.0007
311607	PI	574756	Kachilon	Bangladesh	Southern_Asia	1993-7-28	AUS	0.0002	0.0030	0.0035	0.9930	0.0003
311608	PI	574758	Bowalia	Bangladesh	Southern_Asia	1993-7-28	AUS	0.0003	0.0003	0.0033	0.9955	0.0005
311609	PI	574796	Goria	Bangladesh	Southern_Asia	1993-7-28	AUS	0.0007	0.0009	0.0032	0.9947	0.0005
311610	PI	584587	BISER 2	Macedonia	Eastern_Europe	1991-10-31	TRJ	0.8666	0.0446	0.0009	0.0003	0.0876
311611	PI	70304	Chang Chun Ah Wulissu	China	China	1926-12-1	AUS	0.0001	0.0002	0.0004	0.9992	0.0000
311612	CIor	7253	WC 2843	Indonesia	South_Pacific	1928-3-1	TRJ	0.9738	0.0014	0.0093	0.0006	0.0149
311613	PI	127076	Spin Mere	Afghanistan	Southern_Asia	1938-2-1	AUS	0.0024	0.0012	0.0118	0.9811	0.0036
311614	PI	143747	Djauh	Liberia	Africa	1942-1-5	TRJ	0.9991	0.0005	0.0002	0.0002	0.0001
311615	PI	160457	Yang Hsien Tao	China	China	1947-11-25	IND	0.0052	0.0056	0.9881	0.0009	0.0002
311616	PI	160551	Fan Ho Chan	China	China	1947-11-25	IND	0.0003	0.0002	0.9990	0.0004	0.0001
311617	PI	160865	WC 517	China	China	1947-11-25	TEJ-TRJ	0.3833	0.5801	0.0330	0.0028	0.0009
311618	PI	162365	Ziok Do 49	Korea_ South	North_Pacific	1948-2-1	TEJ	0.0039	0.9652	0.0291	0.0005	0.0013
311619	PI	184386	Baros	Guyana	South_America	1949-9-13	TRJ	0.9990	0.0007	0.0001	0.0001	0.0001
311620	PI	189460	Romeno	Portugal	Western_Europe	1950-5-1	TEJ	0.0781	0.9018	0.0002	0.0010	0.0190
311621	PI	220270	Surang Intan	Malaysia	South_Pacific	1954-8-6	AUS	0.0002	0.0001	0.0011	0.9985	0.0001
311622	PI	223490	GPNO 22570	Guatemala	Central_America	1955-1-24	AUS	0.0038	0.0019	0.3659	0.6280	0.0005
311623	PI	224810	GINBOZU CHUSEI	Japan	North_Pacific	1955-4-20	AUS	0.0004	0.0021	0.0004	0.9971	0.0001
311624	PI	266097	SUDUWI 305	Sri Lanka	Southern_Asia	1960-6-7	IND	0.0008	0.0025	0.6280	0.3685	0.0002
311625	PI	267999	Sraguna Brunca de Nos Violaceos	Portugal	Western_Europe	1960-9-7	TEJ	0.0080	0.9905	0.0002	0.0003	0.0010
311626	PI	282387	MAYANG EBOS 80	Malaysia	South_Pacific	1962-7-26	AUS	0.0002	0.0002	0.0086	0.9910	0.0001
311627	PI	351117	Dikwee	Nigeria	Africa	1970-6-22	IND	0.0015	0.0025	0.7109	0.2848	0.0002
311628	PI	353648	IARI 5828	India	Southern_Asia	1970-5-4	TEJ	0.0076	0.9881	0.0018	0.0022	0.0004
311629	PI	373043	62-355	Sri Lanka	Southern_Asia	1972-3-27	IND	0.0001	0.0001	0.7136	0.2861	0.0000
311630	PI	373122	Hatadawee	Sri Lanka	Southern_Asia	1972-3-27	IND	0.0001	0.0003	0.6500	0.3495	0.0000
311631	PI	373179	Yanayanan	Philippines	South_Pacific	1972-3-27	IND	0.0006	0.0006	0.9588	0.0398	0.0001
311632	PI	373259	Wanni Dahanala	Sri Lanka	Southern_Asia	1972-3-27	IND	0.0018	0.0760	0.6901	0.2319	0.0002

311633	PI	373272	Khao Panh	Laos	Southeast_Asia	1972-3-27	TRJ-TEJ	0.4944	0.3888	0.0090	0.0271	0.0808
311634	PI	373331	Patchaiperumal	Sri Lanka	Southern_Asia	1972-3-27	IND	0.0001	0.0003	0.6586	0.3410	0.0000
311635	PI	373335	AMANE	Sri Lanka	Southern_Asia	1972-3-27	IND	0.0001	0.0002	0.6518	0.3478	0.0000
311636	PI	373349	Kaluheenati	Sri Lanka	Southern_Asia	1972-3-27	IND	0.0004	0.0009	0.8662	0.1324	0.0001
311637	PI	373351	Kahatawee	Sri Lanka	Southern_Asia	1972-3-27	IND-AUS	0.0002	0.0002	0.5924	0.4071	0.0000
311638	PI	373363	Badulla	Sri Lanka	Southern_Asia	1972-3-27	IND	0.0014	0.0028	0.7149	0.2808	0.0002
311639	PI	373452	ARC 10303	India	Southern_Asia	1972-3-27	AUS	0.0007	0.0013	0.0007	0.9957	0.0016
311640	PI	373463	ARC 10378	India	Southern_Asia	3-27-1972	AUS	0.0003	0.0001	0.0150	0.9840	0.0005
311641	PI	373589	ARC 10786	India	Southern_Asia	1972-3-27	IND	0.0244	0.0273	0.9431	0.0005	0.0046
311642	PI	373781	Tia Bura	Indonesia	Oceania	1972-3-27	TRJ	0.7205	0.2330	0.0252	0.0004	0.0209
311643	PI	373820	Padi Tarab Arab	Malaysia	South_Pacific	1972-3-27	TRJ	0.8429	0.0562	0.0027	0.0019	0.0963
311644	PI	385697	P 35	India	Southern_Asia	1974-2-20	AUS	0.0003	0.0006	0.0045	0.9921	0.0026
311645	PI	389041	Chi An Tsao	Taiwan	China	1974-9-1	IND	0.0002	0.0002	0.9937	0.0052	0.0007
311646	PI	389088	Pa Yueh Huang	Taiwan	China	1974-9-1	IND	0.0127	0.0004	0.9440	0.0111	0.0318
311647	PI	389874	Siharboei	Indonesia	South_Pacific	1974-9-1	TRJ	0.7363	0.2461	0.0005	0.0046	0.0125
311648	PI	389959	Srav Ankor	Cambodia	Southeast_Asia	1974-9-1	IND	0.0022	0.0025	0.9625	0.0117	0.0211
311649	PI	391936	Ali Combo	Madagascar	Africa	1974-11-27	IND	0.0002	0.0005	0.9936	0.0053	0.0004
311650	PI	392266	Khao Pahk Maw	Thailand	Southeast_Asia	1975-1-13	AUS	0.0037	0.0016	0.0135	0.9718	0.0095
311651	PI	392571	KERR SAIL	India	Southern_Asia	1975-2-3	IND	0.0007	0.0003	0.9970	0.0017	0.0003
311652	PI	392598	ANAK DIDEK	Malaysia	South_Pacific	1975-2-3	IND	0.0032	0.0017	0.7101	0.2846	0.0004
311653	PI	392610	POPEY	Cambodia	Southeast_Asia	1975-2-3	AUS	0.0002	0.0002	0.0057	0.9936	0.0003
311654	PI	392630	CAROLINO 164	Chad	Africa	1975-2-3	AUS	0.0002	0.0005	0.0009	0.9982	0.0001
311655	PI	392674	Badal 33	Bangladesh	Southern_Asia	1975-2-3	IND	0.0039	0.0020	0.9875	0.0035	0.0031
311656	PI	392677	*ASWINA 330	Bangladesh	Southern_Asia	1975-2-3	AUS	0.0004	0.0001	0.0083	0.9911	0.0001
311657	PI	392760	Chau Ba In	Cambodia	Southeast_Asia	1975-2-3	IND	0.0006	0.0057	0.6485	0.3441	0.0010
311658	PI	392795	Snet Chek	Cambodia	Southeast_Asia	1975-2-3	AUS	0.0001	0.0001	0.0003	0.9994	0.0001
311659	PI	392796	Tranoeup Krassaing	Cambodia	Southeast_Asia	1975-2-3	IND-TEJ-AUS	0.0015	0.3496	0.4687	0.1735	0.0066
311660	PI	392932	NACHIN 11	Malaysia	South_Pacific	1975-2-3	TRJ	0.9443	0.0497	0.0002	0.0025	0.0033
311661	PI	393135	Suduwee	Sri Lanka	Southern_Asia	1975-2-3	IND	0.0016	0.0006	0.6571	0.3405	0.0002
311662	PI	400080	DINALAGA	Philippines	South_Pacific	1975-5-7	TRJ	0.9932	0.0059	0.0001	0.0006	0.0001
311663	PI	400273	516	Uruguay	South_America	1975-3-24	AUS	0.0025	0.0025	0.3697	0.6242	0.0010
311664	PI	402525	SHIMOKITA	Japan	North_Pacific	1975-6-19	AUS	0.0140	0.0015	0.0043	0.9793	0.0008
311665	PI	402991	DA 24	Bangladesh	Southern_Asia	1975-8-4	AUS	0.0002	0.0001	0.0006	0.9991	0.0001
311666	PI	403128	DK 12	Bangladesh	Southern_Asia	1975-8-4	AUS	0.0001	0.0000	0.0004	0.9995	0.0000
311667	PI	403469	HKG 98	Mali	Africa	1975-8-4	AUS	0.0268	0.0116	0.0011	0.9573	0.0033
311668	PI	412790	Daudzai Field Mix	Pakistan	Southern_Asia	1976-6-30	AUS	0.0012	0.0007	0.0030	0.9793	0.0158
311669	PI	412811	JP 5	Pakistan	Southern_Asia	1976-6-30	AUS-IND	0.0002	0.0004	0.4837	0.5152	0.0004
311670	PI	420993	Yakadawee	Sri Lanka	Southern_Asia	1977-11-30	IND	0.0006	0.0004	0.8159	0.1831	0.0001
311671	PI	430394	Manzano	Zaire	Africa	1978-12-4	TRJ	0.9983	0.0006	0.0004	0.0004	0.0004
311672	PI	430980	Amber 43	Iraq	Mideast	1978-12-29	AUS	0.3777	0.0022	0.0039	0.6159	0.0003
311673	PI	431059	Sadri Tor Misri	Iran	Mideast	1978-12-29	AUS-IND	0.0045	0.0027	0.4778	0.5134	0.0016
311674	PI	431144	KPF-16	Bangladesh	Southern_Asia	1978-12-29	AUS-IND	0.0003	0.0001	0.4995	0.5000	0.0001
311675	PI	431149	Panta Rubera	Portugal	Western_Europe	1978-12-29	AUS	0.0003	0.0003	0.0033	0.9960	0.0002
311676	PI	433792	SL 22-604	Sierra Leone	Africa	1979-6-1	IND-AUS-TRJ	0.1971	0.0020	0.5782	0.2226	0.0001
311677	PI	439674	Karabaschak	Bulgaria	Eastern_Europe	1980-2-1	TEJ	0.0009	0.9980	0.0001	0.0008	0.0002
311678	PI	439693	Mutant 2	Uzbekistan	Central_Asia	1980-2-1	TEJ	0.0019	0.8114	0.0003	0.0025	0.1840
311679	PI	458453	Rikuki	Turkey	Mideast	1981-3-1	TEJ	0.0018	0.9960	0.0001	0.0017	0.0004
311680	PI	458466	IITA 119	Nigeria	Africa	1981-3-1	TRJ	0.8459	0.0016	0.1519	0.0004	0.0002
311681	PI	549249	N-2346	Nepal	Southern_Asia	1984-12-13	AUS	0.0011	0.0006	0.0007	0.9965	0.0011
311682	PI	549254	2002b	Nepal	Southern_Asia	1984-12-13	TEJ-TRJ-ARO	0.2997	0.4477	0.0011	0.0455	0.2060
311683	PI	574793	Thubri	Bangladesh	Southern_Asia	1993-7-28	AUS	0.0002	0.0002	0.0031	0.9963	0.0001
311684	PI	584620	Hi Muke	Kazakhstan	Central_Asia	1992-6-2	AUS	0.0177	0.0008	0.0056	0.9646	0.0112
311685	PI	597033	WIR 911	Russian Federation	Eastern_Europe	1994-4-28	TEJ	0.0040	0.9764	0.0002	0.0003	0.0192
311705	CIor	9494	Stg 567989	United States	North_America	1961-1-1	IND-TRJ	0.4644	0.0030	0.4726	0.0327	0.0273
311707	CIor	12418	PI 168934-2	Spain	Western_Europe	1948-12-1	TEJ	0.0004	0.9995	0.0000	0.0000	0.0000

311710	PI	54344	Lua Chua Chan	Vietnam	Southeast_Asia	1921-9-1	TRJ	0.9683	0.0195	0.0092	0.0022	0.0008
311711	PI	143749	Djubuh	Liberia	Africa	1942-1-5	TRJ	0.9945	0.0047	0.0003	0.0001	0.0004
311712	PI	198143	Patheinwa	Myanmar	Southeast_Asia	1951-9-1	TRJ	0.6681	0.2393	0.0437	0.0225	0.0264
311713	PI	214077	Sereno	Jamaica	Central_America	1954-2-11	IND	0.0162	0.0028	0.9804	0.0004	0.0003
311714	PI	220725	BENONG 130	Indonesia	South_Pacific	1954-9-9	IND	0.0002	0.0003	0.9993	0.0001	0.0001
311715	PI	220758	URANG URANGAN 89	Indonesia	South_Pacific	1954-9-9	TEJ	0.0003	0.9995	0.0001	0.0000	0.0001
311716	PI	224942	BELLARDONE	France	Western_Europe	1955-4-19	TEJ	0.0003	0.9995	0.0001	0.0000	0.0000
311717	PI	226340	C1-101-2-4	Mexico	North_America	1955-6-10	TRJ	0.6853	0.0181	0.2963	0.0002	0.0002
311718	PI	226355	CI-466-3-4	Mexico	North_America	1955-6-10	IND	0.0452	0.0539	0.9006	0.0001	0.0001
311719	PI	226363	C1-507-1-2	Mexico	North_America	1955-6-10	IND	0.0429	0.0566	0.9001	0.0003	0.0002
311720	PI	226370	C1-621-3-4	Mexico	North_America	1955-6-10	TRJ	0.6638	0.0021	0.3331	0.0008	0.0002
311721	PI	263814	81 B-145	Suriname	South_America	1960-3-7	TRJ-IND-AUS	0.5008	0.0014	0.3456	0.1504	0.0019
311722	PI	263820	VD 5096-73-6	Suriname	South_America	1960-3-7	TRJ-IND	0.5407	0.0035	0.4224	0.0219	0.0115
311723	PI	263829	K8C-634-10	Suriname	South_America	1960-3-7	TRJ-IND-AUS	0.5656	0.0022	0.3006	0.1274	0.0042
311724	PI	265115	Erythroceros Ramsz	Poland	Eastern_Europe	1960-4-27	TEJ	0.0205	0.9788	0.0001	0.0001	0.0005
311725	PI	281914	A 36-3	Myanmar	Southeast_Asia	1962-7-13	IND	0.0689	0.0062	0.8629	0.0166	0.0454
311726	PI	282457	Pah Leuaud 111	Thailand	Southeast_Asia	1962-8-3	IND	0.0007	0.0120	0.9869	0.0002	0.0003
311727	PI	285074	Nahng Sawn	Thailand	Southeast_Asia	1962-11-29	IND	0.0004	0.0005	0.9680	0.0305	0.0005
311728	PI	286176	Nilo No. 2	El Salvador	Central_America	1963-1-28	IND-TRJ-AUS	0.2769	0.0038	0.5747	0.1353	0.0093
311729	PI	297578	MARICH BATI	Bangladesh	Southern_Asia	1964-5-8	IND	0.1977	0.0011	0.7999	0.0004	0.0009
311730	PI	373190	Sipde-K	Philippines	South_Pacific	1972-3-27	TRJ	0.9027	0.0958	0.0002	0.0002	0.0011
311731	PI	373275	Kh. Malenh	Laos	Southeast_Asia	1972-3-27	TRJ-TEJ-ARO	0.4495	0.4105	0.0064	0.0019	0.1316
311732	PI	373287	Nam Manhchanh	Laos	Southeast_Asia	1972-3-27	TRJ-TEJ-ARO	0.5432	0.2648	0.0389	0.0009	0.1523
311733	PI	373320	Khao Hom	Laos	Southeast_Asia	1972-3-27	IND	0.0059	0.0012	0.8020	0.1904	0.0005
311734	PI	373536	ARC 10633	India	Southern_Asia	1972-3-27	IND	0.0325	0.0012	0.7526	0.2131	0.0006
311735	PI	373798	Simpor	Brunei	South_Pacific	1972-3-27	TRJ	0.9139	0.0283	0.0003	0.0520	0.0055
311736	PI	373899	Coppocina	Bulgaria	Eastern_Europe	1972-3-27	TRJ	0.9964	0.0034	0.0001	0.0001	0.0000
311737	PI	385419	*Basmati	Pakistan	Southern_Asia	1974-2-20	ARO	0.0004	0.0003	0.0002	0.0009	0.9983
311738	PI	388303	Ziong Do No. 23	Korea	North_Pacific	1974-3-5	TEJ	0.0004	0.9995	0.0000	0.0001	0.0000
311739	PI	388917	FUJISAKA 5	Japan	North_Pacific	1974-9-1	IND	0.0021	0.0020	0.9947	0.0005	0.0007
311740	PI	389135	Sampao Tong 22	Thailand	Southeast_Asia	1974-9-1	IND	0.0024	0.0005	0.9940	0.0008	0.0023
311741	PI	389150	SOC NAU	Vietnam	Southeast_Asia	1974-9-1	IND	0.0004	0.0003	0.9980	0.0006	0.0007
311742	PI	389152	VE VANG	Vietnam	Southeast_Asia	1974-9-1	IND	0.0005	0.0003	0.9980	0.0008	0.0005
311743	PI	389238	Tra	Vietnam	Southeast_Asia	1974-9-1	IND	0.0002	0.0001	0.9992	0.0005	0.0001
311744	PI	389267	Heo Trang	Vietnam	Southeast_Asia	1974-9-1	IND	0.0276	0.0312	0.9380	0.0004	0.0027
311745	PI	389360	WONG CHIM	Hong Kong	China	1974-9-1	IND	0.0057	0.0064	0.9873	0.0004	0.0002
311746	PI	389365	Hung Tau Keng	China	China	1974-9-1	IND	0.1398	0.0008	0.8410	0.0162	0.0021
311747	PI	391279	Gambiaka	Burkina Faso	Africa	1974-11-20	IND	0.0006	0.0013	0.9959	0.0019	0.0002
311748	PI	391280	Bogarigbeli	Burkina Faso	Africa	1974-11-20	IND	0.0003	0.0009	0.9917	0.0069	0.0001
311749	PI	391352	SDF	Mali	Africa	1974-11-20	IND	0.0047	0.0028	0.7129	0.2792	0.0004
311750	PI	391865	16-Feb	Tanzania	Africa	1974-11-27	IND	0.0007	0.0010	0.9971	0.0009	0.0004
311751	PI	391904	Magoti	Burundi	Africa	1974-11-27	IND	0.0008	0.0010	0.8518	0.1299	0.0165
311752	PI	391938	Geant W7	Netherlands	Western_Europe	1974-11-27	TRJ-IND-AUS	0.4001	0.0026	0.4485	0.1485	0.0003
311753	PI	392583	EKARIN	Myanmar	Southeast_Asia	1975-2-3	TRJ	0.9992	0.0005	0.0001	0.0000	0.0002
311754	PI	392780	GPNO 25198	Philippines	South_Pacific	1975-2-3	IND	0.0096	0.0409	0.9185	0.0072	0.0238
311755	PI	401749	Gogo Sirah	Indonesia	South_Pacific	1975-5-21	AUS-IND-TRJ	0.2339	0.0004	0.2550	0.5105	0.0002
311757	PI	403457	HC 1	Malawi	Africa	1975-8-4	IND	0.0011	0.1769	0.7314	0.0905	0.0001
311758	PI	403556	Jambaram	Guinea-Bissau	Africa	1975-8-4	IND	0.0003	0.0002	0.9988	0.0003	0.0003
311759	PI	403557	JANSUSU	Ghana	Africa	1975-8-4	IND	0.0004	0.0002	0.9989	0.0002	0.0002
311760	PI	406049	Dissi Hatif	Senegal	Africa	1975-11-13	IND	0.0023	0.0019	0.7012	0.2934	0.0013
311761	PI	406572	Phar Com En	Mali	Africa	1976-1-6	IND	0.0002	0.0014	0.9979	0.0003	0.0002
311762	PI	412826	Khara Ganja	Pakistan	Southern_Asia	1976-6-30	IND	0.0002	0.0007	0.6132	0.3854	0.0005
311763	PI	414215	Laka	Indonesia	Oceania	1976-12-13	IND	0.0013	0.0002	0.9967	0.0005	0.0012

311764	PI	414237	Mekeo White	Papua New Guinea	Oceania	1976-12-13	IND	0.0287	0.0016	0.9691	0.0006	0.0000
311765	PI	418207	Pa Boup	Sierra Leone	Africa	1977-7-15	AUS	0.0055	0.0346	0.0027	0.9443	0.0129
311766	PI	431086	Sadri Dum Siah	Iran	Mideast	1978-12-29	IND	0.0004	0.0009	0.9963	0.0022	0.0001
311767	PI	431198	Italica Alef Hz Ros 275	Uzbekistan	Central_Asia	1978-12-29	IND	0.0008	0.0023	0.9956	0.0012	0.0001
311768	PI	431236	P 1042	Former Soviet Union	Eastern_Europe	1978-12-29	IND	0.0220	0.0777	0.9000	0.0001	0.0001
311769	PI	431310	Pakkali	Philippines	South_Pacific	1978-12-29	ARO	0.0020	0.0006	0.0025	0.0010	0.9939
311770	PI	431359	P 1309	Turkey	Mideast	1978-12-29	TEJ	0.0006	0.9988	0.0001	0.0003	0.0001
311771	PI	431365	P 1315	Turkey	Mideast	1978-12-29	IND	0.0006	0.0030	0.7029	0.2932	0.0002
311772	PI	433788	Plah Sew	Thailand	Southeast_Asia	1979-6-1	IND	0.0089	0.0066	0.9663	0.0041	0.0142
311773	PI	433812	SL 22-646	Sierra Leone	Africa	1979-6-1	TRJ-IND	0.5268	0.0010	0.4717	0.0003	0.0001
311774	PI	434623	Thimphu Local	Bhutan	Southern_Asia	1979-7-1	IND	0.0006	0.0006	0.9984	0.0002	0.0001
311775	PI	439024	THAVALU	Sri Lanka	Southern_Asia	1980-1-1	AUS	0.0464	0.0264	0.0085	0.9167	0.0019
311776	PI	439631	Pyrocarpa	Kyrgyzstan	Central_Asia	1980-2-1	TEJ	0.0036	0.9051	0.0002	0.0025	0.0887
311777	PI	439632	Erythroceros	Tajikistan	Central_Asia	1980-2-1	TEJ	0.0099	0.6961	0.0002	0.0006	0.2932
311778	PI	439704	N.F. 17	Russian Federation	Eastern_Europe	1980-2-1	TEJ	0.0012	0.9987	0.0000	0.0000	0.0001
311781	PI	473562	Krachek Chap	Indochina	Southeast_Asia	1982-10-1	IND	0.0051	0.0013	0.9930	0.0004	0.0002
311782	PI	473566	Mayhiya	Fiji	Oceania	1982-10-1	IND	0.0002	0.0003	0.8468	0.1526	0.0001
311783	PI	560224	AFAA MWANZA	Tanzania	Africa	1990-1-16	IND	0.0053	0.0025	0.6428	0.3485	0.0009
311784	PI	574997	Fulbadam	Bangladesh	Southern_Asia	1993-7-28	AUS	0.0005	0.0099	0.0231	0.9660	0.0005
311785	PI	578201	WHASEONG	Korea_ South	North_Pacific	1994-2-14	TEJ	0.0002	0.9976	0.0010	0.0010	0.0001
311786	PI	584589	MACEDONIJA	Macedonia	Eastern_Europe	1991-10-31	TEJ	0.0004	0.9994	0.0001	0.0000	0.0001
311787	PI	584632	KRASNODARSKIJ 3352	Russian Federation	Eastern_Europe	1992-6-2	TEJ	0.0008	0.9990	0.0002	0.0000	0.0001
311788	PI	585042	EMBRAPA 1200	Brazil	South_America	1991-3-22	TRJ	0.9976	0.0009	0.0013	0.0001	0.0001
311789	PI	596817	SETO BHAKUNDE	Nepal	Southern_Asia	1992-7-20	TEJ-TRJ-ARO	0.2603	0.4729	0.0058	0.0043	0.2568
311790	PI	602637	WAB462-10-3-1	Cote D'Ivoire	Africa	1996-5-14	TRJ	0.9941	0.0010	0.0044	0.0003	0.0003
311791	PI	590414	NSGC 5945	Sierra Leone	Africa	1995-5-17	IND	0.0061	0.0049	0.8961	0.0926	0.0003
311792	PI	561734	*Cypress	United States	North America	2008-10-9	TRJ	0.9018	0.0353	0.0626	0.0001	0.0001
311793	PI	497682	*IR64	Philippines	South Pacific	2008-10-9	IND	0.0001	0.0001	0.9996	0.0001	0.0001
311794	PI	494105	*M202	United States	North America	2008-10-9	TEJ	0.2169	0.7041	0.0788	0.0001	0.0001
311795	PI	514663	*NIPPONBARE	Japan	North Pacific	2008-10-9	TEJ	0.0003	0.9996	0.0001	0.0000	0.0000
	CIor	12037	*Carolina Gold	United States	North America		TRJ	0.9994	0.0004	0.0002	0.0000	0.0000
	PI	475833	*Lemont	United States	North America		TRJ	0.9986	0.0004	0.0008	0.0001	0.0001
	PI	583278	*Kaybonnet	United States	North America		TRJ	0.9981	0.0006	0.0011	0.0000	0.0001
			*Banks	United States	North America		TRJ	0.9973	0.0006	0.0016	0.0002	0.0003
	PI	636726	*Cybonnet	United States	North America		TRJ	0.9920	0.0029	0.0041	0.0002	0.0007
	PI	527707	*Katy	United States	North America		TRJ	0.9862	0.0008	0.0118	0.0003	0.0008
	PI	606331	*Cocodrie	United States	North America		TRJ	0.9792	0.0122	0.0080	0.0003	0.0003
			*Wells	United States	North America		TRJ	0.9498	0.0218	0.0088	0.0189	0.0006
			*Cl161	United States	North America		TRJ	0.9481	0.0082	0.0429	0.0007	0.0001
			*Adair	United States	North America		TRJ	0.9445	0.0011	0.0539	0.0003	0.0001
			*Francis	United States	North America		TRJ	0.9352	0.0052	0.0495	0.0098	0.0003
			*Priscilla	United States	North America		TRJ	0.8643	0.0067	0.1277	0.0006	0.0006
	PI	633624	*Saber	United States	North America		TRJ	0.8139	0.0069	0.1788	0.0002	0.0002
	CIor	9945	*Mars	United States	North America		TRJ	0.7199	0.2799	0.0001	0.0000	0.0001
			*Bengal	United States	North America		TRJ	0.7097	0.2884	0.0017	0.0001	0.0001
	PI	636725	*Medark	United States	North America		TRJ-TEJ	0.5182	0.4782	0.0034	0.0001	0.0001
			*Farm Buster	United States	North America		TRJ-TEJ	0.5863	0.3597	0.0465	0.0072	0.0002
	CIor	9980	*M201	United States	North America		TEJ	0.2252	0.6857	0.0888	0.0002	0.0001
	PI	615014	*Shufeng 109	China	China		IND	0.0001	0.0001	0.9995	0.0001	0.0001
	PI	629016	*Zhe 733	China	China		IND	0.0004	0.0002	0.9989	0.0004	0.0002
	PI	536047	*Teqing	China	China		IND	0.0006	0.0004	0.9988	0.0001	0.0001
	PI	595927	*Jasmine85	United States	North America		IND	0.0003	0.0013	0.9980	0.0002	0.0002
	PI	615205	*Jing185_7	China	China		IND	0.0001	0.0004	0.9862	0.0124	0.0009

Vol.2, No.4, 292-297 (2010)
doi:10.4236/ns.2010.24037

Natural Science

DNA damage in hemocytes of *Schistocerca gregaria* (Orthoptera: Acrididae) exposed to contaminated food with cadmium and lead

Hesham A. Yousef[1*], Amira Afify[1], Hany M. Hasan[2], Afaf Abdel Meguid[1]

[1]Entomology Department, Faculty of Science, Cairo University, Cairo, Egypt; heshamyousef.eg@gmail.com
[2]Agriculture Research Center, Ministry of Agriculture, Cairo, Egypt

Received 9 December 2009; Revised 4 January 2010; accepted 5 February 2010.

ABSTRACT

We measured in a comet assay the damage of DNA in the hemocytes of various stages of the grasshopper *Schistocerca gregaria* after exposing them to various doses of Cd and Pb in the food. The mechanisms of Cd and Pb toxicity for grasshopper are discussed. The accumulation of heavy metals and stage of the insect may play important roles in causing the DNA damage. *S. gregaria* may be considered a valuable bio-indicator for evaluation the genotoxicity of environmental pollutants.

Keywords: Comet Assay; Heavy Metals (Cd, Pb); DNA Damage; *Schistocerca gregaria*

1. INTRODUCTION

Heavy metals are among the most problematic causes of water, soil and plant pollution. Genetic and biochemical effects of pollutants on organisms are important in establishing species as bioindicators for environmental hazards [1,2]. Heavy metals have been found to induce genotoxic effects in chironomids which are used as a good bioindicator group for aquatic pollution [3]. Terrestrial insects that develop in the soil are also exposed directly to metal ions present in the soil. Grasshopper species may provide good systems to evaluate the mutagenic effects of some environmental contaminants [4-6].

Cadmium and lead are widespread and dangerous heavy metals that are released into the environment from many sources. Their accumulation in the soils can become dangerous to all kinds of organisms, including plants and human life, causing many genotoxic effects [7-9]. They are highly toxic and have been recognized as poison and a probable carcinogen [10]. Clinically, they can adversely affect human health, especially the blood and the renal system [11].

Changes in the cell genome caused by genotoxic agents leading to mutations and possibly tumor formation are some of the lethal or sub-lethal effects induced by a complex mixture of pollutants. Among recently used methods to identify DNA damage is the comet assay (SCGE-single cell gel electrophoresis). The comet assay provides a rapid, sensitive, and inexpensive method to detect DNA strand breaks in individual eukaryotic cells [12]. Despite some difficulties in obtaining cell/nuclei suspension, this method has been used to detect and evaluate DNA damage caused by double strand breaks, single strand breaks, alkali labile sites, oxidative base damage, and DNA cross-linking with DNA or protein. It has been successfully applied to cells of various animal groups [13]. Only a few studies have been reported on DNA damage in insects, including *D. melanogaster* [14], and in the weevil Curculio sikkimensis [15], and in grasshoppers *Chorthippus brunneus* [16].

The aim of the present work was to determine the genotoxic effect of cadmium and lead on the locust *S. gregaria* and to evaluate its potential as a biomonitor for detecting a heavy-metal polluted environment.

2. MATERIALS AND METHODS

2.1. Colonization of *S. Gregaria*

Locusts were reared in wooden cages at 32 ± 2C°, 50-60% RH and 16 hrs day light in our Entomology Department since about 10 years ago. A daily supply of fresh grass, clover plant was supplied to the locusts. Packed moist sterilized sand in suitable glass containers about 7 cm in diameter and 10 cm deep were prepared for egg-laying.

2.2. Heavy Metals Treatment and Sample Preparation for Alkaline Single Cell Gel (SCG) Assay

Living individuals of *S. gregaria* of the 4^{th}, 5^{th} instars, and newly emerged (NEA)(4 days old) and mature (15 days old) adult (MA), fed on treated clover (their stems were previously immersed for 24 hrs in distilled water containing 25 mg and 50 mg/L of $CdCl_2$ and $PbCl_2$, to allow the clover to absorb contaminated water) or on untreated clover, were collected from their respective cage. Haemolymph samples were withdrawn from the collected insects by means of micropipettes at incision made near the 3rd coxae. Five insects were used for each sample.

2.3. Detection of DNA Damage Using Alkaline SCG Assay

Biochemical techniques for detecting DNA single strand breaks (frank strand breaks and incomplete excision repair sites), alkali-labile sites, and cross-linking with the single cell were done according to the alkaline (pH 13) SCG assay, and developed [17].

The alkaline version of comet assay was used to analyze the level of DNA damage in the hemocytes of *S. gregaria* to estimate the genotoxic effects of Cd^{2+} and Pb^{2+}. 20 μL of hemolymph from the pool of 5 insects were centrifuged at 1000 rpm for 10 min. Isolated hemocytes were immediately suspended in cooled 50 µL Ringer solution and kept on ice, in darkness. 10 μL of isolated cells were mixed with 90 μL of 0.75% low melting point agarose (LMPA), and placed on a microscope slides, pre-coated with 1.5% normal melting point agarose (NMA). A cover slip was added, and the slides were immediately placed on ice. After agarose solidified, cover slips were removed, and the slides were immersed in a lyses buffer (2.5 M NaCl, 100 mM EDTA, 10 mM Tris, 0.25 M NaOH, 1% TritonX-100, and 10% dimethylsulfoxide (DMSO), pH 10.0) for 2h at 4°C. After the lysis, the slides were placed in a horizontal gel electrophoresis tank and DNA was allowed to unwind for 20 min in electrophoresis buffer (300 mM NaOH and 1 mM EDTA, pH 13). Electrophoresis was carried out at 21 V and 270 mA, at 4°C, for 15 min. Then the slides were neutralized in 0.4 M Tris–HCl (pH 7.4), fixed with methanol and allowed to dry overnight at room temperature before staining with ethidium bromide (2 μg/mL). Comets were analyzed with Axio fluorescence microscope (Carl Zeiss, Germany) with an excitation filter of 524 nm and a barrier filter of 605 nm. Three replicates were prepared and each of them consisted of a pool of 5 individuals.

2.4. Evaluation of DNA Damage

DNA damage was visualized with fluorochrome stain of DNA with the fluorescent microscope and a 40X objective (depending on the size of the cells being scored). A Komet analysis system 4.0 developed by Kinetic Imaging, LTD (Liverpool, UK) linked to a CCD camera was used to measure the length of DNA migration (Tail length) (TL), and the percentage of migrated DNA (DNA %). To distinguish between populations of cells differing in size nuclear diameter was measured. Finally, the program calculated tail moment. 50-100 randomly selected cells are analyzed per sample (at least 25 cells per slid and 3 slide per treatment were evaluated).

Statistical analysis for data was done using ANOVA and T-test analysis, based on a minimum of 4 individual insects per group. In addition, numbers of cells were analyzed to exhibit values greater than the 95 or 99% confidence limits for the distribution of control data.

3. RESULTS

3.1. Comet Assay of DNA Damage

The typical DNA damage of haemolymph cells of *S. gregaria* exposed to low and high concentrations of cadmium chloride ($CdCl_2$) and lead chloride ($PbCl_2$) in the food can be seen in **Figure 1.** The haemolymph cells of the control showed almost rounded nuclei (**Figure 1(a)**). In the haemolymph cells of the heavy metals contaminated insects, the nuclei with a clear tail like extension were observed indicating that the haemolymph cells of the insect were damaged and DNA strand breaks had occurred (**Figure 1**).

The typical DNA comet for hemocytes of *S. gregaria* showed illustration of rounded nuclei of control and maximum length of tail formed and migration of DNA in this tail under the effect of contamination with different concentrations of $CdCl_2$ and $PbCl_2$ (**Figure 1**).

The DNA damage of the hemocytes of different stages of *S. gregaria* fed on clover exposed to low and high concentrations (25 and 50 mg/L) of $CdCl_2$ and $PbCl_2$ was analyzed quantitatively by comet assay and expressed as tail length (TL), DNA % and tail moment (TM) (**Table 1**, and **Figures 2** and **3**). It was found that low concentration

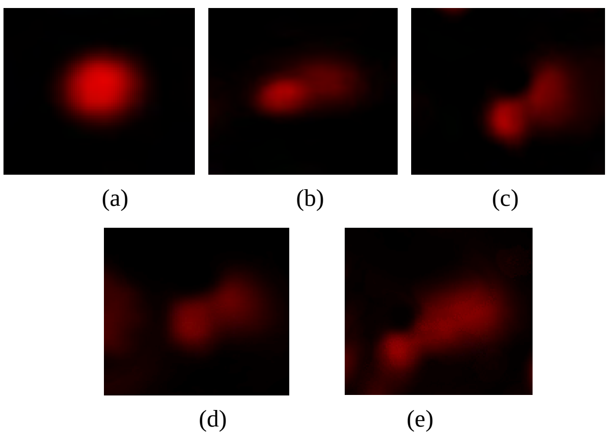

Figure 1. Typical DNA comet from haemocytes of 4th instar *S. gregaria.* (a) Control; (b,c) Low and high concentrations of $CdCl_2$ respectively; (d,e) Low and high concentrations of $PbCl_2$, respectively.

Table 1. Detection of DNA damage by the comet assay, assessed as tail moment (TM) in hemocytes of 4th, 5th, NEA, and MA of *S. gregaria* exposed *in vivo* to $CdCl_2$ and $PbCl_2$, at different doses in the food.

Agent / Dose	4th instar	5th instar	NEA	MA
Control	**0.028** ± 4.4 × 10^{-3}	**0.095** ± 5.8 × 10^{-3}	**0.009** ± 2.3 × 10^{-3}	**0.073** ± 3.5 × 10^{-3}
$CdCl_2$ (mg/L) 25	**0.092** ± 0.02*	**0.16** ± 0.017*	**0.04** ± 3.5 × 10^{-4}*	**0.29** ± 0.0133*
50	**0.057** ± 3.3 × 10^{-3}*	**0.07** ± 6.9 × 10^{-3}	**0.08** ± 3.9 × 10^{-3}*	**0.45** ± 0.03*
$PbCl_2$ (mg/L) 25	**0.081** ± 0.022*	**0.124** ± 0.012	**0.05** ± 5.8 × 10^{-3}*	**0.32** ± 3.5 × 10^{-3}*
50	**0.7** ± 8.8 × 10^{-3}*	**0.11** ± 0.017	**0.021** ± 8.8 × 10^{-3}*	**0.44** ± 0.035*

Significant at $*P < 0.05$; in all cases significance was tested with respect to 0 (control) using t-test, (N = 3). Values are expressed as means ± S.E.

of $CdCl_2$ (25 mg/L) caused a significant increase in the values of TM in the hemocytes of different stages. While, the high concentration (50 mg/L) of $CdCl_2$ caused a lower significance increase in TM in the 4th instar, somewhat insignificant increase or decrease in 5th instar and led to a significant higher increase of these values in the adult stage (NEA and MA). Low and high concentrations of $PbCl_2$ caused a significant increase in TM, generally in all developmental stages with few insignificant changes. The effect of the $PbCl_2$ concentration was not clear as in $CdCl_2$ (**Table 1**).

The damage of hemocyte DNA expressed as TL and DNA% under the effect of different concentrations of $CdCl_2$ and $PbCl_2$, analyzed by the comet assay (**Figures 2** and **3**). It was found that 25 mg/L of $CdCl_2$ caused a significant increase in the values of TL, DNA% in the hemocytes of different stages. The high concentration (50 mg/L) of $CdCl_2$ caused a lower significance increase in TL in the 4th and 5th instar. Low and high concentrations of $PbCl_2$ caused a significant increase in TL, and DNA%. The prominent increase in the values of TL and DNA% in response to contamination with Cd and Pb was observed in the mature adult stage (MA). The dose concentration of Cd and Pb had insignificant effect on the values of TL and DNA % (**Figures 2** and **3**).

The analysis of variance of the two factors (stage and heavy metal concentrations) showed that, the stage of the insect had a clear significant effect on the DNA damage (TL, DNA % and TM). A less significant effect of the dose (concentration of heavy metals) was observed (**Table 2**).

3. DISCUSSIONS

In the present study, the treated clover exposed to $CdCl_2$ and $PbCl_2$, at doses of 10 and 20 mg/L, contained 10 and 20 μg/g plant tissues, respectively to each dose (data not presented). The exposure of *S. gregaria* to Cd and Pb in the food caused an increase in damage (expressed as TL, TM, and DNA%) of DNA of hemocytes. However, the obtained data were sometimes ambiguous; for instance, the TL was not proportional to the Cd dose in the 4th and 5th instars but was true in the NEA and MA (**Figure 2**). The available data from the literature are from assays on cell cultures (mostly human or rat lymphocytes) and many of them concerning genotoxicity of Cd, As, Pb, and Hg [13,18,19].

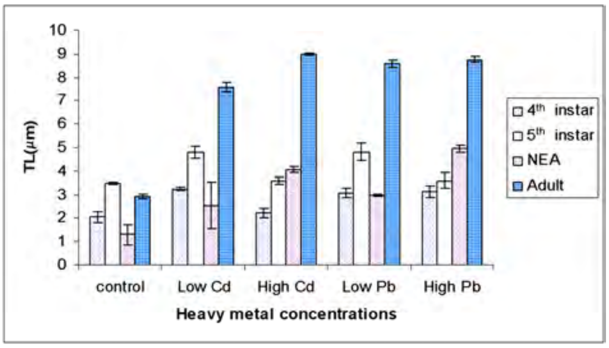

Figure 2. Comet TL data of hemocytes from different instars of *S. gregaria* exposed to food with low (25 mg/L) and high concentration (50 mg/L) of Cd and Pb.

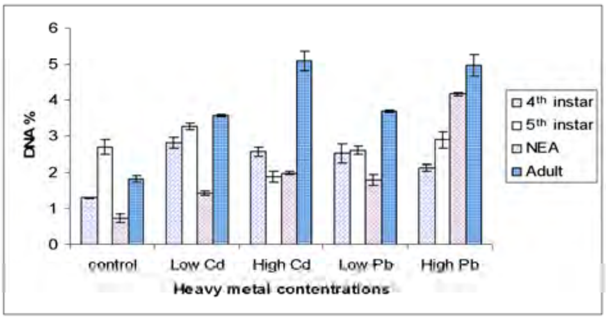

Figure 3. Comet DNA% data of hemocytes from different instars of *S. gregaria* exposed to food with low (25 mg/L) and high concentration (50 mg/L) of Cd and Pb.

Table 2. Analysis of variance (Two Way ANOVA) for tail length (TL), DNA %, and tail moment (TM) in *S. gregaria* with heavy metal treatment as categorical factors.

Source of Variation	TL			DNA %		TM	
	Df	F	P	F	P	F	P
Stage (1)	3	181.3	0.00001	133.6	0.00001	358.3	0.00001
Heavy metal Concentration (2)	4	44.1	0.00001	78.1	0.00001	73.9	0.00001
Interaction 1 × 2	12	12.4	0.00001	29.7	0.00001	36.1	0.00001

The no increased or even decreased DNA migration using comet assay may reflect the cells with DNA cross-linking lesions [19,20]. The higher DNA damage in the mature adults with respect to the long period of exposure to heavy metals (**Figures 2** and **3**) reflects the absence of repair mechanism in this insect at the used concentrations of $CdCl_2$ and $PbCl_2$.

3.1. Cadmium Genotoxicity

Exposure of *S. gregaria* to Cd in their food leads to accumulation of the metal in the insect body of 10, 20, 10, and zero μg/g insect body in the 4th, 5th, NEA, and MA (data not presented data). The accumulation factors of heavy metals in grasshoppers were found in the order Cd > Hg > Pb indicating a greater affinity for Cd accumulation. With the growth of muscle tissues and fat bodies during post-embryonic development (nymph to adult), the concentration of Cd was found to be steadily increasing [21]. It has been suggested that the molecular mechanism for the genotoxicity of cadmium may involve either indirect or direct interaction of with DNA [22], such as DNA strand breaks [10], DNA protein-cross linking [23], Oxidative DNA damage [24], enhanced proliferation, depressed apoptosis and inhibition of DNA repair [24-26].

Many metals, including cadmium, in biological systems form complexes with nucleophilic ligands of target molecules [27]. The affinity of cadmium is higher for biomolecules containing more than one binding site such as metallothionein [7]. Another factor of cadmium toxicity is that it replaces zinc in enzymes, thereby inhibiting their activity [28]. Some insects as *D. melanogaster* have tolerance to heavy metals [27], and their natural populations differed in amplification of the metallothionein gene [29]. By binding to plasma membrane receptors, cadmium stimulates release of calcium from intracellular storage sites [7]. Moreover elevated cadmium levels may inhibit Ca-ATPase working in the plasma and endoplasmic reticulum membranes, leading to disturbance of calcium homeostasis [7,25]. Also, it nhibits DNA repair enzymes, such as DNA polymerases by binding to nucleic acids and chromatin [25].

3.2. Lead Genotoxicity

The exposure of grasshoppers to Pb in the food caused an increase of DNA damage in haemolymph cells. The increase of TL values was proportional to the Pb dose in the food in 4th nymphal instars, newly emerged, and mature adults but not proportional in 5th instars (**Figure 2**). This may be due to high retention of metals in the 5th instar as compared to the other stages. Dietary factors greatly influence lead retention. Several mechanisms could intervene in these effects. Low dietary calcium and lead-binding proteins at the sites of absorption [30] influence lead retention, because lead interferes with the regulation of calcium metabolism [31]. An interaction of lead and calcium can occur on the sites of toxic action by binding to phosphate groups, or by interfering with uptake in organelles etc.

There are several mechanisms how lead might interfere with repair process. Their ions may interfere with calcium regulated processes involved in the regulation of DNA replication and repair [32], induced genome damage includes DNA single- strand and double-strand breaks, DNA-DNA crosslinks, induction of reactive oxygen intermediates [33], and consequently acts as co-clastogens or co-mutagens [34].

The present work clearly shows that, the significant increase of genotoxicity in relation to the development of nymph to adult stage may be due to accumulation of heavy metals in the tissues and blood. This suggests that the DNA damage increased with Pb in blood. Likewise, a significant correlation was found between Pb accumulated in the blood and genotoxic effects in Pb exposed workers [35].

In conclusion, the genotoxicity of cadmium and lead in *S. gregaria* was very high in the mature adult stage; irrespective of the heavy metal dose and accumulation in the cells. So this may reflects the role played by *S. gregaria* as a valuable bioindicator for environmental genotoxic pollutants.

4. ACKNOWLEDGEMENTS

Authors are grateful to Professor Dr. James. L. Nation (Department of Entomology and Nematology, University of Florida, USA) and Professor Dr. John Trumble (Entomology Department, California University, USA), for valuable reviewing the manuscript.

REFERENCES

[1] Michailova, P., Petrova, N., Bovero, S., Cavicchioli, O., Ramella, L. and Sella, G. (2000a) Effect of environmental pollution on the chromosome variability of *Chi-*

ronomus riparius Meigen (1804) (Diptera, Chironomidae) larvae from two Piedmont stations. *Genetica*, **108(2)**, 171-180.
[2] Michailova, P., Petrova, N., Bovero, S., Sella, G. and Ramella, L. (2000b) Structural and functional rearrangements in polytene chromosomes of Chironomids (Diptera) as biomarkers for heavy metal pollution in aquatic ecosystems. *International Conference on Heavy Metals in the Environment*, Michigan University, Michigan, 70-79.
[3] Michailova, P., Ilkova, J., Petrova, N. and White, K. (2001) Rearrangements in the salivary gland chromosomes of Chironomus riparius Mg. (Diptera, Chironomidae) following exposure to lead. *Caryologia*, **4**, 349-363.
[4] Barsiene, J. (1994) Chromosome set changes in molluscs from highly polluted habitats in: A.R. beaumont, editors, genetics and evolution of aquatic organisms. Chapman & Hall, London, 434-447.
[5] Barsyte, D. (1999) The analysis of genotoxic damage of industrial pollution in freshwater mollusc tissues. Summery Doctoral Thesis, Institute of Ecology, Vilnius, 1-20.
[6] Warchalowska–Sliwa, E., Niklinska, M., Görlich, A., Michailova, P. and Pyza, E. (2005) Heavy metal accumulation, heat shock protein expression and cytogenetic changes in Tetrix tenuicornis (L.) (Tetrigidae, Orthoptera) from polluted areas. *Environmental Pollution*, **133(2)**, 373-381.
[7] Goering, P.L., Waalkes, M.P. and Klaassen, C.D. (1995) Toxicology of cadmium. Goyer, R.A. and Cherian, M.G., Ed., *Toxicology of Metals*, Springer-Verlag, Berlin, 189-214.
[8] Sanita di Toppi, L. and Gabbrieli, R. (1999) Responses to cadmium in higher plants. *Environmental and Experimental Botany*, **41(2)**, 105-130.
[9] Panda, B.B. and Panda, K.K. (2002) Genotoxicity and mutagenicity of metals in plants. Prasad, K.N.V. and Strzalka, K., Ed., *Physiology and BioChemistry of Metal Toxicity and Tolerance in Plants*, Kluwer Academic Publishers, Netherlands, **15**, 395-414.
[10] Waalkes, M. and Misra, R. (1996) Cadmium carcinogenicity and genotoxicity. Chang, L.W., Ed., *Toxicology of Metals*, CRC Press, Boca Raton, 231-241.
[11] Arcadio, P.S. and Gregoria, A.S. (2002) Physical-chemical treatment of water and waste water. CRC Press, Boca Raton, IWA Publishing, London.
[12] Rojas, E., Lopez, M.C. and Valverde, M. (1999) Single cell gel electrophoresis assay: Methodology and applications. *Journal of Chromatography B*: *Biomedical Sciences and Applications*, **722(1-2)**, 225-254.
[13] Woźniak, K. and Blasiak, J. (2003) In vitro genotoxicity of lead acetate: Induction of single and double DNA strand breaks and DNA-protein cross-links. *Mutation Research*, **535(2)**, 127-139.
[14] Siddique, H.R., Chowdhuri, D.K., Saxena, D.K. and Dhavan, A. (2005) Validation of Drosophila melanogaster as an in vivo model for genotoxicity assessment using modified alkaline comet assay. *Mutagenesis*, **20(4)**, 285-290.
[15] Todoriki, S., Hasan, M., Miyanoshita, A., Imamura, T. and Hayashi, T. (2006) Assessment of electron beam-induced DNA damage in larvae of chestnut weevil. Curculio sikkimensis (Coleoptera: Curculionidae) using comet assay. *Radiation Physics and Chemistry*, **75(2)**, 292-296.
[16] Augustyniak, M., Juchimiuk, J., Przybylowicz, W.J., Mesjasz-Przybylowicz, J., Babczynska, A. and Migula, P. (2006) Zinc-induced DNA damage and the distribution of metals in the brain of grasshoppers by the comet assay and micro-PIXE. *Comparative Biochemistry and Physiology - Part C*, **144(3)**, 242-251.
[17] Singh, N.P., McCoy, M.T., Tice, R.R. and Schneider, E.L. (1998) A simple technique for quantitation of low levels of DNA damage in individual cells. *Experimental Cell Research*, **175(1)**, 184-191.
[18] Grover, S.A., Coupal, L., Zowall, H., Alexander, C.M., Weiss, T.W. and Gomes, D.R.J. (2001) How cost-effective is the treatment of dyslipidemia in patients with diabetes but without cardiovascular disease? *Diabetes Care*, **24(1)**, 45-50.
[19] Mourón, S.A., Golijow, C.D. and Dulout, F.N. (2001) DNA damage by cadmium and arsenic salts assessed by the single cell gel electrophoresis assay. *Mutation Research*, **498(1-2)**, 47-55.
[20] Tice, R., Agurell, E., Anderson, D., Burlinson, B., Hartmann, A., Kobayashi, H., Miyamae, Y., Rojas, E., Ryu, J.C. and Sasaki, Y. (2000) Single cell gel/comet assay: Guidelines for in vitro and in vivo genetic toxicology testing. *Environmental and Molecular Mutagenesis*, **35(3)**, 206-221.
[21] Devkota, B. and Schmidt, G.H. (2000) Accumulation of heavy metals in food plants and grasshoppers from the Taigetos Mountains. *Greece Agriculture, Ecosystems and Environment*, **78(1)**, 85-91.
[22] Hossain, Z. and Huq, F. (2002) Studies on the interaction between Cd(2+) ions and nucleobases and nucleotides. *Journal of Inorganic Biochemistry*, **90(3-4)**, 97-105.
[23] Misra, R., Smith, G. and Waalkes, M. (1998) Evaluation of the direct genotoxic potential of cadimium in four different rodent cell lines. *Toxicology*, **126(2)**, 103-114.
[24] Dally, H. and Hartwig, A. (1997) Induction and repair inhibition of oxidative DNA damage by nickel (II) and cadmium (II) in mammalian cells. *Carcinogenesis*, **18**, 1021-1026.
[25] Beyersmann, D. and Hechtenberg, S. (1997) Cadmium, gene regulation, and cellular signaling in mammalian cells. *Toxicology and Applied Pharmacology*, **144(2)**, 247-261.
[26] Waalkes, M., Fox, D., States, C., Patierno, S. and McCabe, M. (2000) Metals and disorder of cell accumulation: Modulation of apoptosis and cell proliferation. *Toxicological Sciences*, **56(2)**, 255-261.
[27] Korsloot, A., van Gestel, C.A.M. and van Straalen, N.M. (2004) Environmental stress and cellular response in arthropods. CRC Press, Boca Raton.
[28] Hamer, D.H. (1986) Metallothionein. *Annual Review of Biochemistry*, **55**, 931-951.
[29] Maroni, G.J., Wise, J., Young, J.E. and Otto, E. (1987) Metallothionein gene duplications and metal tolerance in natural populations of Drosophila melanogaster. *Genetics*, **117(4)**, 739-744.
[30] Barltop, D. and Meek, F. (1987) Effect of particle size on lead absorption from the gut. *Archives of Environmental Health*, **34(4)**, 280-286.
[31] Peng, T., Gitelman C.H. and Garner, S.C. (1979) Acute

lead induced increase in serum calcium in the rat without increased secreation of calcitonin. *Proceedings of the Society for Experimental Biology and Medicine*, **160(1)**, 114-117.

[32] Johnson, L. and Pellicciari, C.E. (1988) Lead induced changes in the stabilization of the mouse sperm chromatin. *Toxicology*, **51(1)**, 11-24.

[33] Ariza, M.E., Bijur, G.N. and Williams, M.V. (1998) Lead and mercury mutagenesis: Role of H_2O_2 superoxide dismutase and xanthine oxidase. *Environmental and Molecular Mutagenesis*, **31(4)**, 352-361.

[34] Miadoková, E., Vlčková, V., Jendraššaková, N., Vlček, D. and Šucha, V. (2000) Mutagenic and comutagenic effects of acid-mine water containing heavy metals. *Journal of Trace and Microprobe Techniques*, **18**, 201-207.

[35] Duydu, Y., Suzen, H.S., Aydin, A., Cander, O., Uysal, H., Isimer, A. and Vural, N. (2001) Correlation between lead exposure indicators and sister chromatid exchange (SCE) frequencies in lymphocytes from inorganic lead exposed workers. *Archives of Environmental Contamination and Toxicology*, **41(2)**, 241-246.

Vol.2, No.4, 298-306 (2010)
doi:10.4236/ns.2010.24038

Natural Science

Wave processes-fundamental basis for modern high technologies

Viktor Sergeevich Krutikov

Institute of Pulse Processes and Technologies at NAS of Ukraine, Nikolaev, Ukraine; iipt@iipt.com.ua

Received 28 December 2009; Revised 21 January 2010; accepted 16 February 2010.

ABSTRACT

Problems of moving boundaries, moving permeable boundaries, questions of control over wave processes are fundamental physical problems (acc. to V.L.Ginzburg) that exist for a long time from the moment of the wave equation emergence, for over three hundred years. This paper for the first time states a brief, but clear and quite integral disclosure of the author's approaches, and also a physical essence of analytical methods of functions evaluation of wave processes control - the basic processes of the Nature and the natural sciences, characteristic for all objects of the surrounding world without exception and able to occur only in the regions with moving and moving permeable boundaries. Absolutely immovable boundaries do not exist in the nature. Certain examples which are fundamental in theoretical physics of spherical, cylindrical and flat waves, including the waves induced by dilation of the final length cylinder, demonstrate physical, mathematical and engineering lucidity and simplicity (the solution comes to a quadratic equation), and, therefore, the practical value of definition of control function for the predetermined (based on engineering requirements) functions of effect. This paper is designated for a wide range of scientific readers, with aim to render to the reader first of all the physical sense of the studied phenomenon, to show the novelty that it has introduced in the development of the corresponding direction, to show that the way of the research (it is more important than the result) has not arisen "out of nothing", and the gained results are only "a stone which cost him a whole life" (H.Poincar).

Keywords: Waves; Mobility; Permeability; Boundary; Control; Inverse Problems

1. INTRODUCTION

"No recipes and prescriptions exist guiding how to move in an unknown sphere. Steps are taken by the method of attempts and mistakes. The winner will be the master of a better intuition and ability to solve a complicated task. However, it seems that luck and chance are of no less significance, unless we speak of such giants as Einstein." (V.L. Ginsburg, Nobel Prize winner) [1].

The "technologies" of getting scientific results, the logic of scientific discoveries are particularly individual. These questions are not solved exhaustively and for the present it is impossible to teach it. Special analysis shows that only a small percentage (about two) of all defended Ph.D. and doctoral theses contains a scientific novelty. The same small percent-about two and a half–is observed among the successful businessmen among the enormous quantity of those who carry on business in America. For all seeming triviality, the stated questions have a great scientific and applied significance. Therefore, it is rightful to describe and enumerate at one time not only scientific results, but also the technology, the logic of scientific discoveries which are especially relevant for wave processes and immediately relate to the theme of this paper. At present, one has just to accumulate and comprehend an individual philosophy of each researcher[1].

It is important to get an outstanding, great result, and it is more important to conceive the ways of its acquisition. These questions interested many people a long time ago, for example, Leibniz. The works of Henri Poincar "Science and hypothesis", "Value of science", "Science and method", "Last thoughts", "On science" [2], etc. are devoted to examination of cognition routs in mathematics, mechanics, physics. It seems that a lot of researchers, including Poincar, got scientific results at first, and then, looking back at their and not only their own traversed

[1]The American Biographical Institute USA and International Biographical Centre Cambridge CB2 3QP England, whose questionnaires contain the paragraph "Individual philosophy of success" and whose staff is more than 14000 of highly experienced and high-paid experts and specialized scientific institutions are engaged with it (see Great Minds of 21st Century).

path, they comprehended it. This process is essential and productive. Some basic ideas are selected and extracted to the epigraphs with similar purpose. It is worth to pay attention to how harmoniously they blend with the sequence of operations as for the problem-solving of moving permeable boundaries and the problems of wave processes control. It is the evidence of many things and first of that is the knowledge put in them which helps to get a new knowledge, new truths.

This article is not a systematic statement on the given question. The purpose of this publication is an opportunity kindly rendered by the editors of journal of ***Natural Science*** **(*NS*)** to share some considerations connected with attempts to solve the most difficult problems of mathematical physics which existed from the moment of wave equation creation. Scientific *results* for the solution to physical problems of moving boundaries (MB), moving permeable boundaries (MPB) and wave processes control are rather explicitly stated in the following studies: V. S. Krutikov: Technical Physics Letters 1988, 1989, 1990, 1999, 2000, 2003, 2003, 2005, 2005 (Chief editor Zh.I. Alferov); Doklady Physics 1993, 1999, 2006; Doklady Mathematics 1999; Acoustic Physics 1996; Applied Mathematics and Mechanics 1991; Izvestiya Russian Academy of Sciences MTT 1992, etc. This would serve the continuation of accumulation of information as for the comprehension of cognition ways by the personal example of complicated scientific problems solving.

2. WAVE PROCESSES

2.1. Mathematical Models

Wave process is one of the most important forms of substance motion. To some extent, wave movements are inherent to all objects of the material world without exception. Wave processes are the fundamental basis for the development of natural science, modern techniques and high technologies. Therefore, the problems-solving of mathematical physics with its most complicated problems of moving boundaries (MB), moving permeable boundaries (MPB) and the problems of wave processes control acquire great importance. Such problems for the regions with moving boundaries are complicated and little-studied [3].

Both linear and non-linear wave processes are intensively studied in electrodynamics, plasma physics, optics, fluid dynamics, acoustics, etc. The mechanisms of disturbance propagation naturally differ greatly from each other. The difference of physical mechanisms which realize a wave process leads to various different features in equation systems. However, there is often no necessity to analyze the initial often complicated equations systems in order to understand the most fundamental phenomena characteristic for the waves of different nature (interference, diffraction, dispersion, reverberation, refraction, dispersion, etc). As a rule, elementary effects are described with the help of simple and, therefore, universal mathematic models. Hence it is obviously possible to make a conclusion that the purpose of the research has to be not only the composition of especially complicated systems of differential equations in partial derivatives and their solution with the help of powerful computers, but also the reduction of task solution to the simplest mathematical model and acquisition of an analytical solution with the determination of its (model) validity limits [4,5].

It is a wave equation that serves such a universal mathematical model describing a lot of physical processes. It is also necessary to take it into account that due to some factors, the direct considering of all factors determining the complex phenomenon is a rather difficult task, and the task solution is achieved by combining the data on simpler model problems discovered at the analysis stage. Such models are studied by various methods with outstanding analytical methods of solution which give the most precious results of an absolute character. At the same time, physical experiment has a criterion value, and the potent side of numerical methods of solution is their efficiency. This statement enhances the role and shows the importance of solutions of a wave equation in the regions with moving boundaries, as rather often the simplest model problems lead directly to it.

However, even if the process under consideration is described with the help of a linear equation, the presence of moving boundaries makes the problem substantially nonlinear, the sum of two solutions is not a solution, and the method of superposition is inapplicable. The essential nonlinearity of the problem of moving boundaries for parabolic equations known as the problem of Stephen is analyzed in the works of G.A. Grinberg; for the wave equation it is shown in the works of the author [6,7]. It was the explanation why there were no methods of an exact analytical solution to such tasks. Exact solutions of this sort of problems retrieved mainly due to successful conjectures are known only for some particular kind of boundary conditions. Regarding the wave equation, this is the only one J. Taylor's solution (1946) [8] of a particular kind of a direct problem of sphere expansion with steady speed in a compressible medium. Direct problem when the conditions are specified at the moving boundary, inverse problem when the additional conditions are specified at a fixed point of wave zone, it is necessary to determine the functions under consideration in other points, including the near-field zone and the surface of moving boundaries. At the same time, the law of boundary moving is unknown and should be determined; and it can be non-linear. The presence of permeability of moving boundaries amends these concepts, new concepts–compound additional conditions–appear [9,10]. Let us give a definition to some terms: wave zone, near-field region, moving boundaries surface. While describing the processes in terms of mathematics due to the wave equation, and when the additional conditions are defined correctly, the following cases are distinguished: *a* – wave zone, when the given function (e.g. the pressure function) is determined through Langrange- Cauchy linear integral; *b* – near-field region – the given function (of pressure) is determined through Langrange- Cauchy linear integral; *c* – the predetermined function on the moving boundary surface is determined through Langrange-Cauchy nonlinear integral (nonlinear additional clause), at the same time nonlinear law of radius change of the moving surface of the boundary, which is known beforehand, is included in compound arguments of these functions on the moving boundary. Nonlinear additional clauses are the first nonlinearity; the presence of moving boundaries is the second nonlinearity; if these two nonlinearities exist, the problem is supposed to be twice nonlinear.

Interaction of arguments means the following: the functions of an additional clause with one sort of arguments are put in an interim decision having another sort of arguments. As a result, we get the solution with the third sort of the argument.

The researches had to accept various assumptions: to change the boundary conditions, to transfer the boundary conditions to fixed boundaries or to replace the actions of moving boundaries by the system of peculiarities. This leads to the limited nature of decisions, and sometimes to unacceptable results. It is indicative that the solution to the wave equation was got by d'Alember (1747): Cauchy problem-initial conditions are known, boundary conditions are missing, and the functions form that depended on boundary conditions remained unknown. In a known summarizing of a general method of terminal integral transformations (Koshlyakov N.S., Grinberg G.A.) for direct problems, "momentary" eigenfunctions expansion is used. However, it leads to the solution to the infinite system of first-order differential equations. Traditional approaches appeared to be unacceptable for the solution to the moving boundaries problem, and it was necessary to seek for the new ones.

2.2. Interaction of Complicated Non-Linear Arguments

The basis for mathematic physics is three main equations: heat conduction equation, wave and Laplace's equation. The largest quantity of processes are described with the help of wave equations.

Before it could be solved only numerically, that is in the regions with moving boundaries. Let us ask ourselves the following question: why the main equation of mathematical physics was not solved, that is the wave equation in the regions with moving boundaries. In the author's opinion, there are two reasons. The first one is that only the direct problems were solved (G. Taylor), which resulted in insuperable mathematical difficulties under voluntary boundary conditions. The second one is that the fundamental fact of all wave phenomena in compressible spheres of disturbances propagation with finite speed was not taken into account. The author managed to overcome theses difficulties in the following way. First of all, let us examine the fact of disturbances propagation in a compressible sphere with the finite speed which is directly connected with the concept of a lag, and in its mathematical describing it is connected with the concepts of compound arguments, the quantity of compound arguments, and with the interaction of compound nonlinear arguments. It is impossible to get accurate analytical solutions of inverse and direct wave problems in the regions with moving boundaries without the comprehension of these concepts and their application. Let disturbance appears at some point of time on the surface of finite size of initial radius, for example, on the surface of sphere with the source of its expansion. Waves generated in this way are used in different technologies. Then in the point of wave zone in some distance from the center of the sphere the disturbance appears not in the moment of beginning of wave expansion but after some dead time, which is equal to the quotient from the division of distance from the source surface of the sphere to the point of wave zone by the speed of disturbance expansion according to the certain medium [6]. Thus, logical considerations would give us some more varieties of arguments with lags which interact when mathematical operations are carried out. There appears to be five such arguments for the wave problem of sphere expansion (see [6]). There are sixteen of them for the problem with two moving boundaries. It is significant that this information is got without the solution to the equation itself. Having determined all varieties of compound arguments with the lags, it is natural to try to find that succession of mathematical operations in solving an equation for wave problems which keeps all kinds of found arguments. For the first time, such a succession was found by the author and named as the methods of inverse problems with regard for the interaction of nonlinear arguments. This is the ground to the second reason. At the same time it is meant that it is impossible to solve the pointed problems just with the help of the methods of inverse problems. These problems are also necessarily solved with regard for a great number of compound arguments, including nonlinear ones with various lags and also taking into consideration the fact that they interact.

Here the following question may appear: having determined, for example five varieties of arguments with lags, on what ground, on what is the confidence based that all these kinds of arguments would correspond the internal structure of wave equation?

Such a confidence appears already if one examines d'Alember's solution (of Cauchy problem) of wave equation. There already exists, though the only one, variety of lag [11]. It is possible to become firmly convinced in it when an accurate analytical development of wave equation in the regions with moving boundaries with all found varieties of arguments, the substitution of which turns the left side of the wave equation into zero. It is significant that for the first time in mathematical physics the author determined all compound arguments, and the fact of their interaction. It allowed fro the first time to create the methods of inverse problems with regard to the interaction of nonlinear arguments and for the first time it allowed to get accurate analytical developments of wave problems with moving boundaries and moving permeable boundaries.

As we can see in this case, the truth inherent to the nature itself is the fact of disturbance expansion in continuum with the finite speed in which mathematical description gave grounds to various arguments with delays.

2.3. Deeply Hidden Mathematical Truths

The author understands this in the following way. On the one hand, the study of the done by other people is meant. Historical, consecutive, according the chronology of events, approach to the study of the material is based on it. On the other hand, it is necessary to begin to gather information for reflection gradually while studying something unknown and solving more simple particular problems. Since it is clear that particular solutions bear the marks of accurate development and help to comprehend the ways of its receipt. Such an accumulation can be carried out by the generations of scientists. It can be also done and by the only one scientist in the course of his whole life. For example, Gauss K.F. worked in such a way. As is well known, Gauss was an incomparable calculator and, just as other outstanding arithmeticians did, he usually got his new results from extensive numerical calculations which helped him to notice new, deeply concealed mathematical truths, the proofs of which he got quite often only in the result of painstaking, enduring, sometimes long-term work. The succession of accumulation of information is also observed in technique. For instance, stitching: awl - threads - needle with an eye - sewing machine. Or another example: wheel - axle – axle with blades - screw propeller - turbine.

As it turned out, in solving the problems of moving and moving permeable boundaries, both of these methods are examined, but in the main the example of Gauss is closer to what has really happened [6].

2.4. What was Done for the First Time in Solving of Problems of Moving and Moving Permeable Boundaries

The author considers the main result to be the fact that for the first time the new non-traditional author's method for solving the problem of moving boundaries of mathematical physics equations was proposed and devised—these are the methods of inverse problems with regard for the interaction of nonlinear arguments. The new method of moving boundaries problem solving, just as the wave equation itself lie outside the scope of use in the problems which describe pulse processes. It let to get universal analytical solutions of intricate nonlinear problems. They are suitable for inverse and direct problems for a wave equation with one and two moving boundaries, one of them moves and another one is fixed [13]; with nonlinear conditions and moving boundaries [12]; with nonlinear conditions at moving boundaries. Two latter cases are twice nonlinear problems. At the same time the laws of change of boundary moving speed, data of initial radiuses and displacements may be voluntary. Received results reflect the wave processes of various physical natures. It is necessary to point out that the name of the nontraditional approach to the solution to moving boundaries equations of mathematical - the methods of inverse problems involving interaction of nonlinear arguments - reflects physical and mathematical essence of the author's method very successfully and exactly [6,10,14].

The prospects of the developed method considerable: analytically direct and inverse problems of special difficulty with permeable (radiant) moving boundaries are posed and solved [6,10,15], the laws of change of permeability speed and speed of boundary moving may be voluntary. Such problems in mathematical physics were not examined. The developed system is a methodological basis for the study of the influence of new, similar off-center boundary conditions. At the same time, the solution to twice-nonlinear problems is brought to the algebraic equation solving. Trustworthiness of findings is proved by the comparison with the results of experiment and solutions of more complicated equations and systems of nonlinear equations with the help of known methods (characteristics, dimensions and similarity, small parameter etc.), the correctness of current inverse problems is shown. Substitution of received solutions into the wave equation turns its left side in zero. Developed analytical methods of compound wave problems solution may be used to give solution to new problems of theoretical fluid mechanics, theoretical physics and mathematical physics.

2.5. Wave Processes Control. The Mobility and Permeability of Moving Boundaries as the Principle of Control

To the author's mind, the control is possible when the study of the process reached certain level and when all possible control consequences are conceived. The proposed and developed method of solution to moving permeable boundaries problems of mathematical physics equations allowed to proceed from the processes of cognition of wave phenomena to more complex and important processes of wave phenomena control.

The wave equation serves as the mathematical model of a great number of physical processes, the necessity of their control appears, as a rule, simultaneously with the study of these phenomena. The abilities of control are determined both by the availability of exact analytical solutions of inverse wave problems (control problems), and to a greater extent — by the formulating of mathematical models, which let to describe practically all possible variety, all conceivable wave fields in a theoretical way. Wave equation realized in the regions with moving and moving permeable boundaries is such an important mathematical model.

As is well known, control, in the general case, is the function of organized systems of various nature (biological, physical, technical, social etc.), which describes the preservation of their definite structure, maintenance of activity regulations, realization of the program, and purposes of the activity. The task of control is the determination of control function. In the context of the examined mathematical model under control is understood the following: the first one – velocity function (moving and permeable moving boundary) or the second – pressure function (at the moving boundary). The purpose of investigations at the control problems is the definition of control functions of the first and second cases, which supply the receipt of adjusted wave regions of velocity and pressure in necessary points, including the near-field region and moving surfaces of boundaries (where the experimental determination passes with difficulty or impossible), and also their purposeful change during certain period of time.

The main, basic concepts which explain properties and possibilities (to control) of named mathematical model, are mobility and permeability of moving boundaries, what is the control principle by definition.

The methods of inverse problems with regard for the interaction of nonlinear arguments allowed to get exact analytical solutions of inverse wave problems with moving boundaries. In inverse problems solving the investigated pressure function is defined, reasoning from technological necessities, the pressure function (or velocity) under consideration in the point of wave zone. The received solutions determine the examined functions in any points and at moving boundary. The knowledge of pressure and velocity functions at moving boundaries is the knowledge of control functions of wave processes; thereby the control problem becomes decided. In applications, using the energy balance equations, which connect pressure and velocity at moving boundary of plasma piston with the quantity of input energy in the channel, we get accurate analytical dependences. They let to know the law of input energy in plasma channel of discharge or laser impulse, for example, for the receipt of adjusted pressure and velocity wave fields in a compressible medium [16].

Thus, we see that it is possible to control wave processes in an accurate way only on reaching the definite level of knowledge of the process. In this case, the knowledge of exact analytical dependences of control functions of the first and second cases (velocity and pressure functions at moving boundaries). Without this exact knowledge of control functions, the control itself turns into the series of attempts to determine the wishful (required) thing through attempts and mistakes, mostly accidentally. Frequently this leads to time and funds losses, and even lives. As is well known, especially tragic are the attempts to implement such a control in a social sphere.

As we see, the conclusions concerning the possibility of wave processes control also have a more general character. They also contain information (signs) on other more complicated control processes, including the ones of a social character. At present, there is no possibility to define control functions with the help of such complex systems, because of their extreme difficulty. Their study may take place on the stage of examination of simpler models.

Registration and use of permeability (radiation) of moving boundaries are greatly significant for the receipt of the adjusted forms of examined functions that is the control problems solution. Such problems belong to complex unexplored essentially nonlinear class of problems of mathematical physics. Mathematical formulating and involvement of permeability of moving boundaries are executed at first by the author [6,7,15].

Received solutions are fit for inverse and direct problems for voluntary values of initial radius, displacements, laws of change of rate of movement and permeability of boundaries. Such problems appear, in particular, in fluid dynamics, seism acoustics, at examination of a dynamite source, for instance, of electric discharge, laser pulse etc. in fluid, which has the temperature close to critical one. The effect of dynamite source results in intense vaporization from the moving surface of plasma cavity. In this case wave phenomena under research may be described with the help of mathematical model with a moving permeable boundary.

It should be noted that the most complex and unexplored is the definition of control function for the wave equation with moving boundaries and nonlinear conditions at moving boundary. At the same time, the law of motion of moving boundaries is unknown, is to be defined, and may be nonlinear. The problems with nonlinear additional conditions and moving boundaries are twice nonlinear problems and they are of great interest, their applied importance is so great that they become in the number of the issues of the day of mathematics, physics, and mechanics. Such problems in mathematical physics were not examined. The methods of inverse problems with due regard for interaction of nonlinear arguments allowed to get analytical solutions of theses twice nonlinear wave problems, and their solution is for the first time reduced to the solution to the algebraic quadratic equation [13].

The definition of validity limits of physical and mathematical models and their solutions is the requirement of completeness of every elaboration. The wave equation is the mathematical model of many physical processes. However for all that it is necessary to take into account that the validity limits of its solutions may be different in every particular case, for every process under investigation. The absence of exact analytical solutions for wave equations with moving boundary and moving permeable boundary did not allow to define its validity limits in impulse fluid dynamics and acoustics, for example, to present day. These two disciplines, two scientific trends began before the year 1717 – the time of creation of wave equation (Taylor Brook). These limits were vague and were system according the pressure from several hundreds to several thousands atmospheres. Such a dispersion in dozens of times is intolerable. Exact analytical solutions, received with the help of inverse problems methods with regard for the interaction of nonlinear arguments, allowed to define the validity limits of wave equation with moving boundaries и moving permeable boundary in impulse fluid dynamics and acoustics for the first time and unambiguously [6,7]. It was carried out in a nontraditional form - not according the pressure, what cannot be produced unambiguously, but according the velocity of boundary moving in compressible medium.

These limits are also defined for the cases of moving permeable boundaries, what has great scientific and applied significance.

Thus, we come to a conclusion that the logic of investigations lies basically in the following sequence of priorities. Victory, achieved in search of truth, heads the list of all achievements. Naturally, the preference is given not to knowledge hoarding, but to sincere, outstanding search for the new knowledge. Mathematical models and their solutions are built on basis of the truths inherent to the nature itself, which is highly important. Gathering and using both the information of the ancestors and the one got in the process of particular problems solution in a purposeful way, to create new untraditional methods. New methods are the tool used to accept an infinite number of valuable results.

A non-traditional approach to wave problems solution in the regions with moving boundaries – the methods of inverse problems with the regard of nonlinear arguments interaction is fundamentally new in the development of mathematical physics. It allowed to solve not only direct wave problems with moving boundaries, but also inverse problems which were not solved before; system and solve complex substantially nonlinear problems with moving permeable boundary – both direct and inverse; to solve analytically twice nonlinear problems (with moving boundaries and nonlinear additional conditions); to reduce the solutions of twice nonlinear problems to algebraic equation. It allows to solve the new classes of problems of theoretical fluid mechanics and theoretical physics, mathematical physics.

Moreover, the method allowed making a big qualitative step forward: to pass from the learning of wave phenomena to more important and complicated wave phenomena control process. It is shown that the correct wave processes control is possible only when certain level of knowledge of the process is achieved–the knowledge of exact analytical dependence of control functions.

3. FUNDAMENTAL BASIS FOR MODERN HIGH TECHNOLOGIES

3.1. Some Aspects (Illustrating) of the Received Results Application

Pulse processes may serve as an illustration of application of received results. Electric discharge, laser pulse, explosion of charge and premixed gases, a blow against the surface etc. in compressible media belong to them. They are one of the essential principles of modern high technologies including informational ones (geophysics, geoacoustics etc., mineral exploration overland and at sea etc.). Many outstanding scientists were engaged in the theory of pulse processes, amidst them are the following: Sedov, L.I., Lavrentiev, M.A., Christianovich, S.A., Kochin, N.E., Shemyakin, E.I., Landau, L.D., Okun, I.Z., Yakovlev, Y.S., Baum, F.S., Stanyukovich, K.P., Laurentiev, M.M., Alekseev, A.S, Korobeynikov, V.P., Naugolnych, K.A., Roy, N.A., Lyamshev, L.M., Kurant, R., Fridrichs, K., Chariton, Y.B., Zeldovich, M.A., Rozhdestvensky, B.L., Yanenko, N.N., Lighthill and many others.

Characteristic feature of pulse processes in compressible media is the presence of moving boundaries of phase division plasma-fluid, gas-fluid (and also of moving explosions, barriers etc.). Taking into account the influence of this peculiarity and also of the initial radius value is necessary while studying the plasma of electric discharge channel, laser pulse etc. in fluid, while studying wave processes, including the ones of the near-field region of the expanding boundary of plasma cavity, the solution to the problems of pulse processes control; modeling of disruption (breakdown) of a spark gap (being a separate complex problem) and in many other cases, for example, at materials surface cleaning and treatment, punching, fragmentation, investigations of behavior of bubbles in a two-phase media, etc.; growth of wear-resistance and corrosion resistance, influence on crystallizing alloy, interaction with plates and jackets and many others. Hence we see that there is no such a technology on base of pulse processes, where the main equation of mathematical physics – wave with moving boundaries – would not be used at the heart of the processes. There will also be other technologies based on wave processes, but wave equation with moving boundaries would also be at their heart. This is an imperishable value wave equation with moving boundaries, and its exact solutions, which were at first acquired with the help of inverse problems methods with regard of nonlinear arguments interaction.

It is necessary to pay attention to known important circumstances. Technologies developed on basis of experimental data without support of fundamental theoretical elaborations have narrow orientation, cannot be widely used, are not replicate, that is expensive experiments will be again necessary for another allied technologies, a considerable waste of time and funds. However, for all that rather often when experiments are made the physical sense of phenomena is not comprehensible and studied enough because of their great difficulty. For instance, physics of perturbation effects on crystallizing metal, development physics and “healing” of cracks formed during pulse processing etc., with all following negative consequence. Besides, nowadays, as a rule, workable technologies do not find manufacturing application and become out-of-date because of an economical grave condition. Minor number of high technologies and industrial standards are used in modern manufacture. As soon as the results of fundamental researches do not become out-of-date, are of imperishable value and will always be wanted for the elaboration of new high technologies both now and then. Therefore, it is evident that fundamental researches should have priorities for elaborations and financing, it is the most efficient and economically profitable, advantageous and purposeful way.

In the presence of high technological culture some countries spend dozens of milliards of dollars on the creation of their fundamental science.

3.2. New Ways of Use of Particular Wave Processes in Particular High Technologies

A lot of high technologies border on art, for example, cooking, formulation of drugs, wine making, preparation of paints, “Greek fire”, damask, the technologies of treatment etc., many products of defense technology, “technology” of performance of musical compositions, creation of artistic masterpieces, “technologies” of getting of new scientific truths, discoveries etc. Coming in the form of complete product even to the country with high technological culture, the products of high technologies cannot be reproduced for a long time, sometimes never at all. Yet, some of them cannot be described with the help of physico-mathematical models.

At the same time, it does not require proves that modern high technologies are impossible without mathematical physics. They are the concentration of scientific discoveries of many scientists, sometimes of the whole generations, engineering and technological developments. One of the main physical phenomena of modern higher technologies based on pulse processes is the motion of moving boundaries of the division of plasma-fluid phase, gas-fluid, which generate shock waves, perturbation waves, media waves etc., used in various technologies, at which mathematical description we come to the problems of moving permeable boundaries. Among the described pulse processes, underwater electric explosion is the most powerful controlled generator of cavitation phenomena, which exceeds the possibilities of mechanic oscillators. Recently it was established that underwater electric explosion in its acoustic spectrum generates not only low-frequency vibrations, but also ultrasound ones to the extend of a hundred kHz.

Here are some examples of new methods of use of wave processes, induced by electric discharge in fluid: the explosion of thin coal conductors (fibers) - the receipt of fullerenes, necessary for manufacture, for example, of special radio technical products; the receipt of metals oxides, which find their application in the production of paint, structural ceramics, used, for example, in mechanical engineering, covering of spacecrafts of nonexpendable usage, the production of superconducting materials (superconductor) etc.; discharge-pulse technology of pure decomposition of various radio materials, namely of phosphor; the receipt of high quality flax fibers with the purpose of their application in textile manufacture and at production of medicinal cotton, and also of other strategic materials; breaking up of gravel, cement blocks, wastes of porcelain manufacture etc. in a wide spectrum from lumpy breaking up of non- metallic materials to ultrafine pounding; moulding refinement–removal of core sand mixture from mouldings; electroblasting diameter extension (extension of size), ends fixity of tubes in tube plates of heat-exchange apparatuses by means of electroblasting diameter extension (extension of size); sputter-ion processing of oil and water wells on purpose of rising of their flow rate (increase of oil recovery of plates etc.); protection of young fish from getting to water supply points of water supply systems; stamping of goods from plate stock; the creation of acoustic resistance devises in seas and oceans; the creation of generative probing signal, used at mineral exploration; catalysts preparation and intensification of catalytic processes; the preparation device of subsided rocks for the construction of buildings and erections; electroblasting technology of water conditioning and sterilization of sewage by means of generation of high-level cavitation processes; layer-by-layer sputter-ion sparing release of high-radiation lavas safety fourth block Chernobyl nuclear power-station from depositions and lots of others. See works [17] and [18] to learn in details about these and other technologies having no world analogs on basis of electric discharge in fluid.

The significance of the solution to moving permeable boundaries problems and wave processes control problems is not limited by their usage for the elaboration of new technologies. New developed approaches to the creation of analytical methods of complex wave problems solution, including twice nonlinear, can be used for the creation of new methods of mathematical physics to solve the problems within the spheres of theoretical fluid mechanics and theoretical physics.

The content of paragraphs 1-5 which contain the investigations development descriptions and mentioned in epigraphs, composes the necessary conditions of getting the new truths. It is evident that non-observance of the only one of them is impossible. From the author's point of view, sufficient conditions are in individual philosophy of success.

4. CONCLUSIONS

General concepts, views, theories, laws and principles should be considered of the first importance [19]. To this extent, the most significant ones are the wave processes and the questions regarding their control. This article is devised for a wide circle of scientific readers with aim to render to them first of all the physical ground of the examined phenomena, and also to manifest the novelties which it brought into the development of a respective tendency, and that the way of the investigation did not emerge "out of nothing", and the retrieved results are only "the stone which cost him a whole life" [2]. This study is the synopsis of the information covering author's publications.

Furthermore, it is necessary to mention the following. Astonishing exceptional number of applications of the wave equation "from the waves in the oceans of water, air and ether", as Russell [20] would tell, to the waves, describing the elementary particles. Nowadays the wave equation became so customary and usual, that nobody is surprised at its effectiveness any longer. However, if one tries to comprehend in one's mind everything that has been done with the help of this equation, simply to imagine what a wealth of natural phenomena is hiding behind such a simple formula, the epithets "astonishing" and "extraordinary" would seem inappropriate. Once, an eminent contemporary physicist wrote a popular article "On the incomprehensible effectiveness of mathematics in natural sciences". [21] There is surely something incomprehensible in the effectiveness of the wave equation, no matter what everything-can-explain people say [20]. Evidently, now the effectiveness of the wave equation rises repeatedly due to the presence of exact analytical solutions of inverse (and direct) wave problems in the regions with MB and MPB, which were for the first time received by the methods of inverse problems involving interaction of nonlinear arguments. So far, the simple truth is that neither measurement, nor experiment and observation are possible without a respective **theoretical** scheme [22]. At development of such schemes a significant role is played by control functions described above. Without these control functions it is impossible to develop such schemes. Moreover, in case when a successful model of physical phenomenon is designed, i.e. the model which allows to make accurate calculations and predictions, then the mathematical structure of the model itself reveals new sides of these phenomena. As the result, the "studies of an internal structure of a model" can change and broaden our notions of physical phenomena [23] Vol.1, p.7.

The following statement brings surety. Wave equation and its accurate analytical solutions are devised on basis of the phenomena adherent to the nature itself, the phenomena of agitations propagation in continuum with a final velocity. It is evident in terms of physics that wave phenomena – the basic phenomena characteristic for all objects without exception – reflection in a wave equation, "a marvelous basic equation of mathematical physics". Other equations, e.g. parabolic, etc. are "unphysical", since they describe the agitations which propagate instantaneously [24].

A wonderful correspondence of mathematical language to the laws of physics [21] is actually a real gift. But it is not a mystery and we can and are able and dignified to accept it, which is demonstrated on the example of the fore-mentioned physical problems solution. Optimism is bred from an enormous role of mathematical methods for the solution to **physical problems**, e.g. the known scheme of three steps [25] for the solution to **various** problems: the problem of any kind comes to mathematical problem; mathematical problem of any kind comes to algebraic problem; any algebraic problem comes to solution to one single equation. This is demonstrated by the formulas, e.g. stated in work [13].

It is worth citing the optimistic words of d'Alember instead of conclusion: work, work, absolute comprehension comes later. As we see, it took three hundred years to understand the essence to take into consideration the influence of mobility and permeability of moving boundaries on wave processes [7,9,10,14,26].

REFERENCES

[1] Ginsburg, V.L. (1985) O fizike i astrofizike. *Physics and Astrophysics*, **400**, 100.

[2] Poincar, H. (1983) O nauke. *Science*, **270**, 218.

[3] Tikhonov, A.N. and Samarskiy, A.A. (1972) Uravneniya matematicheskoy fiziki *Equations of Mathematical Physics*, **735**.

[4] Lavrent'yev, M.M. (1964) On one inverse problem for a wave equation. *Doklady Akademii Nauk SSSR*, **157(3)**, 520-521.

[5] Lavrent'yev, M.A., Shabat, B.V. (1973) Problems of hydrodynamics and their mathematical models. *Nauka*, **416**.

[6] Krutikov, V.S. (1985) Odnomernye zadachi mekhaniki sploshnoi sredy s podvizhnymi granitsami (One-dimensional problems in continuum mechanics with moving boundaries). *Kiev, Izdatel'stvo Naukova Dumka*, **125**, 128.

[7] Krutikov, V.S. (1996) Validity Limits of solutions to the wave equation for regions with moving permeable boundaries in impulse fluid dynamics and acoustics. *Acoustical Physics*, **42(4)**, 471-477.

[8] Taylor, G. (1946) The airwave surrounding an expanding sphere. *Proceedings of the Royal Society A, Mathematical and Physical Sciences*, London, **186(1006)**, 273-292.

[9] Krutikov, V.S. (1999) Waves surrounding an expanding permeable cylinder in a compressible medium. *Doklady Physics*, **44(10)**, 674-677.

[10] Krutikov, V.S. (1993) Wave phenomena with finite displacements of permeable boundaries. *Doklady Akademii Nauk*, **333(4)**, 512-514.

[11] Isakovich, M.A. (1973). Obschaya akustika. *Fundamental Acoustics*, **495**.

[12] Krutikov, V.S. (1992) Interaction of weak shock waves with a spherical shell involving motion of the boundaries. *Mekhanika Tverdogo Tela*, **2**, 178-186.

[13] Krutikov, V.S. (1991) A Solution to the Inverse problem for the wave equation with nonlinear conditions in regions with moving boundaries. *Prikladnaia Matematika i Mekhanika*, **55(6)**, 1058-1062.

[14] Krutikov, V.S. (1999) A new approach to solution to inverse problems for a wave equation in domains with moving boundaries. *Doklady Mathematics*, **59(1)**, 10-13.

[15] Krutikov, V.S. (1999) Waves surrounding an expanding permeable cylinder in a compressible medium. *Doklady Physics*, **44(10)**, 674-677.

[16] Krutikov, V.S. (2003) An exact analytical solution to the inverse problem for a plasma cylinder expanding in a compressible medium. *Technical Physics Letters*, **29(12)**, 1014-1017.

[17] Gulyi, G.A. (1990) Scientific fundamentals of pulse-discharge technologies. *Naukova Dumka*, Kiev, **208**.

[18] Shvets, I.S. (2002) 40th Anniversary of the institute of pulse processes and technologies at NAS of Ukraine. Science and production. *Theory, Experiment, Practice of Electrodischarge Technologies*, **4**, 3-6.

[19] Ginsburg, V.L. (2000) Physics: Past, present, and future. *Priroda*, **3**.

[20] Philippov, A.T. (1990) Mnogolikiy soliton. *Nauka*, **297**.

[21] Wigner, E. (1968) On Incomprehensible efficiency of mathematics in natural sciences. *Uspekhi Phizicheskikh Nauk*, **94(3)**, 540.

[22] Prigozhin, I. and Stengers I. (1986) Order out of Chaos. Bantam Dell Publishing Group, Moskow, **364**.

[23] Reed, M. and Simon, B. (1977-1982) Methods of contemporary mathematical physics. Springer, Moscow, **1-4**.

[24] Krutikov, V.S. (1995) Development of the method and solutions of pulse problems of continuum mechanics with moving boundaries. Dissertation by the Doctor of Physico-mathematical Sciences, Institute of Geophysics NAS of Ukraine, Kiev, **343**.

[25] Poya, D. (1970) Mathematical invention. *Nauka*, **45**.

[26] Krutikov, V.S. (2006) On an inverse problem for the wave equation in regions with mobile boundaries and an iteration method for the determination of control functions. *Doklady Physics*, **51(1)**, 1-5.

Vol.2, No.4, 307-319 (2010)
doi:10.4236/ns.2010.24039

Natural Science

The thermoanalytical, infrared and pyrolysis-gas chromatography-mass spectrometric sifting of poly (methyl methacrylate) in the presence of phosphorus tribromide

Muhammad Arshad[1*], Khalid Masud[2], Muhammad Arif[3], Saeed-ur-Rehman[4], Jamshed H. Zaidi[1], Muhammad Arif[1], Aamer Saeed[5], Tariq Yasin[6]

[1]Chemistry Division, Directorate of Science, PINSTECH, Islamabad, Pakistan; marshads53@yahoo.com.sg
[2]New Laboratories Pinstech, Islamabad, Pakistan
[3]Department of Chemistry, Bahauddin Zakariya University, Multan, Pakistan
[4]Institute of Chemical Sciences, University of Peshawar, Peshawar, Pakistan
[5]Department of Chemistry, Quaid-i-Azam University, Islamabad, Pakistan
[6]DCME, Pakistan Institute of Engineering & Applied Sciences, Islamabad, Pakistan

Received 23 December 2009; revised 25 January 2010; accepted 29 January 2010.

ABSTRACT

The behaviour of poly(methyl methacrylate) was examined in the presence of phosphorus tribromide (PBr_3) with varying concentrations. Films were cast from common solvent and subjected to TG, DTA, DTG, IR and Py-GC-MS for evaluating the degradation routes. Despite early decomposition of the blends, certain temperature zones were identified for stabilization of the system. New products were found and mechanisms of their formation were proposed. Pyrolysis of the blends was also carried out at different temperatures to ascertain the nature of interaction between the constituents of the system.

Keywords: PMMA; PBr_3; Thermoanalytical Study; IR Spectroscopy; GC-MS Investigation

1. INTRODUCTION

The thermal degradation and flammability characteristics of poly (methyl methacrylate) chemically modified with silicon-containing groups, functionalized by phosphorus-containing groups and also neat poly(methyl methacrylate) with a number of additives have been reported by several researchers [1-12].

Poly (methyl methacrylate) is widely used and studied poly alkyl methacrylate thermoplastic polymer, but it is highly flammable owing to the ease with which it degrades thermally (depolymerise), releasing large quantities of highly flammable volatile, monomeric and oligomeric frangments. Thermal decomposition characteristics of PMMA are well-understood [2,9,10,13,14] and a lot of research work is underway to improve its flammability as well as other features by additive-route technique.

Our interest in the thermal behaviour of polymeric/ copolymeric systems and these systems in combination with additives (organometallics) has resulted in a number of publications [15-21]. It was observed with overwhelming evidence that polymers/ copolymers showed markedly different thermal behaviour when heated even in the presence of minor amounts of additives. The interaction between the constituents was chemical as well as physical. The products of degradation were identified as either completely different (new ones) or if same, exhibited variation in amounts when this feature of the neat and blended systems was compared. Physical nature of interaction was noticed due to the sublimation of additives in addition to the heat- sinking property of stable residues from the degradation of additives. The shifting of T_i (temperature corresponding to the first weight-loss), T_{50} (temperature which designates the 50% weight-loss of the system) and T_{max} (temperature which gives the maximum weight-loss) clearly indicates the effects of additives on the degradation of polymers/copolymers. Recently, our research activities have seen a shift in the nature of additives, *i.e.*, from organometallics, we have started introducing purely inorganic compounds in polymers/copolymers of commercial importance [22,23]. This change in approach is based on the fact that the degradation of organometallics also results in the production of those species which are themselves flammable, whereas our aim is to modify the degradation mechanism in such a way as not only to increase the temperature of degradation but also to seek the formation of non-flammable or less flammable degradation products.

This paper is concerned with the influence of phosphorus tribromide—a non-metal halide—on the PMMA for the course of degradation with the aim to establish possible chemical interaction between the components by using different ratios of polymer and additive. Emphasis is laid on the mechanism of the observed effects, in particular, on the formation and identification of degradation products.

2. EXPERIMENTAL

2.1. Chemicals

All the reagents and solvents obtained from standard source suppliers (E. Merck) were of analytical grade. The monomer, methyl methacrylate, was freed from inhibitor (hydroquinone) by washing with aqueous 5% sodium hydroxide followed by de-ionised water until neutral and then it was dried over anhydrous calcium chloride for 24 hours [24]. It was distilled under reduced pressure prior to use, only middle portion was chosen for polymerization. 2, 2'-azobisisobutyronitrile (AIBN) was selected as radical initiator for polymerization and was purified by re-crystallizing from absolute ethanol. The crystals obtained were dried under vacuum and kept in refrigerator (black paper wrapped around bottle). Phosphorus tribromide was prepared by the standard procedure [25]. All solvents were distilled by standard literature procedures before use.

2.2. Preparation of Poly (Methyl Methacrylate)

The homopolymer was synthesized by free radical polymerization by the reported procedure [26]. The purified monomer was de-aerated and vacuum-distilled into the calibrated dilatometer containing sufficient amount of 2, 2'-azobisisobutyronitrile initiator to give 0.7% w/v in the solution. The dilatometer was sealed under vacuum and polymerization was carried to 10% conversion at 60^{o}C in hot water bath. The mixture was then added to 100 mL of toluene and the polymer was precipitated from 1 liter of methanol. The polymer was collected by filtration, vacuum dried, purified by reprecipitation (thrice) and finally dried in a vacuum oven at 50^{o}C for 24 hours.

2.3. Formulation of Blend for Analysis

The blends with varying compositions of PMMA and phosphorus tribromide in the form of thin films were prepared by employing common solvent, *i.e.*, acetone. The known amounts of polymer and additive were mixed separately in a sufficient quantity of acetone and were left overnight in closed Pyrex tubes to dissolve completely at ambient temperature. Both the solutions were mixed, shaken thoroughly, placed for 24 hours in dark place to mix completely and then poured into a well-cleaned transparent Pyrex dish. Complete evaporation of the solvent was effected at STP. The resultant film was transparent in the dish confirming the compatibility of the components of the pair studied.

2.4. Procedure to Prepare Strip for Flammability Test

For neat PMMA sample, the polymer was added to acetone and kept overnight to dissolve completely. The solution thus obtained, was poured into an aluminum mold with the dimensions, 1 mm × 7 mm × 150 mm, the inside cavity of which was covered with high density polythene sheet. The mold was left for 48 hrs in dark for complete dryness. For the blends, both polymer and additive in definite ratios were dissolved in acetone separately and set aside for 24 hrs. Individual solutions were then intermingled and placed in dark place for complete miscibility. This solution was then poured in the mold and allowed to dry for 48 hrs in a thoroughly-cleaned dark place. The dry sample was removed and kept in desiccator for the required test.

2.5. Physiochemical Methods

Thermoanalytical (TG-DTA-DTG) curves were obtained using Netzsch Simultaneous Thermal Analyzer STA 429. All the measurements were carried out with samples having 30-60 mg initial mass. These were heated over the temperature range from ambient to 800^{o}C in an inert atmosphere (nitrogen), using kaolin as reference material. The heating rate was 10^{o}C min^{-1}.

Infrared (IR) spectra of polymer, additive and those of residues produced after heating the blends at various temperatures were recorded with Nicolet 6700 FT-IR spectrometer in the range 4000-400cm^{-1}.

The liquid chromatograph, Hitachi 655-A-11 with GPC software and integrator (D-2200 GPC) along with column GLA-100m (Gelko), was employed for molecular weight determination of polymer at room temperature. The detector system consisted of Hitachi 655-A UV variable wavelength monitor (= 254 nm) and SE-51 (Shodex) refractive index detector. Polystyrene standards were used for calibration curves and HPLC grade tetrahydrofuran (Aldrich) was used as solvent. The molecular weight was found 120000.

The samples were subjected to an Agilent 6890N type GC-MS coupled with 5973 inert MSD, by Agilent Analytical Instruments, Agilent Technologies, USA. Analysis of the products in acetone was performed with a DB-5MS column. The injection volume was 1 μL. The temperature program entailed an initial increase of temperature from 120-150^{o}C at 10^{o}C min^{-1} and from 150-280^{o}C at 15^{o}C min^{-1}. The mass spectrometer was operated in the electron-impact (EI) mode at 70 eV.

Horowitz and Metzger method [27] was used to calculate activation energy (E_o) and order of reaction (n) of polymer and its blends. A plot of ln ln Wo/Wt (where Wo = initial weight of material and Wt = weight of material at temperature T) against θ (θ = T – Ts) resulted in a straight line. The activation energy was determined from its slope which was equal to E_o/RTs^2 (where R = gas constant and Ts = temperature (from DTG peak) at which maximum weight-loss occurs). Order of reaction was calculated by using the relation between reaction order and concentration at maximum slope.

The horizontal burning test (HBT) of homopolymer and its blend was conducted in accordance with the ASTM standards [28,29]. The blend compositions given in **Table 1** were prepared by mixing the polymer with additive in an aluminum mold with the specified dimensions.The specimen was held horizontally and a flame fuelled by natural gas was supplied to light one end of it. The time for the flame to reach from the first reference mark (25 mm from the end) to the second reference mark at 100 mm from the end, was measured. The results are reproduced in **Figure 12**.

3. RESULTS AND DISCUSSION

3.1. Thermogravimetry, Derivative Thermogravimetry and Differential Thermal Analysis

The thermal traces of additive (X), neat polymer (A) and blends, B1-B5, are shown in **Figures 1-4**, while thermoanalytical data are given in **Table 1**. The TG curve of neat phosphorus tribromide gives a single step weight-loss. This additive begins to lose weight around 60°C and the whole process completes around 178°C (**Figure 1**). The first fifty per cent of the original weight requires heating of 105°C to disappear whereas the remaining

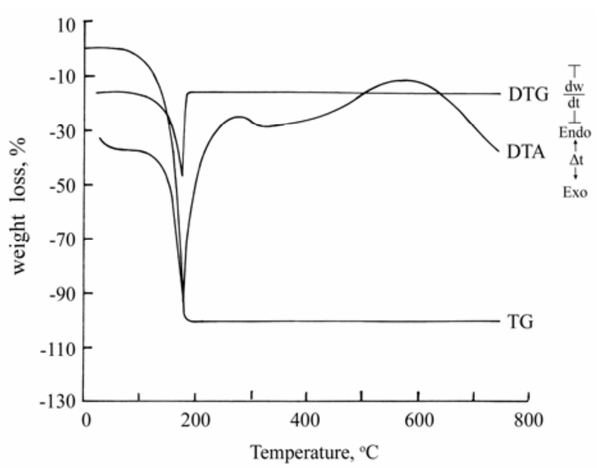

Figure 1. Thermal (TG-DTA-DTG) traces (dynamic nitrogen, heating rate 10°C/min) for phosphorus tribromide additive (X) in nitrogen atmosphere.

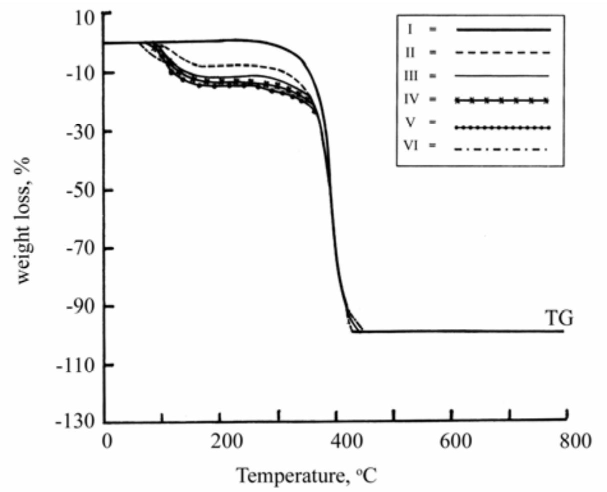

Figure 2. Thermogravimetry curves (dynamic nitrogen, heating rate 10°C/min) for PMMA-PBr_3 blends: (I) A, (II) B1, (III) B2, (IV) B3, (V) B4 and (VI) B5.

fifty per cent leaves the crucible within a temperature range of just 15°C. A DTG peak is found at 178°C while DTA peak is noted at 176°C. When PBr_3 approaches its boiling point (175°C), the weight-loss (evaporation) becomes brisk. This is also evident from the preceding observation. At the termination of weight- loss step, no residue is encountered.

This blend (PMMA 97.5%: PBr_3 2.5%–hereafter designated as B1) begins to degrade around 81°C and the first stage comes to an end at 169°C (**Figure 2(II)**). Nine per cent weight-loss is observed. The products evolved at this stage clearly indicate the interaction between the two components of the system (GC-MS results). The neat polymer exhibits T_0 (temperature corresponding to the detection of first weight-loss) at 250°C (**Figure 2(I)**), whereas additive starts losing weight around 60°C when heated alone. This is another clue for interaction. From 169°C to 279°C the system remains intact thereby showing the stability of the intermediate. This intermediate is not pure PMMA as neat polymer commences to decompose around 250°C. So it is believed that bonds between PBr_3 and PMMA are formed which result in the stabilization of intermediate (169-279°C). The second stage which terminates at 430°C accounts for 91% weight-loss. No residue is noticeable at the completion of degradation process. One DTG peak (**Figure 3(II)**) at 393°C and one DTA peak (**Figure 4(II)**) at 408°C are noted for the final (second) stage. The sharp fall in TG traces for the second stage manifests the rupture of all types of bonds as the rising energy content cannot be resisted.

The second blend of this series B2 (PMMA 95%: PBr_3 5%) starts losing weight around 80°C and by the end of the first stage (165°C), accounts for 12% weight-loss (**Figure 2(III)**). It is clear now that by increasing the

Table 1. Comparative thermoanalytical data for PMMA(A), PBr_3(X) and blends, B1-B5.

Blend composition (%) PMMA-PBr_3	Temperature range, °C	Stage	Weight loss, %	TG, °C				DTG, °C		DTA, °C, Thermal Effect
				T_0	T_{25}	T_{50}	T_{100}	I	II	
A (100-00)	250-440	I	100	250	378	390	440	396	--	319 (Endo), 412 (Exo)
B1 (97.5-2.5)	81-169 279-430	I II	9 91	81	378	392	430	110	393	130 (Exo), 350 (Endo), 408 (Exo)
B2 (95-5)	80-165 262-440	I II	12 88	80	380	390	440	111	396	120 (Exo), 363 (Endo), 407 (Exo)
B3 (92.5-7.5)	70-175 280-445	I II	14 86	70	370	390	445	115	397	118 (Exo), 350 (Endo), 404 (Exo)
B4 (90-10)	70-190 260-441	I II	16 84	70	365	390	441	110	393	124 (Exo), 365 (Endo), 406 (Exo)
B5 (87.5-12.5)	62-192 243-448	I II	11 89	62	370	394	448	123	397	136 (Exo), 365 (Endo), 415 (Exo)
X (00-100)	60-178	I	100	60	155	168	178	178	--	176 (Exo)

Endo = Endothermic, Exo = Exothermic.

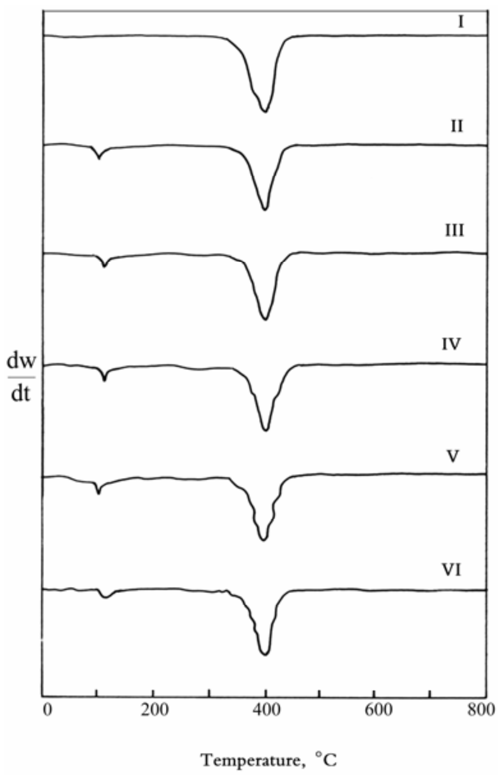

Figure 3. Derivative thermogravimetry curves (dynamic nitrogen, heating rate 10°C/min) for PMMA-PBr_3 blends: (I) A, (II) B1, (III) B2, (IV) B3, (V) B4 and (VI) B5.

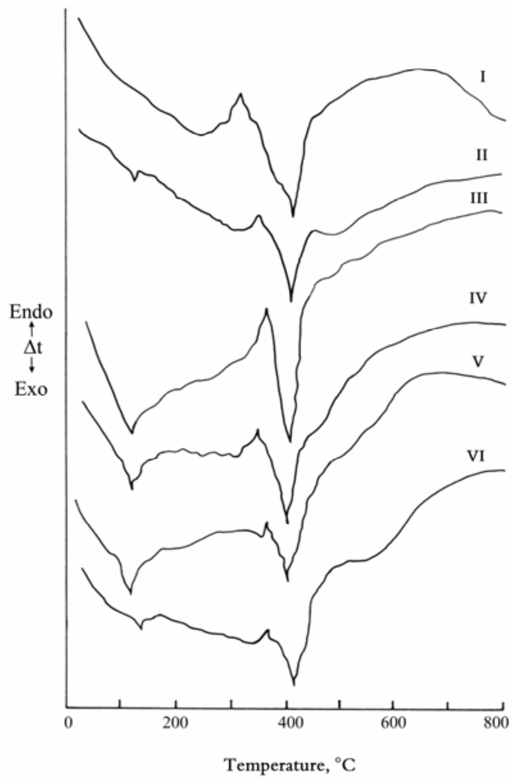

Figure 4. Differential thermal analysis curves (dynamic nitrogen, heating rate 10°C/min) for PMMA-PBr_3 blends: (I) A, (II) B1, (III) B2, (IV) B3, (V) B4 and (VI) B5.

concentration of additive (PBr_3), the T_0 does not show any change, however, the per cent weight-loss has increased. Same type of interaction is believed to have occurred for this blend as was observed for B1. The range of temperature for stable residue (165-262°C) in this case exhibits a reduction when compared with the same range for the first member of this series (B1). It may be due to less number of bonds/links formed between the constituents of the system despite the presence of relatively higher concentration of additive. The last stage (262-440°C) gives a weight-loss of 88 %. From 262°C to 360°C, the weight-loss is only 7% which is attributed to the strength of bonds/interactions developed in the earlier part of the degradation between the components of the system resulting in the stable intermediate. For first stage, one DTG peak (111°C) and one DTA peak (120°C) appear. For second step, one DTG (**Figure 3(III)**) and two DTA (**Figure 4(III)**) peaks are noticed at 396°C, 363°C and 407°C, respectively. No residue is found at the termination of the degradation process.

B3 (PMMA 92.5%: PBr_3 7.5%) begins to degrade around 70°C and loses 14 % of original weight in the first stage which terminates at 175°C (**Figure 2(IV)**). The intermediate formed at this stage is stable up to 280°C after which the pyrolysis again starts and the second step shows a weight-loss of 86 % with no residue at the completion of the decomposition (445°C). From 280°C to 338°C, only 6% weight-loss is observed which is indicative of the toughness of bonds that developed during the early part of pyrolysis. One DTG (**Figure 3(IV)**) and one DTA (**Figure 4(IV)**) peak appear for first stage (115 and 118°C, respectively), however, for second stage one DTG and two DTA peaks at 397°C , 350°C and 404°C, respectively, arise.

B4 (PMMA 90%: PBr_3 10%) shows a weight-loss of 16 % for first stage. It commences to decompose around 70°C and stops losing weight around 190°C (**Figure 2(V)**). Single DTG (**Figure 3(V)**) and DTA (**Figure 4(V)**) peaks are found at 110°C and 124°C, respectively. The intermediate withstands a temperature of 70°C (190-260°C) before the inception of second stage of degradation. The second step comes to an end at 441°C marking a weight-loss of 84%. The first 6% weight-loss of second stage requires heating of 96°C which is due to the strong bonds/links produced in the early part of the degradation. One DTG and two DTA peaks are observed at 393, 365 and 406°C, respectively. No residue is noticeable at the completion of degradation process.

B5 (PMMA 87.5%: PBr_3 12.5%) commences its weight-loss around 62°C for first stage which comes to an end at 192°C (**Figure 2(VI)**). One DTG and one DTA peak appear for this step at 123°C and 136°C, respectively. Eleven per cent weight-loss is evident from TG traces (**Figure 2(VI)**). The intermediate that is stable up to 243°C, starts decomposing as the temperature increases. The second stage terminates at 448°C. One DTG (**Figure 3(VI)**) and two DTA (**Figure 4(VI)**) peaks are found at 397°C, 365°C and 415°C, respectively. The first 8% weight-loss for the second step (out of 89%) requires heating of 109°C (from 243 to 352°C) whereas the remaining larger portion (81 %) leaves the scene for a heating of 96°C (352-448°C). This is basis of the types of bonds present in the intermediate. There was no residue at the end of pyrolysis of this blend.

The interaction is clear between the components of the system throughout the series, *i.e.*, B1-B5. The nature of interaction seems to be same for all members of the series with effectiveness decreasing down the series. The percentage of degradation for first stage is higher than the total percentage of additive in the blends B1-B4. The molecular level mixing of the constituents favours the development of links between them which, in turn, influences the degradation of both parts from the beginning. The evolution of new products (GC-MS results) in the early part of pyrolysis confirms the chemical interaction and mutual effect of the ingredients on each other's decomposition.

3.2. Blend's Composition Effect on Thermal Behaviour

Figure 5 shows the graph between temperature and weight % of additive. The results reveal a very clear trend of destabilization when T_0 is considered. It is observed that as the percentage of additive in the blends is increased, a slight stabilization of 20°C is noted which may be attributed to the number of links which are developed between phosphorus and pendent oxygens of polymer per unit volume of additive. For T_{25} (temperature at which 25% weight-loss occurs), the trend in destabilization is not so different for blends when weight percentage of additive goes from 2.5 to 12.5. This seems to be due to the less number of interactions, *i.e.*, cumulative impact to lowers. At T_{50} (temperature at which 50% weight-loss is observed), a very inappreciable stabilization is observed as energy content is too great to be resisted by the different types of interactions or bonds between additive and polymer irrespective of the weight percentage of additive. T_{100} (temperature for 100 weight-loss) does not show much difference for polymer and blends which may be due to very high temperature region signifying the completion of decomposition process. In this zone, almost all kinds of bonds are prone to breakage.

3.3. Activation Energy (E_o) and Order of Reaction (n) Determination

Table 2 presents the activation energy and order of reaction of thermal decomposition of polymer, additive and polymer-additive systems. A decreasing trend of activation energy is noticed with the increasing percentage of

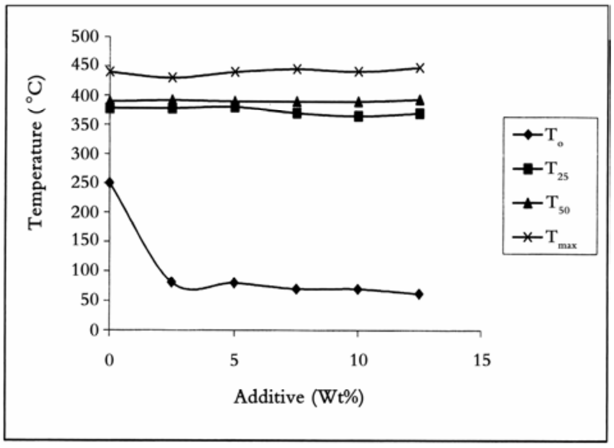

Figure 5. Effect of blend composition on T_0, T_{25}, T_{50} and T_{100} values of A and B1-B5 blends.

Table 2. Activation energies and order of reaction for A, X and PMMA-additive blends.

Blend composition (%) PMMA-PBr_3	E_o* (KCal/mol)	Order of reaction (n)
A	138.9	3/2
B1	43.68	1/2
B2	42.17	1/2
B3	40.29	1
B4	37.65	1
B5	38.03	3/2
X	93.32	0

* = overall activation energy.

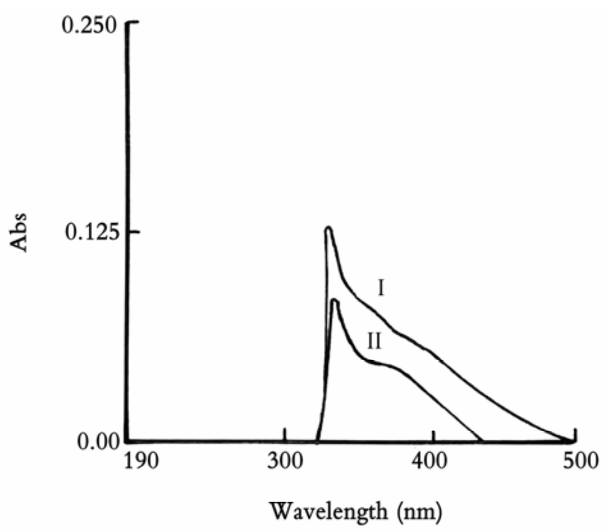

Figure 6. UV-spectra of X (I) and B4 (II) blend in acetone.

additive (2.5-12.5%) in the blends. These results were computed from TG curves. It is believed that decrease in the activation energy is due to the destabilization of the blended system observed in the earlier part of pyrolysis keeping T_0 in view. The interaction at the outset of degradation between the components of blends triggers an early loss of weight which is attributed to the decreasing trend this parameter exhibits down the series (B1→B5). The shifting of T_0 to lower temperatures from B1 to B5 is quite evident in the current thermal investigation.

3.4. UV Findings

It is well-known fact that PMMA does not absorb in UV region. On the contrary, PBr_3 gives a distinct peak at 325 nm (in acetone) whereas its blend with PMMA also absorbs in UV range (**Figure 6**). The shift in wavelength for PMMA-PBr_3 (330 nm) clearly indicates interaction between the components of the system. This shift is attributed to the establishment of links between phosphorus of additive and carbonyl oxygen of polymer and bromines of additive and carbons of polymer backbone (main chain).

3.5. IR Spectra

Poly(methyl methacrylate) is a widely-studied polymer and its IR spectrum (**Figure 7(I)**) gives the characteristic peaks for the presence of ester linkages (1730-1735 cm^{-1}). The absence of peaks in the region of 1630-1640 cm^{-1} confirms the formation of polymer. The stretchings attributed to C-H bonds can be observed around 3000 cm^{-1}.

The IR of PBr_3 (**Figure 7(II)**) shows a broad band at 3362 cm^{-1} which is due to water absorption (all our endeavors to save PBr_3 from taking moisture from surroundings failed as the humidity was high at the time of IR run). The remaining peaks (485, 476, 458, 442, 418, 407 cm^{-1}) are assigned to P-Br bond [30]. The IR peaks for blend (B4–PMMA 90%:PBr_3 10%—selected arbitrarily to represent the whole series) exhibit some interesting features (**Figure 7(III)**). "Free" PBr_3 is either completely absent or if present, is only at trace levels. The absence of peaks around 3362 cm^{-1} (O-H stretching for water) overrules the presence of free PBr_3. The shift observed for ester linkages of PMMA (IR peak at 1718 cm^{-1}) and appearance of some sharp peaks at 1434, 1386, 1141 cm^{-1} suggest formation of a 'complex-type' arrangement involving carbonyl oxygen of PMMA pendent groups (either of the same chain or two different chains) and phosphorus of PBr_3. The following structures are proposed.

Few more peaks at 1238, 667, 599, 564 cm^{-1} indicate that Br of P-Br bond 'experiences' a pull from nearby carbons (backbone as well as ester carbons) [30-33]. For true C-Br and CH_3-Br bonds, the stretchings are found at 515-680 and ~1230 cm^{-1}, respectively. This may result in the weakening of this bond (P-Br) as Br 'moves' closer to the more electropositive carbon atoms. The results of GC-MS point towards these types of developments.

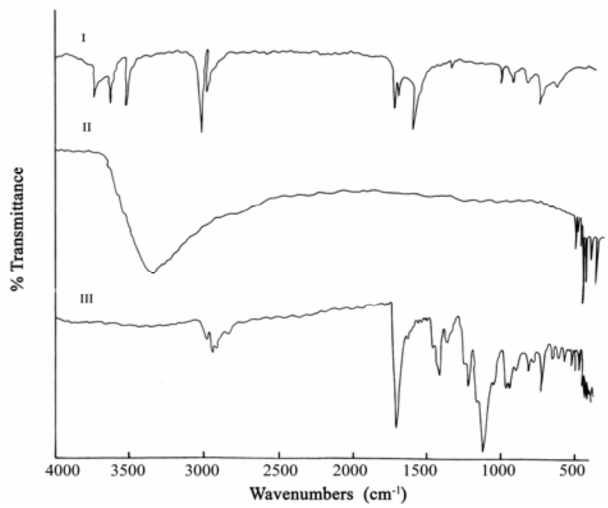

Figure 7. (I) Infrared spectra of PMMA; (II) Additive, PBr_3; (III) Blend, B4, PMMA (90%) + PBr_3 (10%).

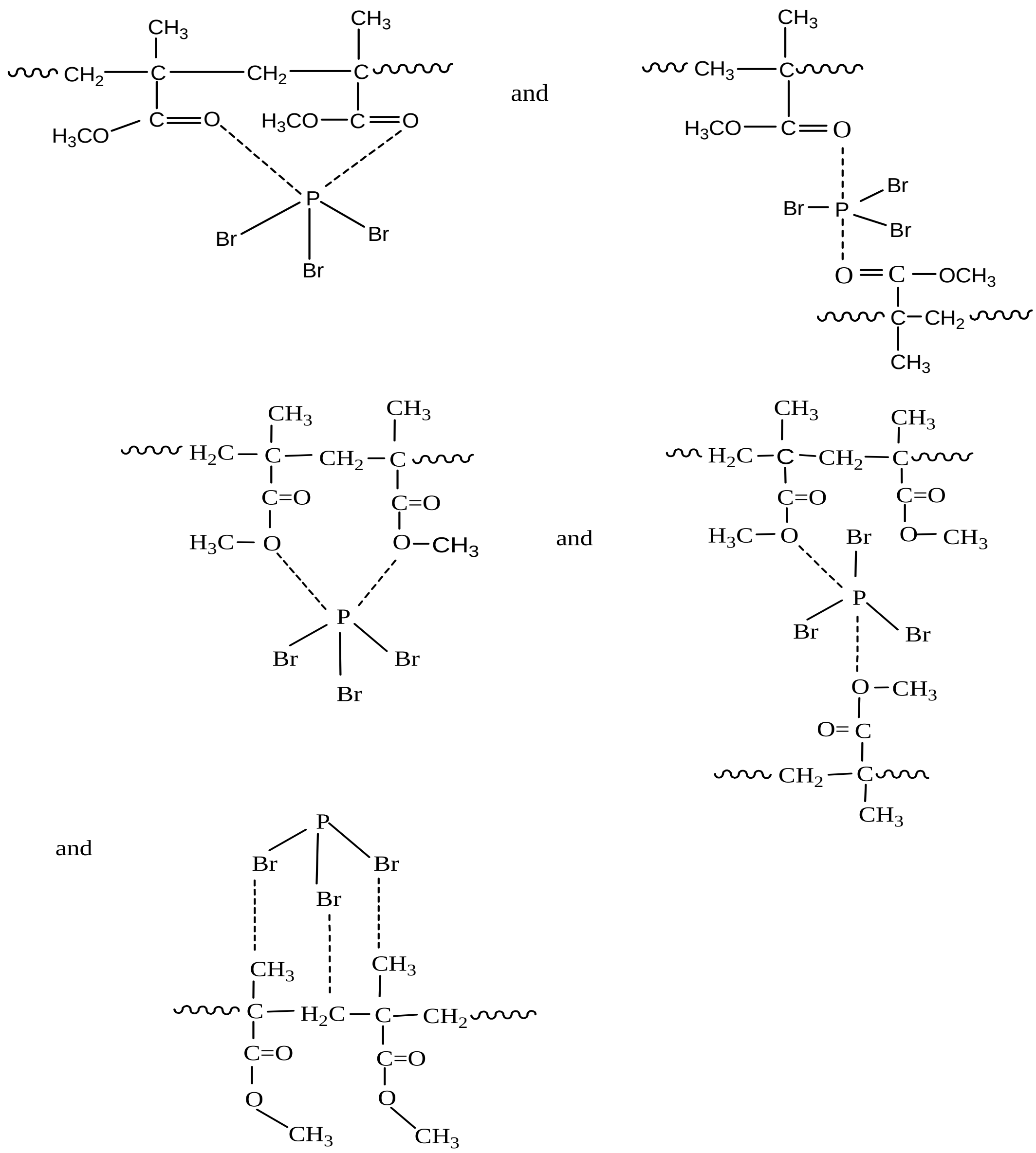

3.6. Pyrolysis-Gas Chromatography-Mass Spectrometry Behaviour

The blend B4 (PMMA:PBr_3, 90%:10%) was heated to 250°C for a minute and after bringing the residue to room temperature, GC-MS was taken in acetone to check the nature of degrading blend around this temperature. B4 was selected arbitrarily to represent the present series. Since the blends show stability at or around 250°C (TG traces, **Figure 2**), the identification of products is expected to shed light on the interactions developed by the constituents of blends at this stage.

GC-MS of this blend (**Figure 8**) shows a number of peaks. The products identified clearly indicate the interaction between the components of the system from an early stage of degradation. The absence of PBr_3 in the degradation products (it could not be found in a trap at -196°C) after heating B4 up to 250°C suggests its involvement with the pendent groups of the neat polymer or even with the backbone of the PMMA. However, the early weight-loss is attributed to the decomposition of some 'free' PBr_3 which initiates the degradation of polymer. The formation of $Br^{\cdot}$ (free radicals) may result in the products of peaks at 1, 3, and 4. Peak number 7, gives the bromine radicals replacing the methyls attached to the backbone carbons. The other peaks hint at either the contacts developed by one constituent (P) of the additive (PBr_3) or both. The product at peak 8 provides the convincing clue for the stability of the system in the region unfolded by TG curves (**Figure 2**). The

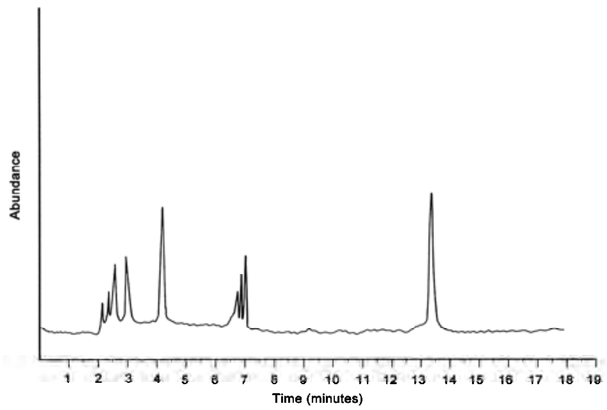

Figure 8. GC-MS results of blend, B4 (PMMA (90%) + PBr_3 (10%)), heated at 250°C.

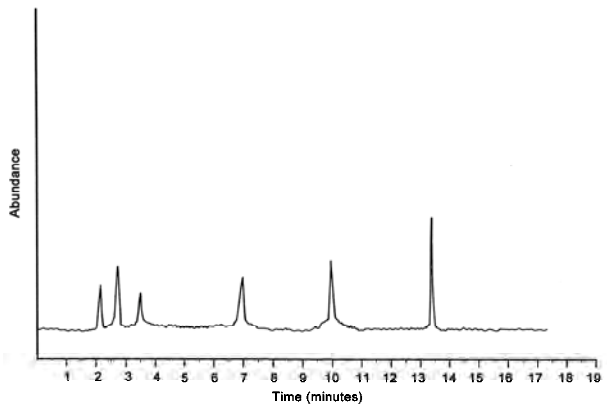

Figure 9. GC-MS results of blend, B4 (PMMA (90%) + PBr_3 (10%)), heated at 300°C.

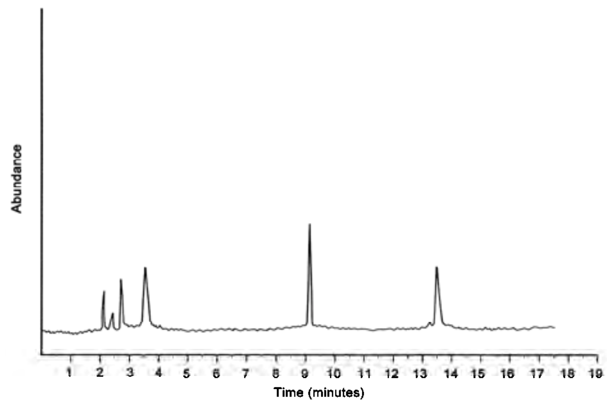

Figure 10. GC-MS results of blend B4, (PMMA (90%) + PBr_3 (10%)), heated at 400°C.

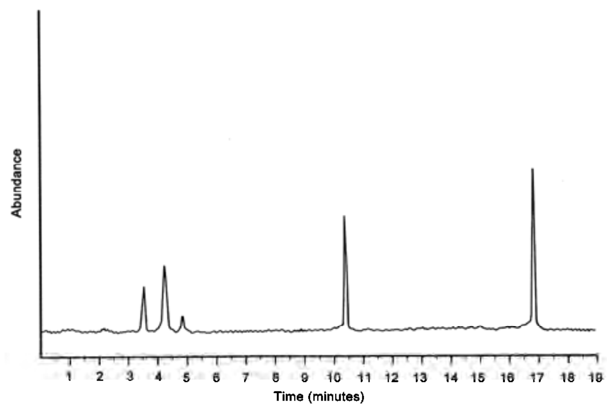

Figure 11. GC-MS results of blend B4 (PMMA (90%) + PBr_3 (10%)), heated to boiling, cooled and mixed with acetone.

interactions proposed as per IR studies (**Figure 7**) may be taken as proof now supported by GC-MS studies. The 'binding' of pendent groups of PMMA by phosphorus of additive may stop the degradation of polymer in certain temperature ranges furnishing stability to the system. The strength of the overall system lies in the 'engagement' of various chains by undegraded or partially degraded additive. The mechanism of the production of these compounds is presented in **Schemes I-IV**. Peak no. 9 provides a clue (which may also be regarded as the reason of stability of the system around this temperature, *i.e.*, 250 °C) whereby phosphorus is found as part of the backbone. It is worth-noting that phosphorus present in backbone of polymer is attached to carbon and hydrogen whereas bromine replaces either the $–OCH_3$ of pendent group or $–CH_3$ attached to backbone carbons. The formation of $–PH_2$ and –PH- from PBr_3 appears to have taken place along the degrading polymer. This also explains the "blockades" experienced by the degrading polymer [15,20,21].

The GC-MS taken after heating the blend (B4) up to 300°C is to get insight into the nature of products arisen, after the decomposition of stable intermediate (**Figure 9**). The product identified at peak number 5 does provide enough information about the stable intermediate. Phosphorus seems to be linked to two separate chains (**Scheme V**). Another product (peak no. 6) suggests as if $Br^·$ (free radicals) blocks the depolymerisation of the chains (**Scheme VI**).

The products identified (**Table 3**) after heating the blend (B4) to 400°C also furnish evidence of the mechanism of degradation close to the completion of decomposition process (GC-MS, **Figure 10**). Despite inclusion of phosphorus in the chain (peak 3), replacement of some of the part of pendent group by phosphorus (peak 6) and presence of bromine (peak 6) at the end of few modified MMA units, the breaking of bonds takes place owing to the energy content of this temperature zone (at or around 400°C). Unzipping of the chains cannot be hindered by phosphorus or bromine. Oligomers of neat MMA are absent which is another indication of interaction between the components of the system.

Another GC-MS (**Figure 11**) of this blend was recorded after heating to boiling for two minutes, cooling and then dissolving it in acetone. This was performed to check the overall behaviour of the blend subjecting it to

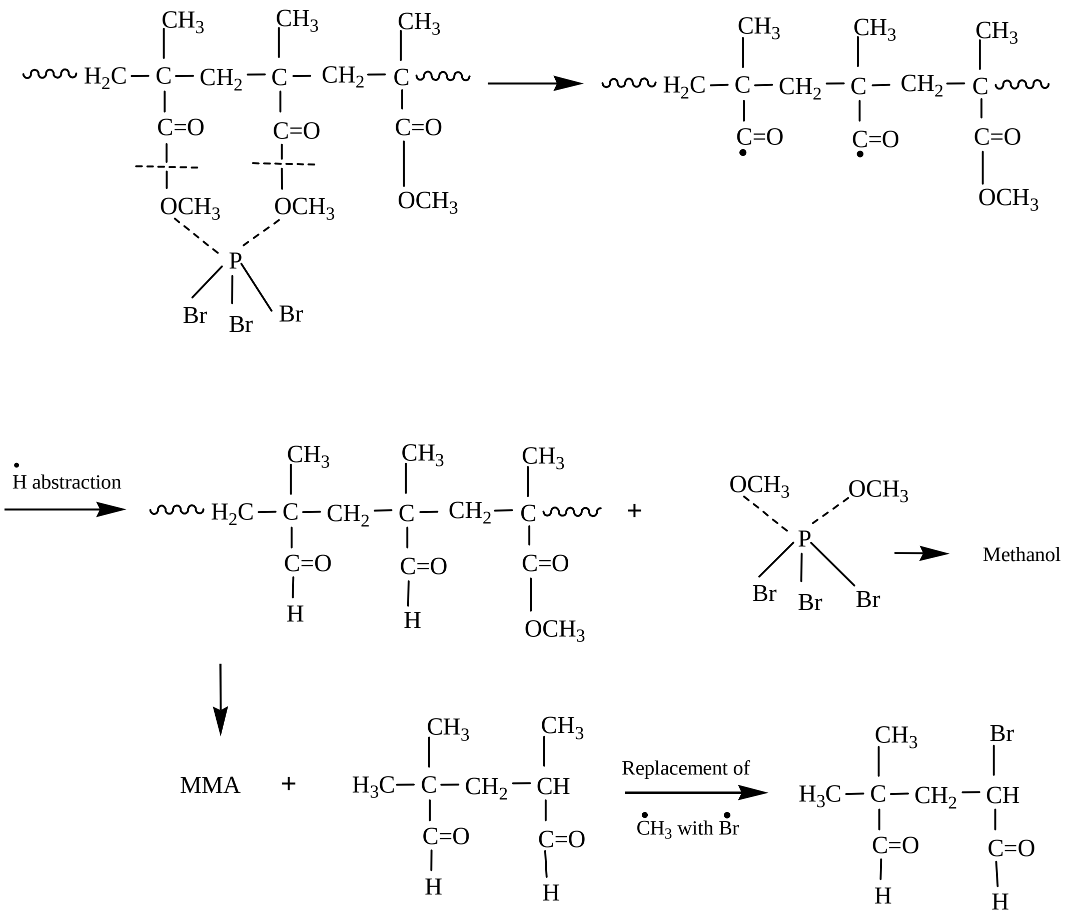

Scheme I

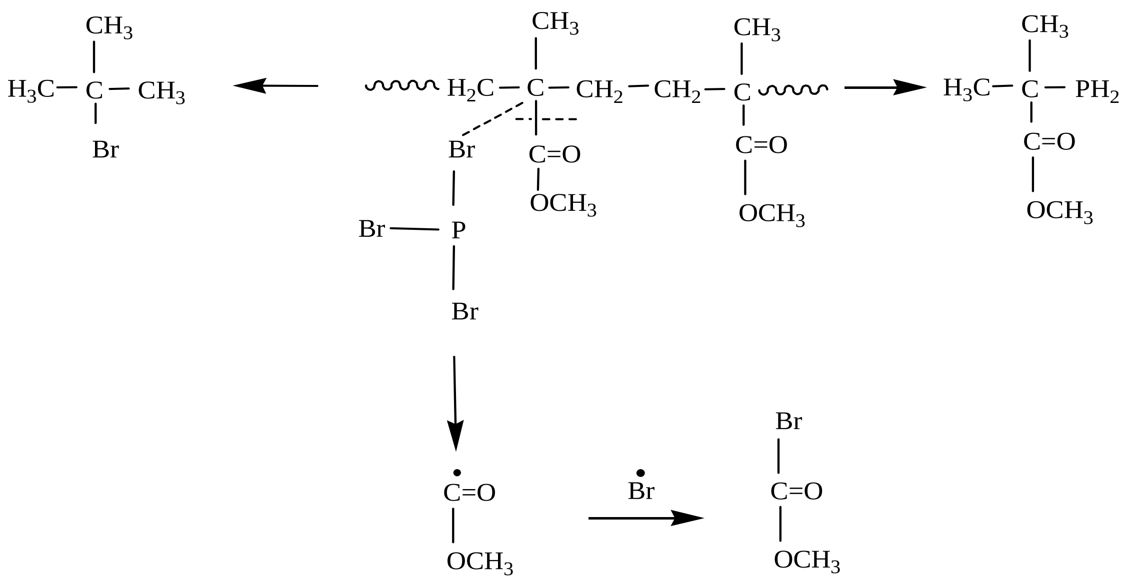

Scheme II

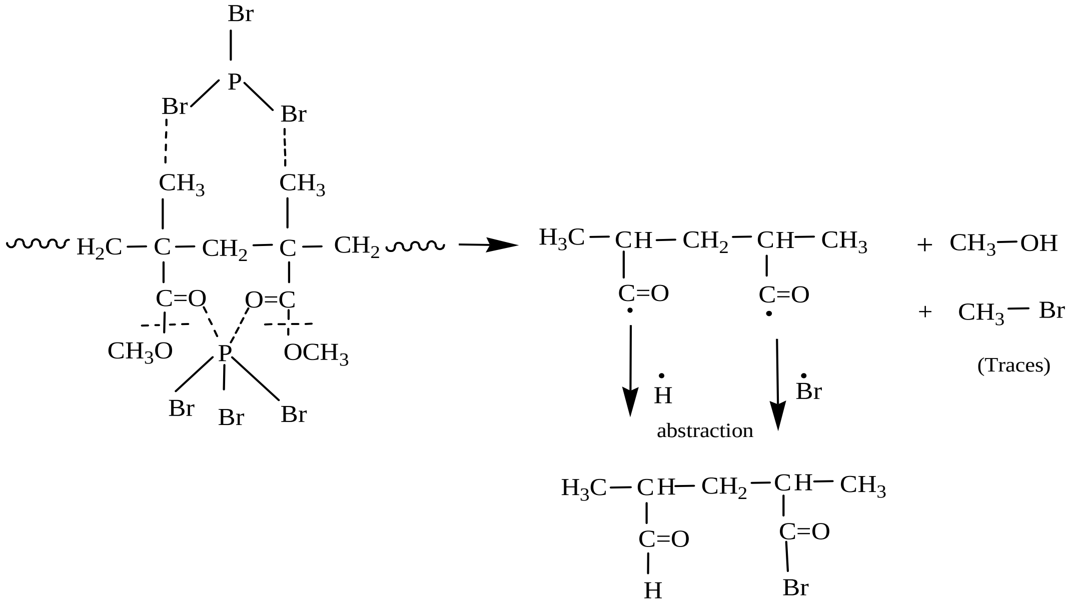

Scheme III

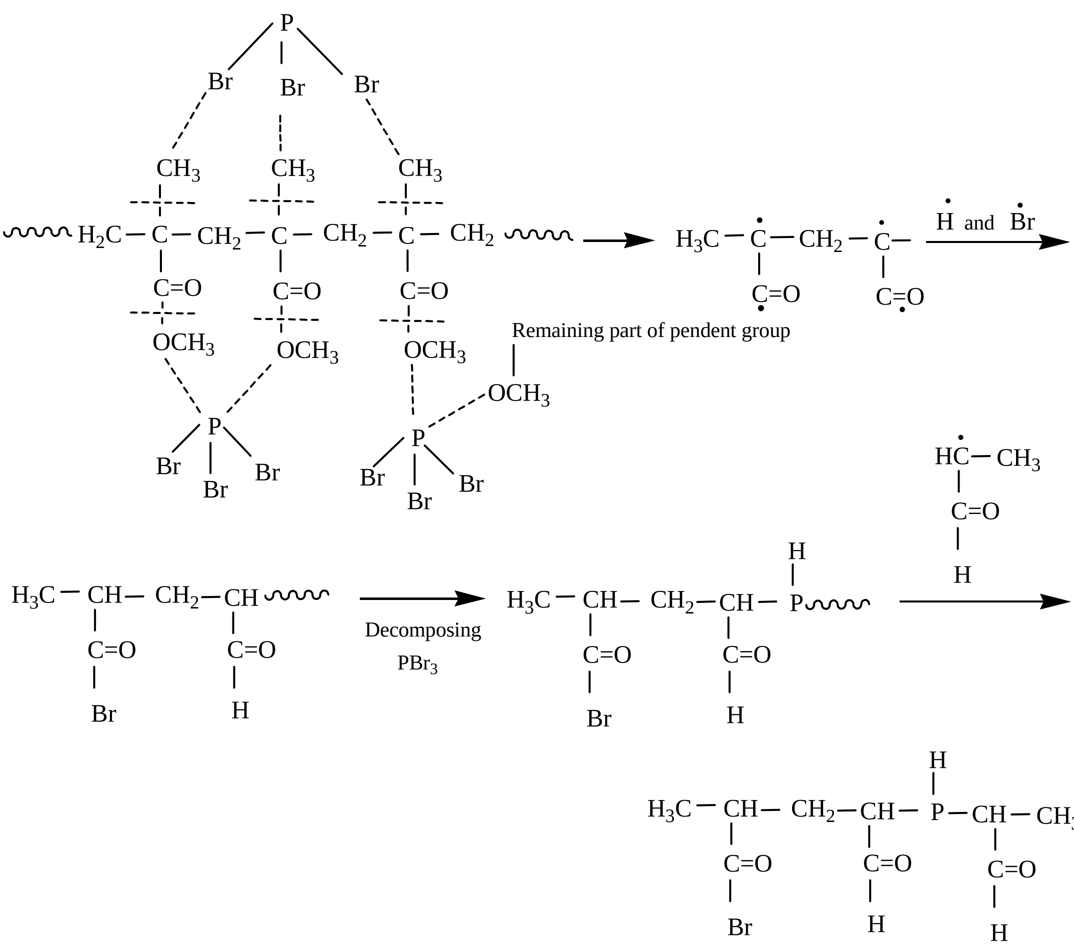

Scheme IV

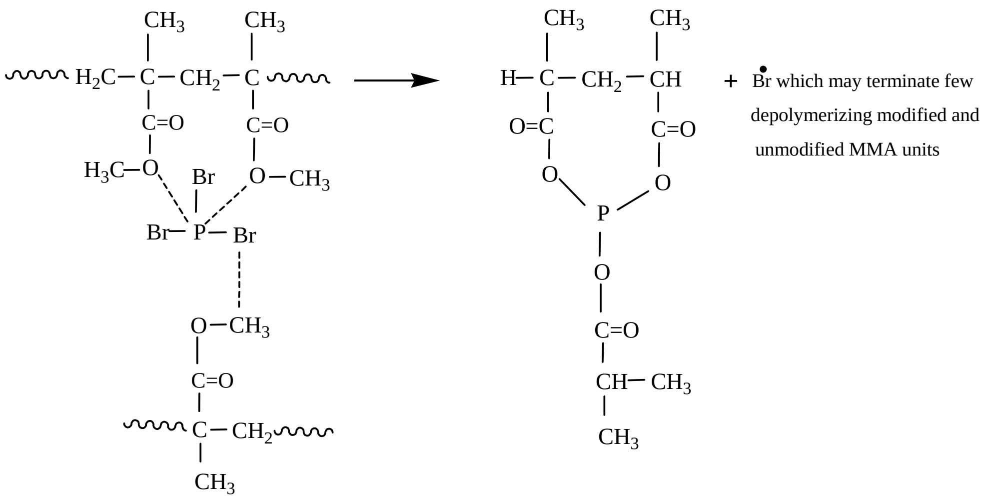

Scheme V

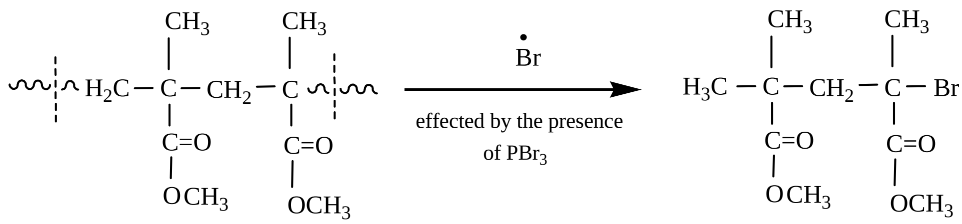

Scheme VI

Table 3. GC-MS results of blend, B4 after heating at 250°C, 300°C and 400°C.

Blend heated at 250°C		Blend heated at 300°C		Blend heated at 400°C	
Peak no.	Product identified	Peak no.	Product identified	Peak no.	Product identified
1	$C_2H_3O_2Br$, C_3H_6O, CH_4O	1	C_2H_3OBr	1	C_5H_9Br
2	$C_5H_{11}O_2P$	2	C_2H_4OPBr	2	C_2H_4PBr or CH_2OPBr
3	C_3H_8PBr	3	CH_3OBr	3	$C_7H_{14}O_3P_2$, $C_8H_{13}O_4P$
4	C_4H_9Br	4	$C_6H_{12}PBr$	4	$C_7H_{11}O_2Br$
5	Unidentified	5	$C_{11}H_{17}O_6P$	5	$C_8H_{11}O_2PBr$
6	Unidentified	6	$C_{10}H_{17}O_4Br$	6	$C_{12}H_{21}O_3P_2Br$
7	$C_4H_5O_2Br$	--	--	--	--
8	$C_4H_7Br_2$	--	--	--	--
9	$C_9H_{14}O_3PBr$	--	--	--	--

high temperature for short time. Modified MMA units were found confirming the products identified in different temperature zones earlier. Traces of MMA units were also detected which is in accordance with earlier findings. It is further concluded (peak 5) that parts of the pendent groups of MMA units are equally liable to replacement by bromine and phosphorus.

The interaction between additive and polymer is established. The GC-MS studies help in understanding the mechanism of degradation of the blended system. This interaction imparts stability to the system in certain regions (TG curves). The orientation of PBr_3 in the system appears to have profound impact on the formation of the products identified during degradation at different temperatures. The cross-linking of adjacent chains by the presence of phosphorus gives stability to the system. In addition to this, phosphorus and bromine when terminate the degrading polymer also play role in the formation of these products which 'block' further degradation in the regions of stability.

3.7. Flammability Behaviour of Neat Polymer and its Blends

Horizontal burning rate (HBR) and time to burn neat

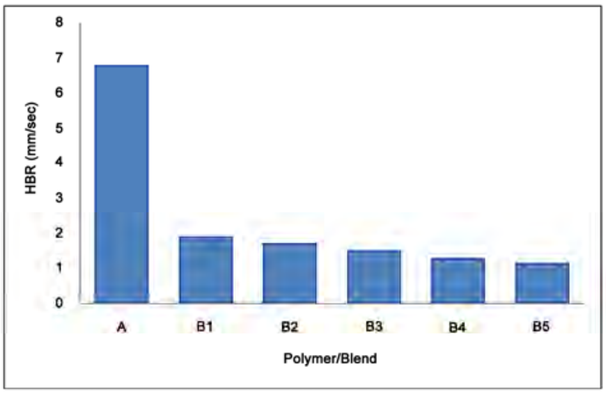

Figure 12. Horizontal burning rate of polymer and its blends.

Table 4. Horizontal burning rate (HBR) for polymer (A) and blends, B1-B4.

Polymer/Blend code number	A	B1	B2	B3	B4	B5
Time to burn (sec)	11	39	43	49	58	65
Length of strip (mm)	75	75	75	75	75	75
HBR (mm/sec)	6.8	1.9	1.7	1.5	1.29	1.15

mm = millimeter, sec = second.

polymer and its blends are tabulated in **Table 4**. The trend is clearly a linear one (**Figure 12**). Higher the concentration of additive in the blend, lower is the rate of burning obtained. It has been observed that burning rate of blend (B5) decreases to 6 times compared to neat polymer (A). Reduction in burning rate is much more pronounced even with the lowest proportion of additive (B1) and this is easily explained by the retardency caused by the additive towards polymer's flammability. The uniform distribution of all concentrations of additive throughout polymer is also confirmed.

4. CONCLUSIONS

1) The blends (PMMA-PBr_3) lose weight at lower temperatures than neat polymer.

2) Despite early destabilization, the blends exhibit stabilization temperature zones.

3) The interaction between the components appears to be purely chemical.

4) The earlier decomposition is attributed to the splitting of PBr_3 releasing bromine free radicals ($Br^{\cdot}$).

5) The formation of products involving phosphorus as part of degrading polymer imparts stability to the blends.

6) The "engaging" of separate polymer chains by phosphorus is another reason of stabilization of the binary system.

7) It seems that free radicals ($Br^{\cdot}$) not only start the early depolymerization of the polymer but also inhibits this process, thus, providing one more point for stabilization.

8) The pendent groups of polymer or a part of them are equally liable to replacement by phosphorus and bromine.

9) The production of monomer has decreased significantly furnishing ample evidence for chemical interaction between the constituents of the system.

5. ACKNOWLEDGEMENTS

The authors would like to express their gratitude to PINSTECH, Islamabad, Pakistan for providing the opportunity to undertake this research work. Messrs Nehad Ali (Senior Tech. IAD, PINSTECH), Nadeem Ahmad and Muhammad Adeel Khattak are acknowledged for drawing of figures and technical help.

REFERENCES

[1] Laachachi, A., Cochez, M., Ferriol, M., Leroy, E., Lopez, C.M. and Oget, N. (2004) Influence of Sb_2O_3 particles as filler on the thermal stability and flammability properties of poly (methyl methacrylate) (PMMA). *Polymer Degradation and Stability*, **85(1)**, 641-646.

[2] Ebdon, J.R., Hunt, B.J. and Joseph, P. (2004) Thermal degradation and flammability characteristics of some polystyrenes and poly (methyl methacrylate) chemically modified with silicon-containing groups. *Polymer Degradation and Stability*, **83(1)**, 181-185.

[3] Gentilhomme, A., Cochez, M., Ferriol, M., Oget, N. and Mieloszynski, J.L. (2003) Thermal degradation of methyl methacrylate polymers functionalized by phosphorus – containing molecules – II: Initial flame retardance and mechanistic studies. *Polymer Degradation and Stability*, **82(2)**, 347-355.

[4] Price, D., Pyrah, K., Hull, T.R., Milnes, G.J., Ebdon, J.R., Hunt, B.J. and Joseph P. (2002) Flame retardance of poly (methyl methacrylate) modified with phosphorus – containing compounds. *Polymer Degradation and Stability*, **77(2)**, 227-233.

[5] Price, D., Pyrah, K., Hull, T.R., Milnes, G.J., Ebdon, J.R., Hunt, B.J., Joseph, P. and Konkel, C.S. (2001) Flame retarding poly (methyl methacrylate) with phosphorous – containing compounds: Comparison of an additive with a reactive approach. *Polymer Degradation and Stability*, **74(3)**, 441-447.

[6] Ebdon, J.R., Price, D., Hunt, B.J., Joseph, P., Gao, F., Milnes, G.J. and Cunliffe, L.K. (2000) Flame retardance in some polystyrene and poly (methyl methacrylate) with covalently bound phosphorus – containing groups: Initial screening experiments and some laser pyrolysis mechanistic studies. *Polymer Degradation and Stability*, **69(3)**, 267-277.

[7] Chang, T.C. and Wu, K.H. (1997) The effect of silicon and phosphorus on the thermo-oxidative degradation of poly (methyl methacrylate). *Polymer Degradation and Stability*, **57(4)**, 325-330.

[8] Nair, C.P.R., Clouet, G. and Guilbert, Y. (1989) Flame and thermal resistance of phosphorous – functionalized poly (methyl methacrylate) and polystyrene. *Polymer*

Degradation and Stability, **26(4)**, 305-331.

[9] Chandrasiri, J.A. and Wilkie, C.A. (1994) Thermal degradation of poly (methyl methacrylate) in the presence of tin (IV) chloride and tetraphenyltin. *Polymer Degradation and Stability*, **45(1)**, 91-96.

[10] Chandrasiri, J.A., Roberts, D.E. and Wilkie, C.A. (1994) The effect of some transition metal chlorides on the thermal degradation of poly (methyl methacrylate): A study using TGA–FTIR spectrometry. *Polymer Degradation and Stability*, **45(1)**, 97-101.

[11] McNeill, I.C. and McGuiness, R.C. (1984) The effect of zinc bromide on the thermal degradation of poly (methyl methacrylate): Part I – Thermal analysis studies and general nature of the interaction. *Polymer Degradation and Stability*, **9(3)**, 167-183.

[12] McNeill, I.C. and McGuiness, R.C. (1984) The effect of zinc bromide on the thermal degradation of poly (methyl methacrylate): Part 2 – Reaction products, structural changes and degradation mechanism. *Polymer Degradation and Stability*, **9(4)**, 209-224.

[13] Song, J., Fischer, C. H. and Schnabel, W. (1992) Thermal oxidative degradation of poly (methyl methacrylate). *Polymer Degradation and Stability*, **36(3)**, 261-266.

[14] Wochnowski, C., Eldin, M. A. S. and Metev S. (2005) UV-laser-assisted degradation of poly (methyl methacrylate). *Polymer Degradation and Stability*, **89(2)**, 252-264.

[15] Zulfiqar, S., Paracha, A. and Masud, K. (1996) The thermal degradation of poly (allyl methacrylate). *Polymer Degradation and Stability*, **52(1)**, 89-93.

[16] Zulfiqar, S., Masud, K., Siddique, B. and Paracha, A. (1996) Thermal degradation of phenyl methacrylate-styrene copolymers. *Polymer Degradation and Stability*, **52(3)**, 293-299.

[17] Zulfiqar, S., Masud, K., Piracha, A. and McNeill, I.C. (1997) Thermal degradation of allyl methacrylate-methyl methacrylate copolymers. *Polymer Degradation and Stability*, **55(3)**, 257-263.

[18] Zulfiqar, S. and Masud, K. (2000) Thermal degradation of blends of allyl methacrylate-methyl methacrylate copolymers with aluminum ethoxide. *Polymer Degradation and Stability*, **70(2)**, 229-236.

[19] Zulfiqar, S., Masud, K. and Ameer, Q. (2002) Thermal degradation of blends of phenyl methacrylate-styrene copolymers with aluminum ethoxide. *Polymer Degradation and Stability*, **77(3)**, 457-464.

[20] Zulfiqar, S. and Masud, K. (2002) Thermal degradation of blends of allyl methacrylate-methyl methacrylate copolymers with aluminum isopropoxide. *Polymer Degradation and Stability*, **78(2)**, 305-313.

[21] Zulfiqar, S., Masud, K. and Ameer, Q. (2003) Thermal degradation behavior of blends of phenyl methacrylate-styrene copolymers with aluminum isopropoxide. *Journal of Thermal Analysis and Calorimetry*, **73(3)**, 877-886.

[22] Arshad, M., Masud, K., Arif, M., Rehman, S., Chohan, Z.H., Arif, M., Qureshi, A.H., Saeed, A., Salma, U. and Awan, M.S. (2008) A comparative study of roles played by aluminum tribromide and aluminum acetylacetonate on the thermal degradation of PMMA by simultaneous thermoanalytical techniques. *The Nucleus*, **45(1-2)**, 63-72.

[23] Arshad, M., Masud, K., Arif, M., Rehman, S., Arif, M., Zaidi, J.H., Chohan, Z.H., Saeed, A. and Qureshi, A.H. (2009) The effect of $AlBr_3$ additive on the thermal degradation of PMMA: A study using TG–DTA–DTG, IR and Py–GC–MS techniques. *Journal of Thermal Analysis and Calorimetry*, **96(3)**, 873-881.

[24] Riddick, J.A., Bunger, W.B. and Sakano, T.K. (1986) Organic solvents – physical properties and methods of purification. John-Wiley and Sons, New York.

[25] Furniss, B.S. and Vogel, A.I. (1978) Vogel's textbook of practical organic chemistry. Longman Group, London, 458-459.

[26] Grassie, N., McNeill, I.C. and Cooke, I. (1968) Thermal degradation of polymer mixtures. I. Degradation of polystyrene-poly (methyl methacrylate) mixtures and a comparison with the degradation of styrene-methyl methacrylate copolymers. *Journal of Applied Polymer Science*, **12**, 831-837.

[27] Horowitz, H. H. and Metzger, G. A. (1963) New analysis of thermogravimetric traces. *Analytical Chemistry*, **35**, 1464-1468.

[28] Flammability Test. UL94, ASTM D 635.

[29] Sain, M., Park, S.H., Suhara, F. and Law, S. (2004) Flame retardant and mechanical properties of natural fibre-PP composites containing magnesium hydroxide. *Polymer Degradation and Stability*, **83(2)**, 363-367.

[30] Smith, A.L. (1979) Applied infrared spectroscopy fundamentals, techniques and analytical problem-solving. John Wiley and Sons, A Wiley-Interscience Publication, New York, 297&308.

[31] Sadtler Research Laboratories (1974) The Sadtler Standard Spectra. PA 5, Philadelphia.

[32] Robinson, J.W. (1974) CRC Handbook of spectroscopy. CRC Press, Inc., USA, **2**.

[33] Szymanski, H.A. and Erikson, R. E. (1970) Infrared band handbook. 2nd Edition, IFI/Plenum, New York, **1-2**.

Vol.2, No.4, 320-328 (2010)
doi:10.4236/ns.2010.24040

Natural Science

Sufficient noise and turbulence can induce phytoplankton patchiness

Hiroshi Serizawa[1], Takashi Amemiya[2], Kiminori Itoh[1]

[1] Graduate School of Engineering, Yokohama National University, Yokohama, Japan; seri@qb3.so-net.ne.jp; itohkimi@ynu.ac.jp
[2] Graduate School of Environment and Information Sciences, Yokohama National University, Yokohama, Japan; amemiyat@ynu.ac.jp

Received 25 November 2009; revised 28 December 2009; accepted 3 February 2010.

ABSTRACT

Phytoplankton patchiness ubiquitously observed in marine ecosystems is a simple phy- sical phenomenon. Only two factors are required for its formation: one is persistent variations of inhomogeneous distributions in the phytoplankton population and the other is turbulent stirring by eddies. It is not necessary to assume continuous oscillations such as limit cycles for realization of the first factor. Instead, a certain amount of noise is enough. Random fluctuations by environmental noise and turbulent advection by eddies seem to be common in open oceans. Based on these hypotheses, we propose seemingly the simplest method to simulate patchiness formation that can create realistic images. Sufficient noise and turbulence can induce patchiness formation even though the system lies on the stable equilibrium conditions. We tentatively adopt the two-component model with nutrients and phytoplankton, however, the choice of the mathematical model is not essential. The simulation method proposed in this study can be applied to whatever model with stable equilibrium states including one-component ones.

Keywords: Eddy; Fluctuation; Noise; Patchiness; Reaction-Advection-Diffusion Model; Turbulence

1. INTRODUCTION

Patchiness is the inhomogeneous distribution of phytoplankton observed all over the oceans from the tropic to the boreal zone (**Figure 1**). The characteristic pattern with stretched and curled structures appears in the mesoscale or sub-mesoscale region from one to hundreds of kilometers, where the surface flow is approximately two-dimensional, *i.e.*, horizontal [1]. This observation suggests that the main cause of the phenomenon is referred to the physical factors such as lateral turbulent stirring and mixing by currents and eddies.

It is well known that the spatially inhomogeneous patterns can be generated in reaction-diffusion or reaction-advection-diffusion systems with equal diffusivities. One of the remarkable studies using reaction-diffusion equations was conducted by Medvinsky *et al.* [2]. They demonstrated that the diffusive instability can lead the system to spatiotemporal chaos even though starting from simple initial conditions. However, the chaotic patterns arising from reaction-diffusion systems do not necessarily mimic the real phytoplankton patchiness as seen in **Figure 1**. Without advection terms, stretched and curled structures characteristic of marine patchiness are not properly reproduced.

The situation is much improved by incorporating the effects of advection into the model. The simulation images created by reaction-advection-diffusion systems seem to show a closer similarity to real patchiness patterns than those by reaction-diffusion systems [3-6]. The studies by reaction-advection-diffusion systems usually adopt the seeded-eddy model to represent two-dimensional turbulent flows, which is developed by Dyke and Robertson [7].

However, the controversy is that the above mentioned studies using reaction-diffusion or reaction-advection-diffusion equations assume the limit cycle oscillations as the origin of heterogeneity in phytoplankton distributions. Considering that the system with the stable equilibrium state is meant to be homogeneous even though the initial state is heterogeneous [8], any pattern formation seems to require some kind of mechanisms such as limit cycles that continue to oscillate the system. However, it is not clear whether the limit cycle oscillations are usual events in natural aquatic ecosystems. Limit cycle oscillations could be too severe for the precondition of patchiness formation. To avoid the contradiction, it is necessary to seek the alternative mechanism other than the limit cycle oscillation.

One of the candidates that can replace the limit cycle oscillation could be persistent noise, which also can provide continuous changes of phytoplankton population.

Recently, Vainstein *et al*. [9] examined the stochastic population dynamics in the turbulent field, using a two-component reaction-advection-diffusion model with phytoplankton and zooplankton. In their model, the equation of zooplankton only contains the noise term for the reason that the population of zooplankton is considerably smaller than that of phytoplankton and thus subject to stochastic processes. The zooplankton distribution shows the finer structure than the phytoplankton distribution in their simulations, which is consistent with field observations. However, the phytoplankton distribution reproduced by their model does not seem to resemble real satellite images such as **Figure 1**.

Ecological systems are open systems in which the interactions with the external environment are noisy [10,11]. Thus, it is natural to incorporate random fluctuations into the model. However, proper incorporation of noise is not easy. For example, there are mathematically two types of noise: one is the additive noise and the other is the multiplicative noise [12]. The multiplicative noise is dependent on the dynamical variables, while the additive noise is independent of them. The multiplicative noise is thought to be caused by the interaction between the corresponding component and the external environment [10,13]. However, clear criteria do not necessarily exist for which type of noise should be used in a given situation. The decision rests more or less on the individual modeler.

The technical problem in computer simulations is more crucial. The stochastic spatiotemporal simulations of the partial differential equation model are strongly affected by such factors as the spatial correlation length and the temporal frequency of random noise. Therefore, it is important to determine appropriate values for these parameters in order that the effects of noise are properly reflected to simulation processes. In particular, the temporal frequency of noise is subtle to be handled. If the changing speed of noise is too fast or the period of subsequent noise is too short, successful pattern formation cannot be expected.

The goal of this paper is to specify the ultimate causes for patchiness formation and to propose a simple and convenient simulation method for its reproduction. We construct the model on the basis of the same concept as that by Vainstein *et al*. [9]. That is, the model includes the effect of temporally fluctuating noise as well as those of diffusion and advection. However, the substantial difference lies on the way to incorporate noise into the model. The simulation images obtained by our method seem to show a striking resemblance to real patchiness patterns as seen in **Figure 1**.

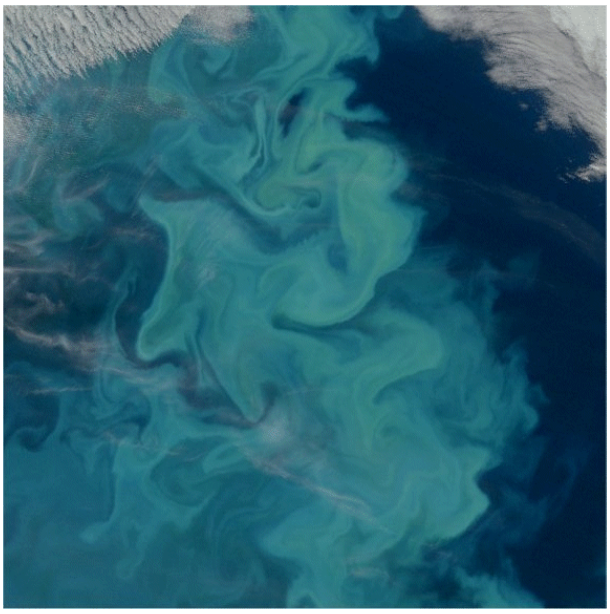

Figure 1. Algal blooms in the Barents Sea (Credit: NASA Goddard Space Flight Center).

Our two-component model consists of nutrients and phytoplankton. However, the model itself is not essential. The simulation method used in this study is not only effective for a wide range of parameter settings but also applicable to other mathematical models. Robustness and applicability could afford considerable credibility to our method.

2. MATHEMATICAL MODEL

2.1. Mean-Field Model

First, we present the mean-field model that describes the biological interaction. The ordinary differential equations are given as follows:

$$\frac{dN}{dt} = I_N - k\mu \frac{N}{H_N + N} P - m_N N, \tag{1}$$

$$\frac{dP}{dt} = I_P + \mu \frac{N}{H_N + N} P - f_P \frac{P}{H_P + P} - m_P P. \tag{2}$$

Two state variables N and P represent the nutrient concentration (the unit is mmol/m^3) and the phytoplankton density (the unit is g/m^3), respectively. The other variable t is actual time (the unit is day). With regard to the parameters, I_N and I_P are the input rates of nutrients and phytoplankton from the external environment, μ is the maximum growth rate of phytoplankton, k is the nutrient content in phytoplankton, f_P is the maximum predation rate of zooplankton on phytoplankton, m_N is the removal rate of nutrients from the system, m_P is the natural mortality rate of phytoplankton, and H_N and H_P are the half-saturation constants of nutrients and phyto-

Table 1. Parameters in minimal NP models **Eqs.1** and **2** and **Eqs.7-9**.

Parameters	Meanings	Set I	Set II	Units
I_N	Input rate of nutrients	0.4	0.15	$mmol \cdot m^{-3} \cdot day^{-1}$
k	Nutrient content in phytoplankton	0.2	0.2	mmol/g
H_N	Half-saturation constant of nutrients	0.2	0.2	$mmol/m^3$
m_N	Removal rate of nutrients	0.1	0.02	day^{-1}
I_P	Input rate of phytoplankton	0.04	0.04	$g \cdot m^{-3} \cdot day^{-1}$
μ	Maximum growth rate of phytoplankton	0.5	0.5	day^{-1}
f_P	Maximum feeding rate of zooplankton on phytoplankton	2.0	2.0	$g \cdot m^{-3} \cdot day^{-1}$
H_P	Half-saturation constant of phytoplankton	4.0	4.0	g/m^3
m_P	Mortality rate of phytoplankton	0.1	0.1	day^{-1}
D	Diffusion coefficient	0.125	0.125	km^2/day
r_c	Radius of eddies	10.0 (20.0)	10.0	km
V_{max}	Maximum velocity	10.0 (10.0)	10.0	km/day
V_{av}	Average velocity	2.98 (3.50)	2.98	km/day
L	Half length of square domain side	100	100	km

The Set I is used for the simulations in **Figures 5**, **6** and **7**, while the Set II is used in **Figure 8**. The values within parentheses in the Set I correspond to the VF I in **Figure 2(a)**, which is used only for the simulation in **Figure 6(a)**.

plankton, respectively. The mathematical model **Eqs.1** and **2**, named the minimal NP model in the present study, is known to show both bistability and limit cycle oscillations for the parameter values within the realistic range [6,8]. The meanings and the units of these parameters are listed in **Table 1** together with their values.

It is worth pointing out that the input term of phytoplankton I_P and the removal term of nutrients $m_N N$ contribute to stabilizing the system. For example, the situation that the phytoplankton density $P = 0$, where phytoplankton continue to be extinct, can be avoided by the parameter I_P. Moreover, even if $P = 0$, the other unfavorable situation that the nutrient concentration N continues to increase unlimitedly can be avoided by the term $m_N N$.

2.2. Velocity Field

Turbulent stirring is considered to be a crucial factor in creating phytoplankton patchiness in marine ecosystems. In this study, we use a simplified version of the seeded-eddy model as two-dimensional turbulent flows [3,6,7,9, 14]. The stream function ψ and fluid velocity $\boldsymbol{V}$ are described as follows:

$$\psi(x,y) = A\sum_i \sigma_i r_i^2 \exp\left\{-\frac{(x-x_i)^2+(y-y_i)^2}{2r_i^2}\right\},$$
$$\sigma_i = 1 \text{ or } -1, \quad \boldsymbol{V} = (V_x, V_y) = \left(-\frac{\partial\psi}{\partial y}, \frac{\partial\psi}{\partial x}\right). \tag{3}$$

Suppose that the number of eddies is denoted by n. Then, the velocity field is composed of n eddies, the half of which rotate clockwise, while the other half rotate counter-clockwise. The center of each eddy (x_i, y_i) is randomly dispersed within the domain. For simplicity, we use a constant value of the radius r_i for all eddies without considering a distribution of variant eddy sizes. Thus, $r_i = r_c$ (constant). It is supposed that the velocity field is mainly composed by eddies with larger radii, because the stream function ψ is proportional to the square of the radius r_i^2. The use of the constant radius can be justified for this reason. In fact, no essential difference is observed in the final appearance of patchiness patterns as compared to the case in which the eddy sizes are varied. The adoption of the constant radius is for the sake of speedy simulations. The scaling constant A is introduced for the adjustment of the maximum velocity V_{max}.

Figure 2 shows the velocity fields $\boldsymbol{V}$ used in the present study. The number and the radius of eddies are $n = 40$ and $r_c = 20$ km in **Figure 2(a)**, while $n = 100$ and $r_c = 10$ km in **Figure 2(b)**. The former velocity field is referred to as the VF I, and the latter is as the VF II. In most of the simulations except for **Figure 6(a)**, the VF II is employed. The domain is a 200 km × 200 km square, that is, a half length of each side is $L = 100$ km. The maximum velocity V_{max} is set up at 10 km/day for both velocity fields by varying the scaling parameter A. Then, the average velocities become 3.50 km/day in the VF I, while 2.98 km/day in the VF II. Both velocity fields are stationary and remain temporally unchanged, and also meet the periodic boundary conditions.

2.3. White Noise Process

Random fluctuations are constructed as explained in our previous study [8]. First, we provide a fluctuation function to describe a spatially smoothed deviation. The fluctuation function is formulated using the following Gaussian distribution function:

$$G_{x_i,y_i}(x,y)=\exp\left\{-\frac{(x-x_i)^2+(y-y_i)^2}{2s^2}\right\} \qquad (4)$$

The function G depicts a convex curved surface whose peak locates at (x_i, y_i), and the peak value equals 1. Here, the parameter s denotes the correlation length of fluctuations. The convex Gaussian function G is named the plus-type, and we can also formulate the minus-type Gaussian function, denoted as $-G$, that creates a concave valley.

Thereafter, a total of 100 Gaussian functions are provided with different (x_i, y_i) values, which consist of 50 plus-type ones and 50 minus-type ones. As the location of the peak or the valley (x_i, y_i) is randomly dispersed within the domain, the unevenly waved surface can be generated by the superposition of these Gaussian functions, the average height of which equals 0. Then, the fluctuation function F is defined as follows:

$$F(x,y)=\sum_i \sigma_i G_{x_i,y_i}(x,y), \quad \sigma_i=1 \text{ or } -1. \qquad (5)$$

The position coordinates of peaks and valleys (x_i, y_i) are different depending on the index i.

Assuming that the peak position (x_i, y_i) is a function of time t, the fluctuation function F is also a function of t, thus, $F(x, y, t)$. Then, we can use the function $F(x, y, t)$ as time-dependent fluctuations $\delta_{N,P}(x, y, t)$ for both the nutrient concentration N and the phytoplankton density P according to the following equation:

$$\delta_{N,P}(x,y,t)=A_{N,P}F(x,y,t). \qquad (6)$$

Here, the parameter A_N and A_P denote the scale factors of fluctuations for nutrients and phytoplankton. The functions $\delta_{N,P}(x, y, t)$ are referred to as the noise distribution function in this study. For example, the noise distributions for phytoplankton by $\delta_P(x, y, t)$ are shown in **Figure 3** for three elapsed time, where **Figure 3(a)** is the initial distribution of $\delta_P(x, y, t)$ when t = 0. The noise distribution function $\delta_P(x, y, t)$ continues to change alike, thereafter, and $\delta_N(x, y, t)$ changes as well.

2.4. Reaction-Advection-Diffusion Model

Finally, we construct the reaction-advection-diffusion model that synthesizes the above-mentioned factors, that is, the biological interaction, turbulence and noise. Using the right side of the **Eqs.1** and **2**, we can formulate the following two-dimensional reaction-advection-diffusion model:

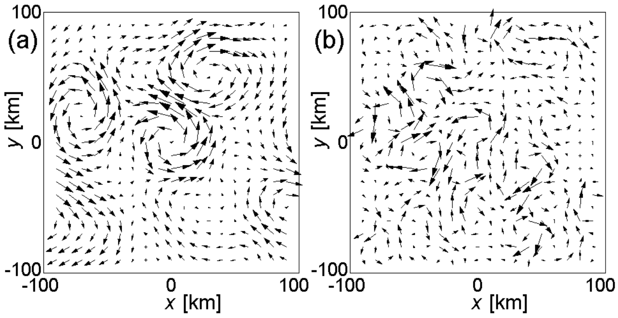

Figure 2. Velocity fields by turbulent stirring. The velocity field is constructed by the superimposition of n eddies with the constant radius r_c. (a) n = 40, r_c = 20 km. (b) n = 100, r_c =10 km. These are named the VF I and the VF II, respectively. The velocity fields meet the periodic boundary conditions.

$$\frac{\partial N}{\partial t}=D\nabla^2 N-\nabla\cdot(\boldsymbol{V}N)+I_N-k\mu\frac{N}{H_N+N}P \qquad (7)$$
$$-m_N N+N\delta_N(x,y,t),$$

$$\frac{\partial P}{\partial t}=D\nabla^2 P-\nabla\cdot(\boldsymbol{V}P)+I_P+\mu\frac{N}{H_N+N}P$$
$$-f_P\frac{P}{H_P+P}-m_P P+P\delta_P(x,y,t). \qquad (8)$$

The Laplacian operators are described as follows:

$$\nabla=\left(\frac{\partial}{\partial x},\frac{\partial}{\partial y}\right), \quad \nabla^2=\frac{\partial^2}{\partial x^2}+\frac{\partial^2}{\partial y^2}. \qquad (9)$$

The variables x and y are the horizontal position coordinates (the unit is km). The parameter D denotes the lateral diffusivity, which is equal for two components. Further, the vector $\boldsymbol{V}$ represents the velocity field shown in **Figure 2**. It should be noted that the units of state variables N and P are changed to mmol/m^2 and g/m^2 due to the adoption of the two-dimensional model.

As stated previously, there are two types of noise, the additive noise and the multiplicative noise. The mathematical model **Eqs.7-9** contains the stochastic fluctuation terms in the right-hand sides of the partial differential equations, which are described in the multiplicative forms as $+N\delta_N(x, y, t)$ for nutrients and $+P\delta_P(x, y, t)$ for phytoplankton. This is because we assume the interactions with the external environment for both nutrients and phytoplankton. However, even if the additive noise is added for both components, the results are hardly affected. Thus, which type of noise is used is not essential in the current study. What is important is to set the amplitude of noise within adequate values by adjusting the scale parameters A_N and A_P in order to avoid the situation

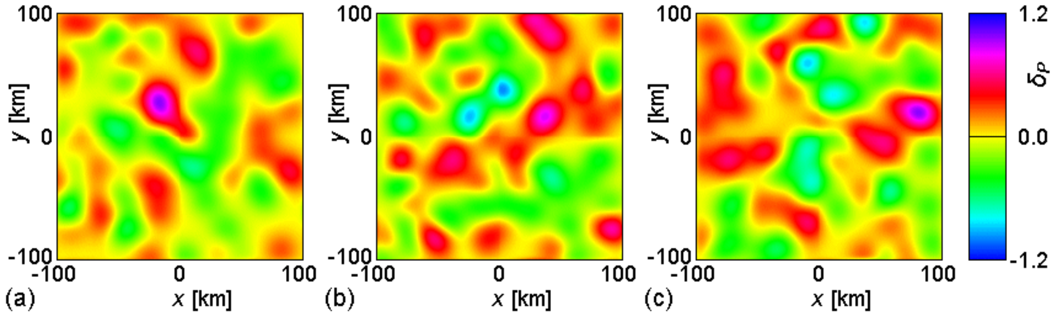

Figure 3. Spatiotemporal variation of noise distribution for phytoplankton. The distribution of noise for the phytoplankton density P is represented by the noise distribution function $\delta_P(x, y, t)$. (a) shows the initial distribution $\delta_P(x, y, 0)$, which is changed to (b) and (c) consecutively. The noise distributions also meet the periodic boundary conditions.

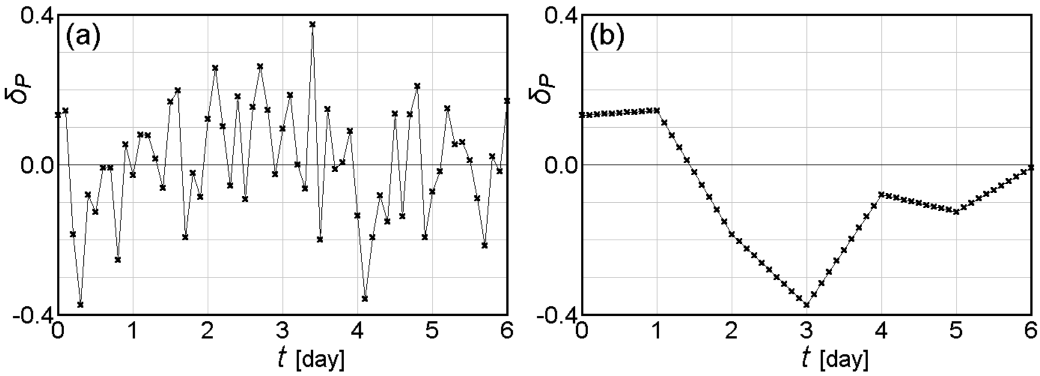

Figure 4. White noise processes at (0, 0). These line graphs show the temporal change of the noise distribution function $\delta_P(x, y, t)$ for phytoplankton at the center of the domain, *i.e.*, $\delta_P(0, 0, t)$. The time step of the simulations Δt = 0.1 day, meaning that the calculation is carried out 10 times a unit time, which equals a day. Renewed noise distribution functions are provided every time step in (a) and every 10 time steps, *i.e.*, everyday in (b), respectively. Also in (b), the amplitude of noise is changed linearly at each time step between two days. The white noise processes described in (a) and (b) are named the WN I and the WN II, respectively.

that the population of the component falls to the negative values.

In white noise processes, the amplitude of the fluctuation, *i.e.*, deviation from the mean value is randomly distributed within a certain range at each cell and each unit time. If the difference of the amplitude between adjacent cells or subsequent time steps is too large, the system is often led to divergence.

The temporal change of fluctuations is determined as follows. According to the noise distribution functions $\delta_{N,P}(x, y, t)$, the amplitudes of fluctuations for both nutrients and phytoplankton change independently at each cell. Assuming that the time step of the simulation Δt = 0.1 day, the calculations are conducted ten times a unit time, *i.e.*, a day. Further, the noise distribution functions $\delta_{N,P}(x, y, t)$ are renewed every time step (**Figure 4(a)**) or every ten time steps (**Figure 4(b)**). In the latter case, the renewal of $\delta_{N,P}(x, y, t)$ is performed every unit time, *i.e.*, everyday, and the amplitude of fluctuations varies linearly between successive two distributions. The temporal change of random noise for the phytoplankton density *P* at the center of the domain $\delta_P(0, 0, t)$ is depicted in **Figure 4** for these two cases, which are referred to as the WN I and the WN II, respectively. The WN I is used only for the simulation in **Figure 7(a)**. Otherwise, the WN II is employed.

In our spatiotemporal simulations, the domain is a 200 km × 200 km square, and a half length of each side *L* = 100 km. Then, the two-dimensional square domain is divided into a rectangular grid of 200 × 200 cells. Therefore, each cell is a 1.0 km × 1.0 km square, and the noise distribution functions $\delta_{N,P}(x, y, t)$ are allocated to each cell. In the initial state, the distribution of both components are homogeneous, however, inhomogeneous distributions are realized just after the onset of simulations due to random fluctuations. The fourth order Runge-Kutta integrating method is applied with a time step Δt = 0.1 day, and the periodic boundary conditions are imposed.

It is confirmed that the results with smaller time steps remain the same for each program, ensuring the accuracy of the simulations.

3. RESULTS

3.1. Simulations with Noise (Set I)

Prior to spatiotemporal simulations of the reaction-advection-diffusion model **Eqs.7-9**, we conduct the stability analyses of the mean-field model **Eqs.1** and **2**. The results are shown in **Table 2**. For the parameter Set I in **Table 1**, the systems **Eqs.1** and **2** have only one fixed point. As the real parts of two eigenvalues are both negative, this fixed point is identified as an attractor that represents the stable equilibrium state. Therefore, even if the initial state is heterogeneous, the system is damped out to the uniform distribution in the course of time without continuous fluctuations.

Figure 5 shows the spatiotemporal variation of phytoplankton density P for the parameter Set I, in which the effects of turbulence and noise are both considered. The VF II given by **Figure 2(b)** and the WN II described in **Figure 4(b)** are applied for the simulations. While the initial state is homogeneous, the spatial distribution of phytoplankton begins to be disturbed soon due to the combined effects of furious turbulence and random noise. Then, as early as the ninth day, patchiness formation is perfectly completed, and continues to change, thereafter. It should be noted that the same pattern does not occur again, because the stochastic perturbation is not periodic.

Table 2. Stability analyses in minimal NP model **Eqs.1** and **2.**

	Set I	Set II
(N_0, P_0)	(0.259, 6.631)	(1.656, 1.31)
Eigenvalues	-0.309 ± 0.029i	0.017 ± 0.037i
Stability	Stable	Unstable
State	Convergence	Limit cycle

The minimal NP model **Eqs.1** and **2** generates only one fixed point (N_0, P_0) for both Sets I and II within the region $N_0 > 0$ and $P_0 > 0$, showing the convergence for the Set I and the limit cycle oscillation for the Set II, respectively.

The dependence of the patchiness pattern on the turbulence fields are examined in **Figure 6**. The velocity fields used in **Figure 6(a)** and **(b)** are the VF I and the VF II in **Figure 2**, respectively. The broadly extended structures observed in **Figure 6(a)** are probably due to the mildness of currents in the VF I. In contrast, the stormy velocity field such as the VF II seems to generate the patchiness pattern with fine structures as seen in **Figure 6(b)**, showing a clear resemblance with real satellite images such as **Figure 1**.

Meanwhile, the dependence on the noise processes is investigated in **Figure 7**. The white noise processes corresponding to **Figures 7(a)** and 7**(b)** are the WN I and the WN II in **Figure 4**, respectively. Too frequent change in the noise distributions could obscure the patchiness pattern as seen in **Figure 7(a)**. On the contrary, the patchiness image in **Figure 7(b)** shows a clear difference in phytoplankton density. Slowly changing fluctuations

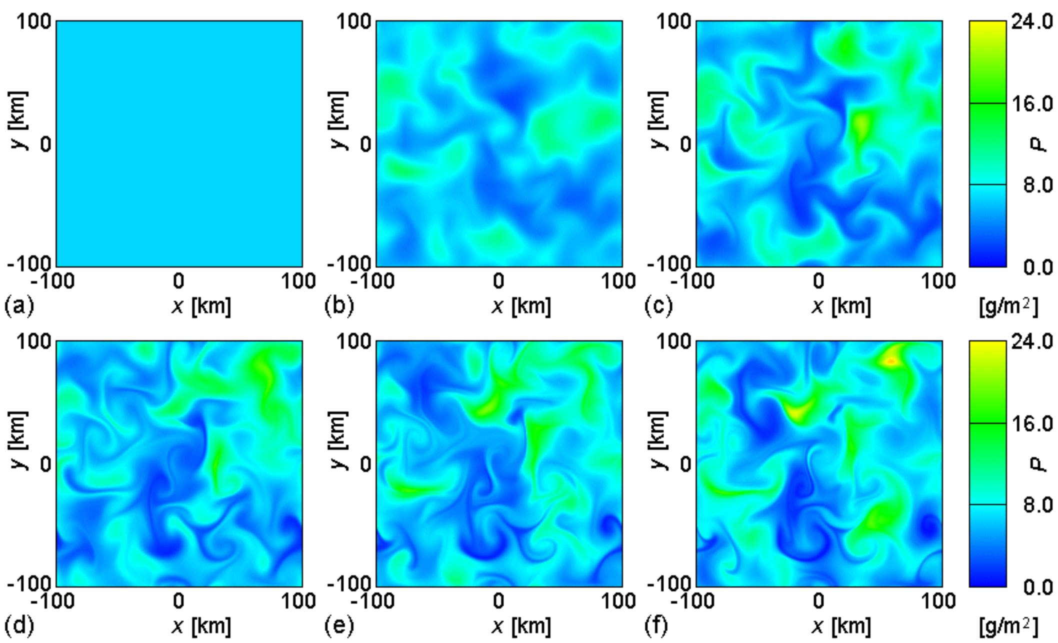

Figure 5. Spatiotemporal variation of phytoplankton distribution in minimal NP model **Eqs.7-9**. Without noise, the system shows a convergence to a stable equilibrium state for the parameter Set I in **Table 1**. However, incorporating random fluctuations into the model, patchiness formation is induced by the combined effects of turbulence and noise. The VF II and the WN II are employed. (a) t = 0 day, (b) t = 3 day, (c) t = 6 day, (d) t = 9 day, (e) t = 12 day, (f) t = 15 day.

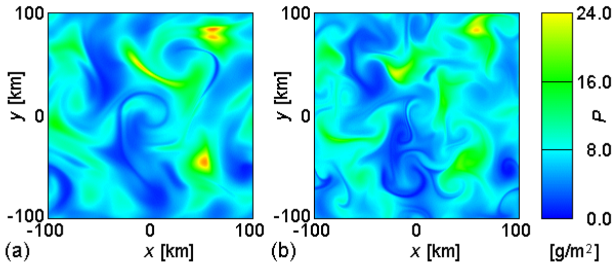

Figure 6. Dependence of phytoplankton distribution on velocity field in minimal NP model **Eqs.7-9**. The parameters are given by the Set I, and the WN II is employed. t = 15 day. (a) VF I, (b) VF II (same as **Figure 5(f)**).

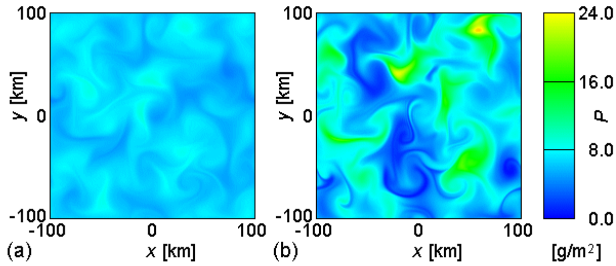

Figure 7. Dependence of phytoplankton distribution on white noise process in minimal NP model **Eqs.7-9**. The parameters are given by the Set I, and the VF II is employed. t = 15 day. (a) WN I, (b) WN II (same as **Figure 5(f)**).

intensify the effects of random noise, facilitating the emergence of both the densely populated and the sparsely populated areas.

3.2. Simulations with Limit Cycle Oscillation (Set II)

For the comparison, we also survey the pattern formation in the oscillatory regime. According to the stability analysis for the parameter Set II, the fixed point of the system becomes unstable as shown in **Table 2**, and the limit cycle is formed around it. In this case, random noise is not necessary, because the continuous oscillation encourages the pattern formation unless the initial distribution is homogeneous [6].

The spatiotemporal variation of phytoplankton density P for the parameter Set II is shown in **Figure 8**. Only the effect of turbulence is considered employing the VF II. Instead, the initial distributions of both components are not homogeneous but randomly dispersed. Patchiness patterns are formed also in this case for the almost same period as in **Figure 5**. However, it could be happened that the similar patterns appear repeatedly with the period of the limit cycle oscillation, which was the case in our previous study [6].

4. DISCUSSIONS

4.1. Comparison with Field Observations

Our simulation results seem to show a close similarity with satellite images such as **Figure 1**. Stretched and curled patterns characteristic of marine patchiness are clearly reproduced particularly in **Figure 5**, which employs energetic turbulence as the VF II and slowly changing white noise process as the WN II.

We attempt some kinds of numerical comparisons. First, the size of our simulation images are comparable to that of the satellite images in **Figure 1**, which covers the area of some hundreds kilometers. Considering that most of the patchiness images supplied by NASA are of a similar size with **Figure 1**, we can insist that the velocity field and the noise process adopted in our method are suitable for patchiness simulations.

Comparing the horizontal diffusivity to experimental data, two types of diffusion must be distinguished [6,14]. The first type of diffusion is usual diffusion originating from a tendency toward homogeneity. This type of diffusion is represented by the second order differential for position coordinates. Thus, the diffusion coefficient D used in the minimal NP model **Eq.7-Eq.9** corresponds to this type. However, this type of diffusion does not stand for real diffusion in marine ecosystems. In the context of computer simulations, diffusion of this type merely functions as a smoothing factor that prevents divergence of the system.

Meanwhile, there exists another type of diffusion originating from advection by currents and eddies, which is represented by the first order differential for position coordinates. It is this type of diffusion that is responsible for patchiness formation in oceanic environments. Thus, the real diffusion coefficient must be recalculated from the velocity fields $\boldsymbol{V}$ in **Figure 2**.

The real diffusion coefficient D_{ad} can be evaluated by the following equation:

$$D_{ad} = \mu L_D{}^2. \tag{10}$$

As a rough approximation, suppose that the characteristic scale of diffusion L_D is given by the average velocity V_{av}. In the case the VF II in **Figure 2(b)** is L_D ~3.0 km. Then, we can estimate the value of turbulent diffusivity D_{ad} as about 4.5 km^2/day. This value is converted to about 5×10^5 cm^2/sec, which is in agreement with the empirical data estimated by Okubo [15] that range from 5×10^2 to 2×10^6 cm^2/sec.

4.2. Crucial Factors for Patchiness Formation

Turbulence and persistent variation of phytoplankton population are two essential factors for creating marine patchiness. Particularly as for turbulence, many researchers take it for granted that lateral advection and mixing by currents and eddies plays a constructive role for patchiness formation [1]. However, there seems to be no consensus for another factor at the present time. According to our simulations, both random noise and limit cycle oscillations can cause persistent variation, and promote patchiness formation as shown in **Figures 5** and **8**. It is not yet clear about which is the ultimate cause for persistent variation of phytoplankton population. Which is more probable as a crucial factor in patchiness formation, noise or limit cycles? It seems difficult to judge from the appearance of simulation images.

Becks *et al*. [16] reported that a defined chemostat system with bacteria and ciliate showed dynamic behaviors such as chaos and stable limit cycles. In their two-prey, one-predator system, the changes of the bifurcation parameter (the dilution rate) trigger the population dynamics such as stable coexistence at high dilution rates, chaos at intermediate dilution rates and stable limit cycles at low dilution rates.

However, there is still a lack of field evidence that limit cycle oscillations or chaotic behaviors surely occur in the natural seas and oceans. It seems unnatural to adopt limit cycle oscillations as a precondition of population variations. Thus, it is reasonable to conclude as follows. That is, random noise ubiquitously observed in the natural world is the source of persistent variations of inhomogeneous phytoplankton distributions, which plays a crucial role in patchiness formation together with turbulent stirring and mixing.

It is worth noting that random noise and limit cycles are not exclusive. A possibility cannot be denied that these two contribute together to patchiness formation. Indeed, further simulations show that the system containing both the noise process and the limit cycle oscillation can successfully produce realistic patchiness patterns. However, we can insist that the crucial factor is not limited cycles but noise processes that are responsible for phytoplankton patchiness in marine ecosystems.

From the technical point of view in computer simulations, appropriate incorporation of turbulence and noise into the model is indispensable. The effects of these factors must be fully reflected in the simulations. The velocity field should be sufficiently energetic as the VF II (**Figure 2(b)**) rather than the VF I (**Figure 2(a)**). The white noise process should be slow enough as the WN II (**Figure 4(b)**) rather than the WN I (**Figure 4(a)**).

4.3. Extension to One-Component Model

In order to confirm robustness and applicability of the method, we finally attempt the simulation of patchiness formation using the different model. The exemplified mathematical model is a partial differential equation system with one variable, which is described as follows:

$$\frac{\partial P}{\partial t} = D\nabla^2 P - \nabla\cdot(\mathbf{V}P) + I_P + \mu P\left(1-\frac{P}{K}\right) - f_P\frac{P}{H_P+P} - m_P P + P\delta_P(x,y,t). \quad (11)$$

The reaction-advection-diffusion model **Eq.11** contains only one state variable P, which represents the phytoplankton density (the unit is g/m^2). The parameter K is the carrying capacity of the environment, and the meanings of the other parameters are the same as in the minimal NP models **Eqs.1** and **2** and **Eqs.7-9**. Moreover, the same velocity field (the VF II) and the same multiplicative white noise process (the WN II) as in **Figure 5** are employed in the simulation. It should be noted that limit cycles are impossible due to the use of the one-variable model. The system can give rise to only a convergence to the attractor, unless it diverges.

Figure 9 is an example of patchiness formation in the mathematical model **Eq.11**. The similar pattern formation with that in **Figure 5** proceeds, ensuring robustness and extensive applicability of the method described in this study.

5. CONCLUSIONS

1) Phytoplankton patchiness in marine ecosystems is essentially the physical phenomenon independent of

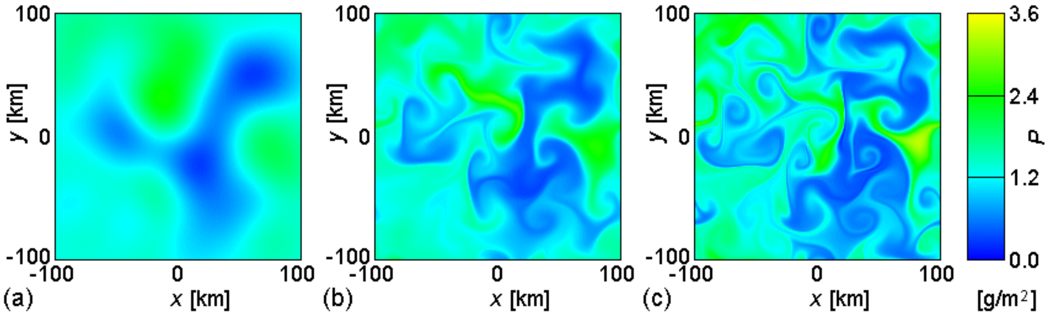

Figure 8. Spatiotemporal variation of phytoplankton distribution in minimal NP model **Eqs.7-9**. Without noise, the system shows a limit cycle oscillation for the parameter Set II in **Table 1**. In this case, patchiness formation is induced without fluctuations, supposing that the initial distribution is inhomogeneous. The VF II is employed. (a) $t = 0$ day, (b) $t = 6$ day, (c) $t = 12$ day.

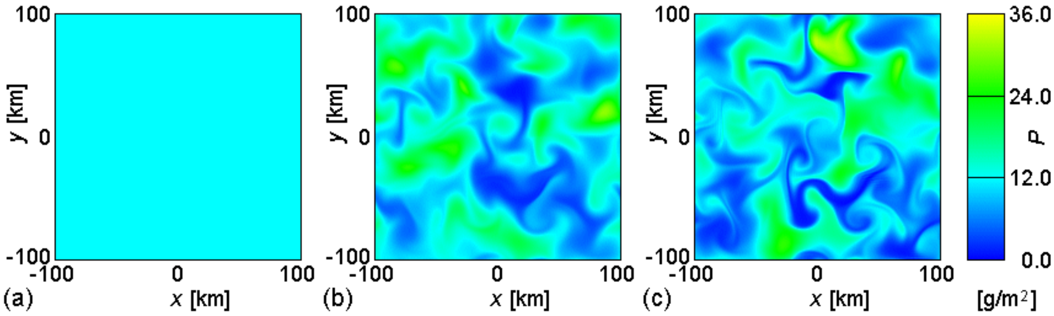

Figure 9. Spatiotemporal variation of phytoplankton distribution in mathematical model **Eq.11**. Without noise, the system shows a convergence to a stable equilibrium state for the following parameters: $I_P = 0.1$ g·m^{-2}·day^{-1}, $\mu = 0.5$ day^{-1}, $K = 20.0$ g/m^2, $f_P = 1.6$ g·m^{-2}·day^{-1}, $H_P = 2.4$ g/m^2, $m_P = 0.1$ day^{-1}. The units are altered to those of the two-dimensional model. The VF II and the WN II are employed. (a) $t = 0$ day, (b) $t = 6$ day, (c) $t = 12$ day.

each biological process. Turbulence and noise are two major factors that promote patchiness formation in oceanic environments. The pattern formation is guaranteed by persistent variations of the phytoplankton population. Stochastic noise is one of the most probable causes responsible for continuous variations. In addition, stirring and mixing by currents and eddies facilitate the creation of stretched and curled structures characteristic of phytoplankton patchiness.

2) Patchiness formation can be simulated in the spatially extended reaction-advection-diffusion system that properly integrates the turbulence field and the noise process. Sufficiently furious turbulence such as the VF II (**Figure 2(b)**) and slowly changing fluctuations such as the WN II (**Figure 4(b)**) are the key to reproduce realistic images of patchiness.

3) The simulations of patchiness formation can be performed by whatever model with the stable equilibrium state. Robustness in model simulations and applicability to various models could explain the universality of the phenomenon that is observed worldwide on Earth.

6. ACKNOWLEDGEMENTS

This study is supported by the Global COE Program "Global Eco-Risk Management from Asian View Points" by the Ministry of Education, Culture, Sports, Science and Technology, Japan.

REFERENCES

[1] Martin, A.P. (2003) Phytoplankton patchiness: The role of lateral stirring and mixing. *Progress in Oceanography*, **57(2)**, 125-174.

[2] Medvinsky, A.B., Petrovskii, S.V., Tikhonova, I.A., Malchow, H. and Li, B.-L. (2002) Spatiotemporal complexity of plankton and fish dynamics. *SIAM Review*, **44(3)**, 311-370.

[3] Abraham, E.R. (1998) The generation of plankton patchiness by turbulent stirring. *Nature*, **391(6667)**, 577-580.

[4] Neufeld, Z., Haynes, P.H., Garçon, V. and Sudre, J. (2002) Ocean fertilization experiments may initiate a large scale phytoplankton bloom. *Geophysical Research Letters*, **29(11)**, 1-4.

[5] Tzella, A. and Haynes, P.H. (2007) Small-scale spatial structure in plankton distributions. *Biogeosciences*, **4(2)**, 173-179.

[6] Serizawa, H., Amemiya, T. and Itoh, K. (2008) Patchiness in a minimal nutrient-phytoplankton model. *Journal of Biosciences*, **33(3)**, 391-403.

[7] Dyke, P.P.G. and Robertson, T. (1985) The simulation of offshore turbulent dispersion using seeded eddies. *Applied Mathematical Modelling*, **9(6)**, 429-433.

[8] Serizawa, H., Amemiya, T. and Itoh, K. (2009) Noise-triggered regime shifts in a simple aquatic model. *Ecological Complexity*, **6(3)**, 375-382.

[9] Vainstein, M.H., Rubí, J.M. and Vilar, J.M.G. (2007) Stochastic population dynamics in turbulent fields. *The European Physical Journal-Special Topics*, **146(1)**, 177-187.

[10] Spagnolo, B., Valenti, D. and Fiasconaro, A. (2004) Noise in ecosystems: A short review. *Mathematical Biosciences and Engineering*, **1(1)**, 185-211.

[11] Provata, A., Sokolov, I.M. and Spagnolo, B. (2008) Editorial: Ecological complex systems. *The European Physical Journal B*, **65(3)**, 307-314.

[12] Guttal, V. and Jayaprakash, C. (2007) Impact of noise on bistable ecological systems. *Ecological Modelling*, **201 (3-4)**, 420-428.

[13] Spagnolo, B., Fiasconaro, A. and Valenti, D. (2003) Noise induced phenomena in Lotka-Volterra systems. *Fluctuation and Noise Letters*, **3(2)**, 177-185.

[14] Serizawa, H., Amemiya, T. and Itoh, K. (2009) Patchiness and bistability in the comprehensive cyanobacterial model (CCM). *Ecological Modelling*, **220(6)**, 764-773.

[15] Okubo, A. (1971) Oceanic diffusion diagram. *Deep Sea Research and Oceanographic Abstracts*, **18(8)**, 789-802.

[16] Becks, L., Hilker, F.M., Malchow, H., Jürgens, K. and Arndt, H. (2005) Experimental demonstration of chaos in a microbial food web. *Nature*, **435(30)**, 1226-1229.

Vol.2, No.4, 329-337 (2010)
doi:10.4236/ns.2010.24041 Natural Science

Orbital effects of Sun's mass loss and the Earth's fate

Lorenzo Iorio

INFN-Sezione di Pisa, Viale Unità di Italia 68, Bari (BA), Italy; lorenzo.iorio@libero.it

Received 22 November 2009; revised 28 November 2009; accepted 13 January 2010.

ABSTRACT

I calculate the classical effects induced by an isotropic mass loss $\dot{M}/M$ of a body on the orbital motion of a test particle around it; the present analysis is also valid for a variation $\dot{G}/G$ of the Newtonian constant of gravitation. I perturbatively obtain negative secular rates for the osculating semimajor axis *a*, the eccentricity *e* and the mean anomaly $\mathcal{M}$, while the argument of pericenter *ω* does not undergo secular precession, like the longitude of the ascending node *Ω* and the inclination I. The anomalistic period is different from the Keplerian one, being larger than it. The true orbit, instead, expands, as shown by a numerical integration of the equations of motion in Cartesian coordinates; in fact, this is in agreement with the seemingly counter-intuitive decreasing of *a* and *e* because they only refer to the osculating Keplerian ellipses which approximate the trajectory at each instant. By assuming for the Sun $\dot{M}/M = -9 \times 10^{-14}\ \mathrm{yr}^{-1}$, it turns out that the Earth's perihelion position is displaced outward by 1.3 cm along the fixed line of apsides after each revolution. By applying our results to the phase in which the radius of the Sun, already moved to the Red Giant Branch of the Hertzsprung-Russell Diagram, will become as large as 1.20 AU in about 1 Myr, I find that the Earth's perihelion position on the fixed line of the apsides will increase by $\approx 0.22-0.25$ AU (for $\dot{M}/M = -2 \times 10^{-7}\ \mathrm{yr}^{-1}$); other researchers point towards an increase of $\approx 0.37-0.63$ AU. Mercury will be destroyed already at the end of the Main Sequence, while Venus should be engulfed in the initial phase of the Red Giant Branch phase; the orbits of the outer planets will increase by $1.2-7.5$ AU. Simultaneous long-term numerical integrations of the equations of motion of all the major bodies of the solar system, with the inclusion of a mass-loss term in the dynamical force models as well, are required to check if the mutual N-body interactions may substantially change the picture analytically outlined here, especially in the Red Giant Branch phase in which Mercury and Venus may be removed from the integration.

Keywords: Gravitation; Stars; Mass-Loss; Celestial Mechanics

1. INTRODUCTION

I deal with the topic of determining the classical orbital effects induced by an isotropic variation $\dot{M}/M$ of the mass of a central body on the motion of a test particle; my analysis is also valid for a change $\dot{G}/G$ of the Newtonian constant of gravitation. This problem, although interesting in itself, is not only an academic one because of the relevance that it may have on the ultimate destiny of planetary companions in many stellar systems in which the host star experiences a mass loss, like our Sun [1]. With respect to this aspect, my analysis may be helpful in driving future researches towards the implementation of long-term N-body simulations including the temporal change of *GM* as well, especially over timescales covering paleoclimate changes, up to the Red Giant Branch (RGB) phase in which some of the inner planets should be engulfed by the expanding Sun. Another problem, linked to the one investigated here, which has recently received attention, is the observationally determined secular variation of the Astronomical Unit [2-5]. Moreover, increasing accuracy in astrometry pointing towards microarcsecond level [6], and long-term stability in clocks [7] requires to consider the possibility that smaller and subtler perturbations will be soon detectable in the solar system. Also future planetary ephemerides should take into account $\dot{M}/M$. Other phenomena which may show connections with the problem treated here are the secular decrease of the semimajor axes of the LAGEOS satellites, amounting to 1.1 mm d^{-1} [8], and the increase of the lunar orbit's eccentricity [9]. However, a detailed analysis of all such issues is beyond the scope of this paper.

Many treatments of the mass loss-driven orbital dynamics in the framework of the Newtonian mechanics, based on different approaches and laws of variation of the central body's mass, can be found in literature [2,4,10-18] and references therein.

The plan of the paper is as follows. Section 2 is devoted to a theoretical description of the phenomenon in a two-body scenario. By working in the Newtonian framework, I will analytically work out the changes after one orbital revolution experienced by all the Keplerian orbital elements of a test particle moving in the gravitational field of a central mass experiencing a variation of its GM linear in time. Then, I will clarify the meaning of the results obtained by performing a numerical integration of the equations of motion in order to visualize the true trajectory followed by the planet. Concerning the method adopted, I will use the Gauss perturbation equations [19,20], which are valid for generic disturbing accelerations depending on position, velocity and time, the "standard" Keplerian orbital elements (the Type I according to [16]) with the eccentric anomaly E as "fast" angular variable. Other approaches and angular variables like, e.g. the Lagrange perturbation equations [19,20], the Type II orbital elements [16] and the mean anomaly $\mathcal{M}$ could be used, but, in my opinion, at a price of major conceptual and computational difficulties[1]. With respect to possible connections with realistic situations, it should be noted that, after all, the Type I orbital elements are usually determined or improved in standard data reduction analyses of the motion of planets and (natural and artificial) satellites. Instead, my approach should, hopefully, appear more transparent and easy to interpret, although, at first sight, some counter-intuitive results concerning the semimajor axis and the eccentricity will be obtained; moreover, for the chosen time variation of the mass of the primary, no approximations are used in the calculations which are quite straightforward. However, it is important to stress that such allegedly puzzling features are only seemingly paradoxical because they will turn out to be in agreement with numerical integrations of the equations of motion, as explicitly shown by the Figures depicted. Anyway, the interested reader is advised to look also at [16] for a different approach. In Section 3, I will apply our results to the future Sun-Earth scenario and to the other planets of the solar system. Section 4 summarizes my results.

2. ANALYITICAL CALCULATION OF THE ORBITAL EFFECT OF $\dot{\mu}/\mu$

By defining $\mu \doteq GM$ at a given epoch t_0, the acceleration of a test particle orbiting a central body experiencing a variation of μ is, to first order in $t - t_0$,

$$\boldsymbol{A} = -\frac{\mu(t)}{r^2}\hat{\boldsymbol{r}} \approx -\frac{\mu}{r^2}\left[1 + \left(\frac{\dot{\mu}}{\mu}\right)(t - t_0)\right]\hat{\boldsymbol{r}}, \quad (1)$$

with $\dot{\mu} \doteq \dot{\mu}|_{t=t_0}$. $\dot{\mu}$ will be assumed constant throughout the temporal interval of interest $\Delta t = t - t_0$, as it is the case, e.g., for most of the remaining lifetime of the Sun as a Main Sequence (MS) star [1]. Note that $\dot{\mu}$ can, in principle, be due to a variation of both the Newtonian gravitational constant G and the mass M of the central body, so that

$$\frac{\dot{\mu}}{\mu} = \frac{\dot{G}}{G} + \frac{\dot{M}}{M}. \quad (2)$$

Moreover, while the orbital angular momentum is conserved, this does not happen for the energy.

By limiting ourselves to realistic astronomical scenarios like our solar system, it is quite realistic to assume that

$$\left(\frac{\dot{\mu}}{\mu}\right)(t - t_0) \ll 1 \quad (3)$$

over most of its remaining lifetime: indeed, since $\dot{M}/M$ is of the order of[2] $10^{-14}\ \mathrm{yr}^{-1}$, for the Sun [1], the condition (3) is satisfied for the remaining[2] ≈ 7.58 Gyr before the Sun will approach the RGB tip in the Hertzsprung-Russell Diagram (HRD). Thus, I can treat it perturbatively with the standard methods of celestial mechanics.

The unperturbed Keplerian ellipse at epoch t_0, assumed coinciding with the time of the passage at perihelion t_p, is characterized by

$$\begin{cases} r = a(1 - e\cos E), \\ dt = \left(\frac{1 - e\cos E}{n}\right) dE, \\ \cos f = \frac{\cos E - e}{1 - e\cos E}, \\ \sin f = \frac{\sqrt{1-e^2}\sin E}{1 - e\cos E}, \end{cases} \quad (4)$$

where a and e are the semimajor axis and the eccentricity, respectively, which fix the size and the shape of the unchanging Keplerian orbit, $n \doteq \sqrt{\mu/a^3}$ is its unperturbed Keplerian mean motion, f is the true anomaly, reckoned from the pericentre, and E is the eccentric anomaly. **Eq.4** characterizes the path followed by the particle for any $t > t_p$ if the mass loss would suddenly cease at t_p. Instead, the true path will be, in general, different from a closed ellipse because of the perturbation induced by $\dot{\mu}$, and the orbital parameters of the osculating ellipses approximating the real trajectory at each instant of time will slowly change in time.

[1]Think, e.g., about the cumbersome expansions in terms of the mean anomaly and the Hansen coefficients, the subtleties concerning the choice of the independent variable in the Lagrange equations for the semimajor axis and the eccentricity [19].

[2]About 80% of such a mass-loss is due to the core nuclear burning, while the remaining 20% is due to average solar wind.

[3]The age of the present-day MS Sun is 4.58 Gyr, counted from its zero-age MS star model [1].

2.1. The Semimajor Axis and the Eccentricity

The Gauss equation for the variation of the semimajor axis a is [19,20]

$$\frac{da}{dt}=\frac{2}{n\sqrt{1-e^2}}\left[eA_r\sin f+A_\tau\left(\frac{p}{r}\right)\right], \tag{5}$$

where A_r and A_τ are the radial and transverse, *i.e.* orthogonal to the direction of $\hat{\boldsymbol{r}}$, components, respectively, of the disturbing acceleration, and $p\doteq a(1-e^2)$ is the semilatus rectum. In the present case

$$A=A_r=-\frac{\dot\mu}{r^2}\left(t-t_p\right), \tag{6}$$

i.e. there is an entirely radial perturbing acceleration. For $\dot\mu<0$, *i.e.* a decrease in the body's *GM*, the total gravitational attraction felt by the test particle, given by (1), is reduced with respect to the epoch t_p.

In order to have the rate of the semimajor axis averaged over one (Keplerian) orbital revolution (6) must be inserted into (5), evaluated onto the unperturbed Keplerian ellipse with (4) and finally integrated over $ndt/2\pi$ from 0 to 2π because $n/2\pi\doteq 1/P^{\rm Kep}$ (see below). Note that, from (4), it can be obtained

$$t-t_p=\frac{E-e\sin E}{n}. \tag{7}$$

As a result, I have [4]

$$\left\langle\frac{da}{dt}\right\rangle=-\frac{ea}{\pi}\left(\frac{\dot\mu}{\mu}\right)\int_0^{2\pi}\frac{(E-e\sin E)\sin E}{(1-e\cos E)^2}dE \tag{8}$$
$$=\frac{2ea}{1-e}\left(\frac{\dot\mu}{\mu}\right).$$

Note that if μ decreases, a gets reduced as well: $\langle\dot a\rangle<0$. This may be seemingly bizarre and counter-intuitive, but, as it will be shown later, it is not in contrast with the true orbital motion.

The Gauss equation for the variation of the eccentricity is [19,20]

$$\frac{de}{dt}=\frac{\sqrt{1-e^2}}{na}\left\{A_r\sin f+A_\tau\left[\cos f+\frac{1}{e}\left(1-\frac{r}{a}\right)\right]\right\} \tag{9}$$

For $A=A_r$ it reduces to

$$\frac{de}{dt}=\left(\frac{1-e^2}{2ae}\right)\frac{da}{dt}, \tag{10}$$

so that

$$\left\langle\frac{de}{dt}\right\rangle=(1+e)\left(\frac{\dot\mu}{\mu}\right); \tag{11}$$

also the eccentricity gets smaller for $\dot\mu<0$.

As a consequence of the found variations of the osculating semimajor axis and the eccentricity, the osculating orbital angular momentum per unit mass, defined by $L^2\doteq\mu a(1-e^2)$, remains constant: indeed, by using (8) and (11), it turns out

[4]Recall that the integration is taken over the unperturbed Keplerian ellipse: that is why a and e are kept out of the integral in (8) and in the following averages.

$$\left\langle\frac{dL^2}{dt}\right\rangle=\mu\langle\dot a\rangle(1-e^2)-2\mu ae\langle\dot e\rangle=0. \tag{12}$$

The osculating total energy $\mathcal{E}\doteq-\mu/2a$ decreases according to

$$\left\langle\frac{d\mathcal{E}}{dt}\right\rangle=\frac{\mu}{2a^2}\langle\dot a\rangle=\frac{e\dot\mu}{a(1-e)}. \tag{13}$$

Moreover, the osculating Keplerian period

$$P^{\rm Kep}\doteq 2\pi\sqrt{\frac{a^3}{\mu}}, \tag{14}$$

which, by definition, yields the time elapsed between two consecutive perihelion crossings in absence of perturbation, *i.e.* it is the time required to describe a fixed osculating Keplerian ellipse, decreases according to

$$\left\langle\frac{dP^{\rm Kep}}{dt}\right\rangle=\frac{3}{2}P^{\rm Kep}\frac{\langle\dot a\rangle}{a}=\frac{6\pi e\dot\mu}{(1-e)}\left(\frac{a}{\mu}\right)^{3/2}. \tag{15}$$

As I will show, also such a result is not in contrast with the genuine orbital evolution.

2.2. The Pericenter, the Node and the Inclination

The Gauss equation for the variation of the argument of pericentre ω is [19,20]

$$\frac{d\omega}{dt}=\frac{\sqrt{1-e^2}}{nae}\left[-A_r\cos f+A_\tau\left(1+\frac{r}{p}\right)\sin f\right]-\cos I\frac{d\Omega}{dt}, \tag{16}$$

where I and Ω are the inclination and the longitude of the ascending node, respectively, which fix the orientation of the osculating ellipse in the inertial space. Since $d\Omega/dt$ and dI/dt depend on the normal component A_ν of the disturbing acceleration, which is absent in the present case, and $A=A_r$, I have

$$\left\langle\frac{d\omega}{dt}\right\rangle=\frac{\sqrt{1-e^2}}{2\pi e}\left(\frac{\dot\mu}{\mu}\right)\int_0^{2\pi}\frac{(E-e\sin E)(\cos E-e)}{(1-e\cos E)^2}dE=0. \tag{17}$$

The osculating ellipse does not change its orientation in the orbital plane, which, incidentally, remains fixed in the inertial space because $A_\nu=0$ and, thus, $d\Omega/dt=dI/dt=0$.

2.3. The Mean Anomaly

The Gauss equation for the mean anomaly $\mathcal{M}$, defined as $\mathcal{M}\doteq n\left(t-t_p\right)$, [19,20] is

$$\frac{d\mathcal{M}}{dt}=n-\frac{2}{na}A_r\frac{r}{a}-\sqrt{1-e^2}\left(\frac{d\omega}{dt}+\cos I\frac{d\Omega}{dt}\right). \tag{18}$$

It turns out that, since

$$-\frac{2}{na}A_r\frac{r}{a}dt=\frac{2\dot\mu}{(na)^3}(E-e\sin E)dE, \tag{19}$$

then

$$\langle\frac{d\mathcal{M}}{dt}\rangle = n + 2\pi\left(\frac{\dot{\mu}}{\mu}\right); \quad (20)$$

the mean anomaly changes uniformly in time at a slower rate with respect to the unperturbed Keplerian case for $\dot{\mu} < 0$.

2.4. Numerical Integration of the Equations of Motion and Explanation of the Seeming Contradiction with the Analytical Results

At first sight, the results obtained here may be rather confusing: if the gravitational attraction of the Sun reduces in time because of its mass loss the orbits of the planets should expand (see the trajectory plotted in **Figure 1**, numerically integrated with MATHEMATICA), while I obtained that the semimajor axis and the eccentricity undergo secular decrements. Moreover, I found that the Keplerian period P^{Kep} decreases, while one would expect that the orbital period increases.

In fact, there is no contradiction, and my analytical results do yield us realistic information on the true evolution of the planetary motion. Indeed, a, e and P^{Kep} refer to the osculating Keplerian ellipses which, at any instant, approximate the true trajectory; it, instead, is not an ellipse, not being bounded. Let us start at t_p from the osculating pericentre of the Keplerian ellipse corresponding to chosen initial conditions: let us use a heliocentric frame with the x axis oriented along the osculating pericentre. After a true revolution, *i.e.* when the true radius vector of the planet has swept an angular interval of 2π, the planet finds itself again on the x axis, but at a larger distance from the starting point because of the orbit expansion induced by the Sun's mass loss. It is not difficult to understand that the osculating Keplerian ellipse approximating the trajectory at this perihelion passage is oriented as before because there is no variation of the (osculating) argument of pericentre, but has smaller semimajor axis and eccentricity. And so on, revolution after revolution, until the perturbation theory can be applied, *i.e.* until $\dot{\mu}/\mu\ (t - t_p) \ll 1$. In **Figure 1** the situation described so far is qualitatively illustrated. Just for illustrative purposes I enhanced the overall effect by assuming $\dot{\mu}/\mu \approx 10^{-2}\ \text{yr}^{-1}$ for the Sun; the initial conditions for the planet correspond to an unperturbed Keplerian ellipse with $a = 1$ AU, $e = 0.8$ with the present-day value of the Sun's mass in one of its foci. It is apparent that the initial osculating red dashed ellipse has larger a and e with respect to the second osculating blue dash-dotted ellipse. Note also that the true orbital period, intended as the time elapsed between two consecutive crossings of the perihelion, is larger than the unperturbed Keplerian one of the initial red dashed osculating ellipse, which would amount to 1 yr for the Earth: indeed, after 2 yr the planet has not yet reached the perihelion for its second passage.

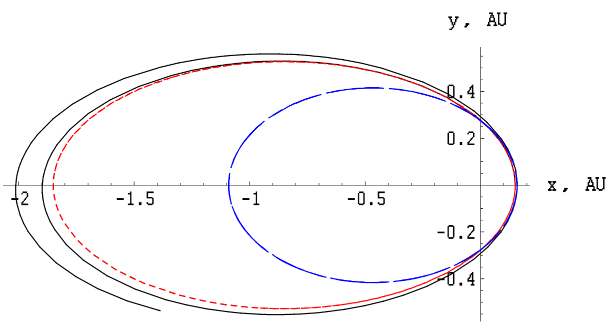

Figure 1. Black continuous line: true trajectory obtained by numerically integrating with MATHEMATICA the perturbed equations of motion in Cartesian coordinates over 2 yr; the disturbing acceleration (1) has been adopted. The planet starts from the perihelion on the x axis. Just for illustrative purposes, a mass loss rate of the order of $10^{-2}\ \text{yr}^{-1}$ has been adopted for the Sun; for the planet initial conditions corresponding to a = 1 AU, e = 0.8 have been chosen. Red dashed line: unperturbed Keplerian ellipse at $t = t_0 = t_p$. Blue dash-dotted line: osculating Keplerian ellipse after the first perihelion passage. As can be noted, its semimajor axis and eccentricity are clearly smaller than those of the initial unperturbed ellipse. Note also that after 2 yr the planet has not yet reached the perihelion as it would have done in absence of mass loss, *i.e.* the true orbital period is longer than the Keplerian one of the osculating red ellipse.

Now, if I compute the radial change $\Delta r(E)$ in the osculating radius vector as a function of the eccentric anomaly E I can gain useful insights concerning how much the true path has expanded after two consecutive perihelion passages. From the Keplerian expression of the Sun-planet distance in (4) one gets the radial component of the orbital perturbation expressed in terms of the eccentric anomaly E

$$\Delta r(E) = (1 - e\cos E)\Delta a - a\cos E\,\Delta e + ae\sin E\,\Delta E; \quad (21)$$

It agrees with the results obtained in [21]. Since

$$\begin{cases} \Delta a = -\frac{2ae}{n}\left(\frac{\dot{\mu}}{\mu}\right)\left(\frac{\sin E - E\cos E}{1 - e\cos E}\right), \\ \Delta e = -\frac{(1-e^2)}{n}\left(\frac{\dot{\mu}}{\mu}\right)\left(\frac{\sin E - E\cos E}{1 - e\cos E}\right), \\ \Delta E = \frac{\Delta\mathcal{M} + \sin E\Delta e}{1 - e\cos E} = \frac{1}{n}\left(\frac{\dot{\mu}}{\mu}\right)[\mathcal{A}(E) + \mathcal{B}(E) + \mathcal{C}(E)], \end{cases} \quad (22)$$

with

$$\begin{cases} \mathcal{A}(E) = \frac{E^2 + 2e(\cos E - 1)}{1 - e\cos E}, \\ \mathcal{B}(E) = \left(\frac{1-e^2}{e}\right)\left[\frac{1 + e - (1+e)\cos E - E\sin E}{(1 - e\cos E)^2}\right] \\ \mathcal{C}(E) = -\frac{(1-e^2)\sin E(\sin E - e\cos E)}{(1 - e\cos E)^2}, \end{cases} \quad (23)$$

It follows

$$\Delta r(E) = \frac{a}{n}\left(\frac{\dot{\mu}}{\mu}\right)[\mathcal{D}(E) + \mathcal{F}(E)], \quad (24)$$

with

$$\mathcal{D}(E) = e\left\{\begin{array}{c} -2(\sin E - E\cos E) + \\ +\frac{\sin E\left[E^2+2e(\cos E-1)\right]}{1-e\cos E} - \\ -\frac{(1-e^2)\sin^2 E(\sin E - e\cos E)}{(1-e\cos E)^2} \end{array}\right\}, \quad (25)$$

and

$$\mathcal{F}(E) = \left(\frac{1-e^2}{1-e\cos E}\right)\left\{\begin{array}{c} \cos E(\sin E - E\cos E) + \\ +\sin E\left[\frac{1+e-(1+e)\cos E - E\sin E}{1-e\cos E}\right] \end{array}\right\}. \quad (26)$$

It turns out from (25) and (26) that, for $E > 0$, $\Delta r(E)$ never vanishes; after one orbital revolution, *i.e.* after that an angular interval of 2π has been swept by the (osclating) radius vector, a net increase of the radial (osculating) distance occurs according to[5]

$$\Delta r(2\pi) - \Delta r(0) = \Delta r(2\pi) = -\frac{2\pi}{n}\left(\frac{\dot{\mu}}{\mu}\right)a(1-e) \quad (27)$$

This analytical result is qualitatively confirmed by the difference[6] $\Delta r(t)$ between the radial distances obtained from the solutions of two numerical integrations of the equations of motion over 3 yr with and without $\dot{\mu}/\mu$; the initial conditions are the same. For illustrative purposes I used $a = 1$ AU, $e = 0.01$, $\dot{\mu}/\mu = -0.1$ yr^{-1}. The result is depicted in **Figure 2**.

Note also that (25) and (26) tell us that the shift at the aphelion is

$$\Delta r(\pi) = \frac{1}{2}\left(\frac{1+e}{1-e}\right)\Delta r(2\pi), \quad (28)$$

in agreement with **Figure 1** where it is 4.5 times larger than the shift at the perihelion.

Since **Figure 1** tells us that the orbital period gets larger than the Keplerian one, it means that the true orbit must somehow remain behind with respect to the Keplerian one. Thus, a negative perturbation $\Delta\tau$ in the transverse direction must occur as well; see **Figure 3**.

Let us now analytically compute it. According to [21], it can be used

$$\Delta\tau = \frac{a\sin E}{\sqrt{1-e^2}} + a\sqrt{1-e^2}\Delta E + r(\Delta\omega + \cos I\,\Delta\Omega). \quad (29)$$

By recalling that, in the present case, $\Delta\Omega = 0$ and using

$$\Delta\omega = -\frac{\sqrt{1-e^2}}{ne}\left(\frac{\dot{\mu}}{\mu}\right)\left[\frac{1+e-(1+e)\cos E - E\sin E}{1-e\cos E}\right], \quad (30)$$

it is possible to obtain from (22) and (30)

$$\Delta\tau(E) = \frac{a}{n}\left(\frac{\dot{\mu}}{\mu}\right)\frac{\sqrt{1-e^2}}{1-e\cos E}\left[\mathcal{G}(E) + \mathcal{H}(E) + \mathcal{I}(E) + \mathcal{J}(E) + \mathcal{K}(E)\right], \quad (31)$$

with

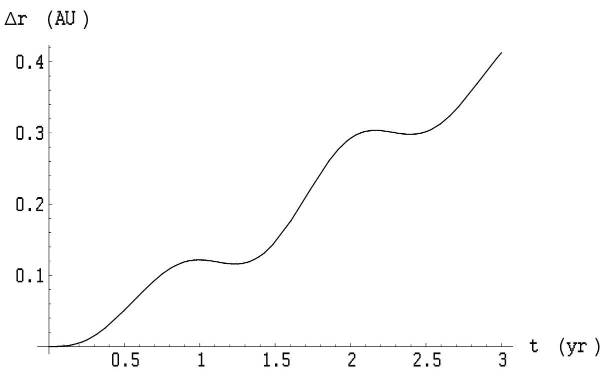

Figure 2. Difference $\Delta r(t)$ between the radial distances obtained from the solutions of two numerical integrations with MATHEMATICA of the equations of motion over 3 yr with and without $\dot{\mu}/\mu$; the initial conditions are the same. Just for illustrative purposes a mass loss rate of the order of $\dot{\mu}/\mu = -0.1$ yr^{-1} has been adopted for the Sun; for the planet initial conditions corresponding to $a = 1$ AU, $e = 0.01$ have been chosen. The cumulative increase of the Sun-planet distance induced by the mass loss is apparent.

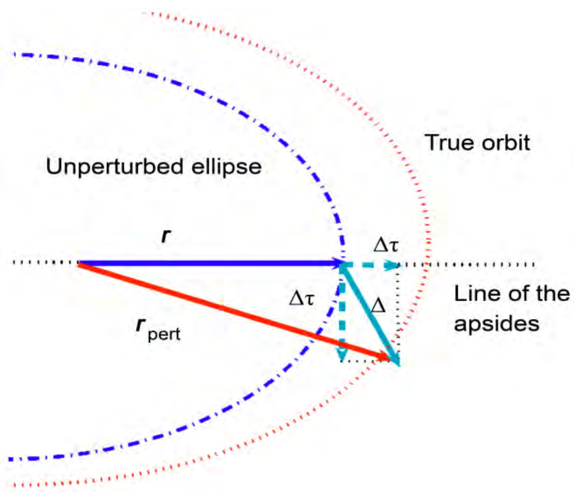

Figure 3. Radial and transverse perturbations Δr and $\Delta\tau$ of the Keplerian radius vector (in blue); the presence of the transverse perturbation $\Delta\tau$ makes the real orbit (in red) lagging behind the Keplerian one.

$$\left\{\begin{array}{c} \mathcal{G}(E) = \sin E\,(E\cos E - \sin E), \\ \mathcal{H}(E) = \frac{(1-e\cos E)}{e}\left[(1+e)(\cos E - 1) + E\sin E\right], \\ \mathcal{I}(E) = E^2 + 2e(\cos E - 1), \\ \mathcal{J}(E) = \sin E\left[\frac{(1-e^2)(e\cos E - \sin E)}{1-e\cos E}\right], \\ \mathcal{K}(E) = \left(\frac{1-e^2}{e}\right)\left[\frac{(1+e)(1-e\cos E) - E\sin E}{1-e\cos E}\right]. \end{array}\right. \quad (32)$$

It turns out from (31) and (32) that, for $E > 0$, $\Delta\tau(E)$ never vanishes; at the time of perihelion passage

$$\Delta\tau(2\pi) - \Delta\tau(0) = \frac{4\pi^2}{n}a\left(\frac{\dot{\mu}}{\mu}\right)\sqrt{\frac{1+e}{1-e}} < 0. \quad (33)$$

[5] According to (25) and (26), $\Delta r(0) = 0$.

[6] Strictly speaking, Δr and the quantity plotted in **Figure 2** are different objects, but, as the following discussion will clarify, I can assume that, in practice, they are the same.

This means that when the Keplerian path has reached the perihelion, the perturbed orbit is still behind it. Such features are qualitatively confirmed by **Figure 1**. From a vectorial point of view, the radial and transverse perturbations to the Keplerian radius vector $\boldsymbol{r}$ yield a correction

$$\Delta = \Delta r\hat{\boldsymbol{r}} + \Delta\tau\hat{\boldsymbol{\tau}}, \quad (34)$$

so that

$$\boldsymbol{r}_{\rm pert} = \boldsymbol{r} + \Delta. \quad (35)$$

The length of Δ is

$$\Delta(E) = \sqrt{\Delta r(E)^2 + \Delta\tau(E)^2}. \quad (36)$$

Eqs.27 and **31** tell us that at perihelion it amounts to

$$\Delta(2\pi) = \Delta r(2\pi)\sqrt{1 + 4\pi^2\frac{(1+e)}{(1-e)^3}}. \quad (37)$$

The angle ξ between Δ and $\boldsymbol{r}$ is given by

$$\tan\xi(E) = \frac{\Delta\tau(E)}{\Delta r(E)}; \quad (38)$$

at perihelion it is

$$\tan\xi(2\pi) = -2\pi\frac{\sqrt{1+e}}{(1-e)^{3/2}}, \quad (39)$$

i.e. ξ is close to 90 deg; for the Earth it is 81.1 deg. Thus, the difference δ between the lengths of the perturbed radius vector $r_{\rm pert}$ and the Keplerian one r at a given instant amounts to about

$$\delta \approx \Delta\cos\xi; \quad (40)$$

in fact, this is precisely the quantity determined over 3 yr by the numerical integration of **Figure 2**. At the perihelion I have

$$\delta = \Delta r(2\pi)\sqrt{1 + 4\pi^2\frac{(1+e)}{(1-e)^3}}\cos\xi. \quad (41)$$

Since for the Earth

$$\sqrt{1 + 4\pi^2\frac{(1+e)}{(1-e)^3}}\cos\xi = 1.0037, \quad (42)$$

it holds

$$\delta \approx \Delta r(2\pi). \quad (43)$$

This explains why **Figure 2** gives us just Δr.

Concerning the observationally determined increase of the Astronomical Unit, more recent estimates from processing of huge planetary data sets by Pitjeva point towards a rate of the order of 10^{-2} m yr^{-1} [22,23]. It may be noted that my result for the secular variation of the terrestrial radial position on the line of the apsides would agree with such a figure by either assuming a mass loss by the Sun of just -9×10^{-14} yr^{-1} or a decrease of the Newtonian gravitational constant. $\dot{G}/G \approx -1\times10^{-13}$ yr^{-1}. Such a value for the temporal variation of G is in agreement with recent upper limits from Lunar Laser Ranging [24]. $\dot{G}/G = (2\pm7)\times10^{-13}$ yr^{-1}. This possibility is envisaged in [25] whose authors use $\dot{a}/a = -\dot{G}/G$ by speaking about a small radial drift of $-(6\pm13)\times10^{-2}$ m yr^{-1} in an orbit at 1 AU.

3. THE EVOLUTION OF THE EARTH-SUN SYSTEM

In this Section I will not consider other effects which may affect the final evolution of the Sun-Earth system like the tidal interaction between the Earth and the tidal bulges of the giant solar photosphere, and the drag friction in the motion through the low chromosphere [1]. For the Earth, by assuming the values a = 1.00000011 AU, e = 0.01671022 at the epoch J2000 (JD 2451545.0) with respect to the mean ecliptic and equinox of J2000 and $\dot{\mu}/\mu = -9\times10^{-14}$ yr^{-1}, (24) yields

$$\Delta r(2\pi) = 1.3\times10^{-2}\,{\rm m}. \quad (44)$$

This means that at every revolution the position of the Earth is shifted along the true line of the apsides (which coincides with the osculating one because of the absence of perihelion precession) by 1.3 cm. This result is confirmed by our numerical integrations and the discussion of Section 2; indeed, it can be directly inferred from **Figure 2** by multiplying the value of Δr at t = 1 yr by 9×10^{-13}. By assuming that the Sun will continue to lose mass at the same rate for other 7.58 Gyr, when it will reach the tip of the RGB in the HR diagram [1], the Earth will be only 6.7×10^{-4} AU more distant than now from the Sun at the perihelion. Note that the value 9×10^{-14} yr^{-1} is an upper bound on the magnitude of the Sun's mass loss rate; it might be also smaller [1] like, e.g., 7×10^{-14} yr^{-1} which would yield an increment of 5.5×10^{-4} AU. Concerning the effect of the other planets during such a long-lasting phase, a detailed calculation of their impact is beyond the scope of the present paper. By the way, I wish to note that the dependence of $\Delta r(2\pi)$ on the eccentricity is rather weak; indeed, it turns out that, according to (24), the shift of the perihelion position after one orbit varies in the range $1.1-1.3$ cm for $0\le e\le 0.1$. Should the interaction with the other planets increase notably the eccentricity, the expansion of the orbit would be even smaller; indeed, for higher values of e like, e.g., e = 0.8 it reduces to about 3 mm. By the way, it seems that the eccentricity of the Earth can get as large as just 0.02 – 0.1 [26-28] over timescales of $\approx$ 5 Gyr due to the N-body interactions with the other planets. In **Table 1**, I quote the expansion of the orbits of the other planets of the solar system as well.

It is interesting to note that Mercury[7] and likely Venus are fated at the beginning of the RGB; indeed, from **Figure 2** of [1] it turns out that the Sun's photosphere will reach about 0.5-0.6 AU, while the first two planets of the solar system will basically remain at 0.38 AU and 0.72 AU, respectively, being the expansion of their orbits negligible according to **Table 1**.

After entering the RG phase things will dramatically change because in only $\approx$ 1 Myr the Sun will reach the tip of the RGB phase loosing mass at a rate of about -2×10^{-7} yr^{-1} and expanding up to 1.20 AU [1]. In the meantime, according to our perturbative calculations, the perihelion distance of the Earth will increase by 0.25 AU. I have used as initial conditions for μ, a and e their final values of the preceding phase 7.58 Gyr-long. In **Table 2**, I quote the expansion experienced by the other planets as well; it is interesting to note that the outer planets of the solar system will undergo a considerable increase in the size of their orbits, up to 7.5 AU for Neptune, contrary to the conclusions of the numerical computations in [29] who included the mass loss as well. I have used as initial conditions the final ones of the previous MS phase. Such an assumption seems reasonable for the giant planets since their eccentricities should be left substantially unchanged by the mutual N-body interactions during the next 5 Gyr and more [26-28]; concerning the Earth, should its eccentricity become as large as 0.1 due to the N-body perturbations [26-28], after about 1 Myr its radial shift would be smaller amounting to 0.22 AU. Mutual N-body interactions have not been considered. Thus, orbital hardly preventing our planet to escape from engulfment in the expanding solar photosphere. Concerning the result for the Earth, it must be pointed out that it remains substantially unchanged if I repeat the calculation by assuming a circularized orbit during the entire RGB phase. Indeed, it is possible to show that by adopting as initial values of a and μ the final ones of the previous phase I get that after $\approx$ 1.5 Myr Δr has changed by 0.30 AU. Note that my results are in contrast with those in [1] whose authors obtain more comfortable values for the expansion of the Earth's orbit, assumed circular and not influenced by tidal and frictional effects, ranging from 1.37 AU ($|\dot{\mu}/\mu| = 7\times10^{-14}$ yr^{-1}) to 1.50 AU ($|\dot{\mu}/\mu| = 8\times10^{-14}$ yr^{-1}) and 1.63 AU ($|\dot{\mu}/\mu| = 9\times10^{-14}$ yr^{-1}). However, it must be noted that such a conclusion relies upon a perturbative treatment of (1) and by assuming that the mass loss rate is constant throughout the RGB until its tip; in fact, during such a Myr the term $(\dot{\mu}/\mu)\,\Delta t$ would get as large as 2×10^{-1}. In fact, by inspecting **Figure 4** of [1] it appears that in the last Myr of the RGB a moderate variation of $\dot{M}/M$ occurs giving rise to an acceleration of the order of $\ddot{M}/M \approx 10^{-13}$ yr^{-2}. Thus, a further quadratic term of the form

$$\left(\frac{\ddot{\mu}}{\mu}\right)\frac{(t-t_0)^2}{2} \tag{45}$$

should be accounted for in the expansion of (1). A perturbative treatment yields adequate results for such a phase 1 Myr long since over this time span (45) would amount to $\approx 5\times10^{-2}$. However, there is no need for detailed calculations: indeed, it can be easily noted that the radial shift after one revolution is

$$\Delta r(2\pi) \propto \left(\frac{\ddot{\mu}}{\mu}\right)\frac{a^4}{\mu}. \tag{46}$$

After about 1 Myr (46) yields a variation of the order of 10^{-9} AU, which is clearly negligible.

Table 1. Expansion of the orbits, in AU, of the eight planets of the solar system in the next 7.58 Gyr for $\dot{M}/M = -9\times10^{-14}$ yr^{-1}. I have neglected mutual N-body interactions.

Planet	Δr(AU)
Mercury	2×10^{-4}
Venus	5×10^{-4}
Earth	7×10^{-4}
Mars	9×10^{-4}
Jupiter	3×10^{-3}
Saturn	6×10^{-3}
Uranus	1×10^{-2}
Neptune	2×10^{-2}

Table 2. Expansion of the orbits, in AU, of the eight planets of the solar system in the first 1 Myr of the RGB for $\dot{M}/M = -2\times10^{-7}$ yr^{-1}. I have neglected mutual N-body interactions and other phenomena like the effects of tidal bulges and chromospheric drag for the inner planets.

Planet	Δr(AU)
Mercury	7×10^{-2}
Venus	1.8×10^{-1}
Earth	2.5×10^{-1}
Mars	3.4×10^{-1}
Jupiter	1.24
Saturn	2.25
Uranus	4.57
Neptune	7.46

[7] It might also escape from the solar system or collide with Venus over 3.5 Gyr from now [26-28].

4. CONCLUSIONS

I started in the framework of the two-body Newtonian dynamics by using a radial perturbing acceleration linear in time and straightforwardly treated it with the standard Gaussian scheme. I found that the osculating semimajor axis a, the eccentricity e and the mean anomaly $\mathcal{M}$ secularly decrease while the argument of pericentre ω remains unchanged; also the longitude of the ascending node Ω and the inclination I are not affected. The radial distance from the central body, taken on the fixed line of the apsides, experiences a secular increase Δr. For the Earth, such an effect amounts to about 1.3 cm yr^{-1}. By numerically integrating the equations of motion in Cartesian coordinates I found that the real orbital path expands after every revolution, the line of the apsides does not change and the apsidal period is larger than the unperturbed Keplerian one. I have also clarified that such results are not in contrast with those analytically obtained for the Keplerian orbital elements which, indeed, refer to the osculating ellipses approximating the true trajectory at each instant. I applied our results to the evolution of the Sun-Earth system in the distant future with particular care to the phase in which the Sun, moved to the RGB of the HR, will expand up to 1.20 AU in order to see if the Earth will avoid to be engulfed by the expanded solar photosphere. My answer is negative because, even considering a small acceleration in the process of the solar mass-loss, it turns out that at the end of such a dramatic phase lasting about 1 Myr the perihelion distance will have increased by only $\Delta r \approx$ 0.22-0.25 AU, contrary to the estimates in [1] whose authors argue an increment of about 0.37-0.63 AU. In the case of a circular orbit, the osculating semimajor axis remains unchanged, as confirmed by a numerical integration of the equations of motion which also shows that the true orbital period increases and is larger than the unperturbed Keplerian one which remains fixed. Concerning the other planets, while Mercury will be completely engulfed already at the end of the MS, Venus might survive; however, it should not escape from its fate in the initial phase of the RGB in which the outer planets will experience increases in the size of their orbits of the order of 1.2- 7.5 AU.

As a suggestion to other researchers, it would be very important to complement my analytical two-body calculation by performing simultaneous long-term numerical integrations of the equations of motion of all the major bodies of the solar system by including a mass-loss term in the dynamical force models as well to see if the N-body interactions in presence of such an effect may substantially change the picture outlined here. It would be important especially in the RGB phase in which the inner regions of the solar system should dramatically change.

5. ACKNOWLEDGEMENTS

I thank Prof. K.V. Kholshevnikov, St. Petersburg State University for useful comments and references.

REFERENCES

[1] Schröder, K.P. and Smith, R.C. (2008) Distant future of the Sun and Earth revisited. *Monthly Notices of the Royal Astronomy Society*, **386(1)**, 155-163.

[2] Krasinsky, G.A. and Brumberg, V.A. (2004) Secular increase of astronomical unit from analysis of the major planet motions, and its interpretation. *Celestial Mechanics and Dynamical Astronomy*, **90(3-4)**, 267-288.

[3] Standish, E.M. (2005) The astronomical unit now. *Transits of Venus: New Views of the Solar System and Galaxy. Proceedings of the IAU Colloquium* 196, Kurtz, D.W., Ed., Cambridge University Press, Cambridge, 2004, 163-179.

[4] Noerdlinger, P.D. (2008) Solar mass loss, the astronomical unit, and the scale of the solar system. http://arxiv.org/abs/0801.3807

[5] Klioner, S.A. (2008) Relativistic scaling of astronomical quantities and the system of astronomical units. *Astronomy and Astrophysics*, **478**, 951-958.

[6] Jin, W., Imants, P. and Perryman, M. (2008) A giant step: From milli- to micro-arcsecond astrometry. *Proceedings of the IAU Symposium* 248, Cambridge University Press, Cambridge, 2007.

[7] Oskay, W.H., Diddams, S.A., Donley, E.A., Fortier, T. M., Heavner, T.P., Hollberg, L., Itano, W.M., Jefferts, S.R., Delaney, M.J., Kim, K., Levi, F., Parker, T.E. and Bergquist, J.C. (2006) Single-atom optical clock with high accuracy. *Physical Review Letters*, **97(2)**, 1-4.

[8] Rubincam, D.P. (1982) On the secular decrease in the semimajor axis of Lageos's orbit. *Celestial Mechanics and Dynamical Astronomy*, **26(4)**, 361-382.

[9] Williams, J.G. and Boggs, D.H. (2008) DE421 lunar orbit, physical librations, and surface coordinates. 16*th International Workshop on Laser Ranging*, Poznań, 13-17 October 2008.

[10] Strömgren, E. (1903) Über die bedeutung kleiner massenänderungen für die newtonsche centralbewegung. *Astronomische Nachrichten*, **163**, 129-136.

[11] Jeans, J.H. (1924) Cosmogonic problems associated with a secular decrease of mass. *Monthly Notices of the Royal Astronomy Society*, **85**, 2-11.

[12] Jeans, J.H. (1961) Astronomy and cosmogony. Dover, New York.

[13] Armellini, G. (1935) The variation of the eccentricity in a binary system of decrasing mass. *The Observatory*, **58**, 158-159.

[14] Hadjidemetriou, J.D. (1963) Two-body problem with variable mass: A new approach. *Icarus*, **2**, 440-451.

[15] Hadjidemetriou, J.D. (1966) Analytic solutions of the two-body problem with variable mass. *Icarus*, **5**, 34-46.

[16] Kholshevnikov, K.V. and Fracassini, M. (1968) Le problème des deux corps avec G variable selon l'hypothèse de dirac. *Conferenze dell' Osservatorio Astronomico di Milano-Merate*, **1(9)**, 5-50.

[17] Deprit, A. (1983) The secular accelerations in Gylden's problem. *Celestial Mechanics and Dynamical Astronomy*, **31(1)**, 1-22.

[18] Kevorkian, J. and Cole, J.D. (1966) Multiple scale and singular perturbation methods. Springer, New York and Berlin.

[19] Bertotti, B. Farinella, P. and Vokrouhlický, D. (2003) Phyiscs of the solar system. Kluwer, Dordrecht.

[20] Roy, A.E. (2005) Orbital motion. 4th Edition, Institute of Physics, Bristol.

[21] Casotto, S. (1993) Position and velocity perturbations in the orbital frame in terms of classical element perturbations. *Celestial Mechanics and Dynamical Astronomy*, **55**, 209-221.

[22] Pitjeva, E.V. (2005) The astronomical unit now. *Transits*

of Venus: New Views of the Solar System and Galaxy. Proceedings of the IAU Colloquium 196, 2004, Kurtz, D. W., Ed., Cambridge University Press, Cambridge, 177.

[23] Pitjeva, E.V. (2008) Personal communication to P. Noerdlinger.

[24] Müller, J. and Biskupek, L. (2007) Variations of the gravitational constant from lunar laser ranging data. *Classical and Quantum Gravity*, **24**, 4533-4538.

[25] Williams, J.G., Turyshev, S.G. and Boggs, D.H. (2007) Williams, Turyshev, and Boggs reply. *Physical Review Letters*, **98(55)**.

[26] Laskar, J. (1994) Large-scale chaos in the solar system. *Astronomy and Astrophysics*, **287**, L9-L12.

[27] Ito, K. and Tanikawa, K. (2002) Long-term integrations and stability of planetary orbits in our solar system. *Monthly Notices of the Royal Astronomy Society*, **336**, 483-500.

[28] Laskar, J. (2008) Chaotic diffusion in the solar system. *Icarus*, **196**, 1-15.

[29] Duncan, M.J. and Lissauer, J.J. (1998) The effects of post-main-sequence solar mass loss on the stability of our planetary system. *Icarus*, **134**, 303-310.

Vol.2, No.4, 338-356 (2010)
doi:10.4236/ns.2010.24042

Application of analytic functions to the global solvabilty of the Cauchy problem for equations of Navier-Stokes

Asset Durmagambetov

Ministry of Education and Science of the Republic of Kazakhstan, Buketov Karaganda State University, Institute of Applied Mathematics, Buketov Karaganda, Kazakhstan; asset.durmagambetov@gmail.com

Received 14 December 2009; revised 29 January 2010; accepted 3 February 2010.

ABSTRACT

The interrelation between analytic functions and real-valued functions is formulated in the work. It is shown such an interrelation realizes nonlinear representations for real-valued functions that allow to develop new methods of estimation for them. These methods of estimation are approved by solving the Cauchy problem for equations of viscous incompressible liquid.

Keywords: Shrödinger; Cauchy Problem; Navier-Stokes'; Inverse; Analytic Functions; Scattering Theory

1. INTRODUCTION

The work of L. Fadeyev dedicated to the many- dimensional inverse problem of scattering theory inspired the author of this article to conduct this research. The first results obtained by the author are described in the works [1-3]. This problem includes a number of subproblems which appear to be very interesting and complicated. These subproblems are thoroughly considered in the works of the following scientists: R. Newton [4], R. Faddeyev [5], R. Novikov and G. Khenkin [6], A. Ramm [3] and others. The latest advances in the theory of SIPM (Scattering Inverse Problem Method) were a great stimulus for the author as well as other researchers. Another important stimulus was the work of M. Lavrentyev on the application of analytic functions to Hydrodynamics. Only one-dimensional equations were integrated by SIPM. The application of analytic functions to Hydrodynamics is restricted only by bidimensional problems. The further progress in applying SIPM to the solution of nonlinear equations in R 3 was hampered by the poor development of the three-dimensional inverse problem of scattering in comparison with the progress achieved in the work on the one-dimensional inverse problem of scattering and also by the difficulties the researchers encountered building up the corresponding Lax' pairs. It is easy to come to a conclusion that all the success in developing the theory of SIPM is connected with analytic functions, *i.e.*, solutions to Schrodinger's equation. Therefore we consider Schrodinger's equation as an interrelation between real-valued functions and analytic functions, where real-valued functions are potentials in Schrodinger's equation and analytic functions are the corresponding eigenfunctions of the continuous spectrum of Schrodinger's operator. The basic aim of the paper is to study this interrelation and its application for obtaining new estimates to the solutions of the problem for Navier-Stokes' equations. We concentrated on formulating the conditions of momentum and energy conservation laws in terms of potential instead of formulating them in terms of wave functions. As a result of our study, we obtained non-trivial nonlinear relationships of potential. The effectiveness and novelty of the obtained results are displayed when solving the notoriously difficult Chauchy problem for Navier-Stokes' equations of viscous incompressible fluid.

2. BASIC NOTIONS AND SUBSIDIARY STATEMENT

Let us consider Shrödingerse equation

$$-\Delta_x\varphi + q\varphi = |k|^2\varphi \tag{1}$$

where q is a bounded fast-decreasing function,

$$k \in R^3, \qquad |k|^2 = \sum_{j=1}^{3} k_j^2.$$

Definition 1. *Rolnik's Class* $\boldsymbol{R}$ *is a set of measurable functions* q,

$$||q||_{\mathbf{R}} = \int_{R^6} \frac{q(x)q(y)}{|x-y|^2}\,dxdy < \infty.$$

It is considered to be a general definition ([7]).

Theorem 1. *Suppose that* $q \in \boldsymbol{R}$*; then a exists a unique solution of* **Eq.1**, *with asymptotic form* (2) *as* $|x| \to \infty$.

$$\varphi_{\pm}(k,x) = e^{i(k,x)} + + \frac{e^{\pm i|k||x|}}{|x|} A_{\pm}(k,k') + 0\left(\frac{1}{|x|}\right) \quad (2)$$

where

$$x \in R^3, k' = |k|\frac{x}{|x|}, (k,x) = \sum_{j=1}^{3} k_j x_j,$$

$$A_{\pm}(k,\lambda) = \frac{1}{(2\pi)^3}\int_{R^3} q(x)\varphi_{\pm}(k,x)e^{-i(\lambda,x)}dx.$$

The proof of this theorem is in [7].

Consider the operators $H = -\Delta_x + q(x)$, $H_0 = -\Delta_x$ defined in the dense set $W_2^2(R^3)$ in the space $L_2(R^3)$. The operator H is called Schrodinger's operator. Povzner [8] proved that the functions $\varphi \pm (k,x)$ form a complete orthonormal system of eigenfunctions of the continuous spectrum of the operator H, and the operator fills up the whole positive semi-axis. Besides the continuous spectrum the operator H can have a finite number N of negative eigenvalues Denote these eigenvalues by $-E_j^2$ and conforming normalized egenfunctions by

$$\psi_j(x, -E_j^2)(j = \overline{1,N}),$$

where $\psi_j(x, -E_j^2) \in L_2(R^3)$.

Theorem 2 (*About Completeness*). *For any vector-function $f \in L_2(R^3)$ and eigenfunctions of the operator H, we have Parseval's identity*

$$\|f\|_{L_2}^2 = \sum_{j=1}^{N} |f_j|^2 + \int_{R^3} |\bar{f}(s)|^2 ds,$$

where f_j and $\bar{f}$ are Fourier coefficients in case of discrete of and continuous spectrum respectively.

The proof of this theorem is in [8].

Theorem 3 (*Birman - Schwinger's Estimate*). *Suppose $q \in R$. Then the number of discrete eigenvalues of Shrödinger operator satisfies the estimate*

$$N(q) \le \frac{1}{(4\pi)^2}\int_{R^3}\int_{R^3} \frac{q(x)q(y)}{|x-y|^2}dxdy.$$

The proof of this theorem is in [9].

Definition 2. [7]

$$T\pm(k,k') = \frac{1}{(2\pi)^3}\int_{R^3} \varphi_{\pm}(x,k')e^{\mp i(k,x)}q(x)dx.$$

$T\pm(.,.)$ is called T-matrix. Let us take into consideration a series for $T_{\pm}$:

$$T_{\pm}(k,k') = \sum_{n=0}^{\infty} T_{n_{\pm}}(k,k'),$$

where

$$T_{0_{\pm}}(k,k') = \frac{1}{(2\pi)^3}\int_{R^3} e^{i(k'\mp k,x)}q(x)dx,$$

$$T_{n_{\pm}}(k,k') = \frac{1}{(2\pi)^3}\frac{(-1)^n}{(4\pi)^n}\int_{R^{3(n+1)}} e^{\mp i(k,x_0)} \times q(x_0)\frac{e^{\pm i|k'||x_0-x_1|}}{|x_0-x_1|}q(x_1)\dots q(x_{n-1}) \times \frac{e^{\pm i|k'||x_{n-1}-x_n|}}{|x_{n-1}-x_n|}q(x_n)e^{i(k',x_n)}dx_0\dots dx_n.$$

As well as in [7] we formulate.

Definition 3. *Series (4) is called Born's series.*

Theorem 4. *Let $q \in L_1(R^3) \cap \boldsymbol{R}$. If $PqP_{\boldsymbol{R}}^2 \le 4\pi$, then Born's series for $T(k,k')$ converges as $k,k' \in R^3$.*

The proof of the theorem is in [7].

Definition 4. *Suppose $q \in R$; then the function $A(k,\lambda)$, denoted by the following equality*

$$A(k,l) = \frac{1}{(2\pi)^3}\int_{R^3} q(x) \varphi_{+}(k,x)e^{-i(\lambda,x)}dx,$$

is called scattering amplitude

Corollary 1. *Scattering amplitude $A(k,\lambda)$ is equal to T-matrix*

$$A(k,l) = T_{+}(l,k) = \frac{1}{(2\pi)^3}\int_{R^3} q(x)\varphi_{+}(k,x)e^{-i(\lambda,x)}dx.$$

The proof follows from definition 4.

It is a well-known fact [5] that the solutions $\varphi + (k,x)$ and $\varphi - (k,x)$ of **Eq.1** are linearly dependent

$$\varphi_{+} = S\varphi_{-} \quad (3)$$

where S is a scattering operator with the nucleus $S(k,\lambda)$ of the form

$$S(k,\lambda) = \int_{R^3} \varphi_{+}(k,x)\varphi_{+}^{*}(\lambda,x)dx.$$

Theorem 5. (*Conservation Law of Impulse and Energy*). *Assume that $q \in \boldsymbol{R}$, then*

$$SS^* = I, S^*S = I,$$

where I is anunit operator.

The proof is in [5].

Let us use the following definitions

$$\tilde{q}(k) = \int_{R^3} q(x)e^{i(k,x)}dx,$$

$$\tilde{q}(k-\lambda) = \int_{R^3} q(x)e^{i(k-\lambda,x)}dx,$$

$$\tilde{q}_{\text{mv}}(k) = \int_{R^3} \tilde{q}(k-\lambda))\delta(|k|^2 - |\lambda|^2)d\lambda,$$

$$A_{\mathrm{mv}}(k) = \int_{R^3} A(k,l))\delta(|k|^2 - |l|^2)dl,$$

$$\int f(k,l)de_k = \int_{R^3} f(k,l)\delta(|k|^2 - |l|^2)dk,$$

$$\int f(k,l)de_\lambda = \int_{R^3} f(k,l)\delta(k^2 - |l|^2)dl,$$

where $k, \lambda \in R^3$ and $e_k = \frac{k}{|k|}$, $e_\lambda = \frac{\lambda}{|\lambda|}$.

3. ESTIMATE OF AMPLITUDE MAXIMUM

Let us consider the problem of estimating the maximum of amplitude, *i.e.*, $\max_{k\in R^3}|A(k,k)|$. Let us estimate the n term of Born's series $|T_n(k,k)|$.

Lemma 1. $|T_n(k,k)|$ *satisfies the inequality*

$$|T_{n+1}(k,k)| \le \frac{1}{(2\pi)^3}\frac{1}{(4\pi)^{n+1}} \times \frac{\gamma^n}{(2\pi)^{2(n+1)}}\int_{R^3}\frac{|\tilde{q}(k)|^2}{|k|^2}dk,$$

$$\gamma = C\delta||q|| + 4\pi M\tilde{q}\delta, C\delta = 2\frac{\sqrt{\pi}}{\sqrt{\delta}},$$

where δ *-is a small value,* C *is a positive number,* $M\tilde{q} = \max_{k\in R^3}|\tilde{q}|$.

Theorem 6. *Suppose that* $\gamma < 16\pi^3$ *, then* $\max_{k\in R^3}|A(k,k)|$ *satisfies the following estimate*

$$\max_{k\in R^3}|A(k,k)| \le \frac{1}{(2\pi)^3}\frac{1}{16\pi^3 - \gamma}\int_{R^3}\frac{|\tilde{q}(k)|^2}{|k|^2}dk,$$

where $\gamma = C\delta||q|| + 4\pi M\tilde{q}\delta$, δ *is a small value,*

$C\delta = 2\sqrt{\frac{\pi}{\delta}}$, $M\delta = \max_{k\in R^3}|\tilde{q}|$.

4. REPRESENTATION OF FUNCTIONS BY ITS SPHERICAL AVERAGES

Let us consider the problem of defining a function by its spherical average. This problem emerged in the course of our calculation and we shall consider it hereinafter.

Let us consider the following integral equation

$$\int_{R^3}\tilde{q}(t)\delta(|t-k|^2 - |k|^2)dt = f(2k),$$

where $k, t \in R^3$, δ is Dirac's delta function,

$f \in W_2^2(R^3)$, $|k|^2 = \sum_{i=1}^3 k_i^2$, $(k,t) = \sum_{i=1}^3 k_i t_i$.

Let us formulate the basic result.

Theorem 7. *Suppose that* $f \in W_2^2(R^3)$, *then*

$$(2\pi)^2\tilde{q}(r,\xi,\eta) = -\frac{1}{r}\frac{\partial^2}{\partial r^2}\int_0^\pi\int_0^{2\pi}\Big(f\big(\frac{2r}{(e_k,e_s)},e_k\big) + f\big(\frac{2r}{(e_k,e_s)},-e_k\big)\Big)\frac{r^2}{(e_k,e_s)^2}\sin\theta\ d\theta\ d\varphi,$$

where

$$f\big(\frac{2r}{(e_k,e_s)},e_k\big) = \tilde{q}\big(\frac{2r}{(e_k,e_s)},e_k\big),$$
$$\sin\theta\ d\theta\ d\varphi = de_k,$$
$$\sin\xi\ d\xi d\eta = de_s, \qquad r = |t|.$$

Theorem 8. *Fourier transformation of the function q satisfies the following estimate*

$$|\tilde{q}|_{L_1} \le \frac{1}{4}\left|z\frac{\partial\tilde{q}_{mv}}{\partial z^2}\right|_{L_1} + 2\left|\frac{\partial\tilde{q}_{mv}}{\partial z^2}\right|_{L_1} + \left|\frac{\tilde{q}_{mv}}{z}\right|_{L_1},$$

5. CORRELATION OF AMPLITUDE AND WAVE FUNCTIONS

We take the relationship for φ_+, φ_- from (3)

$$\varphi_+(k,x) = \varphi_-(k,x) - 2\pi i\int_{R^3}\delta(|k|^2 - |l|^2) \times A(k,\lambda)\varphi_-(\lambda,x)d\lambda. \quad (4)$$

Let us denote new functions and operators we will use further

$$\varphi_0(\sqrt{z}e_k,x) = e^{i(\sqrt{z}e_k,x)},$$
$$\Phi_0(\sqrt{z}e_k,x) = \varphi_0(\sqrt{z}e_k,x) + \varphi_0(-\sqrt{z}e_k,x),$$
$$\Phi_+(\sqrt{z}e_k,x) = \varphi_+(\sqrt{z}e_k,x) - e^{i(\sqrt{z}e_k,x)} + \varphi_+(-\sqrt{z}e_k,x) - e^{-i(\sqrt{z}e_k,x)},$$
$$\Phi_-(\sqrt{z}e_k,x) = \varphi_-(\sqrt{z}e_k,x) - e^{i(\sqrt{z}e_k,x)} + \varphi_-(-\sqrt{z}e_k,x) - e^{-i(\sqrt{z}e_k,x)},$$
$$D_1 f = -2\pi i\int_{R^3} A(k,\lambda)\delta(z-l)f(\lambda,x)d\lambda,$$
$$D_2 f = -2\pi i\int_{R^3} A(-k,\lambda)\delta(z-l)f(\lambda,x)d\lambda,$$
$$D_3 f = D_1 f + D_2 f,$$

where $z = |k|^2$, $l = |\lambda|^2$, $\pm k = \pm\sqrt{z}e_k$. Let us introduce the operators $T_\pm$, T for the function $f \in W_2^1(R)$ by the formulas

$$T_+ f = \frac{1}{\pi i}\lim_{Imz\to 0}\int_{-\infty}^{\infty}\frac{f(\sqrt{s})}{s-z}ds,$$

where $Imz > 0$,

$$T_- f = \frac{1}{\pi i}\lim_{Imz\to 0}\int_{-\infty}^{\infty}\frac{f(\sqrt{s})}{s-z}ds,$$

where $Imz < 0$,

$$Tf = \frac{1}{2}(T_+ + T_-)f$$

Use (4) and the symbols $e_r = \frac{k}{|k|}$ to come to Riemann' problem of finding a function Φ_+, which is analytic by the variable z in the top half plane, and the function Φ_-, which is analytical on the variable z in the bottom half plane by the specified jump of discontinuity f onto the positive semi axis.

For the jump the discontinuity of an analytical function, we have the following equations

$$f = \Phi_+ - \Phi_- \tag{5}$$

$$f = D_3[\Phi_-] - D_3[\varphi_-] \tag{6}$$

where $\varphi_- = \varphi_-(-\lambda, x)$.

Theorem 9. *Suppose that* $q \in \boldsymbol{R}$,

$\varphi_\pm|_{x=0,z=0} = 0$;

then the functions

$$\Psi_1 = \Phi_\pm(\sqrt{z}e_k, x)|_{x=0} - \Phi_0(\sqrt{z}e_k, x)|_{x=0},$$

$$\Psi_2 = T_\pm f|_{x=0}$$

are coincided according to the class of analytical functions, coincide with bounded derivatives all over the complex plane with a slit along the positive semi axis.

Lemma 2. *There exists* $0 < |\varepsilon| < \infty$ *such that it satisfies the following condition* $\varphi_+|_{x=0,z=0} = 0$ *holds for the potential of the form* $v = \varepsilon q$, *where* $q \in \boldsymbol{R}$.

Now, we can formulate Riemann's problem. Find the analytic function $\Phi_\pm$ that satisfies (5), (6) and its solution is set by the following theorem.

Theorem 10. *Assume that* $q \in \boldsymbol{R}$,

$\varphi_\pm|_{x=0,z=0} = 0$,

then

$$\Phi_\pm = T_\pm f + \Phi_0,$$

$$f = D_3[f[T_- f + \Phi_0]] - D_3\varphi_-,$$

where $\varphi_- = \varphi_-(-\lambda, x)$.

Lemma 3. *Suppose that* $q \in \boldsymbol{R}$, $\varphi_\pm|_{x=0,z=0} = 0$; *then*

$$\Delta_x T_\pm[f]|_{x=0} = T_\pm \Delta_x[f]|_{x=0}.$$

Theorem 11. *Suppose that* $q \in \boldsymbol{R}$,

$\varphi_\pm|_{x=0,z=0} = 0$, $q(0) \neq 0$,

then

$$q(0)f|_{x=0} = D_3 T_-[qf|_{x=0}$$

$$-D_3[q\varphi_-]|_{x=0} + D_3\int_0^\infty f\,ds|_{x=0}.$$

6. AUXILIARY PROPOSITIONS

For wave functions let us use integral representations following from Lippman-Schwinger's theorem

$$\varphi_\pm(k,x) = e^{i(k,x)}$$

$$+\frac{1}{4\pi}\int_{R^3}\frac{e^{\pm i\sqrt{z}|x-y|}}{|x-y|}q(y)\varphi_\pm(k,y)dy,$$

$$\varphi_\pm(-k,x) = e^{-i(k,x)}$$

$$+\frac{1}{4\pi}\int_{R^3}\frac{e^{\mp i\sqrt{z}|x-y|}}{|x-y|}q(y)\varphi_\pm(-k,y)dy.$$

Lemma 4. *Suppose that* $q \in \boldsymbol{R}$,

$\varphi_\pm|_{x=0,z=0} = 0$;

then

$$A(k,k') = c_0\tilde{q}(k-k')$$

$$+\frac{c_0}{4\pi}\int_{R^3}\int_{R^3} e^{-i(k',x)}q(x)\frac{e^{i\sqrt{z}|x-y|}}{|x-y|}$$

$$\times q(y)e^{i(k,y)}dydx + A_3(k,k'),$$

$$A(-k,k') = c_0\tilde{q}(-k-k')$$

$$+\frac{c_0}{4\pi}\int_{R^3}\int_{R^3} e^{-i(k',x)}q(x)\frac{e^{-i\sqrt{z}|x-y|}}{|x-y|}$$

$$\times q(y)e^{-i(k,y)}dydx + A_3(-k,k'),$$

where $c_0 = \frac{1}{(2\pi)^2}$, *and* $A_3(k,k'), A_3(-k,k')$ *are terms of order higher than 2 with regards to* q.

Theorem 12 (*Parseval*). *The functions*

$$f, g \in L_2(R^3)$$

satisfy the equation

$$(f,g) = c_0(\tilde{f}, \tilde{g}^*),$$

where $(\cdot,\cdot)$ *is a scalar product and* $c_0 = \frac{1}{(2\pi)^3}$.

Lemma 5. *Suppose that* $q \in \boldsymbol{R}$, $\varphi_\pm|_{x=0,z=0} = 0$, *then*

$$A(k,k') = c_0\tilde{q}(k-k')$$

$$-c_0^2\int_{R^3}\frac{\tilde{q}(k+p)\tilde{q}(p-k')}{|p|^2 - z - i0}dp$$

$$+A_3(k,k'),$$

$$A(-k,k') = c_0\tilde{q}(-k-k')$$

$$-c_0^2\int_{R^3}\frac{\tilde{q}(-k+p)\tilde{q}(p-k')}{|p|^2 - z - i0}dp$$

$$+A_3(-k,k').$$

Corollary 2. *Suppose that* $q \in \boldsymbol{R}$,

$\varphi_\pm|_{x=0,z=0} = 0$,

then

$$A_{\mathrm{mv}}(k) = c_0\tilde{q}_{\mathrm{mv}}(k)$$

$$-c_0^2\frac{\sqrt{z}}{2}\int_0^\pi\int_0^{2*\pi}\int_{R^3}\frac{\tilde{q}(k+p)\tilde{q}(p-k')}{|p|^2 - z - i0}dp\,de_{k'} + A_{3\mathrm{mv}}(k)$$

where

$$A_{3\text{mv}}(k) = \int_{R^3} A_3(k,k')\delta(z-|k'|^2)dk'$$

and

$$A_{\text{mv}}(-k) = c_0\tilde{q}_{\text{mv}}(-k)$$
$$-c_0^2\frac{\sqrt{z}}{2}\int_0^{\pi}\int_0^{2*\pi}\int_{R^3}\frac{\tilde{q}(-k+p)\tilde{q}(p-k')}{|p|^2-z-i0}dpde_{k'}$$
$$+A_{3\text{mv}}(-k),$$

where

$$A_{3\text{mv}}(-k) = \int_{R^3} A_3(-k,k')\delta(z-|k'|^2)dk'.$$

Lemma 6. *Suppose that* $q \in R$ *and* $x = 0$, *then*

$$\varphi_{\pm}(k,0) = 1+\frac{1}{4\pi}\int_{R^3}\frac{e^{\pm i\sqrt{z}|y|}}{|y|}q(y)e^{i(k,y)}dy$$
$$+\frac{1}{(4\pi)^2}\int_{R^3}\int_{R^3}\frac{e^{\pm i\sqrt{z}|y|}}{|y|}q(y)\frac{e^{\pm i\sqrt{z}|y-t|}}{|y-t|}$$
$$\times q(t)e^{i(k,t)}dtdy+\varphi_{\pm}^{(3)}(k,0),$$

where $\varphi_{\pm}^{(3)}(k,0)$ *are terms of order higher than 2 with regards to* q., *i.e.*,

$$\varphi_{\pm}^{(3)}(k,x) = \frac{1}{(4\pi)^3}\int_{R^3}\int_{R^3}\int_{R^3}\frac{e^{\pm i\sqrt{z}|x-y|}}{|x-y|}q(y)$$
$$\times\frac{e^{\pm i\sqrt{z}|y-t|}}{|y-t|}q(t)\frac{e^{\pm i\sqrt{z}|t-s|}}{|t-s|}q(s)\varphi_{\pm}(k,s)dsdtdy.$$

and

$$\varphi_{\pm}(-k,0) = 1+\frac{1}{4\pi}\int_{R^3}\frac{e^{\mp i\sqrt{z}|y|}}{|y|}q(y)e^{-i(k,y)}dy$$
$$+\frac{1}{(4\pi)^2}\int_{R^3}\int_{R^3}\frac{e^{\mp i\sqrt{z}|y|}}{|y|}q(y)\frac{e^{\mp i\sqrt{z}|y-t|}}{|y-t|}q(t)$$
$$\times e^{-i(k,t)}dtdy+\varphi_{\pm}^{(3)}(-k,0),$$

where $\varphi_{\pm}^{(3)}(-k,0)$ *are terms of or der hi gher than 2 with regards to* q., *i.e.*,

$$\varphi_{\pm}^{(3)}(-k,x) = \frac{1}{(4\pi)^3}\int_{R^3}\int_{R^3}\int_{R^3}\frac{e^{\mp i\sqrt{z}|x-y|}}{|x-y|}q(y)$$
$$\times\frac{e^{\mp i\sqrt{z}|y-t|}}{|y-t|}q(t)\frac{e^{\mp i\sqrt{z}|t-s|}}{|t-s|}q(s)\varphi_{\pm}(-k,s)dsdtdy.$$

Lemma 7. *Suppose that* $q \in \boldsymbol{R}$, $\varphi_{\pm}|_{x=0,z=0} = 0$, *then*

$$\varphi_{\pm}(k,0) = 1-c_0\int_{R^3}\frac{\tilde{q}(k+p)}{|p|^2-z\mp i0}dp$$
$$+c_0^2\int_{R^3}\frac{\tilde{q}(k+p)}{(|p|^2-z\mp i0)} \tag{7}$$
$$\times\int_{R^3}\frac{\tilde{q}(p+p_1)}{(|p_1|^2-z\mp i0)}dp_1dp+\varphi_{\pm}^{(3)}(k,0)$$

$$\varphi_{\pm}(-k,0) = 1-c_0\int_{R^3}\frac{\tilde{q}(-k+p)}{|p|^2-z\mp i0}dp$$
$$+c_0^2\int_{R^3}\frac{\tilde{q}(-k+p)}{(|p|^2-z\mp i0)} \tag{8}$$
$$\times\int_{R^3}\frac{\tilde{q}(p+p_1)}{(|p_1|^2-z\mp i0)}dp_1dp+\varphi_{\pm}^{(3)}(-k,0)$$

Lemma 8. *Suppose that* $q \in R$, $x = 0$; *then*

$$F(k,0) = -\pi ic_0\sqrt{z}\int_0^{\pi}\int_0^{2\pi}\tilde{q}(k-\sqrt{z}e_p)de_p$$
$$+\pi ic_0^2\sqrt{z}\int_0^{\pi}\int_0^{2\pi}V.p.\int_{R^3}\frac{\tilde{q}(k-\sqrt{z}e_p)}{|p_1|^2-z}$$
$$\times\tilde{q}(-\sqrt{z}e_p-p_1)dp_1de_p$$
$$+\pi ic_0^2\sqrt{z}V.p.\int_{R^3}\int_0^{\pi}\int_0^{2\pi}\frac{\tilde{q}(k-p)}{|p|^2-z}$$
$$\times\tilde{q}(-p-\sqrt{z}e_{p_1})de_{p_1}dp$$
$$+\varphi_{+}^{(3)}(k,0)-\varphi_{-}^{(3)}(k,0).$$

and

$$F(-k,0) = -\pi ic_0\sqrt{z}\int_0^{\pi}\int_0^{2\pi}\tilde{q}(-k-\sqrt{z}e_p)de_p$$
$$+\pi ic_0^2\sqrt{z}\int_0^{\pi}\int_0^{2\pi}V.p.\int_{R^3}\frac{\tilde{q}(-k-\sqrt{z}e_p)}{|p_1|^2-z}$$
$$\times\tilde{q}(-\sqrt{z}e_p-p_1)dp_1de_p$$
$$+\pi ic_0^2\sqrt{z}\,V.p.\int_{R^3}\int_0^{\pi}\int_0^{2\pi}\frac{\tilde{q}(-k-p)}{|p|^2-z}$$
$$\times\tilde{q}(-p-\sqrt{z}e_{p_1})de_{p_1}dp$$
$$+\varphi_{+}^{(3)}(-k,0)-\varphi_{-}^{(3)}(-k,0).$$

7. TWO REPRESENTATIONS OF SCATTERING AMPLITUDE

Lemma 9. *Suppose that* $f \in W_2^1(R)$, *then*

$$T_{\pm}f = \mp f+Tf.$$

Lemma 10. *Suppose t hat* $q \in \boldsymbol{R}$, $\varphi_{\pm}|_{x=0,z=0} = 0$, *then*

$$f(k,0) = F(k,0)+F(-k,0).$$

Lemma 11. *Suppose that* $q \in \boldsymbol{R}$, $\varphi_{\pm}|_{x=0,z=0} = 0$, *then*

$$A_{\mathrm{mv}}(k) + A_{\mathrm{mv}}(-k) = c_0(\tilde{q}_{\mathrm{mv}}(k) + \tilde{q}_{\mathrm{mv}}(-k))$$
$$+\pi i c_0^2\sqrt{z}\int_0^{\pi}\int_0^{2\pi}(\tilde{q}(k-\sqrt{z}e_\lambda) + \tilde{q}(-k-\sqrt{z}e_\lambda))$$
$$\times \tilde{q}_{\mathrm{mv}}(\sqrt{z}e_\lambda)de_\lambda$$
$$+\pi i c_0^2\frac{\sqrt{z}}{2}\int_0^{\pi}\int_0^{2\pi}(\tilde{q}(k-\sqrt{z}e_\lambda) + \tilde{q}(-k-\sqrt{z}e_\lambda))$$
$$\times \tilde{q}_{\mathrm{mv}}(-\sqrt{z}e_\lambda)de_\lambda$$
$$-\pi i c_0^2\sqrt{z}\int_0^{\pi}\int_0^{2\pi}(\tilde{q}(k-\sqrt{z}e_\lambda) + \tilde{q}(-k-\sqrt{z}e_\lambda))$$
$$\times (T[\tilde{q}_{\mathrm{mv}}](\sqrt{z}e_\lambda) + T[\tilde{q}_{\mathrm{mv}}](-\sqrt{z}e_\lambda))de_\lambda$$
$$-c_0^2\sqrt{z}\int_0^{\pi}\int_0^{2\pi}(\tilde{q}(k-\sqrt{z}e_\lambda) + \tilde{q}(-k-\sqrt{z}e_\lambda))$$
$$\times V.p.\int_{R^3}\frac{\tilde{q}(-\sqrt{z}e_\lambda - p)}{|p|^2 - z}dp de_\lambda$$
$$+c_0^2\frac{\sqrt{z}}{2}V.p.\int_{R^3}\int_0^{\pi}\int_0^{2\pi}\frac{\tilde{q}(k-\lambda) + \tilde{q}(-k-\lambda)}{l-z}$$
$$\times \tilde{q}(-l-\sqrt{z}e_p)de_p d\lambda - 2\pi i(F^{(3)}(k,0)$$
$$+F^{(3)}(-k,0) + Q_3(k,0) + Q^{(3)}(k,0)),$$

where $Q_3(k,0)$, $Q^{(3)}(k,0)$ *are defined by formulas*

$$Q_3(k,0) = -4\pi^2 c_0^2\int_{R^3}(A_2(k,\lambda) + A_2(-k,\lambda))$$
$$\times \delta(z-l)(\tilde{q}_{\mathrm{mv}}(\lambda) + \tilde{q}_{\mathrm{mv}}(-\lambda))d\lambda$$
$$+2\pi i c_0\int_{R^3}(A_2(k,\lambda) + A_2(-k,\lambda))\delta(z-l)$$
$$\times f_2(l,0)dl + 4\pi^2 c_0^2\int_{R^3}(A_2(k,\lambda) + A_2(-k,\lambda))$$
$$\times \delta(z-l)(T[\tilde{q}_{\mathrm{mv}}](\lambda) + T[\tilde{q}_{\mathrm{mv}}](-\lambda))d\lambda$$
$$-2\pi i c_0\int_{R^3}(A_2(k,l) + A_2(-k,l))$$
$$\times \delta(z-l)T[f_2](\lambda,0)d\lambda. \tag{9}$$
$$Q^{(3)}(k,0) = 2\pi i c_0^2\int_{R^3}(\tilde{q}(k-\lambda) + \tilde{q}(-k-\lambda))$$
$$\times \delta(z-l)\varphi_-^{(2)}(-\lambda,0)d\lambda$$
$$+2\pi i c_0^2\int_{R^3}(A_2(k,\lambda) + A_2(-k,\lambda))$$
$$\times \delta(z-l)(\int_{R^3}\frac{\tilde{q}(-\lambda-p)}{|p|^2 - l + i0}dp$$
$$+\varphi_-^{(2)}(-l,0))d\lambda. \tag{10}$$

correspondingly,

$$F^{(3)}(k,0) = \varphi_+^{(3)}(k,0) - \varphi_-^{(3)}(k,0),$$
$$F^{(3)}(-k,0) = \varphi_+^{(3)}(-k,0) - \varphi_-^{(3)}(-k,0),$$

and $\varphi_\pm^{(3)}(\pm k,0)$ *are terms of order* 3 *and higher w.r.t.* $\tilde{q}$ *in the representations* (7), (8).

Lemma 12. *Suppose that* $q \in \boldsymbol{R}$, $\varphi_{\pm}|_{x=0,z=0} = 0$, *then*

$$A_{\mathrm{mv}}(k) + A_{\mathrm{mv}}(-k)$$
$$= -\frac{i\sqrt{z}}{4\pi q(0)}\int_0^{\pi}\int_0^{2\pi}(A(k,\sqrt{z}e_\lambda) + A(-k,\sqrt{z}e_\lambda))$$
$$\times \int_0^{\infty} f(se_\lambda,0)ds de_\lambda.$$

8. NONLINEAR REPRESENTATION OF POTENTIAL

Let us proceed to the construction of potential nonlinear representation.

Lemma 13. *Assume that* $q \in \boldsymbol{R}$, $\varphi_{\pm}|_{x=0,z=0} = 0$; *then*

$$\tilde{q}_{\mathrm{mv}}(k) + \tilde{q}_{\mathrm{mv}}(-k)$$
$$= -\pi i c_0\sqrt{z}\int_0^{\pi}\int_0^{2\pi}(\tilde{q}(k-\sqrt{z}e_\lambda)$$
$$+\tilde{q}(-k-\sqrt{z}e_\lambda))\tilde{q}_{\mathrm{mv}}(\sqrt{z}e_\lambda)de_\lambda$$
$$-\pi i c_0\frac{\sqrt{z}}{2}\int_0^{\pi}\int_0^{2\pi}(\tilde{q}(k-\sqrt{z}e_\lambda) + \tilde{q}(-k-\sqrt{z}e_\lambda))$$
$$\times \tilde{q}_{\mathrm{mv}}(-\sqrt{z}e_\lambda)de_\lambda$$
$$+\pi i c_0\sqrt{z}\int_0^{\pi}\int_0^{2\pi}(\tilde{q}(k-\sqrt{z}e_\lambda) + \tilde{q}(-k-\sqrt{z}e_\lambda))$$
$$\times (T[\tilde{q}_{\mathrm{mv}}](\sqrt{z}e_\lambda) + T[\tilde{q}_{\mathrm{mv}}](-\sqrt{z}e_\lambda))de_\lambda$$
$$-c_0\sqrt{z}\int_0^{\pi}\int_0^{2\pi}(\tilde{q}(k-\sqrt{z}e_\lambda) + \tilde{q}(-k-\sqrt{z}e_\lambda))$$
$$\times V.p.\int_{R^3}\frac{\tilde{q}(-\sqrt{z}e_\lambda - p)}{|p|^2 - z}dp de_\lambda$$
$$-c_0\frac{\sqrt{z}}{2}V.p.\int_{R^3}\int_0^{\pi}\int_0^{2\pi}\frac{(\tilde{q}(k-\lambda) + \tilde{q}(-k-\lambda))}{l-z}$$

$$\times \tilde{q}(-l-\sqrt{z}e_p)de_p d\lambda$$

$$-\frac{i\sqrt{z}}{4\pi c_0 q(0)}\int_0^{\pi}\int_0^{2\pi}(A(k,\sqrt{z}e_\lambda)+A(-k,\sqrt{z}e_\lambda))$$

$$\times\int_0^{\infty}f(se_\lambda,0)dsde_\lambda+\frac{2\pi i}{c_0}(F^{(3)}(k,0)$$

$$+F^{(3)}(-k,0)+Q_3(k,0)+Q^{(3)}(k,0)),$$

where $Q_3(k,0)$, $Q^{(3)}(k,0)$ *are defined by* **Eqs.9** and **10** *accordingly,*

$$F^{(3)}(k,0)=\varphi_+^{(3)}(k,0)-\varphi_-^{(3)}(k,0),$$

$$F^{(3)}(-k,0)=\varphi_+^{(3)}(-k,0)-\varphi_-^{(3)}(-k,0),$$

and $\varphi_\pm^{(3)}(\pm k,0)$ *are term of order* 3 *and higher w.r.t.* $\tilde{q}$ *in representations* (7), (8).

Lemma 14. *Suppose that* $q\in \boldsymbol{R}$, $\varphi_\pm|_{x=0,z=0}=0$, *then*

$$V.p.\int_{R^3}\int_0^{\pi}\int_0^{2\pi}\frac{(\tilde{q}(k-\lambda)+\tilde{q}(-k-\lambda))}{l-z}$$

$$\times\tilde{q}(-l-\sqrt{z}e_p)de_p dl$$

$$=\pi i\int_0^{\pi}\int_0^{2\pi}(\tilde{q}(k-\sqrt{z}e_\lambda)+\tilde{q}(-k-\sqrt{z}e_\lambda))$$

$$\times\tilde{q}_{\mathrm{mv}}(-\sqrt{z}e_\lambda)de_\lambda.$$

Lemma 15. *Let* $\tilde{q}\in W_2^1(R)$ *and* $q\in R$, *then*

$$\int_0^{\pi}\int_0^{2\pi}(\tilde{q}(k-\sqrt{z}e_\lambda)+\tilde{q}(-k-\sqrt{z}e_\lambda))$$

$$\times(T[\tilde{q}_{\mathrm{mv}}](\sqrt{z}e_\lambda)+T[\tilde{q}_{\mathrm{mv}}](-\sqrt{z}e_\lambda))de_\lambda$$

$$=\int_0^{\pi}\int_0^{2\pi}(\tilde{q}(k-\sqrt{z}e_\lambda)+\tilde{q}(-k-\sqrt{z}e_\lambda))$$

$$\times(\tilde{q}_{\mathrm{mv}}(\sqrt{z}e_\lambda)+\tilde{q}_{\mathrm{mv}}(-\sqrt{z}e_\lambda))de_\lambda,$$

$$\int_0^{\pi}\int_0^{2\pi}(\tilde{q}(k-\sqrt{z}e_\lambda)+\tilde{q}(-k-\sqrt{z}e_\lambda))$$

$$\times V.p.\int_{R^3}\frac{\tilde{q}(-\sqrt{z}e_\lambda-p)}{|p|^2-z}dpde_\lambda$$

$$=\pi i\int_0^{\pi}\int_0^{2\pi}(\tilde{q}(k-\sqrt{z}e_\lambda)+\tilde{q}(-k-\sqrt{z}e_\lambda))$$

$$\times\tilde{q}_{\mathrm{mv}}(-\sqrt{z}e_\lambda)de_\lambda.$$

Theorem 14. *Let* $q\in\boldsymbol{R}$, $\varphi_\pm|_{x=0,z=0}=0$, *then*

$$\tilde{q}_{\mathrm{mv}}(k)+\tilde{q}_{\mathrm{mv}}(-k)$$

$$=-\pi i c_0\sqrt{z}\int_0^{\pi}\int_0^{2\pi}(\tilde{q}(k-\sqrt{z}e_\lambda)+\tilde{q}(-k-\sqrt{z}e_\lambda))$$

$$\times\tilde{q}_{\mathrm{mv}}(-\sqrt{z}e_\lambda)de_\lambda+\mu(k),$$

$$\mu(k)=\frac{2\pi i}{c_0}(F^{(3)}(k,0)+F^{(3)}(-k,0)$$

$$+Q_3(k,0)+Q^{(3)}(k,0)),$$

where $c_0=4\pi$.

Theorem 15. *Suppose* $q\in\boldsymbol{R}$, $\varphi_\pm|_{x=0,z=0}=0$; *then*

$$\mu(k)=\sqrt{z}\int_0^{\pi}\int_0^{2\pi}\int_0^{\pi}\int_0^{2\pi}(\tilde{q}(-k-\sqrt{z}e_\lambda)$$

$$+\tilde{q}(k-\sqrt{z}e_\lambda))\tilde{q}(\sqrt{z}e_\lambda-\sqrt{z}e_s)$$

$$\times\mu_0(\sqrt{z}e_s)de_\lambda de_s,$$

where $|\mu_0|<C|q_{\mathrm{mv}}|$

9. THE CAUCHY PROBLEM FOR NAVIER-STOKES' EQUATIONS

Let us apply the obtained results to estimate the solutions of Cauchy problem for Navier-Stokes' set of equations

$$q_t-\nu\Delta q+\sum_{k=1}^{3}q_k q_{x_k}$$

$$=-\nabla p+F_0(x,t),\ divq=0, \tag{11}$$

$$q|_{t=0}=q_0(x) \tag{12}$$

in the domain of $Q_T=R^3\times(0,T)$. With respect to q_0, assume

$$div\ q_0=0. \tag{13}$$

Problem (11), (12), (13) has at least one weak solution (q,p) in the so-called Leray-Hopf class, see [3].

Let us mention the known statements proved in [10].

Theorem 16. *Suppose that*

$$q_0\in W_2^1(R^3),\quad f\in L_2(Q_T)$$

then there exists a unique weak solution of problem (11), (12), (13), *in* Q_{T_1}, $T_1\in[0,T]$, *that satisfies*

$$q_t,\ q_{xx},\nabla p\in L_2(Q_T)$$

Note that T_1 depends on q_0, f.

Lemma 16. *If* $q_0\in W_2^1(R^3)$, $f\in L_2(Q_T)$, *then*

$$\sup_{0\le t\le T}||q||^2_{L_2(R^3)}+\int_0^t||q_x||^2_{L_2(R^3)}d\tau$$

$$\le||q_0||^2_{L_2(R^3)}+||F_0||_{L_2(Q_T)}$$

Our goal is to prove the global unicity weak solution of (11), (12), (13) irrespective of initial velocity and power smallness conditions.

Therefore let us obtain uniform estimates.

Statement 1. *Weak solution of problem* (11), (12), (13), *from Theorem* 16 *satisfies the following equation*

$$\tilde{q}(z(e_k-e_\lambda),t)=\tilde{q}_0(z(e_k-e_\lambda))$$
$$+\int_0^t e^{-\nu z^2|e_k-e_\lambda|(t-\tau)}([\widetilde{(q,\nabla)}q]+\tilde{F})$$
$$\times(z(e_k-e_\lambda),\tau)d\tau, \qquad (14)$$

where $F=-\nabla p+F_0$.

Proof. The proof follows from the definition of Fourier transformation and the formulas for linear differential equations.

Lemma 17. *The solution of the problem* (11), (12), (13) *from Theorem* 16, *satisfies the following equation*

$$\tilde{p}=\sum_{i,j}\frac{k_ik_j}{|k|^2}\widetilde{q_iq_j}+i\sum_i\frac{k_i}{|k|^2}\tilde{F_i}$$

and the following estimates

$$||p||_{L_2(R^3)}\le 3||q_x||^{\frac{3}{2}}_{L_2(R^3)}||q||^{\frac{1}{2}}_{L_2(R^3)},$$
$$\left|\frac{\partial\tilde{p}}{\partial k}\right|\le\frac{|\tilde{q}^2|}{|k|}+\frac{|\tilde{F}|}{|k|^2}+\frac{1}{|k|}\left|\frac{\partial\tilde{F}}{\partial k}\right|+3\left|\frac{\partial\tilde{q}^2}{\partial|k|}\right|;$$

Proof. We obtain the equation for p using div and Fourier transformation. The estimates follow from the obtained equation.

This completes the proof of Lemma 17.

Lemma 18. *Weak solution of problem* (11), (12), (13), *from Theorem* 16 *satisfies the following inequalities*

$$\sup_{0\le t\le T}\Big[\int_{R^3}|x|^2|q(x,t)|^2dx$$
$$+\int_0^t\int_{R^3}|x|^2|q_x(x,\tau)|^2dxd\tau\Big]\le const,$$
$$\sup_{0\le t\le T}\Big[\int_{R^3}|x|^4|q(x,t)|^2dx$$
$$+\int_0^t\int_{R^3}|x|^4|q_x(x,\tau)|^2dxd\tau\Big]\le const,$$

or

$$\sup_{0\le t\le T}\Big[\left\|\frac{\partial\tilde{q}}{\partial z}\right\|_{L_2(R^3)}$$
$$+\int_0^t\int_{R^3}z^2|\widetilde{q_k}(k,\tau)|^2dkd\tau\Big]\le const,$$
$$\sup_{0\le t\le T}\Big[\left\|\frac{\partial^2\tilde{q}}{\partial z^2}\right\|_{L_2(R^3)}$$
$$+\int_0^t\int_{R^3}z^2|\widetilde{q_{kk}}(k,\tau)|^2dkd\tau\Big]\le const.$$

Proof. The proof follows from Navier-Stokes' equation, the first priori estimate formulated in Lemma 16 and obtained from Lemma 17.

This completes the proof of Lemma 18.

Lemma 19. *Weak solution of problem* (11), (12), (13), *from Theorem* 16, *satisfies the following inequalities*

$$\max_k|\tilde{q}|\le\max_k|\tilde{q}_0|$$
$$+\frac{T}{2}\sup_{0\le t\le T}||q||^2_{L_2(R^3)}+\int_0^t||q_x||^2_{L_2(R^3)}d\tau,$$
$$\max_k\left|\frac{\partial\tilde{q}}{\partial z}\right|\le\max_k\left|\frac{\partial\tilde{q}_0}{\partial z}\right|$$
$$+\frac{T}{2}\sup_{0\le t\le T}\left\|\frac{\partial\tilde{q}}{\partial z}\right\|_{L_2(R^3)}+\int_0^t\int_{R^3}z^2|\widetilde{q_k}(k,\tau)|^2dkd\tau,$$
$$\max_k\left|\frac{\partial^2\tilde{q}}{\partial z^2}\right|\le\max_k\left|\frac{\partial^2\tilde{q}_0}{\partial z^2}\right|$$
$$+\frac{T}{2}\sup_{0\le t\le T}\left\|\frac{\partial^2\tilde{q}}{\partial z^2}\right\|_{L_2(R^3)}+\int_0^t\int_{R^3}z^2|\widetilde{q_{kk}}(k,\tau)|^2dkd\tau.$$

Proof. We obtain these estimates using representation (14), Parseval's equality, Cauchy - Bunyakovskiy inequality (14) by Lemma 18.

This proves Lemma 19.

Lemma 20. *Weak solution of problem* (11), (12), (13), *from Theorem* 16 *satisfies the following inequalities*

$$|\tilde{q}_{\rm mv}(z,t)|\le zM_1,\qquad\left|\frac{\partial\tilde{q}_{\rm mv}(z,t)}{\partial z}\right|\le zM_2,$$
$$\left|\frac{\partial^2\tilde{q}_{\rm mv}(z,t)}{\partial z^2}\right|\le zM_3,$$

where M_1, M_2, M_3 *are limited.*

Proof. Let us prove the first estimate. These inequalities

$$|\tilde{q}_{\rm mv}(z,t)|\le\frac{z}{2}\int_0^\pi\int_0^{2\pi}|\tilde{q}(z(e_k-e_p),t)|de_p$$
$$\le 2\pi z\max_k|\tilde{q}|\le zM_1,$$

where $M_1=const$.

Follows from definition (2) for the average of q and from Lemmas 18, 19.

The rest of estimates are proved similarly.

This proves Lemma 20.

Lemma 21. *Weak solution of problem* (11), (12), (13), *from Theorem 16 satisfies the following inequalities* $C_i \le const$, $(i = \overline{0,2,4})$, *where*

$$C_0 = \int_0^t |\tilde{F}_1|^2 d\tau, \qquad F_1 = (q,\nabla)q + F,$$

$$C_2 = \int_0^t \left|\frac{\partial \tilde{F}_1}{\partial z}\right|^2 d\tau, \qquad C_4 = \int_0^t \left|\frac{\partial^2 \tilde{F}_1}{\partial z^2}\right|^2 d\tau.$$

The proof follows from the apriori estimate of Lemma 16 and the statement of Lemma 18.

This completes the proof of Lemma 21.

Lemma 22. *Suppose that* $q \in R$, $\max_k |\tilde{q}| < \infty$, *then*

$$\int_{R^3}\int_{R^3} \frac{q(x)q(y)}{|x-y|^2} dxdy \le C(|q|_{L_2} + \max_k |\tilde{q}|)^2$$

Proof. Using Plansherel's theorem, we get the statement of the lemma.

This proves Lemma 22.

Lemma 23. *Weak solution of problem* (11), (12), (13), *from Theorem* 16 *satisfies the following inequalities*

$$|\tilde{q}(z(e_k - e_\lambda),t)| \le |\tilde{q}_0(z(e_k - e_\lambda))| + \left(\frac{1}{2\nu}\right)^{\frac{1}{2}} \frac{C_0^{\frac{1}{2}}}{z|e_k - e_\lambda|}, \tag{15}$$

where

$$C_0 = \int_0^t |\tilde{F}_1|^2 d\tau, F_1 = (q,\nabla)q + F.$$

Proof. From Formula (14) we get

$$|\tilde{q}(z(e_k - e_\lambda),t)| \le |\tilde{q}_0(z(e_k - e_\lambda))| + \left|\int_0^t e^{-\nu z^2|e_k-e_\lambda|^2(t-\tau)} \times \tilde{F}_1(z(e_k - e_\lambda),\tau)d\tau\right| \tag{16}$$

where

$$F_1 = (q,\nabla)q + F.$$

Using the denotation

$$I = \left|\int_0^t e^{-\nu z^2|e_k-e_\lambda|^2(t-\tau)} \times \tilde{F}_1(z(e_k - e_\lambda),\tau)d\tau\right|,$$

Taking into account Holder's inequality in I we obtain

$$I \le \left(\int_0^t |e^{-\nu z^2|e_k-e_\lambda|^2(t-\tau)}|^p d\tau\right)^{\frac{1}{p}} \times \left(\int_0^t |F_1|^q d\tau\right)^{\frac{1}{q}}$$

where p, q satisfies the equality $\frac{1}{p} + \frac{1}{q} = 1$.

Suppose $p = q = 2$. Then

$$I \le \left(\frac{1}{2\nu}\right)^{\frac{1}{2}} \frac{\left(\int_0^t |\tilde{F}_1|^2 d\tau\right)^{\frac{1}{2}}}{z|e_k - e_\lambda|}.$$

Taking into consideration the estimate I in (16), we obtain the statement of the lemma.

This proves Lemma 23.

Now, we have the uniform estimates of Rolnik norms for the solution of problems (11), (12), (13). Our further and basic aim is to get the uniform estimates $|\tilde{q}_i|_{L_1(R^3)}$, a component of velocity components in the Cauchy problem for Navier-Stokes' equations. In order to achieve the aim, we use Theorem 8 it implies to get estimates of spherical average.

Lemma 24. *Weak solution of problem* (11), (12), (13), *from Theorem* 16 *satisfies the following inequalities*

$$|\tilde{q}_{\text{mv}}|_{L_1(R^3)} \le \frac{C}{2}\left(A_0^{(1)} + \beta_1|\tilde{q}_{\text{mv}}|_{L_1(R^3)}\right) + |\mu|_{L_1(R^3)} \tag{17}$$

the function μ *is defined in Theorem* 15,

$$A_0^{(1)} = \int_{R^3} z \int_0^\pi \int_0^{2\pi} |\tilde{q}_0(z(e_k - e_\lambda))| \times |\tilde{q}_{\text{mv}}(ze_\lambda,t)| de_\lambda dk, \beta_1 = \left(\frac{1}{\nu}\right)^{\frac{1}{2}} 8\pi C_0^{\frac{1}{2}},$$

and C_0 *is defined in Lemma* 23.

Proof. From the statement of Theorem 14, we get the estimate

$$|\tilde{q}_{\text{mv}}|_{L_1(R^3)} \le \frac{C}{2}\int_{R^3} z \int_0^\pi \int_0^{2\pi} |\tilde{q}(z(e_k - e_\lambda),t)| \times |\tilde{q}_{\text{mv}}(ze_\lambda,t)| de_\lambda dk + |\mu|_{L_1(R^3)}.$$

(15) in the integral, we obtain

$$|\tilde{q}_{\text{mv}}|_{L_1(R^3)} \le \frac{C}{2}\Big(\int_{R^3} z \int_0^\pi \int_0^{2\pi} |\tilde{q}_0(z(e_k - e_\lambda))| \times |\tilde{q}_{\text{mv}}(ze_\lambda,t)| de_\lambda dk + \left(\frac{1}{\nu}\right)^{\frac{1}{2}} C_0^{\frac{1}{2}} \int_{R^3} \int_0^\pi \int_0^{2\pi} |\tilde{q}_{\text{mv}}(k,t)| \times \frac{de_\lambda}{|e_k - e_\lambda|} dk\Big) + |\mu|_{L_1(R^3)}.$$

Let us use the notation

$$A_0^{(1)} = \int_{R^3} z \int_0^{\pi} \int_0^{2\pi} |\tilde{q}_0(z(e_k - e_\lambda))| \times |\tilde{q}_{mv}(ze_\lambda, t)| de_\lambda dk,$$

then

$$|\tilde{q}_{mv}|_{L_1(R^3)} \leq \frac{C}{2}(A_0^{(1)} + \left(\frac{1}{\nu}\right)^{\frac{1}{2}} C_0^{\frac{1}{2}}$$

$$\times \int_{R^3} \int_0^{\pi} \int_0^{2\pi} |\tilde{q}_{mv}(k,t)| \frac{de_\lambda}{|e_k - e_\lambda|} dk) + |\mu|_{L_1(R^3)}.$$

Let us use the notation

$$I_0 = \int_0^{\pi} \int_0^{2\pi} \frac{de_\lambda}{|e_k - e_\lambda|}$$

and obtain I_0. Since

$$|e_k - e_\lambda| = ((e_k - e_\lambda, e_k - e_\lambda))^{\frac{1}{2}} = (1 - \cos\theta)^{\frac{1}{2}}$$

where θ is the angle between the unit vectors e_k, e_λ, it follows that

$$I_0 = 4\pi \int_0^{\pi} \frac{\sin\theta}{(1 - \cos\theta)^{\frac{1}{2}}} d\theta = 2^{\frac{7}{2}}\pi.$$

Using I_0 in the estimate $|\tilde{q}_{mv}|_{L_1(R^3)}$, we obtain the statement of the lemma.

This completes the proof of Lemma 24.

Theorem 17. *Weak solution of problem* (11), (12), (13), *from Theorem* 16 *satisfies the following inequalities*

$$\left|\frac{\tilde{q}_{mv}}{z}\right|_{L_1(R^3)} \leq \frac{C}{2}\left(A_0 + \beta_1 \left|\frac{\tilde{q}_{mv}}{z}\right|_{L_1(R^3)}\right) + \left|\frac{\mu}{z}\right|_{L_1(R^3)}, \tag{18}$$

where

$$A_0 = \int_{R^3} \int_0^{\pi} \int_0^{2\pi} |\tilde{q}_0(z(e_k - e_\lambda))| \times |\tilde{q}_{mv}(ze_\lambda, t)| de_\lambda dk$$

and β_1 *is defined in Lemma* 24.

Proof. Proof follows from (16), (17).

Corollary 3. *Weak solution of problem* (11), (12), (13), *from Theorem* 16 *satisfies the following inequalities*

$$\left|\frac{\tilde{q}_{mv}}{z}\right|_{L_1(R^3)} \leq \left(\frac{C}{2}A_0 + \left|\frac{\mu}{z}\right|_{L_1(R^3)}\right)K,$$

where

$$K = \frac{\nu^{\frac{1}{2}}}{\nu^{\frac{1}{2}} - 4\pi C C_0^{\frac{1}{2}}}.$$

Let's consider the influence of the following large scale transformations in Navier-Stokes' equation on K

$$t' = tA, \quad \nu' = \frac{\nu}{A}, \quad v' = \frac{v}{A}, \quad F_0' = \frac{F_0}{A^2}.$$

Statement 2. Let

$$A = \frac{4}{\nu^{\frac{1}{3}}(CC_0 + 1)^{\frac{2}{3}}},$$

then $K \leq \frac{8}{7}$.

Proof. By the definitions C and C_0, we have

$$K = (\frac{\nu}{A})^{\frac{1}{2}}((\frac{\nu}{A})^{\frac{1}{2}} - \frac{4\pi CC_0}{A^2})^{-1}$$

$$= \nu^{\frac{1}{2}}(\nu^{\frac{1}{2}} - \frac{4\pi CC_0}{A^{\frac{3}{2}}})^{-1} < \frac{8}{7}.$$

This proves Statement 2.

Lemma 25. *Weak solution of problem* (11), (12), (13), *from Theorem* 16 *satisfies the following inequalities*

$$\left|\frac{\partial\tilde{q}(z(e_k - e_\lambda), t)}{\partial z}\right| \leq \left|\frac{\partial\tilde{q}_0(z(e_k - e_\lambda))}{\partial z}\right| + 4\alpha\left(\frac{1}{\nu}\right)^{\frac{1}{2}} \frac{C_0^{\frac{1}{2}}}{z^2|e_k - e_\lambda|} + \left(\frac{1}{2\nu}\right)^{\frac{1}{2}} \frac{C_2^{\frac{1}{2}}}{z|e_k - e_\lambda|}, \tag{19}$$

where

$$C_2 = \int_0^t \left|\frac{\partial\tilde{F}_1}{\partial z}\right|^2 d\tau.$$

Proof. The underwritten inequalities follows from representation (14)

$$\left|\frac{\partial\tilde{q}(z(e_k - e_\lambda), t)}{\partial z}\right| \leq \left|\frac{\partial\tilde{q}_0(z(e_k - e_\lambda))}{\partial z}\right|$$

$$+2\nu z|e_k - e_\lambda|^2| \int_0^t (t-\tau)e^{-\nu z^2|e_k - e_\lambda|^2(t-\tau)} \times \tilde{F}_1(z(e_k - e_\lambda), \tau)d\tau|$$

$$+| \int_0^t e^{-\nu z^2|e_k - e_\lambda|^2(t-\tau)} \times \frac{\partial\tilde{F}_1}{\partial z}(z(e_k - e_\lambda), \tau)d\tau|.$$

Let us introduce the following denotation

$$I_1 = 2\nu z|e_k - e_\lambda|^2| \int_0^t (t-\tau)e^{-\nu z^2|e_k - e_\lambda|^2(t-\tau)} \times \tilde{F}_1(z(e_k - e_\lambda), \tau)d\tau|,$$

$$I_2 = \left| \int_0^t e^{-\nu z^2|e_k-e_\lambda|^2(t-\tau)} \times \frac{\partial \tilde{F}_1}{\partial z}(z(e_k-e_\lambda),\tau)d\tau \right|,$$

then

$$\left|\frac{\partial \tilde{q}(z(e_k-e_\lambda),t)}{\partial z}\right| \le \left|\frac{\partial \tilde{q}_0(z(e_k-e_\lambda))}{\partial z}\right| + I_1 + I_2.$$

Estimate I_1 by means of

$$\sup_t |t^m e^{-t}| < \alpha,$$

where $m > 0$ we obtain

$$I_1 \le \frac{4\alpha}{z}\left| \int_0^t e^{-\nu z^2|e_k-e_\lambda|^2\frac{t-\tau}{2}} \times \tilde{F}_1(z(e_k-e_\lambda),\tau)d\tau \right|.$$

On applying Holder's inequality, we get

$$I_1 \le \frac{4\alpha}{z}\left(\int_0^t |e^{-\nu z^2|e_k-e_\lambda|^2\frac{t-\tau}{2}}|^p d\tau\right)^{\frac{1}{p}} \times \left(\int_0^t |F_1|^q d\tau\right)^{\frac{1}{q}},$$

where p, q satisfy the equality $\frac{1}{p}+\frac{1}{q}=1$.

For $p=q=2$ we have

$$I_1 \le 4\alpha\left(\frac{1}{\nu}\right)^{\frac{1}{2}} \frac{C_0^{\frac{1}{2}}}{z^2|e_k-e_\lambda|},$$

$$I_2 \le \left(\frac{1}{2\nu}\right)^{\frac{1}{2}} \frac{C_2^{\frac{1}{2}}}{z|e_k-e_\lambda|},$$

$$C_2 = \int_0^t \left|\frac{\partial \tilde{F}_1}{\partial z}\right|^2 d\tau.$$

Inserting I_1, I_2 in to $\left|\frac{\partial \tilde{q}}{\partial z}\right|$, we obtain the statement of the lemma.

This completes the proof of Lemma 25.

Theorem 18. *Weak solution of problem* (11), (12), (13), *from Theorem* 16 *satisfies the following inequalities*

$$\left|\frac{\partial \tilde{q}_{\text{mv}}}{\partial z}\right|_{L_1(R^3)} \le \frac{C}{2}(A_0 + A_1 + A_2 + \beta_3|\tilde{q}_{\text{mv}}|_{L_1(R^3)} + (\beta_1+\beta_2)\left|\frac{\tilde{q}_{\text{mv}}}{z}\right|_{L_1(R^3)} + \beta_1\left|\frac{\partial \tilde{q}_{\text{mv}}}{\partial z}\right|_{L_1(R^3)}) + \left|\frac{\partial \mu}{\partial z}\right|_{L_1(R^3)}, \tag{20}$$

where

$$A_1 = \int_{R^3} z \int_0^\pi \int_0^{2\pi} \left|\frac{\partial \tilde{q}_0(z(e_k-e_\lambda))}{\partial z}\right| \times |\tilde{q}_{\text{mv}}(ze_\lambda,t)|de_\lambda dk,$$

$$A_2 = \int_{R^3} z \int_0^\pi \int_0^{2\pi} |\tilde{q}_0(z(e_k-e_\lambda))| \times \left|\frac{\partial \tilde{q}_{\text{mv}}(ze_\lambda,t)}{\partial z}\right| de_\lambda dk,$$

$$\beta_2 = \left(\frac{1}{\nu}\right)^{\frac{1}{2}} 2^{\frac{11}{2}}\pi\alpha C_0^{\frac{1}{2}}, \beta_3 = \left(\frac{1}{\nu}\right)^{\frac{1}{2}} 8\pi C_2^{\frac{1}{2}},$$

and C_2 *is defined in Lemma* 25, $C = const.$

Proof. From the statement of Theorem 14 we get the following estimate

$$\left|\frac{\partial \tilde{q}_{\text{mv}}}{\partial z}\right|_{L_1(R^3)} \le \frac{C}{2}\Bigg(\int_{R^3}\int_0^\pi\int_0^{2\pi} |\tilde{q}(z(e_k-e_\lambda),t)| \times |\tilde{q}_{\text{mv}}(ze_\lambda,t)|de_\lambda dk + \int_{R^3} z\int_0^\pi\int_0^{2\pi} \left|\frac{\partial \tilde{q}(z(e_k-e_\lambda),t)}{\partial z}\right| \times |\tilde{q}_{\text{mv}}(ze_\lambda,t)|de_\lambda dk + \int_{R^3} z\int_0^\pi\int_0^{2\pi} |\tilde{q}(z(e_k-e_\lambda),t)| \times \left|\frac{\partial \tilde{q}_{\text{mv}}(ze_\lambda,t)}{\partial z}\right| de_\lambda dk\Bigg) + \left|\frac{\partial \mu}{\partial z}\right|_{L_1(R^3)}.$$

Let us introduce the following denotation

$$I_1 = \int_{R^3}\int_0^\pi\int_0^{2\pi} |\tilde{q}(z(e_k-e_\lambda),t)| \times |\tilde{q}_{\text{mv}}(ze_\lambda,t)|de_\lambda dk,$$

$$I_2 = \int_{R^3} z\int_0^\pi\int_0^{2\pi} \left|\frac{\partial \tilde{q}(z(e_k-e_\lambda),t)}{\partial z}\right| \times |\tilde{q}_{\text{mv}}(ze_\lambda,t)|de_\lambda dk,$$

$$I_3 = \int_{R^3} z\int_0^\pi\int_0^{2\pi} |\tilde{q}(z(e_k-e_\lambda),t)| \times \left|\frac{\partial \tilde{q}_{\text{mv}}(ze_\lambda,t)}{\partial z}\right| de_\lambda dk,$$

then

$$\left|\frac{\partial \tilde{q}_{\text{mv}}}{\partial z}\right|_{L_1(R^3)} \le \frac{C}{2}(I_1+I_2+I_3) + \left|\frac{\partial \mu}{\partial z}\right|_{L_1(R^3)}.$$

The estimate of I_1 was obtained in theorem 16, therefore from (15), (18), it follows that

$$I_1 \leq A_0 + \beta_1 \left|\frac{\tilde{q}_{\text{mv}}}{z}\right|_{L_1(R^3)}.$$

Inserting inequality (19) into I_2, we get

$$I_2 \leq \int_{R^3} z \int_0^{\pi} \int_0^{2\pi} \left|\frac{\partial \tilde{q}_0(z(e_k - e_\lambda))}{\partial z}\right| \times |\tilde{q}_{\text{mv}}(ze_\lambda, t)| de_\lambda dk$$

$$+4\alpha \left(\frac{1}{\nu}\right)^{\frac{1}{2}} C_0^{\frac{1}{2}} I_0 \int_{R^3} \frac{|\tilde{q}_{\text{mv}}(k,t)|}{z} dk$$

$$+\left(\frac{1}{2\nu}\right)^{\frac{1}{2}} C_2^{\frac{1}{2}} I_0 \int_{R^3} |\tilde{q}_{\text{mv}}(k,t)| dk,$$

Let us take into account the estimate of I_0 obtained in Lemma 25,

$$I_0 = \int_0^{\pi} \int_0^{2\pi} \frac{de_\lambda}{|e_k - e_\lambda|} = 2^{\frac{7}{2}}\pi.$$

Inserting this value in I_2, we obtain

$$I_2 \leq \int_{R^3} z \int_0^{\pi} \int_0^{2\pi} \left|\frac{\partial \tilde{q}_0(z(e_k - e_\lambda))}{\partial z}\right| \times |\tilde{q}_{\text{mv}}(ze_\lambda, t)| de_\lambda dk$$

$$+\left(\frac{1}{\nu}\right)^{\frac{1}{2}} 2^{\frac{11}{2}} \pi \alpha C_0^{\frac{1}{2}} \int_{R^3} \frac{|\tilde{q}_{\text{mv}}(k,t)|}{z} dk$$

$$+\left(\frac{1}{\nu}\right)^{\frac{1}{2}} 8\pi C_2^{\frac{1}{2}} \int_{R^3} |\tilde{q}_{\text{mv}}(k,t)| dk.$$

Let us introduce the following denotation

$$A_1 = \int_{R^3} z \int_0^{\pi} \int_0^{2\pi} \left|\frac{\partial \tilde{q}_0(z(e_k - e_\lambda))}{\partial z}\right| \times |\tilde{q}_{\text{mv}}(ze_\lambda, t)| de_\lambda dk,$$

then

$$I_2 \leq A_1 + \beta_2 \left|\frac{\tilde{q}_{\text{mv}}}{z}\right|_{L_1(R^3)} + \beta_3 |\tilde{q}_{\text{mv}}|_{L_1(R^3)},$$

where

$$\beta_2 = \left(\frac{1}{\nu}\right)^{\frac{1}{2}} 2^{\frac{11}{2}} \pi \alpha C_0^{\frac{1}{2}}, \qquad \beta_3 = \left(\frac{1}{\nu}\right)^{\frac{1}{2}} 8\pi C_2^{\frac{1}{2}}.$$

Using inequality (16) in I_3, we get

$$I_3 \leq \int_{R^3} z \int_0^{\pi} \int_0^{2\pi} |\tilde{q}_0(z(e_k - e_\lambda))| \times \left|\frac{\partial \tilde{q}_{\text{mv}}(ze_\lambda, t)}{\partial z}\right| de_\lambda dk$$

$$+\left(\frac{1}{2\nu}\right)^{\frac{1}{2}} C_0^{\frac{1}{2}} I_0 \int_{R^3} \left|\frac{\partial \tilde{q}_{\text{mv}}(k,t)}{\partial z}\right| dk.$$

Similarly as we estimated I_2, obtain

$$I_3 \leq A_2 + \beta_1 \left|\frac{\partial \tilde{q}_{\text{mv}}}{\partial z}\right|_{L_1(R^3)},$$

where

$$A_2 = \int_{R^3} z \int_0^{\pi} \int_0^{2\pi} |\tilde{q}_0(z(e_k - e_\lambda))| \times \left|\frac{\partial \tilde{q}_{\text{mv}}(ze_\lambda, t)}{\partial z}\right| de_\lambda dk.$$

Inserting I_1, I_2, I_3 $\left|\frac{\partial \tilde{q}_{\text{mv}}}{\partial z}\right|_{L_1(R^3)}$, we obtain the statement of the theorem.

This completes the proof of Theorem 18.

Lemma 26. *Weak solution of problem* (11), (12), (13), *from Theorem* 16 *satisfies the following inequalities*

$$\left|\frac{\partial^2 \tilde{q}(z(e_k - e_\lambda), t)}{\partial z^2}\right| \leq \left|\frac{\partial^2 \tilde{q}_0(z(e_k - e_\lambda))}{\partial z^2}\right| + \left(\frac{1}{\nu}\right)^{\frac{1}{2}} \frac{16\alpha C_0^{\frac{1}{2}}}{z^3|e_k - e_\lambda|} + \left(\frac{1}{\nu}\right)^{\frac{1}{2}} \frac{8\alpha C_2^{\frac{1}{2}}}{z^2|e_k - e_\lambda|} + \left(\frac{1}{2\nu}\right)^{\frac{1}{2}} \frac{C_4^{\frac{1}{2}}}{z|e_k - e_\lambda|}, \tag{21}$$

where

$$\sup_t |t^m e^{-t}| < \alpha,$$

as $m > 0$,

$$C_4 = \int_0^t \left|\frac{\partial^2 \tilde{F}_1}{\partial z^2}\right|^2 d\tau.$$

Proof. From (14) we have the following inequalities

$$\left|\frac{\partial^2 \tilde{q}(z(e_k - e_\lambda), t)}{\partial z^2}\right| \leq \left|\frac{\partial^2 \tilde{q}_0(z(e_k - e_\lambda))}{\partial z^2}\right|$$

$$+4\nu^2 z^2 |e_k - e_\lambda|^4 \left| \int_0^t (t-\tau)^2 \times e^{-\nu z^2 |e_k - e_\lambda|^2 (t-\tau)} \tilde{F}_1(z(e_k - e_\lambda), \tau) d\tau \right|$$

$$+4\nu z |e_k - e_\lambda|^2 \left| \int_0^t (t-\tau) \times e^{-\nu z^2 |e_k - e_\lambda|^2 (t-\tau)} \frac{\partial \tilde{F}_1}{\partial z}(z(e_k - e_\lambda), \tau) d\tau \right|$$

$$+\left| \int_0^t e^{-\nu z^2 |e_k - e_\lambda|^2 (t-\tau)} \frac{\partial^2 \tilde{F}_1}{\partial z^2}(z(e_k - e_\lambda), \tau) d\tau \right|.$$

Let us introduce the following denotation

$$I_1 = 4\nu^2 z^2 |e_k - e_\lambda|^4 \left| \int_0^t (t-\tau)^2 \right.$$

$$\left. \times e^{-\nu z^2 |e_k - e_\lambda|^2 (t-\tau)} \tilde{F}_1(z(e_k - e_\lambda), \tau) d\tau \right|,$$

$$I_2 = 4\nu z |e_k - e_\lambda|^2 \left| \int_0^t (t-\tau) \right.$$

$$\left. \times e^{-\nu z^2 |e_k - e_\lambda|^2 (t-\tau)} \frac{\partial \tilde{F}_1}{\partial z}(z(e_k - e_\lambda), \tau) d\tau \right|,$$

$$I_3 = \left| \int_0^t e^{-\nu z^2 |e_k - e_\lambda|^2 (t-\tau)} \right.$$

$$\left. \times \frac{\partial^2 \tilde{F}_1}{\partial z^2}(z(e_k - e_\lambda), \tau) d\tau \right|,$$

then

$$\left| \frac{\partial^2 \tilde{q}(z(e_k - e_\lambda), t)}{\partial z^2} \right| \le \left| \frac{\partial^2 \tilde{q}_0(z(e_k - e_\lambda))}{\partial z^2} \right|$$

$$+ I_1 + I_2 + I_3.$$

Using the estimate

$$\sup_t |t^m e^{-t}| < \alpha,$$

as $m > 0$, we estimate I_1, I_2

$$I_1 \le \frac{16\alpha}{z^2} \left| \int_0^t e^{-\nu z^2 |e_k - e_\lambda|^2 \frac{t-\tau}{2}} \right.$$

$$\left. \times \tilde{F}_1(z(e_k - e_\lambda), \tau) d\tau \right|,$$

$$I_2 \le \frac{8\alpha}{z} \left| \int_0^t e^{-\nu z^2 |e_k - e_\lambda|^2 \frac{t-\tau}{2}} \right.$$

$$\left. \times \frac{\partial \tilde{F}_1}{\partial z}(z(e_k - e_\lambda), \tau) d\tau \right|.$$

Using Holder's inequality

$$I_1 \le \frac{16\alpha}{z^2} \left(\int_0^t |e^{-\nu z^2 |e_k - e_\lambda|^2 \frac{t-\tau}{2}}|^p d\tau \right)^{\frac{1}{p}}$$

$$\times \left(\int_0^t |\tilde{F}_1|^q d\tau \right)^{\frac{1}{q}},$$

$$I_2 \le \frac{8\alpha}{z} \left(\int_0^t |e^{-\nu z^2 |e_k - e_\lambda|^2 \frac{t-\tau}{2}}|^p d\tau \right)^{\frac{1}{p}}$$

$$\times \left(\int_0^t \left| \frac{\partial \tilde{F}_1}{\partial z} \right|^q d\tau \right)^{\frac{1}{q}},$$

where p, q satisfy the equality $\frac{1}{p} + \frac{1}{q} = 1$.

For $p = q = 2$ we get

$$I_1 \le 16\alpha \left(\frac{1}{\nu}\right)^{\frac{1}{2}} \frac{C_0^{\frac{1}{2}}}{z^3 |e_k - e_\lambda|},$$

$$I_2 \le 8\alpha \left(\frac{1}{\nu}\right)^{\frac{1}{2}} \frac{C_2^{\frac{1}{2}}}{z^2 |e_k - e_\lambda|}.$$

Taking into account Holder's inequality for I_3, we get

$$I_3 \le \left(\frac{1}{2\nu}\right)^{\frac{1}{2}} \frac{C_4^{\frac{1}{2}}}{z|e_k - e_\lambda|}, C_4 = \int_0^t \left| \frac{\partial^2 \tilde{F}_1}{\partial z^2} \right|^2 d\tau.$$

Inserting I_1, I_2, I_3 in $\left|\frac{\partial^2 \tilde{q}}{\partial z^2}\right|$, we get the statement of the lemma.

This completes the proof of Lemma 26.

Theorem 19. *Weak solution of problem* (11), (12), (13), *from Theorem* 16 *satisfies the following estimate*

$$\left| z \frac{\partial^2 \tilde{q}_{\mathrm{mv}}}{\partial z^2} \right|_{L_1(R^3)} \le \frac{C}{2} (2(A_1 + A_2 + A_3)$$

$$+ A_4 + A_5 + (2\beta_2 + \beta_4) \left| \frac{\tilde{q}_{\mathrm{mv}}}{z} \right|_{L_1(R^3)}$$

$$+ (2\beta_3 + \beta_5) |\tilde{q}_{\mathrm{mv}}|_{L_1(R^3)} + \beta_6 |z \tilde{q}_{\mathrm{mv}}|_{L_1(R^3)}$$

$$+ 2(\beta_1 + \beta_2) \left| \frac{\partial \tilde{q}_{\mathrm{mv}}}{\partial z} \right|_{L_1(R^3)} + 2\beta_3 \left| z \frac{\partial \tilde{q}_{\mathrm{mv}}}{\partial z} \right|_{L_1(R^3)}$$

$$+ \beta_1 \left| z \frac{\partial^2 \tilde{q}_{\mathrm{mv}}}{\partial z^2} \right|_{L_1(R^3)}) + \left| z \frac{\partial^2 \mu}{\partial z^2} \right|_{L_1(R^3)}, \quad (22)$$

where

$$A_3 = \int_{R^3} z^2 \int_0^\pi \int_0^{2\pi} \left| \frac{\partial \tilde{q}_0(z(e_k - e_\lambda))}{\partial z} \right|$$

$$\times \left| \frac{\partial \tilde{q}_{\mathrm{mv}}(z e_\lambda, t)}{\partial z} \right| de_\lambda dk,$$

$$A_4 = \int_{R^3} z^2 \int_0^\pi \int_0^{2\pi} \left| \frac{\partial^2 \tilde{q}_0(z(e_k - e_\lambda))}{\partial z^2} \right|$$

$$\times |\tilde{q}_{\mathrm{mv}}(z e_\lambda, t)| de_\lambda dk,$$

$$A_5 = \int_{R^3} z^2 \int_0^\pi \int_0^{2\pi} |\tilde{q}_0(z(e_k - e_\lambda))|$$

$$\times \left| \frac{\partial^2 \tilde{q}_{\mathrm{mv}}(z e_\lambda, t)}{\partial z^2} \right| de_\lambda dk,$$

$$\beta_4 = \left(\frac{1}{\nu}\right)^{\frac{1}{2}} 2^{\frac{15}{2}} \pi \alpha C_0^{\frac{1}{2}},$$

$$\beta_5 = \left(\frac{1}{\nu}\right)^{\frac{1}{2}} 2^{\frac{13}{2}} \pi \alpha C_2^{\frac{1}{2}},$$

$$\beta_6 = \left(\frac{1}{\nu}\right)^{\frac{1}{2}} 8\pi C_4^{\frac{1}{2}},$$

and C_4 *is defined in Lemma* 26.

Proof. From the statement of Theorem 14 we have the estimate

$$\left|z\frac{\partial^2\tilde{q}_{\mathrm{mv}}}{\partial z^2}\right|_{L_1(R^3)} \le \frac{C}{2}(2\int_{R^3} z\int_0^{\pi}\int_0^{2\pi} |\tilde{q}(z(e_k-e_\lambda),t)| \times\left|\frac{\partial\tilde{q}_{\mathrm{mv}}(ze_\lambda,t)}{\partial z}\right| de_\lambda dk$$

$$+2\int_{R^3} z\int_0^{\pi}\int_0^{2\pi}\left|\frac{\partial\tilde{q}(z(e_k-e_\lambda),t)}{\partial z}\right| \times|\tilde{q}_{\mathrm{mv}}(ze_\lambda,t)|de_\lambda dk+$$

$$+2\int_{R^3} z^2\int_0^{\pi}\int_0^{2\pi}\left|\frac{\partial\tilde{q}(z(e_k-e_\lambda),t)}{\partial z}\right| \times\left|\frac{\partial\tilde{q}_{\mathrm{mv}}(ze_\lambda,t)}{\partial z}\right| de_\lambda dk+$$

$$+\int_{R^3} z^2\int_0^{\pi}\int_0^{2\pi}\left|\frac{\partial^2\tilde{q}(z(e_k-e_\lambda),t)}{\partial z^2}\right| \times|\tilde{q}_{\mathrm{mv}}(ze_\lambda,t)|de_\lambda dk+$$

$$+\int_{R^3} z^2\int_0^{\pi}\int_0^{2\pi}|\tilde{q}(z(e_k-e_\lambda),t)| \times\left|\frac{\partial^2\tilde{q}_{\mathrm{mv}}(ze_\lambda,t)}{\partial z^2}\right| de_\lambda dk)$$

$$+\left|z\frac{\partial^2\mu}{\partial z^2}\right|_{L_1(R^3)} = \frac{C}{2}\sum_{j=1}^{5} I_j+\left|z\frac{\partial^2\mu}{\partial z^2}\right|_{L_1(R^3)}.$$

Let us use the estimates for $I_1,\ I_2$

$$I_1 = 2\int_{R^3} z\int_0^{\pi}\int_0^{2\pi}|\tilde{q}(z(e_k-e_\lambda),t)| \times\left|\frac{\partial\tilde{q}_{\mathrm{mv}}(ze_\lambda,t)}{\partial z}\right| de_\lambda dk$$

$$\le 2\left(A_1+\beta_2\left|\frac{\tilde{q}_{\mathrm{mv}}}{z}\right|_{L_1(R^3)}+\beta_3|\tilde{q}_{\mathrm{mv}}|_{L_1(R^3)}\right),$$

$$I_2 = 2\int_{R^3} z\int_0^{\pi}\int_0^{2\pi}\left|\frac{\partial\tilde{q}(z(e_k-e_\lambda),t)}{\partial z}\right| \times|\tilde{q}_{\mathrm{mv}}(ze_\lambda,t)|de_\lambda dk$$

$$\le 2\left(A_2+\beta_1\left|\frac{\partial\tilde{q}_{\mathrm{mv}}}{\partial z}\right|_{L_1(R^3)}\right).$$

Let us use inequality (19) to estimate I_3, then we get

$$I_3 = 2\int_{R^3} z^2\int_0^{\pi}\int_0^{2\pi}\left|\frac{\partial\tilde{q}(z(e_k-e_\lambda),t)}{\partial z}\right| \times\left|\frac{\partial\tilde{q}_{\mathrm{mv}}(ze_\lambda,t)}{\partial z}\right| de_\lambda dk$$

$$< 2(\int_{R^3} z^2\int_0^{\pi}\int_0^{2\pi}\left|\frac{\partial\tilde{q}_0(z(e_k-e_\lambda))}{\partial z}\right| \times\left|\frac{\partial\tilde{q}_{\mathrm{mv}}(ze_\lambda,t)}{\partial z}\right| de_\lambda dk$$

$$+4\alpha\left(\frac{1}{\nu}\right)^{\frac{1}{2}}C_0^{\frac{1}{2}}I_0\int_{R^3}\left|\frac{\partial\tilde{q}_{\mathrm{mv}}(k,t)}{\partial z}\right| dk$$

$$+\left(\frac{1}{2\nu}\right)^{\frac{1}{2}}C_2^{\frac{1}{2}}I_0\int_{R^3} z\left|\frac{\partial\tilde{q}_{\mathrm{mv}}(k,t)}{\partial z}\right| dk).$$

Inserting the value of the integral I_0, from Lemma 18, we get

$$I_3 = 2(\int_{R^3} z^2\int_0^{\pi}\int_0^{2\pi}\left|\frac{\partial\tilde{q}_0(z(e_k-e_\lambda),t)}{\partial z}\right| \times\left|\frac{\partial\tilde{q}_{\mathrm{mv}}(ze_\lambda,t)}{\partial z}\right| de_\lambda dk$$

$$+\left(\frac{1}{\nu}\right)^{\frac{1}{2}}2^{\frac{11}{2}}\pi\alpha C_0^{\frac{1}{2}}\int_{R^3}\left|\frac{\partial\tilde{q}_{\mathrm{mv}}(k,t)}{\partial z}\right| dk$$

$$+\left(\frac{1}{\nu}\right)^{\frac{1}{2}}8\pi C_2^{\frac{1}{2}}\int_{R^3} z\left|\frac{\partial\tilde{q}_{\mathrm{mv}}(k,t)}{\partial z}\right| dk)$$

$$= 2(\int_{R^3} z^2\int_0^{\pi}\int_0^{2\pi}\left|\frac{\partial\tilde{q}_0(z(e_k-e_\lambda))}{\partial z}\right| \times\left|\frac{\partial\tilde{q}_{\mathrm{mv}}(ze_\lambda,t)}{\partial z}\right| de_\lambda dk$$

$$+\beta_2\int_{R^3}\left|\frac{\partial\tilde{q}_{\mathrm{mv}}(k,t)}{\partial z}\right| dk+\beta_3\int_{R^3} z\left|\frac{\partial\tilde{q}_{\mathrm{mv}}(k,t)}{\partial z}\right| dk).$$

Let us introduce the following denotation

$$A_3 = \int_{R^3} z^2\int_0^{\pi}\int_0^{2\pi}\left|\frac{\partial\tilde{q}_0(z(e_k-e_\lambda))}{\partial z}\right| \times\left|\frac{\partial\tilde{q}_{\mathrm{mv}}(ze_\lambda,t)}{\partial z}\right| de_\lambda dk,$$

then

$$I_3 \le 2(A_3+\beta_2\int_{R^3}\left|\frac{\partial\tilde{q}_{\mathrm{mv}}(k,t)}{\partial z}\right| dk +\beta_3\int_{R^3} z\left|\frac{\partial\tilde{q}_{\mathrm{mv}}(k,t)}{\partial z}\right| dk).$$

Applying inequality (21) to estimate I_4, we get

$$I_4 = \int_{R^3} z^2 \int_0^{\pi}\int_0^{2\pi} \left|\frac{\partial^2 \tilde{q}(z(e_k-e_\lambda),t)}{\partial z^2}\right| \times |\tilde{q}_{\mathrm{mv}}(ze_\lambda,t)|de_\lambda dk$$

$$\leq \int_{R^3} z^2 \int_0^{\pi}\int_0^{2\pi} \left|\frac{\partial^2 \tilde{q}_0(z(e_k-e_\lambda))}{\partial z^2}\right| \times |\tilde{q}_{\mathrm{mv}}(ze_\lambda,t)|de_\lambda dk$$

$$+\left(\frac{1}{\nu}\right)^{\frac{1}{2}} 16\alpha C_0^{\frac{1}{2}} I_0 \int_{R^3} \frac{1}{z}|\tilde{q}_{\mathrm{mv}}(k,t)|dk$$

$$+\left(\frac{1}{\nu}\right)^{\frac{1}{2}} 8\alpha C_2^{\frac{1}{2}} I_0 \int_{R^3} |\tilde{q}_{\mathrm{mv}}(k,t)|dk$$

$$+\left(\frac{1}{2\nu}\right)^{\frac{1}{2}} C_4^{\frac{1}{2}} I_0 \int_{R^3} z|\tilde{q}_{\mathrm{mv}}(k,t)|dk.$$

Inserting the value of I_0, we obtain

$$I_4 \leq \int_{R^3} z^2 \int_0^{\pi}\int_0^{2\pi} \left|\frac{\partial^2 \tilde{q}_0(z(e_k-e_\lambda))}{\partial z^2}\right| \times |\tilde{q}_{\mathrm{mv}}(ze_\lambda,t)|de_\lambda dk$$

$$+\left(\frac{1}{\nu}\right)^{\frac{1}{2}} 2^{\frac{15}{2}}\pi\alpha C_0^{\frac{1}{2}} \int_{R^3} \frac{1}{z}|\tilde{q}_{\mathrm{mv}}(k,t)|dk$$

$$+\left(\frac{1}{\nu}\right)^{\frac{1}{2}} 2^{\frac{13}{2}}\pi\alpha C_2^{\frac{1}{2}} \int_{R^3} |\tilde{q}_{\mathrm{mv}}(k,t)|dk$$

$$+\left(\frac{1}{2\nu}\right)^{\frac{1}{2}} 8\pi C_4^{\frac{1}{2}} \int_{R^3} z|\tilde{q}_{\mathrm{mv}}(k,t)|dk.$$

Let us introduce the following denotation

$$\beta_4 = \left(\frac{1}{\nu}\right)^{\frac{1}{2}} 2^{\frac{15}{2}}\pi\alpha C_0^{\frac{1}{2}}, \beta_5 = \left(\frac{1}{\nu}\right)^{\frac{1}{2}} 2^{\frac{13}{2}}\pi\alpha C_2^{\frac{1}{2}},$$

$$\beta_6 = \left(\frac{1}{2\nu}\right)^{\frac{1}{2}} 8\pi C_4^{\frac{1}{2}},$$

then

$$I_4 \leq \int_{R^3} z^2 \int_0^{\pi}\int_0^{2\pi} \left|\frac{\partial^2 \tilde{q}_0(z(e_k-e_\lambda))}{\partial z^2}\right|$$

$$\times |\tilde{q}_{\mathrm{mv}}(ze_\lambda,t)|de_\lambda dk + \beta_4 \int_{R^3} \frac{1}{z}|\tilde{q}_{\mathrm{mv}}(k,t)|dk$$

$$+\beta_5 \int_{R^3} |\tilde{q}_{\mathrm{mv}}(k,t)|dk + \beta_6 \int_{R^3} z|\tilde{q}_{\mathrm{mv}}(k,t)|dk.$$

Introduce the denotation

$$A_4 = \int_{R^3} z^2 \int_0^{\pi}\int_0^{2\pi} \left|\frac{\partial^2 \tilde{q}_0(z(e_k-e_\lambda))}{\partial z^2}\right| \times |\tilde{q}_{\mathrm{mv}}(ze_\lambda,t)|de_\lambda dk,$$

then

$$I_4 \leq A_4 + \beta_4 \int_{R^3} \frac{1}{z}|\tilde{q}_{\mathrm{mv}}(k,t)|dk$$

$$+\beta_5 \int_{R^3} |\tilde{q}_{\mathrm{mv}}(k,t)|dk + \beta_6 \int_{R^3} z|\tilde{q}_{\mathrm{mv}}(k,t)|dk.$$

Using inequality (16) to estimate I_5 , we obtain

$$I_5 = \int_{R^3} z^2 \int_0^{\pi}\int_0^{2\pi} |\tilde{q}(z(e_k-e_\lambda),t)| \times \left|\frac{\partial^2 \tilde{q}_{\mathrm{mv}}(ze_\lambda,t)}{\partial z^2}\right| de_\lambda dk$$

$$\leq \int_{R^3} z^2 \int_0^{\pi}\int_0^{2\pi} |\tilde{q}_0(z(e_k-e_\lambda))| \times \left|\frac{\partial^2 \tilde{q}_{\mathrm{mv}}(ze_\lambda,t)}{\partial z^2}\right| de_\lambda dk$$

$$+\left(\frac{1}{2\nu}\right)^{\frac{1}{2}} C_0^{\frac{1}{2}} I_0 \int_{R^3} z\left|\frac{\partial^2 \tilde{q}_{\mathrm{mv}}(k,t)}{\partial z^2}\right| dk.$$

Inserting the value of the integral I_0, we obtain

$$I_5 \leq \int_{R^3} z^2 \int_0^{\pi}\int_0^{2\pi} |\tilde{q}_0(z(e_k-e_\lambda))| \times \left|\frac{\partial^2 \tilde{q}_{\mathrm{mv}}(ze_\lambda,t)}{\partial z^2}\right| de_\lambda dk + \beta_1 \left|z\frac{\partial^2 \tilde{q}_{\mathrm{mv}}}{\partial z^2}\right|_{L_1(R^3)}.$$

Let us introduce the following denotation

$$A_5 = \int_{R^3} z^2 \int_0^{\pi}\int_0^{2\pi} |\tilde{q}_0(z(e_k-e_\lambda))| \times \left|\frac{\partial^2 \tilde{q}_{\mathrm{mv}}(ze_\lambda,t)}{\partial z^2}\right| de_\lambda dk,$$

then

$$I_5 \leq A_5 + \beta_1 \left|z\frac{\partial^2 \tilde{q}_{\mathrm{mv}}}{\partial z^2}\right|_{L_1(R^3)}.$$

Inserting I_j, $(j=1,\ldots,5)$ in $\left|z\frac{\partial^2 \tilde{q}_{\mathrm{mv}}}{\partial z^2}\right|_{L_1(R^3)}$, we obtain the statement of the theorem.

This completes the proof of Theorem 19.

Lemma 27. *Weak solution of problem* (11), (12), (13), *from Theorem* 16 *satisfies the following estimate*

$$\left|\frac{\tilde{q}_{\mathrm{mv}}}{z}\right|_{L_1(R^3)} \leq B_0 K, \tag{23}$$

$$|\tilde{q}_{\mathrm{mv}}|_{L_1(R^3)} \leq B_1 K, \tag{24}$$

$$|z\tilde{q}_{\text{mv}}|_{L_1(R^3)} \le B_2 K, \tag{25}$$

where

$$K = \frac{\nu^{\frac{1}{2}}}{\nu^{\frac{1}{2}} - 4\pi C C_0^{\frac{1}{2}}}, B_0 = \frac{C}{2}A_0 + \left|\frac{\mu}{z}\right|_{L_1(R^3)},$$

$$B_1 = \tfrac{C}{2}A_0^{(1)} + |\mu|_{L_1(R^3)}, \tag{26}$$

$$B_2 = \frac{C}{2}A_0^{(2)} + |z\mu|_{L_1(R^3)},$$

$$A_0^{(2)} = \int_{R^3}\int_0^{\pi}\int_0^{2\pi} z^2|\tilde{q}_0(z(e_k - e_\lambda))| \times |\tilde{q}_{\text{mv}}(ze_\lambda, t)|de_\lambda dk.$$

Proof. From inequality (15) and estimate (17), we make the sequence of estimates

$$|z^n\tilde{q}_{\text{mv}}|_{L_1(R^3)} \le \frac{C}{2}(A_0^{(n+1)} + \beta_1|z^n\tilde{q}_{\text{mv}}|_{L_1(R^3)}) + |z^n\mu|_{L_1(R^3)},$$

where

$$A_0^{(n+1)} = \int_{R^3}\int_0^{\pi}\int_0^{2\pi} z^{n+1}|\tilde{q}_0(z(e_k - e_\lambda))| \times |\tilde{q}_{\text{mv}}(ze_\lambda, t)|de_\lambda dk.$$

$$\beta_1 = \left(\frac{1}{\nu}\right)^{\frac{1}{2}} 8\pi C_0^{\frac{1}{2}},$$

and n is an exponent of z. From this recurrence formula, as $n = 0$, $n = -1$, we get estimates (17) and (18) accordingly.

For $n = 1$ we have

$$|z\tilde{q}_{\text{mv}}|_{L_1(R^3)} \le \frac{C}{2}(A_0^{(2)} + \beta_1|z\tilde{q}_{\text{mv}}|_{L_1(R^3)}) + |z\mu|_{L_1(R^3)}.$$

Considering estimates (17), (18) and the last estimate, we obtain the statement of the lemma.

This proves Lemma 27.

Lemma 28. *Weak solution of problem* (11), (12), (13), *from Theorem* 16 *satisfies the following estimates*

$$\left|\frac{\partial\tilde{q}_{\text{mv}}}{\partial z}\right|_{L_1(R^3)} \le D_0K^2 + D_1K, \tag{27}$$

$$\left|z\frac{\partial\tilde{q}_{\text{mv}}}{\partial z}\right|_{L_1(R^3)} \le D_2K^2 + D_3K, \tag{28}$$

where

$$D_0 = \frac{C}{2}(\beta_3^{(0)}B_1 + (\beta_1^{(0)} + \beta_2^{(0)})B_0),$$

$$D_1 = \frac{C}{2}(A_0 + A_1 + A_2) + \left|\frac{\partial\mu}{\partial z}\right|_{L_1(R^3)},$$

$$D_2 = \frac{C}{2}(\beta_3^{(0)}B_2 + (\beta_1^{(0)} + \beta_2^{(0)})B_1),$$

$$D_3 = \frac{C}{2}(A_0^{(1)} + A_1^{(1)} + A_2^{(1)}) + \left|z\frac{\partial\mu}{\partial z}\right|_{L_1(R^3)},$$

$$A_1^{(1)} = \int_{R^3} z^2\int_0^{\pi}\int_0^{2\pi}\left|\frac{\partial\tilde{q}_0(z(e_k - e_\lambda))}{\partial z}\right| \times |\tilde{q}_{\text{mv}}(ze_\lambda, t)|de_\lambda dk,$$

$$A_2^{(1)} = \int_{R^3} z^2\int_0^{\pi}\int_0^{2\pi}|\tilde{q}_0(z(e_k - e_\lambda))| \times \left|\frac{\partial\tilde{q}_{\text{mv}}(ze_\lambda, t)}{\partial z}\right| de_\lambda dk,$$

$$\beta_1^{(0)} = \frac{8\pi C_0^{\frac{1}{2}}}{\nu^{\frac{1}{2}}}, \qquad \beta_2^{(0)} = \frac{2^{\frac{11}{2}}\pi\alpha C_0^{\frac{1}{2}}}{\nu^{\frac{1}{2}}},$$

$$\beta_3^{(0)} = \frac{8\pi C_2^{\frac{1}{2}}}{\nu^{\frac{1}{2}}},$$

Proof. From inequality (19) and estimate (20), let us make the sequence of estimates

$$\left|z^n\frac{\partial\tilde{q}_{\text{mv}}}{\partial z}\right|_{L_1(R^3)} \le \frac{C}{2}(A_0^{(n)} + A_1^{(n)} + A_2^{(n)} + \beta_3|z^n\tilde{q}_{\text{mv}}|_{L_1(R^3)} + (\beta_1 + \beta_2)\left|\frac{\tilde{q}_{\text{mv}}}{z^{1-n}}\right|_{L_1(R^3)} + \beta_1\left|z^n\frac{\partial\tilde{q}_{\text{mv}}}{\partial z}\right|_{L_1(R^3)}) + \left|z^n\frac{\partial\mu}{\partial z}\right|_{L_1(R^3)},$$

where

$$A_0^{(n)} = \int_{R^3}\int_0^{\pi}\int_0^{2\pi} z^n|\tilde{q}_0(z(e_k - e_\lambda))| \times |\tilde{q}_{\text{mv}}(ze_\lambda, t)|de_\lambda dk,$$

$$A_1^{(n)} = \int_{R^3} z^{n+1}\int_0^{\pi}\int_0^{2\pi}\left|\frac{\partial\tilde{q}_0(z(e_k - e_\lambda))}{\partial z}\right| \times |\tilde{q}_{\text{mv}}(ze_\lambda, t)|de_\lambda dk,$$

$$A_2^{(n)} = \int_{R^3} z^{n+1}\int_0^{\pi}\int_0^{2\pi}|\tilde{q}_0(z(e_k - e_\lambda))| \times \left|\frac{\partial\tilde{q}_{\text{mv}}(ze_\lambda, t)}{\partial z}\right| de_\lambda dk,$$

and n is an exponent of z. From this recurrence formula, we get estimate (17) and (18) for $n = 0$, $n = 1$, accordingly. And

$$\left|z\frac{\partial\tilde{q}_{\text{mv}}}{\partial z}\right|_{L_1(R^3)} \le \frac{C}{2}(A_0^{(1)} + A_1^{(1)} + A_2^{(1)} + \beta_3|z\tilde{q}_{\text{mv}}|_{L_1(R^3)} + (\beta_1 + \beta_2)|\tilde{q}_{\text{mv}}|_{L_1(R^3)}$$

$$+\beta_1\left|z\frac{\partial\tilde{q}_{\text{mv}}}{\partial z}\right|_{L_1(R^3)})+\left|z\frac{\partial\mu}{\partial z}\right|_{L_1(R^3)},$$

Considering e stimate (17) a nd t he l ast es timate, w e obtain the statement of the lemma.

This completes the proof of Lemma 28.

Lemma 29. *The s olution of t he p roblem* (11), (1 2), (13), *from Theorem* 16, *satisfies the following estimate*

$$\left|z\frac{\partial^2\tilde{q}_{\text{mv}}}{\partial z^2}\right|_{L_1(R^3)}\le P_0K^3$$
$$+P_1K^2+P_2K, \qquad (29)$$

where

$$P_0=C(\beta_3^{(0)}D_2+(\beta_1^{(0)}+\beta_2^{(0)})D_0),$$
$$P_1=\frac{C}{2}((2\beta_2^{(0)}+\beta_4^{(0)})B_0$$
$$+(2\beta_3^{(0)}+\beta_5^{(0)})B_1+\beta_6^{(0)}B_2$$
$$+2\beta_3^{(0)}D_3+2(\beta_1^{(0)}+\beta_2^{(0)})D_1),$$
$$P_2=\frac{C}{2}(2(A_1+A_2+A_3)$$
$$+A_4+A_5)+\left|z\frac{\partial^2\mu}{\partial z^2}\right|_{L_1(R^3)},$$
$$\beta_4^{(0)}=\frac{2^{\frac{15}{2}}\pi\alpha C_0^{\frac12}}{\nu^{\frac12}},\qquad \beta_5^{(0)}=\frac{2^{\frac{13}{2}}\pi\alpha C_2^{\frac12}}{\nu^{\frac12}},$$
$$\beta_6^{(0)}=\frac{8\pi C_4^{\frac12}}{\nu^{\frac12}}.$$

Proof. From (22), we obtain the following estimate

$$\left|z\frac{\partial^2\tilde{q}_{\text{mv}}}{\partial z^2}\right|_{L_1(R^3)}\le\frac{C}{2}(2(A_1+A_2+A_3)$$
$$+A_4+A_5+(2\beta_2^{(0)}+\beta_4(0))\left|\frac{\tilde{q}_{\text{mv}}}{z}\right|_{L_1(R^3)}$$
$$+(2\beta_3(0)+\beta_5(0))|\tilde{q}_{\text{mv}}|_{L_1(R^3)}$$
$$+\beta_6(0)|z\tilde{q}_{\text{mv}}|_{L_1(R^3)}+$$
$$+2(\beta_1(0)+\beta_2(0))\left|\frac{\partial\tilde{q}_{\text{mv}}}{\partial z}\right|_{L_1(R^3)}$$
$$+2\beta_3(0)\left|z\frac{\partial\tilde{q}_{\text{mv}}}{\partial z}\right|_{L_1(R^3)})+\left|z\frac{\partial^2\mu}{\partial z^2}\right|_{L_1(R^3)}.$$

Using e stimates (23)-(28) i n t he l ast i nequality, we obtain the statement of the lemma.

This proves Lemma 29.

Theorem 20. *The solution of the problem* (11), (12), (13), *from Theorem* 16, *satisfies the following estimate*

$$|\tilde{q}|_{L_1(R^3)}\le\left(\gamma_1C_0+\gamma_2C_0^{\frac12}C_2^{\frac12}+\gamma_3C_2\right)K^3$$
$$+\left(\gamma_4C_0^{\frac12}+\gamma_5C_2^{\frac12}+\gamma_6C_4^{\frac12}\right)K^2$$
$$+\left(\gamma_7C_0^{\frac12}+\gamma_8C_2^{\frac12}+\gamma_9\right)K,$$

where

$$K=\frac{\nu^{\frac12}}{\nu^{\frac12}-4\pi CC_0^{\frac12}},C_0=\int_0^t\dagger|\tilde{F}_1|^2d\tau,$$
$$F_1=(q,\nabla)q+F,$$
$$C_2=\int_0^t\dagger\left|\frac{\partial\tilde{F}_1}{\partial z}\right|^2d\tau,C_4=\int_0^t\dagger\left|\frac{\partial^2\tilde{F}_1}{\partial z^2}\right|^2d\tau,$$
$$\gamma_1=\frac{C^22^3\pi^2}{\nu}(1+2^{\frac52})B_0,$$
$$\gamma_2=\frac{C^22^4\pi^2}{\nu}(1+2^{\frac52})B_1,$$
$$\gamma_3=\frac{C^22^3\pi^2}{\nu}B_2,$$
$$\gamma_4=\frac{C2^3\pi}{\nu^{\frac12}}((1+2^{\frac92})B_0+(1+2^{\frac52})D_1),$$
$$\gamma_5=\frac{C2^3\pi}{\nu^{\frac12}}((1+2^{\frac32})B_1+D_3),$$
$$\gamma_6=\frac{C2^3\pi}{\nu^{\frac12}},$$
$$\gamma_7=\frac{C2^2\pi}{\nu^{\frac12}}\left(1+2^{\frac52}\right)B_0,\qquad\gamma_8=\frac{C2^2\pi}{\nu^{\frac12}}B_1,$$
$$\gamma_9=\frac{C}{2}(D_1+P_2),\ B_0=\frac{C}{2}A_0+\left|\frac{\mu}{z}\right|_{L_1(R^3)},$$
$$B_1=\frac{C}{2}A_0^{(1)}+|\mu|_{L_1(R^3)},\ B_2=\frac{C}{2}A_0^{(2)}+|z\mu|_{L_1(R^3)},$$
$$D_1=\frac{C}{2}(A_0+A_1+A_2)+\left|\frac{\partial\mu}{\partial z}\right|_{L_1(R^3)},$$
$$D_3=\frac{C}{2}\left(A_0^{(1)}+A_1^{(1)}+A_2^{(1)}\right)+\left|z\frac{\partial\mu}{\partial z}\right|_{L_1(R^3)},$$
$$P_2=\frac{C}{2}(2(A_1+A_2+A_3)$$
$$+A_4+A_5)+\left|z\frac{\partial^2\mu}{\partial z^2}\right|_{L_1(R^3)},$$
$$\frac{C}{2}=\frac{9\pi}{4(2\pi)^3},$$

the function μ *is defined in Theorem* 15.

Proof. From the Theorem 8

$$|\tilde{q}|_{L_1(R^3)}\le\left|\frac{\tilde{q}_{\text{mv}}}{z}\right|_{L_1(R^3)}$$

$$+2\left|\frac{\partial\tilde{q}_{\mathrm{mv}}}{\partial z}\right|_{L_1(R^3)}+\frac{1}{4}\left|z\frac{\partial^2\tilde{q}_{\mathrm{mv}}}{\partial z^2}\right|_{L_1(R^3)}.$$

Using estimates (23), (27), (29) in the right side of this inequality, we get

$$|\tilde{q}|_{L_1(R^3)} \le B_0K + 2(D_0K^2 + D_1K) + \frac{1}{4}(P_0K^3 + P_1K^2 + P_2K)$$

$$\le \frac{1}{4}P_0K^3 + (2D_0 + P_1)K^2 + (B_0 + D_1 + P_2)K,$$

where B_i, K are defined in Lemma 27, D_i is defined in Lemma 28, and P_i is defined in Lemma 29. Taking into account these notations and calculating the coefficients at C_0, C_2, C_4, we obtain the statement of the theorem.

This proves Theorem 20.

Lemma 30. *The function* μ, *defined in Theorem* 15, *satisfies the following estimates*

$$|\mu|_{L_1(R^3)} \le const, \qquad |z\mu|_{L_1(R^3)} \le const,$$

$$\left|\frac{\partial\mu}{\partial z}\right|_{L_1(R^3)} \le const,$$

$$\left|z\frac{\partial\mu}{\partial z}\right|_{L_1(R^3)} \le const, \qquad \left|z\frac{\partial^2\mu}{\partial z^2}\right|_{L_1(R^3)} \le const.$$

Proof. We can get the estimate of cubic members w.r.t. $\tilde{q}$ in μ if we resume all the methods for estimating square members w.r.t. $\tilde{q}$.

This completes the proof of Lemma 30.

Lemma 31. *Weak solution of problem* (11), (12), (13), *from Theorem* 16 *satisfies the following estimates*

$$A_0 \le 2M_1\int_{R^3}(|\tilde{q}_0(ze_k)|)_{\mathrm{mv}}\,dk,$$

$$A_0^{(1)} \le 2M_1\int_{R^3}z(|\tilde{q}_0(ze_k)|)_{\mathrm{mv}}\,dk,$$

$$A_0^{(2)} \le 2M_1\int_{R^3}z^2(|\tilde{q}_0(ze_k)|)_{\mathrm{mv}}\,dk,$$

$$A_1 \le 2M_1\int_{R^3}z\left(\left|\frac{\partial\tilde{q}_0(ze_k)}{\partial z}\right|\right)_{\mathrm{mv}}dk,$$

$$A_1^{(1)} \le 2M_1\int_{R^3}z^2\left(\left|\frac{\partial\tilde{q}_0(ze_k)}{\partial z}\right|\right)_{\mathrm{mv}}dk,$$

$$A_2 \le 2M_2\int_{R^3}z(|\tilde{q}_0(ze_k)|)_{\mathrm{mv}}\,dk,$$

$$A_2^{(1)} \le 2M_2\int_{R^3}z^2(|\tilde{q}_0(ze_k)|)_{\mathrm{mv}}\,dk,$$

$$A_3 \le 2M_2\int_{R^3}z^2\left(\left|\frac{\partial\tilde{q}_0(ze_k)}{\partial z}\right|\right)_{\mathrm{mv}}dk,$$

$$A_4 \le 2M_1\int_{R^3}z^2\left(\left|\frac{\partial^2\tilde{q}_0(ze_k)}{\partial z^2}\right|\right)_{\mathrm{mv}}dk,$$

$$A_5 \le 2M_3\int_{R^3}z^2(|\tilde{q}_0(ze_k)|)_{\mathrm{mv}}\,dk.$$

Proof. The proof follows from Lemmas 18, 19, 20.

This proves Lemma 31.

Theorem 21. *Suppose that*

$$q_0 \in W_2^1(R^3), F_0 \in L_2(Q_T),$$

$$\tilde{F}_0 \in L_1(Q_T), \frac{\partial\tilde{F}_0}{\partial z} \in L_1(Q_T),$$

$$\frac{\partial^2\tilde{F}_0}{\partial z^2} \in L_1(Q_T), \tilde{q}_0 \in L_1(R^3),$$

$$I_j = \int_{R^3}z^{j-1}(|\tilde{q}_0(ze_k)|)_{\mathrm{mv}}\,dk \le const,$$

$$(j = \overline{1,3}),$$

$$I_j = \int_{R^3}z^{j-3}\left(\left|\frac{\partial\tilde{q}_0(ze_k)}{\partial z}\right|\right)_{\mathrm{mv}}dk \le const,$$

$$(j = \overline{4,5}),$$

$$I_6 = \int_{R^3}z^2\left(\left|\frac{\partial^2\tilde{q}_0(ze_k)}{\partial z^2}\right|\right)_{\mathrm{mv}}dk \le const.$$

Then there exists a unique weak solution of (11), (12), (13), *satisfying the following inequalities*

$$\max_t\sum_{i=1}^{3}|\tilde{q}_i|_{L_1(R^3)} \le const,$$

where $const$ *depends only on the theorem conditions.*

Proof. It is sufficient to get uniform estimates of the maximum q_i to prove that the theorem. These obviously follow from the estimate $|\tilde{q}_i|_{L_1(R^3)}$. Uniform estimates allow to extend the rules of the local existence and unicity local to an interval, where they are correct. To estimate the component of velocity, we use statement 2

$$q_i = \frac{q_i}{\int_0^T||q_x||^2_{L_2(R^3)}dt + A + 1},$$

$$A = \frac{4}{\nu^{\frac{1}{3}}(CC_0+1)^{\frac{2}{3}}}.$$

Using Lemmas 21, 22 for the potential

$$q_i = \frac{q_i}{\int_0^T||q_x||^2_{L_2(R^3)}dt + A + 1}$$

We have $N(q_i) < 1$, *i.e.*, it is not necessary to take into account normalization numbers when proving the theorem. Now the statetement of the theorem follows from Theorems 20, 17, Lemmas 21, 30, 31 and the conditions of Theorem 21, that give uniform of velocity maxima at a specified interval of time.

This comletes the proof of Theorem 21.

Note. In the estimate for $\tilde{q}$ the condition $q(0) > 1$ is used. This conditioncan be obviated if we use smooth and bounded function w and make all the estimates for $q_1 = q + w$ such that $q_1(0) > 1$ is satisfied. Using the function w, we also choose the constant A concordant with the constant ε from Lemma 3.

Theorem 21 proves the global solvability and unicity of the Cauchy problem for Navier-Stokes' equation.

10. CONCLUSIONS

In Introduction we mentioned the authors whose scientific researches we consider appropriate to call the prehistory of this work. The list of these authors may be considerably extended if we enumerate all the predecessors diachronically or by the significance of their contribution into this research. Actually we intended to obtain evident results which were directly and indirectly indicated by these authors in their scientific works. We do not concentrate on the solution to the multi- dimensional problem of quantum scattering theory although it follows from some certain statements proved in this work. In fact, the problem of over-determination in the multi-dimensional inverse problem of quantum scattering theory is obviated since a potential can be defined by amplitude averaging when the amplitude is a function of three variables. In the classic case of the multi- dimensional inverse problem of quantum scattering theory the potential requires restoring with respect to the amplitude that depends on five variables. This obviously leads to the problem of over-determination. Further detalization could have distracted us from the general research line of the work consisting in application of energy and momentum conservation laws in terms of wave functions to the theory of nonlinear equations. This very method we use in solving the problem of the century, the problem of solvability of the Cauchy problem for Navier-Stokes' equations of viscous incompressible fluid. Let us also note the importance of the fact that the laws of momentum and energy conservation in terms of wave functions are conservation laws in the micro-world; but in the classic methods of studying nonlinear equations scientists usually use the priori estimates reflecting the conservation laws of macroscopic quantities. We did not focus attention either on obtaining exact estimates dependent on viscosity, lest the calculations be complicated. However, the pilot analysis shows the possibility of applying these estimates to the problem of limiting viscosity transition tending to zero.

REFERENCES

[1] Durmagambetov, A.A. and Fazylova, L.S. (1997) Some methods of solving nonlinear equations. Herald of the Karaganda University, Publishers KarGU, Karaganda, **1**, 6-17.

[2] Durmagambetov, A.A. (1996) Inverse problem of quantum theory of scattering. *International Conference on Inverse and III-Posed Problems*, Moscow, **57**, 27-30.

[3] Leray, J. (1934) Sur le mouvement d'un liquide visquex emp- lissant l'espace. *Acta Math*, **63**, 193-248.

[4] Novikov, R.G. and Henkin $\overline{\partial}$, G.M. (1987) Equation in multidimensional inverse problem of scattering. *Success in Mathematics*, **N3**, 93-152.

[5] Faddeev, L.D. (1974) Inverse problem of quantum theory of scattering. *Modern Problems of Math-Ematicians*, VINITI, **3**, 93-180.

[6] Ramm, A.G. (1992) Multidimensional inverse scattering problems. *Pitman Monographs and Surveys in Pure and Applied Mathematics*, Longman Scientific Technical, Haplow, **51**, 379.

[7] Rid, M. and Saymon, B. (1982) Methods of modern mathematic physics. *Theory of Scattering*, Vol. 3, M.: Mir.

[8] Povzner, A. (1953) About decomposition of functions, into eigenfunctions of operator $-\Delta u + Cu$. *Mathematics Collection*, **32(74)**, 108-156.

[9] Rid, M. and Saymon, B. (1982) Methods of modern mathematic physics. *Analysis of Operators*, **4**, M.: Mir.

[10] Ladyzhenskaya, O.A. (1970) Mathematic problems of viscous incondensable liquid dynamics. M.: Science.

Vol.2, No.4, 357-367 (2010)
doi:10.4236/ns.2010.24043

Natural Science

Effect of Ba^{2+} in BNT ceramics on dielectric and conductivity properties

Konapala Sambasiva Rao, Kuan China Varada Rajulu, Bollepalli Tilak, Anem Swathi

Centre for Piezoelectric Transducer Materials, Department of Physics, Andhra University, Visakhapatnam, India;
sambasivaraokonapala@yahoo.co.in; konapala@sify.com

Received 11 December 2009; revised 13 January 2010; accepted 19 February 2010.

ABSTRACT

The polycrystalline $(Na_{0.5}Bi_{0.5})_{1-x}Ba_xTiO_3$ (x = 0.026, 0.055 & 0.065) (BNBT) ceramics have been synthesized by conventional solid state sintering technique. The tolerance (t) factor of the BNBT composition have been estimated and found to be 0.988, 0.990 and 0.991 for x = 0.026, 0.055 and 0.065 respectively, revealing system is stable perovskite type structure. The compound has a rhombohedral-tetragonal Morphtropic Phase Boun- dary (MPB) at x = 0.065. XRD results indicated the crystalline structure of the investigated materials are of single phase with rhombohedral structure and the average particle size of the calcined powder is found to lie between 45 nm - 60 nm. The effect of Ba^{2+} on dielectric and conductivity properties in Bismuth Sodium Titanate (BNT) has been studied. The variation of dielectric constant with frequency (45 Hz-5 MHz) and temperature (35℃-590℃) has been performed. The value of T_m and T_d are found to decrease with increase of concentration of Barium in BNT. The value of tanδ in the studied materials is found to be the order of 10^{-2} indicating low loss materials. The evaluated Curie constant in the composition is found to be the order of 10^5 revealing the materials belong to oxygen octahedra ferroelectrics. The theoretical dielectric data of the studied composition have been fitted by using Jonscher's dielectric dispersion relation: $\varepsilon_r' = \varepsilon_\infty + \sin(n(T)\frac{\pi}{2})(\frac{a(T)}{\varepsilon_o})(\omega^{n(T)-1})$. The pre-factor *a(T)*, which indicates the strength of the polarizability showed a maximum at transition temperature (T_m). The exponent *n*(*T*) which gives a large extent of interaction between the charge carriers and polarization is found to be minimum in the vicinity of T_m. The A.C. and d.c conductivity activation energies have been evaluated; the difference in activation energies could be due to the grain boundary effect. The activation enthalpy energies, have been estimated and found to be H_m = 0.37 eV, 0.26 eV and 0.25 eV for BNBT-26, BNBT-55 and BNBT-65 respectively.

Keywords: MPB; Dielectric; Perovskite; Conductivity; Tolerance Factor

1. INTRODUCTION

Recently, according to the stern restriction of environmental pollution such as waste electrical and electronic equipment (WEEE) and restriction of hazardous substance (RoSH), development of lead free piezoelectric ceramics capable of replacing lead-based ceramics is strongly required. The development of lead-free piezoelectric materials has been required. Lead free piezoelectric ceramics have recently attracted great attention for the consideration of environmental protection. Tungsten-Bronze (TB) type, Bismuth Layer-Structured (BLS) type and perovskite type ferroelectrics are known for lead-free piezoelectric ceramics.

Now a days $Na_{0.5}Bi_{0.5}TiO_3$ (NBT) is considered to be a parent component for lead-free ferroelectric and piezoelectric material [1,2]. But Bi ion is highly volatile at high temperature above 1130℃ during sintering and making this material difficult to pole due to its high conductivity [3]. The solution to this problem has been found by many researchers, who were able to modify BNT crystal by the substitution of other A and B-site cations, such as in $(Bi_{0.5}Na_{0.5})_{(1-1.5x)}La_xTiO_3$; (BNLT) [4], BNT-$KNbO_3$(KN) [5], and BNT-Ba(Ti,Zr)O_3 [6] solid-solution ceramic system. The piezoelectric properties of these ceramics were significantly improved.

The piezoelectric property of $Na_{1/2}Bi_{1/2}TiO_3$-$BaTiO_3$ (BNBT) system with perovskite structure was studied by B.J. Chu *et al.* [7]. A simple aqueous route was developed for the preparation of (1-x)$Na_{1/2}Bi_{1/2}TiO_3$x$BaTiO_3$

by D.L. West *et al.* [8] and studied the crystal structure and dielectric properties. Crystallographically textured ferroelectric and piezoelectric ceramics were prepared by tape casting of slurries containing powder particles with shape anisotropy by T. Kimura *et al.* [9]. $(Na_{1/2}Bi_{1/2})_{1-x}Ba_xTiO_3$ powders were synthesized by a citrate method, and the piezoelectric and ferroelectric properties of the ceramics were investigated by Q. Xu [10]. (1-x)$BaTiO_3$-x$Bi_{0.5}Na_{0.5}TiO_3$ for x = 0.01-0.3 ceramics has been prepared by conventional solid state reaction route by Huang *et al.* [11]. Also, crystal structure of the prepared compositions and variation of ε' with temperature and tanδ at different frequencies have been reported. Barium substituted BNT ceramics have been prepared by the usual double sintering method by Qu *et al.* [12]. The crystal structure of the prepared materials and the effect of Ba^{2+} on the temperature dependence of ε' and microstructural by SEM have been reported by the same authors.

It is evident from the above survey that most of the work that has been carried in BNBT system is in its preparative methods, dielectric (variation of ε' with temperature only) and piezoelectric properties only. Further, in ferroelectrics in general, the study of electrical conductivity is very important since the associated physical properties like piezoelectricity, pyroelectricity and also strategy for poling are dependent on the order and nature of conductivity in these materials. However, no work on dielectric spectroscopy (frequency dependent ε', tanδ) and conductivity studies on (BNT-BT) system have been reported in literature. The aim of the present communication is the preparation of $(Bi_{0.5}Na_{0.5})_{1-x}Ba_xTiO_3$ (BNBT) for x = 0.026, 0.055 and 0.065 ceramic compositions and to study the frequency, temperature dependence of dielectric and conductivity properties in the materials with a special emphasis on the Morphotropic Phase Boundary (MPB) of the system.

2. TOLERANCE FACTOR

The concept of tolerance factor (*t*) is the arrangement of interpenetrating octahedra and dodecahedra in perovskite structure (ABO_3 type) introduced by Goldschmidt, which is given by:

$$\text{tolerance } (t) = \frac{R_a + R_O}{\sqrt{2}(R_b + R_O)} \quad (1)$$

Here, R_a, R_b and R_O are the ionic radii of A, B cations and oxygen respectively, for complex perovskite system R_a and R_b are the ionic radii of composed ions normalized by the atomic ratio. The ionic radii refer to those reported by shannon [13]. All perovskites have a *t* value ranging from 0.75 to 1.00. However, it seems that t = 0.75–1.00 is a necessary but not a sufficient condition for the formation of the perovskite structure. The perovskite structure is stable in the region $0.880 < t < 1.090$, [14] and the symmetry is increases as the t value is close 1. The tolerance, *t* also provides an indication about how far the atoms can move from the ideal packing positions in the structure. It reflects the structural modification such as rotation, tilt, distortion of the octahedral [15]. These structure factors consequently affect the electrical property of the material [16-18]. In the Present BNBT system tolerance factors have been estimated to be 0.988, 0.990 and 0.991 for BNBT-26, BNBT-55 and BNBT-65 respectively. The tolerance factors in the studied materials are found to lie well within the limit indicating the materials belong to stable perovskite structure.

3. EXPERIMENTAL

Starting materials, analar grade oxides and carbonate powders of Bi_2O_3, TiO_2, $BaCO_3$, Na_2CO_3 were weighed according to the formula, $(Bi_{0.5}Na_{0.5})_{1-x}Ba_xTiO_3$ (x = 0.026, 0.055 & 0.065). The weighed powers were mixed well in methanol medium using agate mortar. An extra amount of 3 wt% Bi_2O_3 and Na_2CO_3 were added to the initial mixture to compensate the losses of bismuth and sodium at high temperature. The resultant grounded mixture was calcined at 850℃ for 2 hr with intermediate grinding. After calcination, the ceramic powder was mixed with polyvinyl alcohol (5%), as the binder and then pelletized into discs, 13 mm diameter and about 1.1-1.5 mm thickness. After binder burnout, at 600℃ for 1 hr, the green discs have been sintered in a closed platinum crucible at 1150℃/4 hr. Silver paste was fired on both the surfaces of the disc as an electrodes for electrical measurements. The phase purity of the final product was confirmed via the X-ray diffraction (XRD) using CuKα radiation. The densities of the sintered pellets have been determined by the liquid displacement/Archimedes method. The measurement of dielectric constant (ε'), loss tangent (tanδ) and conductivity (σ) as a function of temperature from RT to 590℃ in the frequency range of 45 Hz - 5 MHz using HIOKI 3532-50 LCR Hi-tester, Japan with heating rate of 5℃/min offset temperature 0.2℃ and time period of 1 min for making the above measurements. Following are the chosen compositions which are well below, near and within MPB region.

$(Bi_{0.5}Na_{0.5})_{0.974}Ba_{0.026}TiO_3$ - BNBT-26 (well below MPB).
$(Bi_{0.5}Na_{0.5})_{0.945}Ba_{0.055}TiO_3$ - BNBT-55 (Near MPB).
$(Bi_{0.5}Na_{0.5})_{0.935}Ba_{0.065}TiO_3$ - BNBT-65 (Within MPB).

4. RESULTS AND DISCUSSION

4.1. XRD Analysis

X-ray diffractograms of $(Bi_{0.5}Na_{0.5})_{1-x}Ba_xTiO_3$ (x = 0.026, 0.055 and 0.065) compositions with 2θ values from 10° to 70° along with BNT are shown in **Figure 1**. The structure and lattice parameters of BNBT materials have been determined by using a standard computer program "POWD" (interpretation and indexing program by E. Wu, school of physical sciences, Flinders University of South Australia, Bed Ford Park, Australia). It is obvious from the **Figure 1** all the peaks in the XRD pattern of the BNBT are correspond to the BNT (3.886Å) phase with rhombohedral structure as reported by different researchers [19-21]. All the XRD peaks obtained in compositions are indexed and found to be single phase with rhombohedral structure. XRD pattern of the compositions showed an extra peak, indicating a possible presence of some unidentifiable extra phase due to non-miscibility of substituted ions with the host lattice ion [22]. It is evident from the **Figure 1** that the substitution of Ba^{2+} in BNT shifts the peak position towards lower angle side. Also, the substitution of Ba^{2+} in BNT for x > 0.055 resulted in a splitting of the (2 0 0) peak into two peaks of (0 0 2) and (2 0 0) reflections. This splitting is obvious at x = 0.065 and can be clearly seen in the extended XRD pattern of the corresponding material at 2θ in the range 42° to 49° (**Figure 1(b)**). Splitting in the peak position reveals the composition BNBT-65 is well in MPB region where rhombohedral and tetragonal phase co-exist. The above results are found to be very good agreement with previous work on (1-x) $(Bi_{0.5}Na_{0.5})$ TiO_3-$xBaTiO_3$ [23,24]. Using lattice parameters theoretical densities (ρ_{theor}) of the compositions are evaluated. Average particle size of the calcined powders of the composition is determined using Debye-Scherer formula. Calculated values of lattice parameters, density, average particle size, average grain size and porosity are given in **Table 1**.

It is seen form the **Table 1** that as increasing the Ba content the lattice parameters of the BNBT materials are found to increase where as the lattice distortion decreases. The experimental densities are found to be 5.87 g/cm³, 5.98 g/cm³ and 5.91 g/cm³ for x = 0.026, 0.055 and 0.065 respectively which are 97.2%, 98.9% and 97.8% to that of theoretical value indicating the materials are high dense. Further, an average particle size in the calcined powders is found to be in nanometer range.

4.2. SEM and EDS

In the present Ba substituted BNT compositions experimental density is found to be more than 97% to that of the theoretical one, reveals less porosity. **Figure 2** shows the SEM micrographs on studied compositions. It is seen from the **Figure 2** spherical shape grains with an average grain size 1.25 μm, 1.01 μm and 1.09 μm found in BNBT-

Table 1. Lattice parameters and related properties of BNBT ceramics.

Composition	Lattice Parameters/ distortions		Density (ρ)(g/cm³)			Avg. particle size (nm)	Avg. grain size (μm)	Porosity
	a (Å)	α (angle)	ρ_{exptl}	ρ_{theor}	Density %			
BNBT-26	3.886	89.894	5.87	6.04	97.2	47	1.25	0.028
BNBT-55	3.891	89.891	5.98	6.04	98.9	56	1.01	0.011
BNBT-65	3.892	89.890	5.91	6.04	97.8	48	1.09	0.022

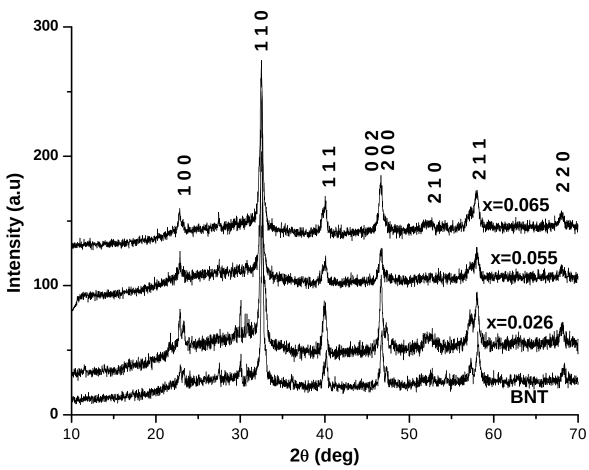

(a)

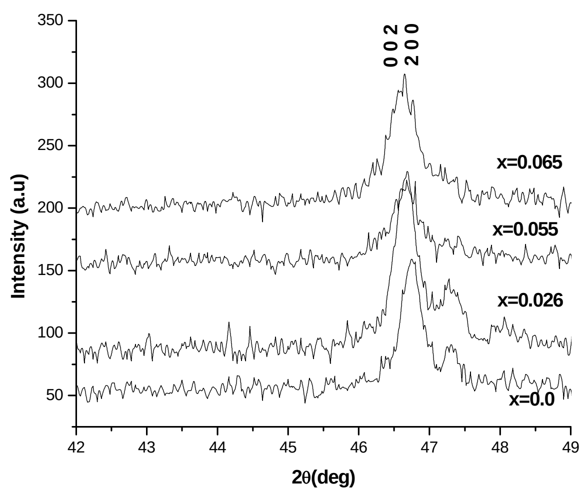

(b)

Figure 1. X-ray diffractograms on BNBT system (a) 2θ, 10°-70°; (b) 2θ, 42°-49°.

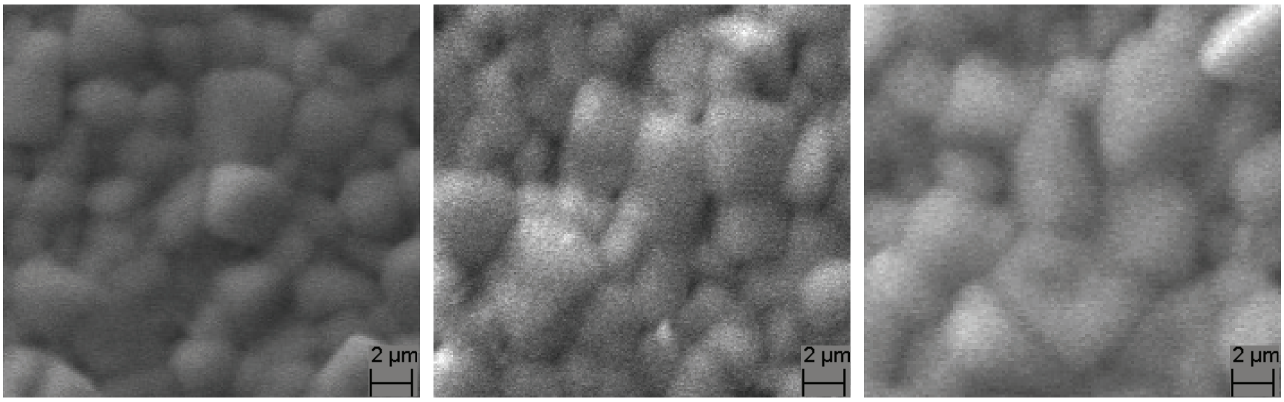

(a) (b) (c)

Figure 2. SEM micrographs of (a) BNBT-26; (b) BNBT-55; (c) BNBT-65.

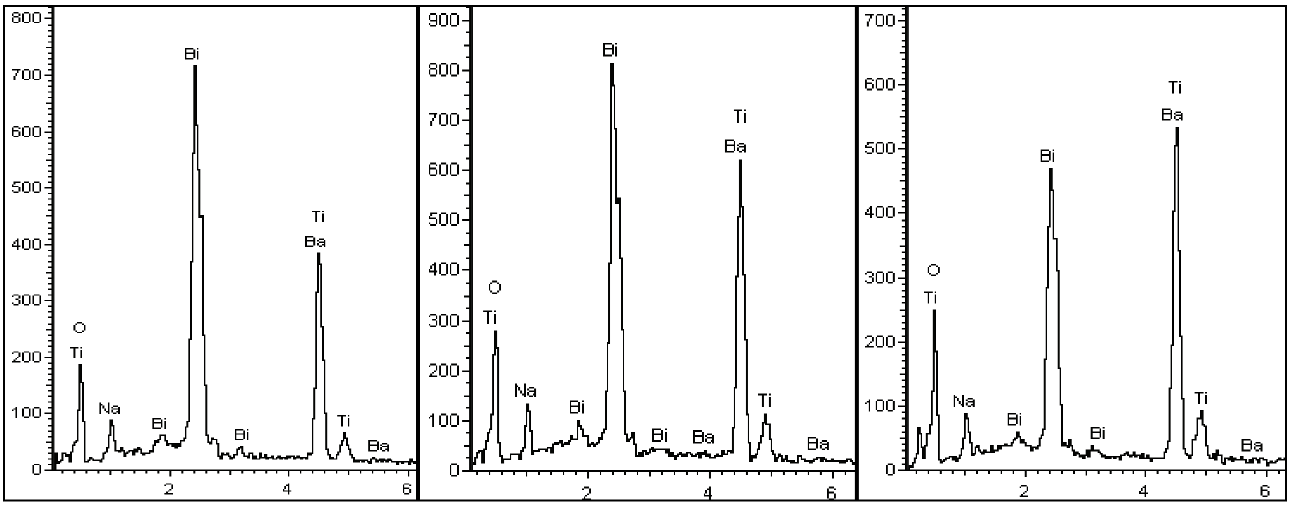

(a) (b) (c)

Figure 3. Energy dispersive X-ray spectrums. (a) BNBT-26; (b) BNBT-55; (c) BNBT-65.

Table 2. Dielectric properties of BNBT ceramics.

Composition	Dielectric constant(ε') (1 kHz)		T_d (℃)	T_m (℃)	Tan δ (1 kHz)		Conductivity (σ)(1 kHz)	Curie Constant ($X10^5$) °K	n(T)	log A(T)
	RT	T_m			RT	T_m				
BNBT-26	541	1625	180	318	0.059	0.05	$1.38x10^{-8}$(s/cm)	1.35	0.285	-9.4
BNBT-55	818	1891	140	313	0.04	0.02	$2.02x10^{-8}$(s/cm)	1.51	0.184	-3.5
BNBT-65	701	1233	100	305	0.06	0.02	$2.46x10^{-8}$(s/cm)	1.0	0.19	-3.6

26, BNBT-55 and BNBT-65 respectively.

Energy Dispersive X-ray Spectroscopy (EDS) is a chemical microanalysis technique used in conjunction with SEM and is not a surface science technique. The EDS technique detects X-rays emitted from the sample during bombardment by an electron beam to characterize the elemental composition of the analyzed volume. **Figure 3** shows the EDS of Ba substituted BNT compositions. The spectrum (**Figure 3**) shows the elements present in the prepared compositions are Na, Bi, Ba, Ti and O only.

4.3. Dielectric

The temperature dependence of dielectric constant ε' and dielectric loss tanδ of Ba substituted BNT system at 1 kHz are shown in **Figure 4**.

It is seen from **Figure 4(a)** that two dielectric peaks have been observed in each composition. The observed two dielectric peaks can be attributed to the factors caused by the phase transitions from ferroelectric to anti-ferroelectric, which is called depolarization temperature (T_d) and from anti-ferroelectric to paraelectric phase, at which the maximum value of dielectric constant corresponding temperature is Curie temperature (T_m) (**Figure 4(a)**). The value of T_d and T_m are found to decrease with increasing the concentration of Ba, indicating the conductivity of the materials is decreased compared with BNT. These results are consistent with previous reports on BNT, BNT-BT, BNT-KBT, BNKLT lead free ferroelectric systems [25-31]. Also it is obvious from the **Figure 4** at high temperatures another dielectric maxima is observed at 520℃ in the compositions. The observed anomaly may be related to the relaxation mechanism in the samples [32]. It is seen from **Table 2** considerable increase in the value of room temperature dielectric constant (ε'_{RT}) as well as at Curie temperature (ε'_{T_m}) are observed in the compositions for x = 0.026 and 0.055 having rhombohedral structure. Whereas decrease in the value of ε'_{RT} and ε'_{T_m} are observed in the composition for x = 0.065 which is in MPB region where rhombohedral and tetragonal phase coexist. The value of dielectric loss (tan δ) in the compositions is found to be the order of 10^{-2} indicating the low loss materials. The important mechanism of conductivity in these ceramics is the movement of ions present in the current carrying conductor. It is well known reason that the alkali ions are good current carriers in ceramics; because these ions play an important role in the conductivity of BNBT ceramics. The Na^+ ions in BNT move easily upon heating, resulting in increase in conductivity with increasing temperature. The present Ba substituted ceramics, Ba^{2+} (large ion) occupies the A-site of BNT, which possibly blocks the passage of Na^+ current carriers. When the temperature is increased above T_m, the value of tanδ is found to increase drastically. Curie constant in the compositions have been evaluated and found to be the order of 10^5 K indicating the materials belong to oxygen octahedra ferroelectrics [33]. The value of ε'_{RT}, ε'_{T_m}, tanδ at RT and T_m, conductivity at RT (σ_{RT}) and Curie constant (K) are given in **Table 2**.

The frequency dependence of the real part of the dielectric constant for BNBT-65 is depicted in **Figure 5** for various temperatures. Two different regions are distinguishable from the **Figure 5(a)**: a plateau region in the high frequency part and a strong dispersion in low frequency region. This phenomenon is commonly observed in conducting materials and is referred to as low frequency dielectric dispersion (LFDD) [34-39]. The same trend has been observed in the remaining compositions BNBT-26 and BNBT-55 as shown in insert **Figures 5(a,b)**. The observed dispersion of the imaginary dielectric constant (ε") (**Figure 5**) is stronger than that of ε'. Slope of the curve ε" Versus frequency (f) is found to be close to -1 in low frequency region, which describes the predominance of the dc conduction. In the high frequency region slope lies between 0 and -1, depending on temperature, as it is observed.

According to the Jonscher's power law, the complex dielectric constant as a function of frequency, ω can be expressed as,

$$\varepsilon^* = \varepsilon_r' - \varepsilon_r'' = \varepsilon_\infty + \left(\frac{\sigma}{i\varepsilon_o\omega}\right) + \left(\frac{a(T)}{\varepsilon_o}\right)(i\omega^{n(T)-1}) \quad (2)$$

From the above equation the real and imaginary parts of ε' and ε" can be written as

$$\varepsilon_r' = \varepsilon_\infty + \sin(n(T)\frac{\pi}{2})(\frac{a(T)}{\varepsilon_o})(\omega^{n(T)-1}) \quad (3)$$

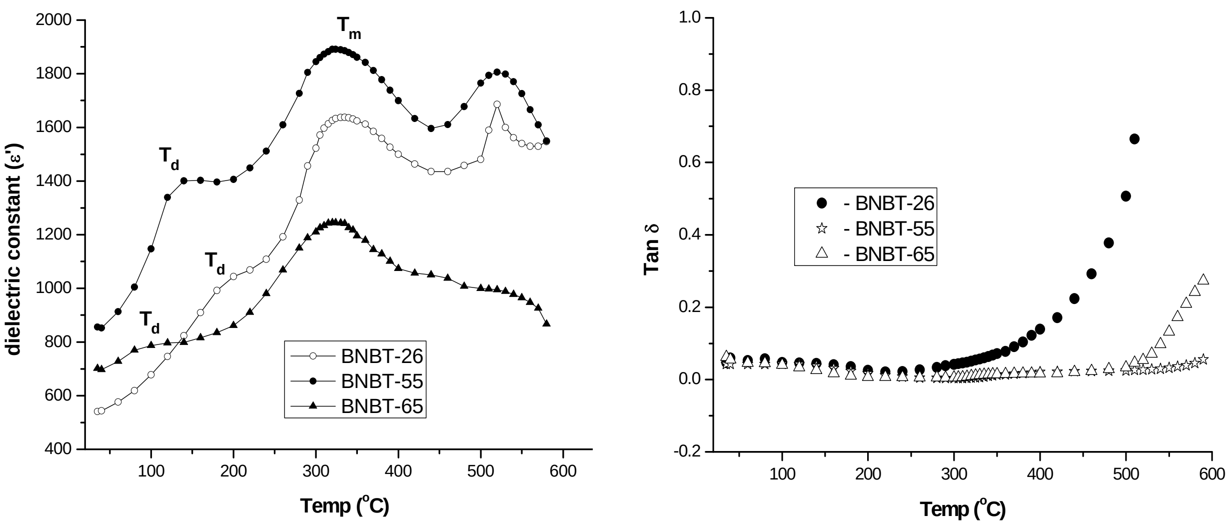

(a) (b)

Figure 4. Variation of (a) ε' and (b) tanδ of BNBT as a function of temperature.

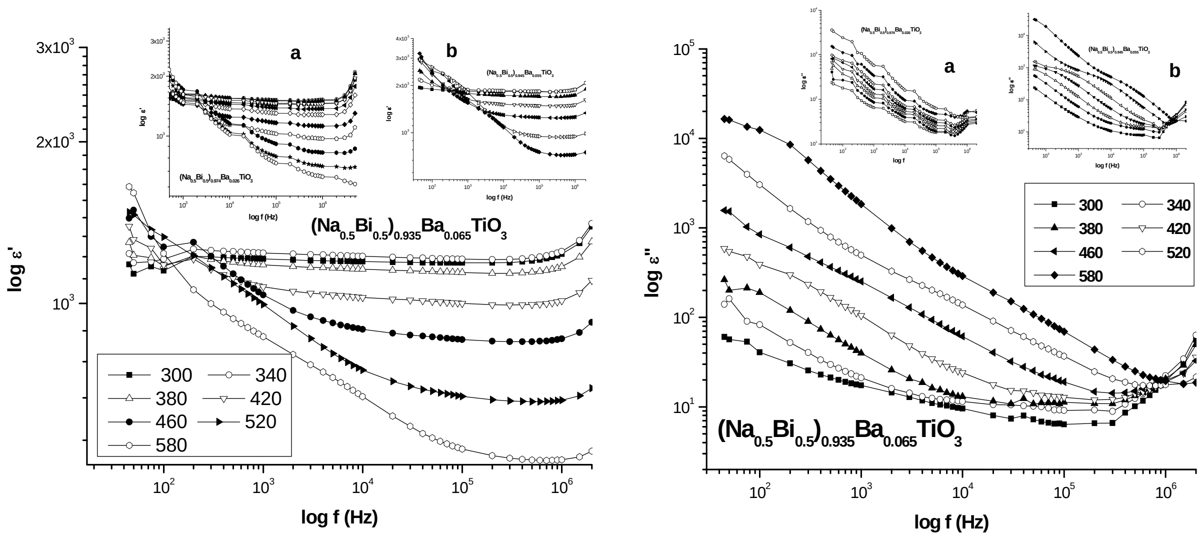

Figure 5. Frequency dependence of ε' and ε'' at various temperatures.

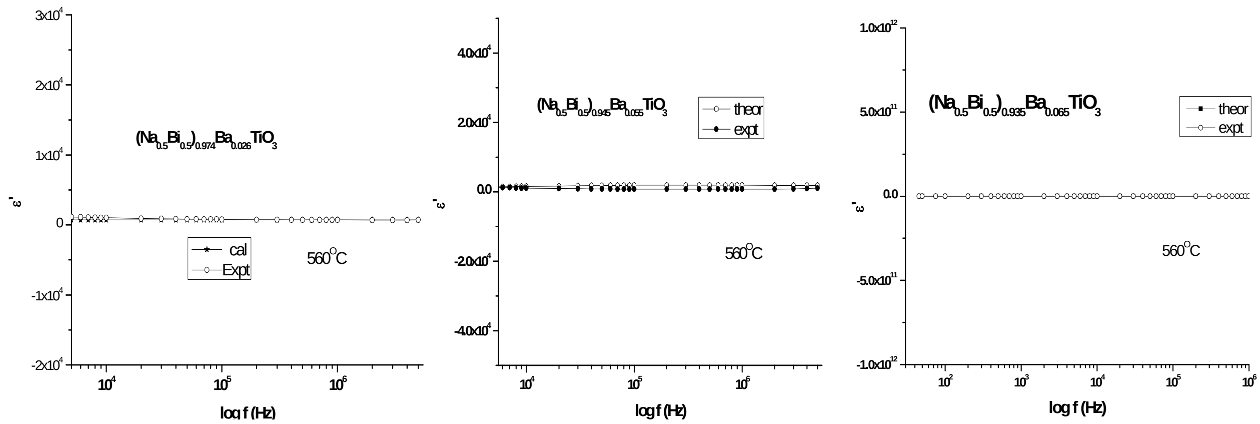

(a) (b) (c)

Figure 6. Fitting curves of dielectric constant as a function of frequency at 560℃.

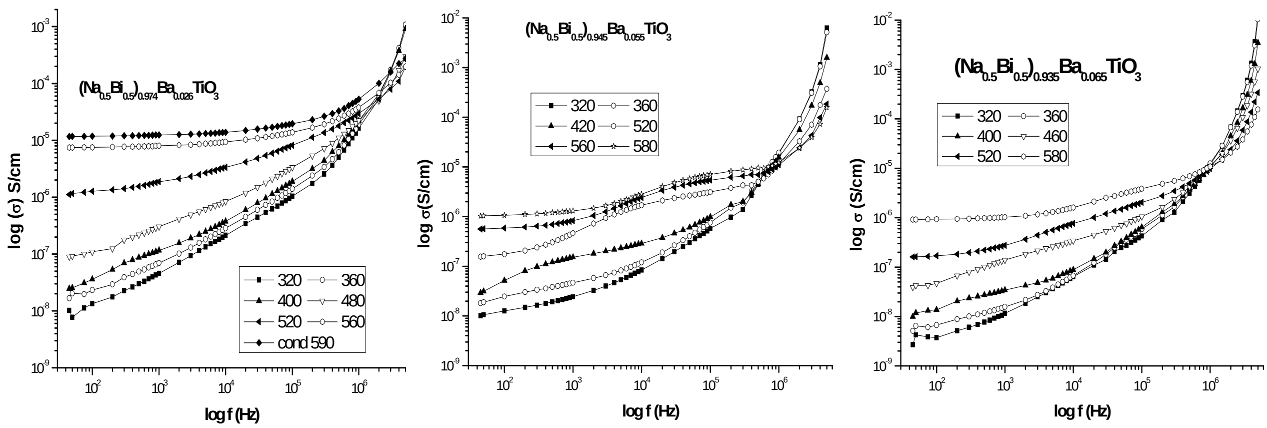

(a) (b) (c)

Figure 7. A.C. conductivity as function of frequency at different temperatures of BNBT system.

$$\varepsilon_r'' = \frac{\sigma}{\varepsilon_o \omega} + \cos(n(T)\frac{\pi}{2})(\frac{a(T)}{\varepsilon_o})(\omega^{n(T)-1}) \quad (4)$$

where ε_∞ is the 'high frequency' value of the dielectric constant, $n(T)$ is the exponent factor, $a(T)$ is prefactor.

Substituting the values of $n(T)$ and $a(T)$ obtained from conductivity measurement in **Eq.3** the theoretical values of ε' has been calculated in the compositions. As the dispersion is negligibly small at higher frequencies, so that the ε_∞ value was chosen as the dielectric constant obtained at 1 MHz. In the studied material the experimental dielectric data have been fitted with theoretical one. The real part of the dielectric constant (ε') at 560℃ and theoretically calculated ε' values for BNBT system as a function of frequency is shown in **Figure 6**. It is seen from the **Figure 6** an excellent agreement between experimental and theoretical values for ε' is observed.

4.4. Conductivity Studies

Figure 7 shows the variation of A.C. conductivity as a function of frequency at different temperatures in BNBT-26, BNBT-55 and BNBT-65. The electric conductivity in ceramics is mainly controlled by the migration of charge species under the action of electric field and by the defect-ion complexes, the polarization field, the relaxation etc. In BNBT-65 the high conductivity is observed where as low conductivity is seen in BNBT-26. The observed high conductivity in BNBT-65 is attributed to the presence of oxygen vacancies and low conductivity in BNBT-26 may be due to an enhancement in barrier properties, suppression of lattice conduction path and local lattice distortion [40-42]. Present BNBT system showed a low frequency dielectric dispersion (LFDD) behavior (discussed in Dielectric analysis). The σ(ω) curves are found to be merging at high frequency and temperature regions, suggesting the less defect mobility and low conductivity in the material. The phenomenon of the conductivity dispersion in the materials is generally analyzed by using A.K. Jonscher's law [43]

$$\sigma(\omega) = \sigma_{dc} + A\omega^n \quad (5)$$

where σ_{dc} is the d.c.conductivity for a particular temperature, n is the power law exponent which varies between 0 and 1 depending on temperature and A is the temperature dependent constant.

The $n(T)$ and $A(aS/L)$ are determined from curve fitting using the **Eq.3**. Temperature dependence of both $n(T)$ and A(aS/L) are shown in **Figures 8(a)** and **(b)** respectively. An interesting feature of **Figure 8** is that the two linear regions have been observed in the studied materials corresponding to the paraelectric and ferroelectric states [44-46]. The value of exponent n value is found to decrease with increasing temperature and shows a minimum near T_m. Similar results have been reported in $SrBi_2NbO_2O_9$ (SBN) and $BaBi_2Nb_2O_9$ (BBN) ceramics [47,48]. The value of prefactor A shows a maximum in the temperature range where n shows a minimum and it decreases with increasing in temperature. According to many body interaction models [43], the interaction between all dipoles participating in the polarization process is characterized by the parameter n. n = 1implies a pure Debye case, where the interaction between the neighboring dipoles is almost negligible. The value of $n(T)$ is observed to be less than one in the studied compositions indicating non-Debye type. The observed minimum $n(T)$ in the vicinity of T_m shows a large extent of interaction between the charge carriers and polarization. The higher value of A in the vicinity of T_m establishes the presence of higher polarizability.

In the materials, the conductivity is found to be independent of frequency at any temperature under study is taken as d.c conductivity. Here, d.c. conductivity indicates hopping of charge carriers after the surrounding environment has relaxed. The jump relaxation theory introduced by Funke (1993) is to account for ionic conduction in solids. The jump relaxation theory yields the Almond-West assumption, from which the A.C. and d.c conductivity activation energies are evaluated in the present compositions. The A.C. conductivity is found to obey the Almond-West relation [49].

$$\sigma(\omega) = \sigma_{dc}(1 + \omega_p / \omega)^n \quad (6)$$

where ω_p is the hopping frequency, the ω_p is the transition region between d.c. and A.C. conductivity.

There have been many attempts [50] to relate σ_{dc} to the A.C. conductivity. Whether they are able to do so in equal numbers is not known but it might be expected that effects such as the blocking of conduction pathways. If anything, lead to fewer ions contributing to the d.c. conductivity than to the A.C. conductivity. The relationship between A and σ:

$$\sigma_{dc} = A\omega_p^n \quad (7)$$

was obtained [51] by taking the assumptions that the electrical response, **Eq.5** is a characteristic of the dynamics of the hopping ions and that the same number of ions contributes to the A.C. and d.c. conductivities. It is well known that ω_p is activated with activation enthalpy, H_m followed by the relation $\omega_p = \omega_e \exp(-H_m/k_BT)$. **Figure 9** shows the typical Arrhenius plot of ω_p for BNBT-65. From these plots the value of H_m = 0.37eV, 0.26eV and 0.25eV has been estimated for BNBT-26, BNBT-55 and BNBT-65 respectively. Activation enthalpy (H_m) is decreasing with increasing the concentration of the Ba. The value of H_m is lowest for BNBT-65 which is in MPB region.

The conductivity (d.c and A.C) behavior in the BNBT system has been shown in **Figure 10**. The conductivity of the materials has been found to increase with increase in temperature, representing the negative temperature coefficient of resistance (NTCR) behavior like semiconductors,

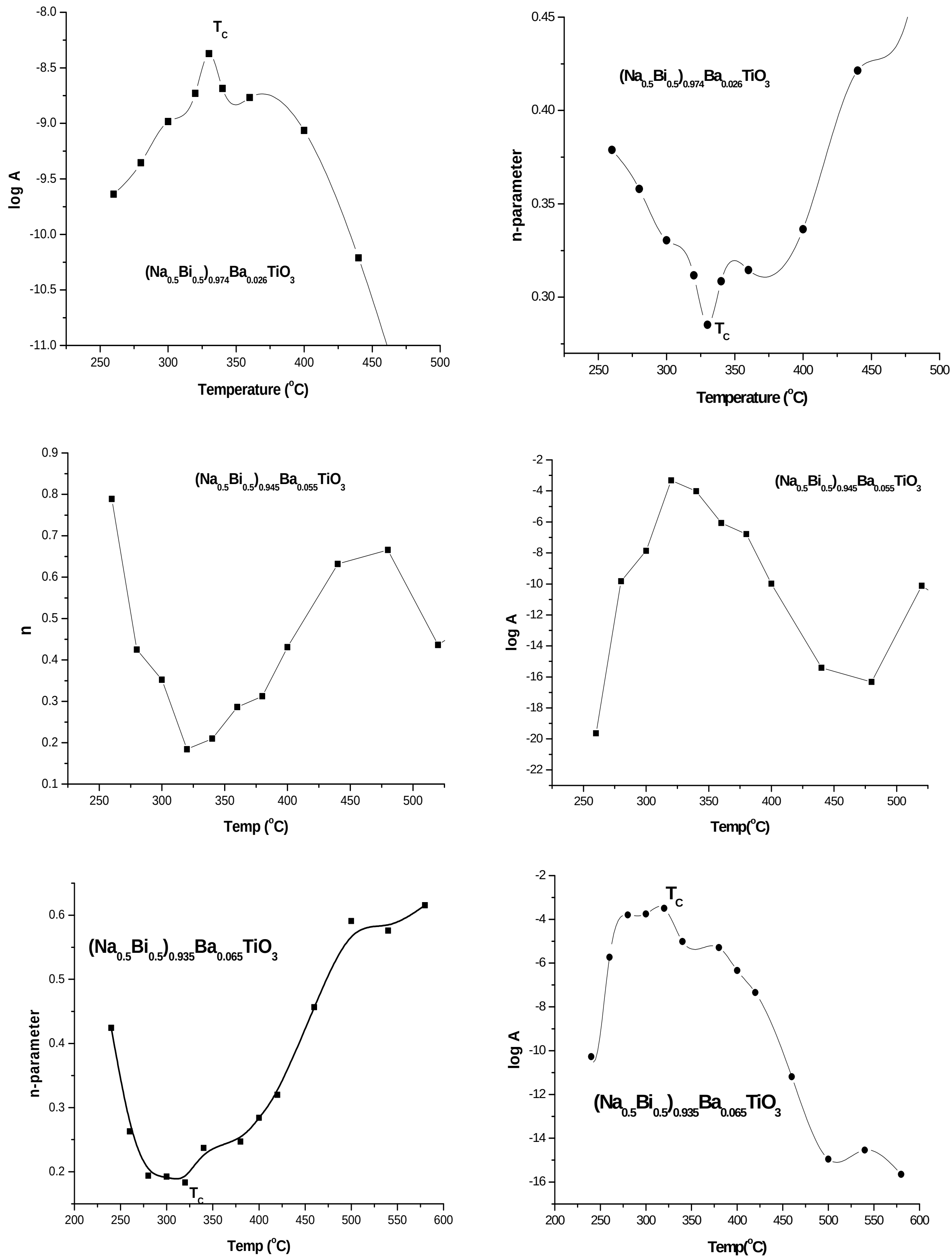

(a) (b)

Figure 8. Temperature depence of (a) $n(T)$ and (b) $A(T)$ parameters of BNBT system.

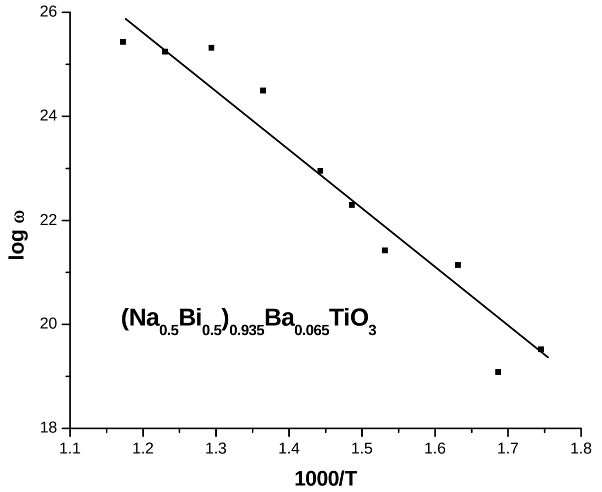

Figure 9. log ω as a function of inverse temperature of BNBT-65.

and it is related to the bound carriers trapped in the sample. Merging of all conductivity curves at higher temperature region results the release of space charge [52,53]. At low temperature, the thermal energy is enough to allow migration of atoms/ions into (oxygen) vacancies already associated in the compound. Hence no clear anomalies appeared in this region. The conductivity values at room temperature are 1.38 × 10^{-8} (s/cm), 2.02 × 10^{-8} (s/cm), 2.46 × 10^{-8} (s/cm) for BNBT-26, BNBT-55 and BNBT65 respectively. It is evident that the conductivity is basically due to the oxygen vacancies. High conductivity is observed in BNBT-65 may be due to it is in MPB region. It represents contribution of the reorientation of Ba^{2+} and Ti^{4+} ions coupling with the thermally activated conduction electrons appear due to ionization of the oxygen vacancies in MPB region.

The A.C. and d.c. conduction activation energies have been calculated from different temperature regions (580-470℃, 470-370℃ and 370-300℃) (**Figures 10(a, b, c)**) and at different frequencies using Arrhenius relation $\sigma = \sigma_{dc}\exp(E_a/K_BT)$ and the obtained values are given in **Table 3**. The activation energy in BNBT-65 is found to be high since it is in MPB region, compare to the other two samples. *i.e.*, below MPB (BNBT-26) and near MPB (BNBT-55). It is seen from the **Figure 10** that a change in the slope of conductivity vs. temperature response of the materials has been observed around the transition temperature may be due to the difference in the activation energy in the ferroelectric and paraelectric regions. This difference in activation energies could be due to the grain boundary effect [54].

The low activation energies found at low temperature and high frequency range in the studied materials suggest the intrinsic conduction may be due to the creation of large number of charge carriers. AC and dc activation energy values at different frequencies and temperature are given in **Table 3**.

5. CONCLUSIONS

The polycrystalline $(Na_{0.5}Bi_{0.5})_{1-x}Ba_xTiO_3$ (x = 0.026, 0.055 & 0.065) (BNBT) ceramics have been synthesized by conventional solid state sintering technique. The tolerance factors (0.988, 0.99 and 0.991) in the studied materials are found to lie well within the limit indicating the materials belong to stable perovskite structure. X-ray powder diffraction patterns of the materials have been indexed and found to be single phase with rhombohedral structure. The evaluated lattice parameters are 3.886Å, 3.891Å and 3.892Å for BNBT-26, BNBT-55 and BNBT-65 respectively. The value of T_m and T_d are found to decrease with increase of concentration of Barium in BNT. The tanδ values in the studied materials are found to be the order of 10^{-2} indicating low loss materials. The evaluated Curie constant in the compositions is found to be the order of 10^5 revealing the materials belong to oxygen octahedra ferroelectrics. A strong low frequency dielectric dispersion has been observed in the studied materials.

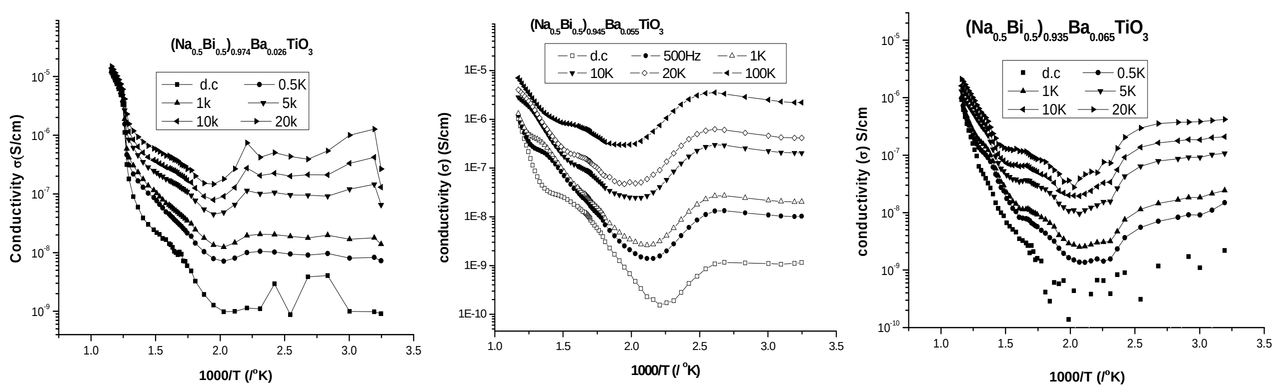

(a) (b) (c)

Figure 10. Conductivity vs. inverse temperature of BNBT-system.

Table 3. Activation energies of BNBT materials.

Composition	BNBT-26 (eV)			BNBT-55 (eV)			BNBT-65 (eV)		
Temperature range	d.c	1kHz	10kHz	d.c	1kHz	10kHz	d.c	1kHz	10kHz
580-470	0.49	0.45	0.37	0.5	0.43	0.43	0.66	0.43	0.32
470-370	0.27	0.21	0.15	0.14	0.31	0.38	0.48	0.41	0.39
370-300	0.24	0.15	0.11	0.07	0.22	0.17	0.20	0.23	0.11

The experimental and theoretical dielectric constant (ε') are fitted well to the Jonscher's power law. The interaction between the charge carriers, exponent $n(T)$ and strength of polarizability, $A(T)$ are observed to be minimum and maximum at T_m respectively. The value of $n(T)$ is observed to be < 1 in the studied compositions indicating non-Debye type. The electrical relaxation process occurring in the materials are observed to be temperature dependent. Temperature dependence of dc conductivity in the compositions exhibits the NTCR behavior. The d.c. conductivity behaviour in the materials indicates hopping of charge carriers after the surrounding environment has relaxed. The value of activation enthalpy (H_m) are evaluated and found to be 0.37eV, 0.26eV and 0.25 eV for BNBT-26, BNBT-55 and BNBT-65 respectively.

6. ACKNOWLEDGEMENTS

Authors K.S. Rao and K.Ch. VaradaRajulu thank to Naval Science & Technological Laboratory (NSTL)-Visak-hapatnam, INDIA for the sanction of a Research Project and providing Research Assistant fellowship.

REFERENCES

[1] Gomah-Pettry, J.R., Marchet, P., Salak, A., Ferriera, V.M. and Mercurio, J.P. (2004) Electrical properties of $Na_{0.5}Bi_{0.5}TiO_3$-$SrTiO_3$ ceramics. *Integrated Ferroelectrics*, **61(1)**, 159-162.

[2] Nageta, H., Yoshida, M., Makiuchi, Y. and Takenaka, T. (2003) Large piezoelectric constant and high curie temperature of lead-free piezoelectric ceramic ternary system based on bismuth sodium titanate-bismuth potassium titanate-barium titanate near the morphotropic phase boundary. *Japanese Journal of Applied Physics*, **42**, 7401-7403.

[3] Takenaka, T. and Nagata, H. (2005) Current status and prospects of lead-free piezoelectric ceramics. *Journal of the European Ceramic Society*, **25(12)**, 2693-2700.

[4] Herabut, A. and Safari, A. (1997) Processing and electromechanical properties of $(Bi_{0.5}Na_{0.5})(1\text{-}1.5x)LaxTiO_3$ ceramics. *Journal of the American Ceramic Society*, **80(11)**, 2954-2958.

[5] Ishii, H., Nagata, H. and Takenaka, T. (2001) Morphotropic phase boundary and electrical properties of bisumuth sodium titanate-potassium niobate solid-solution ceramics. *Japanese Journal of Applied Physics*, **40(9B)**, 5660-5663.

[6] Peng, C., Li, J.F. and Gong, W. (2005) Preparation and properties of $(Bi_{1/2}Na_{1/2})TiO_3$-$Ba(Ti,Zr)O_3$ lead-free piezoelectric ceramics. *Materials Letters*, **59(12)**, 1576-1580.

[7] Chu, B.J., Chen, D.-R., Li. G.-R. and Yin, Q.-R. (2002) Electrical properties of $Na_{1/2}Bi_{1/2}TiO_3$-$BaTiO_3$ ceramics. *Journal of the European Ceramic Society*, **22(13)**, 2115-2121.

[8] West, D.L. and Payne, D.A. (2003) Preparation of $0.95Bi_{1/2}Na_{1/2}TiO_3{\cdot}0.05BaTiO_3$ ceramics by an aqueous citrate-gel route. *Journal of the American Ceramic Society*, **86(1)**, 192-194.

[9] Kimura, T., Takahashi, T., Tani, T. and Saito, Y. (2004) Preparation of crystallographically textured $Bi_{0.5}Na_{0.5}TiO_3$–$BaTiO_3$ ceramics by reactive-templated grain growth method. *Ceramics International*, **30(7)**, 1161-1167.

[10] Xu, Q., Chen, S.T., Chen, W., Wu, S.J., Zhou, J., Sun, H.J. and Li, Y.M. (2005) Synthesis and piezoelectric and ferroelectric properties of $(Na_{0.5}Bi_{0.5})(1\text{-}x)BaxTiO_3$ ceramics. *Materials Chemistry and Physics*, **90(1)**, 111-115.

[11] Gao, L., Huang, Y., Hu, Y. and Du, H. (2007) Dielectric and ferroelectric properties of $(1\text{-}x)BaTiO_3$-$xBi_{0.5}Na_{0.5}TiO_3$ ceramics. *Ceramic International*, **33(6)**, 1041-1046.

[12] Qu, Y., Shan, D. and Song, J. (2005) Effect of A-site substitution on crystal component and dielectric properties in $Bi_{0.5}Na_{0.5}TiO_3$ ceramics. *Materials Science and Engineering B*, **121(1-2)**, 148-151.

[13] Shannon, R.D. (1976) Revised effective ionic radii and systematic studies of interatomic distances in halides and chalcogenides. *Acta Crystallographica Section A*, **32**, 751-767.

[14] Muller, O. and Roy, R. (1974) The major ternary structural families. Springer, New York, 221.

[15] Bhalla, A.S., Guo, R. and Roy, R. (2000) The perovskite structure—a review of its role in ceramic science and technology. *Materials Research Innovations*, **4(1)**, 3-26.

[16] Eitel, R.E., Randall, C.A., Shrout, T.R. and Rehrig, P.W. (2001) New high temperature morphotropic phase boundary piezoelectrics based on $Bi(Me)O_3$-$PbTiO_3$ ce- ramics. *Japanese Journal of Applied Physics*, **40(10)**, 5999-6002.

[17] Reaney, I.M., Colla, E.L. and Setter, N. (1994) Dielectric and structural characteristics of Ba-based and Sr-based complex perovskites as a function of tolerance factor. *Japanese Journal of Applied Physics*, **33(7A)**, 3984-3990.

[18] Suchomel, M.R. and Davies, P.K. (2004) Predicting the position of the morphotropic boundary in new high temperature $PbTiO_3$-$Bi(B'B'')O_3$ based dielectric ceramics. *Journal of Applied Physics*, **96(8)**, 4405-4410.

[19] Isupov, V.A. (2005), Ferroelectric $Na_{0.5}Bi_{0.5}TiO_3$ and $K_{0.5}Bi_{0.5}TiO_3$ perovskites and their solid solutions. *Ferroelectrics*, **315(1)**, 123-147.

[20] Park, S.E. and Chung, S.J. (1994), Phase transition of ferroelectric $(Na_{1/2}Bi_{1/2})TiO_3$ on applications of ferroelectrics. *Proceedings of the* 9*th IEEE International Symposium*, **ISAF'94**, 265-268.

[21] Liu, Y.F., Lv, Y.N., Xu, M., Shi, S.Z., Xu, H.Q. and

Yang, X.D. (2007) Structure and electric properties of (1-x)($Bi_{1/2}Na_{1/2}$) TiO_3-x$BaTiO_3$ systems. *Journal of Wuhan University of Technology - Materials Science Edition*, **22(2)**, 315-319.

[22] Mahboob, S., Prasad, G. and Kumar, G.S. (2007) Impedance spectroscopy and conductivity studies on B site modified ($Na_{0.5}Bi_{0.5}$)(Nd-xTi(1-2x)Nbx)O_{-3} ceramics. *Journal of Material Science*, **42**, 10275-10283.

[23] Takenaka, T. (1999) Piezoelectric properties of some lead-free ferroelectric ceramics. *Ferroelectrics*, **230**, 87- 98.

[24] Liu, Y.F., *et al*. (2007) *Journal of Wuhan University of Technology - Materials Science Edition.*

[25] Takenaka, T. (1989) Piezoelectric properties of some lead-free ferroelectric ceramics. *Ferroelectrics*, **230**, 389.

[26] Yoshii, K., Nagata, H. and Takenaka, T. (2006) Electrical properties and depolarization temperature of ($Bi_{1/2}Na_{1/2}$)TiO_3–($Bi_{1/2}K_{1/2}$)TiO_3 lead-free piezoelectric ceramics. *Japanese Journal of Applied Physics*, **45**, 4493.

[27] Takenaka, T., Okuda, T. and Takegahara, K. (1997) Lead-free piezoelectric ceramics based on ($Bi_{1/2}Na_{1/2}$) TiO_3-$NaNbO_3$. *Ferroelectrics*, **196**, 175.

[28] Li, H.D., Feng, C.D. and Yao, W.L. (2005) Some effects of different additives on dielectric and piezoelectric properties of ($Bi_{0.5}Na_{0.5}$)TiO_3 − $BaTiO_3$ morphotropic phase boundary composition. *Materials Letters*, **58**, 1194-1198.

[29] Nagata, H. and Takenaka, T. (2001) Additive effects on electrical properties of ($Bi_{1/2}Na_{1/2}$)TiO_3 ferroelectric ceramics. *Journal of European Ceramic Society*, **21**, 1299.

[30] Wei, Z., Heping, Z. and Yongke, Y., *et al.* (2007) Dielectric and piezoelectric properties of Y_2O_3 doped ($Bi_{0.5}Na_{0.5}$)0.94$Ba_{0.06}TiO_3$ lead-free piezoelectric ceramics. *Key Engineering Materials*, **105**, 336-338.

[31] Lin, D., Xiao, D., Zhu, J. and Yu, P. (2006) Piezoelectric and ferroelectric properties of [$Bi_{0.5}Na_{1-x-y}K_xLi_{y0.5}$]$TiO_3$ lead-free piezoelectric ceramics. *Applied Physics Letters*, **88**.

[32] Tu, C.S., Siny, I.G. and Schimidt, V.H. (1994) Dielectric, NMR and X-Ray diffraction study of $Cs_{1-x}(NH_4)_xH_2PO_4$. *Physical Review B*, **49**, 11550.

[33] Chowdury, P.R. and Deshpande, S.B. (1984) *Indian Journal of Pure & Applied Physics*, **22**, 708.

[34] Jonscher, A.K. and Dube, D.C. (1978) Low frequency dispersion in tri-glycyne sulphate. *Ferroelectrics*, **17**, 533-536.

[35] Jonscher, A.K. (1989) Interpretation of non-ideal dielectric plots. *Journal of Material Science*, **24**, 372.

[36] Garcia-Martin, S., Veiga, M.L., Pico, C., Santamaria, J., Gonzalez-Diaz, G. and Sanchez-Quesada, F. (1990) Dielectric response and ionic conductivity of Cs(NbTe)O_6. *Materials Research Bulletin*, **25**, 1393.

[37] Jonscher, A.K., Deori, K.L., Reau, J.M. and Moali, J. (1979) The dielectric response of $K_xAl_xTi_{8-x}O_{16}$ and $K_xMg_{x/2}Ti_{8-x/2}O_{16}$. *Journal of Materials Science*, **14**, 1308-1320.

[38] Garcia-Martin, S., Veiga, M.L., Pico, C., Santamaria, J., Gonzalez-Diaz, G. and Sanchez-Quesada, F. (1990) Barrier effects on ionic conductivity and dielectric response of Ti(NbTe)O_6. *Solid State Ionics*, **44**, 131.

[39] Varez, A., Alario-Franco, M.A., Santamaria, J., Gonzalez-Diaz, G. and Sanchez-Quesada, F. (1990) Ionic conductivity of lithium inserted $Ba_{2Y}Cu_3O_{7-y}$. *Solid State Communications*, **76(7)**, 917-920.

[40] Kumar, A., Singh, B.P., Choudary, R.N.P. and Thakur, A.K. (2005) A.C. impedance analysis of the effect of dopant concentration on electrical properties of calcium modified $BaSnO_3$. *Journal of Alloys and Compounds*, **394(1-2)**, 292-302.

[41] Scott, B.A., Geiss, E.A., Olson, B.L., Burns, G., Smith, A.W. and O'Kane, D.F. (1970) The tungsten bronze field in the system $K_2O|Li_2O|Nb_2O_5$. *Materials Research Bulletin*, **5(1)**, 47-56.

[42] Kroger, F.A. and Vink, H.J. (1956) Relations between the concentrations of imperfections in crystalline solids. *Solid State Physics*, **3**, 307.

[43] Jonscherm A.K. (1983) Dielectric relaxation in solids. Chelesa Dielectric Press, London.

[44] Henn, F.E.G., Giuntini, J.C., Zanchetta, J.V., Granier, W. and Taha, A. (1990) Frequency dependent protonic conduction in $N_2H_5Sn_3F_7$ glass and $RbHSeO_4$ single crystal. *Solid State Ionics*, **42(1-2)**, 29-36.

[45] Giuntini, J.C., Deroide, B., Belougne, P. and Zanchetta, J.V. (1987) Numerical approach of the correlated barrier hopping model. *Solid State Communications*, **62**, 739.

[46] Bensimon, Y., Giuntini, J.C., Belougne, P., Deroide, B. and Zanchetta, J.V. (1988) *Solid State Communications*, **68**,189.

[47] Venkataraman, B.H. and Varma, K.B.R. (2004) Frequency-dependent dielectric characteristics of ferroelectric $SrBi_2Nb_2O_9$ ceramics. *Solid State Ionics*, **167**, 197-202.

[48] Krthik, C. and Varma, K.B.R. (2006) Dielectric and AC conductivity behavior of $BaBi_2Nb_{209}$ ceramics. *Journal of Physics and Chemistry of Solids*, **67(12)**, 2437-2441.

[49] Almond, D.P. and West, A.R. (1983) Mobile ion concentrations in solid electrolytes from an analysis of a.c. conductivity. *Solid State Ionics*, **22**, 277.

[50] Hill, R.M. and Jonscher, A.K. (1979) *Journal of Non-Crystalline Solids*, **32**, 53.

[51] Almond, D.P., West, A.R. and Grant, R.J. (1982) Temperature dependence of the a.c. conductivity of Na*β*-alumina. *Solid State Communications*, **44(8)**, 1277-1280.

[52] Sundarkannan, S., Kakimoto, K. and Ohsato, H. (2003) *Journal of Applied Physics*, **9**, 5182.

[53] Lu, Z., Bonnet, J.P., Ravez, J. and Hagenmullar, P. (1992) Correlation between low frequency dielectric dispersion (LFDD) and impedance relaxation in ferroelectric ceramic $Pb_2KNb_4TaO_{15}$. *Solid State Ionics*, **57(3-4)**, 235-244.

[54] Thakur, O.P. and Prakash, C. (2003) Dielectric properties of samarium substituted barium strontium titanate. *Phase Transformation*, **76(6)**, 567-574.

Vol.2, No.4, 368-372 (2010)
doi:10.4236/ns.2010.24044

Natural Science

Interfacial control on microstructure, morphology and optics of beta-AgI nanostructures fabricated on sputter-disordered Ag-Sn bilayers

D. Bharathi Mohan[1], C. S. Sunandana[2]

[1] SEG-CEMUC-Department of Mechanical Engineering, University of Coimbra, Coimbra, Portugal; dhanabharathi@yahoo.com
[2] School of Physics, University of Hyderabad, Hyderabad, India; csssp75@yahoo.com

Received 26 October 2009; revised 7 December 2009; accepted 10 February 2010.

ABSTRACT

We report for the first time a non-template based facile growth of hexagonal (*β*) AgI nanorods and nanoplates easily fabricated by rf magnetron sputtering on Ag/Sn bilayers upon controlled iodination. The structural and morphological evolution of the *β*-AgI nanostructures is characterized by X-Ray Diffraction, Atomic Force Microscopy and optical spectroscopy. Sputtering induced disorder in precursor Ag films, high external stress and high defect concentrations at the Sn-AgI interface particularly facilitates the development of layered hexagonal structure of *β*-AgI nanostructures. Extremely sensitive room temperature optical absorbance involving evolution of $W_{1,2}$ and W_3 exciton transitions and emission spectra involving phonon replica corroborate the formation of *β*-AgI nanostructures with high defect concentrations, are aimed at improving the efficiency of photographic process and looking at microelectrodic and optoelectronic applications.

Keywords: Thin Films; Nanostructures; Crystal Structure; Optical Properties

1. INTRODUCTION

Motivated by an extreme mesoscopic ionic conductivity and superior photographic prowess, lately, many researchers have synthesized Ag/AgI, AgI/γ-Al_2O_3 and AgI nanostructures in with controlled nano feature sizes and shapes by routes, including electrochemical, template-chemical, Ultrasonic pyrolysis, W/O microemulsions and solution methods[1-8]. These works, however, focused on the formation of highly stable β-AgI phase at room temperature [9] and its structural disordering, formation of highly conducting interfacial layers (*i.e.* 7H and 9R polytype of AgI with stacking fault arrangements), shape dependent properties and quantum confinement effects in nanorods. In this work, rf magnetron sputtering is exploited as an innovative technique to fabricate β-AgI nanostructures with different shapes-that could lead to miniaturized nanoscale opto-electronic devices [10]. Sputtering introduces structural disorder in Ag films while doping introduces extra disorder and external stress in the host and thus provides localized states for the nucleation of nanoparticles in an effectively kinetically controlled process [11]. To test and implement these ideas we fabricated Ag/Sn bilayers by sputtering where an ultra thin layer (~3.5 nm to 14 nm) of Sn serves as capping agent for Ag particles that introduces external stress at the Ag/Sn interfaces eventually controlling nanomorphology of silver iodide. Moreover, doping could stabilize the crystal structure by strengthening the cation (or anion) sublattice of the ionocovalent semiconductor (CdS or AgI) and introducing a certain number of donors/acceptors in the forbidden gap of the host semiconductor thereby impacting the electrical and optical properties of the host semiconductor [12]. Sn -with valences 2 and 4- was chosen because it is a covalent metal and mixes well with Ag and could controls the iodization kinetics [13] enabling realization of desired optimized nanostructure even for a single Ag/Sn ratio.

2. EXPERIMENTAL METHODS

Ag/Sn bilayers were produced using rf magnetron sputtering (MagSput-1G2-RF-HOT-UPG) with Sn layer thickness varied from 3.5 nm to 14 nm while Ag layer thickness was fixed as 90 nm. Silver (99.99% purity) and tin (99.99% purity) targets each ~55 nm diameter and ~3 mm thick was used for sputtering; the base pressure was always maintained as 1E-6 mbar. At first, Ag films were sputtered onto commercial float glass substrates under constant Ar flow rate and rf power of 20 sccm and 10 Watt respectively. Then, Sn of 3.5 nm, 7 nm and 14 nm thick was successively deposited on Ag films with rf power: 5 Watt and Ar flow rate: 20 sccm. Substrate rotation and sputtering pressure were maintained as 10 RPM and 1E-2 mBar respectively. Thus, bi-layers of Ag (90 nm)/Sn (3.5 nm), Ag (90 nm)/Sn (7 nm) and Ag (90 nm)/Sn (14 nm) were fabricated and stored under vacuum in order to prevent surface oxidation. As grown Ag film and Ag/Sn bilayers were iodized for selected durations ranging from 3 hrs to 24 hours in a specially made jig [14]. AMBIOS XP-1 profilometer was used to measure the thickness and confirmed equal at different places for the homogeneity. X-ray diffraction patterns were obtained using INEL X-Ray Diffractometer (XRD) with Co K_α (λ = 1.78897 A^0) radiation. Atomic Force Microscopy (AFM) measurements were performed using SPA 400 operated in non-contact Dynamic Force Mode (DFM) mode. Optical absorption and photoluminescence studies were carried out using SHIMADZU UV-3101 and HITACHI: F-3010 Fluorescence spectrophotometers respectively.

3. RESULTS AND DISCUSSIONS

Figure 1 shows XRD patterns of Ag film and Ag/Sn bilayers with increasing thickness of Sn layer. Ag is characterized by (111), (200), (220) and (311) planes corresponds to fcc lattice (JCPDS card No. 7440-22-4). Ag/Sn bilayers exhibit similar pattern that obtained in undoped Ag despite increasing Sn layer thickness. However, intensities are decreased in Ag (90 nm)/Sn (3.5 nm) could be due to the formation of quasi amorphous structure as due to Sn induced disorder in Ag. Increasing Sn layer thickness from 7 nm to 14 nm increases the intensities with significant broadening attributed to smaller particle size possibly controlled by Sn atoms. **Figure 2** shows the initial iodination of Ag (90 nm)/Sn (3.5 nm) encourages both γ-AgI and β-AgI phases simultaneously. With 12 hrs iodination, β-AgI phase became stronger while γ-AgI growth stops gradually. β-AgI phase develops gradually with increasing Sn layer thickness which is characterized by (002), (101), (102), (110), (103), (112), (202), (203), (105), (202), (303) and (006) crystal planes (JPCPDS card No. 75-1528). A facile growth of β-AgI phase is observed on Ag (90 nm)/Sn (14 nm) could be due to the development of hexagonal and allied structures pointing to the role of Sn in modifying the stacking of atomic layers by introducing planar defects. Interestingly, (101), (102), (110), (103) and (112) reflections are predominant than from other planes possibly due to the formation of interfacial highly conducting layers *i.e.* 7H and 9R polytypes of AgI with the stacking fault arrangements. This is expectedly due to high external stress and high defect concentrations occurring especially

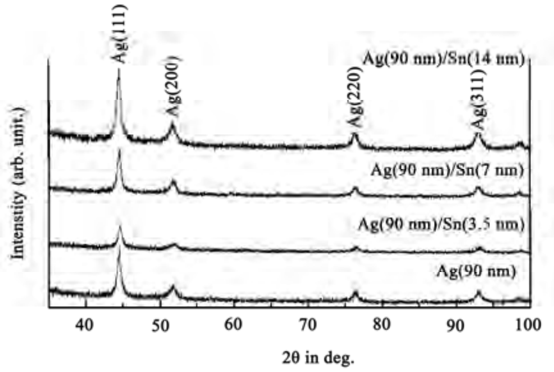

Figure 1. X-ray diffraction patterns of as deposited Ag and Ag/Sn bilayers with increasing Sn layer thickness.

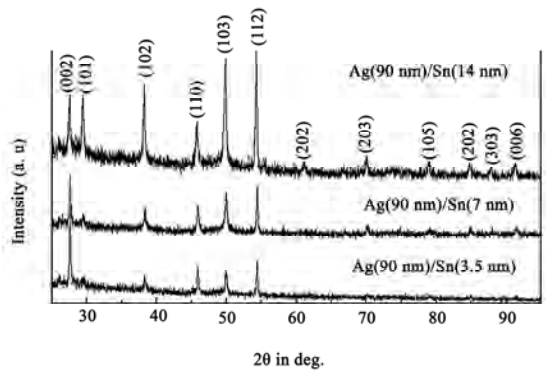

Figure 2. X-ray diffraction patterns of Ag/Sn bilayers iodinated for 24 hrs.

at the Sn/AgI interface [15]. Formations of such polytypes are responsible for the enhanced mesoscopic room temperature ionic conductivity, by as much as four orders of magnitude, compared with bulk β-AgI [16]. Ultra thin ($\leq$ 20 nm) undoped Ag produces γ-AgI while thick ($\geq$ 20 nm) Ag films encourage β-AgI growth [14] however not as neat a structure as observed in bilayers. Lattice parameter increases from 0.408 nm for undoped Ag to 0.409 nm for bilayers as well increases the lattice parameters of *a* (from 0.458 nm to 0.460 nm) and *c* (from 0.751 nm to 0.752 nm) of β-AgI. Increases in lattice parameters possibly reflects the difference in covalent radii of Sn (0.141 nm) and Ag (0.134 nm). Having deposited on glass and Ag surfaces, intrinsic strain could be different for Ag and Sn films as they possess tetragonal and cubic crystal structure respectively. Intrinsic strain determined for iodinated bilayers using Nelson-Reily Function (NRF) [17-18], exhibits zigzag patterns reflecting the presence of intrinsic strain in β-AgI structure (**Figure 3**).

Undoped Ag (**Figure 4(a)**) reveals an inhomogeneous surface with the particle size of about ~20 (±1) nm. Particles are aggregated on the surface as due to lack of thermal energy during deposition. However, Sn layer evens the silver surface (**Figure 4(b)**) by filling pores and

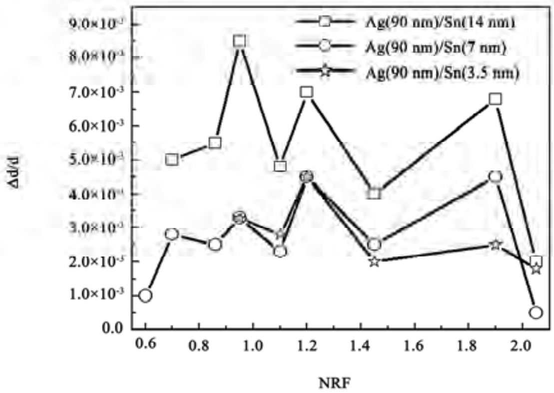

Figure 3. NRF function shows intrinsic strain of β-AgI phase increases with increasing Sn layer thickness.

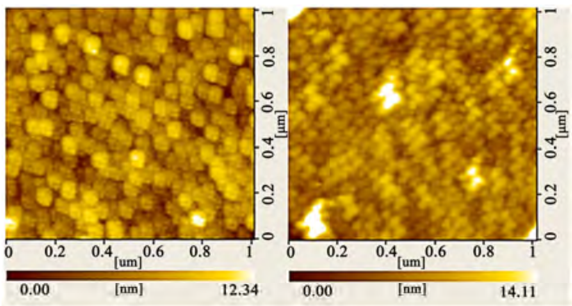

(a) (b)

Figure 4. AFM shows surface morphology of (a) as deposited Ag (90 nm) and (b) as deposited Ag(90 nm) /Sn(7 nm) bilayer.

covering boundaries due to its poor metallicity and higher solubility properties. Iodization of undoped Ag produces spherical shape of AgI particles with the size of about ~150 (±1) nm (**Figure 5(a)**) while Ag/Sn bilayers exhibit rod- and plate- shaped β-AgI particles. Moreover the length of rod increases from 437 (±1) nm to 724 (±1) nm upon increasing tin layer thickness from 3.5 nm to 7 nm (**Figures 5(b)** and **5(c)**). Further increase of doping (14 nm) modifies the morphology from nanorods to nanoplatelets (358 × 353 (±1) nm) (**Figure 5(d)**). Ag atoms need more iodine atoms in order to satisfy the condition ((Ag/I) ≤ 1) for the β-AgI formation and that is indirectly supplied by Sn atoms through unstable SnI_4 tetrahedra.

Uniodized Ag reveals uniodized Ag reveals a broad negative absorption around 320 nm due to Ag reflects the light particularly in opaque films [14,19]. No appreciable changes observed upon Sn doping except some variation in the shape and intensity. At an intermediate stage of iodization process, an evolution of optical absorption at 420 nm occurs due to the dipole forbidden $4d^{10}$-$4d^{9}5s$ transition in AgI allowed by the tetrahedral symmetry of Ag^{+} ion in the wurtzite AgI, attributed to $W_{1,2}$ exciton besides a broad plasmon resonance [14,19, 20] at 500 nm arises due to residual Ag nanoparticles when the films are partially iodized consisting Ag-AgI nanocomposites. After 24 hrs of iodization (**Figure 6**), plasmon resonance disappears while $W_{1,2}$ exciton band enhances alongside a new peak developed at 330 nm due to spin-orbit split I^{-} valence of the spin orbit interaction attributed to W_3 exciton whose degeneracy is lifted due to strain field change at the crystallite surface [21]. These unusual observations are significant because the extremely sensitive room temperature optical absorption on β-AgI has recorded the valence band degeneracy of which is lifted at room temperature which also happens to be the temperature at which iodization is carried out. Absorption becomes very intense, broad and red shifted upon increasing Sn doping [15]. The absorption increases as the length of the nanorods increases from 437 (±1) to 724 (±1) nm however absorption band edge remain same. Surprisingly, absorption is four times intensive for AgI nanoplates as compared to AgI nanospheres. Absorption band is much wider for nanoplates. Band gap [14] decreases from 2.87 eV to 2.83 eV when β-AgI particles change shape from nanospheres to nanoplatelets. The observed red shift arises from not only the different polymorphms of AgI nanoparticles but also due to an increase of Sn layer thickness.

Emission spectra of 24 hrs iodized undoped Ag and Ag/Sn bilayers were performed with the excitation wavelengths 325, 335, 345, 350 and 360 nm. The photoinduced carrier radiative recombination rate is higher for the excitation wavelengths 345 nm and 350 nm. **Figure 7** shows the photoluminescence spectra excited at 350 nm.

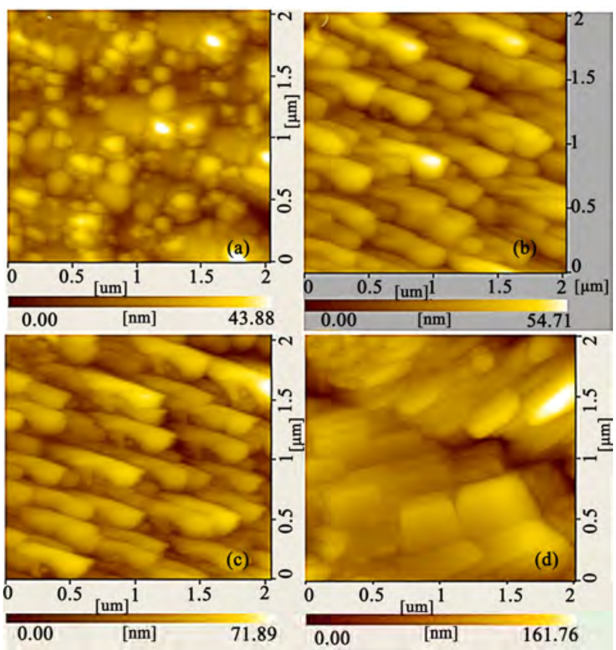

Figure 5. AFM of (a) Ag, (b) Ag(90 nm)/Sn(3.5 nm), (c) Ag(90 nm)/Sn(7 nm) and (d) Ag(90 nm)/Sn(14 nm) iodinated for 24 hrs.

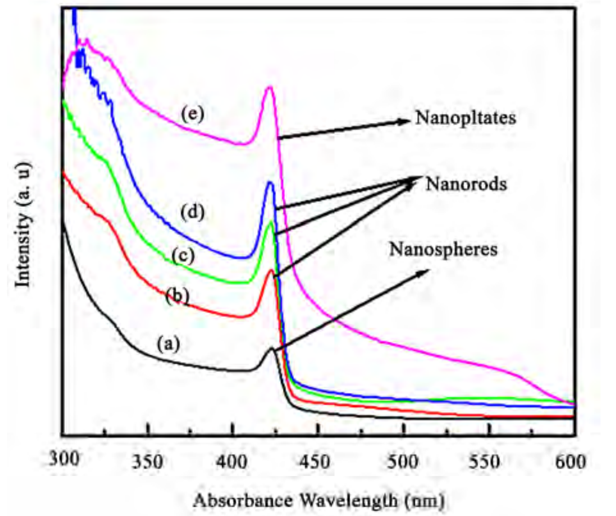

Figure 6. Optical absorbance of 24 hrs iodinated (a) Ag; (b) Ag(90 nm)/Sn(2 nm); (c) Ag(90 nm)/Sn(3.5 nm); (d) Ag(90 nm)/Sn(7 nm); (e) Ag(90 nm)/Sn(14 nm) bilayers.

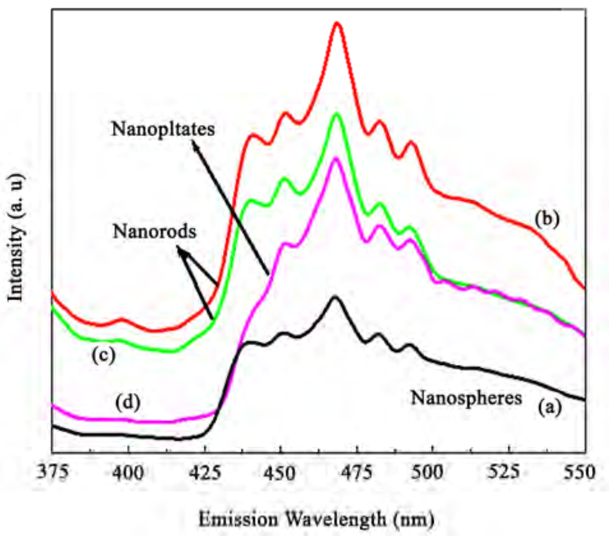

Figure 7. Emission spectra's of 24 hrs iodinated (a) Ag; (b) Ag(90 nm)/Sn(3.5 nm); (c) Ag(90 nm)/Sn(7 nm); (d) Ag(90 nm)/Sn(14 nm) excited at 350 nm.

A sudden jump appears at 426 nm matching with the wavelength of absorbance of the $Z_{1,2}$ exciton [22]. The phonon emission accompanying PL (phonon replica) occurs at 437.8, 450.9, 467.0, 482.5 and 492.2 nm among them the most intense peak centered at 467.0 nm. PL indicates photoexcited electrons at the conduction band edge do not recombine with holes immediately. Instead they undergo many transitions at the shallow trap states or intrinsic near-band edge states slightly below the conduction band involving exciton-phonon and multiphonon interactions. Intrinsic Frenkel defects and impurities could be involved in the formation of trapping states for the recombination. A fundamental reason for the enhancement of probabilities of phonon assisted optical transitions is the essential non-adiabaticity of exciton-phonon systems in quantum dots [23]. The recombination rate increases in nanorods while it is not too high in nanoplates. The relaxation process is apparently slow suggesting that the radiative life time of an exciton is smaller than the time of relaxation between the exciton energy levels. The enhanced trapping of the shallow and deep trap states and the limit of saturation can be visualized from the increase in the full width at half maximum of the inhomogeneously broadened subbands. Accordingly, maximum binding of almost all surface defect sites at low Sn concentration and quenching of radiative emission [24] at higher Sn concentration takes place. Thus, the strong PL features with red shift and multiphonon structure suggests a smaller radiative life time and higher recombination rate with respect to bulk. Reduction in intensity with increasing Sn concentrations saturating the initial traps could further quench the radiative emission, but did not affect the lifetimes effectively. Above a certain limit, Sn effectively blocks charge recombination and decreases the fluorescence quantum efficiency at higher concentrations but does not affect the decay characteristics at all concentrations. This is in accordance with the fact that the presence of higher valency dopant cations strongly reduces the iodination rate of silver under normal conditions. This work therefore has implications for opto-electronic applications.

4. CONCLUSIONS

A non-template based facile growth of hexagonal (β) AgI nanostructures were fabricated on rf magnetron sputtered Ag/Sn bilayers upon controlled iodination. β-AgI phase was strongly observed on Ag (90 nm)/Sn (14 nm) as due to the development of hexagonal and allied structures that eventually proved the possibility of the formation of interfacial highly conducting layers *i.e.* 7H and 9R polytypes of AgI with the stacking fault arrangements. Shapes of the nanoparticles are tailored with respect to the amount of Sn doping onto Ag upon controlled iodization. Evolutions of $W_{1,2}$ and W_3 exciton transitions and phonon replica from absorption and emission spectra respectively corroborates the formation of β-AgI nanostructures with high defect concentrations.

5. ACKNOWLEDGEMENTS

Sincere thanks are due to the University of Hyderabad for the award of research fellowship to D. Bharathi Mohan under UPE programme and for sanctioning publication charges for this paper.

REFERENCES

[1] Liang, C., Terabe, K., Tsuruoka, T., Osada, M., Hasegawa, T. and Aono, M. (2007) AgI/Ag heterojunction

nanowires: Facile electrochemical synthesis, and enhanced ionic conductivity. *Advanced Functional Materials*, **17(9),** 1466-1472.
[2] Lee, W., Yoo, H.-L. and Lee, J.-K. (2001) Template route toward a novel nanostructured superionic conductor film. *Chemical Communications*, **2001(24)**, 2530-2531.
[3] Guo, Y., Lee, J. and Maier, J. (2006) Preparation and characterization of AgI nanoparticles with controlled size, morphology and crystal structure. *Solid State Ionics*, **177(26-32)**, 2467-2471.
[4] Guo, Y.-G., Hu, Y.-S., Lee, J.-S. and Maier, J. (2006) High-performance rechargeable all-solid-state silver battery based on superionic AgI nanoplates. *Electrochemistry Communications*, **8(7)**, 1179-1184.
[5] El-Kouedi, M., Foss, C.A.Jr., Bodolosky-Bettis, S.A. and Bachman, R.E. (2002) Structural analysis of AgI and Au/AgI nanocomposite films by powder x-ray diffraction: Evidence for preferential orientation. *Journal of Physical Chemistry B*, **106(29)**, 7205-7209.
[6] Xu, S. and Lee, Y. (2003) Different morphology at different reactant molar ratios: Synthesis of silver halide low-dimensional nanomaterials in microemulsions. *Journal of Material Chemistry*, **13(1)**, 163-165.
[7] Validzic, I.L., Jankovic, I.A., Mitric, M., Bibic, N. and Nedeljkovic, J.M. (2007) Growth and quantum confinement in AgI nanowires. *Materials Letters*, **61(16)**, 3522-3525.
[8] Validzic, I.L., Jokanovic, V., Uskokovic, D.P. and Nedeljkovic, J.M. (2008) Influence of solvent on the structural and morphological properties of AgI particles prepared using ultrasonic spray pyrolysis. *Materials Chemistry and Physics*, **107(1)**, 28-32.
[9] Chandra, S. (1981) Superionic solids: Principles and applications. North-Holland Publishing Company, Amsterdam.
[10] Mochizuki, S. and Fujishiro, F. (2003) Shallow and deep excited states of mesocopic structure in AgI-γAl_2O_3 composites. *Physica Status Solidi* (*c*), **0(2)**, 763-766.
[11] Mohan, D.B. and Sunandana, C.S. (2007) AgI nanostructure development in sputter-disordered and Al-doped Ag films probed by XRD, SEM, optical absorption and photoluminescence. *Applied Physics A*, **86(1)**, 73-82.
[12] Mohan, D.B. and Sunandana, C.S. (2004) Nanophases in mechanochemically synthesized AgI-CuI system: Structure, phase stability and phase transition. *Journal of Physics and Chemistry of Solids*, **65(10)**, 1669-1677.
[13] Kuiry, S.C., Roy, S.K. and Bose, S.K. (1997) Influence of short circuiting on the kinetics and mechanism of iodide film growth on Ag and Cd-doped Ag. *Metallurgical and Materials Transactions B*, **28(6)**, 1189-1198.
[14] Mohan, D.B. and Sunandana, C.S. (2006) Iodization of rf sputter induced disordered Ag thin films reveals volume plasmon-exciton "transition". *Journal of Applied Physics*, **100(6)**, 4314.
[15] Mohan, D.B. and Sunandana, C.S. (2005) Effect of Sn doping on the growth and optical properties of AgI nanoparticles. *Journal Nanoscience and Nanotechnology*, **5(9)**, 1-5.
[16] Guo, Y.J., Lee, J.-K. and Maier, J. (2005) AgI nanoplates with mesoscopic superionic conductivity at room temperature. *Advanced Materials*, **17(23)**, 2815-2819.
[17] Vook, R.W. and Witt, F. (1965) Structure and annealing behavior of metal films deposited on substrates near 80°K: I. copper films on glass. *Journal of Vacuum Science and Technology*, **2(1)**, 49-57.
[18] Dayal, P.B., Mehta, B.R., Aparna, Y. and Shivaprasad, S.M. (2002) Surface-mediated structural transformation in CdTe nanoparticles dispersed in SiO_2 thin films. *Applied Physics Letters*, **81(22)**, 4254-4256.
[19] Mohan, D.B., Sreejith, K. and Sunandana, C.S. (2007) Surface plasmon-exciton transition in ultra-thin silver and silver iodide films. *Applied Physics B*, **89(1)**, 59-63.
[20] Economou, E.N. (1969) Surface plasmons in thin films. *Physical Review*, **182(2),** 539-554.
[21] Cardona, M. (1963) Optical properties of the silver and cuprous halides. *Physical Review*, **129(1)**, 69-78.
[22] Mochizuki, S. and Fujishiro, F. (2003) Structural, electrical and optical studies on AgI-anatase composites. *Journal of Physics*: *Condensed Matter*, **15(29)**, 5057-5072.
[23] Kumar, P.S. (2002) Ionic and mesoscopic aspects of cation stabilized silver iodide. Ph.D Thesis, University of Hyderabad, Hyderabad, India.
[24] Kumar, P.S. and Sunandana, C.S. (2002) Steady-state photoluminescence characteristics of Sb-doped AgI thin films. *Nano Letters*, **2(9)**, 975-978.

Vol.2, No.4, 373-378 (2010)
doi:10.4236/ns.2010.24045

Natural Science

A nonmonotone adaptive trust-region algorithm for symmetric nonlinear equations*

Gong-Lin Yuan[1], Cui-Ling Chen[2], Zeng-Xin Wei[1]

[1]College of Mathematics and Information Science, Guangxi University, Nanning, China; glyuan@gxu.edu.cn
[2]College of Mathematics Science, Guangxi Normal University, Guilin, China

Received 23 December 2009; revised 1 February 2010; accepted 3 February 2010.

ABSTRACT

In this paper, we propose a nonmonotone adaptive trust-region method for solving symmetric nonlinear equations problems. The convergent result of the presented method will be established under favorable conditions. Numerical results are reported.

Keywords: Trust Region Method; Global Convergence; Symmetric Nonlinear Equations

1. INTRODUCTION

Consider the following system of nonlinear equations:

$$g(x)=0, x\in R^n \tag{1}$$

where $g: R^n \to R^n$ is continuously differentiable, the Jacobian $\nabla g(x)$ of g is symmetric for all $x\in R^n$. Define a norm function by $\varphi(x)=\frac{1}{2}\|g(x)\|^2$. It is not difficult to see that the nonlinear equations problem **Eq.1** is equivalent to the following global optimization problem

$$\min\ \varphi(x),\ x\in R^n \tag{2}$$

Here and throughout this paper, we use the following notations.

- $\|\cdot\|$ denote the Euclidian norm of vectors or its induced matrix norm.
- $\{x_k\}$ is a sequence of points generated by an algorithm, and $g(x_k)$ and $\varphi(x_k)$ are replaced by g_k and φ_k respectively.
- B_k is a symmetric matrix which is an approximation of $\nabla g(x)^T \nabla g(x)$.

It is well known that there are many methods for the unconstrained optimization problem $\min_{x\in R^n} f(x)$ (see [1-7], *etc.*), where the trust-region methods are very successful, *e.g.*, Moré and Sorensen [8]. Other classical references on this topic are [9-12]. Trust- region methods have been applied to equality constrained problems [13-16]. Many authors have studied the trust-region method [2,17-22] too. Zhang [23] combined the trust region subproblem with nonmonotone technique to present a nonmonotone adaptive trust region method and studied its convergence properties.

$$\begin{aligned}&\min\ \nabla f(x_k)^T d+\frac{1}{2}d^T H_k d\\ &s.t.\ \|d\|\le h_k,\ d\in R^n\end{aligned} \tag{3}$$

where H_k is the Hessian of some function $f: R^n\to R$ at x_k or an approximation to it, $h_k=c_1^{p_1}\|\nabla f(x_k)\|M_k'$, $0<c_1<1$, $M_k'=\|B_k'^{-1}\|$, p_1 is a nonnegative integer, they adjust p_1 instead of adjusting the trust radius, and B_k' is a safely positive definite matrix based on Schnabel and Eskow [24] modified cholesky factorization, $B_k'=H_k+E_k$, where $E_k=0$ if H_k is safely positive definite, and E_k is a diagonal matrix chosen to make B_k' positive definite otherwise.

For nonlinear equations, Griewank [25] first established a global convergence theorem for quasi-Newton method with a suitable line search. One nonmonotone backtracking inexact quasi-Newton algorithm [26] and the trust region algorithms [27-30] were presented. A Gauss-Newton-based BFGS method is proposed by Li and Fukushima [31] for solving symmetric nonlinear equations. Inspired by their ideas, Wei [32] and Yuan [33-37] made a further study. Recently, Yuan and Lu [38] presented a new backtracking inexact BFGS method for symmetric nonlinear equations.

Inspired by the technique of Zhang [23], we propose a new nonmotone adaptive trust region method for solving

*Foundation item: National Natural Science Foundation of China (10761001), the Scientific Research Foundation of Guangxi University (Grant No. X081082), Guangxi SF grands 0991028, the Scientific Research Foundation of Guangxi Education Department (Grant No. 200911LX53), and the Youth Backbone Teacher Foundation of Guangxi Normal University.

Eq.1. More precisely, we solve **Eq.1** by the method of iteration and the main step at each iteration of the following method is to find the trial step d_k. Let x_k be the current iteration. The trial step d_k is a solution of the following trust region subproblem

$$\min\ q_k(d) = \nabla \varphi(x_k)^T d + \frac{1}{2} d^T B_k d$$
$$s.\,t.\ \| d \| \le \Delta_k,\ d \in R^n \tag{4}$$

where $\nabla \varphi(x_k) = \nabla g(x_k) g(x_k)$, $\Delta_k = c^p \| \nabla \varphi(x_k) \| M_k$, $0 < c < 1$, $M_k = \| B_k^{-1} \|$, p is a nonnegative integer, and matrix B_k is an approximation of $\nabla g(x_k)^T g(x_k)$ which is generated by the following BFGS formula [31]:

$$B_{k+1} = B_k - \frac{B_k s_k s_k^T B_k}{s_k^T B_k s_k} + \frac{y_k y_k^T}{y_k^T s_k} \tag{5}$$

where $s_k = x_{k+1} - x_k$, $y_k = g(x_k + \delta_k) - g_k$, $\delta_k = g_{k+1} - g_k$. By $y_k = g(x_k + \delta_k) - g_k$, we have the approximate relations

$$y_k = g(x_k + \delta_k) - g_k \approx \nabla g_{k+1} \delta_k \approx \nabla g_{k+1} \nabla g_{k+1} s_k$$

Since B_{k+1} satisfies the secant equation $B_{k+1} s_k = y_k$ and ∇g_k is symmetric, we have approximately

$$B_{k+1} \approx \nabla g_{k+1} \nabla g_{k+1} s_k = \nabla g_{k+1}^T \nabla g_{k+1} s_k$$

This means that B_{k+1} approximates $\nabla g_{k+1}^T \nabla g_{k+1}$ along direction s_k. We all know that the update **Eq.5** can ensure the matrix B_{k+1} inherits positive property of B_k if the condition $s_k^T y_k > 0$ is satisfied. Then we can use this way to insure the positive property of B_k.

This paper is organized as follows. In the next section, the new algorithm for solving **Eq.1** is represented. In Section 3, we prove the convergence of the given algorithm. The numerical results of the method are reported in Section 4.

2. THE NEW METHOD

In this section, we give our algorithm for solving **Eq.1**. Firstly, one definition is given. Let

$$\varphi_{l(k)} = \max_{0 \le j \le n(k)} \{\varphi_{k-j}\},\ k = 0, 1, 2, \cdots \tag{6}$$

where $n(k) = \min\{M, k\}$, $M \ge 0$ is an integer constant. Now the algorithm is given as follows.

- **Algorithm 1.**

Initial: Given constants $\rho, c \in (0,1)$, $p = 0$, $\varepsilon > 0$, $M \ge 0$, $x_0 \in R^n$, $B_0 \in R^n \times R^n$. Let $k := 0$;

Step 1: If $\| \nabla \varphi_k \| < \varepsilon$, stop. Otherwise, go to step 2;

Step 2: Solve the problem **Eq.4** with $\Delta = \Delta_k$ to get d_k;

Step 3: Calculate $n(k)$, $\varphi_{l(k)}$ and the following r_k:

$$r_k = \frac{\varphi_{l(k)} - \varphi(x_k + d_k)}{q_k(0) - q_k(d_k)} \tag{7}$$

If $r_k < \rho$, then we let $p = p + 1$, go to step 2. Otherwise, go to step 4;

Step 4: Let $x_{k+1} = x_k + d_k$, $\delta_k = g_{k+1} - g_k$, $y_k = g(x_k + \delta_k) - g_k$. If $d_k^T y_k > 0$, update B_{k+1} by **Eq.5**, otherwise let $B_{k+1} = B_k$.

Step 5: Set $k := k + 1$ and $p = 0$. Go to step 1.

Remark. i) In this algorithm, the procedure of "Step 2-Step 3-Step 2" is named as inner cycle.

ii) The Step 4 in Algorithm 1 ensures that the matrix sequence $\{B_k\}$ is positive definite.

In the following, we give some assumptions.

Assumption A. j) Let Ω be the level set defined by

$$\Omega = \{x \mid \| g(x) \| \le \| g(x_0) \| \} \tag{8}$$

is bounded and $g(x)$ is continuously differentiable in Ω for all any given $x_0 \in R^n$.

jj) The matrices $\{B_k\}$ are uniformly bounded on Ω_1, which means that there exists a positive constant M such that

$$\| B_k \| \le M,\ \forall k \tag{9}$$

Based on Assumption A and Remark (ii), we have the following lemma.

Lemma 2.1. Suppose that Assumption A(jj) holds. If d_k is the solution of **Eq.4**, then we have

$$-q_k(d_k) \ge \frac{1}{2} \| \nabla \varphi(x_k) \| \min\{\Delta_k, \frac{\| \nabla \varphi(x_k) \|}{\| B_k \|}\} \tag{10}$$

Proof. Using d_k is the solution of **Eq.4**, for any $\alpha \in [0,1]$, we get

$$-q_k(d_k) \ge -q_k(-\alpha \frac{\Delta_k}{\| \nabla \varphi(x_k) \|} \nabla \varphi(x_k))$$

$$= \alpha \Delta_k \| \nabla \varphi(x_k) \| - \frac{1}{2} \alpha^2 \Delta_k^2 (\nabla \varphi(x_k))^T B_k \nabla \varphi(x_k) / \| \nabla \varphi(x_k) \|^2$$

$$\ge \alpha \Delta_k \| \nabla \varphi(x_k) \| - \frac{1}{2} \alpha^2 \Delta_k^2 \| B_k \|$$

Then, we have

$$-q_k(d_k) \ge \max_{0 \le \alpha \le 1} [\alpha \Delta_k \| \nabla \varphi(x_k) \| - \frac{1}{2} \alpha^2 \Delta_k^2 \| B_k \|]$$

$$\ge \frac{1}{2} \| \nabla \varphi(x_k) \| \min\{\Delta_k, \frac{\| \nabla \varphi(x_k) \|}{\| B_k \|}\}$$

The proof is complete.

In the next section, we will concentrate on the convergence of Algorithm 1.

3. CONVERGENCE ANALYSIS

The following lemma guarantees that Algorithm 1 does not cycle infinitely in the inner cycle.

Lemma 3.1. Let the Assumption A hold. Then Algorithm 1 is well defined, *i.e.*, Algorithm 1 does not cycle in the inner cycle infinitely.

Proof. First, we prove that the following relation holds when p is sufficiently large

$$\frac{\varphi_k - \varphi(x_{k+1})}{-q_k(d_k)} \geq \rho \quad (11)$$

Obviously, $\|\nabla\varphi(x_k)\| \geq \varepsilon$ holds, otherwise, Algorithm 1 stops. Hence

$$\Delta_k = \frac{c^p \|\nabla\varphi(x_k)\|}{\|B_k\|} \to 0,\ p \to \infty \quad (12)$$

By Lemma 2.1, we conclude that

$$-q_k(d_k) \geq \frac{1}{2}\|\nabla\varphi(x_k)\| \min\{\Delta_k, \frac{\|\nabla\varphi(x_k)\|}{\|B_k\|}\} \geq \frac{1}{2}\varepsilon\Delta_k,$$
$$\text{as } p \to \infty \quad (13)$$

Consider

$$|\varphi_k - \varphi(x_{k+1}) + q_k(d_k)| = O(\|d_k\|^2) \quad (14)$$

By **Eqs.12-14**, and $\|d_k\| \leq \Delta_k$, we get

$$\left|\frac{\varphi_k - \varphi(x_{k+1})}{-q_k(d_k)} - 1\right| = \left|\frac{\varphi_k - \varphi(x_{k+1}) + q_k(d_k)}{-q_k(d_k)}\right| \leq \frac{2O(\|d_k\|^2)}{\varepsilon\Delta_k} \to 0$$

Therefore, for p sufficiently large, which implies **Eq.11**.

The definition of the algorithm means that

$$r_k = \frac{\varphi_{l(k)} - \varphi(x_{k+1})}{-q_k(d_k)} \geq \frac{\varphi_k - \varphi(x_{k+1})}{-q_k(d_k)} \geq \rho .$$

This implies that Algorithm 1 does not cycle in the inner cycle infinitely. Then we complete the proof of this lemma.

Lemma 3.2. Let Assumption A hold and $\{x_k\}$ be generated by the Algorithm 1. Then we have $\{x_k\} \subset \Omega$.

Proof. We prove the result by induction. Assume that $\{x_k\} \subset \Omega$, for all $k \geq 0$. By using the definition of the algorithm, we have

$$r_{l(k)} \geq \rho > 0 \quad (15)$$

Then we get

$$\varphi_{l(k)} \geq \varphi_{k+1} - \rho q_k(d_k) > \varphi_{k+1} \quad (16)$$

By $l(k) \leq k$, $\varphi_{l(k)} \leq \varphi_0$, from **Eq.16**, we have

$$\varphi_{k+1} \leq \varphi_0,$$

this implies

$$\|g_{k+1}\| \leq \|g_0\|,$$

i.e.,

$$x_{k+1} \in \Omega$$

which completes the proof.

Lemma 3.3. Let Assumption A hold. Then $\{\varphi_{l(k)}\}$ is not increasing monotonically and is convergent.

Proof. By the definition of the algorithm, we get

$$\varphi_{l(k)} \geq \varphi_{k+1},\ \forall k \quad (17)$$

We proceed the proof in the following two cases.

1) $k \geq M$. In this case, from the definition of $\varphi_{l(k)}$ and **Eq.17**, it holds that

$$\begin{aligned}\varphi_{l(k+1)} &= \max_{0 \leq j \leq n(k+1)}\{\varphi_{k+1-j}\} \\ &= \max\{\max_{0 \leq j \leq n(k)-1}\{\varphi_{k-j}\}, \varphi_{k+1}\} \\ &\leq \varphi_{l(k)}\end{aligned} \quad (18)$$

2) $k < M$. In this case, using induction, we can prove that

$$\varphi_{l(k)} = \varphi_0$$

Therefore, the sequence $\{\varphi_{l(k)}\}$ is not increasing monotonically. By Assumption A(j) and Lemma 3.2, we know that $\{\varphi_k\}$ is bounded. Then $\{\varphi_{l(k)}\}$ is convergent.

In the following theorem, we establish the convergence of Algorithm 1.

Theorem 3.1. Let the conditions in Assumption A hold. If $\varepsilon = 0$, then the algorithm either stops finitely or generates an infinite sequence $\{x_k\}$ such that

$$\liminf_{k\to\infty} \varphi_k = 0 \quad (19)$$

Proof. We prove the theorem by contradiction. Assume that the theorem is not true. Then here exists a constant $\varepsilon_1 > 0$ satisfying

$$\varphi_k \geq \varepsilon_1,\ \forall k . \quad (20)$$

By Assumption A(jj) and the definition of B_k, there exists a constant $m > 0$ such that

$$\|B_k^{-1}\| \geq m \quad (21)$$

Therefore, according to Assumption A(j), Lemma 2.1, **Eq.20**, and **Eq.21**, there is a constant $b_1 > 0$ such that

$$-q_k(d_k) \geq b_1 c^{p_k} \quad (22)$$

where p_k is the value of p at which the algorithm gets out of the inner cycle at the point x_k. By step 2, step 3, step 4, and **Eq.22**, we know

$$\varphi_{l(k)} \geq \varphi_{k+1} + \rho b_1 c^{p_k} \tag{23}$$

Then

$$\varphi_{l(k+1)} \leq \varphi_{l(l(k))} - \rho b_1 c^{p_{l(k)}}. \tag{24}$$

By Lemma 3.3 and **Eq.24**, we deduce that

$$p_{l(k)} \to \infty \tag{25}$$

The definition of the algorithm implies that $d'_{l(k)}$ which corresponds to the following subproblem is unacceptable:

$$\min_{d \in R^n} \varphi_{l(k)}^T d + \frac{1}{2} d^T B_{l(k)} d = q_{l(k)}(d),$$

$$s.t. \ \| d \| \leq c^{p_{l(k)}-1} M_{l(k)} \varphi_{l(k)} = \frac{\Delta_{l(k)}}{c} \tag{26}$$

i.e.,

$$\frac{\varphi_{l(l(k))} - \varphi(x_{l(k)} + d'_{l(k)})}{-q_{l(k)}(d'_{l(k)})} < \rho \tag{27}$$

By the definition of $\varphi_{l(k)}$, we have

$$\frac{\varphi_{l(l(k))} - \varphi(x_{l(k)} + d'_{l(k)})}{-q_{l(k)}(d'_{l(k)})} \geq \frac{\varphi_{l(k)} - \varphi(x_{l(k)} + d'_{l(k)})}{-q_{l(k)}(d'_{l(k)})} \tag{28}$$

By step 2, step 3, and step 4, we have that when k is sufficiently large, the following formula holds:

$$\frac{\varphi_{l(k)} - \varphi(x_{l(k)} + d'_{l(k)})}{-q_{l(k)}(d'_{l(k)})} \geq \rho \tag{29}$$

This combines with **Eq.28** will contradicts **Eq.27**. The contradiction shows that the theorem is true. The proof is complete.

Remark. Theorem 3.1 shows that the iterative sequence $\{x_k\}$ generated by Algorithm 1 such that $\nabla g(x_k) g(x_k) \to 0$. If x^* is a cluster point of $\{x_k\}$ and $\nabla g(x^*)$ is nonsingular, then we have $\| g(x_k) \| \to 0$. This is a standard convergence result for nonlinear equations. At present, there is no method that can satisfy $\| g(x_k) \| \to 0$ without the assumption that $\nabla g(x^*)$ is nonsingular.

4. NUMERICAL RESULTS

In this section, results of some preliminary numerical experiments are reported to test our given method.

Problem. The discretized two-point boundary value problem is the same to the problem in [39]

$$g(x) \equiv Ax + \frac{1}{(n+1)^2} F(x) = 0$$

where A is the $n \times n$ tridiagonal matrix given by

$$A = \begin{bmatrix} 3 & -1 & & & & \\ -1 & 3 & -1 & & & \\ & -1 & 3 & -1 & & \\ & & \ddots & \ddots & \ddots & \\ & & & \ddots & \ddots & -1 \\ & & & & -1 & 3 \end{bmatrix}$$

and $F(x) = (F_1(x), F_2(x), \cdots F_n(x))^T$, with

$$F_i(x) = \sin x_i - 1, \ \text{i=1,2,} \cdots nS$$

In the experiments, the parameters were chosen as $c = 0.01$, $M = 10$, and $\rho = 0.8$, B_0 is the unit matrix. Solving the subproblem **Eq.4** to get d_k by *Dogleg* method. The program was coded in MATLAB 7.0. We stopped the iteration when the condition $\| g_k \| \leq 10^{-5}$ was satisfied. The columns of the tables have the following meaning:

Dim: the dimension of the problem.

NG: the number of the function evaluations.

NI: the total number of iterations.

GG: the norm of the function evaluations.

The numerical results (**Table 1**) indicate that the proposed method performs quite well for the Problem. Moreover, the inverse initial points and the initial points don't influence the performance of Algorithm 1 very much. Especially, the numerical results hardly change with the dimension increasing.

Discussion. In this paper, based on [23], a modified algorithm for solving symmetric nonlinear equations is presented. The convergent result is established and the numerical results are also reported. We hope that the proposed method can be a topic of further research for symmetric nonlinear equations.

Table 1. Test results for problem.

x_0	(2, … ,2)	(10, … ,10)	(50, … ,50)	(-10, … ,-10)	(-2, … ,-2)
Dim	NI/NG/GG	NI/NG/GG	NI/NG/GG	NI/NG/GG	NI/NG/GG
n = 49	191/391/9.557342e-006	196/401/6.091920e-006	253/515/7.487518e-006	286/581/9.484488e-006	206/421/9.047968e-006
n = 100	240/505/9.607401e-006	402/829/9.985273e-006	117/259/8.296290e-006	185/395/9.828274e-006	144/313/9.842536e-006
n = 300	223/463/8.060658e-006	260/537/9.470041e-006	241/499/3.894953e-006	246/509/9.915900e-006	233/483/9.705042e-006
n = 500	157/331/9.236809e-006	171/359/9.814318e-006	177/371/9.567563e-006	170/357/9.852428e-006	155/327/7.401986e-006

REFERENCES

[1] Yuan, G.L. and Lu, X.W. (2009) A modified PRP conjugate gradient method. *Annals of Operations Research*, **166(1)**, 73-90.

[2] Yuan, G.L. and Lu, X.W. (2008) A new line search method with trust region for unconstrained optimization. *Communications on Applied Nonlinear Analysis*, **15(1)**, 35-49.

[3] Yuan, G.L. and Wei, Z.X. (2009) New line search methods for unconstrained optimization. *Journal of the Korean Statistical Society*, **38(1)**, 29-39.

[4] Yuan, G.L. and Wei, Z.X. (2008) Convergence analysis of a modified BFGS method on convex minimizations. *Computational Optimization and Applications*.

[5] Yuan, G.L. and Wei, Z.X. (2008) The superlinear convergence analysis of a nonmonotone BFGS algorithm on convex objective functions. *Acta Mathematica Sinica*, English Series, **24(1)**, 35-42.

[6] Yuan, G.L. and Lu, X.W. and Wei, Z.X. (2007) New two-point stepsize gradient methods for solving unconstrained optimization problems. *Natural Science Journal of Xiangtan University*, **29(1)**, 13-15.

[7] Yuan, G.L. and Wei, Z.X. (2004) A new BFGS trust region method. *Guangxi Science*, **11**, 195-196.

[8] Moré, J.J. and Sorensen, D.C. (1983) Computing a trust-region step. *SIAM Journal on Scientific and Statistical Computing*, **4(3)**, 553-572.

[9] Flecher, R. (1987) Practical methods of optimization. 2nd Edition, John and Sons, Chichester.

[10] Gay, D.M. (1981) Computing optimal locally constrained steps. *SIAM Journal on Scientific and Statistical Computing*, **2**, 186-197.

[11] Powell, M.J.D. (1975) Convergence properties of a class of minimization algorithms. Mangasarian, O.L., Meyer, R.R. and Robinson, S.M., Ed., *Nonlinear Programming*, Academic Press, New York, **2**, 1-27.

[12] Schultz, G.A., Schnabel, R.B. and Bryrd, R.H. (1985) A family of trust-region-based algorithms for unconstrained minimization with strong global convergence properties. *SIAM Journal on Numerical Analysis*, **22(1)**, 47-67.

[13] Byrd, R.H., Schnabel, R.B. and Schultz G.A. (1987) A trust-region algorithm for nonlinearly constrained optimization. *SIAM Journal on Numerical Analysis*, **24(5)**, 1152-1170.

[14] Celis, M.R., Dennis, J.E. and Tapia, R.A. (1985) A trust-region strategy for nonlinear equality constrained optimization, in numerical optimization 1984. Boggs, P.R. Byrd, R.H. and Schnabel, R.B., Ed., SIAM, Philadelphia, 71-82.

[15] Liu, X. and Yuan, Y. (1997) A global convergent, locally superlinearly convergent algorithm for equality constrained optimization. Research Report, ICM-97-84, Chinese Academy of Sciences, Beijing.

[16] Vardi, A. (1985) A trust-region algorithm for equality constrained minimization: Convergence properties and implementation. *SIAM Journal of Numerical Analysis*, **22(3)**, 575-579.

[17] Nocedal, J. and Yuan, Y. (1998) Combining trust region and line search techniques. *Advances in Nonlinear Programming*, 153-175.

[18] Sterhaug, T. (1983) The conjugate gradient method and trust regions in large-scale optimization. *SIAM Journal Numerical Analysis*, **20(3)**, 626-637.

[19] Yuan, Y. (2000) A review of trust region algorithms for optimization. *Proceedings of the 4th International Congress on Industrial & Applied Mathematics* (*ICIAM* 99), Edinburgh, 271-282.

[20] Yuan, Y. (2000) On the truncated conjugate gradient method. *Mathematical Programming*, **87(3)**, 561-573.

[21] Zhang, X.S., Zhang, J.L. and Liao, L.Z. (2002) An adaptive trust region method and its convergence. *Science in China*, **45**, 620-631.

[22] Yuan, G.L., Meng, S.D. and Wei, Z.X. (2009) A trust-region-based BFGS method with line search technique for symmetric nonlinear equations. *Advances in Operations Research*, **2009**, 1-20.

[23] Zhang, J.L. and Zhang, X.S. (2003) A nonmonotone adaptive trust region method and its convergence. *Computers and Mathematics with Applications*, **45(10-11)**, 1469-1477.

[24] Schnabel, R.B. and Eskow, R. (1990) A new modified cholesky factorization. *SIAM Journal on Scientific and Statistical Computing*, **11(6)**, 1136-1158.

[25] Griewank, A. (1986) The 'global' convergence of Broyden-like methods with a suitable line search. *Journal of the Australian Mathematical Society Series B*, **28**, 75-92.

[26] Zhu, D.T. (2005) Nonmonotone backtracking inexact quasi-Newton algorithms for solving smooth nonlinear equations. *Applied Mathematics and Computation*, **161(3)**, 875-895.

[27] Fan, J.Y. (2003) A modified Levenberg-Marquardt algorithm for singular system of nonlinear equations. *Journal of Computational Mathematics*, **21**, 625-636.

[28] Yuan, Y. (1998) Trust region algorithm for nonlinear equations. *Information*, **1**, 7-21.

[29] Yuan, G.L., Wei, Z.X. and Lu, X.W. (2009) A nonmonotone trust region method for solving symmetric nonlinear equations. *Chinese Quarterly Journal of Mathematics*, **24**, 574-584.

[30] Yuan, G.L. and Lu, X.W. and Wei, Z.X. (2007) A modified trust region method with global convergence for symmetric nonlinear equations. *Mathematica Numerica Sinica*, **11(3)**, 225-234.

[31] Li, D. and Fukushima, M. (1999) A global and superlinear convergent Gauss-Newton-based BFGS method for symmetric nonlinear equations. *SIAM Journal on Numerical Analysis*, **37(1)**, 152-172.

[32] Wei, Z.X., Yuan, G.L. and Lian, Z.G. (2004) An approximate Gauss-Newton-based BFGS method for solving symmetric nonlinear equations. *Guangxi Sciences*, **11(2)**, 91-99.

[33] Yuan, G.L. and Li, X.R. (2004) An approximate Gauss-Newton-based BFGS method with descent directions for solving symmetric nonlinear equations. *OR Transactions*, **8(4)**, 10-26.

[34] Yuan, G.L. and Li, X.R. (2010) A rank-one fitting method for solving symmetric nonlinear equations. *Journal of Applied Functional Analysis*, **5(4)**, 389-407.

[35] Yuan, G.L. and Lu, X.W. and Wei, Z.X. (2009) BFGS trust-region method for symmetric nonlinear equations.

Journal of Computational and Applied Mathematics, **230(1)**, 44-58.

[36] Yuan, G.L., Wei, Z.X. and Lu, X.W. (2006) A modified Gauss-Newton-based BFGS method for symmetric nonlinear equations. *Guangxi Science*, **13(4)**, 288-292.

[37] Yuan, G.L., Wang, Z.X. and Wei, Z.X. (2009) A rank-one fitting method with descent direction for solving symmetric nonlinear equations. *International Journal of Communications, Network and System Sciences*, **2(6)**, 555-561.

[38] Yuan, G.L. and Lu, X.W. (2008) A new backtracking inexact BFGS method for symmetric nonlinear equations. *Computer and Mathematics with Application*, **55(1)**, 116- 129.

[39] Ortega, J.M. and Rheinboldt, W.C. (1970) Iterative solution of nonlinear equations in several variables. Academic Press, New York.

Vol.2, No.4, 379-387 (2010)
doi:10.4236/ns.2010.24046

Natural Science

Study the effect of formulation variables in the development of timed-release press-coated tablets by Taguchi design

Chikkanna Narendra[1*], Mayasandra Srinavasalyengar Srinath[2]

[1]Department of Pharmaceutics, Visveswarapura Institute of Pharmaceutical Sciences, Bangalore, India; narendragcp@rediffmail.com
[2]Department of Pharmaceutics, SET'S College of Pharmacy, Dharwad, India

Received 30 November 2009; revised 28 December 2009; accepted 3 February 2010.

ABSTRACT

In this investigation, the effect of formulation variables on the release properties of timed-release press-coated tablets was studied using the Taguchi method of experimental design. Formulations were prepared based on Taguchi orthogonal array design with different types of hydrophilic polymers (X_1), varying hydrophilic polymer/ethyl cellulose ratio (X_2), and addition of magnesium stearate (X_3) as independent variables. The design was quantitatively evaluated by best fit mathematical model. The results from the statistical analysis revealed that factor X_1, X_3 and interaction factors between X_1X_2 and X_1X_3 were found to be significant on the response lag time (Y_1), where as only factor X1 was found to be significant on the response percent drug release at 8 hrs (Y_2). A numerical optimization technique by desirability function was used to optimize the response variables, each having a different target. Based on the results of optimization study, HPC was identified as the most suitable hydrophilic polymer and incorporation of hydrophobic agent magnesium stearate, could significantly improve the lag time of the timed-release press-coated tablet.

Keywords: Press-Coated Tablet; Taguchi Design; Hydrophilic Polymers; Timed-Release; Hydrophobic Agents

1. INTRODUCTION

During the recent years timed-release preparations has received increasing attention, which release the drug rapidly and completely after a lag time following oral drug administration. This type of delivery system is not only rate controlled but also time and /or site controlled to deliver the drug when it is required. Such time and/or site controlled formulations has been widely investigated for a number of diseases and therapies [1,2].

Over a period, many different approached have been used for delivering the drugs as time and /or site specific which includes, Timeclock® system [3], Chronotropic® system [4], Pulsincap® sysem [5], Port® system [6], TimeRx® system [7] and Geomatrix® system [8]. These systems are developed with intention to meet the needs of chronopathologies with symptoms mostly recurring at night time or early morning hours. The principal advantage of Chronotherapeutic drug delivery system includes consideration of a person's biological rhythms in determining the timing and the amount of medication to optimize a drug's desired effects and minimize the undesired ones. As a consequence there is reduction of dose requirement and this likely to improve patient compliance [9].

In spite of the difficulties faced by releasing actives due to the variable gastrointestinal environment, orally administered timed-release delivery systems are most preferred because they offer flexibility in dosage-form design and are relatively safe. Press-coated tablet composed of an inner core that contains an active pharmaceutical ingredient and inert excipients surrounded by an outer coating layer. The outer coating material may be compressed onto the inner core as compression coated which dissolves or erodes or disintegrates slowly to produce a lag time before the release of active ingredient.

Several types of hydrophilic polymers have been investigated as a compression coating material including hydroxypropylmethylcellulose [10], L-hydroxypropylcellulose [11], hydroxyethylcellulose [12], polyethyleneoxide/polyethyleneglycol [13], and pectin/ hydroxypropylmethylcellulose [14]. Lin *et al*. [15] studied the effect of hydrophilic excipients (spray-dried lactose and HPMC K4M) along with hydrophobic ethylcellulose as an outer coating shell material and concluded that addition of hydrophilic excipients can be very useful in controlling the lag time adequately. The effect of hydroxylpropylmethylcellulose acetate succinate (HPMCAS) and water soluble/insoluble plasticizers-adsorbent as outer coating material was reported by Fukui *et al*. [16] and the results suggested that the outer shell had a plastic deformation property due to some interaction between HPMCAS and water soluble plasticizers-adsorbent and the same would be useful for colon targeting. In another study, effect of hydrophobic additives were investigated and the results indicated that mixing of HPMCAS, magnesium stearate and calcium stearate at appropriate ratio prolonged the lag time [17].

Design of experiment has been widely used in pharmaceutical field to study the effect of formulation variables and their interaction on dependent (response) variables. [18-20] In the present study an attempt is made to study the effect of formulation variables with the aid of Taguchi design to identify the potential contribution of various types of hydrophilic polymers, varying the hydrophilic/ethylcellulose ratio and presence and absence of magnesium stearate.

2. MATERIALS AND METHODS

2.1. Materials

Theophylline anhydrous was received as gift sample from M/s Eros Pharma Pvt. Ltd., Bangalore, India. Hydroxypropylmethylcllulose (HPMC, Methocel K100M), sodium carboxymethylcellulose (NaCMC, HVP), Hydroxypropylcellulose (HPC, Klucel® EXF Pharm), Hydroxyethylcellulose (HEC, NATROSOL® 250 HX Pharm) and ethylcellulose (EC, Ethocel® 25cPs) were supplied by M/s Strides Arco, Labs Ltd., Bangalore, India as gift samples. Other materials were purchased from commercial source; magnesium stearate (Loba chemicals, Mumbai, India), polyvinylpyrrolidine (PVP K30) (Reidel India chemicals, Mumbai, India), sodium starch glycolate, talc (Nice chemicals, Cochin, India) and directly compressible lactose (S.D. fine chemicals Ltd, Mumbai, India). All other chemicals used in the study were of analytical grade.

2.2. Experimental Design

A Taguchi design [$L_{16}(4^5)$] was implanted to study the effect of formulation variables in the development of timed release press-coated tablet. The Taguchi method utilizes orthogonal arrays are essentially fractional factorial experimental design to study the large number of variables with a small number of experiments. Generally a full factorial design would yield large experiments with replication of centre points.

The levels of the 3 independent variables are as follows;

X_1= Type of Hydrophillic polymer (HPMC, NaCMC, HPC and HEC)

X_2= Hydrophilic polymer/EC (1:1 to 4:1)

X_3= Amount of magnesium stearate (0 to 10%)

The response variables tested include:

Y_1 = Lag time (time required for 10% of drug release in hour)

Y_2 = Percent drug release at 8 hrs.

2.3. Preparation of Core Tablet

A direct compression method was adapted to prepare the core tablet. As shown in **Table 1**, Theophylline anhydrous, lactose, PVP K30 and sodium starch glycolate were mixed in a suitable stainless steel vessel in a tumbler mixer (Rimek, Karnavati Engineering Ltd. Ahmedabad, India) at 100 rpm for 30 min. thoroughly after passing through 80 mesh screen. Further, magnesium stearate and talc were added to the above powder mixture and blended for 10 min. Finally the resulting powder blend was compressed by using a 10-station rotary tablet compression machine (Rimek, Ahmedabad, India) fitted with 8mm standard concave punches. Preparation was performed in 100 tablet batches and compression was controlled to produce 4 ± 0.5kg/cm^2 tablet crushing strength.

2.4. Preparation of Press-Coated Tablet

The formulations were prepared at random following Taguchi design. Prior to compression all the ingredients were passed through 80 mesh screen. The core tablets were press-coated with an appropriate blend of polymers with or with out magnesium stearate as given in **Table 2**. Half the quantity of outer coating material was weighed and transferred into the die; manually the core tablet was placed carefully in the centre of the die. Then, the remaining half quantity of outer coating material was added into the die and compressed by using 10-station rotary tablet compression machine (Rimek, Ahmedabad, India) fitted with 11 mm standard concave punches and compression was controlled to produce 14 ± 0.5kg/cm^2 tablet crushing strength.

2.5. In Vitro Dissolution Studies

The dissolution was performed by using USP dissolution apparatus II paddle assembly (TDT-06T, Electrolab, India) at 37˚C ± 1˚C using 750 ml of pH 1.2 buffer for the first 2 hours and followed by 900 ml of pH 6.8 buffer till the end of dissolution studies. The paddle rotational speed was set to 100 rpm. Aliquots samples were withdrawn at specified time intervals and the samples were

Table 1. Composition of core layer of press-coated tablet.

Ingredients	Quantity (mg/tablet)
Theophylline anhydrous	100
Sodium starch glycolate	10
Polyvinylpyrrolidone	5
Magnesium stearate	1
Talc	2
Lactose	32

Table 2. Composition of coat layer of press-coated tablets based on Taguchi design with observed responses.

Formulation code	X_1 Type	X_2 Ratio	X_3 (%)	Y_1 (Hr)	Y_2 (%)
F1	HPMC	1:1	0	5.3 ± 0.6	10.51 ± 2.01
F2	HPMC	2:1	10	7.5 ± 0.5	10.05 ± 3.16
F3	HPMC	3:1	0	3.4 ± 0.3	12.30 ± 2.37
F4	HPMC	4:1	10	7.1 ± 0.5	42.40 ± 1.15
F5	NaCMC	1:1	0	1.4 ± 1.1	100*
F6	NaCMC	2:1	10	3.1 ± 1.6	100*
F7	NaCMC	3:1	0	2.5 ± 0.9	100*
F8	NaCMC	4:1	10	4.2 ± 0.7	98.14 ± 3.34
F9	HPC	1:1	10	5.5 ± 0.5	100.81 ± 4.22
F10	HPC	2:1	0	2.3 ± 1.3	103.68 ± 3.14
F11	HPC	3:1	10	7.1 ± 0.5	98.87 ± 4.06
F12	HPC	4:1	0	2.8 ± 1.0	114.87 ± 4.13
F13	HEC	1:1	10	4.6 ± 0.3	14.13 ± 4.05
F14	HEC	2:1	0	2.5 ± 0.9	14.32 ± 3.55
F15	HEC	3:1	10	5.2 ± 0.6	11.98 ± 3.22
F16	HEC	4:1	0	2.6 ± 0.5	16.05 ± 3.37

*100% drug release was observed before 8 hrs of dissolution studies.

analyzed spectrophotometrically (UV-1601, Shimadzu, Japan) at 271 nm and the amount of drug released was determined from the calibration curve. The volume of the sample withdrawn each time was replaced with the same volume of the respective buffer solution. The studies were carried out in triplicate and mean values plotted verses time with standard error of mean, indicating the reproducibility of the results.

2.6. Statistical Analysis

The effect of formulation variables on the response variables were statically evaluated by applying one-way ANOVA at 0.05 level using a commercially available software package Design-Expert® version 6.05 (Stat-Ease, Inc.). The design was evaluated by using a suitable model. The best fit model was selected based on the several statistical parameters including multiple correlation coefficient (R^2), adjusted multiple correlation coefficient (adjusted R^2) and the predicted residual sum of square (PRESS). For the model to be chosen as best fit, the PRESS valve should be small relative to the other models.

Linear model

$$Y= b_0 + b_1X_1+ b_2X_2 + b_3X_3$$

Two factor interaction model

$$Y= b_0 + b_1X_1+ b_2X_2 + b_3X_3+ b_4X_1X_2+b_5X_1X_3+b_6X_2X_3$$

where Y is the response variable, b_0 the constant and b_1, b_2, b_3,…,b_5 is the regression coefficient. X_1, X_2 and X_3 stand for the main effect; X_1X_2, X_1X_3 and X_2X_3 are the interaction terms, show how response changes when two factors are simultaneously changed.

3. RESULT AND DISCUSSION

3.1. Experimental Design

Taguchi method as design of experiment was chosen for the organization of the experiments and analysis of the results. Normally a full factorial design for such experiment would yield 4 × 4 × 2 = 32 experiments. In the present case, L_{16} orthogonal array, a mixed-level design (2 factors at 4 levels and one factor at 2 levels) was considered and the size of experimentation was represented by symbolic arrays *i.e.* 16 experiments [21]. The use of more than two factors makes it possible to study some of the eventual non-linear effects with interactions between the factors. The statistical analysis to select the model that best fits the data was obtained by analyzing the results of sequential model given in the **Table 3**. As seen from the table, though the linear model was found to be significant but the PRESS value for a two factor interaction model (2FI) was found to be least hence, 2FI model was considered to analyze the response lag time. For the response percent drug release at 8 hrs, linear model was found be significant with low PRESS value and the same model was further navigated for ANOVA studies.

3.2. Effect of Type of Hydrophilic Polymers

Figures 1-4 show the release profile of press-coated tablets in accordance to type of hydrophilic polymer. If HPMC as type of hydrophilic polymer, increasing the amount of HPMC in the coating layer, formulations F1, F2 and F3 exhibited a minimal drug release at the end of dissolution studies. Such a type of decrease in drug release may be due to increased amount of EC in the coating layer retarded the rate of hydration of HPMC which

Table 3. Comparison of sequential model.

Statistical Parameters	Y_1 (hr)			Y_1 (%)		
	Linear	*2FI*	*Quadratic*	*Linear*	*2FI*	*Quadratic*
R^2	0.8754	0.9940	0.9941	0.9773	0.9910	0.9953
Adjusted R^2	0.8132	0.9704	0.9558	0.9660	0.9550	0.9648
PRESS	16.11724	**9.2977**	20.88	**1907.033**	7752.664	9088.802
p Valve	**0.0003***	0.0522	0.9563	**< 0.0001***	0.713	0.3079

* denotes significant $p < 0.05$.

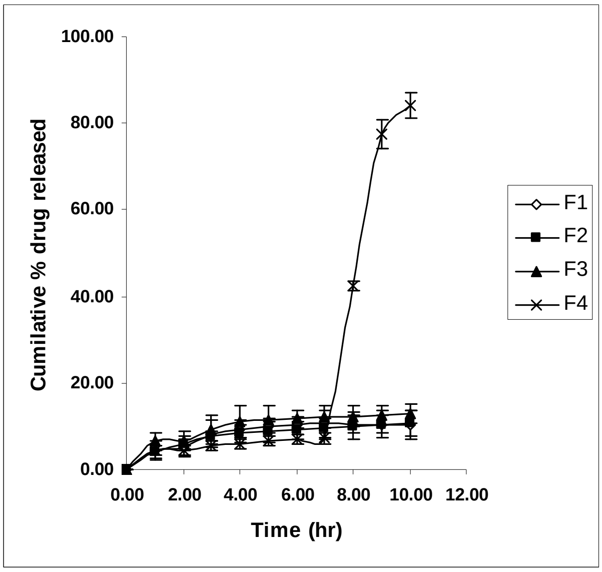

Figure 1. Dissolution profiles of press-coated tablets containing HPMC as type of hydrophilic polymer.

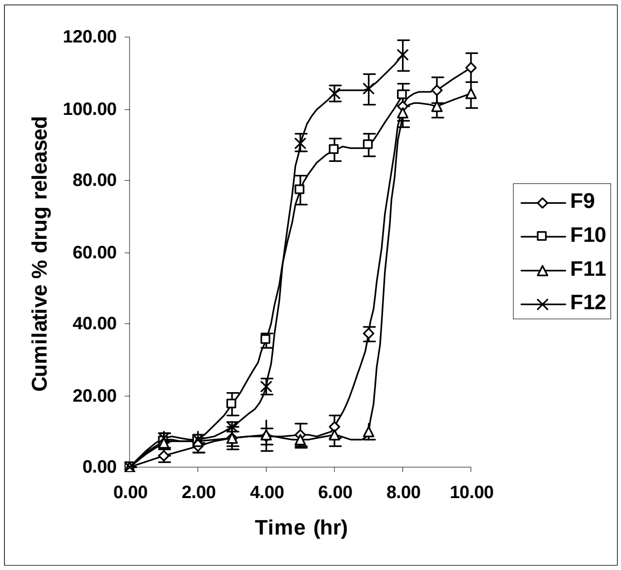

Figure 3. Dissolution profiles of press-coated tablets containing HPC as type of hydrophilic polymer.

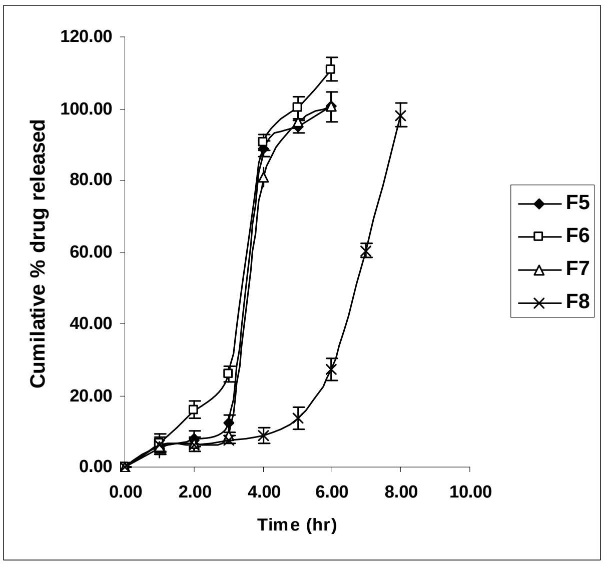

Figure 2. Dissolution profiles of press-coated tablets containing NaCMC as type of hydrophilic polymer.

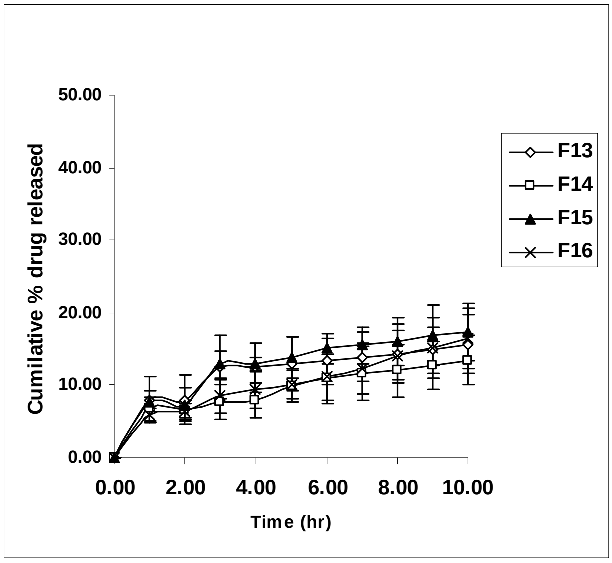

Figure 4. Dissolution profiles of press-coated tablets containing HEC as type of hydrophilic polymer.

in turn hindered the drug release. In case of formulation F4, the release from the tablet was more in a sustained manner than a burst release which may be due to slower hydration of HPMC and also this formulation contains least amount of EC than the other formulations of HPMC.

Similar but opposite result was observed in case of NaCMC, that all the formulations show a relative, slow initial drug release for first 2 hours then the release increases quickly to 100% with in 8 hours of dissolution studies. This behavior of increase in drug release may be due to high solubility of NaCMC at pH 6.8 [22] also this polymer undergoes a quick gel erosion rate and complete disintegration of polymer matrix. In case of HPC as type of hydrophilic polymer, the dissolution behavior was characterized by sigmoid, S-shaped curve release profile with a prolonged lag time and a complete drug release from the core tablet was observed at the end of dissolution studies due to separation of coating layer into two halves allowing the core tablet exposed to dissolution medium (observation made during the dissolution studies). HEC as a type of hydrophilic polymer, the release at the end of dissolution studies were found to be less than 18% which may be due to high viscosity of polymer, decreased water uptake to form a gel matrix [23] and presence of hydrophobic components such as EC and magnesium stearate further prevented the hydration rate.

3.3. Effect of Hydrophilic/EC Ratio

EC, a cellulose ether derivative most widely used as water insoluble polymer for coating of solid dosage forms. Besides as controlled release barrier, they have also been used as moisture barrier to improve stability of hydrolytically liable drugs [24]. The effect of hydrophilic/EC ratio in presence and absence of magnesium stearate on the release properties are summarized in **Table 4**. On comparison of values, increasing the hydrophilic/EC ratio, HPMC containing formulations exhibited a negative effect on lag time where as a positive effect was observed in case of other hydrophilic polymers. HPMC and HEC containing formulations showed no complete drug release from the tablet even at the end of dissolution studies which is probably due to slow hydration rate (because of hydrophobic components) and also the hydrogel layer therefore formed was strong enough and could inhibit further water penetration into the inside of core tablet [25,26].

In case of NaCMC and HPC, they did not show significant difference in their release profile at the end of dissolution studies except that NaCMC containing formulations exhibited shorter lag time with complete drug release with in 8 hours of dissolution studies where as in case of HPC containing formulations exhibited longer lag time with complete drug release at the end of dissolution studies. Such a type of release behavior may be due to faster hydration followed by a combination of disintegration and high erosion rate for the former where as moderate swelling with low erosion rate for the later [26,27].

3.4. Effect of Magnesium Stearte

The effect of magnesium stearate on the lag time and percent drug release at 8 hrs can be visualized from the **Table 4**. The formulations containing magnesium stearate exhibited an improved lag time but no improvement was observed in case of percent drug release at 8 hrs. The beneficial effect of magnesium stearate on the lag time is probably due to its hydrophobic nature prolongs the lag time by significantly decreasing the water uptake and penetration through the coating layer [28].

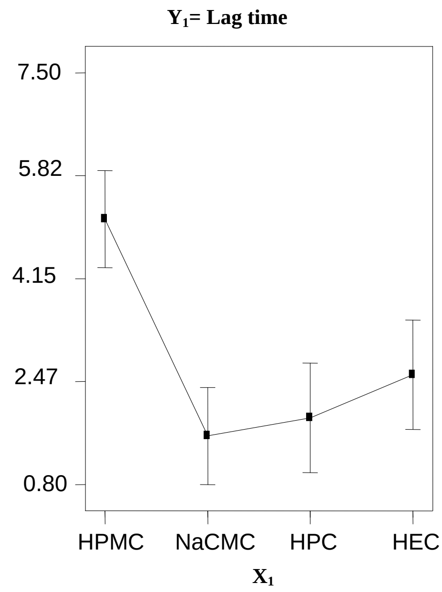

Figure 5. Main effect plot for type of hydrophilic polymer (X_1) on lag time (Y_1) by keeping factors X_2 and X_3 at lower level.

3.5. Statistical Analysis

The model terms for Y_1 (lag time) were found to be significant with an *F* value of 42.10 (0.0052), high R^2 value of 0.9940 indicate the adequate fitting of two factor interaction model. As shown in **Table 5**, factors X_1, X_3 and interaction factors X_1X_2 and X_1X_3 were found to be significant.

At lower level of factors X_2 and X_3, changing the type of hydrophilic polymer from HPMC to HEC the lag time decreases but at higher level of factors X_2 and X_3, the lag time increased to a greater value if HPMC and HPC were used as the type of hydrophilic polymer, where as in case of NaCMC and HEC the effect was found to be negative (**Figures 5** & **6**).

Changing the factor X_3 from lower to higher level, a significant positive effect on the lag time was observed with irrespective of type of hydrophilic polymer and hydrophilic /EC ratio.

The interaction effect between the factors X_1X_2 can be studied with the help of **Figures 7** & **8.**

In presence or absence of magnesium stearate, if X_2 was increased from lower to higher level and by

Table 4. Comparison of release parameters prepared from different types of hydrophilic polymers.

Response	HPMC		NaCMC		HPC		HEC	
	[1]no MgSt	[2]MgSt	[3]no MgSt	[4]MgSt	[5]no MgSt	[6]MgSt	[7]no MgSt	[8]MgSt
Y_1 (Hr)	4.35	7.3	1.95	3.65	2.55	6.3	2.55	4.9
Y_2 (%)	11.405	26.229	100	99.07	109.275	99.84	15.185	13.055

Mean values from the formulations [1]F1-F3, [2]F2-F4, [3]F5-F7, [4]F6-F8, [5]F10-F12, [6]F9-F11, [7]F14-F16, [8]F13-F15.

Table 5. Summary of ANOVA table for dependent variables from Taguchi design.

Source	d.f.	Sum square	Mean square	F value	Probability
Y_1 (Hr)					$R^2 = 0.9940$
Model	12	55.04	4.59	42.10	**0.0052***
X_1	3	19.29	6.43	59.01	**0.0036***
X_2	1	0.46	0.46	4.18	0.1334
X_3	1	26.34	26.34	241.70	**0.0006***
X_1X_2	3	3.30	1.10	10.10	**0.0446***
X_1X_3	3	4.38	1.46	13.41	**0.0304***
X_2X_3	1	0.60	0.60	5.51	0.1005
Y_2 (%)					$R^2 = 0.9773$
Model	5	29611.65	5922.33	86.34	< **0.0001***
X_1	3	29388.78	9796.26	142.82	< **0.0001***
X_2	1	221.52	221.52	3.23	0.1025
X_3	1	1.36	1.36	0.02	0.8910

d.f. denotes degree of freedom; * denotes significant p < 0.05.

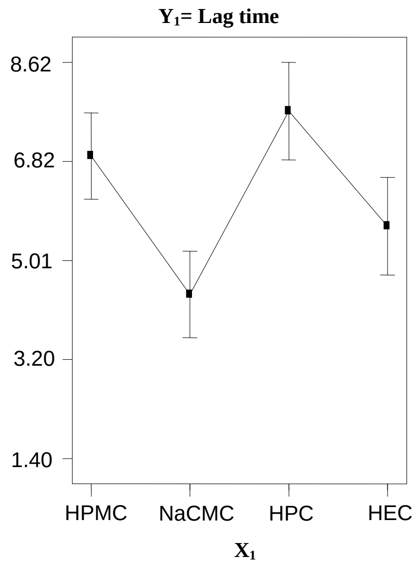

Figure 6. Main effect plot for type of hydrophilic polymer (X_1) on lag time (Y_1) by keeping factors X_2 and X_3 at higher level.

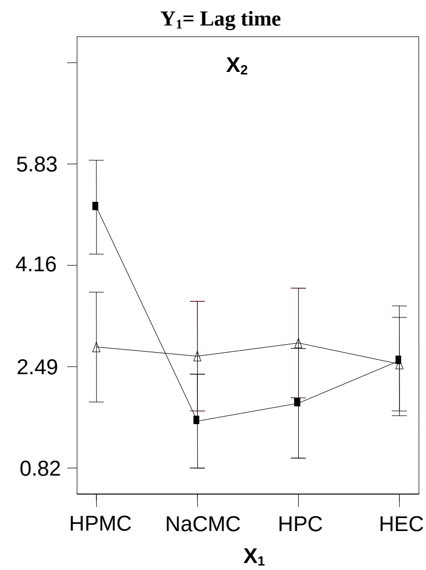

Figure 7. Interaction effect plot between type of hydrophilic polymer (X_1) and hydrophilic polymer/EC ratio (X_2) on lag time (Y_1) at lower level of factor X_3. (▪ Lower level; Δ Higher level).

changing the type of hydrophilic polymer, only HPMC containing formulations showed negative effect where as other hydrophilic polymers showed positive effect on the lag time.

The interaction effect between the factors X_1X_3 can be studied with the help of **Figures 9** & **10.**

From this figures it may be concluded that presence of magnesium stearate in the coating layer exhibited a positive effect on the lag time with irrespective levels of factors X_1 and X_2.

A linear model for Y_2 (percentage drug release at 8 hrs) was found to be significant. In this case, only factor X_1 was found to be significant (**Table 5**). As the factor X_1 was increased from lower to higher level, NaCMC and HPC containing formulations exhibited an increased amount of drug release where as incase of HPMC and HEC containing formulations exhibited very less amount of drug release (**Figures 11** & **12**). This type of behavior may be attributed due to low hydration rate of these polymers in presence to EC and magnesium stearate and if so hydrated they formed a dense layer which further decreases the water diffusion into the core layer and delayed the release of drug from the dosage form [29].

4. OPTIMIZATION

To optimize the studied responses with different targets,

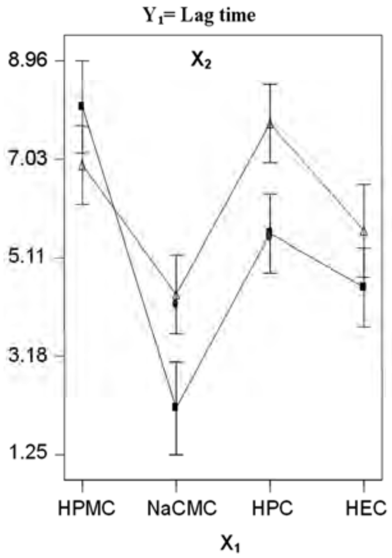

Figure 8. Interaction effect plot between type of hydrophilic polymer (X_1) and hydrophilic polymer/EC ratio (X_2) on lag time (Y_1) at higher level of factor X_3. (▪ Lower level; Δ Higher level).

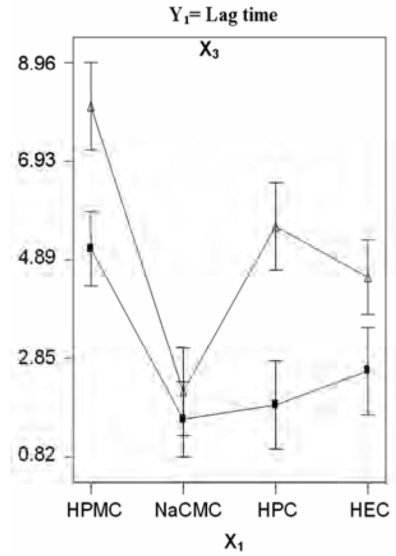

Figure 9. Interaction effect plot between type of hydrophilic polymer (X_1) and amount of magnesium stearate (X_3) on lag time (Y_1) at lower level of factor X_2.(▪ Lower level; Δ Higher level).

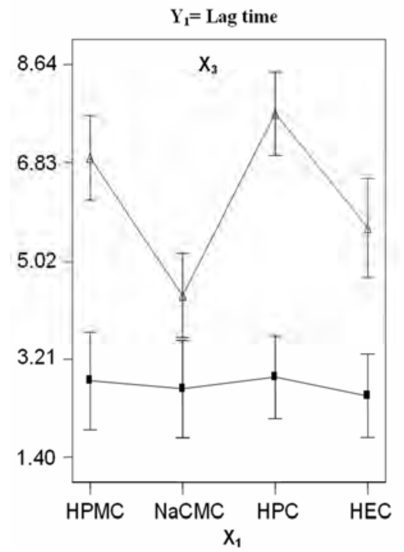

Figure 10. Interaction effect plot between type of hydrophilic polymer (X_1) and amount of magnesium stearate (X_3) on lag time (Y_1) at higher level of factor X_2 (▪ Lower level; Δ Higher level).

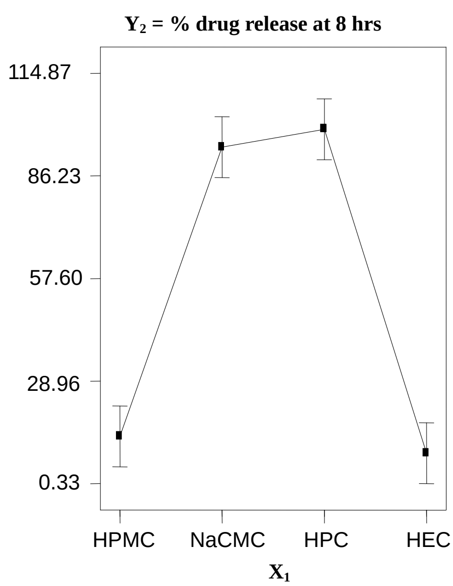

Figure 11. Main effect plot for type of hydrophilic polymer (X_1) on % drug release at 8 hrs (Y_2) by keeping factors X_2 and X_3 at lower level.

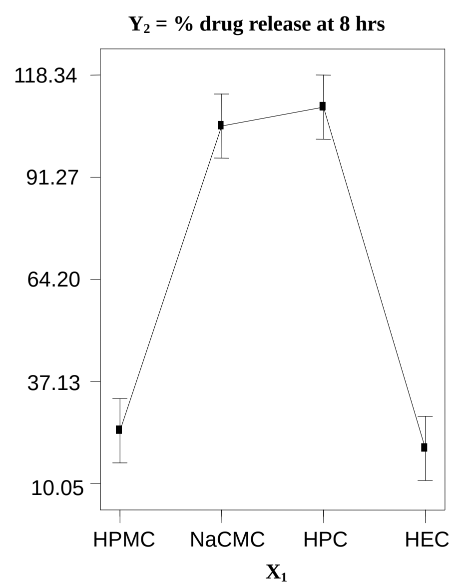

Figure 12. Main effect plot for type of hydrophilic polymer (X_1) on % drug release at 8 hrs (Y_2) by keeping factors X_2 and X_3 at higher level.

a multi-criteria decision approach, like numerical optimization technique by the desirability function was used to generate the optimum settings for the formulation. [30, 31] The variables were optimized for the response Y_1 and Y_2 and the optimized formulation settings were arrived by maximizing the percent drug release at 8 hrs and lag time was kept at range between 6 to 7 hours. According to the statistical prediction, the optimal values obtained was: HPC for type of hydrophilic polymer, hydrophilic polymer/EC ratio ranged between 2.5: 1 to 4: 1 and magnesium stearate also was ranged between 26-30 mg. Since, the Taguchi design is used to screen the formulation variables and to study their significant effect [32], the results from optimization studies was found to be in wider range and suggesting further studies to arrive to the optimal settings.

5. CONCLUSIONS

A Taguchi design was performed to screen the effect of formulation variables on the response lag time and percent drug release at 8 hrs in the development of timed-release press-coated tablets by applying computer optimization technique. Type of hydrophilic polymer was found to be the major factor affecting studied responses and also the results demonstrated that the hydrophobic agent, magnesium stearate could significantly prolonged the lag time. Among the type of different hydrophilic polymers studied, HPC was found to be more suitable and other hydrophilic polymers did not demonstrate beneficial effect (with in the studied variable limits) in the development of timed-release press-coated tablets. Based on the results of optimization studies it was concluded that further studies are required to obtain the optimal settings.

REFERENCES

[1] Ueda, S., Hata, T., Asakura, S., Yamaguchi, H., Kotani, M. and Ueda, Y. (1994) Development of a novel drug release system, time-controlled explosion system (TES). I. Concept and design. *Journal of Drug Targeting*, **2(1)**, 35-44.

[2] Krögel, I. and Bodmeier, R. (1998) Pulsatile drug release from an insoluble capsule body controlled by an erodible plug. *Pharmaceutical Research*, **15(3)**, 474-481.

[3] Pozzi, F., Furlani, P., Gazzaniga, A., Davis, S.S. and Wilding, I.R. (1994) The TIME CLOCK* system: A new oral dosage form for fast and complete release of drug after a predetermined lag time. *Journal of Controlled Release*, **31(1)**, 99-108.

[4] Gazzaniga A., Sangalli, M. and Giordano, F. (1994) Oral chronotropic drug delivery systems: Achievement of time and/or site specificity. *European Journal of Pharmaceutics and Biopharmaceutics*, **40**, 246-250.

[5] McNeil, M.E., Rashid, A. and Stevens, H.N.E. (1994) Dispensing device. U.S. Patent 5,342,624.

[6] Crison, J.R., Siersma, P.R., Taylor, M.D. and Amidon, G.L. (1995) Programmable oral release technology, Port Systems & Mac226: A novel dosage form for time and site specific oral drug delivery. *Proceedings of International Symposium on Control Release of Bioactive Materials*, **22**, 278-279.

[7] Conte, U., Maggi, L., Torre, P., Giunchedi, P. and La-Manna, A. (1993) Press-coated tablets for time programmed release of drugs. *Biomaterials*, **14(13)**, 1017-1023.

[8] Conte, U. and Maggi, L. (1996) Modulation of the dissolution profiles from Geomatrix® multi-layer matrix tablets containing drugs of different solubility. *Biomaterials*, **17(9)**, 889-896.

[9] Lemmer, B. (2007) Chronobiology, drug-delivery, and chronotherapeutics. *Advanced Drug Delivery Reviews*, **59(9-10)**, 825-827.

[10] Wu, B., Shun, N., Wei, X. and Wu, W. (2007) Characterization of 5-fluorouracil release from hydroxypropylmethylcellulose compression-coated tablets. *Pharmaceutical Development and Technology*, **12(2)**, 203-210.

[11] Fukui, E., Uemura, K. and Kobayashi, M. (2000) Studies on applicability of press-coated tablets using hydroxypropylcellulose (HPC) in the outer shell for timed-release preparations. *Journal of Controlled Release*, **68(2)**, 215-223.

[12] Matsuo, M., Arimori, K., Nakamura, C. and Nakano, M. (1996) Delayed-release tablets using hydroxyethylcellulose as a gel-forming matrix. *International Journal of Pharmaceutics*, **138(2)**, 225-235.

[13] Sawada, T., Kondo, H., Nakashima, H., Sako, K. and Hayashi, M. (2004) Time-release compression-coated core tablet containing nifedipine for chronopharmacotherapy. *International Journal of Pharmaceutics*, **280(1-2)**, 103-111.

[14] Ugurlu, T., Turkoglu, M., Gurer, U.S. and Akarsu, B.G. (2007) Colonic delivery of compression coated nisin tablets using pectin/HPMC polymer mixture. *European Journal of Pharmaceutics and Biopharmaceutics*, **67(1)**, 202-210.

[15] Lin, S.Y., Li, M.J. and Lin, K.H. (2004) Hydrophilic excipients modulate the time lag of time-controlled disintegrating press-coated tablets. *AAPS PharmSciTech*, **5(4)**, Article 54.

[16] Fukui, E., Miyamura, N., Yoneyama, T. and Kobayashi, M. (2001) Drug release from and mechanical properties of press-coated tablets with hydroxypropylmethylcellulose acetate succinate and plasticizers in the outer shell. *International Journal of Pharmaceutics*, **217(1-2)**, 33-43.

[17] Fukui, E., Miyamura, N. and Kobayashi, M. (2001) Effect of magnesium stearate or calcium stearate as additives on dissolution profiles of diltiazem hydrochloride from press-coated tablets with hydroxypropylmethylcellulose acetate succinate in the outer shell. *International Journal of Pharmaceutics*, **216(1-2)**, 137-146.

[18] Narendra, C., Srinath M.S. and Rao, B.P. (2005) Development of three layered buccal compact containing metoprolol tartrate by statistical optimization technique. *International Journal of Pharmaceutics*, **304(1-2)**, 102-114.

[19] Lewis, G.A., Mathieu, D. and Phan-Tan-Luu, R. (1999) Pharmaceutical experimental design. Marcel Dekker, New York.

[20] Li, S., Lin, S., Daggy, B.P., Mirchandani, H.L. and Chein, Y.W. (2003) Effect of HPMC and carbopol on the release and floating properties of gastric floating drug delivery system using factorial design. *International Journal of Pharmaceutics*, **253(1-2)**, 13-22.

[21] Nouranian, S., Garambi, H. and Mohammadi, N. (2007) Taguchi-based optimization of adhesion of polyurethane to plasticized poly (vinyl chloride) in synthetic leather. *Journal of Adhesion Science and Technology*, **21(8)**, 705-724.

[22] Conti, S., Maggia, L., Segalea, L., Machiste, E.O., Conte, U., Grenier, P. and Vergnault, G. (2007) Matrices containing NaCMC and HPMC 1. Dissolution performance characterization. *International Journal of Pharmaceutics*, **333(1-2)**, 136-142.

[23] Matsuo, M., Nakamura, C., Arimori, K. and Nakano, M. (1995) Evaluation of hydroxyethylcellulose as a hydrophilic swellable material for delayed release tablets.

Chemical & Pharmaceutical Bulletin, **43(2)**, 311-314.
[24] Mahato, R.I. (2005) Biomaterials for delivery and targeting of proteins and nucleic acids. CRC Press, Florida.
[25] Enayatifard, R., Saeedi, M., Akbari, J. and Tabatabaee, Y.H. (2009) Effect of hydroxypropylmethylcellulose and ethylcellulose content on release profile and kinetics of diltiazem hcl from matrices. *Tropical Journal of Pharmaceutical Research*, **8(5)**, 425-432.
[26] Roy, D.S. and Rohera, B.D. (2002) Comparative evaluation of rate of hydration and matrix erosion of HEC and HPC and study of drug release from their matrices. *European Journal of Pharmaceutical Sciences*, **16(3)**, 193-199.
[27] Hilton, A.K. and Deasy, P.B. (1992) In vitro and in vivo evaluation of an oral sustained-release floating dosage form of amoxycillin trihydrate. *International Journal of Pharmaceutics*, **86(1)**, 79-88.
[28] Durig, T. and Fassihi, R. (1997) Mechanistic evaluation of binary effects of magnesium stearate and talc as dissolution retardants at 85% drug loading in an experimental extended-release formulation. *Journal of Pharmaceutical Sciences*, **86(10)**, 1092-1098.
[29] Minarro, M., Garcia-Montoya, E. and Sune-Negre, J.M. (2001) Study of formulation parameters by factorial design in metoprolol tartrate matrix systems. *Drug Development and Industrial Pharmacy*, **27(9)**, 965-973.
[30] Narendra, C., Srinath, M.S. and Moin, A. (2008) Study the effect of formulation variables on in vitro floating time and release properties of floating drug delivery system by statistical optimization technique. *Chemical Industry & Chemical Engineering Quarterly*, **14,** 17-26.
[31] Sanchez-Lafuente, C., Furlanetto, S., Fernandez-Arevalo, M., Alvarez-Fuentes, J., Rabasco, A.M., Faucci, T., Pinzauti, S. and Mura, P. (2002) Didanosine extended- release matrix tablets: Optimization of formulation variables using statistical experimental design. *International Journal of Pharmaceutics*, **237(1-2)**, 107-118.
[32] Kuo, C.F.J. and Wu, Y.-S. (2006) Optimization of the film coating process for polymer blends by the grey-based Taguchi method. *International Journal of Advanced Manufacturing Technology*, **27(5-6),** 525-530.

Vol.2, No.1, 388-397 (2010)
doi:10.4236/ns.2010.24047

Natural Science

The multiplicity of particle production from hadron-hadron and nucleus-nucleus interaction

Ahmed Abdo Ahmed Al-Haydari[1], Mohmmed Tarek Hussein[2]

[1]Physics Department, Faculty of Applied Science Taiz University, Taiz, Yemen; a_alhaydari@yahoo.com
[2]Physics Department, Faculty of Science, Cairo University, Giza, Egypt; hussein1@mailer.eun.eg

Received 21 October 2009; revised 26 November 2009; accepted 23 February 2010.

ABSTRACT

The particle production in hadron-nucleon (h-N), hadron-nucleus (h-A) and nucleus-nucleus (A-A) collisions at high energies are studied in view of the multi-peripheral model. A multi-peripheral T-matrix element is assumed with multi surface parameter that is functionally dependent on the number of particles in the final state and control the kinematical path of the reaction. A Monte Carlo code is designed to simulate events according to a hypothetical model, the quark structure of the interacting nucleons is considered. The number of possible nucleon collisions inside the target nucleus plays an important role in folding the (h-N) to generate the (h-A) and (A-A) collisions. The predictions of the model give reasonable agreement with the recently examined experimental data.

Keywords: Monte-Carlo Generators; Multiplicity Distribution; Integral Phase Space

1. INTRODUCTION

In the last few years, research work has been concentrated on the possible existence of the quark-gluon plasma phase, considering of unconfined quarks and gluons at high temperature or high density. In the laboratory, nucleus-nucleus collisions at very high energies provide a promising way to produce high temperature or high-density matter. As estimated by Bajorken [1] the energy density can be so high that these reactions might be utilized to explore the existence of the quark-gluon plasma. One of the many factors that lead to an optimistic assessment that matter at high density and high temperature may be produced with nucleus-nucleus collisions is the occurrence of multiple collisions. By this we mean, a nucleon of one nucleus may collide with many nucleons in the other and deposit a large amount of energy in the collision region. In the nucleon-nucleon center of mass system, the longitudinal inter-nucleon spacing between target nucleons is Lorentz contracted and can be smaller than 1 *fm* in high-energy collisions. On the other hand, particle production occurs only when a minimum distance of about 1 *fm* separates the leading quark and antiquark in the nucleon-nucleon center of mass system [2,3]. Therefore when the projectile nucleon collides with many target nucleons, particle production arising from the first N-N collision is not finished before the collision of the projectile with another target nucleon begins. There are models [4-11] that describe how the second collision is affected by the first one. Nevertheless, the fundamental theory of doing that remains one of the unsolved problems. Experimental data suggest that after the projectile nucleon makes a collision, the projectile-like object that emerges from the first collision appears to continue to collide with other nucleons in the target nucleus on its way through the target nucleus. In each collision the object that emerges along the projectile nucleon direction has a net baryon number of unity because of the conservation of the baryon number. One can speak loosely of this object as the projectile or baryon-like object and can describe the multiple collision process in terms of the projectile nucleon making many collisions with the target nucleons. Then, losing energy and momentum in the process, and emerging from the other side of the target with a much diminished energy. The number of collisions depends on the thickness of the target nucleus. Experimental evidence of occurrence of multiple collision process can be best illustrated with the data of *p-A* reactions in the projectile fragmentation region [3,12]. In the present work, we shall investigate the particle production mechanism in heavy ion collision by introducing the multi- peripheral model [13-16,18] which is based on the phase space integral to describe the multi-particle production in the Hadron-Hadron, Hadron-Nucleus and Nucleus-Nucleus interaction at different energies. In this technique the many body system is expanded into subsystems, each one concerns a two body collision where we have used the matrix element of the multi-peripheral nature whose parameters are strongly correlated to the final state multiplicity. The simplified quark-quark interaction picture is considered to improve the results; we suppose that all the quarks which constitute the hadrons contribute in the reaction. It is assumed that each Hadron in the final state is produced at the specific peripheral surface that is characterized by a peripheral parameter.

2. THE MULTI-PERIPHERAL MODEL

We start with the initial single state of center of mass energy $\sqrt{s}$, let us denote by t_i the square of the 4-vectore momentum transferred from the particle p_a of mass m_a to the system of 4-momenta k_{n-1} with mass M_{n-1}. This will reduce the many body problem into $n-1$ iterative diagram, each of them has only two particles in the final state. For example, the i^{th} diagram has two in the final state, the first one is the particle number $n-1$, and the other has an effective mass M_i, equivalent to the rest of the i particles of the system. The general expression for t_i in the center of mass frame of K_{i+1} is Kinematically calculated as,

$$t_i = (p_a - k_i)^2 = ma^2 + M_i^2 - 2E_a^{(i+1)}k_i^0 \\ +2P_a^{(i+1)}K_i\cos\theta_i \tag{1}$$

where K_i and $P^{(i)}$ are the magnitude of the 3-vector momentum of a system of i particles and the i^{th} splitted one, θ_i and k_i^0 are the scattering angle and the energy of the system M_i. The recursion relations of $P^{(i)}$ and K_i are given by,

$$K_i = \frac{\sqrt{\lambda(M^2{}_{i+1}, M^2_i, m^2{}_{i+1})}}{2M_{i+1}} \tag{2}$$

$$P_a^{(i)} = \frac{\sqrt{\lambda(M^2{}_i, t_i, m^2{}_a)}}{2M_i} \tag{3}$$

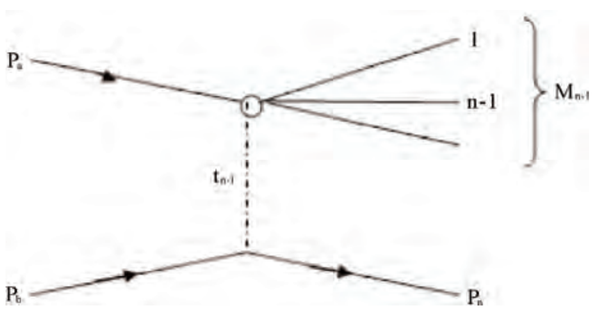

Figure 1. The basic process diagram of $p_a + p_b = K_{n-1} + p_n$ expressed as a sequence of two particles decay.

and the corresponding energies k_i^0 and $E_a^{(i)}$ of the system M_i are given by,

$$k_i^0 = (M_i^2 + K_i^2)^{\frac{1}{2}}, k_n^0 = M_n = \sqrt{s} \tag{4}$$

$$E_a^{(i)} = (P_a^{(i)2} + m_a^2)^{1/2} \tag{5}$$

For the case where $i = n$, we get

$$P_a^{(n)} = \frac{\sqrt{\lambda(s, m_b^2, m_a^2)}}{2\sqrt{s}} \tag{6}$$

where m_a and m_b are the masses of the initially interacting particles. The function denotes the Lorentz invariant function which is defined by,

$$\lambda(x, y, z) = (x - y - z)^2 - 4yz \tag{7}$$

The phase space integral $I_n(S)$ which expresses the probability of obtaining a final state of n-particles with total center of mass (C. M) $\sqrt{s}$ in which energy and momentum are conserved is given by,

$$I_n(s) = \int ....\int d^3 p_i / 2E_i \delta^4 (p_a - p_b - \sum p_i) | T(P_i) |^2 \tag{8}$$

where $T(p_i)$ is the transition matrix element that represents the transition probability from an initial state $p_a + p_b$ to the final state $K_{n-1} + P_{n-1}$ with the definite momentum p_i. Once the phase space integral is defined, one can easily find the reaction cross-section as

$$\sigma_n = (1/F)I_n(s) \tag{9}$$

where F is the flux function defined by,

$$F = 2\sqrt{\lambda(s, m_b^2, m_a^2)}(2\pi)^{2n-4} \tag{10}$$

If $x = x(p_i)$ is any physical quantity depending on the p_i, the differential cross-section $\frac{d\sigma_n}{dx}$ is obtained by transforming the integral in **Eq.8** so that x appears as a variable and then omitting the integration over x. This can be most simply carried out by inserting the constraint $x = x(p_i)$ in the integrand as a δ function so that

$$\frac{d\sigma_n}{dx} = (1/F)\int ....\int \frac{d^3 p_i}{2E_i}\delta^4 (p_a + p_b - \sum p_i)\delta^4 \times \\ (x - x(p_i)) | T(p_i) |^2 \tag{11}$$

The multiperipheral matrix element [17] is introduced in the form,

$$T = \prod_{i=1}^{n-1} g_i(t_i) \tag{12}$$

The function $g_i(t_i)$ cuts of large values of t_i for instance one may choose

$$g_i(t_i) = \exp(-a_i t_i) \tag{13}$$

where a_i is a peripheral parameter that play an important role in converging the particles in phase space and consequently, control the energy of the particles in final state. So that the values of a_i are adjusted to conserve the total energy. The energy $E^{(i)}$ of the particle number *i* is related to its rapidity y_i through the relation,

$$E^{(i)} = m_t = \cosh(y_i)$$

where m_t is defined by,

$$m_t = \sqrt{P_t^2 + m_i^2} \tag{14}$$

so that the total energy of the particles in the final state is

$$\zeta_i^n = \frac{1}{\sigma_n} \int m_t \cosh(y)(d\sigma / dy)dy \tag{15}$$

ζ_i^n, is the function of the parameters a_i which should be compared with the total center of mass energy $\sqrt{s}$ of the initial state. We first start with n=1 to get a_1, which is inserted again in the case n = 3 to get a_2 and so on. These are repeated sequentially to get the values of the rest parameters. The integral phase space **Eq.8** is then calculated as,

$$\begin{aligned} I_n(s) = {} & \frac{1}{2M_n} \cdot \frac{1}{4P_a^{(n)}} \int_{\mu n-1}^{M_n - m_n} dM_{n-1} \int_{t^-_{n-1}}^{t^+_{n-1}} \exp(a_{n-1}t_{n-1})dt_{n-1} \int_0^{2\pi} d\phi_{n-1} \ldots\ldots\ldots\ldots \\ & \ldots\ldots\ldots \frac{1}{4P_a^{(3)}} \int_{\mu 2}^{M_3 - m_3} dM_2 \int_{t_2^-}^{t_2^+} \exp(a_2 t_2)dt_2 \int_0^{2\pi} d\phi_2 \frac{1}{4p_a^{(2)}} \int_{t_1^-}^{t_1^+} \exp(a_1 t_1)dt_1 \int_0^{2\pi} d\phi_1 \end{aligned} \tag{16}$$

The multiple integration in **Eq.16** may be solved by using the Monte-Carlo technique [21-23]. At extremely high energy, **Eq.16** has an asymptotic limit in the form,

$$I_n(s) = \frac{1}{2\sqrt{s}} \prod \{ \frac{\pi}{2P_a^{(i+1)}} \frac{e^{a_i t_i^+} - e^{a_i t_i^-}}{a_i e^{a_i t_i}} \} \frac{(\sqrt{s} - \mu_n)^{n-2}}{(n-2)!} \tag{17}$$

where $\{\frac{e^{a_i t_i^+} - e^{a_i t_i^-}}{a_i e^{a_i t_i}}\}$ is the normalization density and μ_n is defined by,

$$\mu_i = \sum_j m_j, \; j = 1, \ldots\ldots i \tag{18}$$

Let $r^{(i)}$ be a group of ***i***-random numbers, $0 \le r^{(i)} \le 1$, then the invariant mass M_i for a system of ***i***-particles can be generated according to

$$M_i = \mu_i + r^{(i)}(M_{i+1} - \mu_i) \tag{19}$$

It means that, the invariant masses vary between the limits $\mu_i \le M_i \le M_{i+1} - m_{i+1}$, i=2,…, n-1 for the special case where T is constant (no dynamical effect), the momentum transfer t_i should vary homogeneously between the two limiting values $t_i^{\pm}$,

$$t_i^{\pm} = m_a^2 + M_i^2 + 2E_a^{(i+1)} k_i^0 \pm 2P_a^{(i+1)} K_i \tag{20}$$

and the Monte-Carlo will generate the t values according to

$$t_i = t_i^- + r^{(i)}(t_i^+ - t_i^-) \tag{21}$$

The limiting values $t^{\pm}$ define the physical region boundaries of $2 \to 2$ reaction on the Chow-Low plot shown in **Figure 2**.

On the other hand, using a multiperipheral form in T as in **Eq.13**, we can generate events with anisotropic behavior so as to satisfy the simulation identity [16].

$$\int_{t_i^-}^{t_i} \exp(a_i t_i)dt_i \Big/ \int_{t_i^-}^{t_i^+} \exp(a_i t_i)dt_i = r^{(i)}$$

then

$$t_i = (1/a_i)\ln\{r^{(i)}(\exp(a_i t_i^+) - \exp(a_i t_i^-)) + \exp(a_i t_i^-)\} \tag{22}$$

The condition **Eq.22** will spread the points in a confined Zone in the Chow-Low Plot by cutting of the high t values. The parameters a_i are directly reproduced from the comparison with experimental distributions.

2.1. Effect of the Quark Structure

Let use assume that the interaction takes place not with the interacting particles as a whole but rather among

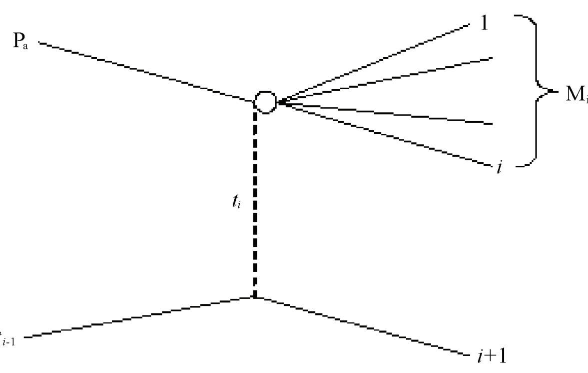

Figure 2. The basic process at stage *i* of iteration.

their minute constituent quarks. Neglecting the spin effect of the quark and considering, for example, πp, system as two bags containing, respectively, two and three quarks each of effective mass m_q, we assume that the reaction goes through one of the following channels:

1) One of the projectile quarks interacts with one of the target quarks. We use the symbols (O—OO) and (O—OO) to describe the two states of the first channel. The number of possible permutation of these states is 3.

2) In the second channel, the two projectile quarks may interact with the three target quarks in a collective manner. This state is symbolized by (O—OOO) with only one possible permutations. The square of the center-of-mass energy of each state is calculated according to;

$$s = (N_a^2 + N_b^2)m_q^2 + 2m_q N_a N_q e_q \tag{23}$$

where N_a and N_b are the number of quarks participating in the reaction from the target and projectile, respectively; m_q is the effective quark mass and e_q is the laboratory energy per quark. The multiplicity distribution $F(n)$ of an n-particle system is calculated in terms of the distribution functions of the different states of the reaction. For our example case ($\pi\, p$-system), let us assume that $f_{11}(n)$ and $f_{12}(n)$ represent the phase space integrals of the state (O—O) and (O—OO) for the first channel, so that the distribution of the first channel is obtained by a restricted superposition of the two functions;

$$f_1(n) = \sum_i \sum_j Z(n)[(f_{11}(i) + f_{12}(j))\delta(n-(i+j))] \tag{24}$$

where the normalization factor, $Z(n)$ is given by

$$Z(n) = [\sum_i \sum_j \delta(n-(i+j))]^{-1} \tag{25}$$

The second channel has only one state (O—OOO) represented by a phase space integral $f_2(n)$, then the overall distribution function $F(n)$ is

$$F(n) = k_1 f_1 + k_2 f_2 \tag{26}$$

where k_1 and k_2 are the number of possible permutations in each channel. The distribution function for any other physical quantity x is simply given by

$$H(x) = k_1 \sum h_{1i}(x) + k_2 h_2(x) \tag{27}$$

2.1.1. Hadron-Nucleus Collision

On extending the model to the hadron-nucleus or nucleus-nucleus collision, we follow the NN-base super position as expected from the features of the experimental data. We should consider the possible interactions with the nucleons forming the target nucleus A_t. The incident hadron makes successive collisions inside the target. The energy of the incident hadron (leading particle) slows down after each collision, producing a number of created hadrons each time which depends on the available energy. The phase space integral I_n^{NA} in this case has the form;

$$I_n^{NA}(s) = \sum_{\nu}^{A_t} I_{n\nu}(s_\nu) P(\nu, A_t)\delta(n - \sum_i^{A_t} n_i) \tag{28}$$

where $P(\nu, A_t)$ is the probability that ν nucleons out of A_t will interact with the leading particle and $I_{n\nu}(s\nu)$ is the phase space integral of NN collision that produces hadrons at energy $\sqrt{s}$. The delta function in **Eq.28** is to conserve the number of particles in the final state. All the nucleons are treated identically, and the X_{NN} is the N-N phase shift function [20,24-26]. Then, according to the eikonal approximation,

$$p(l, A_t) = -\binom{A_t}{l} \sum_j^l (-1)^j \binom{l}{j} \{1 - \exp(2\,\mathrm{Re}\, i(A_t - l + j) X_{NN})\} \tag{29}$$

This approach was then worked out by putting the multi-dimension integration of **Eq.16** and the generated kinematical variables into a Monte-Carlo program which was created by the author. This in turn is restored ν times, where ν is the number of collisions inside the target nucleus that is generated by a Monte-Carlo Generator according to the probability distribution **Eq.29**. In the first one, the incident hadron has its own incident energy and moves parallel to the collision axis ($(Z - axis)\theta_0 = 0$. The output of the program determines the number of created hadrons n_1 as well as the energy $E_1 (< E_0)$ and the direction q_1 of the leading particle. The leading particle leads the reaction in its second round with E_1 and θ_1 as input parameters and creates new number of $n-2$ and so on. The number n_j is determined according to a multiplicity generator which depends on the square of the center of mass energy s_j in the round number j:

$$s_j = 2m_N^2 + 2m_N E_j \tag{30}$$

3. NUCLEUS-NUCLEUS COLLISIONS

The extension of the multi peripheral model to the nucleus-nucleus case is more complicated. The number of available collisions is multi-folded due to the contribution of the projectile nucleons. By analogy of the $N - A$

collision, it is possible to define the phase space integral I_n^{AA} in $A-A$ collisions as,

$$I_n^{NN}(s)=\sum_j^{A_p}\sum_k^{A_t} I_{n_{j,k}}(s_{j,k})P_{AA}(j,A_p,k,A_t)\delta(n-\sum_{j,k}^{A_t}n_{j,k}) \quad (31)$$

where $I_{n_{j,k}}(s_{j,k})$ is the phase space integral due to the knocked on nucleon number j from the projectile and that, number k from the target. The probability that the $A-A$ collision encounters events. So that,

$$P_{AA}(j,A_p,k,A_t)=P(v_p,A_p).\cdot P(v_t,A_t) \quad (32)$$

About 1000 events have been generated for each reaction by the Monte-Carlo according to the decay diagram of **Figure 1**.

4. THEORETICAL CALCULATION

4.1. The Multi-Peripheral Parameters a_i with n Particle Final State

The values of the multi-peripheral parameters a_i play an important role in the calculation of the phase space integrals and the inclusive cross sections. The multi-peripheral parameters carry all the dynamical effects that control the geometrical and kinematical behavior of the reactions. The values of a_i are considered as fitting parameters and are determined to conserve the total energy in the center of mass of the reaction [17]. Taking all possible configurations (pairing) of quark combinations as described in Subsection 2.1.

Referring to equations **Eq.12** and **Eq.13** we find that the parameter a_n, plays the effective role in the dynamic matrix element which controls the generation process of the events according to the assumed number of produced particles n_b and the square of the available energy in the center of mass $\sqrt{s}$. The parameter a_n is just a fitting parameter in the simulation process. Its value is to conserve the energy in the generator G(n).

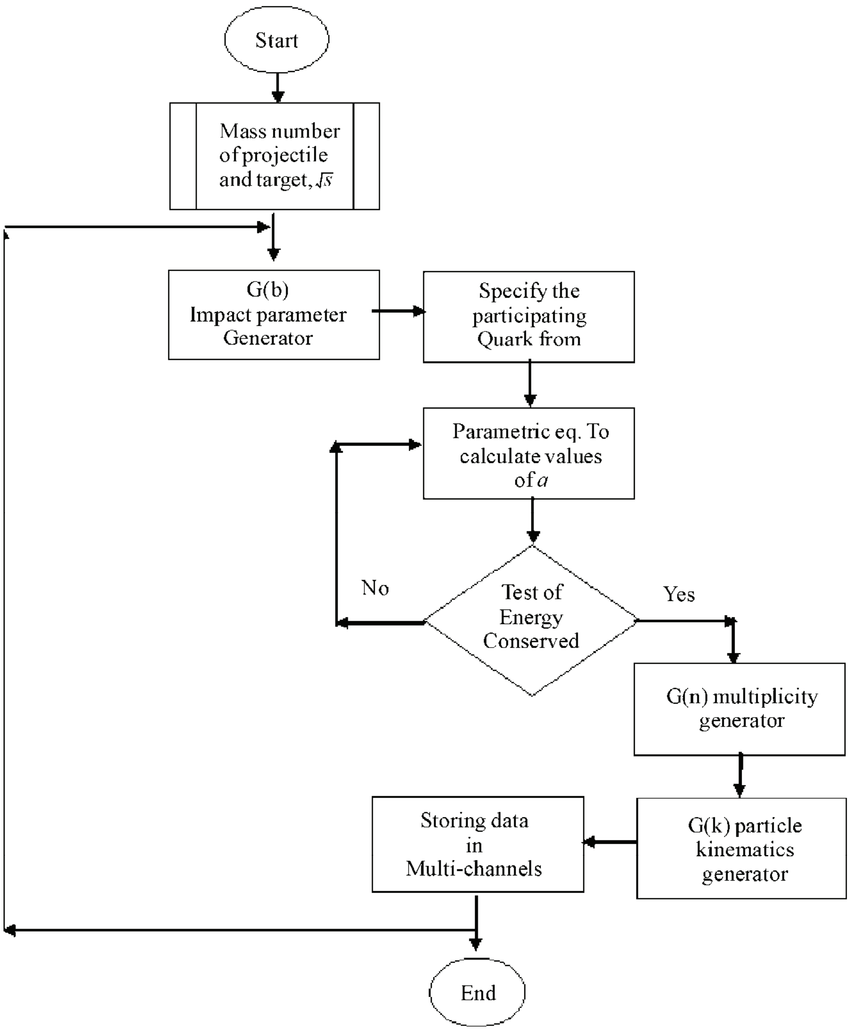

Figure 3. The flow chart of the Monte Carlo code for *p-p* collisions.

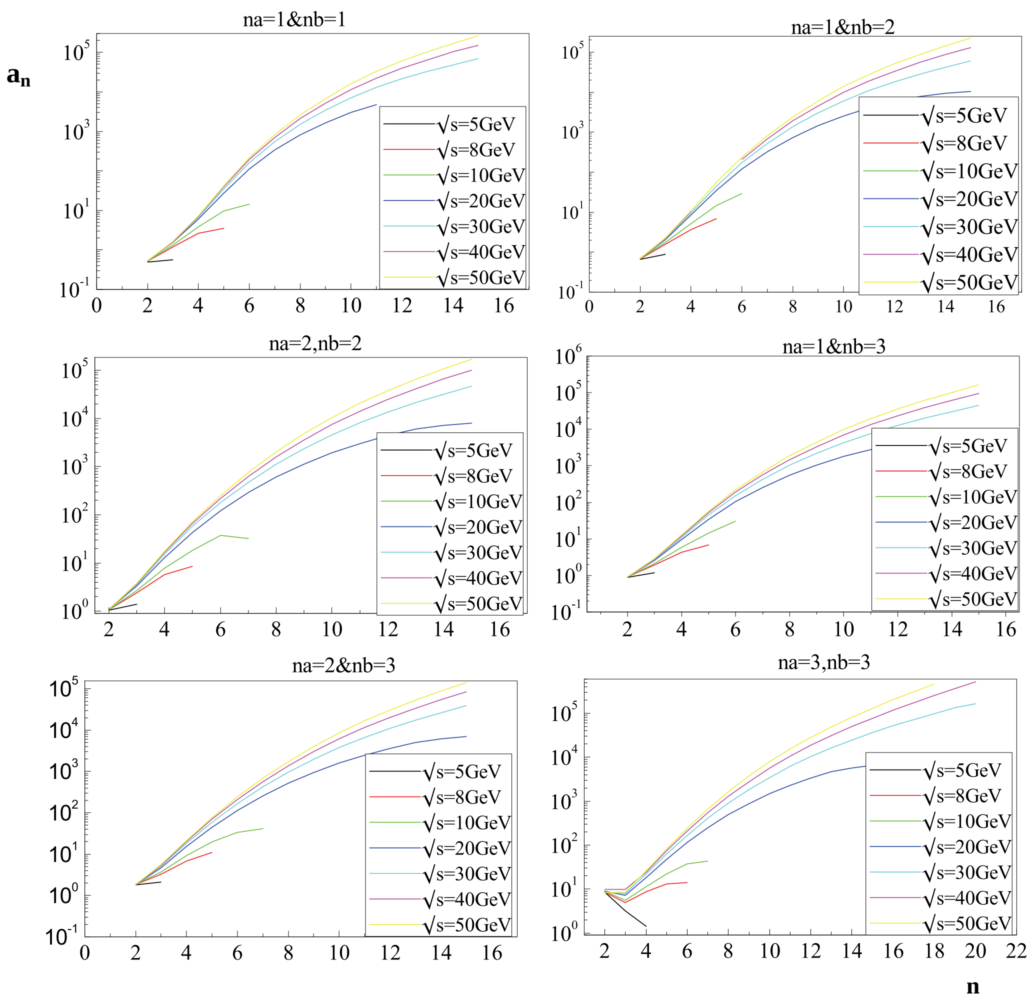

Figure 4. The multi-peripheral parameter (a) deduced for the *n*-particle final state in case of proton -proton collisions.

In **Figure 4** we display the values of the multi-peripheral parameters a_n as a function of number of created particles n in the final state at different center of mass energies, $\sqrt{s}$ = 5,8,10,20,30,50 GeV, for different configurations of participating nucleons from projectile a_n and target n_b. In all cases the value of *a*n increases in general with *n* and $\sqrt{s}$. The relation of a_n with *n* and $\sqrt{s}$ is parameterized in a polynomial form to speed up the simulation process of the generator.

A Monte-Carlo code is designed to generate (*pp*) events at incident energies of 8.8, 102 and 400 GeV. **Figure 3** shows the flow chart of the code generators. We start with the initial incident energy. The projectile and target protons consist of 3-quarks for each. The following generators are considered:

1) -Impact parameter generator G(b) to generate the value of the impact parameter according to simple geometrical aspects.

2) -Specifying the target and projectile number of quark participating in the collision according to the impact parameter value.

3) -Multiplicity Generator G(n) to generate the number of particles in the final state.

4) -The kinematics generator G(k) to generate particle kinematics in the final state according to the Feynman binary diagram **Figure 2**.

5) -Combining the possible number of quarks that participate in the reaction

6) -Storing the kinematical data in multi-channels of momentum-angular and energy spaces.

7) -END.

In dealing with the proton-nucleus (*pA*) and the nucleus-nucleus (*AA*) collisions we considered the Monte-Carlo code of (*pp*) as a subroutine in a more general code. It is assumed that a number of *ν*-binary collisions of (*pp*) type would be carried out inside the (*pA*) or (*AA*) collision. Consequently, the *pp* code is folded *ν*-times for each (*AA*) event. The number *ν* depends mainly upon the effective target mass at the considered impact parameter.

The Monte-Carlo code is run to the case of *p-C* collision at 200 GeV. All possible values of a projectile nucleon participant in the reaction are considered. The case of $n_p = 1$ and $n_t = 1$ refers to the single nucleon-nucleon collision. It rather happened for the conditions of peripheral interactions. As collision orients towards the central collision, more target nucleons contribute to the reaction. **Figure 5(a)** Shows that the shower particle production (created particles) increases with increasing the number of target participant nucleons; where the available center of mass energy increases. The multiplicity distribution of the shower created particles may fit a Gaussian distribution, the peak and the dispersion of which shifts forward as n_t increases. The contribution of each n_t value has a certain weight factor that is related to the impact parameter weight. Averaging over all possible values of the impact parameters results in the overall multiplicity distribution that is displayed in **Figure 5(b)**. It was found that the average value of the charged particle multiplicity is 4.35 and the dispersion is 1.37557 for the *p-C* interaction at 200 GeV. The same procedure is carried out for the He-Be interaction as an example of (*AA*) collision at the same incident energy for the sake of comparison. In this case both the number of projectile and target participant nucleons n_p and n_t have appreciable effect in shaping the charged particle multiplicity distributions. The number n_p plays the role of multiplication factor in the production process.

In **Figure 6** we demonstrate the family of curves representing the results of multiplicity distributions for the case where all projectile nucleons participate the reaction $n_p = 4$ while parts of the target contribute as n_t = 4, 5, 6, 7 and 8.

5. RESULTS AND DISCUSSION

The numerical computation of the charged and negative charged multiplicity distribution of the outgoing particles in (*p-p*) interactions at 8.8 GeV **Figure 7**, 102 GeV **Figure 8**, 400 GeV **Figure 9**, (*p-d*) interaction at 28 GeV **Figure 10** and (*He-He*) interaction at 120 Gev **Figure 11** are calculated. A Monte-Carlo program designed by the authors is used to simulate about 1000 events for each final state of specific *n*-values. The multi-peripheral matrix element is used according to **Eq.12** to calculate the phase space integral and the production cross section. The cut-off boundaries $t_i^{\pm}$ of the physical region is used according to **Eq.22**.

The proposed model is a statistical model in its nature. It assumes a large phase space and consequently large number of quantum states to work in a relevant environment.

Figures 7-11 show that the prediction of the model comes closer to the experimental data as simple as increasing both the available energy and the number of interacting particles (the size of the target and the projectile nuclei) that meets with the increase of the volume of phase space.

Table 1 shows the Chi-square values for the reaction under consideration to test the validity or the behavior of the model against the projectile-target size and the energy of the reaction.

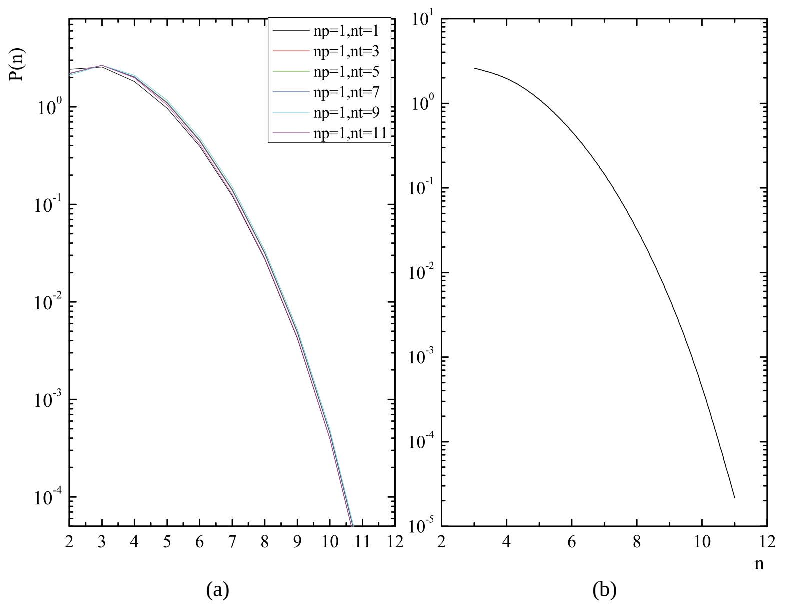

Figure 5. (a) Multiplicity distributions of the produced particles for 200 GeV proton-Carbon *p*-C interactions for different number of target participants; (b) Total multiplicity distribution of the produced particles for 200 GeV *p-C* interactions.

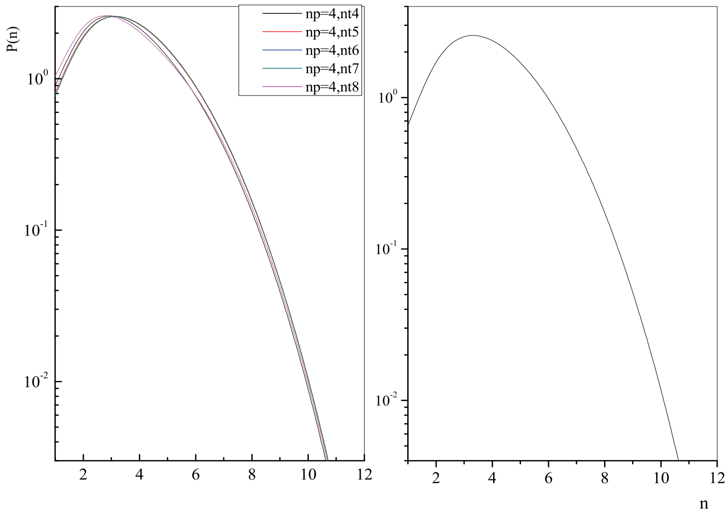

(a) (b)

Figure 6. (a) Multiplicity distributions of the produced particles in *He-Be* interactions at 200 GeV/n for different target participants; (b) Total multiplicity distributions of the produced particles in Helium-Brelium *He-Be* interactions *at* 200 *GeV/n.*

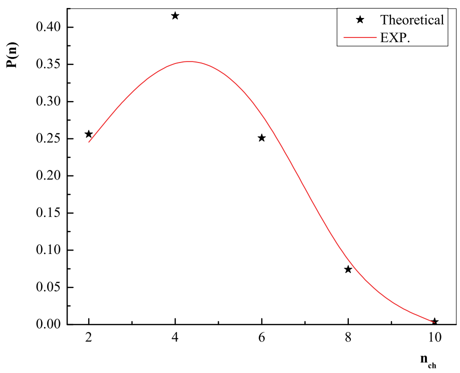

Figure 7. The multiplicity distributions of charged particles produced in p_p interactions at 8.8 GeV.The red curve is the model prediction, the black stars are the experimental data which have been taken from [27].

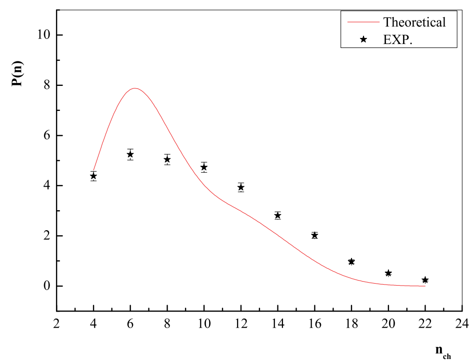

Figure 9. The multiplicity distributions of negative charged particles produced in *p- p* interactions at 400 GeV. The red curve is the model prediction, the black stars with error bars are the experimental data which have been taken from [29].

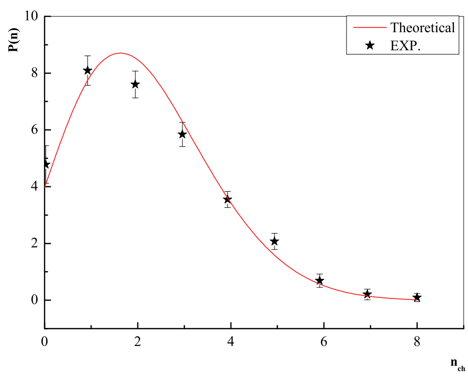

Figure 8. The multiplicity distributions of negative charged particles produced in *p-p* interactions at 102 GeV. The red curve is the model prediction, the black stars with error bars are the experimental data which have been taken from [28].

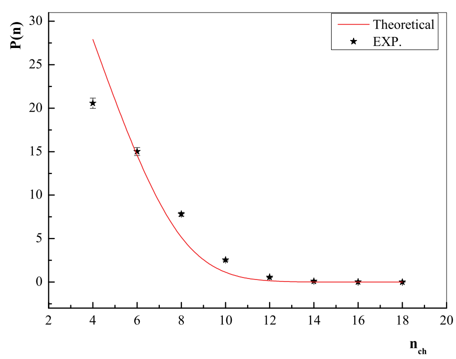

Figure 10. The multiplicity distributions of charged particles produced in *p-d* interactions at 28 GeV. The red curve is the model prediction. The black stars are the experimental data which have been taken from [30].

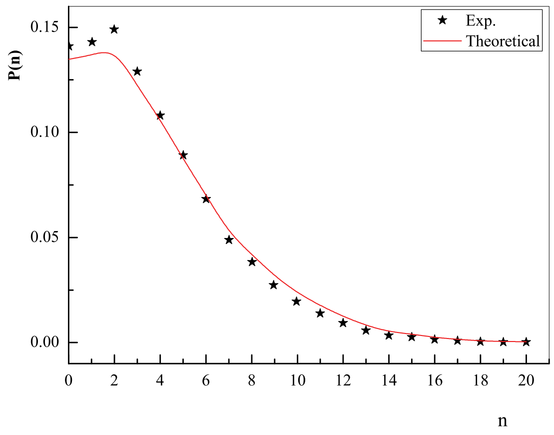

Figure 11. The multiplicity distribution of the particles produced in *He-He* interactions at 120 GeV. The red curve is the model prediction. The black stars are the experimental data which have been taken from [31].

Table 1. The Chi-square of the reactions.

Reaction	Energy	Chi-Square
$p-p$	8.8 GeV	0.005066
$p-p$	102 GeV	0.004561
$p-p$	400 GeV	0.822473
$p-d$	28 Gev	0.034502
He-He	120 GeV	0.000382

5. CONCLUSIONS

The multi-peripheral model is extended to the nucleon-nucleus and the nucleus-nucleus interaction on the basis of nucleon-nucleon collisions, where the phase space integral of the nucleon-nucleon and nucleus-nucleus interaction is folded several times according to the number of encountered nucleons from the target. The number of created particles in each collision is summed over to get the production in the nucleon-nucleon case, where the conservation of number of particles in the final state is taken into consideration. The inclusive cross section is calculated and showed a fair agreement with experimental data.

REFERENCES

[1] Bjorken, J.D. (1983) Principles of opticsoo. *Physical Review D*, **27**, 140.

[2] Busza, W. and Goldhaber, A. (1984) Nuclear stopping power. *Physics Letters B*, **139(4)**, 235-238.

[3] Barton, D.S., *et al*. (1983) Experimental-study of the A-dependence of inclusive hadron fragmentation. *Physical Review D*, **27(11)**, 2580-2599.

[4] Andersson, B., Gustafson, G. and Nilsson-Almqvist, B. (1987) A model for low-pT hadronic reactions with generalizations to hadron-nucleus and nucleus-nucleus collisions. *Nuclear Physics B*, **281(1-2)**, 289-309.

[5] Nilsson-Almqvist, B. and Stenlund, E. (1987) Interactions between hadrons and nuclei: The Lund Monte Carlo - FRITIOF version 1.6. *Computer Physics Communications*, **43(3)**, 387-397.

[6] Sorge, H., Von Keitz, A., Mattiello, R., Stocker, H. and Greiner, W. (1990) Energy density, stopping and flow in 10-20 A GeV heavy ion collisions. *Physics Letters B*, **243**, 7-12.

[7] Mattiello, R., *et al*. (1991) Multistrangeness production in heavy ion collisions. *Nuclear Physics B*, **24(2)**, 221-233.

[8] Wang, X.N. and Gyulassy, M. (1991) HIJING: A Monte Carlo model for multiple jet production in *pp*, *pA*, and *AA* collisions. *Physical Review D*, **44**, 3501-3516.

[9] Geiger, K. and Muller, B. (1992) Dynamics of parton cascades in highly relativistic nuclear collisions. *Nuclear Physics A*, **544(2)**, 467-470.

[10] Geiger, K. (1992) Thermalization in ultrarelativistic nuclear collisions I. Parton kinetics and quark-gluon plasma formation. *Physical Review D*, **46(11)**, 4965.

[11] Geiger, K. (1993) Particle production in high energy nuclear collisions: Parton cascade—cluster hadronization model. *Physical Review D*, **47**, 133.

[12] Brenner, A.E., *et al*. (1982) Experimental study of single-particle inclusive hadron scattering and associated multiplicities. *Physical Review D*, **26**, 1497-1553.

[13] Amati, D., Stanghellini, A. and Fubini, S. (1962) Theory of high-energy scattering and multiple production. *Nuovo Cimento*, **26**, 896-954.

[14] Hassan, N.M. (2007), Charged particle multiplicity produced in neutrino-nucleon interactions at high energies. Scientific Research and Essays, **2(6)**, 171-176.

[15] Hussein, M.T., Hassan, N. M. and Rabea, A. (1994) ICTP, Trieste, internal report IC/93/111. *Nuovo Cimento A*, **107**, 749.

[16] Hussein, M.T. (1993) ICTP, Trieste, internal report IC/92/166. *Nuovo Cimento A*, **106**, 481.

[17] Byckling, E. and Kajantie, K. (1973) Particle kinematics. John Wiley and Sons, New York, 190.

[18] Hussein, M.T., Hassan, N.M. and Rabea, A. (1994) Hadron fragmentation at high energies. *Particle World*, **4(1)**, 4.

[19] Hussein, M.T., Hassan, N.M. and Allam, M.A. (1997) A Multi-cluster model in hadron nucleus interactions at high energies. *Turkish Journal of Physics*, **21**, 241.

[20] Hegab, M.K., Hussein, M.T. and Hassan, N.M. (1990) Nucleus-nucleus collisions at high energies. *Zeitschrift für Physik A*, **336**, 345.

[21] Hussein, M.T. (1996) Monte Carlo simulation for hadron fragmentation at high energies. *Invited Talk, First International Conference on Basic Science and Advanced Technology*, Assiut, 9-12 November 1996.

[22] Hussein, M.T., Rabea, A., El-Naghy, A. and Hassan, N.M. (1995) A string model for hadron interactions at high energies. *Progress of Theoretical Physics Japan*, **93(3)**, 585.

[23] Hassan, N.M., El-Harby, N. and Hussein, M.T. (2000) A Monte Carlo generator for high energy nucleus-nucleus collision. *Acta Physiologica Academiae Scientiarum Hungaricae*, **12**, 33-46.

[24] Meggiolaro, E. (1998) High-energy quark-quark scattering and the eikonal approximation. *Nuclear Physics B-Proceedings Supplements*, **64**, 191.

[25] Pereira, F. and Ferreira, E. (1999) Eikonal profile func-

tions and amplitudes for pp and p¯p scattering. *Physical Review D*, **59(1)**.

[26] Ducati, M.B.G., Goncalves, V.P. (1999) The AGL equation from the dipole picture. *Nuclear Physics B*, **557(1)**, 296-306.

[27] Booth, C.N., Ansorge, R.E. and Carter, J. (1983) Differences between p¯p and pp interactions at 8.8 GeV/c and their relationship to p¯p annihilations. *Physical Review D*, **27**, 2018-2040.

[28] Aznauryan, I.G. and Ter-Isaakyan, N.L. (1980) Anomalous magnetic-moments of quarks in magnetic dipole transitions of hadrons. *Soviet Journal of Nuclear Physics*, **31(6)**, 871-875.

[29] Kass, R.D., Ko, W., Lander, R.L., *et al*. (1979) Charged- and neutral-particle production from 400-GeV/c pp collisions. *Physical Review D*, **20(3)**, 605-614.

[30] Hanlon, J., Panvini, R.S., Walters, J.W., Webster, M.S. and Morris, T.W. (1979) Multiplicity distributions in 28-GeV/c pd interactions and double scattering in deuterium. *Physical Review D*, **19(1)**, 49-54.

[31] Akesson, T., Albrow, M.G., Almehed, S., *et al*. (1982) Multiplicity distributions in *p*-*α* and *α*-*α* collisions in the CERN ISR. *Physics Letters B*, **119**, 464.

Vol.2, No.1, 398-401 (2010)
doi:10.4236/ns.2010.24048

Natural Science

Gauge boson mass generation–without Higgs–in the scalar strong interaction hadron theory

F. C. Hoh

Dragarbrunnsg, 55C, Uppsala, Sweden; hoh@telia.com

Received 6 December 2009; revised 23 December 2009; accepted 5 January 2010.

ABSTRACT

It is shown that the gauge boson mass is naturally generated–without Higgs–in the pion beta decay using the scalar strong interaction hadron theory. This mass generation is made possible by the presence of relative time between quarks in the pion in a fully Lorentz covariant formalism.

Keywords: No Higgs; Gauge Boson Mass; Scalar Strong Interaction

The nonobservation of Higgs, needed in the standard model [1], has led to various supersymmetry models that have no experimental support. This gauge boson mass generation problem is resolved here in the scalar strong interaction hadron theory (SSI) [2,3], an alternative to low energy QCD. The equations of motion of mesons, not yet quantized, read [2,3].

$$\partial_I^{a\dot{b}}\partial_{II}^{f\dot{e}}\chi_{(pr)\dot{b}f}(x_I,x_{II})-\left(M_{mpr}^2-\Phi_m(x_I,x_{II})\right)\psi_{(pr)}^{a\dot{e}}(x_I,x_{II})=0 \tag{1}$$

$$\partial_{I\dot{b}c}\partial_{II\dot{e}d}\psi_{(pr)}^{c\dot{e}}(x_I,x_{II})-\left(M_{mpr}^2-\Phi_m(x_I,x_{II})\right)\chi_{(pr)\dot{b}d}(x_I,x_{II})=0,\quad M_{mpr}=\frac{1}{2}(m_p+m_r) \tag{2}$$

$$\Box_I\Box_{II}\Phi_m(x_I,x_{II})=-\frac{g_s^4}{4}\left(\psi^{b\dot{a}}(x_I,x_{II})\chi_{\dot{a}b}^*(x_I,x_{II})+\psi^{*a\dot{b}}(x_I,x_{II})\chi_{\dot{b}a}(x_I,x_{II})\right) \tag{3}$$

Here, x_I and x_{II} are the quark and antiquark coordinates, $\partial_I=\partial/\partial x_I$, $\partial_{II}=\partial/\partial x_{II}$, χ and ψ are the meson wave functions with the spinor indices a, b,..., undotted and dotted, running from 1 to 2, Φ_m the scalar interquark potential, g_s the strong quark charge, m_p and m_r the quark masses, and p, r the quark flavors (1 for u and 2 for d quark). An epistemological background of this theory has been published earlier this year [4]. **Eqs.1-3** have been rather successfully applied to confinement and meson spectra [5] and some basic meson decays [6-9].

In these references, the transformation

$$x^\mu=x_{II}^\mu-x_I^\mu,\quad X^\mu=(1-a_m)x_I^\mu+a_m x_{II}^\mu,\quad a_m=1/2 \tag{4}$$

has been made. The relative space time $x^\mu=(x^0,\underline{x})$ are hidden variables [4] reflecting the fact that no free quarks exists. Generation of gauge boson mass without Higgs is shown here by the example of pion beta decay $\pi^+\to\pi^0e^+\nu_e$. Formally, this requires a field theoretical treatment but here attempt is made to describe such decays on the quantum mechanical level, analogous to some semiclassical treatments of radiation in quantum mechanics. The justification is that the energies involved are low so that field-theoretical effects such as vacuum polarization are small, just like that analogous effects are small in QED at low energies.

The starting point is the total action [10]

$$S_T=S_{GB}+S_{Ll}+S_{Lr}+S_{Lm}+S_m \tag{5}$$

$$S_{GB}=-\frac{1}{4}\int d^4X\sum_{l=1}^3G_l^{\mu\nu}G_{l\mu\nu} \tag{6}$$

$$G_l^{\mu\nu}(X)=\partial_X^\mu W_l^\nu-\partial_X^\nu W_l^\mu-\varepsilon_{jkl}gW_j^\mu W_k^\nu \tag{7}$$

$$S_{Lr}=-i\frac{1}{4}\int d^4X\,\chi_{La}\partial_X^{a\dot{b}}\chi_{L\dot{b}}+c.c. \tag{8}$$

$$S_{Ll}=-\frac{i}{4}\int d^4X\left(\psi_{\nu L}^{\dot{a}},\psi_L^{\dot{a}}\right)\left[\partial_{X\dot{a}b}+\frac{i}{2}g\begin{pmatrix}W_3 & \sqrt{2}W^-\\ \sqrt{2}W^+ & -W_3\end{pmatrix}_{\dot{a}b}\right]\begin{pmatrix}\psi_{\nu L}^b\\ \psi_L^b\end{pmatrix}+c.c. \tag{9}$$

$$S_{Lm}=-\frac{1}{2}\int d^4Xm_L\left(\psi_L^{\dot{a}}\chi_{L\dot{a}}+c.c.\right) \tag{10}$$

where S_{GB} is the action for the gauge boson fields W^+, W^- and W_3 and S_L the SU(2) part of the lepton action in the standard model. S_m is the SSI meson action generalized to include SU(2) gauge fields

$$S_m = \tfrac{1}{2}\int d^4Xd^4x \begin{pmatrix} -\left(D^{a\dot{b}+}_{I\,ps}\chi^{+}_{(rp)\dot{e}a}\right)\left(D^{f\dot{e}}_{II\,sq}\chi_{(qr)\dot{b}f}\right) - \left(D^{+}_{I\,ps\,\dot{a}b}\psi^{+e\dot{a}}_{(rp)}\right)\left(D_{II\,sq\,\dot{f}e}\psi^{b\dot{f}}_{(qr)}\right) - \\ \chi^{+}_{(rp)\dot{e}a}\left(M^2_{mpr} - \Phi_m\right)\psi^{a\dot{e}}_{(pr)} - \psi^{+a\dot{e}}_{(rp)}\left(M^2_{mpr} - \Phi_m\right)\chi_{(pr)\dot{e}a} + c.c. \end{pmatrix} \tag{11}$$

$$\partial_I^{a\dot{b}} = \frac{1}{2}\partial_X^{a\dot{b}} - \partial^{a\dot{b}} \to D^{a\dot{b}}_{I\,ps} = \frac{1}{2}\left(\partial_X^{a\dot{b}}\delta_{ps} + i\frac{1}{2}g(\sigma_l)_{ps}W_l^{a\dot{b}}(X)\right) - \partial^{a\dot{b}}\delta_{ps}$$
$$= \partial_I^{a\dot{b}}\delta_{ps} + i\frac{1}{4}g(\sigma_l)_{ps}W_l^{a\dot{b}}(X) \tag{12}$$

$$(\sigma_l)_{ps}W_l^{a\dot{b}}(X) = \begin{pmatrix} W_3 & \sqrt{2}W^- \\ \sqrt{2}W^+ & -W_3 \end{pmatrix}^{a\dot{b}}, \quad \sqrt{2}W^{\pm} = W_1 \pm iW_2 \tag{13}$$

The superscript $^+$ in **Eq.11** denotes hermitian conjugation. Lorentz and gauge invariance of **Eqs.4-10** has been established in [2,3]. Here,

$$\psi_{(pr)} \to \begin{pmatrix} \frac{1}{\sqrt{2}}\psi_{(\pi 0)} & \psi_{(\pi +)} \\ \psi_{(\pi -)} & -\frac{1}{\sqrt{2}}\psi_{(\pi 0)} \end{pmatrix}, \quad \psi \to \chi \tag{14}$$

Variation of **Eq.11** with respect to χ^+ and ψ^+, with boundary conditions specified in [12], yields

$$D^{a\dot{b}}_{I\,ps}D^{f\dot{e}}_{II\,sq}\chi_{(qr)\dot{b}f} - \left(M^2_{mpr} - \Phi_m\right)\psi^{a\dot{e}}_{(pr)} = 0 \tag{15}$$

$$D_{I\,ps\dot{c}a}D_{II\,sq\dot{e}d}\psi^{a\dot{e}}_{(qr)} - \left(M^2_{mpr} - \Phi_m\right)\chi_{(pr)\dot{c}d} = 0 \tag{16}$$

In the limit of $g \to 0$, **Eq.15** and **Eq.16** reproduce **Eqs.1** and **2** together with subsidiary conditions, arising from the c.c term in **Eq.11**, that are satisfied at least for plane wave W, which refers to W^+ here.

Following [8], let the meson wave functions be perturbed:

$$\psi^{a\dot{b}}_{(pr)}(X,x) = \left(a_{pr} + a^{(1)}_{pr}(X^0)\right)\times$$
$$\left(\delta^{a\dot{b}}\psi_{0(pr)K}(\underline{x}) - \underline{\sigma}^{a\dot{b}}\underline{\psi}_{(pr)K}(\underline{x})\right)\exp\left(-iE_{prK}X^0 + i\underline{K}_{pr}\underline{X}\right)$$
$$= \psi^{a\dot{b}}_{0(pr)}(X,x) + \psi^{a\dot{b}}_{1(pr)}(X,x) = \left(1 + \frac{a^{(1)}_{pr}(X^0)}{a_{pr}}\right)$$
$$\psi^{a\dot{b}}_{0(pr)}(X,x), \quad \psi \to \chi \tag{17}$$

Here, the index 1 denotes a first order quantity, a_{pr} is unity here but is in a quantized case to be elevated to an annihilation operator annihilating a initial meson with flavor pr. Its complex conjugate a^*_{rs} is also unity and is elevated to a creation operator creating a final state with flavor rs. $a^{(1)}_{ps}(X^0)$ is a small amplitude that varies slowly with time and, in the quantized case, becomes an operator that "slowly" transforms the same initial state meson to some virtual intermediate vacuum state. It is zero at $X^0 = -\infty$. $a^{(1)*}_{rs}(X^0)$ is the complex conjugate of $a^{(1)}_{ps}(X^0)$ and, in the quantized case, becomes an operator that "slowly" creates the same final state as that created by a^*_{rs}. The subscripts pr have also been attached to E_K and $\underline{K}$ of the meson. It has been shown that the last of **Eq.4**, required by decay applications [8], leads to that **Eq.17** is independent of the relative time x^0.

The terms in the actions can now be grouped in powers of the small parameter g. Only the lowest order and independent quantities are listed in the two alternatives below [3]:

$$\text{First order:} \quad g,\ \ a^{(1)}_{pr}(X^0),\ \ \partial_X \text{ in } S_{GB},\ \ \psi_L^{\dot{a}}\psi_L^{b},\ \ \chi_{La}\chi_{L\dot{b}} \tag{18}$$

$$\text{First order:} \quad g,\ \ W,\ \ \partial_X \text{ in } S_{GB},\ \ \psi_L,\ \ \chi_L$$
$$\text{Second order:} \quad a^{(1)}_{pr}(X^0) \tag{19}$$

Insert **Eq.17** into **Eq.15** and **Eq.16**, multiply **Eq.15** by $\chi^*_{0\dot{e}a(rp)}$ and **Eq.16** $\psi^{*d\dot{c}}_{0(rp)}$, add them together, and integrate over X and x. The first order quantities read

$$S'_{md} = S'_{ms} \tag{20}$$

Here, S'_{md} is linear in the first order quantity $a^{(1)}_{ps}(X^0)$,

$$S'_{md} = \int d^4Xdx^4 \begin{bmatrix} \partial_I^{a\dot{b}}\left(a^{(1)}_{pr}(X^0)/a_{pr}\right)\chi^{+}_{0(rp)\dot{e}a}\partial^{f\dot{e}}_{II}\chi_{0(pr)\dot{b}f} \\ +\partial_{I\dot{c}a}\left(a^{(1)}_{pr}(X^0)/a_{pr}\right)\psi^{+d\dot{c}}_{0(rp)}\partial_{II\dot{e}d}\psi^{a\dot{e}}_{0(pr)} \end{bmatrix} \tag{21}$$

The source part S'_{ms} of the first order terms contains the gW terms in **Eq.11**, ignoring the c.c. term there,

$$S'_{ms} = -\int d^4Xdx^4\frac{ig}{4}\begin{Bmatrix} \chi^{+}_{0(rp)\dot{e}a}(\sigma_l)_{ps}W_l^{a\dot{b}}\left(\partial^{f\dot{e}}_{II}\chi_{0(sr)\dot{b}f}\right) \\ -\left(\partial_I^{a\dot{b}}\chi^{+}_{0(rp)\dot{e}a}\right)(\sigma_l)_{ps}W_l^{f\dot{e}}\chi_{0(sr)\dot{b}f} \\ +\psi^{+d\dot{c}}_{0(rp)}(\sigma_l)_{ps}W_{l\dot{c}a}\left(\partial_{II\dot{e}d}\psi^{a\dot{e}}_{0(sr)}\right) \\ -\left(\partial_{I\dot{c}a}\psi^{+d\dot{c}}_{0(rp)}\right)(\sigma_l)_{ps}W_{l\dot{e}d}\psi^{a\dot{e}}_{0(sr)} + R_s \end{Bmatrix} \tag{22}$$

where R_s is a surface term [3] which vanishes upon integration in **Eq.29** below. As a rudimentary quantization procedure, let

$$|i\rangle = \left|P_{i(12)}(E_{12})\right\rangle, \qquad \langle f| = \left\langle P_{f(11-22)}\left(K^{\mu}_{f(11-22)}\right), W\right| \tag{23}$$

where $P_{i(12)}$ represents the initial π^+, $P_{f(11-22)}$ the final state π^0 and W the intermediary boson. The subscript K in **Eq.17** is zero for the initial π^+ and is suppressed.

a_{pr} in **Eq.17** is now elevated to become an annihilation operator according to

$$a_{pr}\left|P_{i(pr)}\left(E_{pr}\right)\right\rangle = \left|0\right\rangle \tag{24}$$

Similarly, a^*_{rs} is interpreted as a equivalent creation operator acting on |0> or an annihilation operator acting on <f|. Along these lines, the decay amplitude has been defined as [3]

$$S_{fi} = \left\langle f\left|a^+_{rp}a^{(1)}_{pr}\left(X^0\to\infty\right)\right|i\right\rangle \tag{25}$$

The zeroth order wave functions for a pseudoscalar meson at rest are obtained by solving **Eqs.1-3** using **Eq.17** and are [3,7]

$$\psi^{a\dot{b}}_{0(pr)}\left(X,x\right) = \delta^{a\dot{b}}\psi_{o(pr)}\left(r\right)\exp\left(-iE_{pr}X^0\right), \qquad \psi\to\chi \tag{26}$$

$$\psi_{o(pr)}\left(r\right) = -\chi_{o(pr)}\left(r\right) = \psi_0\left(r\right) = \sqrt{\frac{d^3_m}{8\pi\Omega}}\exp\left(-d_m r/2\right),$$
$$d_m = 0.864 \text{ Gev} \tag{27}$$

Inserting these into **Eq.17** and **Eq.21** and place **Eq.20** between <f| and |i> yields:

$$S_{fi} = i\frac{2}{E_{pr}\tau_0}\left\langle f\left|S'_{ms}\right|i\right\rangle, \qquad \tau_o = \int dx^0 \to\infty \tag{28}$$

where E_{pr} is the mass of the initial π^+. With **Eq.22** and **Eqs.26** and **27**, **Eq.28** becomes

$$S_{fi} = -\frac{ig}{4\Omega E_{\pi+}}\int d^4X\exp\left(i\left(E_{\pi0}-E_{\pi+}\right)X^0 - i\underline{K}_{\pi0}\underline{X}\right)$$
$$\times\left[\left(E_{\pi+}+E_{\pi0}\right)W^{0+}\left(X\right)+2\underline{K}_{\pi0}\underline{W}^+\left(X\right)\right],$$
$$\Omega = \int d^3X \to\infty \tag{29}$$

This result can also be obtained starting from either **Eq.15** or **Eq.16**, without the addition operation mentioned below **Eq.19**.

Variation of **Eqs.6** and **7** with respect to $W^{-a\dot{b}}$ defined in **Eq.13** yields

$$\delta S_{GB}/\delta W^{-a\dot{b}} = \tfrac{1}{2}\Box W^+_{\dot{b}a} - \tfrac{1}{4}\partial_{X\dot{b}a}\left(\partial^{c\dot{d}}_X W^+_{\dot{d}c}\right) + \tfrac{1}{2}g^2V_{C\dot{b}a}\left(W^+\right) \tag{30}$$

where V_C is trilinear in W. Variation of the same order part of **Eq.11** yields

$$\delta S_m/\delta W^{-a\dot{b}}$$
$$= -\frac{g^2}{16}\int d^4xW^{+f\dot{e}}\begin{bmatrix}\left(\chi^*_{0(12)\dot{e}a}\chi_{0(12)\dot{b}f}+\chi^*_{0(21)\dot{b}f}\chi_{0(21)\dot{e}a}+\chi^*_0\leftrightarrow\chi_0\right)\\ +\left(\psi_{0(21)\dot{e}a}\psi^*_{0(21)\dot{b}f}+\psi_{0(12)\dot{b}f}\psi^*_{0(12)\dot{e}a}+\psi^*_0\leftrightarrow\psi_0\right)\end{bmatrix} \tag{31}$$

Inserting **Eqs.26** and **27** into **Eq.31** yields

$$\delta S_m/\delta W^{-a\dot{b}} = -\frac{g^2}{2}\frac{\tau_0}{\Omega}W^{+\dot{b}a} \tag{32}$$

The same variation applied to **Eqs.8-10** yields

$$\delta S_L/\delta W^{-a\dot{b}} = \frac{g}{2\sqrt{2}}\psi_{\nu L\dot{b}}\psi_{La} \tag{33}$$

where L on the right side refers to e^+. With **Eqs.30-33**, variation of **Eq.5** with respect to $W^{-a\dot{b}}$ gives

$$\Box W^+_{\dot{b}a} - \tfrac{1}{2}\partial_{X\dot{b}a}\left(\partial^{c\dot{d}}_X W^+_{\dot{d}c}\right) + g^2V_{C\dot{b}a}\left(W^+\right) - M^2_W W^{+\dot{b}a} = -\frac{g}{\sqrt{2}}\psi_{\nu L\dot{b}}\psi_{La} \tag{34}$$

$$M^2_W = g^2\frac{\tau_0}{\Omega} \tag{35}$$

M_W is the mass of the charged gauge boson [7] and its square the ratio of an integral over the relative time x^0 between the quarks of the pion and the normalization volume Ω of the pion wave function. By the last of **Eq.28** and **Eq.29**, this ratio is ∞/∞ = finite. The pions here also play the role of the Higgs in the standard model. That Higgs boson is not needed to generate M_W was first shown in [12].

Contracting **Eq.34** by $\delta^{a\dot{b}}$ and $\underline{\sigma}^{a\dot{b}}$ yields

$$-\frac{\partial}{\partial X^0}\left(\frac{\partial}{\partial\underline{X}}\underline{W}^+\right) + g^2V^0_C\left(W^+\right) - M^2_W W^{0+} = -\frac{g}{2\sqrt{2}}\psi_{\nu L\dot{a}}\psi_{La} \tag{36}$$

$$\Box\underline{W}^+ + \frac{\partial}{\partial\underline{X}}\left(\frac{\partial}{\partial X^0}W^{0+} + \frac{\partial}{\partial\underline{X}}\underline{W}^+\right)$$
$$+ g^2\underline{V}_C\left(W^+\right) + M^2_W\underline{W}^+ = -\frac{g}{2\sqrt{2}}\underline{\sigma}^{a\dot{b}}\psi_{\nu L\dot{b}}\psi_{La} \tag{37}$$

Choose the gauge [3] to be the Coulomb type

$$\left(\partial/\partial\underline{X}\right)\underline{W}^+ = 0 \tag{38}$$

Further, the ordering **Eqs.18** and **19** adopted relegates the nonlinear g^2V_C terms in **Eqs.36** and **37** to higher order. In the absence of the lepton source terms on the right of **Eqs.36** and **37**, it yields to lowest order

$$W^{0+} = 0 \tag{39}$$

$$\Box\underline{W}^+ + M^2_W\underline{W}^+ = 0 \tag{40}$$

$\underline{W}^+$ is identified with the observed charged gauge boson $\underline{W}$ [1] with the mass

$$M_W = 80.42 \text{ Gev} \tag{41}$$

The time component W^{0+} associated with $\underline{W}^+$ in **Eqs.39** and **40** vanishes in agreement with the nonobservation of such a singlet charged gauge boson W^{0+} accompanying the observed triplet $\underline{W}^+$. If Higgs boson were used to generate the gauge boson mass, such a singlet W^{0+} with same mass **Eq.41** should also be seen, contrary to observation.

If the Lorentz gauge

$$\partial_X^{cd} W_{dc}^{+} = 0 \qquad (42)$$

were employed, **Eq.40** remains unchanged and **Eq.39** becomes

$$\Box W^{0+} - M_W^2 W^{0+} = 0 \qquad (43)$$

This implies that W^{0+} has an imaginary mass of **Eq.41** and therefore must vanish and **Eq.39** remains in effect valid.

The energy and momentum of the virtual gauge boson in **Eqs.36** and **37** are determined by those of the lepton pair and are small and can be dropped next to the mass terms. Hence, **Eqs.36** and **37** reduces to

$$M_W^2 W^{0+} = \frac{g}{2\sqrt{2}} \psi_{La}^{(-)} \psi_{\nu L\dot{a}}^{(+)} \qquad (44)$$

$$M_W^2 \underline{W}^{+} = -\frac{g}{2\sqrt{2}} \underline{\sigma}^{b\dot{a}} \psi_{\nu L\dot{a}}^{(+)} \psi_{Lb}^{(-)} \qquad (45)$$

While the triplet $\underline{W}^{+}$ can exist freely and hence be seen, as is shown in **Eq.40**, it can also be a virtual intermediate state in **Eq.45**. On the other hand, the singlet W^{0+} cannot be observed by **Eq.39**, but can only be a charged, virtual intermediate singlet as is seen in **Eq.44**. These results are due to that the signs of the M_W^2 terms in **Eqs.36** and **37** are different, which in its turn stems from that the meson wave functions **Eqs.26** and **27** are not scalar but the time component of a four vector in SSI. In pseudoscalar meson decays, only the virtual W^{0+} enters.

Because **Eqs.26** and **27** are independent of flavor, any pseudoscalar meson can generate the same M_W. When the above treatment is generalized to account for kaon decay [3], M_W is unaltered and the neutral gauge boson mass becomes $M_Z=M_W/\cos$ (Weinberg angle)=91.02 Gev. Decay of the $\underline{W}^{+}$ boson into a lepton pair is the same as that in the standard model. Inserting **Eqs.44** and **45** into **Eq.29** leads to a pion beta decay amplitude [3,6] that is $(E_{\pi 0}/E_{\pi +})^{1/2} \cong 1$ times that of the literature [11] assuming conserved vector currents.

The value $M_W = \infty/\infty =$ finite cannot and should not be determined in the present theory so far. If M_W were somehow obtained from some data, it implies a test of the well-established Fermi constant with far reaching consequences. This is due to that Fermi constant is proportional to M_W^{-2} and is hence also is a ratio $\infty/\infty =$ finite.

REFERENCES

[1] Amsler, C., *et al*. (2008) Particle data group. *Physics Letters B*, **667(1-5)**, 1-1340.

[2] Hoh, F.C. (1993) Spinor strong interaction model for meson spectra. *International Journal of Theoretical Physics*, **32(7)**, 1111-1133.

[3] Hoh, F.C. (2009) Scalar strong interaction hadron theory. http://web.telia.com/~u80001955

[4] Hoh, F.C. (2007) Epistemological and historical implications for elementary particle physics. *International Journal of Theoretical Physics*, **46(2)**, 269-299.

[5] Hoh, F.C. (1996) Meson classification and spectra in the spinor strong interaction theory. *Journal of Physics G*, **22(1)**, 85-98.

[6] Hoh, F.C. (1998) Weinberg angle and pion beta decay in the spinor strong interaction theory. *International Journal of Theoretical Physics*, **37(6)**, 1693-1705.

[7] Hoh, F.C. (1999) Normalization in the spinor strong interaction theory and strong decay of vector meson V→PP. *International Journal of Theoretical Physics*, **38(10)**, 2617-2645.

[8] Hoh, F.C. (1999) Radiative decay of vector meson V→Pγ in the spinor strong interaction theory. *International Journal of Theoretical Physics*, **38(10)**, 2647-2664.

[9] Hoh, F.C. (2000) $\pi^0 \to \gamma\gamma$ in the spinor strong interaction theory. *International Journal of Theoretical Physics*, **39**, 1069.

[10] Hoh, F.C. (1997) Meson-lepton interaction in the spinor strong interaction theory. *International Journal of Theoretical Physics*, **36(2)**, 509-531.

[11] Källén, G. (1964) Elementary particle physics. Addison-Wesley, Boston.

[12] Hoh, F.C. (1994) Gauge invariance and quantozation of the spinor strong interaction model. *International Journal of Modern Physics A*, **9(3)**, 365-381.

Vol.2, No.1, 402-408 (2010)
doi:10.4236/ns.2010.24049

Natural Science

Review: the charnockite problem, a twenty first century perspective

Samarendra Bhattacharya

Geological Studies Unit, Indian Statistical Institute, Calcutta, India; samar.bhattacharya@gmail.com

Received 11 December 2009; revised 12 January 2010; accepted 5 February 2010.

ABSTRACT

Beginning of the twentieth century was marked by coinage of a new rock name, Charnockite, first described as a hypersthene-bearing granite from Southern India. Since then charnockites have been described from most of the continents and mostly restricted to high-grade belts. Later half of the last century saw a lively debate over an igneous versus metamorphic origin. However, two factors acted as deterrents for the resolution of the debate. First, charnockites and associated rocks occur in a variety of different structural setting and display diverse field relations, attesting to possible different mode of origin. Second and possibly more important is the lack of consensus on the nomenclature of charnockites and associated rocks and this is commonly linked with the metamorphic versus magmatic perspective. Scanning the literature of this period makes one believe that both metamorphic and magmatic hypotheses are valid, but applicable to different field setting only. Before critically evaluating individual cases, it is imperative that a uniform approach in nomenclature should be agreed upon. It is proposed that name charnockite be adopted for any quartzofeldspathic rock with orthopyroxene, irrespective of its mode of occurrence, structural setting and mode of origin. The associated more mafic varieties, be better described as mafic granulite, rather than basic charnockite. For the patchy charnockites of east Gondwana (including parts of Peninsular India, Sri Lanka and Antarctica), metamorphic transformation from amphibolite facies gneiss, by two different mechanisms: CO_2 ingress from deep level, and drop in fluid pressure, has been proposed. However, all such patchy occurrence is not amenable to explanation by metamorphic transformation. In some instances, migmatisation of older charnockitic rocks is evident. Also progressive charnockitisation relating patchy charnockite to banded variety could be argued against on two counts: grain-size relation and time-relation. Larger bodies or bands have been explained as magmatic, but in many instances, from geochemical consideration alone. The compositional variation, commonly encountered in many high-grade belts, if not described in terms of field relation, may lead to wrong notions of magmatic differentiation of mantle-derived melts. Crustal melting of dry granulite facies source rocks has been proposed from geochemical and isotopic data of charnockitic intrusions. This model proposes high-temperature melting of previously dehydrated and dry granulite source rocks. However, tectonic perturbation subsequent to granulite facies metamorphism that might have been responsible for such high temperatures, is not well constrained in this model. Finally, with advent of high-pressure dehydration-melting experiments in the nineties, dehydration-melting of mafic to intermediate composition, syn-kinematic with granulite facies metamorphism has been proposed.

Keywords: Incipient Growth; Progressive Charnockitisation; Plutonic Charnockite; Partial Melting; Plutonic Metamorphism

1. INTRODUCTION

Holland [1] first described charnockite from south India, as hypersthene-bearing granite; and Howie [2] introduced the concept of plutonic metamorphism: charnockite magma emplaced at lower crustal depth, resulting in slow recrystallisation under great heat and uniform pressure. Recent researches, particularly, dehydration melting under granulite conditions in the deep crust, both experimental and empirical results is compatible with the concept of plutonic metamorphism.

Since then charnockite has been described from most of the continents [3-9]. However, a variety of different mode of occurrence and structural setting, particularly the patchy occurrence first reported by Pichamuthu from Karnataka, south India [10] led to a lively debate over an igneous versus metamorphic origin. The first attempt for resolution of the charnockite problem was made by Ravich [11].

Another contentious issue relates to nomenclature, and to this day, this issue remains unresolved and no consensus among practicing earth scientists is a serious deterrent.

2. NOMENCLATURE

As more and more occurrences are reported, controversies on nomenclature cropped up and the IUGS classification, based on feldspar ratio, could not be uniformly implemented, even for the purported plutonic charnockites. On the one hand, many practicing earth scientists would use IUGS nomenclature, even for purported metamorphic charnockites [12-13]. It is noteworthy that not all the patchy occurrences are charnockite sensu stricto [14,16,17]. On the other hand, many of the reported plutons are enderbite or charno-enderbite, but described as charnockite by some workers [17-18]. Again, it has been noted from many granulite terrenes that large-scale bodies commonly include charnockite and enderbite, along with intermediate varieties, but are not distinguishable in the field [15,19,20]. Lack of consensus on charnockite nomenclature continues and some recent publications use various terms like charnockitic gneiss of tonalite-trondjhemite affinity, enderbite, enderbitic charnockite [21] and charnockites, charnockitic rocks, chemically quartz-monzodiorite, quartz monzonite, granodiorite and granite [22]. It is important to note that orthopyroxene also occurs in high-temperature pelitic granulites, which should not be confused with charnockitic rocks [23].

SUMMARY:
The only plausible solution could be a general name for any quartzofeldspathic rock with orthopyroxene as charnockite (except of course high aluminous pelites), irrespective of the mode of occurrence, structural setting and mineralogical-chemical variations within each occurrence; the associated more mafic varieties may be described as mafic granulite, rather than basic charnockite, as first proposed by us [17]. The chemical classification then may follow Streickeisen's scheme for common plutonic rocks and special names like enderbite etc may be omitted.

3. MODE OF ORIGIN

Naha *et al*. [24] noted that charnockitic rocks in south India occur in a variety of different structural settings, attesting to different styles and time-relations. Since 1960, when Pichamuthu first described patchy charnockites from Kabbaldurga in south India, the focus shifted to metamorphic transformation. Moreover, Newton and Hansen [25] questioned the possibility of slow cooling (and hence magmatic charnockite) and recrystallization of relatively dry granitic to intermediate magma under deep seated conditions, as proposed by Holland and Lambert [26]. Lack of experimental evidence on the primary crystallization of orthopyroxene from such H_2O under saturated SiO_2 rich liquid was their main argument and this created a strong bias in favor of metamorphic transformation. However, Kramers and Ridley [27] considered the evolution of the fluid phase during crystallization in the presence of orthopyroxene, and showed that fluid saturation curve is reached at the field of high CO_2/H_2O ratios and hence fluid inclusions are predicted. They further argued that "the patchy distribution of amphibolite & granulite facies TTG rocks in some high-grade terrains could be accounted for in this way". Melting experiments since the nineties, moreover, have highlighted the possibility of primary crystallization of orthopyroxene by dehydration melting reactions in the deep crust.

3.1. Metamorphic Transformation

From many localities in south India and Sri Lanka, "patchy" charnockites have been described as "arrested growth", "in situ" charnockites or charnockitisation of amphibolite facies gneisses [28-39].

Two suggested mechanisms of this transformation: CO_2-influx and drop in fluid pressure are reviewed in the following paragraphs.

Influx of CO_2 rich fluid from deep mantle source along structural weak zones has been proposed by several workers [25,28,29,32,33,40]. and Newton [15] mentioned three criteria for recognition of charnockitisation by CO_2 influx, namely, 1) diffuseness of patchy alteration, unlike discrete veins; 2) occurrences closely associated with warping of foliation or dilation cracks; 3) open system alteration- often loss of mafic constituents and gain of Na and Si; Y and sometimes Rb are characteristically depleted. Some of these criteria are not ubiquitous, as argued by Bhattacharya and co-workers [14,16, 17]. From Kerala and from Chilka area of the Eastern Ghats belt, these workers have argued that, 1) diffuse boundaries of the charnockite patches could have been produced by migmatisation of older charnockitic bodies by a granitic melt; 2) at Elavattum and Kottavattum quarries in Kerala, the apparent disposition along conjugate fractures [41], are actually disrupted segments of fold limbs (Figure 7 in Reference [14]). In Chilka Lake area the charnockite patches occur as elongate bodies parallel to sub horizontal F_3 fold axis and along shear planes with sub horizontal direction of maximum stretching; hence these weak zones are shallow structures and cannot act as channelways for fluid ingress from deeper levels. From the classical area of south India, Kabbaldurga, Bhattacharya and co-workers argued that the charnockite patches are usually not emplaced along the system of fractures, that are common in this region; and 3) four varieties of Peninsular gneisses: granite, trondhjemite, granodiorite and tonalite and three varieties of charnockite: granite, trondhjemite and tonalite are recognized in the quarry and charnockite patches occur within all varieties of peninsular gneisses; hence chemical similarity between close-pairs, cited as evidence of in- situ transformation by several workers, could be fortuitous [17]. The reported abundance of CO_2-rich fluid inclusions in patchy charnockites has been cited as evidence for the process of charnockitization by fluid- streaming [42] But Sen and Bhattacharya [16] argued that CO_2-enriched fluid inclusions may be due to preferential loss of H_2O by crystal plastic deformation and/or open system processes, as suggested by Hollister [43] and Buick and Holland [44]. For the patchy charnockites in the Eastern Ghats belt, CO_2-rich fluid streaming was also assumed by several workers [45-47]. But the possibility of large-scale influx of CO_2-rich fluids in the Eastern Ghats was ruled out by several workers [48,49]. Also deep mantle source of CO_2-rich fluid is not evident, while Bhowmik *et al*. [49] presented isotopic evidence of local sedimentary source (calc-granulites) in a granulite suite from the Eastern Ghats belt.

Raith and Srikantappa [41] proposed an alternative mechanism of this transformation. According to this hypothesis, arrested charnockitization is internally controlled; during near-isothermal uplift, the release of carbonic fluids from decrepitating inclusions in the host gneiss into developing fracture zones, resulting in a change in fluid regime and development of an initial fluid-pressure gradient, triggering the dehydration reaction. What is common, however, between the two hypotheses, is development of “arrested charnockite” in structural weak zones. For the Kabbaldurga occurrence, Bhattacharya and Sen [17] pointed out that “charnockite veins at Kabbal are usually not emplaced along the system of fractures that are common in this region.”

Time relations between charnockites and enclosing gneisses, as also between patchy occurrence and massive bodies, are important constraints, for validating or otherwise of the hypothesis of in-situ transformation. Naha *et al*. [24] pointed out that charnockites of Dharwar craton have formed in at least two distinct phases separated in time and possibly by different mode of origin. And Bhattacharya and Sen [17] pointed out that “patchy charnockites seen in Kerala and in the Eastern Ghats are mostly non-pegmatitic”; “the coarser-grained patches could very well be modified versions of the smaller patches”; and “… are basically earlier than the enclosing gneisses”. It is imperative, therefore, to consider individual cases of “patchy charnockite”, in terms of field relations and if possible, in terms of isotopic age relations. For the Chilka Lake case in the Eastern Ghats belt, Bhattacharya *et al* [50] reported older zircons in the patchy charnockite to those of the host leptynite/granite gneiss.

Another point of contention is the proposed link between patchy charnockite and massive charnockite, particularly in South India. Srikantappa *et al* [34] proposed progressive charnockitisation, from some locales in the Kerala Khondalite belt. But Sen and Bhattacharya [15] argued that grain-size relation between smaller patches and adjacent larger bands (supposedly final product) does not support this hypothesis. Sen and Bhattacharya [15] further argued on the evidence of field relation between them, that larger bands are actually older. On the other hand, the proposed genetic link between the incipient/arrested charnockite of the transition zone in South India to regional scale granulites (massive charnockite), is strongly influenced by the CO_2-influx hypothesis [19,29,31-33,51]. According to this model ascent of the carbonic fluid front to higher crustal levels, results in pervasive fluid flow and wholescale granulitization of the deeper crustal domains. However, Raith and Srikantappa [41] argued on the evidence of field relations, petrological, geochemical and isotopic data, that development of arrested charnockites is a late-stage phenomenon; and regional-scale granulites could have been generated by dehydration melting processes.

SUMMARY:

Proposed hypothesis of charnockitisation, either by CO_2 influx or drop in fluid pressure, could indeed be applicable for individual cases; but each would require additional data pertaining to structural setting and field structural data attesting to time relation. Additionally, isotopic data would resolve the issue in favor or against the hypothesis of progressive charnockitisation. It is emphasized here that patchy occurrence itself should not be taken as prototypes of incipient charnockite.

3.2. Magmatic Origin

Since Howie [2] proposed the hypothesis of plutonic metamorphism, large-scale charnockitic rocks have been described from many granulite terrenes [20-22,52-57]. Subba Rao and Divakara Rao [53] described charnockitic rocks of intrusive origin from Eastern Ghats Belt, and identified two groups, namely basic granulite and charnockite. From geochemical angle, these authors proposed that protoliths of these charnockitic rocks are the fractionated products of a melt, which was derived from metasomatised mantle, and that these were affected by a depletion event probably coeval with granulite facies metamorphism. Although, two groups were said to be identified "based upon field relations and chemistry", the actual field relation between basic granulite and charnockite is not described in this publication. Moreover, as noted earlier by several workers, local structural setting and sample locations are important criteria, and without these information, the applicability of the mantle melting model proposed by these authors can be questioned. In this context, it is important to note that from detailed field mapping and structural analysis in the Chilka Lake area of the Eastern Ghats belt, India, Bhattacharya *et al* [57] argued that "certainly an igneous protolith which has suffered granulite facies metamorphism (as evidenced by inter-layered basic granulites) is a distinct possibility". It is unfortunate that some workers concluded that in the Eastern Ghats belt, age relations may be deduced from field relations, but neither do they present any data, nor refer to published information; hence their conclusion that "intruding magmas are either mantle-derived (basic granulites, enderbites and charnockites with crustal contribution)….." remains questionable [58]. Bhattacharya and co-workers described two types of field relations between charnockitic rocks and metapelitic rocks. First type is the interbanding of the two lithologies; the time relation is uncertain, though both may have undergone granulite facies metamorphism together [57,59]. The other type of field relation between the two lithologies is all the more complex; large-scale bodies of charnockitic rocks usually occur as separate exposures, and no contact between the two could be observed; no pelitic enclaves were observed in charnockites. Only on the basis of the sequence of deformation structure, a tentative correlation has been proposed: mafic granulite, occurring as folded enclaves in charnockite, could be correlated to intrafolial folds in pelitic granulites [57,60]. Dobmeier and Raith [13] also observed that "since the enderbitic and metasedimentary rocks have identical structural histories, the emplacement (of enderbitic/tonalitic magma) happened prior to the discernible deformation…" in the Chilka Lake area.

Magmatic origin of charnockite is also proposed by several workers in the nineties. Kilpatrick and Ellis [7] described Charnockite Magma Type, or C-type, from different areas, with distinctive geochemical signatures. This C-type magma was considered to be derived by melting of a dry granulite source. It should be noted that this C-type magma is not strictly charnockite sensu stricto, but varies between charno-enderbite and charnockite (see K_2O/Na_2O ratios and SiO_2 values in Table 1 of Reference [7]). Also the melting here is considered to have been post-granulite facies metamorphism and a crustal-melting event. Melting of dry granulite-facies source rocks, for Antarctican charnockites, was also proposed by some workers from geochemical and isotopic data [20,55,61]. On the other hand, Sheraton *et al*. [54] argued that more mafic varieties may be largely mantle-derived. It is important to note that these reports on Antarctican charnockites show a range of composition from quartz monzodiorite through granodiorite to adamelite. Hence, discrimination between charnockite and enderbite magma, in massif-type or intrusive charnockite, was considered inappropriate by these authors. This model proposes high-temperature melting of previously dehydrated and dry granulite source rocks. But tectonic perturbation subsequent to granulite facies metamorphism that might have been responsible for such high-temperatures is not well constrained in this model.

A partial melting interpretation for vein type charnockite was advocated by Hansen and Stuk [62], and these authors reported orthopyroxene-bearing leucosomes, of tonalitic to granodioritic composition, within mafic bodies of granulite facies rocks from California.

Finally, melting experiments, particularly dehydration-melting experiments of mafic to intermediate rocks in the nineties have added a new dimension to the problem of charnockite genesis [63-66]. These experiments demonstrate a) significant melting at 8 to 10 kbar and temperatures in excess of 850^{o}C; these values are commonly recorded from many granulite terrains; b) the residual assemblage of two-pyroxene-plagioclase-quartz ± garnet, clearly resemble mafic granulite, that are frequently found associated with massif-type charnockite; c) melt compositions in hornblende-dehydration melting range from tonalite-granodiorite-trondjhemite, while hornblende-biotite combined melting produced granitic melts.

From the classic area, Kabbaldurga, in South India, Bhattacharya and Sen [17] presented a new interpretation of vein type charnockite. These authors proposed hornblende and biotite dehydration melting in two types of mafic granulites observed in the area, producing two types of charnockitic vein, of tonalitic and granitic compositions respectively. Besides the field features, such as orthopyroxene-bearing leucosomes within mafic granulite enclaves in the peninsular gneiss; these authors presented comparative mineral compositions in the charnockite veins and mafic granulite enclaves and bulk compositions of the charnockite veins, and these are compatible with the results of experimental melting, referred to above.

For the massif-type charnockite in the Eastern Ghats belt, India, Kar *et al*. [56] proposed a hornblende- dehydration melting in mafic rocks, now occurring as cognate xenoliths, under granulite facies conditions. Additionally these authors reported two types of mafic granulites, namely prograde hornblende-bearing mafic granulite, interpreted as restitic granulite and two-pyroxene mafic granulite, interpreted as peritectic segregations.

And unlike Subba Rao and Divakara Rao's [53] mantle-melting model for the Eastern Ghats charnockite, these authors described a crustal melting phenomenon, coeval with granulite facies metamorphism. From pressure-temperature estimates and P-T path constraints, these authors further argued that melting could have occurred in thickened continental crust undergoing decompression. Bhattacharya *et al*. [67] established the link between partial melting and granulite facies metamorphism with isotopic data. Kar *et al*. [56] further pointed out that trace element partitioning in dehydration melting is likely to be complex, because incongruent melting reactions result in two sets of solid mineral phases, residual and peritectic [68]. Hence quantitative modeling is inappropriate when the process involves reactions producing a variety of solid peritectic phases. Trace element partitioning then could be considered as a two stage process; to some extent correlated with different degrees of partial melting. At low degree of melting the main process is melt-restite separation, whereas at higher degrees of melting peritectic-melt separation becomes more important [69-71].

SUMMARY:

Although magmatic origin of charnockites, particularly for the large scale bodies, are evident in many cases, the question relating to either mantle-melting or crustal melting and in case of crustal melting, the actual melting process and conditions remain debatable in many cases. Dehydration-melting in mafic to intermediate rocks under granulite facies conditions could be the most potential hypothesis for the massif-type charnockite, provided prograde hornblende/biotite bearing mafic granulite enclaves are observed. Thus the concept of plutonic metamorphism may return with new vigor.

REFERENCES

[1] Holland, T.H. (1900) The charnockite series, a group of Archaean hypersthenic rocks in Peninsular India. *Memoirs of the Geological Survey of India*, **28**, 119-249.

[2] Howie, R.A. (1954) The geochemistry of the charnockite series of Madras, India. *Transactions of the Royal Society of Edinburgh*, **62**, 725-768.

[3] De Ward, D. (1969) The occurrence of charnockite in the Adirondacks: A note on the origin and definition of charnockite. *American Journal of Science*, **267**, 983-987.

[4] Duchesne, J.C., Caruba, R. and Iacconi, P. (1987) Zircon in charnockitic rocks from Rogaland (Southwest Norway): Petrogenetic implication. *Lithos*, **20(5)**, 357-368.

[5] Condie, K.C. and Allen, P. (1984) Origin of Archaean charnockites from southern India. In: Kroner, A., ed., *Archaean Geochemistry*, Springer, Berlin, 182-203.

[6] Hubbard, F.H. and Whitley, J.E. (1979) REE in charnockite and associated rocks, southwest Sweden. *Lithos*, **12(1)**, 1-11.

[7] Kilpatrick, J.A., Ellis, D.J. and Young, D.N. (1990) Field aspects of the Ardery charnockitic intrusions, Windmill Islands, Antarctica. A dynamic magma chamber. *Geological Society of Australia Abstracts*, **25**, 290.

[8] Sheraton, J.W. (1982) Origin of charnockitic rocks of MacRobertson Land. In. Craddock, C., ed., *Antarctic Geoscience*, Madison University of Wisconsin Press, 489-497.

[9] Schumacher, R. and Faulhaber, S. (1994) Summary and discussion of *P-T* estimates from garnet-pyroxene-plagioclase-quartz-bearing granulite facies rocks from Sri Lanka. *Precambrian Research*, **66(1-4)**, 295-308.

[10] Pichamuthu, C.S. (1960) Charnockite in the making. *Nature*, **188**, 135-136.

[11] Ravich, M.G. (1972) The charnockite problem. In. Adie, R. J., ed., *Antarctic Geology and Geophysics*, Scandinavian University Books, Oslo, 523-526.

[12] Raith, M and Srikantappa, C. (1993) Arrested charnockite formation at Kottavattam, southern India. *Journal of Metamorphic Geology*, **11**, 815-832.

[13] Dobmeier, C. and Raith, M. (2000) On the origin of "arrested" charnokitization in the Chilka Lake area, Eastern Ghats Belt, India: A reappraisal. *Geological Magazine*, **137**, 27-37.

[14] Bhattacharya, S., Sen, S.K. and Acharyya, A. (1993) Structural evidence supporting a remnant origin of patchy charnockites in the Chilka Lake area, India. *Geological Magazine*, **130(3)**, 363-368.

[15] Newton, R. C. (1992) Charnockitic alteration: Evidence for CO_2 infiltration in granulite facies metamorphism. *Journal of Metamorphic Geology*, **10**, 383-400.

[16] Sen, S.K. and Bhattacharya, S. (1993) Patchy charnockites from south Kerala-nascent growths or modified relicts? *Indian Minerals*, **47**, 103-112.

[17] Bhattacharya, S. and Sen, S.K. (2000) New insights into the origin of Kabbaldurga charnockites, Karnataka, South India. *Gondwana Research*, **3**, 489-506.

[18] Rao, A.T. and Vijaykumar, V. (1992) Chemical petrology of charnockites from the Eastern Ghats granulite province, India. In: Kyriakidis, A.B., ed., *High Grade Metamorphics*, Theophrastus Publications, 217-235.

[19] Prasad, K.S.S., Rao, K.L.N. and Murty, M.S. (1992) Charnockites of Obachettapalem, Prakasam district, South India. In: Kyriakidis, A.B., ed., *High Grade Metamorphics*, Theophrastus Publications, 237-261.

[20] Young, D.N., Zhao, J.X., Ellis, D.J. and McCulloch, M.T., (1997) Geochemical and Sr-Nd isotopic mapping of source provinces for the Mawson charnockites, east Antarctica: implications for Proterozoic tectonics and Gondwana reconstruction. *Precambrian Research*, **86**, 1-19.

[21] Santosh, M., Yokoyama, K. and Acharyya, S.K. (2004) Geochronology and tectonic evolution of Karimnagar and Bhopalpatnam Granulite belts, Central India. *Gondwana Research*, **7**, 501-518.

[22] Mendes, J.C., Medeiros, S.R., McReath, I. and Pinheiro de Campos, C.M. (2005) Cambro-Ordovician magmatism in SE Brazil: U-Pb and Rb-Sr ages, combined with Sr and Nd isotopic data of charnockitic rocks from the Varzea Alegre Complex. *Gondwana Research*, **8**, 337-346.

[23] Raith, M., Karmakar, S. and Brown, M. (1997) Ultra-high temperature metamorphism and multi-stage decompressional evolution of sapphirine granulites from the

Palni Hill Ranges, south India. *Journal of Metamorphic Geology*, **15**, 379-399.

[24] Naha, K., Srinivasan, R. and Jayaram, S. (1993) Structural relations of charnockites of the Archaean Dharwar craton, southern India. *Journal of Metamorphic Geology*, **11**, 889-895.

[25] Newton, R.C. and Hansen, E.C. (1983) The origin of Proterozoic and late Archaean charnockites-evidence from field relations and experimental petrology. *Geological Society of America Memorials*, **161,** 167-178.

[26] Holland, J.G. and Lambart, R.S.J. (1975) The chemistry and origin of the Lewisian gneisses of the Scottish mainland: the Scourie and Inver assemblages and sub crustal accretion. *Precambrian Research*, **2(2)**, 161-188.

[27] Kramers, J.D. and Ridley, J.R. (1989) Can Archaean granulites be direct crystallization from a sialic magma layer? *Geology*, **17(5)**, 442-445.

[28] Janardhan, A.S., Newton, R.C. and Smith, J.V. (1979) Ancient crustal metamorphism at low pH_2O: Charnockite formation at Kabbaldurga, south India. *Nature*, **278**, 511-514.

[29] Janardhan, A.S., Newton, R.C. and Hansen, E.C. (1982) The transformation of amphibolite facies gneiss to charnockite in southern Karnataka and northern Tamil Nadu, India. *Contributions to Mineralogy and Petrology*, **79**, 130-149.

[30] Janardhan, A.S., Jayananda, M. and Shankara, M.A. (1994) Formation and tectonic evolution of granulites from Biligirirangam and Nilgiri Hills, south India: Geochemical and isotopic constraints. *Journal of the Geological Society of India*, **44**, 27-40.

[31] Friend, C.R.L. (1981) Charnockite and granite formation and influx of CO_2 at Kabbaldurga. *Nature*, **294**, 550-552.

[32] Hansen, E.C., Newton, R.C. and Janardhan, A.S. (1984) Fluid inclusions in rocks from amphibolite-facies gneiss to charnockite progression in southern Karnataka, India: direct evidence concerning the fluids of granulite metamorphism. *Journal of Metamorphic Geology*, **2**, 249-264.

[33] Hansen, E.C., Janardhan, A.S., Newton, R.C., Prame, W.K.B. and Kumar, G.R.R. (1987) Arrested charnockite formation in southern India and Sri Lanka. *Contributions to Mineralogy and Petrology*, **96**, 225-244.

[34] Srikantappa, C., Raith, M. and Spiering, B. (1985) Progressive charnockitization of a leptynite-khondalite suite in southern Kerala, India: Evidence for formation of charnockites through a decrease in fluid pressure? *Journal of the Geological Society of India*, **26**, 62-83.

[35] Srikantappa, C., Raith, M. and Touret, J.L.R. (1991) Synmetamorphic, high-density carbonic fluids in the lower crust: Evidence from the Nilgiri granulites, southern India. *Journal of Petrology*, **33(4)**, 733-760.

[36] Raith, M. Stahle, H.J. and Hoernes, S. (1988) Kabbaldurga-type charnockitization: a local phenomenon in the granulite to amphibolite grade transition zone. *Journal of the Geological Society of India*, **31**, 116-117.

[37] Raith, M., Srikantappa, C., Ashamanjeri, K.G. and Spiering, B. (1990) The granulite terrene of the Nilgiri Hills (southern India): Characterization of high-grade metamorphism. In: Vielzeuf, D. and Vidal, P., ed., *Granulites and Crustal Evolution*, NATO ASI Series C, Kluwer Academic Publishers, Dordrecht, **311**, 339-365.

[38] Yoshida, M. and Santosh, M. (1994) A tectonic perspective of incipient charnockites in East Gondwana. *Precambrian Research*, **66(1-4)**, 379-392.

[39] Harley, S.L. and Santosh, M. (1995) Wollastonite at Nuliyam, Kerala, South India: A reassessment of CO_2 infiltration and charnockite formation at a classic locality. *Contributions to Mineralogy and Petrology*, **120**, 83-94.

[40] Condie, K.C., Bowling, G.P. and Allen, P. (1986) Origin of granites in an Archaean high-grade terrene, southern India. *Contributions to Mineralogy and Petrology*, **92**, 93-103.

[41] Raith, M and Srikantappa, C. (1993) Arrested charnockite formation at Kottavattam, southern India. *Journal of Metamorphic Geology*, **11**, 815-832.

[42] Santosh, M., Jackson, D.H., Mattey, D.P. and Harris, N.B.W. (1988) Carbon Stable Isotopes of fluid inclusions in the granulites of southern Kerala: Implications for the source of CO_2. *Journal of the Geological Society of India*, **32**, 477-493.

[43] Hollister, L.S. (1993) The role of melt in the uplift and exhumation of orogenic belts. *Chemical Geology*, **108**, 31-48.

[44] Buick, I.S. and Holland, T.J.B. (1991) The nature and distribution of fluids during Amphibolite facies metamorphism, Naxos (Greece). *Journal of Metamorphic Geology*, **9**, 301-314.

[45] Halden, N.M., Bowes, D.R. and Dash, B. (1982) Structural evolution of migmatites in a granulite facies terrene: Precambrian crystalline complex of Angul, Orissa, India. *Transactions of the Royal Society of Edinburgh*, *Earth Science*, **73**, 109-118.

[46] Paul, D.K., Burman, T.R., McNaughton, N.J., Fletcher, I.R., Potts, R.J., Ramakrishnan, M. and Augustine, P.F. (1990) Archaean-Proterozoic evolution of Indian charnockites: Isotopic and geochemical evidence from granulites of the Eastern Ghats Belt. *Journal of Geology*, **98**, 253-263.

[47] Rajesham, T., Nagarajan, K., Murti, K.S., Shirahata, H. and Yoshida, M. (1994) Incipient charnockitisation in Eastern Ghats terrain of Vizianagram area, Andhra Pradesh. *Workshop on Eastern Ghats Mobile Belt*, Vishakapatnam, 43.

[48] Bhattacharya, A. and Sen, S.K. (1991) Pressure, temperature and fluid regime in selected granulites tracts of the Eastern Ghats of India. *Proceedings Seminar on Composition and Evolution of High-Grade Gneiss Terrains*, IGCP Project 304, Lower Crustal Process, Kandy.

[49] Bhowmik, S.K., Dasgupta, S., Hoernes, S. and Bhattacharya, P.K. (1995) Extremely high-temperature calcareous granulites from the Eastern Ghats, India: Evidence for isobaric cooling, fluid buffering, and terminal channelized fluid flow. *European Journal of Mineralogy*, **7**, 689-703.

[50] Bhattacharya, S., Deomurari, M.P. and Teixeira, W. (2003) Grenvillian thermal event and remnant charnockite: Isotopic evidence from the Chilka Lake granulite-migmatite suite in the Eastern Ghats belt, India. *Proceedings of the Indian Academy of Sciences* (*Earth and Planetary Science*), **111**, 391-399.

[51] Harris, N.B.W., Holt, R.W. and Drury, S.A. (1982) Geobarometry, geothermometry and the Late Archaean geotherms from the granulite facies terrain in South India. *Journal of Geology*, **90**, 509-527.

[52] Sriramdas, A. and Rao, A.T. (1979) Charnockites of Vishakapatnam, Andhra Pradesh. *Journal of the Geological Society of India*, **20**, 512-517.
[53] Rao, M.V.S. and Rao, V.D. (1988) Chemical constraints on the origin of the charnockites in the Eastern Ghats mobile belt, India. *Chemical Geology*, **69(1-2)**, 37-48.
[54] Sheraton, J.W., Black, L.P. and Tindle, A.G. (1992) Petrogenesis of plutonic rocks in a Proterozoic granulite facies terrene-The Bunger Hills, East Antarctica. *Chemical Geology*, **97**, 163-198.
[55] Zhao, J., Ellis, D.J., Kilpatrick, J.A. and McCulloch, M.T. **(**1997) Geochemical and Sr-Nd isotopic study of charnockites and related rocks in the northern Prince Charles Mountain, East Antarctica. *Precambrian Research*, **81**, 37-66.
[56] Kar, R., Bhattacharya, S. and Sheraton, J.W. (2003) Hornblende-dehydration melting in mafic rocks and the link between massif-type charnockite and associated granulites, Eastern Ghats Granulite Belt, India. *Contributions to Mineralogy and Petrology*, **145**, 707-729.
[57] Bhattacharya, S., Sen, S.K. and Acharyya, A. (1994) The structural setting of the Chilka Lake granulite-migmatite-anorthosite suite with emphasis on time relation of charnockites. *Precambrian Research*, **66**, 393-409.
[58] Rickers, K., Mezger, K. and Raith, M. (2001) Evolution of the continental crust in the Proterozoic Eastern Ghats Belt, India and new constraints for Rodinia reconstruction: Implications from Sm-Nd, Rb-Sr and Pb-Pb isotopes. *Precambrian Research*, **112**, 183-210.
[59] Bhattacharya, S. (2003) Dehydration melting in mafic rocks in the Eastern Ghats Belt, India: Implications for variable composition of charnockitic melt and heterogeneity of source rocks. *Memoirs of the Geological Society of India*, **52**, 131-144.
[60] Bhattacharya, S. and Kar, R. (2002) High-temperature dehydration melting and decompressive *P-T* path in a granulite complex from the Eastern Ghats, India. *Contributions to Mineralogy and Petrology*, **143**, 175-191.
[61] Sheraton, J.W., Tindle, A.G. and Tingey, R.J. (1996) Geochemistry, origin, and tectonic setting of granitic rocks of the Prince Charles Mountains, Antarctica. *Australian Geological Survey Organisation Journal of Australian Geology and Geophysics*, **16**, 345-370.
[62] Hansen, E.C. and Stuk, M. (1993) Orthopyroxene-bearing mafic migmatites at Cone Peak, California: Evidence for the formation of migmatitic granulites by anatexis in an open system. *Journal of Metamorphic Geology*, **11**, 291-307.
[63] Rushmer, T. (1991) Partial melting of two amphibolites: Contrasting experimental results under fluid absent conditions. *Contributions to Mineralogy and Petrology*, **107(1)**, 41-59.
[64] Skjerlie, K.P., Douce, A.E.P. and Johnston, A.D. (1993) Fluid-absent melting of layered crustal protolith: Implications for the generation of anatectic granites. *Contributions to Mineralogy and Petrology*, **114(3)**, 365- 378.
[65] Douce, A.E.P. and Beard, J.S. (1995) Dehydration melting of biotite gneiss and quartz amphibolite from 3 to 15 kbar. *Journal of Petrology*, **36(3)**, 707-738.
[66] Springer, W. and Seck, H.A. (1997) Partial fusion of basic granulites at 5 to 15 kbar: Implications for the origin of TTG magmas. *Contributions to Mineralogy and Petrology*, **127(1-2)**, 30-45.
[67] Bhattacharya, S., Kar, R., Misra, S. and Teixeira, W. (2001) Early Archaean continental crust in the Eastern Ghats granulite belt, India: Isotopic evidence from a charnockite suite. *Geological Magazine*, **138(5)**, 609-618.
[68] Harris, N., Ayres, M. and Massey, J. (1995) Geochemistry of granitic melts produced during the incongruent melting of muscovite: Implications for the extraction of Himalayan leucogranite magmas. *Journal of Geophysical Research*, **100(8)**, 15767-15777.
[69] Brown, M., Rushmer, T. and Sawyer, E.W. (1995) Mechanisms and consequences of melt segregation from crustal protoliths. *Journal of Geophysical Research*, **100(8)**, 15551-15563.
[70] Vigneresse, J.L., Barbey, P. and Cuney, M. (1996) Rheological transition during partial melting and crystallization with application to felsic magma segregation and transfer. *Journal of Petrology*, **37(6)**, 1579-1600.
[71] Brown, M. and Rushmer, T. (1997) The role of deformation in the movement of granitic melt: Views from the laboratory and the field. In: Holness, M.B., ed., *Deformation-Enhanced Fluid Transport in the Earth's Crust and Mantle*, the Mineralogical Society Series, **8**, 111-144.

Vol.2, No.4, 409-417 (2010)
doi:10.4236/ns.2010.24050

Natural Science

Overview of flooding damages and its destructions: a case study of Zonguldak-Bartin basin in Turkey

Hasan Arman[1,3], Ibrahim Yuksel[2*], Lutfi Saltabas[3], Fatih Goktepe[3], Mehmet Sandalci[3]

[1]College of Science, Department of Geology, United Arab Emirates University, Al-Ain, UAE; Harman@uaeu.ac.ae; harman@sakarya.edu.tr
[2]Faculty of Technology, Department of Construction, Sakarya University, Esentepe Campus, Sakarya, Turkey; yukseli2000@yahoo.com; iyuksel@sakarya.edu.tr
[3]Engineering Faculty Department of Civil Engineering, Sakarya University, Esentepe Campus, Sakarya, Turkey

Received 29 December 2009; revised 26 January 2010; accepted 2 February 2010.

ABSTRACT

A number of devastating flood events have occurred in the various river basins of Turkey in the last decade. Because floods caused deaths, suffering and extensive damages to both public and private properties in the flood areas, the government had to most of the damage in addition to losing significant revenues due to the consequences of costly social and economic disruption. On the other hand, some social structures such as socioeconomic activities, land-use patterns and hydro-morphological processes are destroyed. Whereas flood control structures are considered as one of the basic strategies that can reduce flood damages and in this context flood protection planning should consider the full range of the hazard mitigation activities. In Turkey, between 1945 and 1990, 737 flooding events were occurred and at least 830 people were killed. In 1998, there was a major flooding in Zonguldak-Bartin region located on north of Turkey. Due to this devastated flooding, people lost their life and numbers of engineering structures built on the river and surrounding area were totally destroyed or heavily damaged. Both side of the canal were covered with muddy soil having 0.10-0.15 m thickness. Cleaning up process took sometimes in the region. In this paper, all these subjects have been investigated in the basin and some engineering proposals have been presented.

Keywords: Flood Damages; River Management; Zonguldak-Bartin Basin; Flood Control

1. INTRODUCTION

Beside social, economical, technological, administrative and political gains during the development from primarily communities to our information communities throughout the history some hard to solve problems for the future generations and for us about our environment had occurred, especially because of industrialization and urbanization attempts that do not care about environment in spite of their economical profits. Due to global economic order that overbalance the ecosystem, environment problems, which did not exist in twenty century, exist in last twenty-five year. Problems like population increase, decrease in agriculture land area, reduction of ground water, devastation of forests, disappearing of plants and animal kinds, air-water-soil pollution, increase of temperature because of greenhouse gases, are vital for humanity. As a result of this, because of climatic changes it is expecting that there is a risk of hurricanes, strong precipitations, or long-term drought, risk of lands turning into desert [1]. Floods are due to heavy rainfall on the coastal areas of the western and southern parts of Turkey or to a sudden increase in air temperature, resulting in snow melt in the eastern, mountainous part of southeastern Turkey especially Eastern Black Sea Region [2,3]. In the northern and central parts of the country both factors may occur depending on the time of the year.

In Turkey the precipitation types are frontal, orographic, or convective. During occluded fronts, long lasting, intense rainfall may produce flooding depending on the season of the year. Besides most of the coastal precipitation in the Black Sea region where the range of mountains runs parallel to the shore sea, considering some others properties of the region such as hydraulics, hydrological, meteorological characteristics at least a few floods have occurred in a year in this region [4,5]. Convective precipitation mostly occurs during the transition seasons of spring and autumn and affects central Anatolia. The snow accumulated in the upper reaches of the drainage basins of Anatolian rivers melts, starting from the beginning of February or March, and can cause flooding in downstream areas of the rivers. When the general evaluate of the natural balance irregularities arising at a global scale is made, it can be seen the affecting parameters, which are subject to change, are the hydraulic and hydrological ones due to their activities in the river basin. In some areas almost all the waters of the rivers are used up with in the basin, primarily for the purpose of irrigation.

Flash floods are a common, but it is not easy to estimate its environmental features. A lack of accurate environmental data creates much of the uncertainty associated with flash flooding events. In addition to limiting the understanding of hydrological processes, human use and development in a region cause number of problems. Extreme events often exert a disproportionately large effect on the environment, for larger than that associated with the more commonplace typical events, and are those most associated with hazards to humans [6]. A major concern with flash flooding is the development within a very short period of time. Human life and infrastructures are under a major threat of flash flooding. The lack of understanding sometimes compounds problems of flooding, with settlement, road and other structures inappropriately located and designed relative to the flood risk [6].

It is a general accepted fact that especially the dams constructed at a point very close to the shoreline destroy the natural balance of shoreline by totally changing the flow regimen and therefore the sediment load in the rivers. This point, according to one point of view constitutes the crossing point of the shorelines management and the basin management; according to another point view it constitute the intersection between the two basic purposes of both approaches is to watch the natural balance and maintain development. Then, the problem could easily be solved in case there is sustainable growth. In order to achieve joint management, it is obvious that a good monitoring study has to be done and healthy data must be obtained [7].

In Turkey, it is known that erosion flooding and land sliding events are widespread due to unconsciously destruction of nature, and weathering. In many regions of our country flooding and land sliding cause death, wealth loses every year. Although they are not the only environment problem, it is important to consider about these, which time-to-time influence the daily life [1].

This paper deal with the effectiveness of river flooding and its destructive damages on human and their structures built on the river and its surrounding area. Flooding in the Zonguldak-Bartin region during the summer of 1998 caused extensive damage. Immediately after the 1998 floods the Turkish Government took steps to rescue and remove both people and property from flooding area and built up a temporary bridge on the river to provide access people living on both side of the river.

2. FLOOD INVENTORY AND EXITING FLOOD MEASURES IN TURKEY

The existing flood related measures carried out in the framework of flood management can be summarized as:

- Structural Projects: Structural projects keep flood waters away from an area with a levee or reservoir, or other measure that controls the flow of water.
- Hydrometric and Meteorological Observation Works: In an attempt to determine reverie flood hazard by catchments area characteristics, such as rainfall and stream flows.
- Survey Reports on Past Floods: State Hydraulic Works (DSI) has been preparing survey reports soon after flood events to establish actual flood damage information and area of inundation. These reports also include date, time, duration, place, meteorology, hydrology and hydraulic of each flood event. The study method is based on field interviews, questionnaires, observations and flood records. The survey reports of each year are formed as flood yearly book by DSI.
- Surveys Relating to Land Use Plans: As all settlement and construction areas are subjected to land use planning permission, DSI carries out flood surveys, which are conveyed to municipalities or governmental organizations and institutions for use as data at the planning stage.
- Regional Flood Plans: DSI prepares regional flood plans that have the basin-wide coverage to be integrated to basin disaster plan for using in the emergency management of the future disasters in the basin.
- Stream bed modification by setting up new diversion structures, dykes and groins.
- Reforestation, land improvement.
- Education and information.

However, the methods listed above are available and applied at many places, that does not mean that they are effective everywhere. And the last item education is relatively short-lived. If no practical proof of the theoretical information is given, the knowledge and awareness of the risk will be lost within a few years, even if it was there at the beginning [8]. As long as human continue to built any kind of engineering structures such as dams, highways, bridges, homes and etc. on flood-prone area it can expect continued loss of lives and property. Factors that control the damage cause by floods include:

- Land use on the floodplain,

- Magnitude (depth and velocity of the water and frequency of flooding),
- Rate of rise and duration of flooding,
- Season (for example: crops on floodplain),
- Sediment load deposited,
- Effectiveness of forecasting, warning emergency systems [9].

Primary effects include injury and loss of life, along with damage caused by swift currents, debris and sediment to farms, homes, buildings, railroads, bridges, roads and communication systems. Erosion and deposition of sediment in the rural and urban landscape can also involve a loss of considerable soil and vegetation. Secondary effects can include short-term pollution of rivers, hunger and disease and displacement of people who have lost their home. In addition, fire may be caused by short circuits or broke gas mains [9]. Relationships between land use and flooding of small drainage basin may be quite complex. Use of agricultural land may affect the flooding. Urbanization is not the only type of development that can increase flooding [9]. Land cover has a strong influence on key hydrological variables such as infiltration and evaporation [6].

3. FLOOD AND WATER MANAGEMENT

3.1. The Use of Floodplain and Floodwaters along the Rivers

In the some basin at urban area, flood plains along the rivers crossing cities and towns are used for car parking, recreational purpose and for sporting activities, but at rural areas, the flood plains are used for agricultural or others purpose. The farmers cultivate at their own plots as before the land acquisition, but if the flood occurs, with the help of local legal people, sue the state for repayment. The flood waters are not used under any circumstances; the local people and authorities try to get rid of the water as quickly as possible [8].

3.2. Flood Warning System

Experiences gained from the floods of last decade show that structural measures implemented in the basin-wide are effective but too costly in reducing the risk of flood damages. In this respect, it has been considered that more importance should be given to non-structural measures, particularly modification of traditional land use and updating building code guidelines and design standards, early flood warning system, creation of public awareness, insurance and timely and effective emergency management, in order to be more effective for integrated flood management in the project area and in the whole country. Due to economic limitations, non-structural measures imposed by the local municipalities are not always successful. Because the local municipality authorities had to receive the money from central government for the realization of the infrastructures, for example their budget can not cover the land use modification projects. Briefly, the existing non-structural measures are not always successful because of two main reasons [8]:

- In the present situation, the non-structural measures are mostly dealt with by the local administrations including municipalities and mayors. However, due to the present economic conditions, the implementations of the needed activities by these bodies are limited.
- The local units do not have enough educated and trained personnel to implement the nonstructural measures.

On the other hand, in Turkey, local non-Government Organizations (NGOs) are themselves at developing stage. The other point is that the development stage of local non-governmental organizations (NGOs) is not yet satisfactory in dealing with flood disasters**.**

3.3. Modification in Flood Mitigation

Within the framework of flood management, with the increase of structural measures, it is true that the occurrences of floods and their damages become less in Turkey. However, in the recent years, the more importance is given to the non-structural measures, in a given comprehensive plan, including the arrangement of the human activities, the education of the people and the informing of the stakeholders.

From the last experiences, it is understood that the most of the damages is directly related to the fact that the irregular and uncontrolled urbanization at the high-risk areas in the flood plains. In this regard, this approach gives the more responsibility to the local governments and municipalities. There are also some mitigation activities done during the flooding events. These are mostly related to rescue works and emergency studies.

4. FLOOD AND WATER MANAGEMENT INSTRUMENTS

4.1. Existing Laws Related to Integrated Flood Mitigation Concept

The basic legislation in water sector is the Turkish Constitution, which states that water resources are natural wealth of the country, and under the authority of the State, to be used for the benefit of public. In this direction, the Turkish Civil Code covers water both common waters and private waters. The Red Crescent does the first aid, and the General Directorate of Disaster Affairs

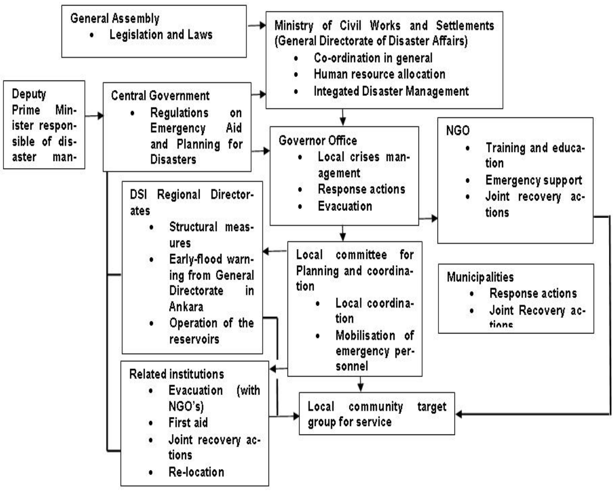

Figure 1. The flow chart in Turkish disaster management system.

(AFET) does the flood mitigation work. With existing laws, the following State organizations deal with the integrated flood management (**Figure 1**).

According to The Republic of Turkey laws:

- DSI is responsible to prevent the disaster effects of both surface and groundwater; and to build protective structures against the floods, and get benefits from its beneficiary uses,
- State Meteorological Institute (DMI) is responsible to supply the meteorological support to the sectors of agriculture, forestry, tourism, transportation, energy, health, and environment, military; on the other hand all kinds of climatic data are collected by DMI during floods,
- The law of General Directorate of Rural Affairs (KHGM**)** states has to prepare and apply some service and investment programs for the requirements of farmers in the rural areas in order to protect, develop and effective use of water and land resources in compliance with the politics and principals determined in the development plan and program. To reclaim the unsuitable land areas for agriculture, belong to the state or private; to prepare the needed reclamation projects for these areas to establish co-operations for the activities of soil conservation, land reclamation and irrigation.

Laws of Bank of Provinces (IB) and municipalities also states the responsibility of local organizations have to fight against the all natural disasters faced at the region under consideration, IB provides the funds and Municipalities spend it properly [8].

4.2. Enforcement of the Laws

The enforcement is realized by the close cooperation of the central government at capital city; and the government's top level representative at the provinces; where the flood disaster is encountered. The basic steps are the first aid, evacuation, safety, and shelter, normalization of the daily routines, rebuilding and recovery of local economy.

When a natural disaster like flood is encountered in a city, then the governor is top decision maker. The experts from various state organizations and mayor and army representatives help the governor to shape up the final decision. This expert group forms are called as "Crises Table (CT)". CT includes deputy governors, mayor, local army commander, the local representatives of DMI, DSI, State Highway Department (TCK), KHGM, civil defense, red crescent, fire brigade and other local non-overnmental organizations, like farmers union, trade union, chamber of commerce etc. In case of flood disasters, DSI and DMI local representatives play the most important role in decision-making [8].

5. COOPERATION FOR FLOOD MANAGEMENT

There should be a good and effective cooperation among the responsible institutes and local interest groups for flood management. A number of governmental and non-governmental organizations have direct and indirect responsibility in integrated disaster management of floods in Turkey. AFET, General Directorate of Civil Defense, Army, Local Administrations and Municipalities. Institutional framework has three levels; namely, decision making, executive and users level. DSI is authorized to plan and manage all aspects and issues of flood management especially after the flood event.

In the long run, all the rehabilitation works are planned and realized by the state, but during the planning stage, all the local interest groups express their views freely. At this stage, local parliamentarians and administrations play the most effective role on deciding the priorities. When a flood disaster is encountered at a province, according to the existing laws, written rules and regulations defining the responsibilities of each organization in emergency case, legislation, administrative principles, hierarchy and the local traditions, Emergency Aid Organizations and Programs Related to Disaster Management initiated the following points:

- Pre-disaster planning,
- Set up some units of the different services in cities for disaster management,
- Set up other special service units and related details.

Generally, there are written rules and regulations defining the responsibilities of each organization in emergency case, but due to human factor, just after the disaster, there may be always chaos, but soon it is over and the system starts to work properly [8]. Of course there some local interest groups or organizations, which are Non-Governmental Organizations (NGOs) such as the unions of farmers, merchants, businessmen, and chamber of commerce. Elected representatives of the local people, mayor, helps to shape up the local public mind to deal with the similar type of floods in future. There may be economic help from the banks, rich local people, some nationwide campaigns to help the disaster hit area but usually these types of helps come afterwards and not sure. There are no written rules to define the type of the service the NGOs are expected to give, but their service is voluntary. So the state is the main healer and organizer of the helps.

6. SOME FLOODS AND LANDSLIDES OCCURRED IN TURKEY

Result of devastation of nature, we have been facing flooding, landslides which causes life and property loses over 80-years period of time. In 1910, it is recorded that after a large rainfall, Tokat-Behzat Stream overflows its blanks and flow over a barrack and cause 2000 people to die in one night. Our country face with 737-flood events during 1945-1990 and has lost 838 people. In 1957, Ankara-Hatip creek flooded and 185 people were died. In 1998 Macka-Catlak landslide is caused 65 deaths [10]. In Rize City, the maximum rainfall recorded as 4045.3 mm/year in 1931, and in Igdır the minimum rainfall recorded as 114.5 mm/year in 1970 [11]. These given examples are the ones, which cause the most death in near history. This does not mean that flooding and landsliding do not cause life loss nowadays. Recently, after a heavy rainfall, number of life or properties loses can occur in many region of our country. However, it is good to say that lost of lives minimized with the gained experiences from past events. On the other hand, it is not possible to say same thing for properties loss.

6.1. Study Area: Zonguldak-Bartin Basin

Zonguldak-Bartin region is located on north of Turkey. In 1998, there was a major flooding in the region (**Figure 2**). Due to this devastated flooding, people lost their life and numbers of engineering structures built on the river and surrounding area were totally destroyed or heavily damaged. The damages caused by flooding may be classified in four categories as follows:

- Heavy damages in both side of river bed and its surrounding areas such as interstate and intercity highways (**Figure 3**).
- Destructive damages on bridge which connect both side of river (**Figure 4**).
- Totally and slight damaged buildings (**Figure 5**).
- Localized landsliding phenomena (**Figure 6**).

Both side of the canal were covered with muddy soil having 0.10-0.15 m thickness (**Figure 1**). This thickness reaches more than 0.50 m in some locations specifically near the riverbed (**Figure 3**). River water rose approximately 3.00 m during flooding. Then, cleaning up process took sometimes in the region.

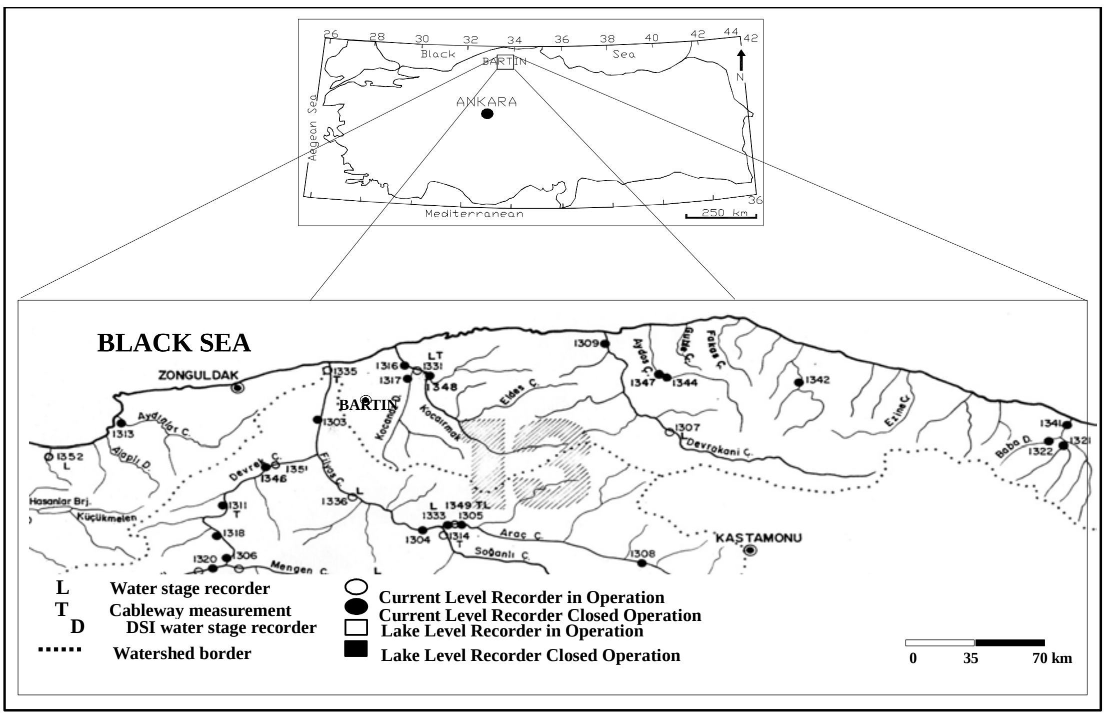

Figure 2. The case study area.

Figure 3. Intensive damages occurred in riverbed [1].

Figure 4. One of the totally damaged bridges [1].

7. RELATION BETWEEN EROSION, FLOODING AND HEAVY PRECIPITATION

In world, 25-billion tons of earth loses through erosion in every year. In the other word, 0.5-2.0 tons of one-hectare earth loses in each year. In last fifteen years, agricultural terrain/person rate decreases 14.3% in developed countries and 40% in developing countries. If this decreasing tendency goes on this rate will decrease by 50% in 2050 [10]. Erosion is one of the most important problems of the world. According to United Nations Environment Program (UNAP), 25% of the world terrain and 900 million people effect from erosion. World soil loss through erosion is 480 billion ton in last 20 years.

Figure 5. Totally destroyed buildings along the riverside [1].

Figure 6. Landslides occurred at some location along the riverbed [1].

Turkey is under erosion condition that all type and intensity of erosion can be seen. Therefore, our country loses 500 million tons of soil, which is enough to fill 150000 trucks, and can cover Sakarya City with a 29 cm thick stratum [12]. 86% of our country soils face with erosion danger [13]. In our country, the dragging material amount in riverbeds is 600 million ton. This is 1.8 times the all Europe's related value, 320 million ton [14]. Erosion or soil weathering is a break down in nature balance occurs with loss of forests and pastures in slopes. After erosion, in erosion zone, it can be seen that water balance changes and (after a rain, by the incoming water from slopes and creeks) there can be floods if the geological structure and other factors are appropriate.

By weathering, soil loses its upper (organic) strata, which is rich in organic materials and fragmental, big pores occur by the effect of this organic material. This upper stratum absorbs much of the rainwater as a sponge so flowing rainwater decreases, by lose of this upper strata approximately all rainwater flows along the surface and in this condition floodplains occur [11]. Because of being in a crossing zone as a geographical location, the half zone climate conditions are dominant. Therefore, majority of precipitations are in short or long time which causes erosion. Although the mean rainfall is 643 mm for Turkey, it is possible to see (according to time and location) rainfall values like 220 mm or 2500 mm as in eastern Black Sea region of Turkey. In inner and eastern region, rainfall mean is less than 400 mm. Between October-January, period that is important for agriculture; rainfall mean was 313.9 mm earlier, this mean decreased to 249.4 mm by 23.8% lose in October 1999-January 2000 period and to 190.1 mm by 39.5% lose in October 2000-January 2001 period [10].

Turkey is not a rich country in water resources. If this decreasing tendency goes on, today's water amount, which is 2860 m^3/person/year, will decrease to 1240 m^3/person/year in 2050 and 700 m^3/person/year in 2100. 2/3 of rainfall dropped on the earth surface starts flooding [10].

8. RECENT CHANGES IN THE FLOOD MANAGEMENT

The floods of the last decade, with their costly results have brought Turkey to a new view-point to reduce and control the susceptibility to the flood damages, namely the "Integrated Flood Management". In this context, a sound underwriting for land use control, flood insurance and early warning system are being considered. It can be said that from the years of experiences gained showed structural measures such as dams, levees and dykes, diversions, channel improvements, implemented in the basin-wide were effective with rather high cost, to reduce the risk in flood damage. Therefore non-structural measures are becoming more important in flood hazard management in the country.

9. CONCLUSIONS AND SUGGESTIONS

Devastation of forests and because of this loses of pastures and plants are fundamental reason for erosion. Then, extensive damages will occur due to flooding and land sliding. The biggest damage caused by erosion is losing the fruitful earth, which formed by thousand year periods. In order to evaluate the important of this, it assists that thinking a tree can produce a benefit, which is 2000 times its wood profit. Erosion is an important reason for agricultural production. Due to erosion and unsuitable use of agricultural terrains, decreasing agricultural terrains become insufficient to rapidly growing population so migration from villages to cities accelerates. The dams and other flood control structures played very important role in protecting the human life. However, flood control and management based on structural solutions could be insufficient. Therefore, effective solutions based on land use control, zoning, building ordinance, modifications in building codes, flood information programs by local communities are needed. This required major restructuring of both present legal systems and institutions responsible for management.

The flood plain use along the narrow valleys, encouraged by local civil administrations, had to be put under control. Otherwise, future human loss will be greater. During a flood, prior to all the state organizations should cooperate. In this respect, DSI, General Directorate of Electric Power Resources Survey and Administration (EIE) and DMI should be able to work together. From the view point of flood, considering the old experiences, to decrease of the flood damages or to take under control the flood some suggestions proposed for countries especially developing countries would be as follows:

- They should improve early warning system,
- They should prepare hazard mitigation plans and strategies and,
- They should be supplied with scientific and technical information about the flood.

REFERENCES

[1] Arman, H. (2004) Overview of flooding damages and its destructive consequences in Turkey: A case study of Zonguldak-Bartin flooding in 1998, Turkey. *NATO Advanced Research Workshop*, Ostrov u Tise.

[2] Yuksel, I. (2003) River erosion in eastern Black Sea region and scientific approaches aimed to prevent those events. *Journal of Engineering Bulletin*, *Chamber of Civil Engineering*, *Trabzon Division*, **17(62)**, 8-9.

[3] Yuksel, I., Onsoy, H. and Yuksek, O. (2005) Analyzing of river and coastal erosions based on the characteristics properties of the eastern Black Sea. 5*th Nationally Coastal Engineering Symposium*, Bodrum, 5-7 May 2005, 75-87.

[4] Yuksel, I. and Yuksek, O. (2003) Analysis of erosion in eastern Black Sea region with the latest developments. *Journal of Natural and Human*, **37(2)**, 2-8.

[5] Yuksel, I. and Yuksek, O. (2004) Studying to prevent of the flood in the settling and agricultural areas in the eastern Black Sea region. *Journal of Natural and Human*, **38(3-4)**, 64-67.

[6] Foody, M.G., Ghoneim, M.E. and Arnell, W.N. (2004) Predicting locations sensitive to flash flooding in an arid environment. *Journal of Hydrology*, **292(1)**, 48-58.

[7] Seker, D.Z., Goksel, C., Kabdaslı, S., Musaoglu, N. and Kaya, S. (2003) Investigation of coastal morphological changes due to river basin characteristics by means of remote sensing and GIS techniques. *Journal of Water Science Technology*, **48(10)**, 135-142.

[8] Gurer, I. and Ozguler, H. (2004) Integrated flood management case study1 Turkey: Recent flood disasters in northwestern Black Sea region. World Meteorological Organization, the Associated Programme on Flood Management.

[9] Keller, E.A. (2000) Environmental geology. 8th Edition, Prentice-Hall, Inc., New Jersey.

[10] Gunay, T. (1997) Forest, Unforestation Soil Erosion. The Turkish Foundation for Computing Soil Erosion for Reforestation and the Protection of Natural Habitats (TEMA), Istanbul.
[11] http://www.meteor.gov.tr (accessible 2008).
[12] http://www.tema.org.tr (accessible 2008).
[13] http://www.agm.gov.tr (accessible 2008).
[14] Burak, S., Duranyildiz, I. and Yetis, U. (1997) National environmental action plan: Management of water resources. State Planning Organization (DPT), Ankara.

Call for Papers

Natural Science

A Journal Published by Scientific Research Publishing, USA
www.scirp.org/journal/ns

Natural Science is an international journal dedicated to the latest advancement of natural sciences. The goal of this journal is to provide a platform for scientists and academicians all over the world to promote, share, and discuss various new issues and developments in different areas of natural sciences. All manuscripts must be prepared in English, and are subject to a rigorous and fair peer-review process. Accepted papers will immediately appear online followed by printed hard copy. The journal publishes original papers including but not limited to the following fields:

- **Astronomy & Space Sciences**
  - Astronomy
  - Astrophysics
  - Atmospheric Science
  - Space Physics
- **Earth Science**
  - Geography
  - Geology
  - Geophysics/Geochemistry
  - Oceanography
- **Chemistry**
  - Analytical Chemistry
  - Biochemistry
  - Computational Chemistry
  - Inorganic Chemistry
  - Organic Chemistry
  - Physical Chemistry
- **Life Science**
  - Cell Biology
  - Computational Biology
  - Genetics
  - Immunology
  - Medicine/Diseases
  - Microbiology
  - Molecular Biology
  - Neuroscience
  - Pharmacology/Toxicology
  - Physiology
  - Psychology
  - Virology
- **Physics**
  - Applied Physics
  - Atomic, Molecular, and Optical Physics
  - Biophysics
  - High Energy/Particle Physics
  - Material Science
  - Plasma Physics
- **Others**
  - Education
  - History of Science
  - Science and Innovations

We are also interested in: 1) Short Reports—2-5 page papers where an author can either present an idea with theoretical background but has not yet completed the research needed for a complete paper or preliminary data; 2) Book Reviews—Comments and critiques.

Notes for Intending Authors

Submitted papers should not be previously published nor be currently under consideration for publication elsewhere. Paper submission will be handled electronically through the website. For more details, please access the website.

Website and E-Mail

http://www.scirp.org/journal/ns   ns@scirp.org

Natural Science, 2010, 2, 247-417
Published Online April 2010 in SciRes (http://www.scirp.org/journal/ns).

TABLE OF CONTENTS

Volume 2, Number 4, April 2010